BERICHTE
aus dem Fachbereich Geowissenschaften
der Universität Bremen

No. 191

Bauer, J.

LATE CENOMANIAN - SANTONIAN CARBONATE PLATFORM EVOLUTION OF SINAI (EGYPT): STRATIGRAPHY, FACIES, AND SEQUENCE ARCHITECTURE

Berichte, Fachbereich Geowissenschaften, Universität Bremen, No. 191,
178 pages, Bremen 2002

ISSN 0931-0800

The "Berichte aus dem Fachbereich Geowissenschaften" are produced at irregular intervals by the Department of Geosciences, Bremen University.

They serve for the publication of experimental works, Ph.D.-theses and scientific contributions made by members of the department.

Reports can be ordered from:

Gisela Boelen

Sonderforschungsbereich 261

Universität Bremen

Postfach 330 440

D 28334 BREMEN

Phone: (49) 421 218-4124

Fax: (49) 421 218-3116

e-mail: boelen@uni-bremen.de

Citation:

Bauer, J.

Late Cenomanian – Santonian carbonate platform evolution of Sinai (Egypt): stratigraphy, facies, and sequence architecture.

Berichte, Fachbereich Geowissenschaften, Universität Bremen, No. 191, 178 pages, Bremen, 2002.

ISSN 0931-0800

BERICHTE
aus dem Fachbereich Geowissenschaften
der Universität Bremen

No. 191

Bauer, J.

LATE CENOMANIAN - SANTONIAN CARBONATE PLATFORM EVOLUTION OF SINAI (EGYPT): STRATIGRAPHY, FACIES, AND SEQUENCE ARCHITECTURE

Berichte, Fachbereich Geowissenschaften, Universität Bremen, No. 191,
178 pages, Bremen 2002

ISSN 0931-0800

Late Cenomanian - Santonian carbonate platform evolution of Sinai (Egypt): stratigraphy, facies, and sequence architecture

Dissertation zur Erlangung des Doktorgrades der Naturwissenschaften am Fachbereich Geowissenschaften, Universität Bremen

Vorgelegt von

Jan Bauer

Bremen, 2001

Tag des Kolloquiums
14.12.2001
Gutachter
Prof. Dr. J. Kuss
Prof. Dr. R. Henrich
Prüfer
Prof. Dr. M. Olesch
Dr. J. Lehmann

PREFACE

The thesis is subdivided into four separate papers, which are submitted, accepted for publication or in press. Several co-authors and collaborators participated in these papers; my own contributions are as follows.

CHAPTER 2: Lithostratigraphy and biostratigraphy of the Cenomanian – Santonian strata of Sinai, Egypt. Bauer, J., Marzouk, A.M., Steuber, T. & Kuss J.; *Cretaceous Research*, **22**; in press.

Own contributions: field work, microfossil extraction, data on benthic and planktic foraminifers and interpretations and discussions of other fossil data (ammonites, calcareous nannofossils, ostracods), all biostratigraphic, lithostratigraphic and geologic interpretations and discussions, correlation, text and figures.

CHAPTER 3: Sequence architecture and carbonate platform configuration (upper Cenomanian Santonian), Sinai, Egypt. Bauer, J., Kuss, J. & Steuber, T.; *Sedimentology*; submitted.

Own contributions: field work; all facies data, interpretations and discussions of facies, sequence stratigraphy, palaeogeography and tectonics, correlations, review and incorporation of published data into the models, text and figures.

CHAPTER 4: Distribution of shallow-water benthics: the Cenomanian – Turonian carbonate platform sequences of Sinai, Egypt. Bauer, J., Steuber, T., Kuss, J. & Heimhofer U.; *Proceedings of the 5th International Congress on Rudists. Courier Forschungsinstitut Senckenberg*; in press.

Own contributions: field work; qualitative and semi-quantitative data on benthic foraminifers and calcareous algae, interpretations and discussions of their distribution patterns and in parts of the rudist distribution patterns, geologic, stratigraphic and facies related interpretations and discussions, text and figures.

CHAPTER 5: Carbonate platform, environments, microfacies and systems tracts (upper Cenomanian - lower Santonian) of Sinai, Egypt. Bauer, J., Kuss, J. & Steuber, T.; *Facies*; submitted.

Own contributions: field work; all microfacies data (qualitative and semi-quantitative), geologic, stratigraphic and facies related interpretations and discussions, most text and all graphics.

The data base of this thesis is stored at Bremen University, department of geosciences (Geochronology). The same is true for the rock samples, ammonites, thin sections, washed microfossil samples and isolated foraminifer samples. Untreated marl samples and isolated ostracod specimens are stored at Ain Shams University (Dr M.M. Morsi), Cairo, Egypt. Smear slides for calcareous nannofossils are stored in the University of Tanta (Dr A.M: Marzouk), Egypt. Rudist specimens are stored at Ruhr-University, Bochum (Dr T. Steuber).

SUMMARY

The interplay of relative sea-level changes, tectonics, and local and large scale environmental perturbations in Sinai left major imprints on late Cenomanian - Santonian carbonate platform configuration and its depositional history. In this thesis, the tectono-sedimentary development of this Sinai platform is reconstructed and important environmental mechanisms on the sedimentary record are investigated with respect to local and regional geological framework. In an integrated approach field observations, palaeontological (macrofossils, microfossils, nannofossils) and thin-section sedimentpetrographical studies are combined. This is documented in four papers (CHAPTERS 2-5) that are in press in or are submitted to international journals.

CHAPTER 2 presents a lithostratigraphic and multibiostratigraphic framework of the sections studied. Five formations (Halal, Raha, Abu Qada, Wata, Matulla) are investigated with respect to age, lithologic variations and depositional environments. The semiquantitative distribution of calcareous nannofossils enable the identification of the biozones CC 10 - CC 16. Abundant ammonites at the base of the Abu Qada Formation are assigned to the uppermost lower Turonian *Mammites nodosoides* Zone. This 'ammonite bed' overlies the Cenomanian Halal and Raha formations respectively and a hiatus across the Cenomanian/Turonian (C/T) boundary is indicated. Keeled planktic foraminifers are only present in the *Dicarinella concavata* and *D. asymetrica* zones (Coniacian - Santonian). The biostratigraphic data sets are supplemented by data on ostracods, smaller benthic foraminifers and rudists (see below). Eleven lithostratigraphic and biostratigraphic units are defined and correlated along a N-S transect. Units within the Halal, Raha, Abu Qada and Wata formations are considered to be synchronous and a more or less coeval formation of the major facies belts is probable. In contrast, the units of the Matulla Formation are most probably diachronous because migrations of the facies belts from the Coniacian onwards are particularly influenced by the structured morphology which originated from syndepositional Syrian Arc tectonics.

In CHAPTER 3, the stratigraphic results provide important information for sequence-stratigraphic and palaeogeographic interpretations. Eight upper Cenomanian - Santonian sequences are manifested in the progradation/retrogradation patterns of major facies belts (supratidal, siliciclastic shoreface, lagoon, shallow subtidal, high-energy subtidal and deep-water). Relative sea-level changes are indicated by the sequence-stratigraphic correlation and by palaeogeographic maps. The palaeogeographic evolution is characterised by (1) the late Cenomanian - early Turonian platform drowning, by (2) the temporal and spatial evolution of the Central Sinai Intrashelf Basin (C-S Basin) in the Turonian and by (3) a Coniacian - Santonian basin and swell morphology. (1) The drowning of the platform is reflected by deep-water deposits above Cenomanian platform carbonates and was due to reduced carbonate production during the late Cenomanian - early Turonian. (2) In the early Turonian deep-water deposits of the C-S Basin covered large parts of north and central Sinai. Since the middle Turonian the synsedimentary subsiding C-S basin was filled by thick accumulations of shallow subtidal deposits. (3) The tectonically induced basin and swell morphology in the Coniacian - Santonian is documented by the interfingering of shallow-subtidal swell deposits and deep-water deposits in rapidly subsiding basins.

Tectonic pulses are documented by laterally varying thickness of the stratal packages. These variations in accommodation are due to tectonically induced uplift and differential subsidence balanced by high accumulation rates. Curves of cumulative sediment thickness allow to detect variations of subsidence. Turonian uplift preceded the main phase of topographic differentiation in the Coniacian - Santonian. Considerable stratigraphic mismatches between our sequence boundaries and those elsewhere on the Tethys margins underline the synsedimentary tectonic influence.

In CHAPTER 4, the stratigraphic and facies-related distribution patterns of rudists, smaller benthic foraminifers and calcareous algae in the upper Cenomanian - Turonian are analysed involving the biostratigraphic and sequence-stratigraphic framework. Diversity of rudist bivalves is generally low; benthic foraminifers are frequent in quiet, low-energy backshoal environments with diverse calcareous algae intercalated between rudist-bearing horizons. Occurrences of rudists and benthic foraminifers, which were both common in the late Cenomanian, declined drastically in the early Turonian and recovered in the middle and late Turonian. Calcareous algae were species-poor during the late Cenomanian and flourished in the early and late Turonian. However, occurrences of these benthics are closely related to the regional distribution of facies belts, which prevail in individual systems tracts. Rudists occur mainly in HSTs (highstand systems tracts), benthic foraminifers and calcareous algae mainly in TSTs (transgressive systems tracts) and HSTs. Thus, relative sea-level changes resulted in repeated reorganisation of the depositional system, which included the benthic communities and their habitats.

In CHAPTER 5, the Cenomanian - Santonian microfacies and semiquantitative distribution patterns of skeletal and non-skeletal components are analysed. The limestones investigated show a wide spectrum of microfacies types which correspond to major inner-platform facies belts (see CHAPTER 3). Local and regional palaeoecological responses to changing sedimentary settings are recognised and the factors controlling grain composition and depositional environments are discussed: (1) ecological conditions varied with increasing distance to the shoreline led to significant proximal-distal distribution gradients. A lateral facies zonation of the platform reflects reduced turbulence and bathymetry as well as high siliciclastic input in the proximal environments in south Sinai. Protected shallow-subtidal environments in central and north Sinai (distal) were less influenced by ecological stress regarding water circulation and siliciclastic input. High-energy deposits are represented by isolated oolitic and bioclastic shoals and carbonate sand sheets, especially in central Sinai along the margins of the C-S Basin. (2) Long term variations reflect variations of the platform morphology and climatic/oceanographic perturbations. The post Turonian lithological break appears to be related to the flooding of the platform by oxygen depleted water at the C/T boundary. A change to a more humid climate and a decrease of water temperature is responsible for an increase of siliciclastics and a decrease of ooids and calcareous algae since the Coniacian. (3) Changes of accommodation favoured the development of specific microfacies types in time and space during, e.g. owing to current intensities and wave-agitation.

ZUSAMMENFASSUNG

Das Zusammenwirken von relativen Meeresspiegelschwankungen, Tektonik und lokalen und regionalen Umwelteinflüssen hatte wesentlichen Einfluss auf die Plattformkonfiguration und die Faziesentwicklung (Obercenoman - Santon) der inneren Plattform der Sinaihalbinsel. In der vorliegenden Arbeit wird die tektono-sedimentäre Entwicklung der Sinai-Plattform rekonstruiert. Die wichtigsten Umwelteinflüsse auf die Fazies werden untersucht und in Bezug zum überregionalen geologischen Rahmen gesetzt. In einem integrierten Ansatz werden Geländebeobachtungen, Paläontologie (Makro-, Mikro- und Nannofossilien) und Dünnschliff-Sedimentpetrographie kombiniert. Dies ist in vier Manuskripten dokumentiert (KAPITEL 2-5), die sich im Druck befinden bzw. bei internationalen Fachzeitschriften eingereicht wurden.

In KAPITEL 2 wird ein litho- und multibiostratigraphischer Rahmen für die untersuchten Profile präsentiert. Fünf Formationen (Halal, Raha, Abu Qada, Wata, Matulla) werden im Hinblick auf Alter, lithologische Variationen und Ablagerungsbedingungen untersucht. Die semiquantitative Verteilung von kalkigen Nannofossilien erlaubt die Identifizierung der Biozonen CC 10 - CC 16. Häufig vorkommende Ammoniten an der Basis der Abu Qada Formation stammen aus der *Mammites nodosoides* Zone des obersten Unterturons. Die "Ammonitenbank" überlagert obercenomane Plattformkarbonate der Halal bzw. Raha Formationen und läßt auf einen Hiatus an der Cenoman/Turon-Grenze (C/T-Grenze) schließen. Gekielte, planktische Foraminiferen treten nur in den *Dicarinella concavata* und *D. asymetrica* Zonen (Coniac - Santon) auf. Die biostratigraphischen Datensätze werden ergänzt durch Daten von Ostrakoden, benthischen Foraminiferen und Rudisten (siehe unten). Elf litho- und biostratigraphische Einheiten werden definiert und entlang eines N-S-Schnittes korreliert. Die Einheiten innerhalb der Halal, Raha, Abu Qada und Wata Formationen werden jeweils als synchron erachtet und eine zeitgleiche Entwicklung der einzelnen Faziesgürtel ist wahrscheinlich. Im Gegensatz dazu sind die Einheiten innerhalb der Matulla Formation höchstwahrscheinlich diachron aufgrund von Faziesverschiebungen im Zuge der "Syrian Arc"-Tektonik.

In KAPITEL 3 liefern die stratigraphischen Ergebnisse wichtige Informationen für sequenzstratigraphische und paläogeographische Interpretationen. Acht Sequenzen (Obercenoman - Santon) sind überliefert und wurden anhand der Progradations- und Retrogradationsmuster der Faziesgürtel (siliziklastische Küste, Lagune, flaches Subtidal, hochenergetisches Subtidal und Tiefwasserfazies) interpretiert. Die sequenzstratigraphische Korrelation und großmaßstäbliche paläogeographischen Karten ermöglichen die Rekonstruktion von relativen Meeresspiegelschwankungen. Die paläogeographische Entwicklung der Sinai-Plattform ist vor allem gekennzeichnet (1) durch das "Ertrinken" der Plattform im Obercenoman - Unterturon, (2) durch die räumliche und zeitliche Entwicklung eines Intraschelf-Beckens im Turon und (3) durch eine Becken- und Schwellen-Morphologie im Coniac - Santon. (1) Das "Ertrinken" der Plattform ist gekennzeichnet durch Tiefwassersedimente, die Plattformkarbonate des Cenomans überlagern, und wird auf eine verminderte Karbonatproduktion im Obercenoman - Unterturon zurückgeführt. (2) Im Unterturon bedeckten Tiefwassersedimente des Intraschelf-Beckens große Teile des Nord- und Zentralsinai. Ab dem Mittelturon wurde das Becken während anhaltender Subsidenz mit mächtigen Flachwassersedimenten gefüllt. (3) Die tektonisch induzierte Becken- und Schwellen-Morphologie im Coniac - Santon ist überliefert durch die Verzahnung von Flachwasser- und Tiefwassersedimenten.

Tektonische Ereignisse sind durch laterale Mächtigkeitsänderungen der Sedimentpakete überliefert. Diese Variationen des Akkommodationraumes sind sowohl durch Hebungen sowie durch unterschiedliche Subsidenz begründet. Die graphische Darstellung der kumulativen Sedimentmächtigkeiten macht Subsidenzvariationen sichtbar. Daneben stellen erste Hebungen im Turon Vorläufer der Hauptphase der topographischen Differenzierung im Coniac - Santon dar. Deutliche stratigraphische Diskrepanzen zwischen unseren Sequenzgrenzen und denen in anderen Regionen der Tethys untermauern den Einfluss synsedimentärer Tektonik.

In KAPITEL 4 werden die stratigraphischen (Obercenoman - Turon) und faziesgebundenen Verteilungsmuster von Rudisten, benthischen Foraminiferen und Kalkalgen analysiert unter Einbeziehung des biostratigraphischen und sequenzstratigraphischen Rahmens. Die Diversität der Rudisten ist generell niedrig; benthische Foraminiferen sind häufig in niederenergetischen Bereichen der inneren Plattform und treten zusammen mit diversen Kalkalgen-Assoziationen und eingeschalteten Rudistenhorizonten auf. Vorkommen von Rudisten und benthischen Foraminiferen sind weit verbreitet im Obercenoman, nehmen im Unterturon deutlich ab und steigen im Mittel- und Oberturon wieder an. Kalkalgen-Assoziationen sind artenarm im Obercenoman und artenreich im Unter- bis Oberturon. Die Verbreitung dieser Benthonten ist jedoch eng verknüpft mit der lateralen Verteilung der Faziesgürtel, die in bestimmten "systems tracts" überwiegen. Das Auftreten von Rudisten ist meist an die HSTs ("highstand systems tracts") gebunden; benthische Foraminiferen und Kalkalgen treten meist in den TSTs ("transgressive systems tracts") und in den HSTs auf. Relative Meeresspiegelschwankungen führten zu einer Reorganisation der Ablagerungssysteme einschließlich der Habitate der benthischen Organismen.

In KAPITEl 5 werden Mikrofazies und semiquantitative Verteilungsmuster von abiogenen und biogenen Komponenten analysiert für das Zeitinterval Obercenoman - Santon. Die untersuchten Kalksteine zeigen ein weites Spektrum an Mikrofaziestypen, die die Faziesgürtel der inneren Plattform (siehe KAPITEl 3) widerspiegeln. Lokale und regionale palökologische Aspekte werden herausgearbeitet und in Bezug zu den sich ändernden Ablagerungsbedingungen gesetzt. Die Kontrollfaktoren der Komponentenzusammensetzungen und der Ablagerungsmilieus werden diskutiert: (1) Die ökologischen Bedingungen variierten mit zunehmender Entfernung zur Küste und führten zu einem signifikanten Verteilungsgradienten von proximal zu distal. Die laterale Fazieszonierung auf der Plattform macht verminderte Turbulenz und Bathymetrie sowie erhöhten siliziklastischen Eintrag in den proximalen Bereichen (Südsinai) deutlich. Geschützte Flachwasserbereiche im Zentral- und Nordsinai (distal) waren weniger beeinflußt von ökologischen Veränderungen in Bezug auf Zirkulation und siliziklastischen Eintrag. Hochenergetische Ablagerungen werden von bioklastischen Ooidbarren und Karbonatsanden repräsentiert, besonders entlang den Rändern des Intrashelf-Beckens im Zentralsinai. (2) Übergeordnete Veränderungen sind mit Änderungen der Plattform-Morphologie und mit klimatischen/ozeanographischen Variationen verknüpft. Der lithologische Einschnitt nach dem Turon ist wahrscheinlich zurückzuführen auf das Fluten der Plattform mit sauerstoffverarmtem Wasser an der C/T Grenze. Ein Wechsel zu humided Klimabedingungen ist verantwortlich für eine Zunahme an Siliziklastika und für eine Abnahme an Ooiden und Kalkalgen ab dem Coniac. (3) Änderungen des Akkomodationsraumes begünstigte die Ausbildung bestimmter Mikrofaziestypen in Raum und Zeit, z.B. aufgrund von Strömungsintensitäten und Wellenbewegungen.

ACKNOWLEDGEMENTS

I am most grateful to Prof. J. Kuss for initiating this project and its financial support. The project benefited from his motivating support, sedimentological experience and the fruitful discussions we had. He reviewed the whole manuscript and improved the quality of this thesis significantly.

Special thanks go to Dr Thomas Steuber (Ruhr University, Bochum) for profitable discussions and critical comments on earlier versions of the submitted papers as well as for his introduction to the rudists. The field trips benefited significantly from Thomas experience.

Thanks are due to Prof. A. M. Bassiouni, Dr Mohsen M. Morsi (both Ain Shams University, Cairo) and Dipl. Geol. Ulrich Heimhofer (ETH Zurich) for their valuable help and assistance during the fieldwork programme in Sinai and during sample preparation at Ain Shams University, Cairo.

Many people have been involved in the preparation of this thesis and provided valuable data and advises. I am indebted to all for the co-operations. Dr Mohsen M. Morsi is thanked for ostracod determinations and for the help in the interpretation of the data. Dr Akmal M. Marzouk (University of Tanta, Egypt) is acknowledged for the identification of the calcareous nannofossils and his patience in investigating even very poorly preserved assemblages. Dr Frank Wiese (FU Berlin) and Dr Peter Luger (TU Berlin) are thanked for the identification of the ammonites.

My colleagues of the working group Geochronology of Bremen University are indebted for the various kinds of assistance and encouragement. Erna Friedel improved the English of this thesis significantly, and helped with all minor and major problems within the department. Ralf Bätzel prepared the thin sections and lended a helping hand for various technical issues. Dr Martina Bachmann, Dr Robert Speijer, and Dr Sebastian Lüning were always willing to answer all (sometimes strange) questions about special English terms, microfacies, sequence stratigraphy, nomenclature, and stratigraphy and gave constructive suggestions and comments on the topics of this thesis. Considerable help and support were provided by my room colleagues Dr Kristin Schnack and Dipl. Geol. Markus Geiger as well as by Dipl. Geol. Frauke Schulze, and Dr Christian Scheibner.

The project was funded by the German Research Foundation (DFG; Ku 642/15-1,2). Further financial support came from the University of Bremen (FNK).

Above all I warmly thank my parents for their extraordinary support throughout my university education. I am grateful for their constant encouragement. Stefanie is thanked for an open ear for all issues. Finally, Silvia encouraged me to overcome all difficulties of various kinds. Silvia is thanked for the continuous support, not only during the busy episodes of this work.

CONTENTS

CHAPTER 1

Introduction

1. Geological Background
2. Research Objectives and Structure of the Thesis
3. References

CHAPTER 1
Introduction

The palaeogeographic evolution of the upper Cenomanian - Santonian carbonate platform of Sinai is investigated with special emphasis on the sedimentologic, biostratigraphic, lithostratigraphic, sequence-stratigraphic and facies development. The interplay of different sedimentologic and geodynamic features on the carbonate platform is deciphered on the basis of field observations and detailed stratigraphic sections, macrofacies and microfacies analyses, fossil distribution patterns, and qualitative and semi-quantitative component analyses. Detailed depositional models integrate the sedimentologic and palaeontologic results. About four months of field work was an essential part of the project. During two field trips in north, central and south Sinai, 30 stratigraphic sections were measured in detail at 13 different localities with a total length of ca. 2700 m. 530 marl samples and 423 rock samples were analysed.

The thesis is subdivided into four separate papers (CHAPTERS 2-5), which are submitted, accepted for publication or are in press. The results were also presented on several international sedimentology and palaeontology meetings. Further closely related sedimentologic and palaeontologic studies appeared or will appear in: Kunow, *Bauer*, Bachmann & Kuss (1998), investigating the distribution patterns of benthic foraminifers and clay-mineral associations of upper Aptian sediments in Sinai; Kuss, Westerhold, Groß, *Bauer*, & Lüning, S. (2000b) presenting a geologic map of the Gebel Areif el Naqa anticline and investigating the sedimentary response to Syrian Arc tectonics; and Morsi & *Bauer* (in press), presenting taxonomic, palaeobiogeographic, biostratigraphic, and palaeoecologic studies on Cenomanian ostracods of Sinai. The abstracts of these papers are presented in the appendix.

1. GEOLOGICAL BACKGROUND

Palaeogeography: During the middle and Late Cretaceous the Sinai Peninsula was part of the Afro-Arabian carbonate platform of the southern margin of the Tethys (Fig. 1 in CHAPTER 3). This platform was located in lower latitudes of the northern hemisphere and extended from Morocco to Oman (Philip & Floquet, 2000). During most of the stratigraphic intervals investigated herein, Sinai was covered by the inner-platform realm. Siliciclastic shoreface and shallow-subtidal facies belts dominated the depositional systems with typical skeletal and non-skeletal constituents of an inner-platform setting (CHAPTERS 3, 4).

A number of Late Cretaceous intrashelf basins developed on the Afro-Arabian Plate margin (Fig. 2 in CHAPTER 5), e.g. in Tunisia and Oman (Harris et al., 1984; Philip et al., 1995; Abdallah et al., 2000). In Sinai, a synsedimentary subsiding intra-platform basin, the Central Sinai Basin (C-S Basin), formed during the latest Cenomanian (CHAPTER 3). Although Lewy (1975), Bartov & Steinitz (1977) and Kuss (1992) noted its importance for palaeogeographic interpretations of Sinai, evolution in time and space of the C-S Basin is still unclear. Its eastward prolongation towards Israel and Palestine, the Eshet-Zenifim Basin (Bentor, 1960; Bartov & Steinitz, 1977), has been studied

previously by Gvirtzman & Garfunkel (1998) and Buchbinder et al. (2000). Facies development through time in the C-S Basin and its lateral extensions have not been investigated in recent publications. In this study this is taken into account by palaeogeographic maps (CHAPTER 3). Moreover, Syrian Arc tectonics (see below) formed a basin and swell morphology since the Coniacian. Shallow-water deposits on the swells interfinger with basin deposits over short distances (CHAPTERS 2, 3). Despite a large amount of published sedimentologic and biostratigraphic data, the exact palaeogeographic positions of the basins and swells is still unclear. This is due to the complicated facies variations (CHAPTER 3) and the sometimes contrasting interpretations in the literature.

Palaeoclimate, palaeoecology, and Cenomanian/Turonian boundary events: The middle - Late Cretaceous was one of the warmest periods in the Late Phanerozoic (Frakes et al., 1992). Ice rafted deposits have not been reported in the high latitudes during Late Cretaceous greenhouse intervals, and thus the polar regions were probably free from large volumes of permanent ice (Huber, 1998; DeConto et al., 2000; Crowley & Zachos, 2000). A low equator to pole temperature gradient (Barron, 1983) probably resulted in a reduced thermohaline circulation (Hay, 1995). In addition the oceans were stratified partly with the development of anoxic bottom waters (see below). However, cooler intervals within this warm period have also been reported (Arthur et al., 1987; Frakes et al., 1992; Huber, 1998; Voigt et al., 1999, Stoll & Schrag, 2000), and are also interpreted in Sinai (CHAPTER 5) and the Near East (Kolodny & Raab, 1988). In addition, wet and temperate conditions of the northern Tethyan carbonate platforms stand in contrast to the tropical and arid climates of the southern Tethyan platforms (Philip & Floquet, 2000), which developed in during the Cenomanian and Turonian (e.g. evidenced by evaporites in Sinai, CHAPTERS 2, 3). The warm, shallow-water environments favoured the formation of broad carbonate platforms on the northern margin of the Afro-Arabian Plate and in southern Europe. Rudists were important carbonate producers together with corals, other bivalves (oysters, chondrodonta) and benthic foraminifers. Towards the Turonian/Coniacian boundary a cooling trend is observed in some low and medium palaeolatitude regions (Frakes et al., 1992).

The C/T boundary is characterised by a demise (drowning) of many Tethyan carbonate platforms in southern Europe, Middle East, and North Africa, including Sinai (CHAPTER 3). As a consequence of drowning, condensed sedimentation and hiati occur at the C/T boundary in these regions, including Sinai (CHAPTER 2). Many of these platform drowning successions are well studied. However, in Sinai, platform drowning, its biosedimentary response, and its mechanisms (CHAPTERS 3, 4) have not been discussed in previously. The demise of carbonate platforms may be linked to the contemporaneous extinction of aragonitic rudist taxa. Benthic foraminifers and other fossil groups also experienced pronounced faunal turnovers in the Middle East and North Africa, including Sinai (CHAPTER 4). The global faunal turnover at the C/T boundary affected 7% of all marine families and 26 % of all genera became extinct (Harries, 1993). This event coincides with a major eustatic sea-level highstand (see below) and with the oceanic anoxic event OAE II (Arthur et al., 1987). The subsequent flooding of the shelves by oxygen-depleted waters gradually demised intermediate and shallow water Cenomanian taxa (Harries, 1993). After the faunal turnover, new species filled the niches and evolved in the Turonian (CHAPTERS 2, 4).

The OAE II was associated with a positive δ13C excursion, deposition of black shales, and global warming (Arthur et al., 1987; Kuypers et al., 1999). A discussion of the C/T boundary events on a global scale and the origin of black shales are beyond the scope of this thesis. However, it is worth mentioning that two general models for the genesis of black shales are widely discussed: (1) the preservation model highlights stratification of the water column and anoxic bottom waters (e.g. Tyson, 1995), owing to circulation patterns or extensive denitrification, and (2) the productivity model (e.g. Pedersen & Calvert, 1990) combines upwelling-induced high productivity and intensification and vertical expansion of the oxygen minimum zone.

Other widespread black shale deposits in the southern Mediterranean are genetically linked to a younger oceanic anoxic event, AOE III (Jenkyns, 1980), in the Coniacian - Santonian. It coincides with a period of enhanced upwelling and high productivity along the eastern Mediterranean coast, which resulted in the deposition of widespread phosphorite belts in Sinai and adjacent regions (Eshet et al., 1994; Kolodny & Garrison, 1994; Lüning et al., 1998; Abed & Amireh, 1999).

Sea-level: Sedimentologic and ecologic changes in Tethyan carbonate platform settings are generally closely linked with eustatic and relative sea-level changes (CHAPTERS 3 - 5). Sequence-stratigraphic interpretations of the mid and Upper Cretaceous platform deposits of North Africa and Arabia (Robaszynski et al., 1990, 1993; Abdallah et al., 2000; Scott et al., 2000; Sharland et al., 2001) show the importance of relative and eustatic sea-level changes. However, few contributions focus on the sequence-stratigraphic evolution of Sinai and adjacent regions (Bachmann & Kuss, 1998; Lüning et al., 1998; Buchbinder et al., 2000; Kuss et al., 2000a).

A long term eustatic sea-level rise started in the Triassic and culminated during the late Cenomanian to early Turonian in the highest sea-level of the Phanerozoic (Haq et al., 1987; Philip & Airaud-Crumiere, 1991; Hancock, 1993). Due to this sea-level maximum, the southern coastline of the Tethys shifted southwards with a maximum transgression reported from Morocco (Philip & Floquet, 2000). Thus, a major expansion of the Afro-Arabian Platform, including the Sinai platform (CHAPTER 3), occurred in this period. Global sea-level reached its climax in the early Turonian *Mammites nodosoides* ammonite biozone (Fig. 13 in CHAPTER 3). Although the sequence chronostratigraphic chart of Haq et al. (1987) was recently recalibrated by Hardenbol et al. (1998), and despite criticism of the 'global' Haq-curve (Miall, 1992), an age equivalent relative sea-level rise is evidenced in Sinai and the Near East from the sedimentary and biostratigraphic record (CHAPTER 2). This relative sea-level rise represents is an important episode of the Turonian carbonate platform evolution (CHAPTER 3). Furthermore, prominent sea-level lowstands in Sinai are recorded in the middle Turonian and in the upper Turonian-Coniacian, which both are correlatable with those of adjacent areas (CHAPTER 3). This contrasts to tectonically influenced relative sea-level changes in Sinai.

Tectonics: The three major stages of geodynamic evolution of Sinai are (1) Triassic rifting in the Neotethyan ocean, (2) post Cenomanian compression, due to the first stage of the collision of the Afro-Arabian and Eurasian plates and (3) the early Miocene establishment of the Gulf of Suez /

Red Sea Rift and Dead Sea fault system, which resulted from the separation and rotation of the Sinai subplate from the African plate from the Oligocene onwards (Badawy & Horváth, 1999).

Triassic - Early Jurassic rifting in the Neotethys caused half grabens and basins in north Sinai (Moustafa & Khalil, 1990), Egypt (Bakr et al., 1999), Israel (Hirsch et al., 1998) and in other eastern Mediterranean regions (e.g. Levantine basin) (Vidal et al., 2000). Late Cretaceous initial closure of the Neotethyan Ocean resulted in northwest - southeast compression and the inversion of most sedimentary basins from Morocco to Oman in (for a review, see Guiraud, 1998). In Sinai, the transpressive inversion along the pre-existing half graben structures involved folding and lateral strike-slip faulting (Guiraud, 1998) since the early Turonian and reached its climax with the formation of the Syrian Arc fold belt (Krenkel, 1924). Domal anticlines are well preserved in northern Sinai, and are part of this fold belt which extends from Syria, Lebanon, Israel to northern Egypt (Moustafa & Khalil, 1990; Walley, 1998; Bosworth et al., 1999). In this thesis, the anticlines Gebel Minsherah, Gebel Risha and Gebel Areif El Naqa were studied. It is important to note that the term ´Arc` is misleading because the structure is not a result of volcanic activities along a plate margin, but of intracontinental deformation. Of course, plate tectonics were unknown to Krenkel and he used the term ´Arc` to express the bent configuration of the fold belt. Detailed reviews of the Syrian Arc evolution are given by e.g. Shahar (1994). There is general agreement about the main folding episode and uplift starting in the Oligocene, which is linked to the opening of the Red Sea and the Gulf of Suez basin. In contrast, the timing of initial movements is still debated and ranges from the early Turonian to Santonian (CHAPTER 3).

Said (1962) introduced the terms ´unstable shelf` for the tectonically active area in north Sinai and ´stable shelf` for the inactive area in central and south Sinai (Fig. 2a in CHAPTER 3). Following this tectonic subdivision, fault reactivation, inversion and folding are expressed on the ´unstable shelf` of Sinai. However, Bosworth et al. (1999) already noted that Late Cretaceous folding also effected the sedimentary cover in the Gulf of Suez region, which was previously considered a stable cratonic setting. Moreover, local depressions along the Gulf of Suez coast and subsidence of the C-S Basin (CHAPTER 3) suggest tectonic activity also on the ´stable shelf`.

2. RESEARCH OBJECTIVES AND STRUCTURE OF THE THESIS

The primary goal of this thesis is to specify the effects of (1) eustatic and relative sea-level changes, (2) platform drowning at the C/T and T/Con boundaries, (3) Syrian Arc tectonics, and (4) Late Cretaceous upwelling on the sedimentary record and on the depositional history in a multidisciplinary approach (stratigraphy, sequence stratigraphy, microfacies analysis and palaeontology); special emphasis is placed on four major themes.

Lithostratigraphy and biostratigraphy: A basic premise is to provide a chronostratigraphic framework of the sections measured (CHAPTER 2). However, as reliable biostratigraphic data are generally rare in shallow carbonate platform settings, the need for an integrated lithostratigraphic and biostratigraphic approach in Sinai is evident. Important questions are: which of the fossil groups recovered from the stratigraphic sections enable best possible biostratigraphic resolution? Are the stratigraphic assignments of the investigated index fossils consistent compared to adjacent regions and

global concepts? Does the combination and inter-correlation of biostratigraphic concepts allow precise biostratigraphic assignments or are the occurrences of the investigated index species stratigraphically inconsistent? Which lithostratigraphic units can be recognised and how do their lithologies vary throughout Sinai? Which lithologic units, marker beds and distribution patterns of characteristic biota are synchronous or diachronous with respect to the stratigraphic framework achieved?

Sequence stratigraphy: Sequence-stratigraphic concepts are useful tools for the determination of the factors controlling lateral and stratigraphic facies evolution and palaeogeography (CHAPTER 3). The interpretation of relative sea-level changes and sequence architectures enable to reconstruct varying accommodation and resulting progradation/retrogradation patterns. Important questions are: how are individual sequences in Sinai organised, and is it possible to recognise typical stacking patterns or other distinct indicators, with respect to the individual systems tracts? How many sequences can be interpreted and are there previously unknown sequence boundaries in Sinai? How do the sequences of Sinai correlate with those of other regions and global charts, and is it possible to differentiate local, regional and eustatic signals.

Palaeogeography and synsedimentary tectonics: Palaeogeographic maps (CHAPTER 3) visualise migration of facies belts in time and space and allow to reconstruct the lateral and stratigraphic platform configuration. Synsedimentary tectonics are documented by laterally varying thicknesses of the stratal packages (CHAPTER 3). Questions of research are: when was the C-S Basin formed and what were its lateral expansions? Is its subsidence history recorded in the sedimentary record and how did it influence the depositional architecture? Are facies belts bounded to specific areas on the platform? How did the depositional system respond to Syrian Arc tectonics?

Lithofacies and biofacies proxies: Lithofacies and biofacies response to local and large scale environmental changes are deduced from facies interpretations, microfacies analysis (CHAPTER 5), and regional and vertical distribution patterns of rudists, benthic foraminifers, and calcareous algae (CHAPTER 4). Correlations of the (sequence) stratigraphic and facies-related distribution patterns of skeletal and non-skeletal components reflect ecological changes within the depositional environments. Moreover, main questions are: how is the lateral zonation of the carbonate platform characterised with respect to lateral distribution of skeletal and non-skeletal components? Which components reacted sensitively on changing platform organisation and relative sea-level changes? Which long-term environmental changes controlled facies composition, biotic turnover (e.g. across the C/T boundary), and evolutionary trends?

To answer these questions a stratigraphic framework for the successions studied (CHAPTER 2) is essential for a lateral correlation of lithofacies and biofacies and inter-regional comparisons of e.g. tectonic episodes, large scale environmental changes, and biotic distribution patterns. On the basis of this combined biostratigraphic and lithostratigraphic correlation a sequence-stratigraphic interpretation (CHAPTER 3) is worked out, which is based on the formation of the major facies belts and their lateral and stratigraphic shifts. The results of the stratigraphic analysis and facies interpretation are integrated into palaeogeographic maps, which show the platform evolution in time and

space including major synsedimentary tectonic episodes. These issues are incorporated in CHAPTER 4. Here, the factors controlling the distribution of benthic carbonate producers are evaluated in the light of platform palaeogeography, sequence-stratigraphic interpretation, and decline and recovery patterns across the Cenomanian/Turonian boundary are documented. The comprehensive microfacies analysis of the upper Cenomanian - Santonian deposits in CHAPTER 5, adds to the information obtained in CHAPTERS 3 and 4, and allows to further specify the effects of lateral facies belts distribution, relative sea-level changes, and large scale environmental perturbations on the lithofacies and biofacies.

3. References

Abdallah, H., Sassi, S., Meister, C. & Souissi, R. (2000): Stratigraphie séquentielle et paléogéographie à la limite Cénomanien-Turonien dans la région de Gafsa-Chott area (Tunisie centrale).- *Cretaceous Research*, **21**, 35-106.

Abed, A.M. & Amireh, B.S. (1999): Sedimentology, geochemistry, economic potential and palaeogeography of an Upper Cretaceous phosphorite belt in southeastern desert of Jordan.- *Cretaceous Research*, **20**, 119-133.

Arthur, M.A., Schlanger, S.O. & Jenkyns, H.C. (1987): The Cenomanian-Turonian Oceanic Anoxic Event, II: Palaeoceanographic controls on organic-matter production and preservation.- In: Marine petroleum source rocks (Eds Brooks, J. & Fleets, A.J.).- *Geological Society, London, Special Publication*, **26**, 401-420.

Bachmann, M. & Kuss, J. (1998): The Middle Cretaceous carbonate ramp of the northern Sinai: sequence stratigraphy and facies distribution.- In: Carbonate ramps (Eds Wright, V. P. & Burchette, T. P.).- *Geological Society, London, Special Publication*, **149**, 253-280.

Badawy, A. & Horváth, F. (1999): The Sinai subplate and tectonic evolution of the northern Red Sea region.- *Geodynamics*, **27**, 433-450.

Bakr, A., Helmy, M. & Baltensperger, P. (1999): Kattaniya fold belt, Western Desert of Egypt; an example of an inverted Jurassic rift basin.- *American Association of Petroleum Geologists Bulletin*, **83**, 1298.

Barron, E.J. (1983): A warm and equable Cretaceous: the nature of the problem.- *Earth Science Reviews*, **19**, 305-338.

Bartov, Y. & Steinitz, G. (1977): The Judea and Mount Scopus Groups in the Negev and Sinai with trend surface analysis of the thickness data.- *Israel Journal of Earth Sciences*, **26**, 119-148.

Bentor, Y. K. (1960): Lexique stratigraphique international, Asie, **3/10 c2** (Israel).- 151 pp. (Centre National de la Recherch Scientifique, Paris).

Bosworth, W., Guiraud, R. & Kessler, L. G. (1999): Late Cretaceous (ca. 84 Ma) compressive deformation of the stable platform of northeast Africa (Egypt): far-field stress effects of the 'Santonian event' and origin of the Syrian Arc deformation belt.- *Geology*, **27**, 633-636.

Buchbinder, B., Benjamini, C. & Lipson-Benitah, S. (2000): Sequence development of Late Cenomanian-Turonian carbonate ramps, platforms and basins in Israel.- *Cretaceous Research*, **21**, 813-843.

Crowley, T.J. & Zachos, J.C. (2000): Comparison of zonal temperatur profiles for past warm time periods.- In: Warm climates in earth history (Eds Huber, B.T., MacLeod, K.G. & Wing, S.L.). - 50-76 (Cambridge University Press).

DeConto, R.M., Brady, E.C., Bergengren J. & Hay, W.W. (2000): Late cretaceous climate vegetation and ocean interactions.- In: Warm climates in earth history (Eds Huber, B.T., MacLeod, K.G. & Wing, S.L.). - 275-296 (Cambridge University Press).

Eshet, Y., Almogi-Labin, A. & Bein, A. (1994): Dinoflagellate cysts, paleoproductivity and upwelling systems: A Late Cretaceous example from Israel.- *Marine Micropaleontology*, **23**, 231-240.

Frakes, L.A., Francis, J.E. & Syktus, J.I. (1992): Climate modes of the Phanerozoic: the history of the earth's climate over the past 600 million years.- 274 pp. (Cambridge University Press).

Guiraud, R. (1998): Mesozoic rifting and basin inversion along the northern African Tethyan margin: an overview.- In: Petroleum geology of North Africa (Eds MacGregor, D.S., Moody, R.T.J. & Clark-Lowes, D.D.).- *Geological Society, London, Special Publication*, **132**, 217-229.

Gvirtzman, Z. & Garfunkel, Z. (1998): The transformation of southern Israel from a swell to a basin: stratigraphic and geodynamic implications for intracontinental tectonics.- *Earth and Planetary Science Letters*, **163**, 275-290.

Hancock, J.M. (1993): Sea-level changes around the Cenomanian-Turonian boundary.-*Cretaceous Research,* **14**, 553-562.

Haq, B.U., Hardenbol, J. & Vail, P.R. (1987): Chronology of fluctuating sea levels since the Triassic.- *Science* **235**, 1156-1167.

Hardenbol, J., Thierry, J., Farley, M.B., Jacquin, T., de Graciansky, P.-C. & Vail, P.R. (1998): Mesozoic and Cenozoic sequence chronostratigraphic framework of European basins, Chart 5.- In: Mesozoic and Cenozoic sequence stratigraphy of European basins (Eds de Graciansky, P.-C., Hardenbol, J., Jacquin, T. & Vail, P.R.).- *SEPM Special Publication* **60**.

Harris, P.M., Frost, S.H., Seiglie, G.A. & Schneidermann, N. (1984): Regional unconformities and depositional cycles, Cretaceous of the Arabian Peninsula.- In: Interregional unconformities and hydrocarbon accumulation (Ed. J.S. Schlee).- *American Association of Petroleum Geologists Memoir, **36**, 67-80.*

Harries, P.J. (1993): Dynamics of survival following the Cenomanian-Turonian (Upper Cretaceous) mass extinction event.- *Cretaceous Research*, **14**, 563 - 583.

Hay, W.W. (1995): Cretaceous Paleoceanography. - Geologica Carpathica, **46**, 257-266.

Hirsch, F., Bassoullet, J.-P., Cariou, E., Conway, B., Feldman, H. R., Grossowicz, L., Honigstein, A., Owen, E.F. & Rosenfeld, A. (1998): The Jurassic of the southern Levant. Biostratigraphy, palaeogeography and cyclic events.- In: Epicratonic basins of Peri-Tethyan platforms (Eds Crasquin-Soleau, S. & Barrier, É.).- *Peri-Tethys Memoir,* **4**, 213-235 (Mémoires du Muséum National d'Histoire Naturelle, Paris).

Huber, B.T. (1998): Tropical paradise at the Cretaceous poles?- *Science*, **282**, 2199-2200.

Jenkyns, H.C. (1980): Cretaceous anoxic events: from continents to oceans.- *Journal Geological Society London*, **137**, 171-188.

Kolodny, Y. & Garrison, R.E. (1994): Sedimentation and diagenesis in paleo-upwelling zones of epeiric sea and basinal settings: a comparison of the Cretaceous Mishash Formation of Israel and the Miocene Monterey Formation of California.- In: Proceedings 29th Geological Congress, Part C (Eds Iijima, A., et al.).- 133-159 (VSP).

Kolodny, Y. & Raab, M. (1988): Oxygen isotopes in phosphatic fish remains from Israel: paleothermometry of tropical Cretaceous and Tertiary shelf waters.- *Palaeogeography, Palaeoclimatology, Palaeoecology*, **64**, 59-67.

Krenkel, E. (1924) Der syrische Bogen.- *Zentralblatt für Mineralogie, Geologie und Palaeontologie, Abhandlungen, B*, **9**, 274-281; **10**, 301-313.

Kunow, R., Bauer, J., Bachmann, M. & Kuss, J. (1998): Verteilungsmuster benthischer Foraminiferen und Tonmineralassoziationen im Oberapt des Sinai.- *Zentralblatt der Geologie und Paläontologie Teil I,* **H1/2**, 353-371.

Kuss, J. (1992): The Aptian-Paleocene shelf carbonates of northeast Egypt and southern Jordan: establishment and break-up of carbonate platforms along the southern Tethyan shores.- *Zeitschrift der Deutschen Geologischen Gesellschaft,* **143**, 107-132.

Kuss, J., Scheibner, C. & Gietl., R. (2000a): Carbonate platform to basin transition along an Upper Cretaceous to Lower Tertiary Syrian Arc uplift, Galala Plateaus, Eastern Desert, Egypt.- *GeoArabia,* **5**, 405-424.

Kuss, J., Westerhold, T., Groß, U., Bauer, J. & Lüning, S. (2000b). Mapping of Late Cretaceous stratigraphic sequences along a Syrian Arc Uplift - examples from the Areif el Naqa/Eastern Sinai.- *Middle East Research Center, Ain Shams University, Earth Science Series,* **14**, 171-191.

Kuypers, M.M.M., Pancost, R.D. & Damsté, J.S.S. (1999): A large and abrupt fall in atmospheric CO2 concentration during Cretaceous times.- *Nature*, **399**, 342-345.

Lewy, Z. (1975): The geological history of southern Israel and Sinai during the Coniacian.- *Israel Journal of Earth Sciences,* **24**, 19-43.

Lüning, S., Marzouk, A. M., Morsi, A. M. & Kuss, J. (1998): Sequence stratigraphy of the Upper Cretaceous of central-east Sinai, Egypt.- *Cretaceous Research,* **19**, 153-196.

Miall, A.D. (1992): Exxon global cycle chart: an event for every occasion?- *Geology,* **20**, 787-790.

Morsi, A.M. & Bauer, J. (in press): Cenomanian ostracode faunas from Sinai peninsula, Egypt.- *Revue Paléobiologie*, **20**.

Moustafa, A.R. & Khalil, M.H. (1990): Structural characteristics and tectonic evolution of north Sinai fold belts.- In: The Geology of Egypt (Ed. Said, R.).- 381-389 (Balkema).

Pedersen, T.F. & Calvert, S.E. (1990): Anoxia vs. productivity: what controls the formation of organic-carbon-rich sediments and sedimentary rocks?- *American Association of Petroleum Geologists Bulletin*, **74,** 454-466.

Philip, J. & Airaud-Crumiere, C. (1991): The demise of the rudist-bearing carbonate platforms at the Cenomanian/Turonian boundary: a global control.- *Coral Reefs*, **10,** 115-125.

Philip, J. & Floquet, M. (2000): Late Cenomanian (94.7-93.5 Ma).- In: Peri-Tethys atlas palaeogeographical maps, explanatory notes (Eds Dercourt, J., Gaetani, M., Vrielynck, B., Barrier, E., Biju-Duval, B., Brunet, M.F., Cadet, J.P., Crasquin, S. & Sandulescu, M.). - 129-136 (CCGM/CGMW).

Philip, J., Borgomano, J. & Al-Maskiry, S. (1995): Cenomanian-early Turonian carbonate platform of northern Oman: stratigraphy and palaeo-environments.- *Palaeogeography, Palaeoclimatology, Palaeoecology,* **119,** 77-92.

Robaszynski, F., Caron, M., Dupuis, C., Amédro, F., Gonzalez Donoso, J.-M., Linares, D., Hardenbol, J., Gartner, S., Calandra, F. & Deloffre, R. (1990): A tentative integrated stratigraphy in the Turonian of central Tunisia: formations, zones and sequential stratigraphy in the Kalaat Senan area.- *Bulletin des Centres de Recherches Exploration - Production Elf Aquitaine,* **14,** 214-384.

Robaszynski, F., Hardenbol, J., Caron, M., Amédro, F., Dupuis, C., González Donoso, J.-M., Linares, D., & Gartner, S. (1993): Sequence stratigraphy in a distal environment: the Cenomanian of the Kalaat Senan region (Central Tunisia).- *Bulletin des Centres de Recherches Exploration - Production Elf Aquitaine,* **17,** 395-433.

Said, R. (1962): The Geology of Egypt.- 377 pp. (Elsevier).

Scott, R.W., Schlager, W., Fouke, B. & Nederbragt, S.A. (2000): Are mid-Cretaceous eustatic events recorded in Middle East carbonate platforms?- In: Middle East models of Jurassic/Cretaceous carbonate systems (Eds A.S. Alsharhan & R.W. Scott).- *SEPM Special Publication,* **69,** 77-88.

Shahar, J. (1994): The Syrian Arc system: an overview. -*Palaeogeography, Palaeoclimatology, Palaeoecology,* **112,** 125-142.

Sharland, P.R., Archer, R., Casey, D.M., Davies, R.B., Hall, S.H., Heward, A.P., Horbury, A.D. & Simmons, M.D. (2001): Arabian Plate sequence stratigraphy. -*GeoArabia Special Publication,* **2,** 371 pp.

Stoll, H.M. & Schrag, D.P. (2000): High-resolution stable isotope records from the Upper Cretaceous rocks of Italy and Spain: glacial episodes in a greenhouse planet?- *Geological Society of America Bulletin,* **112,** 308-319.

Tyson, R.V. (1995): Sedimentary organic matter: organic facies and palynofacies. - 615 pp. (Chapmann & Hall).

Vidal, N., Alvarez-Marrón, J. & Klaeschen, D. (2000): Internal configuration of the Levantine Basin from seismic reflection data (eastern Mediterranean).- *Earth and Planetary Science Letters,* **180,** 77-89.

Voigt, S., Hay, W.W., Höfling, R. & DeConto, R.M. (1999): Biogeographic distribution of late Early to Late Cretaceous rudist-reefs in the Mediterranean as climate indicators.- In: Evolution of the Cretaceous ocean-climate system (Eds Barrera, E. & Johnson, C. C.).- *Geological Society of America Special Paper,* **332,** 91-103.

Walley, C.D. (1998): Some outstanding issues in the geology of Lebanon and their importance in the tectonic evolution of the Levantine region.- *Tectonophysics,* **298,** 37–62.

CHAPTER 2

Lithostratigraphy and biostratigraphy of the Cenomanian - Santonian strata of Sinai, Egypt

Jan Bauer, Akmal M. Marzouk, Thomas Steuber & Jochen Kuss

In press in
Cretaceous Research (2001) ***22***

CHAPTER 2
Lithostratigraphy and biostratigraphy of the Cenomanian - Santonian strata of Sinai, Egypt.

***Jan Bauer, **Akmal M. Marzouk, #Thomas Steuber & *Jochen Kuss**

*Cretaceous Research (2001) **22,** in Press*

* Bremen University, Department of Geoscience, PO Box 330440, D-28334 Bremen, Germany
** Tanta University, Faculty of Science, Geology Department, ET 31527, Tanta, Egypt
\# Ruhr-University Bochum, Institute of Geology, Mineralogy and Geophysics, Universitätsstr. 150, D-44801 Bochum, Germany

ABSTRACT

The Cenomanian - Santonian successions of Sinai mainly consist of inner-shelf siliciclastics and carbonates. Five formations (Halal, Raha, Abu Qada, Wata, Matulla) have been recognized and a multibiostratigraphic framework has been constructed. The biostratigraphic assignments of the formations are mainly based on calcareous nannofossils. Their semiquantitative distribution within nine sections is presented, enabling us to identify the biozones CC 10 - CC 16 in some cases. Ammonites are abundant in the uppermost lower Turonian *Mammites nodosoides* Zone only. Planktic foraminifera of the Coniacian - Santonian *Dicarinella concavata* and *D. asymetrica* zones have been found. In addition to these groups, ostracods are used to differentiate between the stages supplemented by data in the literature on benthic foraminifera and rudists. Some modifications of previous lithostratigraphic schemes are proposed for the sections studied: from the ammonite data, a hiatus is proposed between the Halal / Raha and Abu Qada formations (Cenomanian / Turonian boundary); the Abu Qada Formation is considered to range from the *M. nodosoides* Zone to the lowermost upper Turonian; and the base of the Matulla Formation is uppermost Turonian (CC 13). A combined lithostratigraphic and biostratigraphic correlation of ten sections along a N-S transect allows to distinguish eleven stratigraphic units. Units 1 - 8 within the Cenomanian - Turonian Halal, Raha, Abu Qada and Wata formations are considered to be synchronous. In contrast, 'Syrian Arc' tectonics most probably led to diachronous deposition of units 9 - 11 within the Coniacian - Santonian Matulla Formation.

KEY WORDS: Sinai Carbonate Platform; lithostratigraphy; biostratigraphy; correlations; ammonites; calcareous nannofossils.

1. INTRODUCTION

The aim of this study is to enhance the lithostratigraphic and biostratigraphic schemes for the Cenomanian - Santonian deposits of Sinai and to provide a chronostratigraphic basis for facies interpretation and lateral correlation. We present a correlation of five formations (Halal, Raha, Abu

Qada, Wata, Matulla) on the basis of a multibiostratigraphic framework and discuss their depositional features. The deposits studied mostly reflect shallow inner-shelf conditions and, as in similar Tethyan depositional settings, continuous biostratigraphically reliable data are rare. Extensive studies of published data show a wide variety of lithostratigraphic subdivisions in Sinai and neighbouring Israel / Palestine (for reviews, see e.g. Lewy, 1989; Kora & Genedi, 1995; Issawi *et al.*, 1999). However, the biostratigraphic data in these contributions contain many uncertainties. Moreover, the different usage of 'informal' lithostratigraphic subdivisions and local biostratigraphic schemes gives rise to misinterpretations of the sedimentary settings, the biofacies and their correlation. On the other hand, common large-scale geological maps of Sinai and their explanatory notes (e.g., Klitzsch & Hermina, 1989; Geological Survey of Egypt, 1992 - 1994) naturally refer only to rather broadly defined mappable formations. The need for an integrated lithostratigraphic and biostratigraphic approach is evident to achieve the best possible chronostratigraphic resolution.

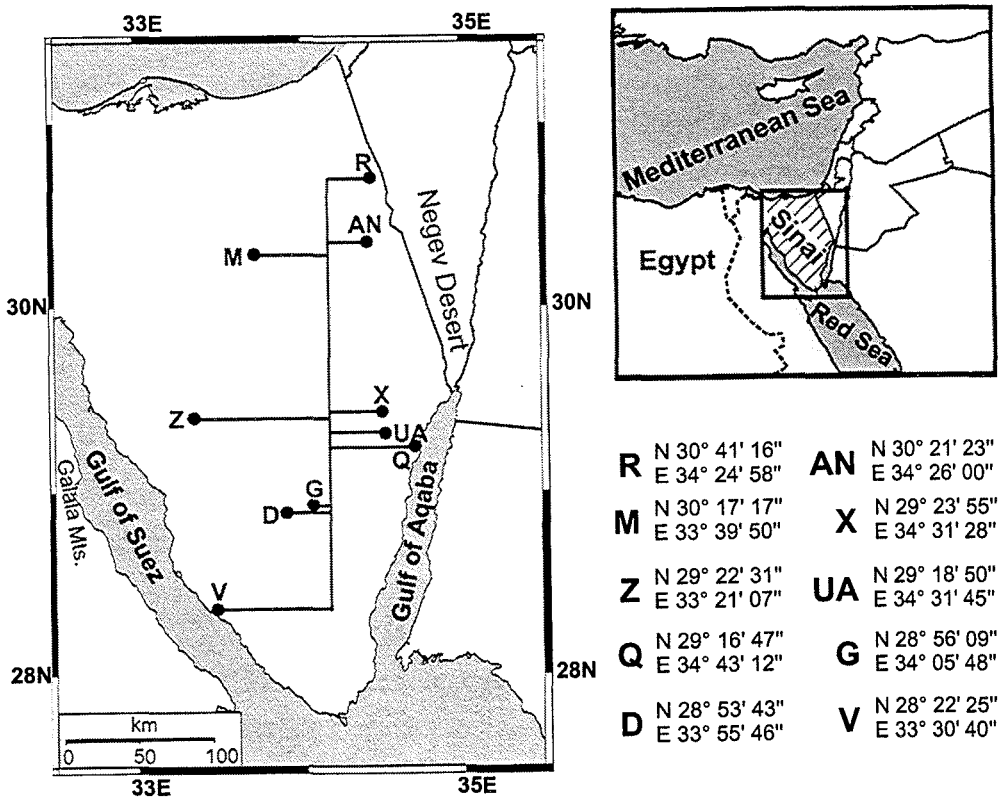

Fig. 1: Location map and co-ordinates of sections referred to in the text. R, Gebel Risha; AN, Gebel Areif El Naqa; M1, M2, Gebel Minsherah; X4, Wadi Gidira; Z, Gebel Abu Zurub; UA, Gebel Um Alda; Q, Ain Quseiyib; G, Gebel Gunna; D, Gebel Dhalal; V, Gebel Arabah.

Calcareous nannofossils and ammonites, yield the best biostratigraphic resolution in the sections studied. In this paper, special emphasis is placed on the lateral and vertical distribution of calcareous nannofossils, even though their frequencies are normally low, and long, continuous distribution patterns are not observed. Planktic foraminifera as well as benthic foraminifera, ostracods and rudists supplement the biostratigraphic data base (the latter groups are presented by Bauer *et al.* in prep.). In order to apply inter-regional comparisons, we use the standard biostratigraphic schemes for each fossil group studied. Previous studies on ammonites of Egypt and Sinai that

have been published by, among others, Allam & Khalil (1988), Luger & Gröschke (1989), Abdel-Gawad *et al.* (1992), Ziko *et al.* (1993) and Kassab (1994) supplement the earlier studies of Parnes (1964), Freund & Raab (1969), Lewy (1975) and Lewy & Raab (1976). Only a few studies have been published on Cretaceous calcareous nannofossils of Sinai (e.g., Arafa, 1991; Faris, 1991; El-Sheikh, 1995; Marzouk & Lüning, 1998) and western Egypt (e.g., Andrawis *et al.*, 1986). Further studies have been carried out in the Near East (e.g., Reiss *et al.*, 1986; Gvirtzman *et al.*, 1989; Almogi-Labin *et al.*, 1991; Eshet & Moshkovitz, 1995; Eshet & Almogi-Labin, 1996). Cretaceous benthic and planktic foraminifera of Sinai have been considered by various authors (for references, see Lüning *et al.*, 1998a, b), and planktic foraminifera have been reported in detail from neritic deposits of the Near East (e.g., Lipson-Benitah, 1980, 1994; Almogi-Labin *et al.*, 1986; Lipson-Benitah *et al.*, 1997).

2. METHODS

This paper is based on ten stratigraphic sections located in different parts of Sinai (Figure 1). Bed-by-bed field studies of sedimentary structures and stacking patterns were supplemented by 450 rock samples from which thin sections were prepared. Additionally, 550 marl and shale samples were collected for microfossil and nannofossil analyses. For microfossil extraction the dried marl samples were soaked in a 0.5 molar Na_2CO_3 solution. After disintegration, the samples were washed over a 63 μm mesh sieve. The dried samples were further fractionated into three grain sizes (63 - 125 μm, 125 - 630 μm, > 630 μm) for easier microfossil identification under a light microscope. For calcareous nannofossils, smear slides were prepared using techniques described by Bramlette & Sullivan (1961) and Hay (1965). The nannofossils were examined at a magnifica-tion of x1000 under a light microscope (cross-polarised and phase-contrast illumination). State of preservation (poor, moderate, good), total floral content and species frequencies were estimated semiquantitatively, and grouped into abundance classes: common, 1 specimen per 2 - 10 fields of view (FOV); few, 1 specimen per 11 - 100 FOV; rare, 1 specimen per 101 - 1000 FOV; very rare, 1 - 2 specimens per slide.

3. GEOLOGICAL SETTING

In mid and Late Cretaceous times Sinai was a broad carbonate shelf with siliciclastic intercalations on the passive margin of the Southern Tethys. The Cenomanian deposits consist of carbonates (Halal Formation) with southward increasing quartzose deposits (Raha Formation). The lower - middle Turonian Abu Qada Formation is composed of marls at the base, overlain by dolostones and marls. The upper Turonian Wata Formation consists of cyclically bedded dolostones and limestones. Sandstones, siltstones and marls dominate in the Coniacian - Santonian Matulla Formation.

The Cenomanian - Santonian depositional history of the region was markedly controlled by: (1) the extensive, probably global eustatic sea-level rise (Haq *et al.*, 1987; Hancock, 1993) at the Cenomanian / Turonian boundary; (2) regional relative sea-level changes of different orders (Flexer *et al.*, 1986; Lewy, 1990; Kuss & Bachmann, 1996; Bachmann & Kuss, 1998; Lüning *et al.*, 1998b);

(3) early 'Alpine' movements, which resulted in the structural inversion of older graben structures and the onset of uplift movements.

3.1. Depositional setting

In Aptian - Albian times a carbonate ramp, influenced by relative sea-level changes and deltaic deposition of siliciclastics, characterized the area of deposition (Bachmann & Kuss, 1998; Kunow *et al.*, 1998). Since the Cenomanian, predominantly shallow inner-shelf environments established in Sinai, consisting of subtidal and peritidal calcareous sediments, over a maximum north - south (distal - proximal) extension of about 200 km. In northernmost Sinai, the Near East and in the Mediterranean Sea, outer shelf and basin sediments were deposited (Lipson-Benitah, 1980, 1994; Alsharhan & Salah, 1996). The coastline was located in southern Sinai, and there is no indication of a particular inclination of the inner shelf realm, in contrast to the Aptian - Albian ramp morpho-logy. The extensive dolomitisation at some localities is interpreted to be a marine signature of circu-lating sea water at a shallow burial depth, and later burial dolomitisation (Tucker *et al.*, 1999). In contrast, Zalat (1999) assumed an early diagenetic clay-derived dolomite origin and a later phase of dolomitization during burial.

Following minor sea-level oscillations in the late Cenomanian, the prominent global eustatic sea-level rise at the Cenomanian / Turonian boundary influenced the depositional settings of many regions of the Mediterranean Tethys (Philip & Airaud-Crumiere, 1991; Abdallah & Meister, 1997). In northern and central Sinai this sea-level rise coincided with the deposition of deep-water deposits and the establishment of an intrashelf basin, the Central Sinai Basin (Bartov & Steinitz, 1977), and its eastward prolongation in the Negev Desert, the Eshet-Zenifim Basin (Bentor, 1960; Bartov & Steinitz, 1977; Gvirtzman & Garfunkel, 1998; Buchbinder *et al.*, 2000).

In the middle and late Turonian, an extended calcareous shelf system governed the area of deposition, which was more or less stable until the early Coniacian, although prominent third order sea-level changes affected the depositional settings (Kuss & Bachmann, 1996). During the Coniacian, siliciclastic input from the hinterland increased. From the late Coniacian onwards, a significant southward retreat of the inner-shelf facies is obvious, and deep-water facies of chalks and marls developed in northern and central Sinai.

3.2. Hiatus at the Cenomanian / Turonian boundary

A hiatus at the Cenomanian / Turonian boundary has been reported from Sinai (see sections 4 and 5.1) and the Near East (Lewy, 1989; Buchbinder *et al.*, 2000), but its origin remains unclear. In Sinai, it is interpreted to have been related to syndepositional uplift of domal anticline structures of northern Sinai (Bartov *et al.*, 1980; Kuss *et al.*, 2000b), with respect to the initial phase of the 'Syrian Arc' movements. However, latest Cenomanian - early Turonian hiatuses and extreme condensation are not local phenomena, but have been recorded from many Mediterranean platforms as a result of platform drowning (e.g., Philip & Airaud-Crumiere, 1991; Drzewiecki & Simo, 1997; Schlager, 1999). Thus, it cannot be excluded that a global control as a result of long term oceanographic changes linked with the eustatic sea-level rise possibly also influenced the formation of the hiatus in Sinai.

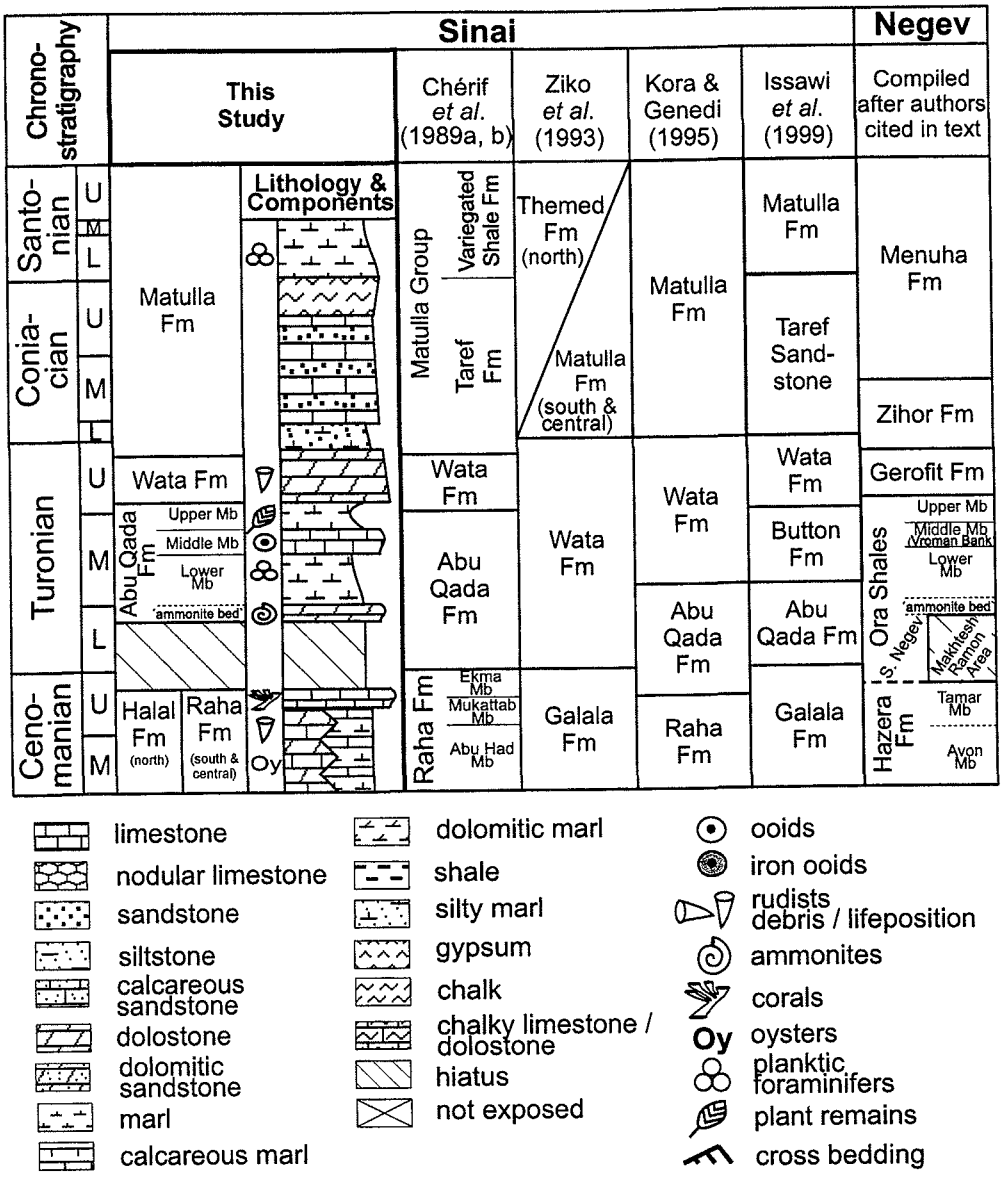

Fig. 2: Lithostratigraphic subdivision of the Cenomanian - Santonian strata. The standard section on the left shows a compilation of the generalized lithologies. Comparisons with other subdivisions in Sinai and the Negev show some differences in the chronostratigraphic assignments, especially with respect to the Abu Qada Formation and the Wata Formation. The hiatus at the Cenomanian-Turonian boundary is discussed in the text. A key to the symbols and lithologies used here and in Figures 3, 4, and 11 - 13 is given beneath.

3.3. Tectonic development

The geodynamic evolution of the region is characterized by: (1) late Triassic - early Jurassic rifting and opening of the Neotethyan ocean; (2) compression since the Turonian, owing to the initial collision of the Afro-Arabian and Eurasian plates.

Neotethyan rifting during the Triassic led to the formation of half grabens and basins on the 'unstable shelf' (*sensu* Said, 1962) in northern Sinai (Kuss, 1989; Moustafa & Khalil, 1990), Egypt (Kuss, 1992; El-Hawat, 1997; Bakr *et al.*, 1999; El-Toukhy *et al.*, 1999), the Near East (Hirsch *et al.*, 1998) and in other eastern Mediterranean regions (Garfunkel, 1998; Vidal *et al.*, 2000). In the eastern Mediterranean, transpressive inversion along the pre-existing half graben structures since

the Turonian involved strike-slip faulting (Guiraud, 1998) and the formation of the 'Syrian Arc' fold belt (Krenkel, 1924). The domal anticlines in northern Sinai are part of this intraplate fold belt which extends from Syria over Lebanon, the Near East, to northern Egypt (Moustafa & Khalil, 1995; Guiraud & Bosworth, 1997; Walley 1998; Bosworth *et al.*, 1999). From the Coniacian onwards, a complex morphology of basins and highs developed in Sinai (Kuss & Bachmann, 1996), the Near East (Rosenthal *et al.*, 2000) and in the Galala area in Egypt (Kuss *et al.*, 2000a), which mirrored these 'Syrian Arc' movements. However, the timing of the initial movements is still controversial and ranges from the Cenomanian to Campanian (Bosworth *et al.*, 1999). Detailed reviews of the evolution of the 'Syrian Arc' are given by Keeley (1994), Shahar (1994), El-Hawat (1997), Guiraud & Bosworth (1997), Keeley & Massoud (1998) and Walley (1998).

4. LITHOSTRATIGRAPHY

The formations used herein are: Raha, Halal (Cenomanian); Abu Qada, Wata (Turonian); and Matulla (Coniacian - Santonian). These are differentiated here based on their stratigraphic ranges, lithofacies, regional distributions and depositional settings (Figure 2). A large number of formations and members has been defined previously, some of which only refer to small localities or even to single sections (e.g., Ziko *et al.*, 1993; Akarish, 1999). Here, we only refer to commonly used formations in Sinai based on Egyptian nomenclature mainly after Ghorab (1961) but supplemented by Chérif *et al.* (1989a, b), Ziko *et al.* (1993) and Kora & Genedi (1995). These are compared with schemes from the Near East (Figure 2) by, e.g., Bartov & Steinitz (1977), Bartov *et al.* (1980) and Lewy (1989). Figure 3 compiles the results in a chronostratigraphic correlation of ten sections along a N-S transect (Figure 1). The biostratigraphic data are discussed in detail in the following sections.

Halal Formation

Author, type section. Said (1971), Gebel Halal (northern Sinai).

Stratigraphic range. Middle Albian - Cenomanian. In this contribution the focus is on the upper Cenomanian deposits of the formation (calcareous nannofossil zones CC 10 - lower CC 11; Figure 4a).

Upper boundary marker bed. Uppermost bed underlying the 'ammonite bed' of the Abu Qada Formation.

Regional distribution. The formation is limited to northern Sinai. Sections studied are M2 and AN (Figure 4a). The successions examined are 90 m thick in M2 and 48 m in AN.

Lithofacies. Although few bioclastic limestone and marl beds are intercalated, the lithology is relatively uniform, owing to intense dolomitization. Silty marls are occasionally present in the lower part but are absent towards the top, where carbonate rocks prevail. Shallow-water benthic organisms such as rudists (Figure 5h), and especially oysters are abundant; corals may occur. Limestones show a diverse assemblage of abundant benthic foraminifera in thin sections (Bauer *et al.*, in prep.).

Depositional setting. Protected subtidal and open lagoonal deposits dominated this shallow-water environment, in contrast to the overlying Turonian deposits, where more high-energy environments occurred.

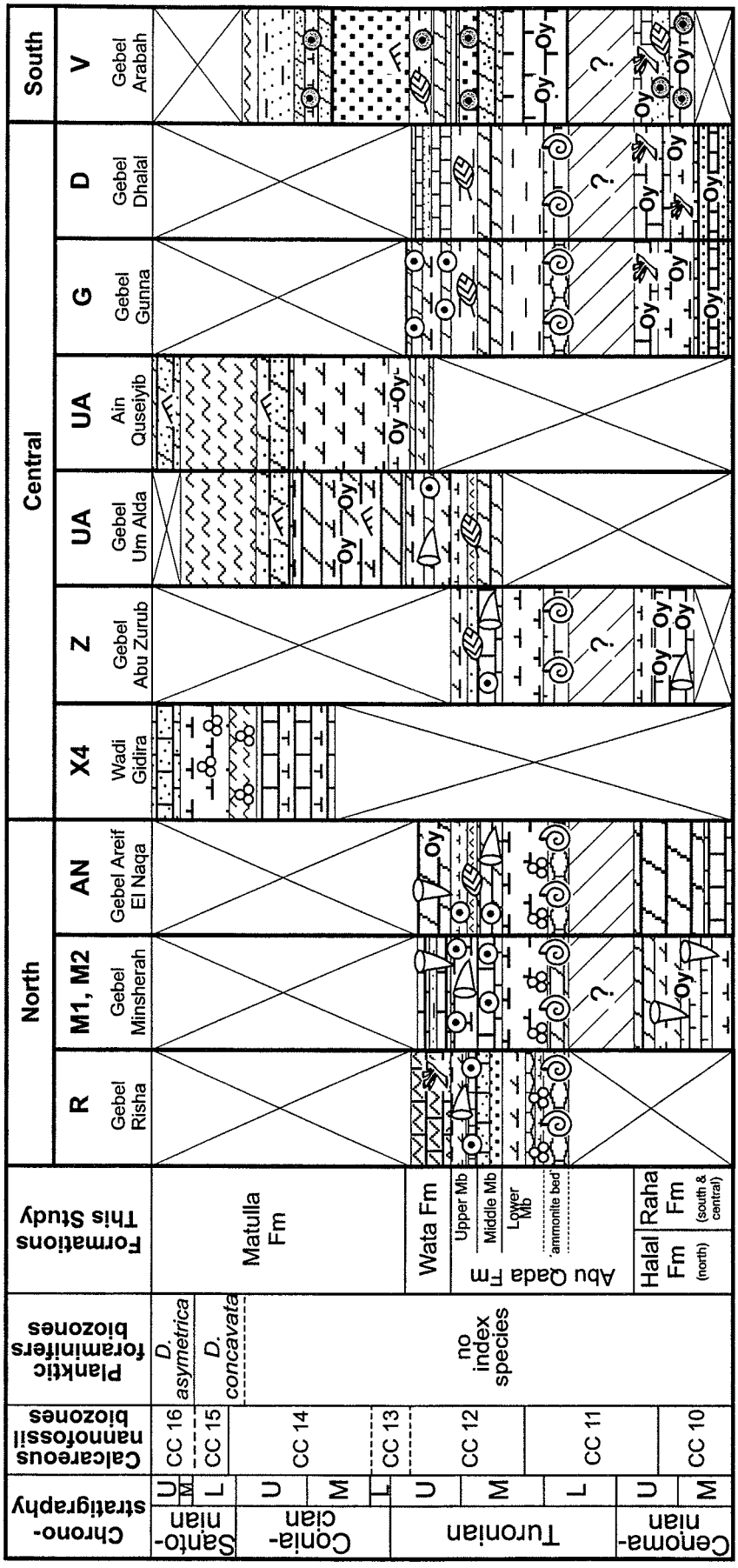

Fig. 3: Chronostratigraphic correlation of five Cenomanian - Santonian formations along a N-S transect based on ten sections (Figure 1). For key to symbols and lithologies, see Figure 2.

Discussion. Said (1971) named the Halal Formation as a counterpart to the Raha Formation in central Sinai, based on different lithofacies. Bartov & Steinitz (1977) attributed the Cenomanian deposits of entire Sinai to the synonymous Hazera Formation of the southern Negev and subdivided it into five members (following Arkin & Braun, 1965), of which the upper two members have been assigned to the middle - upper Cenomanian (Figure 2). In Sinai, a late Cenomanian age is indicated for the top of the formation based on the presence of the ammonite *Neolobites vibrayeanus* at the type locality (Kerdany & Chérif, 1990). For detailed studies on the sedimentological characteristics and depositional history of the lower part of the formation (lower and middle Cenomanian), see Bachmann & Kuss (1998) and Lüning *et al.* (1998a).

Raha Formation

Author, type section. Ghorab (1961), Raha scarp and Raha plateau (west-central Sinai).

Stratigraphic range. Middle Albian - Cenomanian. In this contribution the focus is on the upper Cenomanian deposits of the formation (CC 10 - lower CC 11; Figure 4a).

Upper boundary marker bed. A limestone bed with branching octocorals is a characteristic marker of the uppermost beds of the formation in southern and central Sinai.

Regional distribution. The formation occurs throughout southern and central Sinai (sections Z, G, D and V; Figures 3, 4a). The thickness of the successions examined varies from 75 m (section Z) to 43 m (section V).

Lithofacies. Fossiliferous limestones, dolostones, marls and quartzose sediments alternate. A characteristic green marl succession (Ekma Member *sensu* Chérif *et al.*, 1989a) appears in the upper part of the formation in section Z (Figure 4a). In contrast to the coeval Halal Formation of northern Sinai, marls and shales are more frequent in the Raha Formation. Sandstones and siltstones are observed in central and southern Sinai.

Depositional setting. A shallow subtidal environment of deposition is indicated by abundant oysters in parts of the formation in addition to rudists, echinoderms and gastropods. As in the Halal Formation, high-energy deposits (e.g., oolites and grainstones) are nearly absent. The siliciclastic input increased markedly from west to east and from north to south Sinai, underlining the more coastward position of the depositional area of the Raha Formation compared to that of the Halal Formation.

Discussion. Ghorab (1961) and Chérif *et al.* (1989a) named the following members in ascending order: Abu Had (lower - middle Cenomanian siliciclastics), Mukattab (upper Cenomanian carbonates) and Ekma (upper Cenomanian marls). Further subdivisions of this formation were proposed by Ziko *et al.* (1993), and for the age equivalent Hazera Formation in the Negev by Arkin & Braun (1965). We do not use these members, because of their indistinct separation and only local importance. The Raha Formation contains the oysters *Exogyra olisiponensis* (Cenomanian) as well as *Ceratostreon flabellatum* and *Liymatogyra africana* (upper Cenomanian) in the upper beds throughout Sinai (Allam & Khalil, 1988, 1989; Chérif *et al.*, 1989a; Abdel-Gawad *et al.*, 1992; Hamza *et al.*, 1994; Kora & Genedi, 1995).

Abu Qada Formation

Author, type section. Ghorab (1961), Wadi Abu Qada (west-central Sinai).

Stratigraphic range. Uppermost lower Turonian (upper CC 11 and *M. nodosoides* ammonite biozone) - lowermost upper Turonian (middle CC 12; Figure 4a).

Members. Lower (including basal 'ammonite bed'), Middle and Upper, analogues of subdivisions of the Ora Shales in the Negev (Bartov & Steinitz, 1977; Bartov *et al.*, 1980).

Lower boundary marker bed. 'Ammonite bed' (Figure 5d, j) or first deposits above the coral-bearing bed of the uppermost Raha Formation.

Regional distribution. The formation can be traced from north to south Sinai. However, the 'ammonite bed' occurs in northern and central Sinai, but is absent in southern Sinai (Figure 4a). It is interesting to note that it is also recorded in the Wadi Qena area and Galala Plateau in the Eastern Desert of Egypt (Kuss & Malchus, 1989; Issawi *et al.*, 1999), in the Near East (e.g., Bartov *et al.*, 1972; Lewy, 1989) and in Jordan (Khalil, 1992; Schulze & Kuss, 2000). The thickness of the Abu Qada Formation varies from 75 m (section R) to 50 m (section V).

Lithofacies. The formation mainly consists of marls and shales (Lower and Upper members) separated by a package of thick-bedded limestones and dolostones (Middle Member; Figure 5a). The base of the Lower Member consists of nodular limestones and dolostones, which are separated by thin reddish impregnations and contain densely packed lower Turonian ammonites ('ammonite bed'). The overlying shales and marls contain frequent non-keeled planktic foraminifera in the lower parts. Well-bedded fossiliferous dolostones and limestones of the Middle Member (equivalent to the 'Vroman Bank' in the Negev; Bartov *et al.*, 1972) often contain rudists (Hippuritidae and Radiolitidae) and gastropods. Hardgrounds are common. Bioclastic packstones with diverse benthic foraminifera, calcareous algae and/or ooids and oncoids may occur. The base of the Upper Member is generally characterized by palaeosols, gypsum layers, shales with plant remains and/or siltstones, sometimes overlain by shales with hypersaline or brackish-water ostracods (e.g., *Neocyprideis vandenboldi*). The overlying marls sometimes contain rare non-keeled planktic foraminifera and intercalated oolites or bioclastic packstones.

Depositional setting. The Lower Member represents a significant relative sea-level rise in the early Turonian. An increase in water depth is indicated by its rich ammonite fauna and planktic foraminifera-bearing deposits above shallow subtidal deposits of the Halal and Raha formations. The shallow subtidal deposits of the Middle Member represent an extended calcareous shelf system, which re-established during the following highstand (Bauer *et al.*, in prep.). A prominent sea-level fall is recorded in very shallow subtidal to supratidal deposits at the base of the Upper Member. This shallowing event has also been reported from the Near East by a contemporaneous angiosperm flora (Dobruskina, 1997) and a siliciclastic-evaporite facies ('clastic unit') discussed by Sandler (1996). Overlying subtidal marls and limestones record a later transgression. The deposits of the Lower Member are interpreted herein as the marginal facies of the Central Sinai Basin. The depocenter of the basin is not exposed in Sinai, but equivalent deposits of the Eshet-Zenifim Basin in the Negev have been described in detail by Buchbinder *et al.* (2000). After the hiatus across the Cenomanian / Turonian boundary, sedimentation started in the late early Turonian (see section 5.1) with condensed deposits of the Lower Member. Condensation is indicated by reddish hard-

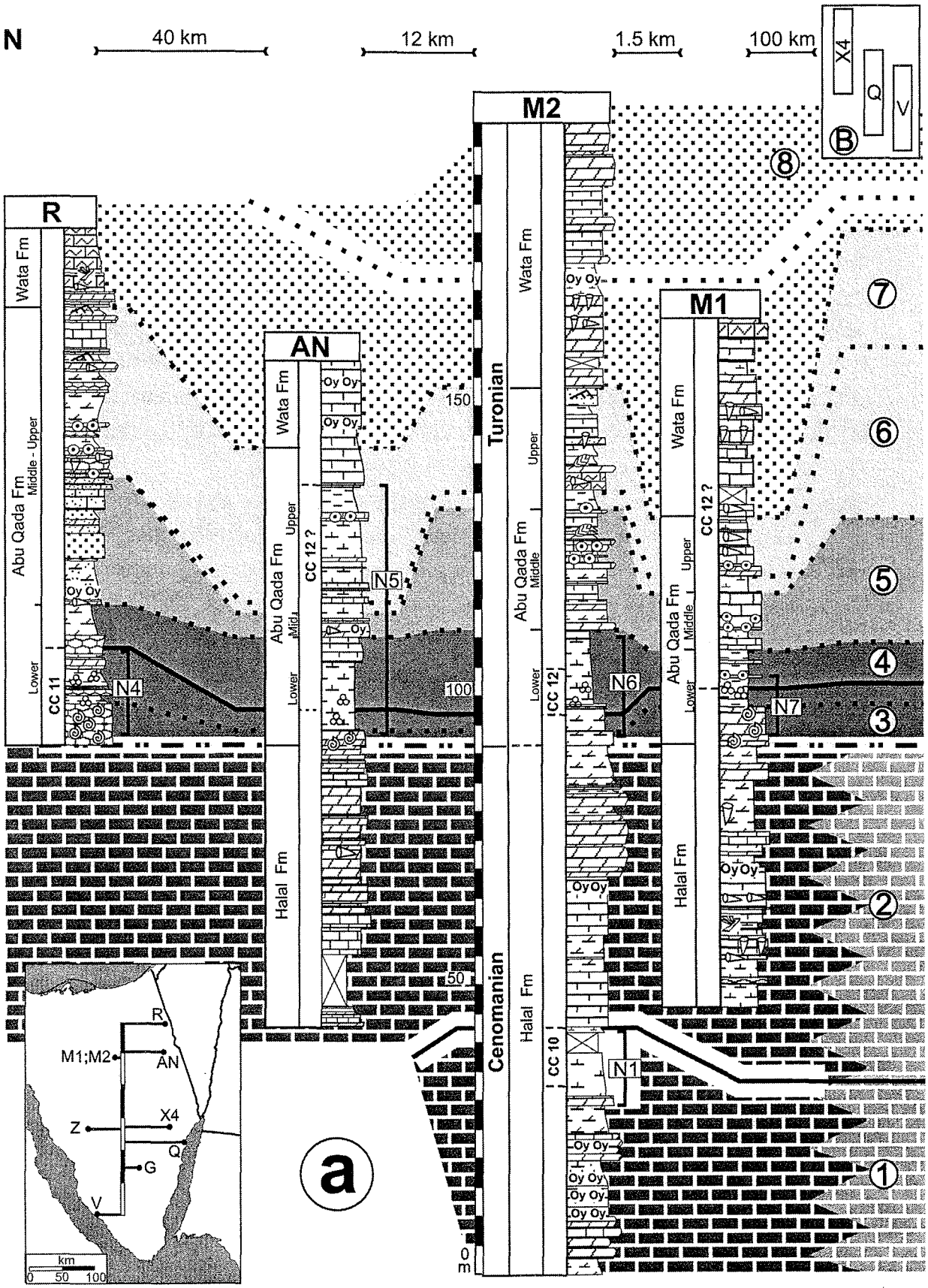

Fig. 4: Two facing pages. Combined lithostratigraphic and biostratigraphic correlation of the Cenomanian - Turonian (a) and upper Turonian - Santonian (b) successions along a N-S transect. The correlated units 1 - 11 are discussed in the text. Intervals that contain calcareous nannofossils are indicated and the corresponding calcareous nannofossil distribution charts are shown in Figures 11-13. For key to symbols and lithologies, see Figure 2.

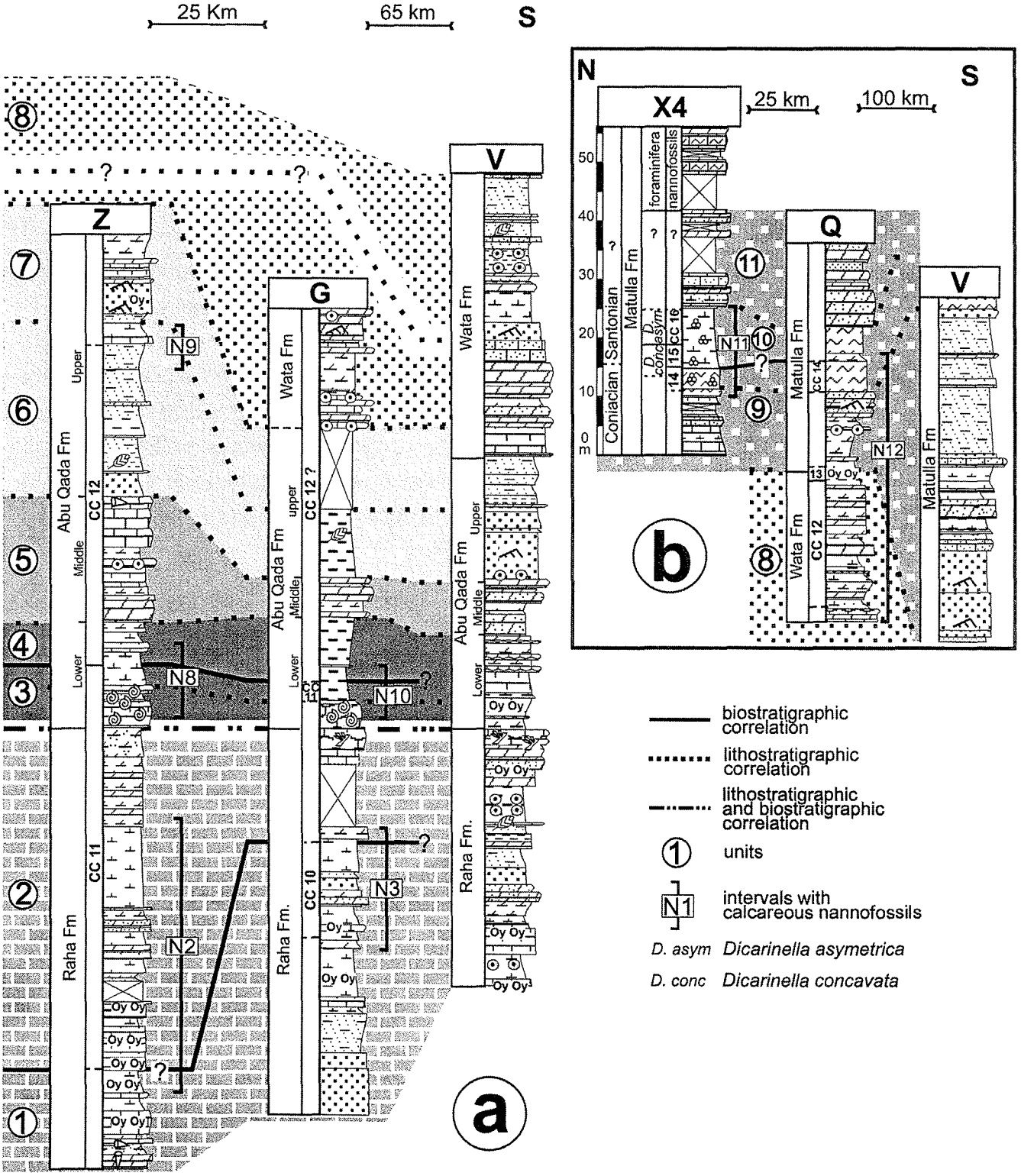
25 Km
65 km
S
N
S
X4
25 km
100 km
Z
G
V
Q
Abu Qada Fm
Wata Fm
Raha Fm
Matulla Fm
Upper
Middle
Lower
CC 12
CC 11
CC 10
CC 12 ?
CC 14
CC 15
CC 16
foraminifera
nannofossils
Coniacian
Santonian
D. asym
D. conc
N1
N2
N3
N8
N9
N10
N11
N12
Oy
a
b
biostratigraphic correlation
lithostratigraphic correlation
lithostratigraphic and biostratigraphic correlation
units
intervals with calcareous nannofossils
D. asym Dicarinella asymetrica
D. conc Dicarinella concavata

grounds, oysters which are frequently found encrusted on ammonites, and superimposed glauconite-bearing marls.

Discussion. The stratigraphic range of the Abu Qada Formation is controversial, especially the definition of its base. We propose a late early Turonian age for the 'ammonite bed' in the sections studied (see section 5.1). Kora & Genedi (1995) and Kassab & Ismael (1994), among others, placed the lower part of the Abu Qada Formation in the Cenomanian, supported by findings of the Cenomanian oyster *Exogyra olisiponensis* in a marly unit underlying the 'ammonite bed'. However, we follow Chérif *et al.* (1989a) and Orabi (1991), and attribute this marly unit (section Z; Figure 4a) to the more marly succession of the Cenomanian Raha Formation (Ekma Member; see above). The, in parts, more calcareous lower and middle Turonian succession in east-central Sinai encouraged some authors (e.g., Abdel-Gawad & Zalat, 1992; Ziko *et al.*, 1993) to neglect the Abu Qada Formation in central Sinai to the benefit of the Wata Formation. In the Negev, the onset of the Ora Shales depends on the geographic and structural setting in the various areas of deposition. Near the depocenter of the Eshet-Zenifim Basin in southern Negev, sedimentation of the Ora Shales started in the late Cenomanian (Lewy, 1989), whereas at its margins in the central Negev (area of Makhtesh Ramon), sedimentation was interrupted until the late early Turonian (Lewy, 1989), as it was also in Sinai (Figure 2).

Wata Formation

Author, type section. Ghorab (1961), Wadi Wata (west-central Sinai).

Stratigraphic range. Upper Turonian (middle - upper CC 12, Figure 4a, b).

Lower boundary marker bed. Onset of cyclically bedded dolostones and limestones.

Regional distribution. The formation is present throughout Sinai. Its thickness varies between > 70 m (section AN) and 45 m (section V).

Lithofacies. Cliff-forming, cyclically bedded dolostones, limestones and calcareous / dolomitic marlstones dominate (Figure 5a, b). Where calcareous deposits are preserved, bioclastic packstones and grainstones with ooids and diverse benthic foraminifera and calcareous algae mostly occur. In southern Sinai, siliciclastics prevail (section V; Figure 4a). Hardgrounds, emersion horizons and quartzose beds (Figure 5e, f) occasionally interrupt the cyclic stacking patterns. Rudists (silicified in parts), gastropods and oysters form the macrofossil assemblages. Laminations, bioturbation and reworking textures occur.

Depositional setting. The formation reflects shallow subtidal to intertidal environments, as indicated by shallow-water biota and abiogenic components (calcareous algae, oysters, rudists, ooids) as well as emersion horizons. The thick succession in northern Sinai reflects a northward increasing accommodation space which may have been related to high subsidence rates of the Central Sinai Basin. A similar interpretation has been given by Buchbinder *et al.* (2000) for the age-equivalent Gerofit Formation within the synsedimentary subsiding Eshet-Zenifim Basin in the Negev. The periodic repetition of stacking patterns, mainly thinning-upwards cycles, of the Wata Formation were most likely caused by high order relative sea-level changes. A larger scale shallowing event is preserved in emersion surfaces, hardgrounds (Figure 5g) and intercalated siltstone/sandstone beds

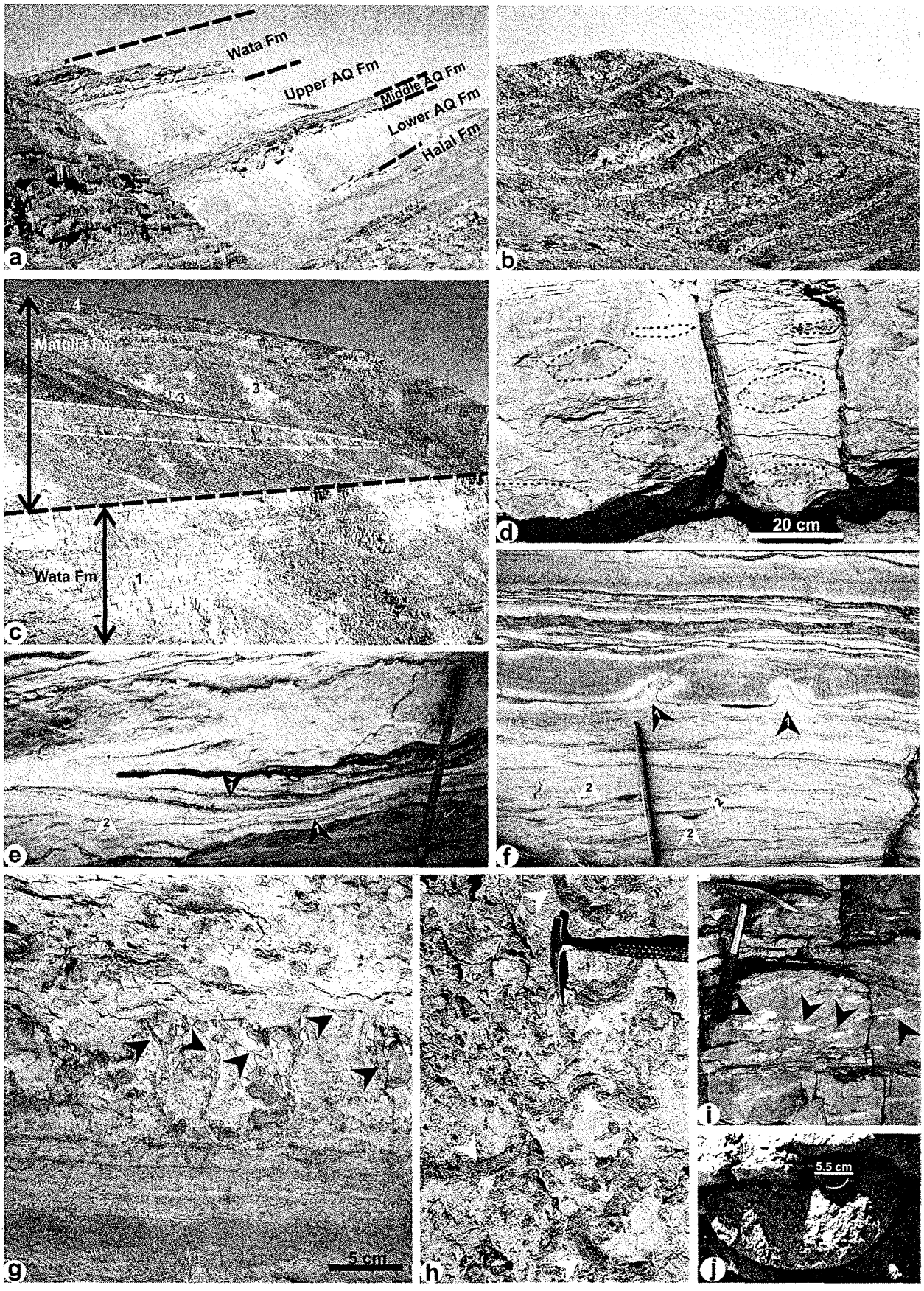
Wata Fm
Upper AQ Fm
Middle AQ Fm
Lower AQ Fm
Halal Fm
a
b
4
Matulla Fm
3
3
Wata Fm
1
c
d
20 cm
e
2
f
2
2
g
5 cm
h
i
5.5 cm
j

Fig. 5: (previous page) Field photographs. For sections and localities mentioned, see Figures 1, 4a, b. a, Halal Formation overlain by the Abu Qada Formation (AQ Fm) showing the marly Lower Member, dolomitic Middle Member and marly Upper Member, and the overlying lowermost part of the Wata Formation; Gebel Areif El Naqa. b, cyclically bedded dolostones of the Wata Formation, Gebel Areif El Naqa. c, cyclically bedded chalky limestones and dolostones of the Wata Formation (1) and calcareous Matulla Formation with lateral thinning sandstone beds (2), chalks (3) and cherts (4); the Matulla Formation is covered by dark chert debris; Gebel Um Alda. d, 'Ammonite bed'; the stippled lines surround transaxial planes of ammonites; section Z. e, f, siltstones with small scale channels (e, 1), cross bedding (e, 2), convolute bedding (f, 1) and small scale ripple cross stratification (f, 2); Wata Formation, section M2 at 150 m; length of pencil is 17 cm. g, hard-ground within dolostones of the Wata Formation; the arrows mark vertical borings; stromatolitic structures are visible in the lower part; section Z. h, bedding-plane view of *Ichthyosarcolites triangularis* in recumbent life position; upper Halal Formation; section M1 at 30 m; length of hammer is 30 cm. i, rip-up structures (arrows) in dolostone layer of lower Matulla Formation; section X4 at 3 m; length of hammer is 28 cm. j, large ammonite within the 'Ammonite bed'; section M1.

which interrupt the carbonate succession in the middle part of the formation. The shallowing event can be traced over wide areas of Sinai.

Discussion. Some authors (e.g., Abdel-Gawad & Zalat ,1992; Ziko *et al.*, 1993) assigned the lower and middle Turonian deposits of west Sinai to the Wata Formation and ignored the Abu Qada Formation. Our sedimentological and biostratigraphic data do not support this interpretation. In addition to the different biostratigraphic assignments, the depositional settings differ significantly and palaeogeographic reconstructions and correlations between different localities in Sinai are more problematic, when mixing the nomenclature. Furthermore, the general lithological trends of the Abu Qada and Wata formations are clearly recognizable in the sections studied herein (Figure 4a), and thus, we prefer to refer to the Wata Formation only in connection with the calcareous deposits of the upper Turonian.

A cyclostratigraphic interpretation of the cyclic stacking patterns seems ambiguous to us at present. In general, bed thickness analyses alone are not reliable for differentiating between shallowing- or deepening-upwards cycles (Strasser *et al.*, 1999). Dolomitization has often destroyed former components and sedimentary structures and, thus, the recognition of cycle bases and tops is often highly subjective when attempting to define shallowing-upwards and/or deepening-upwards cycles and their duration.

Matulla Formation

Author, type section. Ghorab (1961), Wadi Matulla (west-central Sinai).

Stratigraphic range. Uppermost Turonian - Santonian (CC 13 - CC 16 and *Dicarinella Concavata* - *Dicarinella asymetrica* zones; Figures 3, 4b).

Lower boundary marker bed. First marls or quartzose sediments above the Wata Formation.

Regional distribution. The formation is restricted to central and southern Sinai (sections X4, Q, UA, V; Figures 3, 4b) and is 40 - 50 m thick.

Lithofacies. The formation shows highly variable lithologies: cross-bedded sandstones, siltstones, marls, limestones (often with bioclasts, phosphorites and glauconites), dolostones, chalks and chalky limestones with chert concretions (Figure 5c). Siliciclastic detritus prevails in most of the rock-types.

Depositional setting. During the Coniacian, chalks, limestones and marls were deposited on a rapidly subsiding outer shelf in northern Sinai, northern Israel and Palestine. In central Sinai, siliciclastically influenced shallow, inner-shelf deposits prevailed. The biogenic components such as gastropods, echinoderms, ostracods, bivalves, bryozoans, calcareous algae (dasycladaceans and udoteaceans) and miliolids document shallow marine conditions. Cross-bedding, winnowed textures and coarse sandstones indicate local high-energy environments. Towards the south, the siliciclastic input increased successively as a result of the more coastward area of deposition. A conspicuous decrease in water depth across the Turonian / Coniacian boundary in central Sinai is sometimes indicated by rip-up clasts (Figure 5i) and by the onset of siliciclastics above the Wata Formation, which defines the lower boundary of the Matulla Formation.

In the upper Coniacian - upper Santonian, a coastward retreat of the inner-shelf facies is indicated by deeper water sediments (chalks and marls with keeled planktic foraminifera) in east-central Sinai (e.g., section X4, Figure 4b), northern Sinai (Bartov *et al.*, 1980; Lüning *et al.*, 1998a) and the Near East (Menuha Formation; Lewy, 1975) because of a prominent relative sea-level rise. These facies shifts are well documented in the palaeogeographic maps of Lewy (1975), Said (1990), Kuss & Bachmann (1996) and Lüning *et al.* (1998b). Moreover, the interfingering of deep-water sediments with shallow-marine deposits over short distances in Sinai and the Near East, indicate swell and basin morphologies. The morphologies originated from synsedimentary tectonics (Lewy, 1975; Flexer & Honigstein, 1984; Rosenthal *et al.*, 2000) related to 'Syrian Arc' movements from the middle Coniacian onwards. This is supported by indications of syndepositional uplift at the Gebel Areif El Naqa anticline (Bartov *et al.*, 1980; Lüning *et al.*, 1998a; Kuss *et al.*, 2000b).

Discussion. In previous publications, various biostratigraphic data from macrofossils and microfossils have been presented for the formation. In contrast to other schemes (Figure 2), we propose a latest Turonian age (CC 13) for its base. Our biostratigraphic data do not confirm a hiatus across the Turonian / Coniacian boundary, as has been reported from other localities in central Sinai (Chérif *et al.*, 1989b; Orabi 1991). A Coniacian - Santonian age of large parts of the formation is generally accepted (Chérif *et al.*, 1989b; Kora & Genedi, 1995; Abdel-Gawad, 1999), but as in other Tethyan settings, a convincing proposal for the boundary between both stages is still controversial (for references, see e.g. Abdel-Gawad, 1999).

Based on their calcareous nature, Allam & Khalil (1988) and Ziko *et al.* (1993) defined the Mezera and Themed formations, respectively, as age equivalent counterparts to the Matulla Formation in northern Sinai. In this sense, the Coniacian strata of sections Q and X4 (Figure 4b) of east-central Sinai represent a transitional lithofacies between the siliciclastic Matulla Formation in the south to the more calcareous Themed or Mezera formations further to the north. Different subdivisions of the Matulla Formation (and the equivalent Zihor and Menuha formations of the Near East; Lewy, 1975) into members have been attempted previously by Lewy (1975), Refaat (1993), Ziko *et al.* (1993), Enani *et al.* (1994) and Orabi & Ramadan (1995) based on individual lithological characteristics. Chérif *et al.* (1989b) combined three well-known formations of the Western and Eastern Desert of Egypt (Taref Sandstone, Quseir Variegated Shale and Duwi Formation) into a Matulla Group, ranging from upper Coniacian to lower Campanian. However, their type sections are located several hundreds of kilometers southwest of Sinai and are, therefore, not used herein.

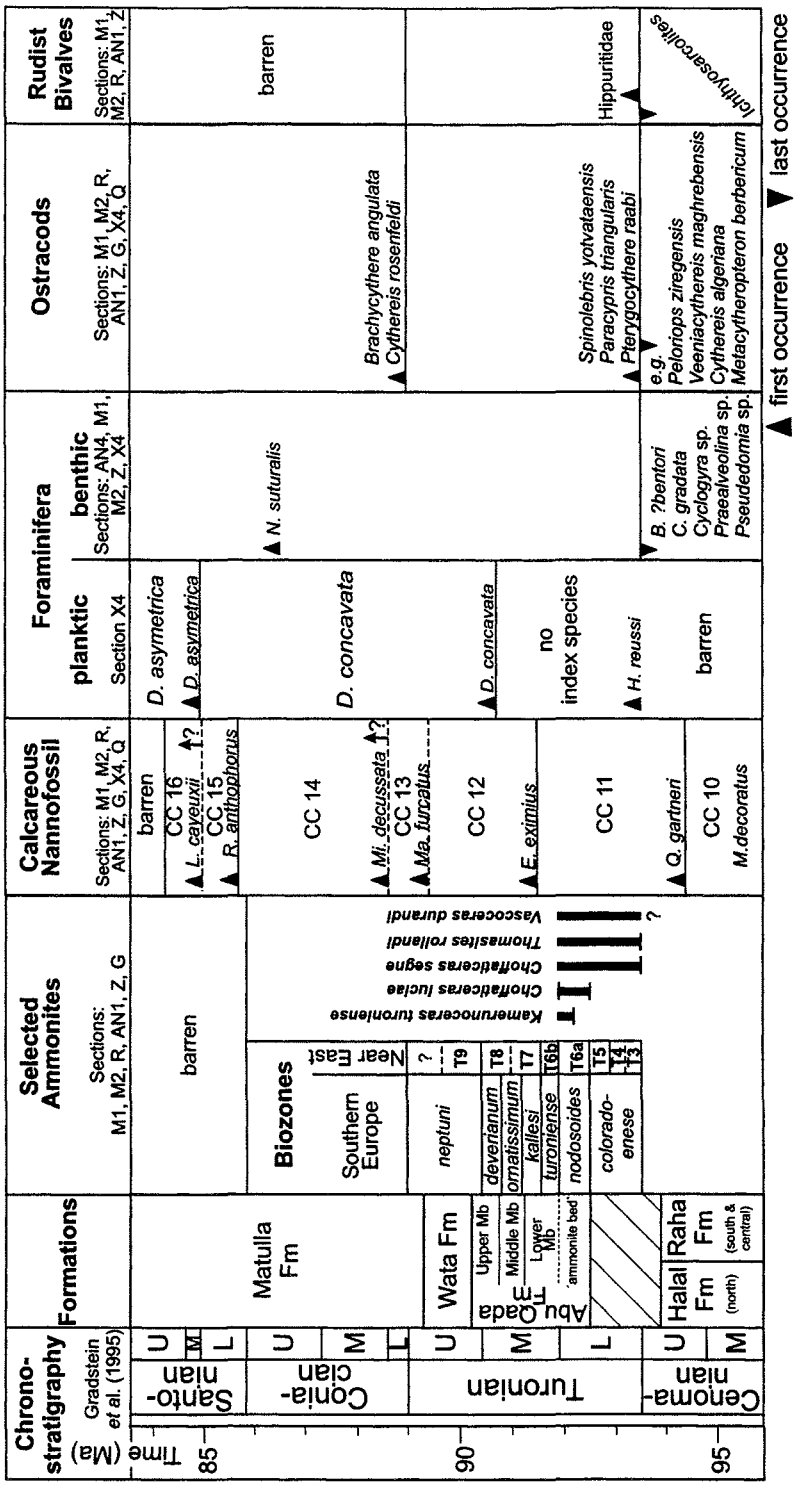

Fig. 6: Multibiostratigraphic framework for the sections studied. Discussions of the ammonite biozones and calcareous nannofossil are given in the text. Regional comparisons of the stratigraphic ranges of the Turonian ammonites (from the ´ammonite bed` of the Lower Abu Qada Formation) are shown in Figure 7. Some biostratigraphically indicative benthic foraminifers, ostracods and rudist bivalves enable differentiation of the stages. Abbreviations: calcareous nannofossils: *E.*, *Eiffellithus*; *L.*, *Lucianorhabdus*; *M.*, *Microrhabdulus*; *Ma.*, *Marthasterites*; *Mi.*, *Micula*; *Q.*,*Quadrum*; *R.*, *Reinhardtites*; planktic foraminifers: *D.*, *Dicarinella*; *H.*, *Heterohelix*; benthic foraminifers: B., *Biconcava*; *C.*, *Chrysalidina*; *N.*, *Neoflabellina*.

5. BIOSTRATIGRAPHY

The biostratigraphic subdivision of the predominantly shallow-water Cenomanian - Santonian platform successions of Sinai is limited. This is because of the long stratigraphic ranges and scarceness or absence of biostratigraphic markers in many of the intervals studied. Thus, we propose a multibiostratigraphic framework for the sections investigated, in order to achieve the best possible biostratigraphic resolution (Figure 6).

5.1. Ammonites

The base of the Lower Abu Qada Formation is marked by a diverse association of densely packed ammonites in northern and central Sinai. This 'ammonite bed' directly overlies Cenomanian deposits of the Raha Formation or Halal Formation, respectively (Figure 4a), and contains, among others, lower Turonian species such as *Choffaticeras luciae, C. segne, Kamerunoceras turoniense, Thomasites rollandi* and *Vascoceras durandi* (determined by F. Wiese and P. Luger, Berlin). The ranges of these species (Figure 7) are based on regional biozonation schemes for Egypt (Kassab, 1994), the Near East (Freund & Raab, 1969, modified by Lewy, 1989 and Buchbinder *et al.*, 2000), Tunisia (Robaszynski *et al.*, 1990; Chancellor *et al.*,1994) and southern Europe (Thomel, 1992; Thierry *et al.* in Hardenbol *et al.*, 1998).

Hiatus across the Cenomanian / Turonian boundary. The 'ammonite bed' is placed in the upper lower Turonian in the northern sections (M1 and AN) because of the presence of *C. luciae*, the index fossil of the biozone T6a in the Near East (Lewy, 1989). This biozone correlates with the *Mammites nodosoides* total range zone (Figure 6) in Tunisia and southern Europe according to Robaszynski *et al.* (1990) and Thomel (1992). We did not find this species, although Bartov *et al.* (1980) and Allam & Khalil (1988) reported its occurrence together with *C. luciae* in the 'ammonite bed' at Gebel Areif El Naqa. *K. turoniense* was found within the ammonite assemblage at this locality and yields further evidence for the presence of the *M. nodosoides* Zone, because the first occurrence (FO) of *K. turoniense* is within the *M. nodosoides* Zone (Figure 7), e.g., in Tunisia and southern Europe (Robaszynski *et al.*, 1990; Thomel, 1992; Chancellor *et al.*,1994; Wiese & Wilmsen, 1999). This corresponds well with the co-occurrence of *C. luciae, M. nodosoides* and *K. turoniense* in the Near East (Freund & Raab, 1969). In contrast, Lewy (1989) placed the FO of *K. turoniense* at the base of the middle Turonian (biozone T6b) and above the last occurrence (LO) of *C. luciae* and *M. nodosoides* (Figure 7). The 'ammonite bed' follows directly above upper Cenomanian deposits at Gebel Minsherah and Gebel Areif El Naqa (Lüning *et al.*, 1998a, Bartov *et al.*, 1980), and thus, a hiatus or a highly condensed interval across the Cenomanian / Turonian boundary is proposed herein, spanning at least the lower Turonian *Watinoceras coloradoense* Zone (Figure 6).

The 'ammonite bed' can be traced further south to central Sinai (Figures 3, 4a). Here, occurrences of *C. segne, C. quaasi, T. rollandi* and *V. durandi* indicate an early Turonian age, but the assemblages do not allow a more precise assignment. Therefore, an extension of the hiatus from northern to central Sinai cannot be proven by our results. Nevertheless, recovery of *K. turoniense* within the 'ammonite bed' in section G and reports of Ziko *et al.* (1993) of *M. nodosoides* in the

Themed area (east-central Sinai) also indicate a late early to middle Turonian age and strongly suggests contemporaneous deposition for the 'ammonite bed'.

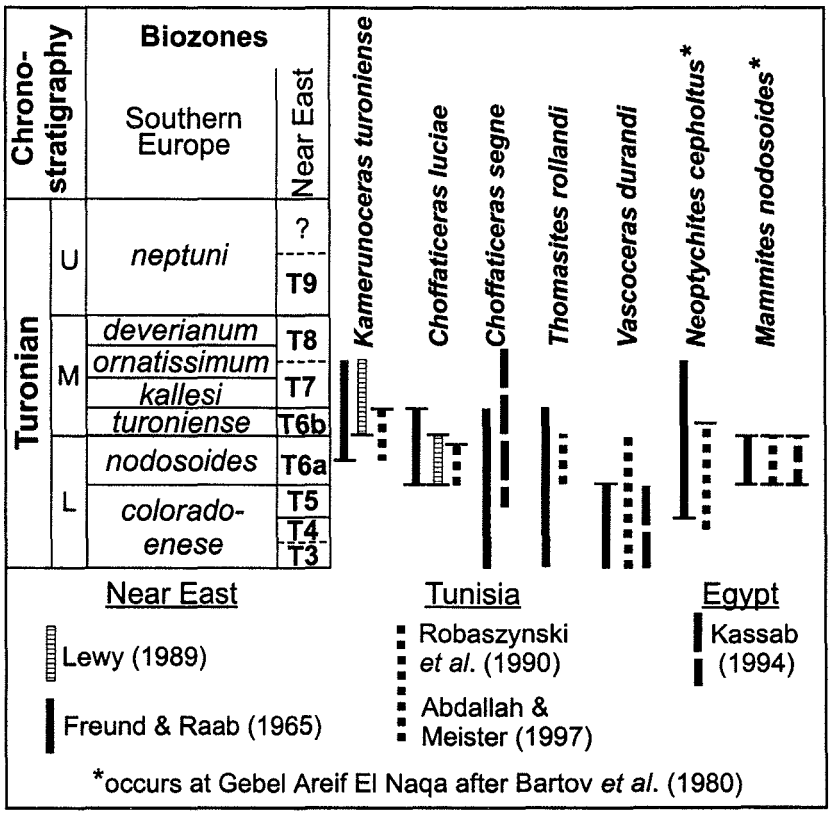

Fig. 7: Comparison of the biostratigraphic ranges of the Turonian ammonites found in the 'ammonite bed' of the Lower Abu Qada Formation with those of Egypt, the Near East and Tunisia. Additionally, the ranges of *Neoptychites cepholtus* and *Mammites nodosoides* are given; these are important index species in the 'ammonite bed' at Gebel Areif El Naqa (after Bartov *et al.*, 1980).

5.2. Calcareous nannofossils

Calcareous nannofossils (mainly identified after descriptions by Perch-Nielsen, 1985) are generally scarce and poorly preserved in the Cenomanian - Turonian successions and are limited to distinct lithostratigraphic units. The total number of species is 28 (Figure 8). Diversity and frequencies increase successively in the Coniacian - Santonian strata (maximum of 35 species). Index taxa are present in the upper Cenomanian - Santonian and allow a reasonable biostratigraphic resolution. In this contribution, we mainly follow the biozone concept of Sissingh (1977), supplemented by Perch-Nielsen (1979, 1985), and use the chronostratigraphic calibration for the Tethyan realm by von Salis in Hardenbol *et al.* (1998). However, some discrepancies in the chronostratigraphic assignments of the bio-events are obvious in the study area and adjacent regions (e.g., *Sinai*: Faris, 1991, 1992; Marzouk & Lüning 1998; *Egypt:* Andrawis *et al.*, 1986; *Near East*: Flexer & Honigstein, 1984; Reiss *et al.*, 1986; *Tunisia:* Robaszynski *et al.*, 1990; Nederbragt & Fiorentino, 1999) as well as in global schemes (Burnett, 1996; Norris *et al.*, 1998) as shown in Figure 9. Photomicrographs

of selected species are shown in Figure 10. Distribution charts of the calcareous nannofossils examined are given in Figures 11-13.

Calcareous nannofossil biozones.

CC 10. Interval zone from FO of *Microrhabulus decoratus* (Figure 10j) to FO of *Quadrum gartneri* (Figure 10s).

Sections. M2, G (Figures 4a, 11).

Formations. Halal and Raha formations.

Stratigraphic range. Middle - upper Cenomanian (e.g., Norris *et al.*, 1998; von Salis in Hardenbol *et al.*, 1998). The index fossil *Lithraphidites actus* of the sub-biozone CC 10a of Burnett (1996) is not recorded.

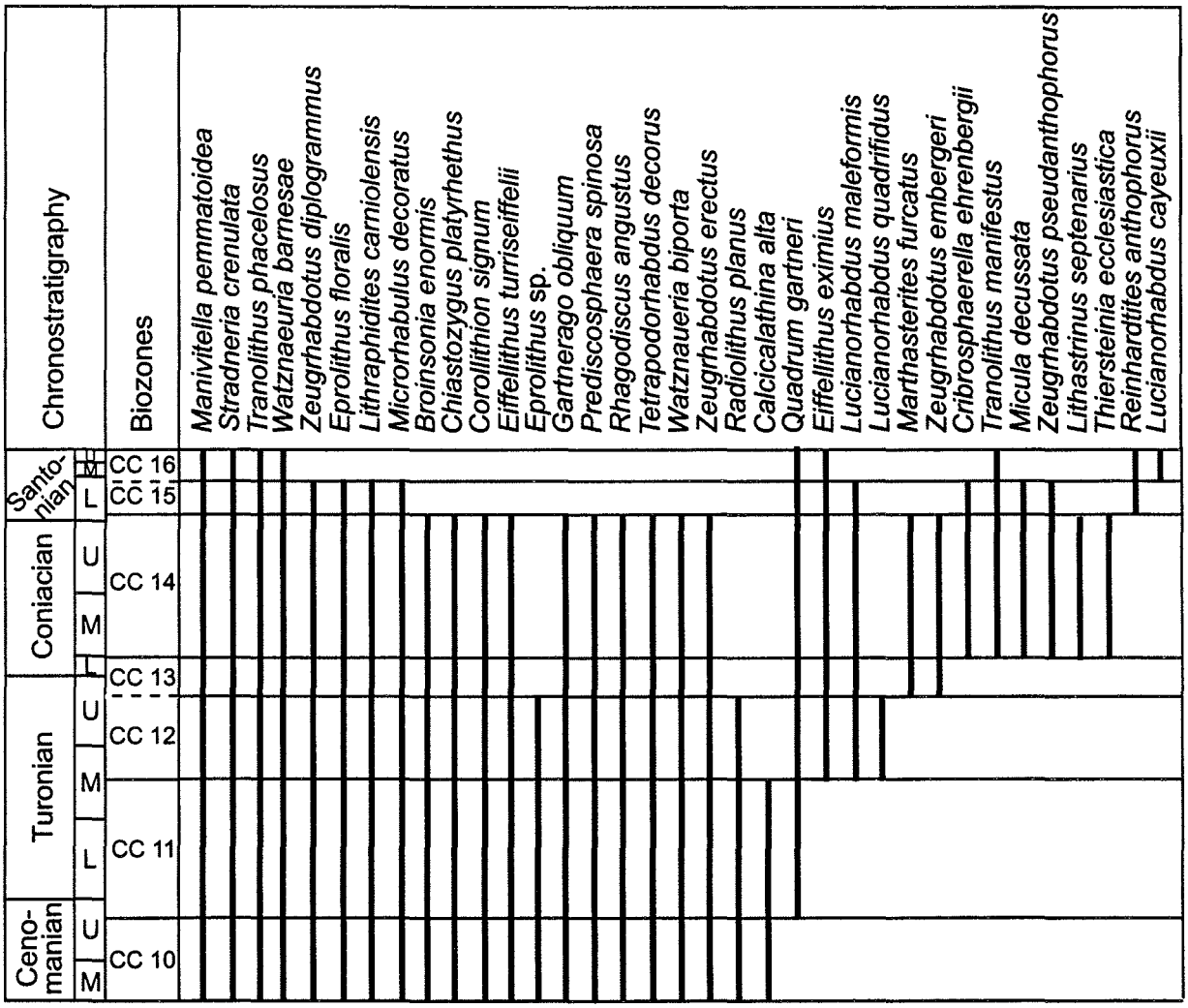

Fig. 8: Range chart of calcareous nannofossils recorded. The LO of most species here is related to ecological conditions and lithology, rather than a result of evolution.

CC 11. Interval zone from FO of *Quadrum gartneri* to FO of *Lucianorhabdus maleformis* (Figure 10d) and/or *Eiffellithus eximius* (Figure 10i, k).

Sections. R, M1, Z, G (Figures 4a, 11, 12).
Formations. Halal, Raha and Lower Abu Qada formations.
Stratigraphic range. The base of CC 11 corresponds to the Cenomanian / Turonian boundary according to global schemes of Perch-Nielsen (1985) and Norris *et al.* (1998) and regional studies (e.g., *Tethyan realm:* von Salis in Hardenbol *et al.*, 1998; *Tunisia:* Nederbragt & Fiorentino, 1999; Robaszynski *et al.*, 1990). In contrast, our own findings of *Q. gartneri* are associated with Cenomanian ostracods (see section 5.4) and/or Cenomanian benthic foraminifera. This may indicate that either the correlation of the Cenomanian - Turonian bio-event datums of the different fossil groups differ in their chronostratigraphic position, leading to uncertainties in stage-boundary determination, or the FO of *Q. gartneri* is already present in the uppermost Cenomanian. The latter matches proposals of the Second Symposium on Cretaceous Stage Boundaries, Brussels 1995 (summarized by Burnett, 1996; Figure 9) as well as reports by Bralower (1988) and assumptions by Sissingh (1977). We discuss these aspects below.

CC 12. Interval zone from FO of *Lucianorhabdus maleformis* and/or *Eiffellithus eximius* to FO of *Marthasterites furcatus* (Figure 10b, c).
Sections. M2, Q, Z (Figures 4a, b, 12).
Formations. Middle and Upper Abu Qada Formation, Wata Formation.
Stratigraphic range. In sections M2 and Z, the FO of both *E. eximius* and *L. maleformis* is 3 m above the upper lower Turonian 'ammonite bed' (Figure 12), indicating a middle Turonian lower boundary of CC 12 within the Lower Abu Qada Formation. This conforms with results from the El Qusaima region (Faris, 1992), 30 km north of Gebel Areif El Naqa. Sissingh (1977) originally assigned CC 12 to the late Turonian and Perch-Nielsen (1979, 1985) used *L. maleformis* and *E. eximius* as interchangeable markers for the lower boundary of CC 12. However, in more recent publications, the FO of *Eiffellithus eximius* is also placed in the middle Turonian (Figure 9), whereas *L. maleformis* was regarded as an unreliable biostratigraphic marker by Burnett (1996) and Nederbragt & Fiorentino (1999). The occurrence of *E. eximius* and *L. maleformis* in the Abu Qada Formation is only occasional (e.g., sections M2, Z; Figure 12). In some sections (M1, AN, G) the 'ammonite bed' is overlain by marls with rare and poorly preserved nannofossils including rare specimens of *Q. gartneri*, but devoid of *E. eximius* and *L. maleformis*. Consequently, only CC 11 or younger can be assumed. We believe that especially sections M1 and AN were effected by strong diagenetic dissolution which eliminated *E. eximius* and *L. maleformis* and other nannofossils (see below).

CC 13. Interval zone from FO of *Marthasterites furcatus* to FO of *Micula decussata* (Figure 10i, m).
Section. Q (Figures 4b, 13).
Formation. Matulla Formation.
Stratigraphic range. The FO of *M. furcatus* is placed within the upper Coniacian deposits of Sinai (Faris, 1991) and the Near East (Reiss *et al.*, 1986), whereas according to the schemes of Sissingh (1977) and Perch-Nielsen (1979, 1985), it marks the Turonian / Coniacian boundary. Burnett (1998) proposed that the FO of the species is diachronous on a global scale. However, in this

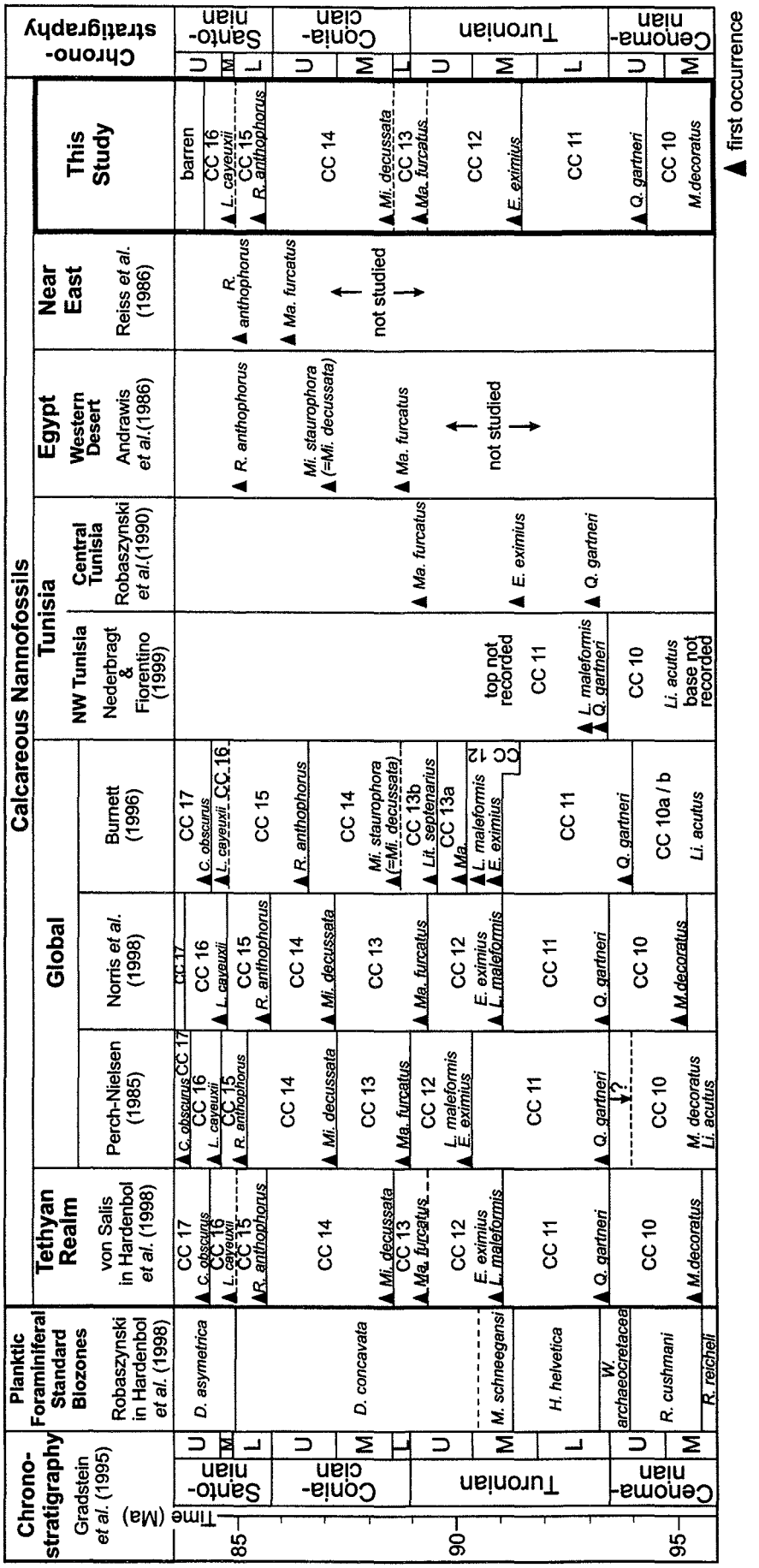
Calcareous Nannofossils
Chrono-stratigraphy
Chrono-stratigraphy Gradstein et al. (1995)
Time (Ma)
Planktic Foraminiferal Standard Biozones Robaszynski in Hardenbol et al. (1998)
Tethyan Realm von Salis in Hardenbol et al. (1998)
Global
Perch-Nielsen (1985)
Norris et al. (1998)
Burnett (1996)
Tunisia
NW Tunisia Nederbragt & Fiorentino (1999)
Central Tunisia Robaszynski et al.(1990)
Egypt Western Desert Andrawis et al.(1986)
Near East Reiss et al. (1986)
This Study
Santo-nian
Conia-cian
Turonian
Cenoma-nian
D. asymetrica
D. concavata
M. schneegansi
H. helvetica
W. archaeocretacea
R. cushmani
R. reicheli
CC 17
CC 16
CC 15
CC 14
CC 13
CC 12
CC 11
CC 10
C. obscurus
L. cayeuxii
R. anthophorus
Mi. decussata
Ma. furcatus
E. eximius
L. maleformis
Q. gartneri
M.decoratus
Li. acutus
Lit. septenarius
Mi. staurophora (=Mi. decussata)
R. anthophorus
Ma. furcatus
E. eximius
Q. gartneri
not studied
top not recorded
base not recorded
barren
▲ first occurrence

Fig. 9: (Previous page) Comparison of chronostratigraphic assignments of the middle Cenomanian - Santonian calcareous nannofossil biozones and bio-events recorded herein with adjacent regional and global schemes. Some discrepancies are obvious, especially with respect to CC 13 - CC 15; note, e.g., the differing FO of *Q. gartneri* in the upper Cenomanian in the study-area and in the global scheme of Burnett (1996). The standard Tethyan planktic foraminiferal biozones are also listed. Abbreviations: calcareous nannofossils: *C.*, *Calculites*; *E.*, *Eiffellithus*; *L.*, *Lucianorhabdus*; *Li*, *Lithraphidites*; *Lit.*, *Lithastrinus*; *M.*, *Microrhabdulus*; *Ma.*, *Marthasterites*; *Mi.*, *Micula*; *Q.*, *Quadrum*; *R.*, *Reinhardtites*; planktic foraminifera: *D*, *Dicarinella*; *H.*, *Helvetoglobotruncana*; *M.*, *Marginotruncana*; *R.*, *Rotalipora*; *W.*, *Whiteinella*.

study, we follow proposals of von Salis in Hardenbol *et al.* (1998) and Norris *et al.* (1998) and place the FO of *M. furcatus* in the uppermost Turonian (Figure 9). The chronostratigraphic position of the upper boundary of CC 13 is uncertain (see below).

CC 14. Interval zone from FO of *Micula decussata* to FO of *Reinhardtites anthophorus* (Figure 10g).

Sections. X4, Q (Figures 4b, 13).

Formation. Matulla Formation.

Stratigraphic range. The Coniacian / Santonian boundary lies within CC 14. Uncertainties exist with respect to the age of the FO of *M. decussata*: e.g., late Coniacian after Perch-Nielsen (1985) in a twofold subdivision of the Coniacian, middle Coniacian according to von Salis in Hardenbol *et al.* (1998), and late middle Coniacian after Norris *et al.* (1998). In this study, the lower boundary of the biozone could not be fixed. We follow studies for Sinai (Faris, 1991) and global concepts (von Salis in Hardenbol *et al.*, 1998) and place the FO of the index species in Sinai within the middle Coniacian (Figure 9).

CC 15. Interval zone from FO of *Reinhardtites anthophorus* to FO of *Lucianorhabdus cayeuxii* (Figure 10a).

Section. X4 (Figures 4b, 13).

Formation. Matulla Formation.

Stratigraphic range. The FO of *R. anthophorus* is mostly attributed to the lower Santonian (Figure 9). In contrast, Andrawis *et al.* (1986) and Reiss *et al.* (1986) placed its FO in the upper Santonian in Egypt and the Near East.

CC 16. Interval zone from FO of *Lucianorhabdus cayeuxii* to FO of *Calculites obscurus*. The top of the zone is not recorded in the sections studied.

Section. X4 (Figures 4b, 13).

Formation. Matulla Formation.

Stratigraphic range. The FO of *L. cayeuxii* is between the uppermost lower Santonian and lower middle Santonian (Figure 9).

Discussion: dissolution

Taphonomic effects, such as diagenetic dissolution, have extensively influenced the frequency and diversity of the original flora and consequently have to be considered for the biostratigraphic inter-

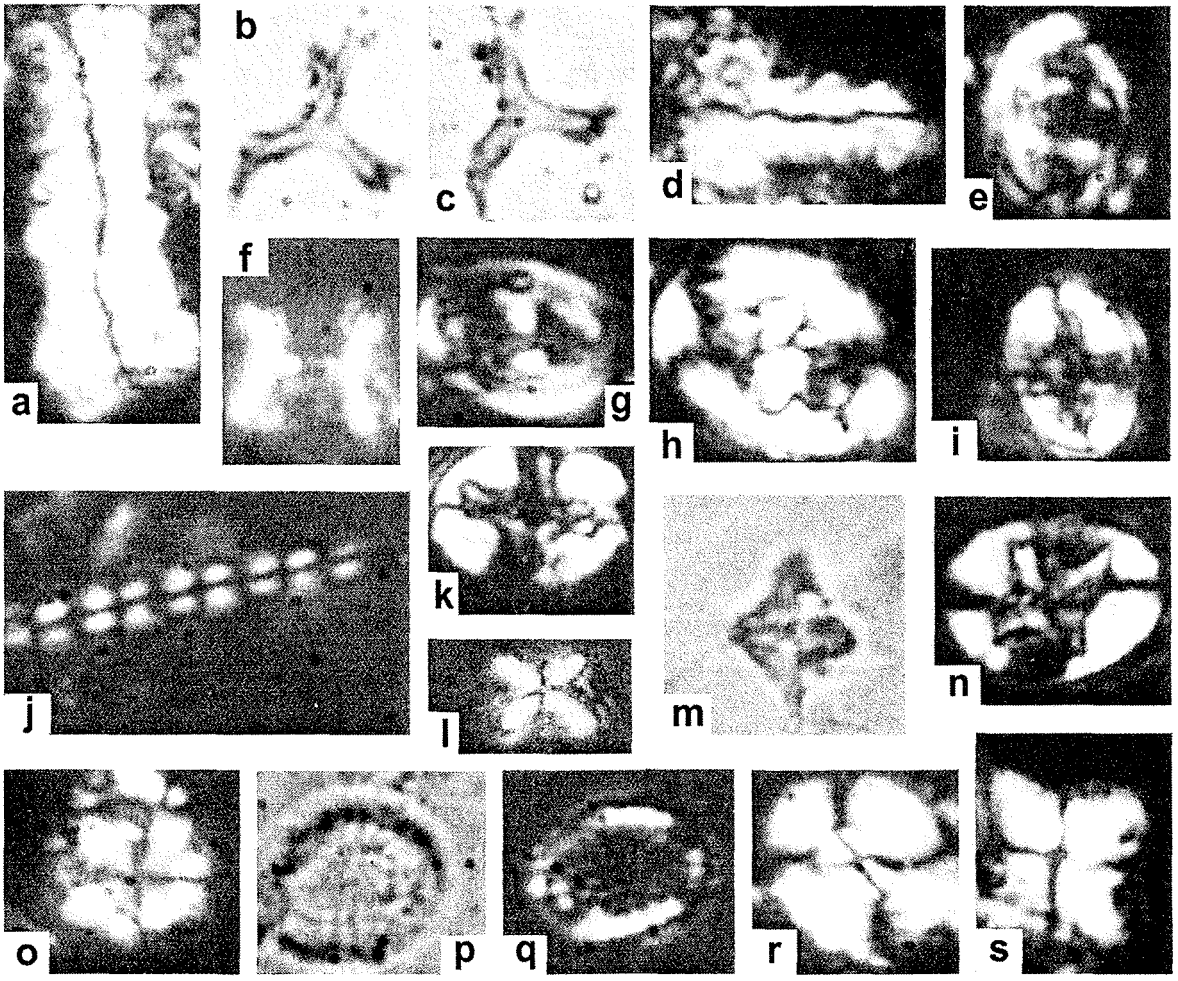

Fig 10: Photomicrographs of selected calcareous nannofossil species; magnification x3300. For sections and samples, refer to Figures 4a, b, and 11 13. a, *Lucianorhabdus cayeuxii*; section X4, sample X4-32. b, c, *Marthasterites furcatus* both from section Q, sample Q-13. d, *Lucianorhabdus maleformis*; section M2, sample M2-25. e, *Tranolithus phacelosus*; section G, sample G-20. f, *Eprolithus floralis*; section G, sample G-22. g, *Reinhardtites anthophorus*; section X4, sample X4-25. h, *Zeugrhabdotus pseudanthophorus*; section X4, sample X4-20. i, k, *Eiffellithus eximius*; section M2, sample M2-20. j, *Microrhabdulus decoratus*; section M2, sample M2-11. l, m, *Micula decussata*; section Q, sample Q-15. n, *Eiffellithus turriseiffelii*; section G, sample G-20. o, *Radiolithus planus*; section G, sample G-22. p, q, *Cribosphaerella ehrenbergii*; section X4; sample X4-22. r, *Watznaeuria barnesae*; section Z, sample Z-23. s, *Quadrum gartneri*; section Z, sample Z-23.

pretation of the nannofossil assemblages studied. This is apparent in the correlation of sections Z and M2 with AN and M1 (Figures 4a, 12). The base of the Abu Qada Formation is characterized by the isochronous 'ammonite bed' (upper lower Turonian *M. nodosoides* Zone), and the overlying deposits of the Abu Qada Formation correspond well concerning the facies evolution of the sections studied. Thus, isochronous deposition during late CC 11 to early CC 12 is most likely, even though *E. eximius* and *L. maleformis* are not recorded in all sections (e.g., sections AN and M1; Figure 12) and marked differences in nannofossil diversity and frequency are obvious. In section Z (Figure 12), *E. eximius* and *L. maleformis* confirm CC 12 within the marls of the Lower Abu Qada Formation and are associated with an abundant, fairly well-preserved and very diverse nannofossil assemblage with no indication of dissolution. In contrast, the Lower and Upper Abu Qada Formation in sections AN and M1 lack these index fossils. Here, the nannofossils are very rare, poorly preserved and of low diversity. Environmental restriction of the index fossil of CC 12 at those positions is unlikely, because other sections of the Abu Qada Formation were deposited in comparable sedimentary settings and contain *E. eximius* and *L. maleformis*. We believe that diagenetic dissolution seriously affected the flora, most probably including *E. eximius* and *L. maleformis,* since the genus *Eiffellithus* is considered to be prone to dissolution (Roth & Krumbach, 1986; Henriksson & Malmgren, 1999). The abundance of *Watznaueria barnesae* (Figure 10r) is generally used as a preservation index because assemblages affected by dissolution are enriched in this dissolution-resistant species (Roth & Krumbach, 1986), although ecological factors may also have affected its distribution (Eshet & Almogi-Labin, 1996; Street & Bown, 2000). Assemblages with more than 40% of this species most probably indicate strong dissolution rather than ecological factors (Roth & Krumbach, 1986). In sections AN and M1 (Figure 12) *W. barnesae* occurs together with *Eprolithus floralis* (Figure 10f), which is also considered to have been relatively resistant against dissolution by various authors (e.g., Thierstein, 1980; Roth & Krumbach, 1986; Bralower, 1988). Moreover, species that are more susceptible to dissolution, such as *Tranolithus phacelosus* (Paul *et al.*, 1999) and *Prediscosphaera spinosa* (Thierstein, 1980; Henriksson & Malmgren, 1999) are absent (but present in M2 and Z; Figure 12). On the other hand, the question as to why other species like *Corollithion signum* or *Radiolithus planus* (Figure 10o) are present in these sections remains unanswered; these species are not more resistant to dissolution than many other nannofossil taxa.

Discussion: chronostratigraphic assignments

The chronostratigraphic variabilities of the herein-detected calcareous nannofossil biozones on regional and global scales (Figure 9) were attributed by Burnett (1996) to the distinct usage of the first appearance datum (FAD) of a taxon on an evolutionary level and the first occurrence (FO) of the taxon, which may be specific to a particular section without global relevance. Gradstein & Agterberg (1998) also pointed out the fact that not observing an event in a given sedimentary record does not necessarily mean that it is absent (owing to, e.g., ecological reasons, sediment supply or taphonomic effects). This is important, especially concerning the detection of index fossils of interval biozones. Moreover, Perch-Nielsen (1985) pointed to different species concepts, state of preservation and uncertain chronostratigraphic assignments of samples studied and the sometimes poor nannofossil content within the stratotypes of the stages.

As the definition of stage boundaries differs historically and some Cretaceous stratotypes may be incomplete (Sissingh, 1977; Burnett, 1998), discrepancies may occur in integrated biostratigraphies and inter-correlation of bio-events of different fossil groups. For example, the FAD of *Q. gartneri* (CC 11) marks the Cenomanian / Turonian boundary in most schemes of Figure 9. However its FAD lies within the ammonite biozone *Neocardioceras judii* of the upper Cenomanian (Symposium on Cretaceous Stage Boundaries, Copenhagen 1983, in Birkelund *et al.*, 1984), which corresponds well with the upper Cenomanian FO of this species in the sections studied.

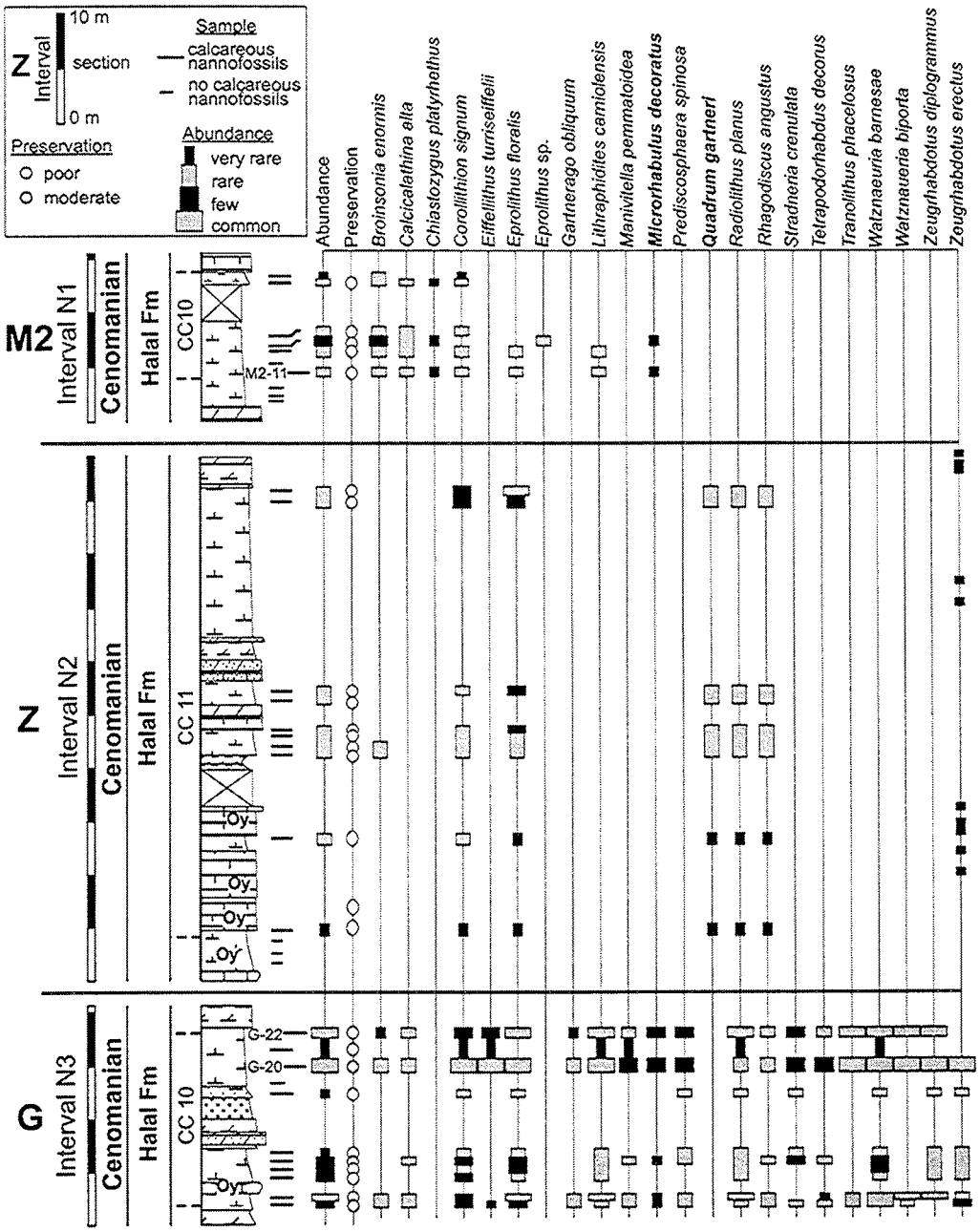

Fig. 11: Cenomanian calcareous nannofossil distribution charts. The positions of the enlarged intervals of sections M2, Z and G are shown in Figure 4a. The sample numbers refer to Figure 10. Specimens in bold are index fossils for the biozones. For key to symbols and lithologies, see Figure 2. The intervals are arranged with respect to the positions of the sections in Figure 4a and not in stratigraphic order.

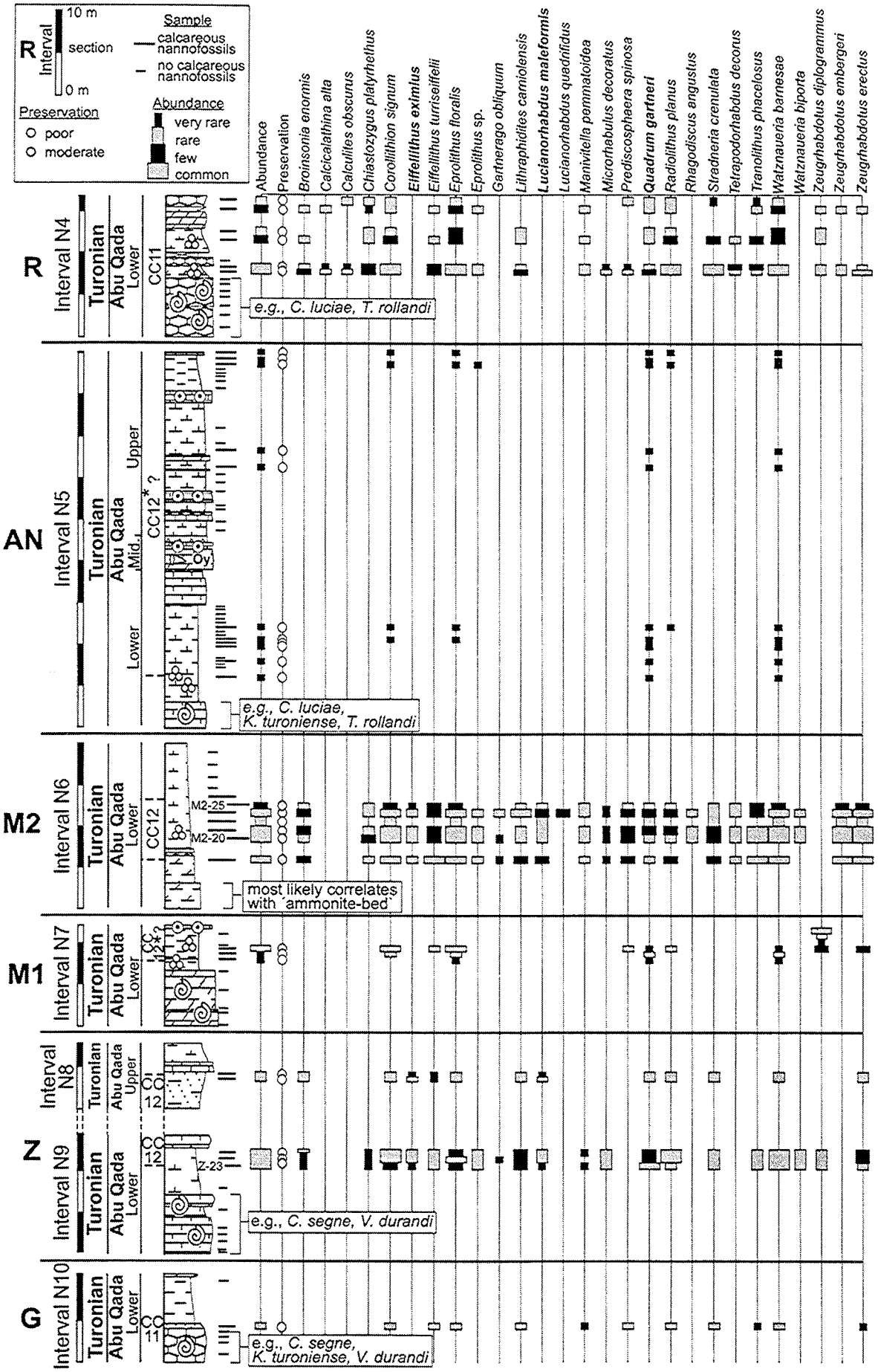

*Dissolution probably destroyed index species

Fig. 12: (Previous page) Turonian calcareous nannofossil distribution charts of enlarged parts of sections R, AN, M1, M2, Z, G, the locations of which are shown in Figure 4a. Characteristic ammonites in the 'ammonite bed' are listed. The sample numbers refer to Figure 10. Specimens in bold are index fossils for the biozones. For key to symbols and lithologies, see Figure 2. The intervals are arranged with respect to the positions of the sections in Figure 4a and not in stratigraphic order.

5.3. Foraminifera

Benthic foraminifera

Benthic foraminifera are frequent in the Cenomanian-Turonian limestones of the sections studied. Their qualitative and semiquantitative distribution patterns have already been studied by Bauer *et al.* (in prep.). Within these diverse assemblages *Chrysalidina gradata*, *Pseudedomia* sp., *Praealveolina* sp., *Biconcava bentori*, and *Cyclogyra* sp. are biostratigraphically indicative of the Cenomanian (e.g., Saint-Marc, 1974; Schröder & Neumann, 1985; Chérif *et al.*, 1989a; Salaj & Maamouri, 1998), and *Neoflabellina suturalis* of the Coniacian (Reiss *et al.*, 1986; Figure 6). A higher biostratigraphic resolution on the basis of the distribution of benthic foraminifera does not seem possible (see discussion below).

Planktic foraminifera

Planktic foraminifera are mostly absent from the Cenomanian successions studied. In the Turonian, planktic foraminifera are restricted to the marginal facies of the Central Sinai Basin within the Lower Abu Qada Formation with varying amounts of hedbergellids (e.g., *Hedbergella delrioensis, H. simplex*), whiteinellids (*Whiteinella archaeocretacea, W. baltica*) and heterohelicids (*Heterohelix globulosa = H. reussi:* late Cenomanian - Maastrichtian according to Nederbragt, 1991), which are unsuitable for high-resolution biostratigraphy because of their long chronostratigraphic ranges (compare Robaszynski & Caron, 1979; Caron, 1985; Sliter, 1989; Abdel-Kireem *et al.*, 1996; Robaszynski in Hardenbol *et al.*, 1998). Above the hiatus at the Cenomanian / Turonian boundary, high amounts of globular foraminifera occur in thin sections of the isochronous 'ammonite bed' and in the overlying marls of the Lower Abu Qada Formation. These microfaunal patterns are observed in northern Sinai (sections R, AN, M1, M2) in upper CC 11 - lower CC 12; therefore, we consider this interval to be chronostratigraphically correlatable.

Keeled planktic foraminifera, generally considered to be deeper water taxa (Hart, 1999), are extremely rare in all of the Turonian samples studied as a result of relatively shallow palaeoenvironments. Deeper marine, Cenomanian - Turonian assemblages occur only in drillcore samples in northernmost Sinai, in the Near East, and offshore in the Mediterranean Sea (e.g., Lipson-Benitah, 1980, 1994). Thus, we cannot confirm reports by Ayyad *et al.*, (1996) of a diverse and well-preserved assemblage of keeled species in the Abu Qada Formation at Gebel Areif El Naqa (for discussion, see Lüning *et al.*, 1998a). Only in Coniacian - Santonian samples of section X4 (Figure 4b), a moderately diverse fauna of keeled species (e.g., *Dicarinella concavata, D. asymetrica, D. primitiva*) is present in the Matulla Formation. The following two standard Tethyan biozones (Caron, 1985, revised by Robaszynski & Caron, 1995 and Robaszynski in Hardenbol *et al.*, 1998) are recognized.

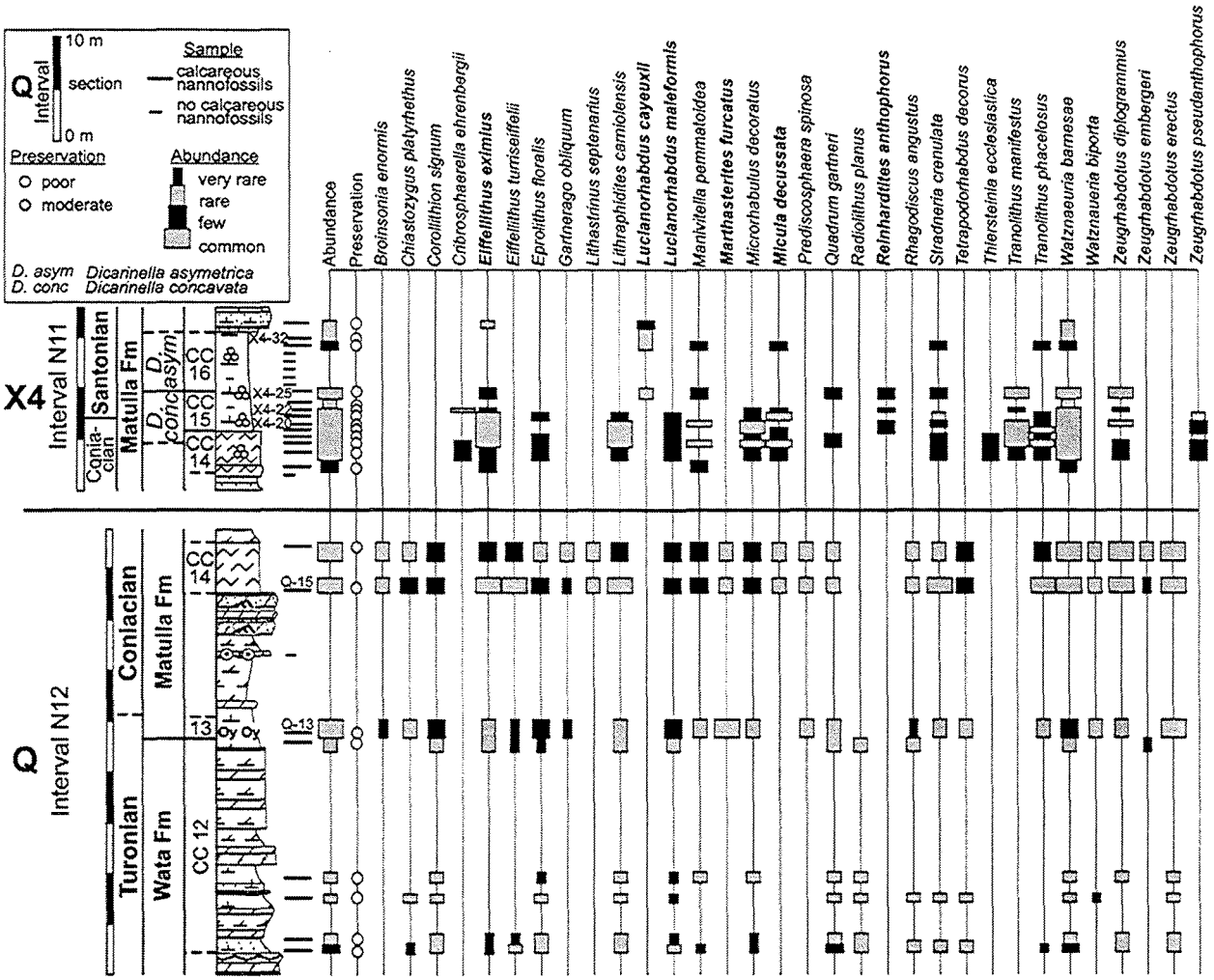

Fig. 13: Upper Turonian - Santonian calcareous nannofossil distribution charts. The locations of the enlarged parts of sections X4 and Q are shown in Figure 4a. The sample numbers refer to Figure 10. Specimens in bold are index fossils for the biozones. For key to symbols and lithologies, see Figure 2.

Dicarinella concavata Zone. Interval zone from FO of *D. concavata* to FO of *D. asymetrica.*

Stratigraphic range. Upper Turonian - upper Coniacian. According to Robaszynski & Caron (1995) *D. concavata* appears together with *D. primitiva.* Thus, the previously used *D. primitiva* Zone of Caron (1985) is unnecessary.

Dicarinella asymetrica Zone. Interval zone from FO of *D. asymetrica* to FO of *Globotruncanita elevata* (the top of the zone has not been found in the sections investigated).

Stratigraphic range. The lower boundary of the zone corresponds to the lower / middle Santonian boundary and the upper boundary lies within the lowermost Campanian (Robaszynski in Hardenbol *et al.*, 1998).

Discussion

Because keeled planktic foraminifera are extremely rare in the Cenomanian - Coniacian successions in Sinai, the Tethyan standard biozone schemes cannot be applied generally. This has led to a wide range of informal biostratigraphic subdivisions in Sinai based on the varying occurrences of planktic and benthic foraminifera (e.g., Chérif *et al.*, 1989a; Shahin & Kora 1991; Hewaidy & El-Ashwah, 1993; Hamza *et al.*, 1994; Kora *et al.*, 1994; Ismail & El-Saadany, 1995). However, these studies refer to single localities or relatively small areas of the Sinai and focus on local features, owing to the frequent lack of species that would allow correlation on a regional scale. Small-scale palaeoenvironmental and palaeogeographic factors most likely influenced the distribution of the species reported. Thus, the stratigraphic reliability of these previously presented subdivisions are of limited use compared to the biostratigraphic framework achieved in the present contribution. Moreover, the subdivisions cited above generally allow a broad biostratigraphic resolution at stage level.

5.4. Ostracods

Ostracods are generally common to abundant in the samples studied. The assemblages are highly diverse. About 75 species have been observed (preliminary determinations by A. M. Morsi, Cairo). The taxonomic and systematic research is still continuing and will be the subject of a future publication. However, the records of biostratigraphically important species based on van den Bold (1964), Bassoullet & Damotte (1969) and Rosenfeld & Raab (1974) are reported here. In the Near East, ostracod biozones and events have been defined and chronostratigraphically calibrated with co-occurring ammonites (Lewy *et al.*, 1988). In Sinai, however, ammonites are less frequent, and thus, a similar high-resolution calibration of the stratrigraphic distribution of ostracods is not possible. An adoption of these biozones seems ambiguous to us at present because we cannot exclude ecologically controlled distribution patterns of some species. Nevertheless, comparisons with data in the literature allow the differentiation of Cenomanian from Turonian levels in terms of ostracod bio-events. Among others, *Cythereis algeriana, Metacytheropteron berbericum, Peloriops ziregensis,* and *Veeniacythereis maghrebensis* occur up to the Cenomanian and *Paracypris triangularis, Pterygocythere raabi,* and *Spinoleberis yotvataensis* first occur in the Turonian (e.g., Rosenfeld & Raab, 1974; Figure 6). With respect to the calcareous nannofossil biozones discussed above, it is important to note that within CC 11 of section Z (Figure 4a), the Cenomanian ostracods *C. algeriana, P. ziregensis* and *V. maghrebensis* still occur, and CC 11 probably straddles the Cenomanian / Turonian boundary. Only a few species (e.g., *Brachycythere angulata; Cythereis rosenfeldi*) indicate a post-Turonian or Coniacian - Santonian age (Figure 6) according to van den Bold (1964), Honigstein *et al.* (1984) and Honigstein & Rosenfeld (1985). However, they do not allow further subdivision of the stages.

5.5. Rudists

The distribution of Cenomanian and Turonian rudists in Sinai has been studied in detail by Bauer *et al.* (in prep.). Post-Turonian rudists have not been recorded in Sinai and are also almost absent

above the Turonian elsewhere on the northeast African shelf of the Tethys (Steuber & Löser, 2000). During the Cenomanian, typical faunal constituents of circum-Mediterranean carbonate shelves such as the Caprinidae were absent in Sinai, but the canaliculate *Ichthyosarcolites* (Figure 5h) were abundant. The first Hippuritidae occur in the Middle Abu Qada Formation of sections UA, AN and G (Figures 3, 4a). These sections yield species that are common in the Turonian of the Mediterranean Tethys, and the FO of *Hippurites requieni* in the Middle Abu Qada Formation is only little later than its first appearance in the Periadriatic region, at the base of the middle Turonian (Philip in Hardenbol *et al.*, 1998). Rudists from this level at Gebel Risha (Figure 1) have been described in detail by Parnes (1987), and they correspond to species that were widely distributed in the Mediterranean Tethys (Steuber, 1999). In Sinai, there was a distinct north-south gradient in diversity of rudists during the Cenomanian - Turonian. Diversity is generally low in northern Sinai. In southern Sinai, monospecific associations of *Eoradiolites* are common, and *Durania* is the only Turonian genus. We cannot confirm the records of upper Turonian rudists reported by Kora & Hamama (1987) from southern Sinai.

6. COMBINED LITHOSTRATIGRAPHIC AND BIOSTRATIGRAPHIC CORRELATION

The well-defined Cenomanian - Santonian lithostratigraphy of Sinai contrasts with a less precise biostratigraphy, because of the lack of consistent biostratigraphically dated successions. In the combined lithostratigraphic and biostratigraphic correlation in Figure 4a, b, the units 1 - 11 used for correlation are based on (in descending order of importance) biozones, formations and members, biota distribution patterns and characteristic stacking patterns. Former palaeoenvironmental interpretations of Bauer *et al.* (in prep.) and Lüning *et al.* (1998a, b) are also considered.

Units 1 and 2, Halal and Raha formations, Cenomanian

Units 1 and 2 (CC 10 - lower CC 11) are composed of mainly calcareous rocks in the northern areas (Halal Formation) and interfinger with more quartzose deposits towards the south (Raha Formation). Unit 1 is characterized by short intervals of frequent calcareous nannofossils in sections M2 and G (Figure 11). The boundary between the two units is marked by the upper limit of *Microrhabulus decoratus* (the index species of CC 10) in sections G and M2, and by the FO of *Quadrum gartneri* (the index species of CC 11) in section Z (Figure 11). Additionally, the benthic foraminiferal assemblages in Unit 1 in sections M2 and AN are very similar (Bauer *et al.*, in prep.).

Unit 3, 'ammonite bed', basal Lower Abu Qada Formation, upper lower Turonian

Unit 3 represents the upper lower Turonian 'ammonite bed', including a short interval of marly deposits (CC 11) of the basal Lower Abu Qada Formation. The species encountered suggest synchronous deposition of the 'ammonite bed' in the late early Turonian (*M. nodosoides* Zone) throughout northern and central Sinai and reflect a flooding of the area of deposition (section 4).

Unit 4, upper part of the Lower Abu Qada Formation, middle Turonian

Unit 4 is within the middle Turonian Lower Abu Qada Formation (CC 12). The lower boundary of Unit 4 is defined by the onset of CC 12 (section Z; Figure 12). Because dissolution most probably

greatly affected the original calcareous nannofossil assemblage (see section 5.2), the index species of CC 12 may be absent and the lower boundary of Unit 4 is uncertain in some sections. Additionally, assemblages of frequent planktic foraminifera are characteristic in unit 4 in the northern sections (M1, M2, AN), interpreted as a response to rising relative sea-level (section 4).

Unit 5, Middle Abu Qada Formation, middle Turonian

Unit 5 of the Middle Abu Qada Formation (middle Turonian) consists of cliff-forming calcareous deposits with intercalated beds of oolites and rudists. Biostratigraphically indicative specimens are missing. The lithofacies is relatively uniform and a nearly identical composition of the rudist associations within the Middle Abu Qada Formation at Gebel Risha and Gebel Um Alda (Figure 3) is reported by Bauer *et al.* (in prep.), suggesting synchronous deposition of the unit.

Unit 6, basal Upper Abu Qada Formation, middle Turonian

Unit 6 is composed of supratidal or very shallow water deposits (gypsum beds, red and green shales with plant remains, emersion horizons) of the basal Upper Abu Qada Formation (middle Turonian, CC 12). In common with Unit 5, Unit 6 is not well-defined biostratigraphically, except for section Z, where CC 12 is recorded (Figure 12). Unit 6 represents a significant relative sea-level lowstand (Lüning *et al.*, 1998b) that is recognizable in all sections studied.

Unit 7, upper part of the Upper Abu Qada Formation, middle - upper Turonian

Unit 7 is placed within the upper part of the Upper Abu Qada Formation (middle - upper Turonian, CC 12). Its lower boundary is defined by the onset of shallow subtidal deposits with oolites, rudists and oysters in places, and with a high glauconite content in most of the sections. The deposits of Unit 7 were formed during a relative sea-level rise (section 4).

Unit 8, Wata Formation, upper Turonian

Unit 8 is equivalent to the Wata Formation (upper Turonian to middle CC 13). The lower boundary is characterized by the onset of cyclically bedded, shallow subtidal carbonates. They often show thinning-upwards cycles, which are probably related to high-order relative sea-level changes. A major shallowing event is indicated by emersion surfaces and intercalated siltstones and sandstones in the middle part of the formation in sections M2 and V.

Unit 9, lower part of the Matulla Formation, Coniacian

Unit 9 is composed of (quartzose) limestones, dolostones and sandstones in the lower part, overlain by chalks (Figure 5b) within the Coniacian part of Matulla Formation in sections X4, Q, and V. Here, CC 13 and CC 14 can be traced as well as the *Dicarinella concavata* Zone (Figure 4b). The upper part of Unit 9 represents a deepening of the depositional system and a southward retreat of the inner-shelf facies of Unit 8, which may correspond with the post-CoSin TST described by Lüning *et al.* (1998b).

Units 10 and 11, upper part of the Matulla Formation, Santonian

Unit 10 is dominated by planktic foraminifera-bearing marls representing the Santonian succession of the Matulla Formation (sections X4, Q). It includes biozones CC 15 and CC 16 as well as the *Dicarinella asymetrica* Zone (section X4). Its lower boundary corresponds with the lower boundary of CC 15. Unit 10 is attributed to a depositional setting similar to that of Unit 9. An increase in siliciclastics, owing to a relative sea-level fall, is documented by calcareous sandstones and dolostones in Unit 11. This lithological break may coincide with sequence boundary Sa/CaSin of Lüning *et al.* (1998b). Both units are characterized by the interfingering of deeper-shelf sediments with shallower marine deposits owing to the interplay of relative sea-level changes and swell and basin morphologies resulting from 'Syrian Arc' tectonics (see sections 3.3 and 4).

The question as to what extent lithostratigraphic units or bedding planes are time transgressive is still a subject of debate (Schwarzacher, 2000), especially with regard to the responses of sedimentary systems to relative sea-level changes. In terms of sequence stratigraphy, Mancini & Tew (1997) underlined the synchroneity of maximum flooding surfaces (*sensu* Van Wagoner *et al.*, 1988) and the diachronous nature of transgressive surfaces and sequence boundaries. According to Strasser *et al.* (1999) sea-level falls may lead to diachronous emersion, but transgressive or maximum flooding events may allow correlation. We assume a more or less coeval onset of most of the major facies changes (e.g., relative sea-level changes) that define the lithostratigraphic units and marker beds of the section studied. The sea-floor topography is considered to have been rather flat during the late Cenomanian, and middle and late Turonian, because the areas of deposition ranged from shallow subtidal to exposure within the wide (proximal-distal extension) inner-platform realm. We believe that the deposits on this flat topography reacted contemporaneously to environmental changes (units 1 - 8), and were exposed or flooded even with low amplitude relative sea-level changes (compare Hunt & Tucker 1993; Strasser *et al.*, 1999). In contrast, units 9 - 11 are probably diachronous owing to the basin and swell morphology during the Coniacian and Santonian ('Syrian Arc' movements), although this can not be confirmed by the biostratigraphic data.

7. CONCLUSIONS

1. Five Cenomanian - Santonian formations (*Cenomanian*: Halal and Raha; *Turonian*: Abu Qada and Wata; *Coniacian - Santonian*: Matulla) have been recognized in Sinai. Lithofacies are mainly controlled by relative sea-level changes or tectonically created differences in relief.
2. A major hiatus straddles the Cenomanian / Turonian boundary, indicated by the first appearance of late early Turonian ammonites above Cenomanian deposits. It is probably related to initial intracratonic compression and inversion of former extensional structures ('Syrian Arc' tectonics).
3. Within a multibiostratigraphic framework, the following biozones are recognized. Ammonites: *M. nodosoides* (sections R, M1, AN, G, Z); calcareous nannofossils: CC 10 (sections M2, G), CC 11 (sections R, Z, G), CC 12 (sections M2, Z), CC 13 (section Q), CC 14 (sections X4, Q), CC 15 - CC 16 (section X4); planktic foraminifera: *D. concavata, D. asymetrica* (section X4).

Certain ostracods allow differentiation at stage-level, as well as benthic foraminifera and rudists from data in the literature.

4. Calcareous nannofossils have been examined semiquantitatively. The biostratigraphic assignment of the index species and the chronostratigraphic positions of the biozones partly differ when compared to the results of other authors, owing to ecological factors, taphonomic effects or taxonomic discrepancies. Selective dissolution has been important in some of the sections studied (AN, M1) and has hampered precise biostratigraphic correlation.
5. A combined biostratigraphic and lithostratigraphic correlation is presented. Within the biostratigraphic resolution achieved we have proposed a chronostratigraphic synchroneity within lithological units, marker beds and distribution patterns of characteristic biota (units 1 - 8). Units 9 - 11 are probably diachronous as a response to 'Syrian Arc' tectonics.

ACKNOWLEDGEMENTS

This study has been funded by the German Research Foundation (DFG; Ku 642/15-1,2). We thank M. M. Morsi and A. M. Bassiouni (both Ain Shams University, Cairo) for ostracod determinations and help in preparing the field work programme in Sinai; U. Heimhofer (ETH Zurich) for his assistance in the field; and F. Wiese (FU Berlin) and P. Luger (TU Berlin) for the identification of the ammonites. D. J. Batten, H. Gebhart, E. Schrank and an anonymous reviewer are kindly acknowledged for having improved this paper by their constructive suggestions and comments. R. Speijer, E. Friedel and R. Bätzel (all Bremen University) are thanked for various kinds of helpful assistance and comments.

8. REFERENCES

Abdallah, H. & Meister, C. 1997. The Cenomanian-Turonian boundary in the Gafsa-Chott area (southern part of central Tunisia): biostratigraphy, palaeoenvironments. *Cretaceous Research* **18**, 197-236.

Abdel-Gawad, G. I. 1999. Biostratigraphy and macrofossil assemblages of the Matulla Formation (Coniacian-Santonian) west central Sinai, Egypt. *Middle East Research Center, Ain Shams University, Earth Science Series* **13**, 187-202.

Abdel-Gawad, G. I., Aboul-Ela, N. M. & Gameil, M. 1992. Molluscan biostratigraphy of the Cenomanian-Turonian strata of Gebel Nezzazat area, west central Sinai, Egypt. In *1 st International Conference on the Geology of the Arab World, Cairo University* (ed. Sadek, A.), pp. 321-332.

Abdel-Gawad, G. I. & Zalat, A. 1992. Some Upper Cretaceous macroinvertebrates from Gebel El-Hamra and Gebel Um Heriba, Mitla Pass, western-central Sinai, Egypt. In *1 st International Conference on the Geology of the Arab World, Cairo University* (ed. Sadek, A.), pp. 333-344.

Abdel-Kireem, M. R., Ibrahim, M. I. A. & Samir, A. M. 1996. Late Cretaceous Heterohelicidae (planktic foraminifera) from the northern part of the Western Desert of Egypt. *Neues Jahrbuch für Geologie und Paläontologie, Abhandlungen* **200**, 237-257.

Akarish, A. I. M. 1999. Microfacies analysis of the Cenomanian-Paleocene exposures of Taba-Nuweiba area, east Sinai. *Middle East Research Center, Ain Shams University, Earth Science Series* **13**, 135-152.

Allam, A. & Khalil, H. 1988. Geology and stratigraphy of the Arif El-Naqa area, Sinai, Egypt. *Egyptian Journal of Geology* **32**, 199-218.

Allam, A. & Khalil, H. 1989. Geology and stratigraphy of Gebel Qabeliat area, southwestern Sinai, Egypt. *Journal of African Earth Sciences* **9**, 59-67.

Almogi-Labin, A., Eshet, Y., Flexer, A., Honigstein, A., Moshkovitz, S. & Rosenfeld, A. 1991. Detailed biostratigraphy of the Santonian/Campanian boundary interval in northern Israel. *Journal of Micropalaeontology* **10**, 39-50.

Almogi-Labin, A., Reiss, Z. & Caron, M. 1986. Senonian Globotruncanidae from Israel. *Ecolgae Geologicae Helvetiae* **79**, 849-895.

Alsharhan, A. S. & Salah, M. G. 1996. Geologic setting and hydrocarbon potential of north Sinai, Egypt. *Bulletin of Canadian Petroleum Geology* **44**, 615-631.

Andrawis, S. F., Faris, M. & El-Sheikh, H. 1986. Biostratigraphic studies on the Upper Cretaceous (Senonian) rocks of East Mubarak Well No. 1, Western Desert, Egypt. *Egyptian Journal of Geology* **30**, 121-130.

Arafa, A. 1991. Biostratigraphic zonation of the Late Cretaceous sediments of Gabal Nazzazat, south-west Sinai, Egypt. *Annals of the Geological Survey of Egypt* **17**, 173-182.

Arkin, Y. & Braun, M. 1965. Type sections of Upper Cretaceous formations in the northern Negev (southern Israel). *Israel Geological Survey, Stratigraphic Sections* **2a**, 19 pp.

Ayyad, S. N., Abed, M. M. & Abu Zied, R. H. 1996. Biostratigraphy and correlation of Cretaceous rocks in Gebel Arif El-Naga, northeastern Sinai, Egypt, based on planktonic foraminifera. *Cretaceous Research* **17**, 263-291.

Bachmann, M. & Kuss, J. 1998. The Middle Cretaceous carbonate ramp of the northern Sinai: sequence stratigraphy and facies distribution. In *Carbonate ramps* (eds Wright, V. P. & Burchette, T. P.), *Geological Society, London, Special Publication* **149**, 253-280.

Bakr, A., Helmy, M. & Baltensperger, P. 1999. Kattaniya fold belt, Western Desert of Egypt; an example of an inverted Jurassic rift basin. *American Association of Petroleum Geologists, Bulletin* **83**, 1298.

Bartov, Y. & Steinitz, G. 1977. The Judea and Mount Scopus Groups in the Negev and Sinai with trend surface analysis of the thickness data. *Israel Journal of Earth Sciences* **26**, 119-148.

Bartov, Y., Eyal, Y., Garfunkel, Z. & Steinitz, G. 1972. Late Cretaceous and Tertiary stratigraphy and paleogeography of southern Israel. *Israel Journal of Earth Sciences* **21**, 69-97.

Bartov, Y., Lewy, Z., Steinitz, G. & Zak, I. 1980. Mesozoic and Tertiary stratigraphy, paleogeography and structural history of the Gebel Areif en Naqa area, eastern Sinai. *Israel Journal of Earth Sciences* **29**, 114-139.

Bassoullet, J.-P. & Damotte, R. 1969. Quelques ostracodes nouveaux du Cénomano-Turonien de l'atlas saharien occidental (Algérie). *Revue de Micropaléontologie* **12**, 130-144.

Bentor, Y. K. 1960. *Lexique stratigraphique international, Asie* **3/10 c2** (Israel) 151 pp. (Centre National de la Recherch Scientifique, Paris).

Birkelund, T., Hancock, J. M., Hart, M. B., Rawson, P. F., Remane, J., Robaszynski, F., Schmid, F. & Surlyk, F. 1984. Cretaceous stage boundaries - proposals. *Bulletin of the Geological Society of Denmark* **33**, 3-20.

Bosworth, W., Guiraud, R. & Kessler, L. G. 1999. Late Cretaceous (ca. 84 Ma) compressive deformation of the stable platform of northeast Africa (Egypt): far-field stress effects of the 'Santonian event' and origin of the Syrian Arc deformation belt. *Geology* **27**, 633-636.

Bralower, T. J. 1988. Calcareous nannofossil biostratigraphy and assemblages of the Cenomanian-Turonian boundary interval: implications for the origin and timing of oceanic anoxia. *Paleoceanography* **3**, 275-316.

Bramlette, M. N. & Sullivan, F. R. 1961. Coccolithophorids and related nannoplankton of the early Tertiary in California. *Micropaleontology* **7**, 129-188.

Buchbinder, B., Benjamini, C. & Lipson-Benitah, S. 2000. Sequence development of Late Cenomanian-Turonian carbonate ramps, platforms and basins in Israel. *Cretaceous Research* **21**, 813-843.

Burnett, J. A. 1996. Nannofossils and Upper Cretaceous (sub-)stage boundaries - state of the art. *Journal of Nannoplankton Research* **18**, 23-32.

Burnett, J. A. 1998. Upper Cretaceous. In *Calcareous nannofossil biostratigraphy* (ed. Bown, P. R.), pp. 132-199 (Chapman & Hall, London).

Caron, M. 1985. Cretaceous planktic foraminifera. In *Plankton stratigraphy* (eds Bolli, H. M., Saunders, J. B. & Perch-Nielsen, K.), pp. 17-86 (Cambridge University Press, Cambridge).

Chancellor, G. R., Kennedy, W. J. & Hancock, J. M. 1994. Turonian ammonite faunas from central Tunisia. *Special Papers in Palaeontology* **50**, 118 pp.

Chérif, O. H., Al-Rifaiy, I. A., Al-Afifi, F. I. & Orabi, O. H. 1989a. Foraminiferal biostratigraphy and paleoecology of some Cenomanian-Turonian exposures in west-central Sinai, (Egypt). *Revue de Micropaléontologie* **31**, 243-262.

Chérif, O. H., Al-Rifaiy, I. A., Al-Afifi, F. I. & Orabi, O. H. 1989b. Planktonic foraminifera and chronostratigraphy of Senonian exposures in west-central Sinai, Egypt. *Revue de Micropaléontologie* **32**, 167-184.

Dobruskina, I. A. 1997. Turonian plants from the southern Negev, Israel. *Cretaceous Research* **18**, 87-107.

Drzewiecki, P. A. & Simo, J. A. 1997. Carbonate platform drowning and oceanic anoxic events on a mid-Cretaceous carbonate platform, south-central Pyrenees, Spain. *Journal of Sedimentary Research* **67**, 698-714.

El-Hawat, A. S. 1997. Sedimentary basins of Egypt: an overview of dynamic stratigraphy. In *African basins.* (ed. Selley, R. C.), pp. 39-85 (Sedimentary basins of the World 3, Elsevier, Amsterdam).

El-Sheikh, H. A. 1995. Foraminifera and calcareous nannofossil biostratigraphy of Late Cretaceous sediments

in Wadi Taba, southeastern Sinai, Gulf of Aqaba, Egypt. *Egyptian Journal of Geology* **39**, 295-311.

El-Toukhy, M., Mahmoud, A., El-Barkooky, A. N. & Gouda, S. 1999. Tectono-stratigraphic evolution of the North Western Desert, Egypt; implications for hydrocarbon prospectivity. *American Association of Petroleum Geologists, Bulletin* **83**, 1310.

Enani, N., Rizk, R. & Anwar, A. 1994. Sedimentological model of the exposed lower Senonian Matulla Formation and its application in Belayim and Rudeis oil fields, Gulf of Suez. In *Proceedings 12th Petroleum Exploration and Production Conference, Cairo,* pp. 387-411 (Egyptian General Petroleum Corporation, Cairo).

Eshet, Y. & Almogi-Labin, A. 1996. Calcareous nannofossils as paleoproductivity indicators in Upper Cretaceous organic-rich sequences in Israel. *Marine Micropaleontology* **29**, 37-61.

Eshet, Y. & Moshkovitz, S. 1995. New nannofossil biostratigraphy for Upper Cretaceous organic-rich carbonates in Israel. *Micropaleontology* **41**, 321-341.

Faris, M. 1991. Late Cretaceous calcareous nannofossils and stage boundaries in East Mubarak, Well No. 1, Western Desert, Egypt. *Annals of the Geological Survey of Egypt* **17**, 213-221.

Faris, M. 1992. Calcareous nannoplankton from the Turonian - Maastrichtian sequence east of El Qusaima, NE Sinai, Egypt. *Qatar University Science Journal* **12**, 166-175.

Flexer, A. & Honigstein, A. 1984. The Senonian succession in Israel - lithostratigraphy, biostratigraphy and sea-level changes. *Cretaceous Research* **5**, 303-312.

Flexer, A., Rosenfeld, A., Lipson-Benitah, S. & Honigstein, A. 1986. Relative sea-level changes during the Cretaceous in Israel. *American Association of Petroleum Geologists, Bulletin* **70**, 1685-1699.

Freund, R. & Raab, M. 1969. Lower Turonian ammonites from Israel. *Special Papers in Palaeontology* **4**, 83 pp.

Garfunkel, Z. 1998. Constraints on the origin and history of the Eastern Mediterranean basin. *Tectonophysics* **298**, 5–35.

Geological Survey of Egypt 1992-1994. Geological map of Sinai, Egypt, 1:25,000, Sheet Nos. 1-5.

Ghorab, M. A. 1961. Abnormal stratigraphic feature in Ras Gharib oil field. In *3rd Arab Petroleum Congress, Alexandria, Egypt,* 10 pp.

Gradstein, F. M. & Agterberg, F. P. 1998. Uncertainty in stratigraphic correlation. In *Sequence stratigraphy - concepts and applications* (eds Gradstein, F. M., Sandvik, K. O. & Milton, N. J.), *Norwegian Petroleum Society (NPF) Special Publication* **8**, 9-29.

Gradstein, F. M., Agterberg, F. P., Ogg, J. G., Hardenbol, J., Van Veen, P., Thierry, J. & Huang, Z. 1995. A Triassic, Jurassic and Cretaceous time scale. In *Geochronology, time scales and global stratigraphic correlation* (eds Berggren, W. A., Kent, D. V., Aubry, M.-P. and Hardenbol, J.), *SEPM (Society for Sedimentary Geology) Special Publication* **54**, 95-126

Guiraud, R. 1998. Mesozoic rifting and basin inversion along the northern African Tethyan margin: an overview. In *Petroleum geology of North Africa* (eds MacGregor, D. S., Moody, R. T. J. & Clark-Lowes, D. D.), *Geological Society, London, Special Publication* **132**, 217-229.

Guiraud, R. & Bosworth, W. 1997. Senonian basin inversion and rejuvention of rifting in Africa and Arabia: synthesis and implications to plate-scale tectonics. *Tectonophysics* **282**, 39-82.

Gvirtzman, Z. & Garfunkel, Z. 1998. The transformation of southern Israel from a swell to a basin: stratigraphic and geodynamic implications for intracontinental tectonics. *Earth and Planetary Science Letters* **163**, 275-290.

Gvirtzman, G., Almogi-Labin, A., Moshkovitz, S., Lewy, Z., Honigstein, A. & Reiss, Z. 1989. Upper Cretaceous high-resolution multiple stratigraphy, northern margin of the Arabian platform, central Israel. *Cretaceous Research* **10**, 107-135.

Hamza, F. H., Ismail, A. A. & El-Saadany, M. A. 1994. Biostratigraphy and paleoecology of some Cretaceous exposures in northern Sinai, Egypt. In *Proceedings, 12th Petroleum Exploration and Production Conference, Cairo,* pp. 482-495 (Egyptian General Petroleum Corporation, Cairo).

Hancock, J. M. 1993. Sea-level changes around the Cenomanian-Turonian boundary. *Cretaceous Research* **14**, 553-562.

Haq, B. U., Hardenbol, J. & Vail, P. R. 1987. Chronology of fluctuating sea levels since the Triassic. *Science* **235**, 1156-1167.

Hardenbol, J., Thierry, J., Farley, M. B., Jacquin, T., de Graciansky, P.-C. & Vail, P. R. 1998. Mesozoic and Cenozoic sequence chronostratigraphic framework of European basins, Chart 5. In *Mesozoic and Cenozoic sequence stratigraphy of European basins* (eds de Graciansky, P.-C., Hardenbol, J., Jacquin, T. & Vail, P. R.), *SEPM (Society for Sedimentary Geology) Special Publication* **60**.

Hart, M. B. 1999. The evolution and biodiversity of Cretaceous planktonic Foraminiferida. *Geobios* **32**, 247-255.

Hay, W. W. 1965. Calcareous nannofossils. In *Handbook of paleontological techniques.* (eds Kummel, B. & Raup, D.), pp. 3-7 (Freeman & Co., San Francisco).

Henriksson, A. S. & Malmgren, B. A. 1999. Ranking of differential dissolution of terminal Cretaceous calcare-

ous nannofossils using a statistical approach. *Revista Española de Micropaleontología* **31**, 289-296.

Hewaidy, A. E. G. & El-Ashwah, A. A. 1993. Faunal and environment studies on the Upper Cretaceous sequence in El Qusaima area, north-east Sinai, Egypt. *Annals of the Geological Survey of Egypt* **19**, 261-288.

Hirsch, F., Bassoullet, J.-P., Cariou, E., Conway, B., Feldman, H. R., Grossowicz, L., Honigstein, A., Owen, E. F. & Rosenfeld, A. 1998. The Jurassic of the southern Levant. Biostratigraphy, palaeogeography and cyclic events. In *Peri-Tethys Memoir 4: epicratonic basins of Peri-Tethyan platforms* (eds Crasquin-Soleau, S. & Barrier, É.), *Mémoires du Muséum National d'Histoire Naturelle, Paris* **179**, 213-235.

Honigstein, A. 1984. Senonian ostracods from Israel. *Geological Survey of Israel, Bulletin* **78**, 48 pp.

Honigstein, A. & Rosenfeld, A. 1985. Late Turonian-early Coniacian ostracodes from the Zihor Formation, southern Israel. *Revista Española de Micropaleontología* **17**, 447-466.

Hunt, D. & Tucker, M. E. 1993. Sequence stratigraphy of carbonate shelves with an example from the mid-Cretaceous (Urgonian) of southeast France. In *Sequence stratigraphy and facies associations.* (eds Posamentier, H. W., Summerhayes, C. P., Haq, B. U. & Allen, G. P.), *International Association of Sedimentologists, Special Publication* **18**, 307-341.

Ismail, A. A. & El-Saadany, M. A. 1995. Some Cretaceous foraminifera from northern Sinai, Egypt. *Middle East Research Center, Ain Shams University, Earth Science Series* **9**, 173-203.

Issawi, B., El-Hinnawi, M., Francis, M. & Mazhar, A. 1999. The Phanerozoic geology of Egypt: a geodynamic approach. *Egyptian Geological Survey, Special Publication* **76**, 462 pp.

Kassab, A. S. 1994. Upper Cretaceous ammonites from the El Sheikh Fadl - Ras Gharib Road, Northeastern Desert, Egypt. *Neues Jahrbuch für Geologie und Paläontologie, Monatshefte* **1994**, 108-128.

Kassab, A. S. & Ismael, M. M. 1994. Upper Cretaceous invertebrate fossils from the area northeast of Abu Zuneima, Sinai, Egypt. *Neues Jahrbuch für Geologie und Paläontologie, Abhandlungen* **191**, 221-249.

Keeley, M. L. 1994. Phanerozoic evolution of the basins of northern Egypt and adjacent areas. *Geologische Rundschau* **83**, 728-742.

Keeley, M. L. & Massoud, M. S. 1998. Tectonic controls on the petroleum geology of NE Africa. In *Petroleum geology of North Africa* (eds MacGregor, D. S., Moody, R. T. J. & Clark-Lowes, D. D.), *Geological Society, London, Special Publication* **132**, 265-281.

Kerdany, M. T. & Chérif, O. H. 1990. Mesozoic. In *The geology of Egypt* (ed. Said, R.), pp. 407-438 (Balkema, Rotterdam).

Khalil, B. 1992. The geology of the Ar Rabba area. *1:50,000 Geological Mapping Series Bulletin (Jordan)* **22**, 106 pp.

Klitzsch, E. & Hermina, M. 1989. The Mesozoic. In *Stratigraphic lexicon and explanatory notes to the geological map of Egypt 1:500 000* (eds Hermina, M., Klitzsch, E. & List, F. K.), pp. 77-140 (Conoco Inc., Cairo).

Kora, M. & Genedi, A. 1995. Lithostratigraphy and facies development of the Upper Cretaceous carbonates in east central Sinai, Egypt. *Facies* **32**, 223-236.

Kora, M. & Hamama, H. 1987. Biostratigraphy of the Cenomanian-Turonian of Gabal Gunna, southeastern Sinai. *Mansoura Science Bulletin* **14**, 289-301.

Kora, M., Shahin, A. & Semiet, A. 1994. Biostratigraphy and paleoecology of some Cenomanian successions in the west central Sinai, Egypt. *Neues Jahrbuch für Geologie und Paläontologie, Monatshefte* **1994**, 597-617.

Krenkel, E. 1924. Der syrische Bogen. *Zentralblatt für Mineralogie, Geologie und Palaeontologie, Abhandlungen B*, **9**, 274-281; **10**, 301-313.

Kunow, R., Bauer, J., Bachmann, M. & Kuss, J. 1998. Verteilungsmuster benthischer Foraminiferen und Tonmineralassoziationen im Oberapt des Sinai. *Zentralblatt der Geologie und Paläontologie Teil I* **H1/2**, 353-371.

Kuss, J. 1989. Facies and paleogeographic importance of the pre-rift limestones from NE-Egypt/Sinai. *Geologische Rundschau* **78**, 487-498.

Kuss, J. 1992. The Aptian-Paleocene shelf carbonates of northeast Egypt and southern Jordan: establishment and break-up of carbonate platforms along the southern Tethyan shores. *Zeitschrift der Deutschen Geologischen Gesellschaft* **143**, 107-132.

Kuss, J. & Bachmann, M. 1996. Cretaceous paleogeography of the Sinai peninsula and neighbouring areas. *Comptes Rendus de l'Académie des Sciences, Serie IIa* **322**, 915-933.

Kuss, J. & Malchus, N. 1989. Facies and composite biostratigraphy of Late Cretaceous strata from northeast Egypt. In *Cretaceous of the Western Tethys. Proceedings 3 rd International Cretaceous Symposium, Tübingen 1987* (ed. Wiedmann, J.), pp. 879-910 (Schweizerbart, Stuttgart).

Kuss, J., Scheibner, C. & Gietl., R. 2000a. Carbonate platform to basin transition along an Upper Cretaceous to Lower Tertiary Syrian Arc uplift, Galala Plateaus, Eastern Desert, Egypt. *GeoArabia* **5**, 405-424.

Kuss, J., Westerhold, T., Groß, U., Bauer, J. & Lüning, S. (2000b). Mapping of Late Cretaceous stratigraphic sequences along a Syrian Arc Uplift - examples from the Areif el Naqa/Eastern Sinai. *Middle East Research Center, Ain Shams University, Earth Science Series* **14**, 171-191.

Lewy, Z. 1975. The geological history of southern Israel and Sinai during the Coniacian. *Israel Journal of Earth Sciences* **24**, 19-43.

Lewy, Z. 1989. Correlation of lithostratigraphic units in the upper Judea Group (late Cenomanian - late Coniacian) in Israel. *Israel Journal of Earth Sciences* **38**, 37-43.

Lewy, Z. 1990. Transgressions, regressions and relative sea level changes on the Cretaceous shelf of Israel and adjacent countries. A critical evaluation of Cretaceous global sea-level correlations. *Paleoceanography* **5**, 619-637.

Lewy, Z. & Raab, M. 1976. Mid-Cretaceous stratigraphy of the Middle East. *Annales du Muséum d'Histoire Naturelle de Nice* **4**, 1 -20.

Lewy, Z., Rosenfeld, A. & Honigstein, A. 1988. Ostracodes from Sinai (Egypt) and southern Israel dated by late Turonian - Coniacian ammonites. *Journal of African Earth Sciences* **7**, 903-913.

Lipson-Benitah, S. 1980. Albian to Coniacian zonation of the western coastal plain of Israel. *Cretaceous Research* **1**, 3-12.

Lipson-Benitah, S. 1994. Cenomanian stratigraphical micropaleontology of shelf deposits - Israel. *Revista Española de Micropaleontología* **26**, 83-100.

Lipson-Benitah, S., Almogi-Labin, A. & Saas, E. 1997. Cenomanian biostratigraphy and palaeoenvironments in the northwest Carmel region, northern Israel. *Cretaceous Research* **18**, 469-491.

Luger, P. & Gröschke, M. 1989. Late Cretaceous ammonites from the Wadi Qena area in the Egyptian Eastern Desert. *Palaeontology* **32**, 355-407.

Lüning, S., Kuss, J., Bachmann, M., Marzouk, A. M. & Morsi, A. M. 1998a. Sedimentary response to basin inversion: Mid Cretaceous - Early Tertiary pre- to syndeformational deposition at the Areif El Naqa anticline (Sinai, Egypt). *Facies* **38**, 103-136.

Lüning, S., Marzouk, A. M., Morsi, A. M. & Kuss, J. 1998b. Sequence stratigraphy of the Upper Cretaceous of central-east Sinai, Egypt. *Cretaceous Research* **19**, 153-196.

Mancini, E. A. & Tew, B. E. 1997. Recognition of maximum flooding events in mixed siliciclastic-carbonate systems: key to global chronostratigraphic correlation. *Geology* **25**, 351-357.

Marzouk, A. M. & Lüning, S. 1998. Comparative biostratigraphy of calcareous nannofossils and planktonic foraminifera in the Paleocene of the eastern Sinai, Egypt. *Neues Jahrbuch für Geologie und Paläontologie, Abhandlungen* **207**, 77-105.

Moustafa, A. R. & Khalil, M.H. 1990. Structural characteristics and tectonic evolution of north Sinai fold belts. In *The Geology of Egypt* (ed. Said, R.), pp. 381-389 (Balkema, Rotterdam).

Moustafa, A. R. & Khalil, S.M. 1995. Rejuvenation of the Tethyan passive continental margin of northern Sinai: deformation style and age (Gebel Yelleq area). *Tectonophysics* **241**, 225-238.

Nederbragt, A. J. 1991. Late Cretaceous biostratigraphy and development of Heterohelicidae (planktic foraminifers). *Micropaleontology* **37**, 329-372.

Nederbragt, A. J. & Fiorentino, A. 1999. Stratigraphy and palaeoceanography of the Cenomanian-Turonian boundary event in Oued Mellegue, north-western Tunisia. *Cretaceous Research* **20**, 47-62.

Norris, R. D., Kroon, D., Klaus, A. & Shipboard Scientific Party 1998. Explanatory notes. *Proceedings of the Ocean Drilling Program, Initial Reports* **171B** (eds Norris, R. D., Kroon, D. & Klaus, A.), 11-44.

Orabi, O. H. 1991. A study of paleoecology and bathymetry of the subsurface formations of the Late Cretaceous sequences encountered in the Abu Rudeis-Belayim area, western Sinai, Egypt. *Science Journal of the Faculty of Science of Menoufia University, Egypt* **5**, 131-160.

Orabi, O. H. & Ramadan, F. S. 1995. Contribution to the stratigraphy and microfacies of the Matulla Formation in southern Wadi Feiran and Wadi Abuira, west-central Sinai, Egypt. *Egyptian Journal of Geology* **39**, 339-360.

Parnes, A. 1964. Coniacian ammonites from the Negev (southern Israel). *Geological Survey of Israel, Bulletin* **39**, 42 pp.

Parnes, A. 1987. Radiation of species of the genus *Radiolites* from the Upper Turonian at Gebel Er-Risha (NE Sinai, Egypt). *Israel Journal of Earth Sciences* **36**, 133-153.

Paul, C. R. C., Lamolda, M. A., Mitchell, S. F., Vaziri, M. R., Gorostidi, A. & Marshall, J. D. 1999. The Cenomanian - Turonian boundary at Eastbourne (Sussex, UK): a proposed European reference section. *Palaeogeography, Palaeoclimatology, Palaeoecology* **150**, 83-121.

Perch-Nielsen, K. 1979. Calcareous nannofossils from the Cretaceous between the North Sea and the Mediterranean. In *Aspekte der Kreide Europas* (ed. Wiedmann, J.), *IUGS Series A* **6**, pp. 223-264 (Schweizerbart, Stuttgart).

Perch-Nielsen, K. 1985. Mesozoic calcareous nannofossils. In *Plankton stratigraphy* (eds Bolli, H. M., Saunders, J. B. & Perch-Nielsen, K.), pp. 329-426 (Cambridge University Press, Cambridge).

Philip, J. M. & Airaud-Crumiere, C. 1991. The demise of the rudist-bearing carbonate platforms at the Cenomanian/Turonian boundary: a global control. *Coral Reefs* **10**, 115-125.

Refaat, A. A. A. 1993. Facies development of the Coniacian-Santonian sediments along the Gulf of Suez,

Egypt. *Berliner Geowissenschftliche Abhandlungen A* **150**, 146 pp.

Reiss, Z., Almogi-Labin, A., Lewy, Z. & Moshkovitz, S. 1986. Biostratigraphic datums in the Senonian of Israel. *Proceedings of the Koninklijke Nederlandse Akademie van Wetenschappen B* **86**, 95-104.

Robaszynski, F. & Caron, M. 1979. Atlas de foraminifères planctoniques du Crétacé moyen (mer Boréale et Téthys). *Cahiers de Micropaléontologie* **1**, 186 pp. **2**, 181 pp. (Centre National de la Recherche Scientifique, Paris).

Robaszynski, F. & Caron, M. 1995. Foraminifères planctoniques du Crétacé: commentaire de la zonation Europe-Méditerrenée. *Bulletin de la Société Géologique de France* **166**, 681-692.

Robaszynski, F., Caron, M., Dupuis, C., Amédro, F., Gonzalez Donoso, J.-M., Linares, D., Hardenbol, J., Gartner, S., Calandra, F. & Deloffre, R. 1990. A tentative integrated stratigraphy in the Turonian of central Tunisia: formations, zones and sequential stratigraphy in the Kalaat Senan area. *Bulletin des Centres de Recherches Exploration - Production Elf Aquitaine* **14**, 214-384.

Rosenfeld, A. & Raab, M. 1974. Cenomanian-Turonian ostracodes from the Judea Group in Israel. *Geological Survey of Israel, Bulletin* **62**, 64 pp.

Rosenthal, E., Weinberger, G., Almogi-Labin, A. & Flexer, A. 2000. Late Cretaceous-early Tertiary development of depositional basins in Samaria as a reflection of Eastern Mediterranean tectonic evolution. *American Association of Petroleum Geologists, Bulletin* **84**, 997-1014.

Roth, P. H. & Krumbach, K. R. 1986. Middle Cretaceous calcareous nannofossil biogeography and preservation in the Atlantic and Indian Oceans: implications for palaeoceanography. *Marine Micropaleontology* **10**, 235-266.

Said, R. 1962. *The Geology of Egypt*, 377 pp. (Elsevier, Amsterdam).

Said, R. 1971. Explanatory notes to accompany the geological map of Egypt. *Egyptian Geological Survey Papers* **56**, 123 pp.

Said, R. 1990. Cretaceous paleogeographic maps. In *The Geology of Egypt* (ed. Said, R.), pp. 439-449 (Balkema, Rotterdam).

Saint-Marc, P. 1974. Étude stratigraphique et micropaléontologique de l'Albien, du Cénomanien et du Turonien du Liban. *Muséum National d'Histoire Narturelle, Paris, Notes et Mémoires sur le Moyen-Orient* **13**, 298 pp.

Salaj, J. & Maamouri, A.-L. 1998. Upper Cretaceous microbiofacies of Tunisia. III. part. In *Atlas of Tunisian microbiofacies and its relation to some circum-tethydian types* (eds Salaj, J. & Maamouri, A.-L.), *Zemný Plyn A Nafta* (MND, Hodonín, Czech Republic) **43**, 339-433.

Sandler, A. 1996. A Turonian subaerial event in Israel: karst, sandstone and pedogenesis. *Geological Survey of Israel, Bulletin* **85**, 52 pp.

Schlager, W. 1999. Type 3 sequence boundaries. In *Advances in carbonate sequence stratigraphy: application to reservoirs, outcrops and models* (eds Harris, P. M., Saller, A. H. & Simo, J. A.), *SEPM (Society for Sedimentary Geology) Special Publication* **63**, 35-45.

Schröder, R. & Neumann, M. (eds) 1985. Les grandes foraminifères du Crétacé moyen de la région Méditerranéenne. *Geobios, Mémoire Spécial* **7**, 160 pp.

Schulze, F. & Kuss, J. 2000. Biostratigraphy and cyclicities of the late Albian to Turonian carbonate platform in central Jordan. *Abstracts, 6th International Cretaceous Symposium, Vienna*, p. 133.

Schwarzacher, W. 2000. Repetitions and cycles in stratigraphy. *Earth-Science Reviews* **50**, 51-75.

Shahar, J. 1994. The Syrian Arc system: an overview. *Palaeogeography, Palaeoclimatology, Palaeoecology* **112**, 125-142.

Shahin, A. & Kora, M. 1991. Biostratigraphy of some Upper Cretaceous successions in the eastern central Sinai, Egypt. *Neues Jahrbuch für Geologie und Paläontologie, Monatshefte* **1991**, 671-692.

Sissingh, W. 1977. Biostratigraphy of Cretaceous calcareous nannofossils. *Geologie en Mijnbouw* **56**, 37-65.

Sliter, W. V. 1989. Biostratigraphic zonation for Cretaceous planktonic foraminifers examined in thin section. *Journal of Foraminiferal Research* **19**, 1-19.

Steuber, T. & Löser, H. 2000. Species richness and abundance patterns of Tethyan Cretaceous rudist bivalves (Mollusca: Hippuritacea) in the central-eastern Mediterranean and Middle East, analysed from a palaeontological database. *Palaeogeography, Palaeoclimatology, Palaeoecology* **162**, 75-104.

Steuber, T. 1999. Cretaceous rudists of Boeotia, central Greece. *Special Papers in Palaeontology* **61**, 229 pp.

Strasser, A., Pittet, B., Hillgärtner, H. & Pasquier, J.-B. 1999. Depositional sequences in shallow carbonate-dominated sedimentary systems: concepts for a high-resolution analysis. *Sedimentary Geology* **128**, 201-221.

Street, C. & Bown, P. R. 2000. Palaeobiogeography of Early Cretaceous (Berriasian-Barremian) calcareous nannoplankton. *Marine Micropaleontology* **39**, 265-291.

Thierstein, H. R. 1980. Selective dissolution of Late Cretaceous and earliest Tertiary calcareous nannofossils: experimental evidence. *Cretaceous Research* **2**, 165-176.

Thomel, G. 1992. *Ammonites du Cenomanien et du Turonien du Sud-Est de la France*. Part 1, 422 pp.; Part 2., 383 pp. (Serre, Nice).

Tucker, M., Khalil, M. & Philobbos, E. 1999. Dolomitization and sequences: the Cretaceous of northern Egypt. *11 th Bathurst Meeting, Cambridge, Journal of Conference Abstracts* **4**, unpaginated (available on http://www.campublic.co.uk/science/publications/JConfAbs/4/976.html).

van den Bold, W. A. 1964. Ostracoden aus der Oberkreide von Abu-Rawash, Ägypten. *Palaeontographica* **123**, 111-136.

Van Wagoner, J. C., Posamentier, H. W., Mitchum, R. M., Vail, P. R., Sarg, J. F., Loutit, T. S. & Hardenbol, J. 1988. An overview of the fundamentals of sequence stratigraphy and key definitions. In *Sea-level changes - an integrated approach* (eds Wilgus, C. K., Hastings, B. S., Kendall, C. G. St C., Posamentier, H. W., Ross, C. A. & Van Wagoner, J. C.), *Society of Economic Palaeontologists and Mineralogists, Special Publication* **42**, 39-45.

Vidal, N., Alvarez-Marrón, J. & Klaeschen, D. 2000. Internal configuration of the Levantine Basin from seismic reflection data (eastern Mediterranean). *Earth and Planetary Science Letters* **180**, 77-89.

Walley, C. D. 1998. Some outstanding issues in the geology of Lebanon and their importance in the tectonic evolution of the Levantine region. *Tectonophysics* **298**, 37–62.

Wiese, F. W. & Wilmsen, M. 1999. Sequence stratigraphy in the Cenomanian to Campanian of the North Cantabrian Basin (Cantabria, N-Spain). *Neues Jahrbuch für Geologie und Paläontologie, Abhandlungen* **212**, 131-173.

Zalat, A. A. 1999. Dolomitization of Cenomanian-Turonian limestones in central Sinai, Egypt. *Middle East Research Center, Ain Shams University, Earth Science Series* **13**, 173-186.

Ziko, A., Darwish, M. & Eweda, S. 1993. Late Cretaceous - Early Tertiary stratigraphy of the Themed area, east central Sinai, Egypt. *Neues Jahrbuch für Geologie und Paläontologie, Monatshefte* **1993**, 135-149.

9 APPENDIX

Alphabetical list of species mentioned in this work.

Ammonites

Choffaticeras luciae (Pervinquiére, 1907)
Choffaticeras segne (Solger, 1903)
Kamerunoceras turoniense (d'Orbigny, 1850)
Mammites nodosoides (Schlüter, 1871)
Neocardioceras judii Barrois & Guerne, 1878
Neolobites vibrayeanus (d'Orbigny, 1841)
Neoptychites cepholtus (Courtiller, 1860)
Thomasites rollandi (Thomas & Péron, 1889)
Vascoceras durandi (Thomas & Péron, 1890)
Watinoceras coloradoense Wright & Kennedy, 1981

Calcareous nannofossils

Broinsonia enormis (Shumenko, 1968) Manivit, 1971
Calcicalathina alta Perch-Nielsen, 1979
Calculites obscurus (Deflandre, 1959) Prins & Sissingh, in Sissingh, 1977
Chiastozygus platyrhethus Hill,1976
Corollithion signum Stradner, 1963
Cribosphaerella ehrenbergii (Arkhangelsky, 1912) Deflandre, in Piveteau, 1952
Eiffellithus eximius (Stover, 1966) Perch-Nielsen, 1968
Eiffellithus turriseiffelii (Deflandre, in Deflandre & Fert, 1954) Reinhardt, 1965
Eprolithus floralis (Stradner, 1962) Stover, 1966
Eprolithus sp.
Gartnerago obliquum (Stradner, 1963) Noel, 1970
Lithastrinus septenarius Forchheimer, 1972
Lithraphidites actus Verbeek & Manivit, in Manivit *et al.*, 1977
Lithraphidites carniolensis Deflandre, 1963
Lucianorhabdus cayeuxii Deflandre, 1959
Lucianorhabdus maleformis Reinhardt, 1966
Lucianorhabdus quadrifidus Forchheimer, 1972
Manivitella pemmatoidea (Deflandre, in Manivit, 1965) Thierstein, 1971
Marthasterites furcatus (Deflandre, in Deflandre & Fert, 1954) Deflandre, 1959
Microrhabulus decoratus Deflandre, 1959

Micula decussata Vekshina, 1959
Prediscosphaera spinosa (Bramlette & Martini, 1964) Gartner, 1968
Quadrum gartneri Prins & Perch-Nielsen, in Manivit *et al.*, 1977
Radiolithus planus Stover, 1966
Reinhardtites anthophorus (Deflandre, 1959) Perch-Nielsen, 1968
Rhagodiscus angustus (Stradner, 1963) Reinhardt, 1971
Stradneria crenulata (Bramlette & Martini, 1964) Noel, 1970
Tetrapodorhabdus decorus (Deflandre, in Deflandre & Fert, 1954) Wind & Wise, in Wise & Wind, 1977
Thiersteinia ecclesiastica Wise & Watkins, in Wise, 1983
Tranolithus manifestus Stover, 1966
Tranolithus phacelosus Stover, 1966
Watznaeuria barnesae (Black, 1959) Perch-Nielsen, 1984
Watznaueria biporta Bukry, 1969
Zeugrhabdotus diplogrammus (Deflandre, in Deflandre & Fert, 1954) Gartner, 1968
Zeugrhabdotus embergeri (Noel, 1959) Perch-Nielsen, 1984
Zeugrhabdotus erectus (Deflandre, in Deflandre & Fert, 1954) Reinhardt, 1965
Zeugrhabdotus pseudanthophorus (Bramlette & Martini, 1964) Perch-Nielsen, 1984

Foraminifera

Biconcava bentori Hamaoui & Saint Marc, 1970
Chrysalidina gradata d'Orbigny, 1850
Cyclogyra sp.
Dicarinella asymetrica Sigal, 1952
Dicarinella concavata Brotzen, 1934
Dicarinella primitiva (Dalbiez, 1955)
Globotruncanita elevata Brotzen, 1934
Hedbergella delrioensis Carsey, 1926
Hedbergella simplex Morrow, 1934
Heterohelix reussi Cushman, 1983
Heterohelix globulosa Ehrenberg, 1840
Neoflabellina suturalis Cushman, 1935
Praealveolina sp.
Pseudedomia sp.
Whiteinella archaeocretacea Pessagno, 1967
Whiteinella baltica Douglas & Rankin, 1969

Ostracods

Brachycythere angulata (Grékoff, 1951)
Cythereis algeriana Bassoullet & Damotte, 1969
Cythereis rosenfeldi Honigstein, 1984
Metacytheropteron berbericum (Bassoullet & Damotte, 1969)
Neocyprideis vandenboldi Gerry & Rosenfeld, 1973
Paracypris triangularis Rosenfeld, 1974
Peloriops ziregensis Bassoullet & Damotte, 1969
Pterygocythere raabi Rosenfeld, 1974
Spinoleberis yotvataensis Rosenfeld, 1974
Veeniacythereis maghrebensis Bassoullet & Damotte, 1969

Oysters

Ceratostreon flabellatum (Goldfuss, 1837)
Exogyra olisiponensis (Sharpe, 1850)
Liymatogyra africana (Lamarck, 1801)

Rudists

Hippurites requieni Matheron, 1842
Ichthyosarcolites triangularis Desmarest, 1817

CHAPTER 3

Sequence architecture and carbonate platform configuration (upper Cenomanian - Santonian), Sinai, Egypt

Jan Bauer, Jochen Kuss & Thomas Steuber

Submitted to Sedimentology

CHAPTER 3
Sequence architecture and carbonate platform configuration (upper Cenomanian - Santonian), Sinai, Egypt

***Jan Bauer, *Jochen Kuss & #Thomas Steuber**

Sedimentology, submitted

* Bremen University, Department of Geoscience, PO Box 330440, D-28334 Bremen, Germany
\# Ruhr-University Bochum, Institute of Geology, Mineralogy and Geophysics, Universitätsstr. 150, D-44801 Bochum, Germany

ABSTRACT

Upper Cenomanian to Santonian relative sea-level changes on the mixed carbonate-siliciclastic platform of Sinai are manifested in the establishment and shifts of distinct facies belts (deep-water facies, high-energy subtidal, shallow subtidal, lagoon, shallow shoreface siliciclastics, supratidal) and are interpreted in terms of sequence stratigraphy. Eight sedimentary sequences are interpreted for the upper Cenomanian to Santonian. Their correlation along a north-south transect reveals distinct changes of lithofacies and progradation/retrogradation patterns within the individual systems tracts. Considerable stratigraphic mismatches between some interpreted sequence boundaries and those elsewhere in the Tethys underline the influence of tectonics on the depositional system: sequence boundaries in the uppermost Cenomanian (CeSin 7), upper Turonian (TuSin 2) and upper Coniacian (CoSin 1) are diachronous with respect to corresponding sequence boundaries in adjacent areas and reflect differing subsidence of the Central Sinai Basin and Syrian Arc tectonics. Patterns of increased basin subsidence are documented since the late Cenomanian by increased thickness of the stratal packages (post-CeSin 7 HST, post-TuSin 1 LST and HST, post-TuSin 2 LST) and are balanced by varying accumulation rates. Curves of cumulative sediment thickness allow periods of subsidence (late Cenomanian, middle and late Turonian) and uplift (latest Cenomanian) to be reconstructed. Based on new sedimentologic and biostratigraphic data, new large-scale palaeogeographic maps and cross-sections show: (1) the temporal and spatial evolution of the Central Sinai Basin, e.g. latest Cenomanian initial formation, lower Turonian deep-water facies, middle Turonian to Coniacian synsedimentary subsidence; (2) the drowning of the Cenomanian platform coinciding with the early Turonian relative sea-level rise; (3) the re-establishment of the platform in middle - late Turonian times and (4) the Coniacian basin and swell morphology.

KEYWORDS: carbonate platform, sequence stratigraphy, palaeogeographic maps, tectonics.

1. INTRODUCTION

The aim of this study is: (1) to enhance the sequence-stratigraphic interpretations of the upper Cenomanian - Santonian mixed carbonate-siliciclastic platform deposits of Sinai; (2) to reconstruct the palaeogeographic evolution involving neighbouring areas, and (3) to determine environmental and tectonic issues controlling the sequence architecture and platform configuration.

Several publications have focussed on the sedimentology and stratigraphy of the middle and Upper Cretaceous strata of Sinai (Bartov & Steinitz, 1977; Bartov *et al.,* 1980; Chérif *et al.,* 1989a,b; Kuss 1992; Ziko *et al.,* 1993; Kora & Genedi, 1995; Issawi *et al.,* 1999). Only some contributions focus on the sequence-stratigraphic evolution of Sinai (e.g. Bachmann & Kuss, 1998; Lüning *et al.,* 1998a,b), the Eastern Desert of Egypt (Kuss *et al.,* 2000a), and the Near East (Buchbinder *et al.,* 2000). However, the new sedimentologic and stratigraphic data presented herein allow to detect previously unknown sequence boundaries in Sinai and to verify the existing sequence-stratigraphic interpretations. This study incorporates the factors controlling facies distribution of ten sections within a sequence-stratigraphic framework, such as relative sea-level changes, platform drowning and tectonics.

Regional sequence-stratigraphic studies (Robaszynski *et al.,* 1990, 1993; Van Buchem *et al.,* 1996; Kuhnt *et al.,* 1997; Abdallah *et al.,* 2000; Scott *et al.,* 2000) show the important impact of relative and eustatic sea-level changes in North Africa and Arabia. Among them, the well known late Cenomanian to early Turonian global sea-level rise perhaps resulted in the highest sea-level stand of the entire Phanerozoic (Haq *et al.,* 1987; Philip & Airaud-Crumiere, 1991; Hancock, 1993). Early Turonian platform drowning has been recorded on many Tethyan platforms in North Africa (Camoin, 1991; Saidi, *et al.,* 1997), Near East (Buchbinder *et al.,* 2000), Arabian Peninsula (Philip *et al.,* 1995; Scott *et al.,* 2000) and Europe (Philip & Airaud-Crumiere, 1991; Drzewiecki & Simo, 1997; Philip 1998; Davey & Jenkyns, 1999). They are mostly attributed to flooding of the platforms by oxygen-depleted waters, related to oceanic anoxia (Arthur *et al.,* 1987; Jarvis *et al.,* 1988; Philip & Airaud-Crumiere, 1991; Drzewiecki & Simo, 1997; Weissert *et al.,* 1998). In contrast, only minor attention has been paid to the drowning of the Cenomanian platform in Sinai previously.

The sedimentary and tectonic evolution of Sinai was predominantly controlled by the establishment and evolution of the Central Sinai Basin (C-S Basin) and the Syrian Arc system. While the latter has been studied extensively (Said, 1962; Shahar, 1994; Moustafa & Khalil, 1990; Guiraud & Bosworth, 1997), recent investigations neglect the C-S Basin. Although Lewy (1975), Bartov & Steinitz (1977) and Kuss (1992) noted its importance for palaeogeographic interpretations, its evolution in time and space is still unclear. Our new palaeogeographic maps for specific systems tracts document the platform configuration and the migrations of the facies belts, and thus differ from previously published palaeogeographic maps (Lewy, 1975; Said, 1990; Kuss & Bachmann, 1996; Lüning *et al.,* 1998b). Additional data from Sinai, the Near East and Jordan are incorporated in the palaeogeographic reconstructions presented herein.

2. GEOLOGICAL SETTING

Tectonics. Late Triassic - Early Jurassic opening of the Neotethys (Fig. 1) resulted in ENE-trending flexural basins and halfgrabens (Fig. 2b) in north Sinai (Moustafa & Khalil, 1990), Egypt (Kuss, 1992;

El-Hawat, 1997), the Near East (Hirsch *et al.*, 1998; Vidal *et al.*, 2000), and Jordan (Abu-Jaber *et al.*, 1989). In Sinai, convergence of the Afro-Arabian and Eurasian plates resulted in the transpressive inversions along the pre-existing halfgraben structures since the Turonian and involved several phases of lateral strike-slip faulting and gentle folding, referred to as the Syrian Arc (Krenkel, 1924). Domal anticlines in north Sinai (Fig. 2a) are part of this intraplate fold belt, which extends from northern Egypt to the Near East, Syria, and Lebanon. Said (1962) introduced the terms 'unstable shelf' for the inversion and folding zone in north Sinai and 'stable shelf' for the tectonically more inactive area of central and south Sinai (Fig. 2a). Detailed discussions of the Syrian Arc evolution and comparisons with other regions of North Africa are given by Moustafa & Khalil (1990), Shahar (1994), Guiraud & Bosworth (1997), Guiraud (1998), Walley (1998), Bosworth *et al.* (1999), and Rosenthal *et al.* (2000). It is generally accepted that the major period of deformation was in the Late Cretaceous, but the timing of first compressional pulses is controversially debated and ranges from the Cenomanian to Campanian. The major episode of reverse faulting probably correlates with compressional deformations in large parts of North Africa and Arabia referred to as the 'Santonian tectonic event' (Guiraud & Bosworth, 1997).

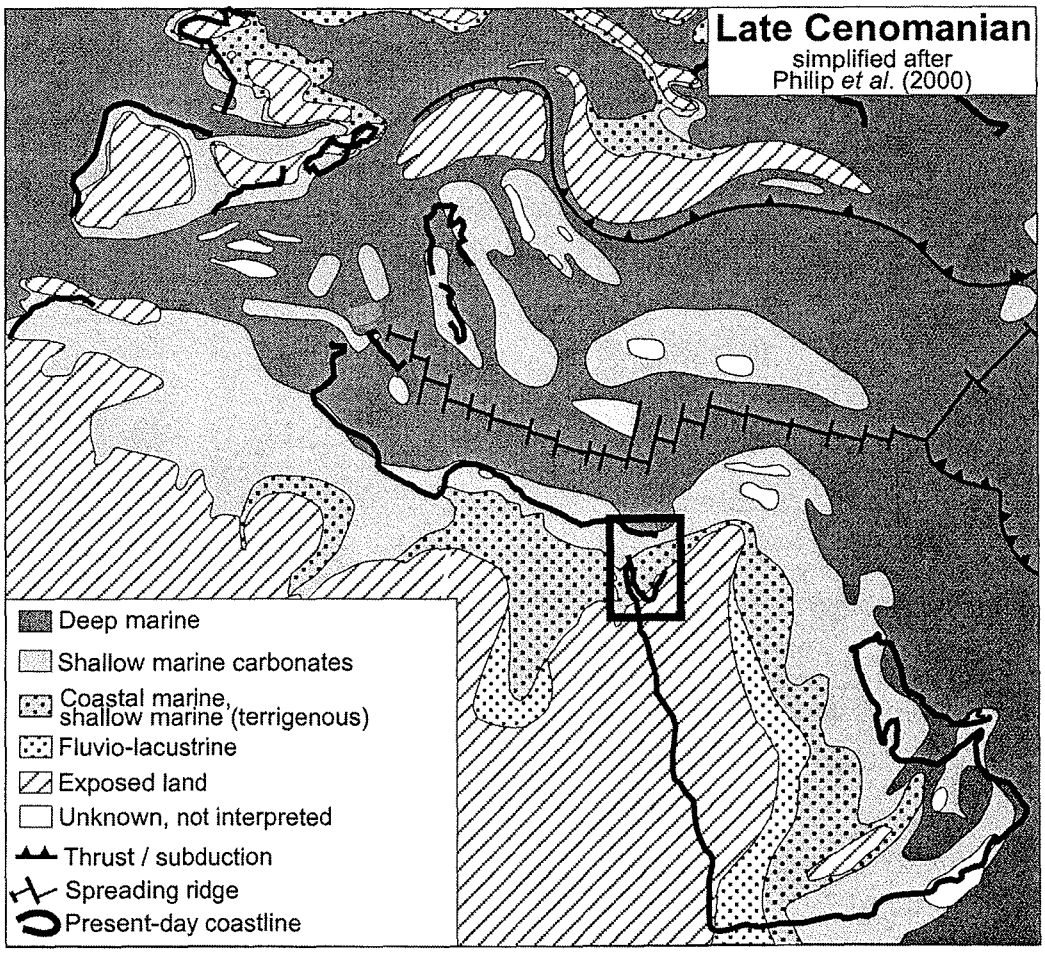

Fig. 1: Palaeogeographic reconstruction of the late Cenomanian Tethys between southern Europe and North Africa. The Sinai Peninsula is indicated.

Palaeogeography. During the Cretaceous, Sinai belonged to the pericratonic Arabo-African carbonate platform, which extended from Morocco to Oman along the southern margin of the Tethys (Philip *et al.*, 2000; Fig. 1). In Aptian times, a delta-dominated carbonate ramp established in north Sinai, and the depositional setting switched to a carbonate-dominated ramp in Albian and early Cenomanian times (Bachmann & Kuss, 1998; Kunow *et al.*, 1998). During the late Cenomanian - early Turonian extensive sea-level rise (Haq *et al.*, 1987; Philip & Airaud-Crumiere, 1991; Hancock, 1993), mainly shallow inner-shelf environments established on a mixed siliciclastic-carbonate platform. In contrast to the preceding ramp morphology, the platform extended over 200 km from north to south Sinai without a recognisable inclination until the late Turonian. In the Coniacian, a basin and swell morphology developed and the siliciclastic input from the southerly exposed hinterland increased markedly. From the late Coniacian onwards, the inner-shelf facies retreated southwards and deep-water deposits developed in north and central Sinai. Hemipelagic chalks dominate the Santonian - Maastrichtian lithologies.

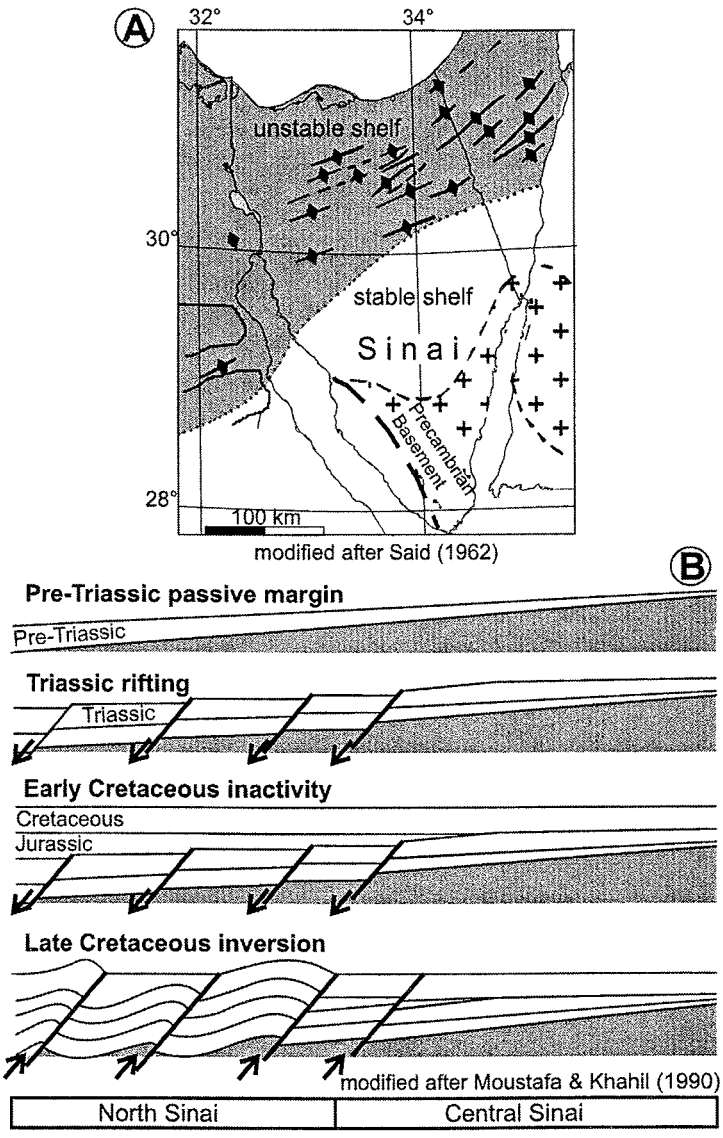

Fig. 2 (Previous page): (A) Syrian Arc anticlines in Sinai and in neighbouring areas on the 'unstable shelf' (grey area). The 'stable shelf' (white area) is located to the south. (B) sketch of the Mesozoic tectonic evolution of Sinai. See text for explanations.

Central Sinai Basin. Since the late Cenomanian, a synsedimentary subsiding intrashelf basin, the Central Sinai Basin (C-S Basin), formed in Sinai. Because upper Cenomanian deposits of the C-S Basin are not exposed, its upper Cenomanian configuration is unclear. However, upper Cenomanian basinal deposits occur in its eastward prolongation, the Eshet-Zenifim Basin (Bentor, 1960; Bartov & Steinitz, 1977), and are also expected further west in the C-S Basin. This is also indicated by isopach maps of Bartov & Steinitz (1977). Moreover, Kassab & Obaidalla (2001) reported a diverse assemblage of upper Cenomanian planktic foraminifers and ammonites in a single section in West Sinai (Wadi Feiran), suggesting a deep-water facies, locally restricted within the Cenomanian carbonate platform.

In the early Turonian, deep-water deposits of the C-S Basin covered north and central Sinai and interfingered with inner-platform deposits. From the middle Turonian - Coniacian, shallow-subtidal sediments prevailed in the C-S Basin throughout Sinai. However, ongoing basin subsidence is reflected by enlarged thickness of the Turonian - Coniacian sedimentary cover (Bartov & Steinitz 1977).

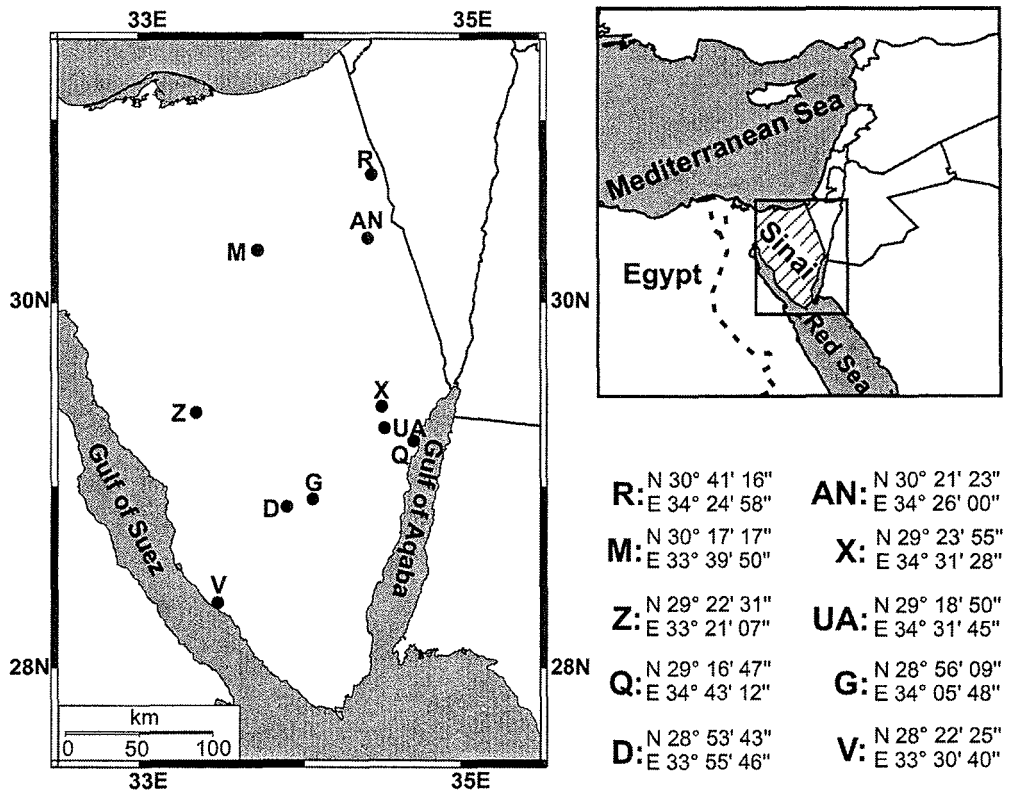

Fig. 3: Locations of sections studied: R, Gebel Risha; AN, Gebel Areif El Naqa; M, Gebel Minsherah; Z, Gebel Abu Zurub; X, Gebel Gidira; UA, Gebel Um Alda; Q, Ain Quseiyib; G, Gebel Gunna; D, Gebel Dhalal; V, Gebel Arabah.

3. METHODS

Detailed sedimentologic and palaeontologic studies were performed on ten sections throughout Sinai (Fig. 3). The sequence-stratigraphic interpretation follows the 'Exxon concepts', e.g. Van Wagoner *et al.* (1988) and Vail *et al.* (1991). Special attention was paid to indicative surfaces (hardgrounds, subaerial exposures, drowning surfaces), sedimentary stacking patterns and lateral and vertical facies distribution patterns. The interpreted sequence boundaries and systems tracts were numbered after the system of Hardenbol & Robaszynski (1998), applied by Lüning *et al.,* (1998a,b), e.g. sequence boundary TuSin 1: Tu= Turonian, Sin= Sinai, 1= first sequence boundary in the Turonian. The systems tracts are differentiated by the prefixes 'post' and the underlying sequence boundary (e.g. post-TuSin 1 LST = LST above sequence boundary TuSin 1).

4. BIOSTRATIGRAPHY AND LITHOSTRATIGRAPHY

Biostratigraphy. A detailed biostratigraphic framework of the sections studied was previously given by Bauer *et al.* (in press2) and is compiled in Fig. 4. The stratigraphic ranges of selected lower Turonian ammonites (Fig. 4) are based on comparisons of range charts and regional biozonation schemes of Egypt (Kassab & Obaidalla 2001), the Near East (Freund & Raab, 1969, verified by Lewy, 1989), Tunisia (Robaszynski *et al.,* 1990; Chancellor *et al.,*1994), and southern Europe (Thierry *et al.* in Hardenbol *et al.,* 1998). A stratigraphic gap in large parts of Sinai spans at least the lower Turonian *Watinoceras coloradoense* biozone, because upper lower Turonian *Mammites nodosoides* directly overlie upper Cenomanian strata in north and central Sinai (Bartov *et al.,* 1980; Allam & Khalil, 1988; Ziko *et al.,* 1993). Co-occurring *Choffaticeras luciae* and *Kamerunoceras turoniense* also underline this stratigraphic gap (Bauer *et al.,* in press2) as well as other biostratigraphic data of, e.g., Chérif *et al.* (1989a) and Kassab (1996). *Paratexanites desmondi* is characteristic for the late Coniacian successions studied.

Concerning calcareous nannofossil biostratigraphy (Fig. 4), this paper follows the biozone concepts of Salis in Hardenbol *et al.* (1998) with two exceptions: the lower boundary of CC 11 is placed in the uppermost Cenomanian, in agreement with Bralower (1988) and Burnett (1996); the lower boundary of CC 12 is considered as lowermost middle Turonian after Robaszynski *et al.* (1990).

Some benthic foraminifers and ostracods enable to differentiate the stages (Fig. 4) according to Van den Bold (1964), Bassoullet & Damotte (1969), Rosenfeld & Raab (1974), Saint-Marc (1974), Schröder & Neumann (1985), Morsi & Bauer (in press). The distribution of rudist bivalves allows the differentiation of Cenomanian and Turonian strata. The last occurrence of *Ichthyosarcolites* and the first occurrence of the Hippuritidae mark the Cenomanian / Turonian (C/T) boundary (Philip & Airaud-Crumiere, 1991).

Lithostratigraphy. The lithostratigraphic units used herein are shown in Fig. 4. The Cenomanian (CC 10 - lower CC 11) Halal Formation in north Sinai mainly consists of dolomites, with some intercalations of marls and bioclastic limestones. The Raha Formation is the equivalent of the Hala Formation in central and south Sinai. It consists of fossiliferous limestones, dolomites, marls and sandstones. Marls

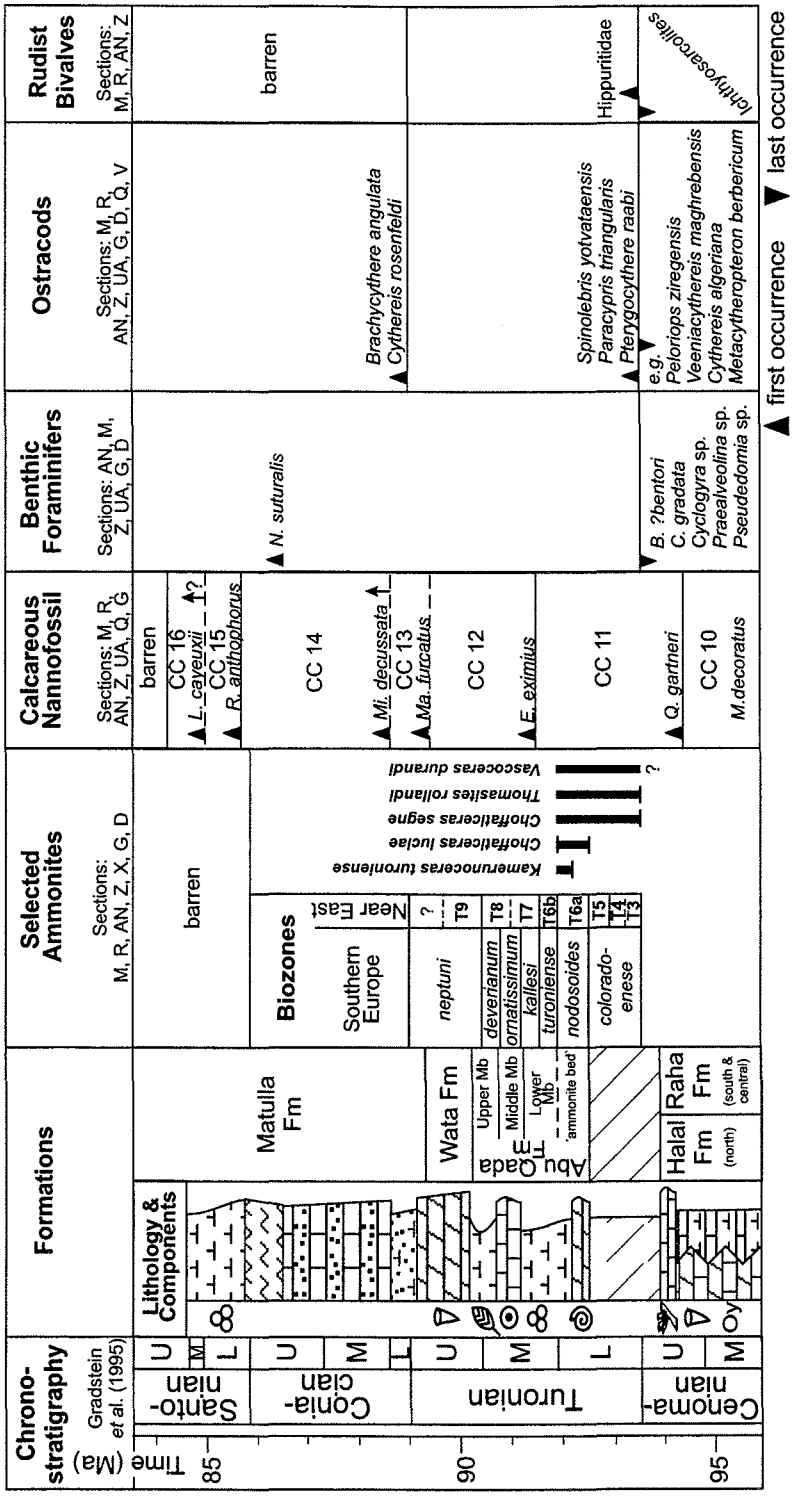

Fig. 4. Lithostratigraphy and multibiostratigraphic framework for the sections studied. The standard section on the left is compiled from Figs. 5, 6 (for key to symbols and lithologies, see Fig. 6). The stratigraphic ranges of the taxa are based on range charts and regional biozonation schemes cited in the text. Southern European ammonite zones are after Thierry *et al.* in Hardenbol *et al.* (1998), those of the Near East are after Freund & Raab (1969, verified by Lewy 1989); calcareous nannofossil zones are after Salis in Hardenbol *et al.* (1998), note exceptions regarding lower boundaries of CC 11 and CC 12. Abbreviations: calcareous nannofossils: *E., Eiffellithus; L., Lucianorhabdus; M., Microrhabdulus; Ma., Marthasterites; Mi., Micula; Q., Quadrum; R., Reinhardtites*; benthic foraminifers: B., *Biconcava C., Chrysalidina; N., Neoflabellina.*

and quartzose sediments are more frequent in comparison to the Halal Formation. The Abu Qada Formation ranges from the upper lower Turonian (upper CC 11or *M. nodosoides* Zone) to the middle and upper Turonian (middle CC 12). It is subdivided herein into three members: marls and a nodular dolomite layer with densely packed lower Turonian ammonites ('ammonite bed') at the base (Lower Member) are overlain by well bedded dolomites and limestones (Middle Member), and by marls with intercalated oolites and bioclastic packstones (Upper Member). The upper Turonian (middle - upper CC 12) Wata Formation is dominated by cliff-forming, cyclically bedded dolomites and bioclastic limestones. The Coniacian - Santonian (CC 13 - CC 16) Matulla Formation shows highly variable lithologies with cross-bedded sandstones, marls, bioclastic limestones, dolomites and chalks with chert concretions. Siliciclastic detritus is common in most of the latter lithologies.

Facies Belts	**North Sinai** (sections R, AN, M)	**Central Sinai** (sections Z, X, UA, Q, G, D)	**South Sinai** (section V)	**Systems Tracts**
supratidal	- emersion surfaces, karstification evaporites and foliated claystones with plant remains		- emersion surfaces, plant remains, silicified wood, caliche beds	LSTs
shallow shoreface siliciclastics	- reddish mottled siltstone and fine sandstones - coarse and medium grained sandstones - bioclastic (cross-bedded) calcareous sandstones		- reddish siltstones and sandstones with ironooids - (cross-bedded) bioclastic sandstones	LSTs, also HSTs in central / south Sinai
lagoon	- marls, monospecific, hypersaline to brackish ostracods and oysters assemblages	- stromatolitic and laminated calcareous marls - wackestones and packstones with miliolids, ostracods peloids, birds eyes - foraminiferal mudstones	- marls with monospecific ostracods assemblages	LSTs, also in HSTs in central Sinai
shallow subtidal	- coarse bioclastic, dolomites, limestones and calcareous marls with bivalves (e.g. rudists, oysters), corals, chaetatids, gastropods, echinoderms - bioclastic packstones and wackestones (benthic foraminifers, calcareous algae, ostracods, echinoderms, bivalves, peloids)		- bioclastic marls and packstones (e.g. oysters, gastropods)-peloidal, wackestones with benthic foraminifers and ostracods	TSTs and HSTs
high-energy subtidal	- winnowed packstones and grainstones with ooids, oncoids, reworked debris (e.g. algae debris, ostracods) - cross-bedding, channels, rip-up structures, reworking textures		*not developed*	TSTs and HSTs
deep-water	- marls and chalks with frequent ammonites, planktic foraminifers and calcareous nannofossils.		*not developed*	TST

Tab: 1. Lithologic and palaeontologic characteristics of six major facies belts and their local occurrences in Sinai. The facies belts dominate in certain systems tracts as indicated in the right column.

5. SEQUENCE-STRATIGRAPHIC INTERPRETATION

The sequence-stratigraphic interpretation of the sections studied is shown in Figs 5 - 8. Correlation of sequence boundaries and systems tracts within the biostratigraphic and lithostratigraphic framework was possible along a north-south transect (Figs 5, 6). Lithofacies descriptions of the facies belts are compiled in Tab. 1.

5.1 Surfaces and systems tracts

Sequence boundaries (SB). Emersion surfaces are characterised by thin palaeosols or sometimes by diagenetic alterations such as caliche or meteoric cements. Additionally, reddish mottled, ferruginous and sometimes bored hardgrounds indicate nondeposition accompanied with subaerial exposure. However, significant emersion surfaces are often missing at the respective SBs, which is attributed to their low preservation potential.

Lowstand systems tracts (LST). In the sections studied, LSTs are composed of very shallow-water deposits, such as red and green foliated claystones or reddish mottled siltstones and sandstones. Ironooids were common features of siliciclastic lowstand deposits in the palaeo-coast areas in southern Sinai. Stromatolitic and laminated calcareous marls, wackestones and packstones with miliolids, peloids and birdseyes occurred in lagoons. Supratidal and restricted environments are characterised by claystones with plant remains or with monospecific, abnormal hypersaline to brackish ostracod and oyster assemblages. Ponded evaporites formed in local sabkhas.

Transgressive systems tracts (TST). In the sections studied, indicators of reduced sedimentation rates of transgressive surfaces (ts) and of TST-deposits are hardgrounds, masses of disarticulated ostracod-valves, glauconite accumulations or highly bioturbated and nodular sediments. Within the TSTs, shallow-subtidal deposits prevail, which are merely composed of calcareous marls and coarse bioclastic limestones with a rich benthic assemblage. High-energy packstones and grainstones are often intercalated. They contain ooids, oncoids and reworked components; rip-up structures, cross-bedding and channels are common. Protected subtidal or open lagoonal settings established in the proximal areas of deposition. Deep-water TST-deposits occur only in the lower Turonian and upper Coniacian successions studied. They are composed of marls and chalks with frequent planktic foraminifers, calcareous nannofossils as well as ammonites.

Highstand systems tracts (HST). The maximum flooding surfaces (mfs) sometimes feature indicators of condensation similar to those described above. The HST-deposits are characterised by aggradational or progradational stacking patterns of shallow-subtidal deposits. The lithologies differ depending on the distance to the palaeo-shoreline. In north and central Sinai shallow-subtidal environments were governed by: (1) thick bedded, massive dolomites with frequent shallow-water macrofossils (rudists, oysters) in the northern, more basinwards realm, (2) bioclastic packstones and wackestones, with echinoderms, oysters, benthic foraminifers, calcareous algae, ostracods and peloids in central Sinai, and (3) cross-bedded, winnowed, oolitic grainstones in both, north and central Sinai. In south Sinai, shallow-water siltstones and sandstones predominate.

5.2 Upper Cenomanian - Santonian sequences

Sequence post-CeSin 5

The upper Cenomanian (CC 10) sequence post-CeSin 5 is equivalent to the upper Halal and Raha formations. It has been completely measured in central and south Sinai (Sections G, D and V, Fig. 6); only the HST has been investigated in Sections M and Z (Fig. 5). Sequence post-CeSin 5 represents one of the oldest preserved sequences in south Sinai, because Proterozoic metamorphic and magmatic basement rocks are exposed only a few tens of meters below the SB (Fig. 7). In north Sinai, the underlying Aptian - Cenomanian units are several hundreds of meters thick and were studied in detail by, e.g., Bachmann & Kuss (1998) and Lüning *et al.* (1998a).

SB and LST. The SB CeSin 5 is placed at the base of alternating beds of siltstones and claystones (LST), which overlie coarse-grained sandstones in Sections G and D (Fig. 6).

ts and TST. The onset of calcareous and marly deposits with oysters and echinoderms characterises the ts in Sections G, D, V (Fig. 6). Washed packstones with frequent miliolids and peloids occur in the shallow-subtidal TST-deposits (Fig. 7).

mfs and HST. The mfs in Sections V, D and G is probably marked by the lithologic break from calcareous TST-deposits to more quartzose HST-sediments. Hardgrounds indicate reduced sedimentation rates at the mfs in Section V (Fig. 6). In Sections M and Z, thickly bedded, massive dolomites with limestone intercalations predominate in the HST. The limestones are sometimes characterised by bioclastic, peloidal packstones and wackestones with a species-rich association of benthic foraminifers, rudists and less frequent calcareous algae and are assigned to a protected marine environment. In Section V (Fig. 6), the neighbouring palaeo-coastline is reflected by quartzose HST-sediments, which interfinger with shallow-subtidal, calcareous deposits in Sections G and D in central Sinai.

Sequence post-CeSin 6

The upper Cenomanian (CC 10 to lower part of CC 11) sequence post-CeSin 6 (upper Halal and Raha formations) has been studied in Sections AN, M, G, D, Z and V (Figs 5, 6).

LST. Very shallow-subtidal siliciclastics of the LST in Sections M, Z and G grade southwards into supratidal deposits, which are composed of red and green foliated claystones with high contents of ironooids (Fig. 7). These deposits witness a relative sea-level lowstand with respect to the underlying HST-deposits of sequence post-CeSin 5.

ts and TST. The ts and TST only clearly recognisable in Section M. The ts placed above the uppermost LST-siltstones. Calcareous and dolomitic marls of the TST contain frequent oysters and document a shallow-subtidal, low-energy environment during the TST.

Fig. 5: (Following page) Sequence-stratigraphic correlation of sections in north and central Sinai. The datum line is placed at sequence boundary TuSin 1. In some sections certain systems tracts could not be differentiated. Question marks indicate uncertain correlation. For key to symbols, lithologies, and correlation lines, see Fig. 6.

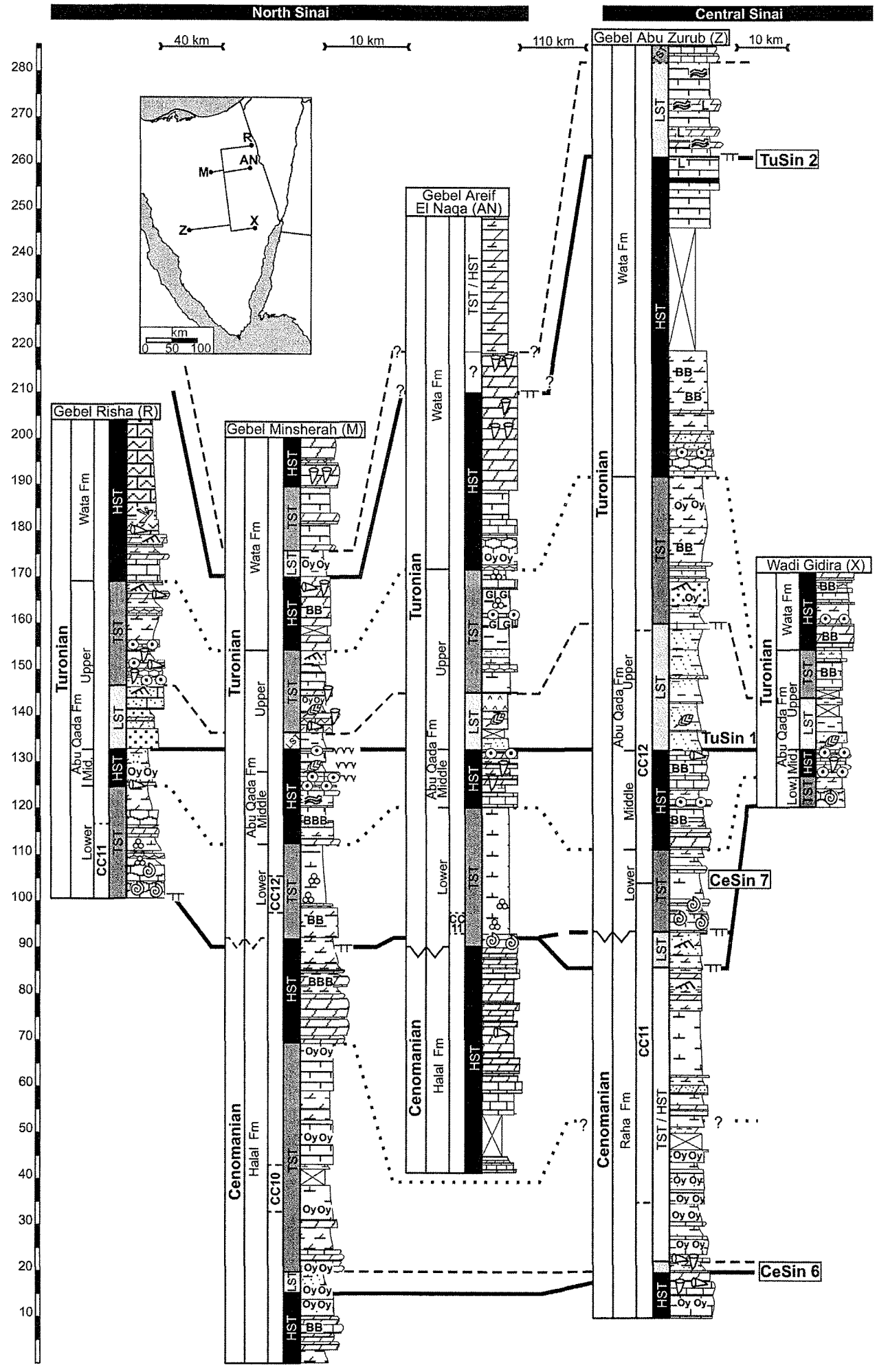
North Sinai
Central Sinai
40 km
10 km
110 km
10 km
Gebel Risha (R)
Gebel Minsherah (M)
Gebel Areif El Naqa (AN)
Gebel Abu Zurub (Z)
Wadi Gidira (X)
TuSin 2
TuSin 1
CeSin 7
CeSin 6
R
AN
M
Z
X
km
0 50 100
Turonian
Cenomanian
Wata Fm
Abu Qada Fm
Halal Fm
Raha Fm
Upper
Middle
Lower
CC10
CC11
CC12
HST
TST
LST
TST / HST
BB
Oy
GI
BBB

mfs and HST. The onset of massive, thick bedded dolomites characterises the mfs in north Sinai (Sections AN, M; Fig. 5). Bioclastic packstones and wackestones with diverse assemblages of benthic foraminifers are associated with rare rudists, chaetatids and corals and characterise the shallow-subtidal HST-facies.

In central and southern Sinai (Section Z, G, D and V) TSTs and HSTs could not be differentiated, because relatively uniform shallow-subtidal successions are composed of alternating marls, dolomite and limestone beds above the respective LST, without distinct changes in lithofacies. Furthermore, candidates for an eventual mfs are not preserved.

Sequence post-CeSin 7

The uppermost Cenomanian (lower CC 11) to upper Turonian (CC 12) sequence post-CeSin 7 corresponds to the Lower and Middle Abu Qada Formation and is traced throughout Sinai in the sections studied.

SB, LST, ts and TST. As LST-sediments are not observed, the ts consequently falls together with the SB in most sections studied. The deep-water TST-deposits are composed of the 'ammonite bed' in Sections R, AN, X, Z, G, D (Figs 5, 6) and marls with frequent planktic foraminifers (hedbergellids, whiteinellids, heterohelicids, Sections R, M, AN and Z) of the Lower Abu Qada Formation. Condensation is indicated by hardgrounds and frequent oyster-encrustations on the ammonites, as well as glauconite grains in the lower marls of the TST. The TST-sediments mark a pronounced relative sea-level rise, coinciding with a drowning of the Cenomanian shallow platform during the early Turonian (see below). They overlie shallow-subtidal deposits of the Cenomanian post-CeSin 6 HST; the two systems tracts are separated by thin reddish mottled hardgrounds, which are interpreted as SB CeSin 7.

In the southern Section V, a deep-water facies is not observed (Fig. 7). Protected shallow-subtidal TST-deposits (Fig. 7) are indicated by coarse bioclastic (oysters, gastropods and bivalves) marls and packstones, as well as by peloidal wackestones with benthic foraminifers and ostracods. In Section Z, the elsewhere missing LST may be represented by a silty dolomite layer underlain by a hardground (Fig. 5). These LST-deposits are likely to correlate with marls, shales and sandstones of tidal-flat to fluviomarine environments at the Gulf of Suez coast (Ekma Member, *sensu* Chérif *et al.,* 1989a), which were deposited in locally restricted depressions (Chérif *et al.,* 1989a; Kora *et al.,* 1994). It is important to note that *Ceratostreon flabellatum* (Chérif *et al.,* 1989a) and *Neolobites vibrayeanus* (Eweda & El-Sorogy, 1999) occur, indicating a late Cenomanian age.

Fig. 6: (Following Page)Sequence-stratigraphic correlation of sections in central and south Sinai. Note, the different datum line (sequence boundary TuSin 2) compared to Fig. 5 for graphical reasons. Some undifferentiated systems tracts are combined, question marks indicate uncertain correlation. For key to symbols, lithologies and correlation lines, see Fig. 6.

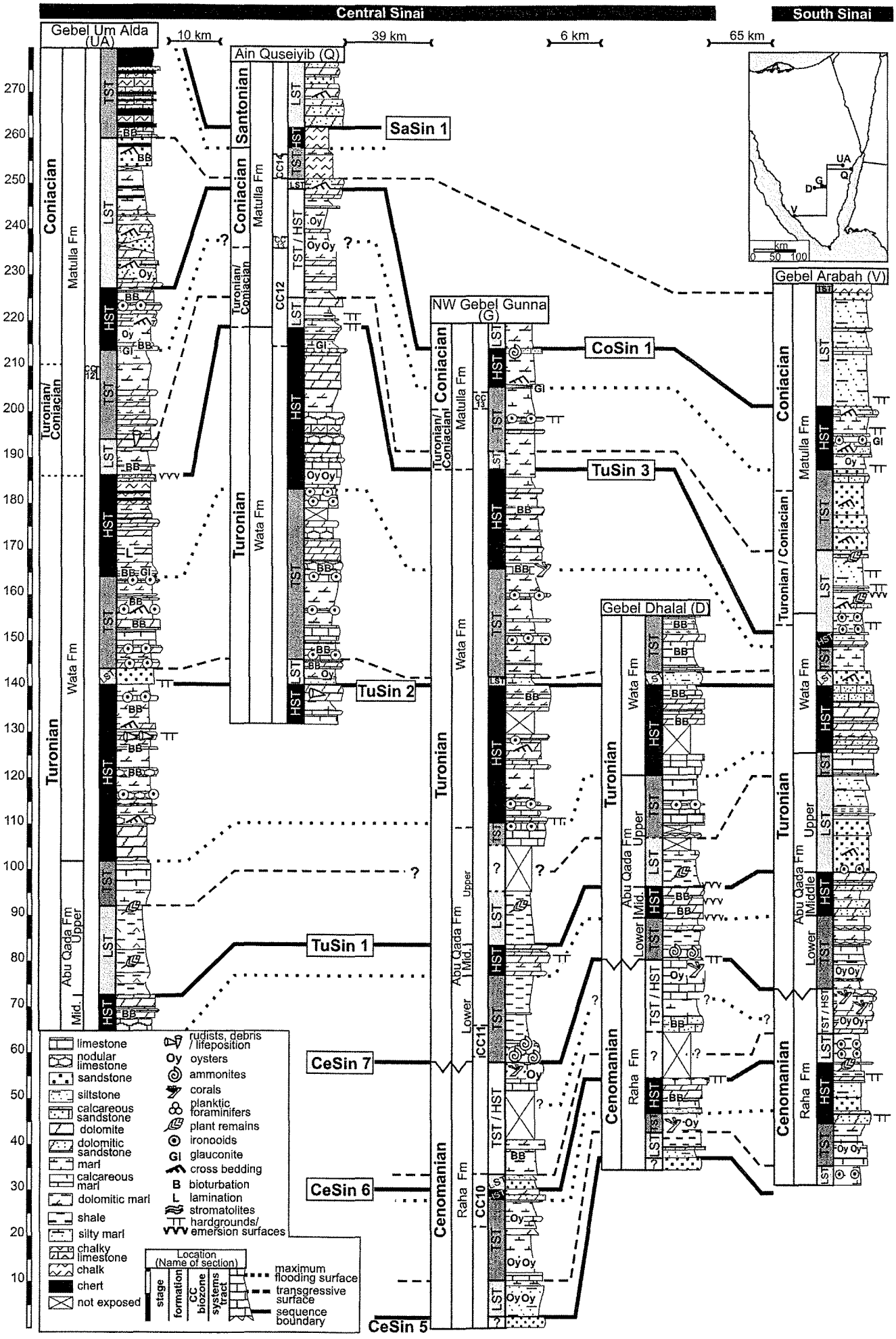
Central Sinai
South Sinai
Gebel Um Alda (UA)
10 km
Ain Quseiyib (Q)
39 km
6 km
65 km
NW Gebel Gunna (G)
Gebel Dhalal (D)
Gebel Arabah (V)
SaSin 1
CoSin 1
TuSin 3
TuSin 2
TuSin 1
CeSin 7
CeSin 6
CeSin 5
Coniacian
Santonian
Turonian
Cenomanian
Turonian/ Coniacian
Matulla Fm
Wata Fm
Abu Qada Fm
Upper
Mid.
Lower
Raha Fm
LST
TST
HST
TST / HST
BB
Oy
Gl
limestone
nodular limestone
sandstone
siltstone
calcareous sandstone
dolomite
dolomitic sandstone
marl
calcareous marl
dolomitic marl
shale
silty marl
chalky limestone
chalk
chert
not exposed
rudists, debris / lifeposition
oysters
ammonites
corals
planktic foraminifers
plant remains
ironooids
glauconite
cross bedding
bioturbation
lamination
stromatolites
hardgrounds/ emersion surfaces
Location (Name of section)
stage
formation
CC biozone
systems tract
maximum flooding surface
transgressive surface
sequence boundary

After the stratigraphic gap across the C/T boundary (Fig. 4), the first TST-deposits are placed in the upper lower Turonian (*M. nodosoides* Zone) to middle Turonian (CC 12). The question remains unsolved, whether the SB CeSin 7 lies above or below the stratigraphic gap, and thus has to be placed in the Cenomanian or in the Turonian (Fig. 9). The lacuna may have been caused either: (1) by erosion or nondeposition during the Turonian lowstand after a Cenomanian SB (´hypothesis 1` in Fig. 9), or (2) by erosion in the Cenomanian late HST followed by a Turonian SB and TST (´hypothesis 2` in Fig. 9). ´Hypothesis 1` seems more convincing, especially owing to the late Cenomanian age of the LST-deposits in Section Z and correlation with more complete successions in the Near East (Fig. 9). Therefore a Cenomanian SB is proposed and consequently it has been given the prefix ´Ce` for Cenomanian although the following deposits are mostly Turonian.

mfs and HST. The mfs is marked by the onset of cliff-forming, fossiliferous dolomites and limestones of the HST, which correspond to the Middle Abu Qada Formation. They represent a re-established carbonate platform (see below). The protected shallow-subtidal HST-deposits contain diverse assemblages of rudists and gastropods (Bauer *et al.*, in press1). Peloidal packstones with calcareous algae and bryozoans, ostracods, echinoderms and bivalves are common as well as hardgrounds. Occasional high-energy deposits (oolitic and oncolitic winnowed packstones and grainstones with ooids, oncoids and reworked bioclasts), established predominantly in the northern Sections AN, M, X and Z (Fig. 7), while quartzose carbonates prograded in the nearshore environments (Section V).

Sequence post-TuSin 1

The middle and upper Turonian (CC 12) sequence post-TuSin 1 (Upper Abu Qada Formation to Wata Formation) is recorded in all sections studied (Figs 5, 6), except for Section Q.

SB and LST. Emersion surfaces correspond to the SB and are well recognisable in Sections AN, M, D (Figs 5, 6), where thin palaeosols or meteoric cements evidence subaerial exposure. Shallow-water and supratidal deposits of the LST (lower part of the Upper Abu Qada Formation) are traced throughout Sinai (Fig. 7). Local supratidal and sabkha deposits in Section AN (Fig. 5) are composed of dark claystones with plant remains and ponded evaporites, which are overlain by marls with monospecific ostracod assemblages (*Neocyprideis vandenboldi*) indicating abnormal hypersaline to brackish environments. According to Bartov *et al.* (1980), this is also indicated by the oysters *Cerithium* sp. and *Caryocorbula* sp. at this locality in the same interval. In Section R, shallow-subtidal sandstones and intercalated reddish mottled siltstone beds occur.

In central Sinai, the LST is composed of bright red and green claystones with rare caliche layers and reddish siltstone beds. Siltstones increase successively southwards towards the palaeocoast and grade into sandstones and siltstones in Section V (Fig. 7).

ts and TST. The ts is placed at lithologic breaks, which indicate a transition from supratidal deposits (LST) to shallow-subtidal environments and an increase of turbulence (oolitic deposits, cross-bedding, rip-up clasts in Section R; reworked rudist debris in Section M, Fig. 5). In Section AN, the ts is interpreted by marl beds with frequent glauconite grains, as well as very abundant, disarticulated ostracods valves, both suggesting condensation.

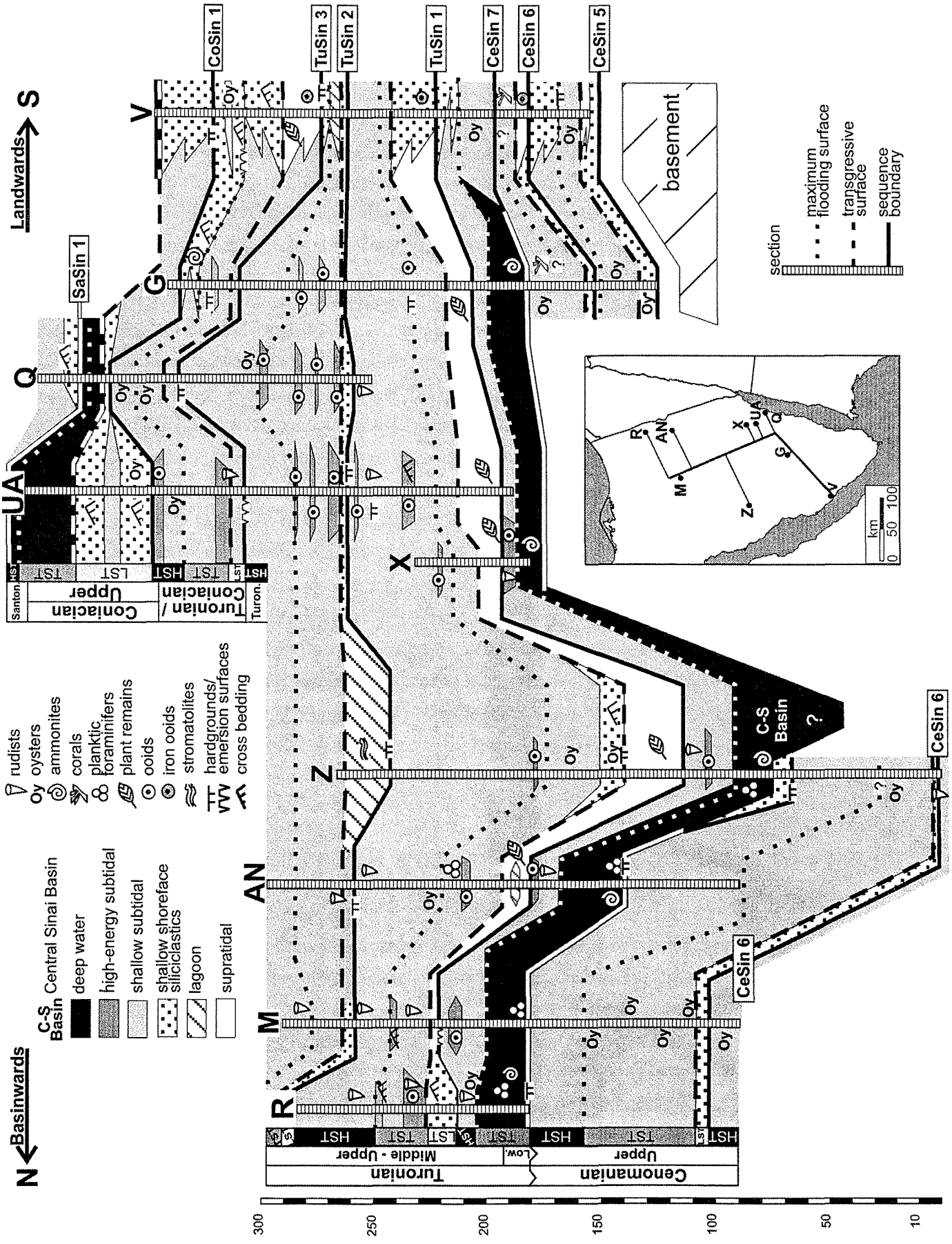

Fig. 7. Sequence architecture and platform and basin configuration along a N-S transect, based on large-scale facies patterns; the sections (vertical bars) refer to lithologic columns of Figs. 5, 6.

In north Sinai, the TST-deposits of the Upper Abu Qada Formation are characterised by marls with occasional intercalations of rudist biostromes and oolitic and bioclastic limestones, that indicate a shallow-subtidal environment with temporally high-energy conditions (Fig. 7). Planktic foraminifers (heterohelicids in Section AN) and glauconite grains rarely occur.

The shallow-subtidal TST-deposits in central and south Sinai (Sections X, Z; Fig. 5 and Sections UA, G, D and V, Fig. 6) are mainly composed of calcareous and dolomitic marls with frequent gastropods, echinoderms and oysters. Bioclastic packstones, rare oolitic grainstones (Sections G and D) as well as occasional cross-bedded sandstones (Section Z) are intercalated.

mfs and HST. The mfs is placed at the base of cyclically bedded dolomites, calcareous marls and limestones of the Wata Formation (HST); reworking structures or condensation features (e.g. hardgrounds and iron impregnations) are, however, rarely preserved at the mfs. Most HST-deposits reflect shallow-subtidal to lagoonal environments throughout the study area with diverse assemblages of benthic foraminifers, calcareous algae, rudists, and oysters as well as minor amounts of corals, ooids, and oncoids. However, distinct differences are obvious between the sections studied, regarding (1) composition and (2) thickness of the HST-sediments: (1) Especially rudists and calcareous algae show a clear decrease in frequency and diversity from north to south (Bauer *et al.*, in press1). Moreover, subordinately occurring ooids, oncoids and cross-bedding in central Sinai (Sections X in Fig. 5 and UA, G in Fig. 6) suggest an occasional increase of turbulence. In Section D (Fig. 6), lagoonal mudstones and foraminiferal packstones dominate the HST-deposits while thickly bedded, sometimes quartzose dolomites occur in Section V; (2) in comparison to sections in central and south Sinai, the HST-deposits of Sections AN, M, UA and Z are considerably thicker (Fig. 7), which strongly suggests higher subsidence. The thick dolomite packages of Sections AN and M were most probably caused by aggradation, owing to a constant high subsidence coeval with sediment accumulation close to sea-level (see below).

Sequence post-TuSin 2

The upper Turonian (CC 12) sequence post-TuSin 2 is represented by the Wata Formation in most sections (Figs 5 - 7).

SB and LST. Emersion surfaces at the SB are rarely preserved in hardgrounds in Sections AN, Z (Fig. 5) and UA (Fig. 6). A thin interval of predominant sandstones, siltstones or claystones often interrupts the uniform calcareous succession of the Wata Formation. These LST-deposits are traced over wide areas of Sinai (Fig. 7). Lagoonal stromatolitic and laminated calcareous marls in Section Z (Fig. 6) strongly confirm the lowstand, above subtidal deposits of the post-TuSin 1 HST. In contrast to the other sections, the LST and the SB have not been recognised in Section AN. This is because erosion or nondeposition during the lowstand; alternatively, dolomitisation may have prevented the recognition of eventual lowstand deposits.

ts and TST. The ts is marked by the first occurrences of winnowed calcareous sediments (e.g. Sections UA, Q, G; Fig. 6). The TST is uniformly composed of dolomites in north Sinai, while in central and south Sinai it features fossiliferous marls and limestones. Here, the TST is also characterised by

water-energy deposits. In Sections M and AN, cyclically bedded dolomites dominate, as in the post-TuSin 2 HST beneath. It is proposed, that the interference of higher-order relative sea-level changes hampered the establishment of significant TST-deposits in northern Sinai, which explains the more or less identical lithofacies of the TST compared with the post-TuSin 2 HST. Yet, the intercalated siliciclastic LST-deposits in Section M reflect a pronounced sea-level fall and the transition to dolomitic deposits may be a potential ts. In Section AN, the ts may coincide with the SB, because LST-deposits are not distinguishable. Alternatively, the ts may be placed at the onset of rudist patches within the dolomitic succession (Fig. 5).

In central Sinai, fossiliferous dolomitic marls alternate with winnowed packstones with high amounts of ooids, oncoids and reworked components throughout the TST. The latter are associated with cross-bedding, channels and rip-up structures (Fig. 7). Additionally, episodes of reduced sedimentation rates are indicated by highly bioturbated and nodular calcareous intercalations and glauconite occurrences. Towards the south, a lagoonal facies belt (Sections D, V, Fig. 6) is composed of lagoonal peloidal wackestones and packstones with birdseyes and marls.

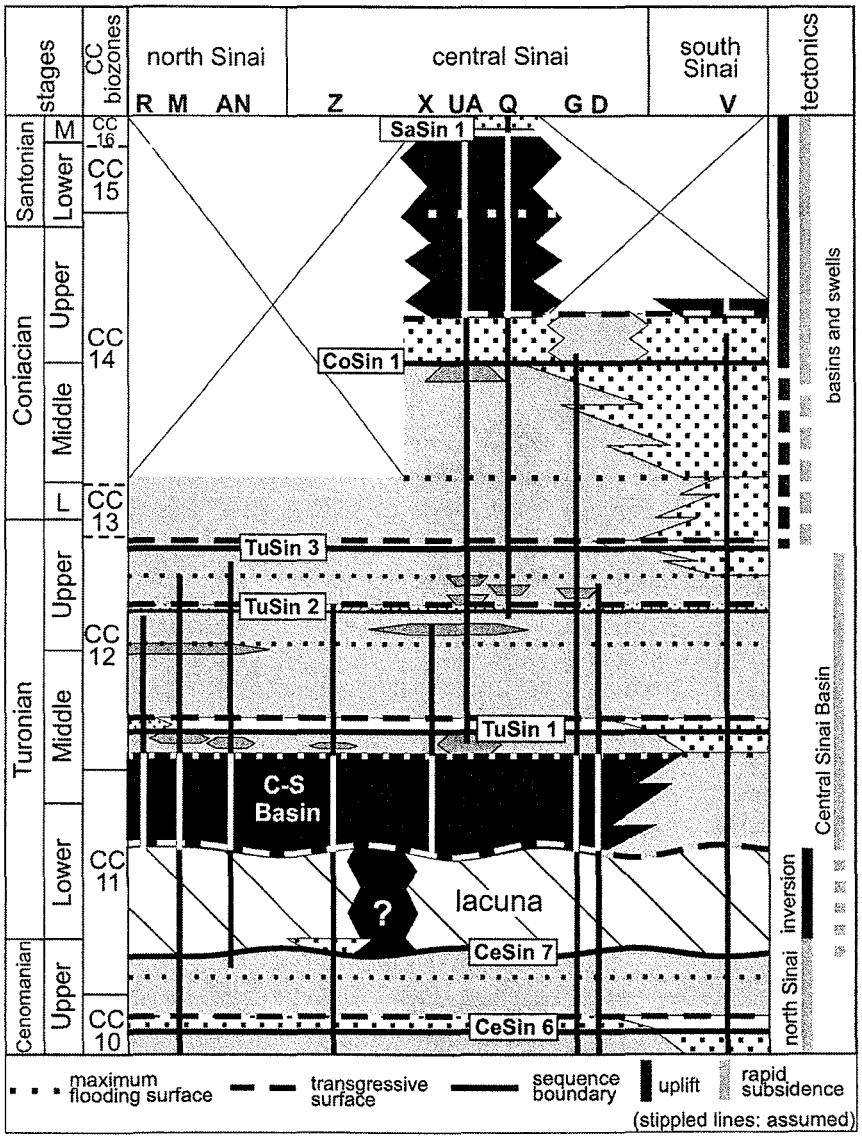

Fig. 8: (Previous page) Lateral and chronostratigraphic distribution of six major facies belts (for key to fill patterns and symbols, see Fig. 7). Systems tracts and surfaces are indicated; durations of major tectonic events are given in the right column.

mfs and HST. The mfs is placed at the onset of protected, shallow-subtidal HST-deposits. Thickly bedded dolomites, limestones and dolomitic marls of the Wata Formation aggrade in the HST in north (Section M, Fig. 5) and central Sinai (Sections UA, Q, G, Fig. 6). The HST-deposits are characterised by bioclastic (echinoderms, gastropods, oysters, ostracods miliolids, calcareous algae) and peloidal wackestones and packstones. Winnowed or reworked textures are scarce, compared with the underlying TST. In Section V, quartzose intercalations dominate in the HST, owing to high siliciclastic influxes from the hinterland. The reduced thickness of the HST in Section V is due to the limited accommodation space in this nearshore setting.

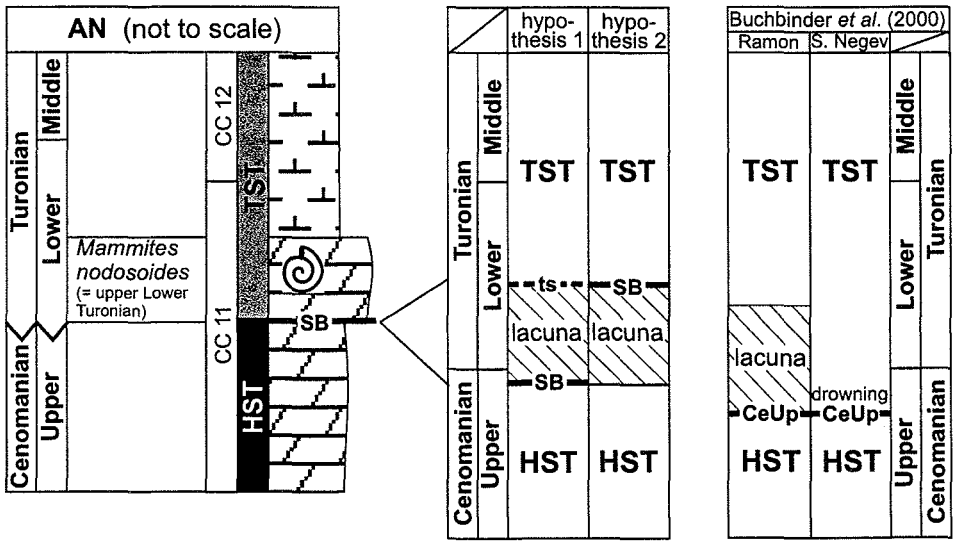

Fig. 9: Two possible age assignments of sequence boundary CeSin 7. The generalised outcrop stacking pattern of Section AN (compare Fig. 5) shows a coinciding sequence boundary (SB) and transgressive surface (ts) at the C/T boundary, which implies a lacuna (left column). Chronostratigraphic interpretations are (middle column): hypothesis 1, after a late Cenomanian SB, the lacuna originated from nondeposition during the early Turonian lowstand; hypothesis 2, erosion during the late highstand (late Cenomanian) caused the lacuna, the SB (early Turonian) is overlain by the TST, and LST-sediments were not deposited. This paper follows hypothesis 1. Interpretations of coeval successions in the Near East are shown for comparison (right column).

Sequence post-TuSin 3

The uppermost Turonian (CC 12) to lower Coniacian (CC 13) sequence post-TuSin 3 is attributed to the lower part of the Matulla Formation and measured in central and south Sinai (Sections UA, Q, G, V; Fig. 6).

SB and LST. Hardgrounds (Section UA) and karstification structures (Section Q) or caliche beds (Section V) at the base of the LST-deposits are considered as SB TuSin 3. In central and south Sinai, the LST is composed of marls and claystones with intercalations of siltstones and dolomites (Fig. 6); the latter may exhibit gypsum nodules. The siliciclastic LST-deposits of Section V contain, plant remains,

ironooids, silicified wood, a caliche bed, two hardgrounds, and an emersion surface; these features suggest short-term switches from silty mudflats to supratidal conditions.

ts and TST. The ts is marked by the first appearance of high-energy deposits with oolites and occasional reworked bioclasts debris, channels or rip-up structures. Subtidal to intertidal dolomites and dolomitic marls with oysters are interpreted as TST. The calcareous deposits of central Sinai interfinger with thickly bedded, occasionally cross-bedded, bioclastic sandstones in the proximal Section V.

mfs and HST. Reduced sedimentation rates at the mfs are indicated by hardgrounds and intense bioturbation in Sections UA and V. In the HST, dolomites and dolomitic marls alternate with scarce calcareous sandstone beds. In contrast to the underlying TST, the HST-deposits lack indicators for high-energy environments, apart from occasional cross-bedding. In Section Q, the TST and HST are not clearly discernible because marked changes in facies are not observed and potential candidates for a mfs are missing. In Section V, marls dominate the HST. Although some calcareous sandstones intercalations are present, a reduced quartz input is obvious in comparison to the TST.

Sequence post-CoSin 1

The sequence post-CoSin 1 is upper Coniacian (CC 14) to Santonian (CC 15 - 16), and comprises the Matulla Formation. The sequence has been studied in central Sinai (Sections UA, Q, and G) and in south Sinai (Section V), but it is only completely measured in Section Q (Fig. 6).

SB and LST. The boundary between quartzose LST-deposits and dolomites of the post-TuSin 2 HST mark the SB CoSin 1, owing to the lack of other indicative discontinuities. In Section V, the SB is characterised by a thin interval of several hardgrounds.

ts and TST. The lithologic break from siliciclastic LST-deposits to chalky limestones and chalks (TST) marks the ts in Sections UA, Q and V (Fig. 6). The TST-deposits reflect a marked deepening of the depositional system, and coincide with a southward retreat of the inner-shelf facies beyond Section V.

HST. The HST is only exposed in Section Q, and it is again composed of hard chalks. A mfs is not discernible in these chalks. The HST is interpreted herein, owing to comparisons with studies of Bauer *et al.* (in press2) and Lüning *et al.* (1998b).

Sequence post-SaSin 1

The LST (uppermost Matulla Formation) in Section Q (Fig. 6) is the only part of the sequence post-SaSin 1 studied. Calcareous sandstones above the chalks of the post-CoSin 1 HST reflect lowstand conditions. The lithologic break most probably coincides with the post-Sa/CaSin LST of Lüning *et al.* (1998b). A middle to late Santonian age is proposed for the LST, because corresponding siliciclastics at Wadi Gidira are assigned to the biozone CC 16 and the *Dicarinella asymetrica* Zone, respectively, by Bauer *et al.* (in press2).

6. VARIATIONS OF SUBSIDENCE

Curves of cumulative sediment thickness against time of the Cenomanian - Turonian successions of Sections AN, M, Z, G, D are shown in Fig. 10. Changing inclinations reflect variations of accommodation and indicate tectono-sedimentary changes, considering that sediment accumulation kept more or less pace with basin-subsidence and sea-level changes. However, varying compaction rates of different lithologies may also have major influence on the varying curve slopes. Moreover, the completeness of the stratigraphic section is a limiting factor in the precision of accumulation (Sadler, 1981).

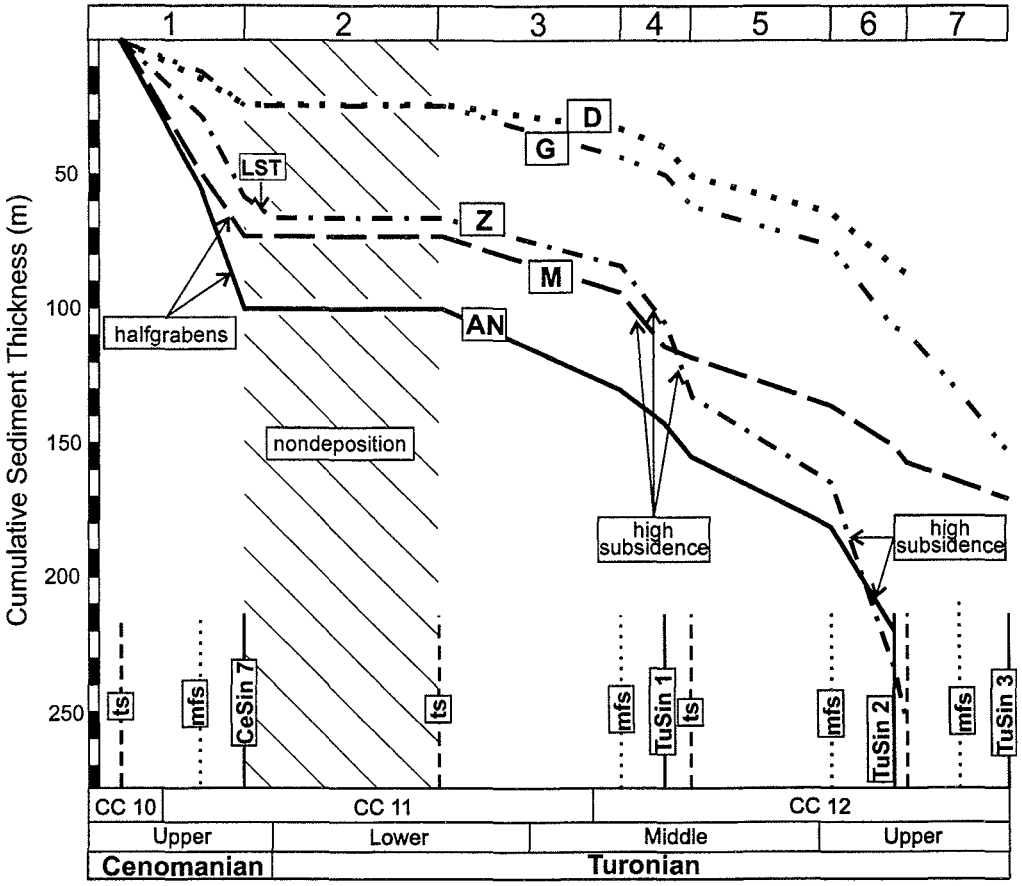

Fig. 10: Curves of cumulative Cenomanian - Turonian sediment thickness against time of Sections AN, M, Z, G, D. Steepened curve slopes indicate increasing subsidence. Note, sediment compaction is not considered. The segments 1 - 7 are discussed in the text.

Despite these restrictions, distinct variations of the curve slopes are interpreted with respect to differing subsidence rates during seven time slices (curve segments 1 - 7). Because steepened curve segments are more pronounced in the basinal, it is assumed that they mirror periods of increased basin subsidence. In curve segment 1, steep slopes of curves M and AN represent high accumulation in the rapidly subsiding halfgrabens in north Sinai during sequence post-CeSin 6, while the flatter slopes of G and D indicate subordinate subsidence in central Sinai. After the stratigraphic gap (curve segment 2) across the C/T boundary (despite rudimentary lowstand deposits in Section Z), maximum

sediment accumulation occurs in Section Z, which indicates the proximity to the depocenter. Furthermore, the curve segments 3 - 7 of AN, M and Z vary particularly, which points to repeating periods of increased (steep slopes) and reduced (flat slopes) subsidence of the C-S Basin. Peaks of subsidence are therefore assumed during segment 4 (middle Turonian post-CeSin 7 HST and post-TuSin 1 LST) and segment 6 (upper Turonian post-TuSin1 HST and post-TuSin 2 LST), especially towards the depocenter (curve Z). In contrast, decreasing sediment accumulations of segments 3, 5, and 7 suggest periods of moderate subsidence. The coeval curves of Sections D and G south of the C-S Basin are more linear, despite small variations. This indicates a constant subsidence, which was predominantly driven by sediment loading rather than rapid tectonic pulses.

7. PALAEOGEOGRAPHY

The new sequence-stratigraphic interpretations presented herein allow to reconstruct detailed palaeogeographic maps (Figs 11, 12). General assumptions of other palaeogeographic interpretations (Said, 1990; Kuss & Bachmann, 1996; Lüning *et al.*,1998b) are incorporated. Regions, where the palaeogeographic setting remains unclear or where biostratigraphic data is imprecise, are blank. For the geographic locations mentioned in the text , refer to Fig. 12D.

7.1 Late Cenomanian platform

The late Cenomanian palaeogeography (Fig. 11A) is governed by a broad carbonate platform with a flat topography and a wide proximal - distal extension of the inner shelf realm. The halfgrabens shown in Fig. 11A were caused by extension, probably owing to Tethyan rifting.

Sinai and Eastern Desert. During the late Cenomanian (post-CeSin 6 TST and HST, Fig. 11A), shallow-subtidal, calcareous deposits (Raha and Halal formations) covered almost entire Sinai (Bartov & Steinitz, 1977; Chérif *et al.,* 1989; Kora *et al.,* 1994; Lüning *et al.,* 1998a) and the Eastern Desert (Bandel *et al.,* 1987; Kuss, 1992). In north Sinai, shoal carbonates were attached to the shelf edge (Kuss & Bachmann, 1996), and slope and basin sediments are known from the northernmost subsurface of Sinai and offshore only (Jenkins, 1990). In south Sinai and in the Eastern Desert, a thin belt of nearshore sandstones interfingered with fluviatile deposits (Bandel *et al.,* 1987; Kuss & Bachmann, 1996), but are out of the range of the transect studied. Therefore, the post-CeSin 6 TST and HST retrogradation and progradation patterns (cross-sections in Fig. 11A) are proposed on the basis of the general context, but are not proven by own observations.

Near East. Middle Cenomanian to lower upper Cenomanian outer-shelf sediments dominated the TST, pre-dating the SB CeUp (Fig. 13) of Buchbinder *et al.* (2000). During the following highstand (equivalent to post-TuSin 6 HST), dolomitic inner-platform deposits with rudists and oysters prograded in the Negev (Braun & Hirsch, 1994). They interfingered northwards with outer-shelf and basinal chalks and marls (Lewy, 1990; Lipson-Benitah, 1994) from the Judean Hills to the Carmel region (Fig. 12D). Further north in Galilee, again a prograding, carbonate platform was attached (Bogoch *et al.,* 1994).

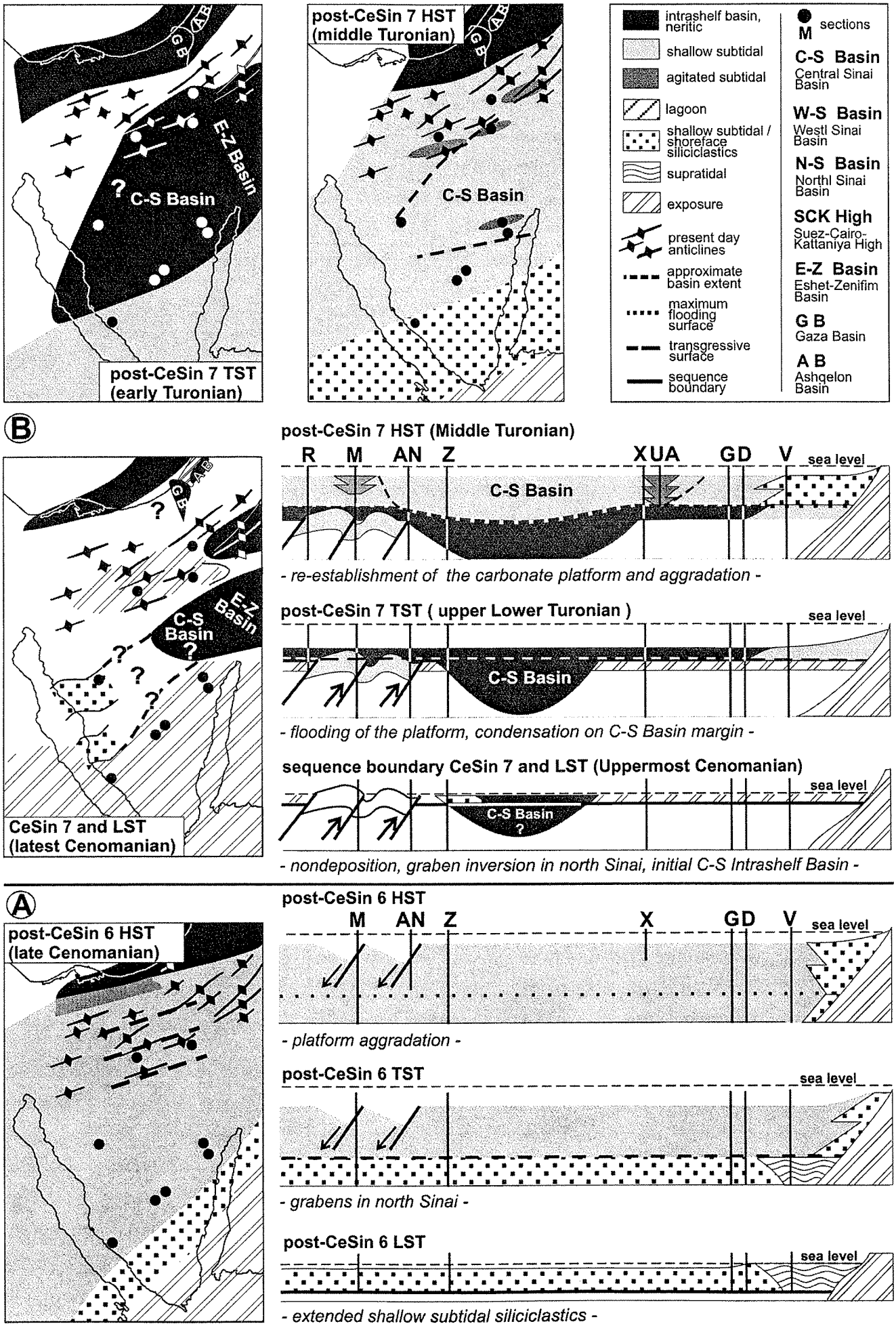
post-CeSin 7 TST
(early Turonian)
E-Z Basin
C-S Basin
G B
A B
post-CeSin 7 HST
(middle Turonian)
intrashelf basin, neritic
shallow subtidal
agitated subtidal
lagoon
shallow subtidal / shoreface siliciclastics
supratidal
exposure
present day anticlines
approximate basin extent
maximum flooding surface
transgressive surface
sequence boundary
sections
C-S Basin
Central Sinai Basin
W-S Basin
Westl Sinai Basin
N-S Basin
Northl Sinai Basin
SCK High
Suez-Cairo-Kattaniya High
E-Z Basin
Eshet-Zenifim Basin
G B
Gaza Basin
A B
Ashqelon Basin
B
CeSin 7 and LST
(latest Cenomanian)
post-CeSin 7 HST (Middle Turonian)
R M AN Z XUA GD V
sea level
- re-establishment of the carbonate platform and aggradation -
post-CeSin 7 TST (upper Lower Turonian)
- flooding of the platform, condensation on C-S Basin margin -
sequence boundary CeSin 7 and LST (Uppermost Cenomanian)
- nondeposition, graben inversion in north Sinai, initial C-S Intrashelf Basin -
A
post-CeSin 6 HST
(late Cenomanian)
post-CeSin 6 HST
M AN Z X GD V
- platform aggradation -
post-CeSin 6 TST
- grabens in north Sinai -
post-CeSin 6 LST
- extended shallow subtidal siliciclastics -

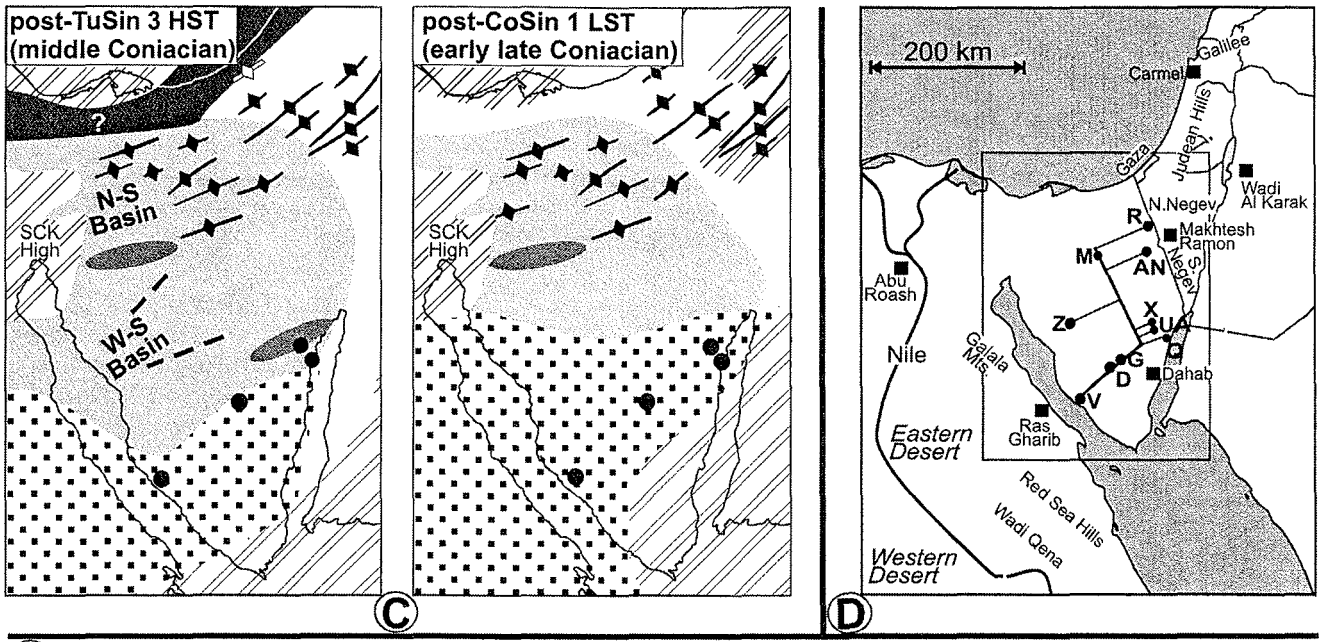
post-TuSin 3 HST
(middle Coniacian)
?
N-S
Basin
W-S
Basin
SCK
High
post-CoSin 1 LST
(early late Coniacian)
SCK
High
C
200 km
Carmel
Galilee
Judean Hills
Gaza
N.Negev
Wadi
Al Karak
R
Makhtesh
Ramon
M
AN
Negev
S.
Abu
Roash
Z
X
UA
Q
Nile
Galala
Mts
G
D
Dahab
V
Ras
Gharib
Eastern
Desert
Red Sea Hills
Wadi Qena
Western
Desert
D

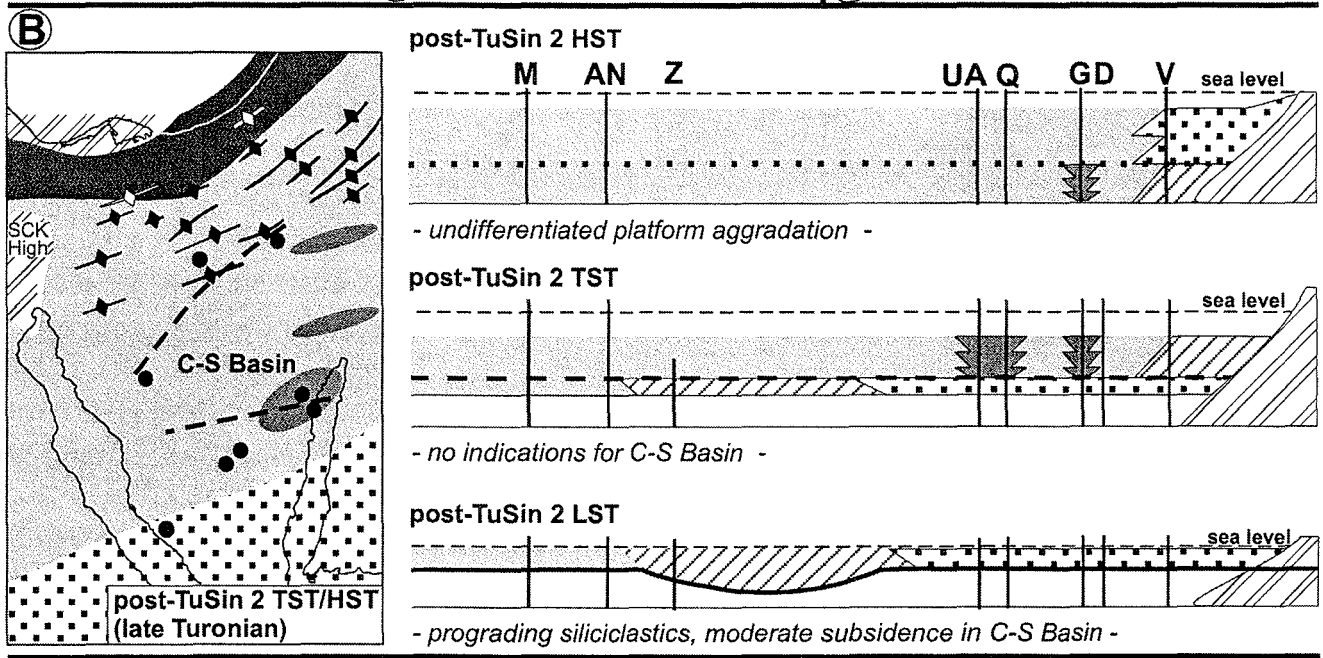
B
SCK
High
C-S Basin
post-TuSin 2 TST/HST
(late Turonian)
post-TuSin 2 HST
M AN Z UA Q GD V
sea level
- undifferentiated platform aggradation -
post-TuSin 2 TST
sea level
- no indications for C-S Basin -
post-TuSin 2 LST
sea level
- prograding siliciclastics, moderate subsidence in C-S Basin -

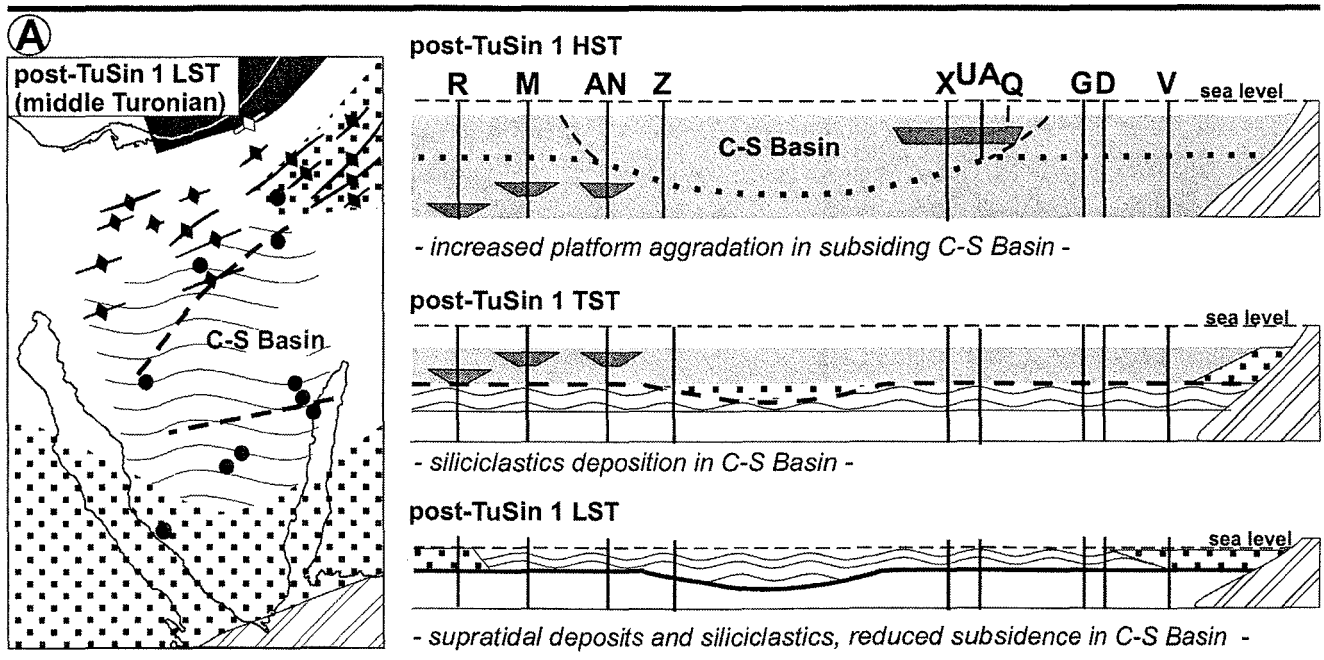
A
post-TuSin 1 LST
(middle Turonian)
C-S Basin
post-TuSin 1 HST
R M AN Z X UA Q GD V
sea level
C-S Basin
- increased platform aggradation in subsiding C-S Basin -
post-TuSin 1 TST
sea level
- siliciclastics deposition in C-S Basin -
post-TuSin 1 LST
sea level
- supratidal deposits and siliciclastics, reduced subsidence in C-S Basin -

Previous pages:

Fig. 11. Palaeogeographic maps of Sinai (including parts of Egypt, the Near East, Jordan and Saudi Arabia) during post-CeSin 6 HST (A), and post-CeSin 7 LST, TST, HST (B). Schematic cross-sections illustrate changing facies belt distributions and C-S Basin configurations within certain systems tracts (compare Figs. 7, 8). Additional data is cited in the text. For location of sections and line of correlation, see Fig. 11d. Note, some abbreviations in the legend refer to Fig. 11 only.

Fig. 12. Palaeogeographic maps during post-TuSin 1 LST (A), post-TuSin 2 TST and HST (B) and post-TuSin 3 HST and post-CoSin 1 LST (C). The schematic cross-sections of the facies-belt distributions and platform configurations within the systems tracts were constructed in analogy to Fig. 10. Owing to the limited amount of Coniacian sections, cross-sections for the maps in (C) were not constructed. The line of correlation and further important localities referred to in the text are given in (D). For legend, see Fig. 6.

Jordan. In southern Jordan, Kuss (1992) and Schulze & Kuss (2000) recognised upper Cenomanian limestones, very similar to those of Sinai. Frequent foraminifers, calcareous algae and oysters within wackestones, as well as high-energy facies belts and coral biostromes indicate a shallow inner-shelf environment. More restricted environments occurred nearshore.

7.2 Latest Cenomanian - middle Turonian: platform drowning, lacuna, intrashelf basins

Important palaeogeographic changes coincide with the early Turonian sea-level rise (Fig. 11B). Large parts of the Cenomanian platform were drowned, and the formation of the C-S Basin and Eshet-Zenifim Basin affected the facies evolution in Sinai and the Near East notably (Bartov & Steinitz, 1977).

Sinai and Eastern Desert. A stratigraphic gap occurs across the C/T boundary in large parts of Sinai, apart from ,e.g., slope and basin deposits in the subsurface of northernmost Sinai (Jenkins, 1990). In north Sinai, this gap is probably related to submarine nondeposition or exposure on isolated highs, which reflect the initial pulses of the Syrian Arc movements (Bartov *et al.*, 1980; Kuss *et al.*, 2000b). However, in central and south Sinai it rather reflects the northward retreat of the coastline during the late Cenomanian lowstand. Uppermost Cenomanian siliciclastics of the elsewhere missing post-CeSin 7 LST are preserved in Section Z (Fig. 7), and in other areas along the Gulf of Suez. They are probably bounded to local, tectonically induced depressions (Chérif *et al.,* 1989a), which are interpreted herein as the westward extension of the C-S Basin (Fig. 11B). In the Eastern Desert, local channels at Wadi Qena (Fig. 12D) transported conglomerates and siliciclastics from the elevated Red Sea Hills south-westwards (Bandel *et al.,* 1987). Although biostratigraphically not well dated, these deposits presumably also represent locally restricted lowstand deposits, similar to those in West Sinai.

During the following early Turonian relative sea-level rise, the exposed areas were flooded and large parts of the platform were drowned, documented by the condensed deep-water deposits of C-S Basin (post-CeSin 7 TST). These deposits mark the minimum N-S extension of the C-S Basin from Section R in the north to Section D in central Sinai (Fig. 11B). The minimum westward position of the basin margin is confirmed by very similar lithofacies in Section Z and in other areas along the Gulf of Suez coast (Chérif *et al.,* 1989; Kora *et al.,* 1994), as well as by condensed, organic-rich shales in the subsurface (Mostafa, 1999) near Ras Gharib (Gulf of Suez coast, Fig. 12D).

Beyond the southern margin of the basin, protected shallow-subtidal or open lagoonal environments prevailed (Section V, Fig. 6). Parts of the Red Sea Hills (Fig. 12D) were also inundated (Bandel *et al.,* 1987) and transgressive deposits similar to those of north and central Sinai (including 'ammonite bed') dominated in the Eastern Desert (Kuss & Malchus, 1989), but they were probably deposited in more shallower water-depths when compared to Sinai. In northern Egypt, shallow-subtidal environments established on submarine highs, e.g. the Abu Roash area (Hamza, 1993).

Near East. During the late Cenomanian - middle Turonian, a morphologic differentiation in swells and NNE striking basins has been recorded in the Near East (Lewy, 1989; Sandler, 1996). Sedimentation in the depocenters of the Eshet-Zenifim Basin started in the late Cenomanian (Lewy, 1989). In the northern and southern Negev, a condensed deep-water facies with planktic foraminifers and ammonites (post-CeUp TST of Buchbinder *et al.,* 2000) overlies Cenomanian platform deposits. The depocenters in southern and northern Negev were separated by an uplifted area in central Negev (Makhtesh Ramon, Figs 11B, 12D), which is regarded as the eastward prolongation of the Gebel Areif El Naqa structure (Lewy, 1989). As in Section AN, uppermost Cenomanian - lower Turonian deposits are missing at Makhtesh Ramon. A conspicuous upper Cenomanian omission surface (Fig. 9) indicates extreme submarine condensation (Buchbinder *et al.,* 2000) or even local exposure (Lewy & Avni, 1988). After this stratigraphic gap, the inundation of the uplift started in late early Turonian times, slightly earlier than in Section AN, and the basinal sedimentation persisted until the middle Turonian (Lewy, 1989). Owing to extreme condensation on further highs, stratigraphic gaps of similar ages are also recorded from the Judean Hills, the Mediterranean coast (Lipson-Benitah, 1994) as well as from the Carmel and Galilee regions (Buchbinder *et al.,* 2000). The highs separated several local intrashelf basins (e.g. Gaza Basin, Ashqelon Basin; Fig. 11B) with monotonous neritic, and in parts dysoxic deposits (Honigstein *et al.,* 1989; Lipson-Benitah *et al.,* 1990) prevailed in the basins.

Jordan. Swells and rapidly subsiding basins are recorded especially in central Jordan. Organic-rich beds accumulated in these basins and in grabens in Syria (Abu-Jaber *et al.,* 1989). Compared to Sinai, a stratigraphically more complete succession of upper Cenomanian - lower Turonian deep-water deposits with restricted black-shale occurrences (Schulze & Kuss 2000) is locally exposed in the vicinity of Wadi al Karak (Fig. 12D). This basin possibly formed the eastward extension of the Eshet-Zenifim Basin, before it was displaced northwards along the sinistral 'Dead Sea transform fault' in post Cretaceous times. A marked inundation during the early Turonian relative sea-level rise, is also manifested by an interval of frequent lower Turonian ammonites and planktic foraminifers throughout Jordan (Khalil, 1992; Schulze & Kuss 2000), very similar to the Lower Abu Qada Formation of Sinai.

7.3 Middle - late Turonian platform recovery

After the early Turonian drowning, the platforms recovered in the regions considered. Subtidal calcareous deposits again dominated in the middle to late Turonian (Figs 12A, B), interrupted by a pronounced middle Turonian shallowing event.

Sinai and Eastern Desert. The offset of deep-water deposits marks a further important feature of the depositional history in the middle Turonian. On the newly established platform (post-CeSin 7 HST, Middle Abu Qada Formation), mainly protected shallow-subtidal deposits aggraded in north and central Sinai, and high-energy conditions prevailed along the margins of the C-S Basin (Fig. 11B). The C-S Basin margins are placed between Sections M and AN in north Sinai and Sections UA and G in central Sinai, owing to increased sediment accumulations of sequences post-TuSin 1 and 2 (Fig. 7) in the basin (Sections AN, UA). In the southern nearshore realm, a siliciclastic facies belt prograded.

Exposure surfaces at SB TuSin 1 reflect a pronounced middle Turonian relative sea-level fall, and shallow-subtidal to supratidal LST-deposits (Fig. 8) covered large parts of Sinai (Fig. 12A; Bartov & Steinitz, 1977; Lüning *et al.,* 1998a,b). Coeval siliciclastic mud flats were attached in south Sinai (Fig. 12A). A local feature is the siliciclastic dominated LST in Section R (Figs 5, 7); the close lithologic similarities to the 'clastic unit' in the Near East (Sandler, 1996) suggest a previously unreported westward extension of the latter. The generalised middle Turonian facies of (1) shallow-subtidal and locally high-energy deposits in north and central Sinai and (2) prograding / retrograding siliciclastic facies belts in the south (Figs 8, 12B) persisted until the late Turonian (Upper Abu Qada Formation and Wata Formation). A hiatus across the Turonian / Coniacian (T/ C) boundary has been reported from central Sinai (Chérif *et al.,* 1989b; Kassab & Ismael, 1994). Although its precise biostratigraphic position cannot be confirmed in this study, nondeposition, due to emersion, corresponds to SB TuSin 3 close to the T/C boundary (Fig. 8). A correlatable sea-level drop is also proposed in Egypt by Issawi *et al.* (1999, p. 215).

In the Eastern Desert, shallow-subtidal facies associations of limestones and dolomites mixed with siliciclastics prevailed in the Turonian. Although relative sea-level fluctuations controlled the sedimentary compositions intensely (Kuss, 1992; Kuss & Bachmann, 1996), biostratigraphically well constrained correlations are scarcely published. Nevertheless, the middle Turonian shallowing event is recorded by: (1) fluviomarine siliciclastic intercalations (Kuss & Malchus, 1989; Issawi *et al.,* 1999, p. 215), (2) a probable disconformity and hiatus between the lower and upper Turonian deposits (Kuss & Malchus, 1989), and (3) prograding fluvial sandstones in southern Egypt (Wadi Qena; Said, 1990). The uplift of the Abu Roash structure (Hamza, 1993), the Suez-Cairo-Kattaniya High, the coastal areas of Sinai (Said, 1990), and other isolated areas (Fig. 12B) persisted in the middle and late Turonian (Kerdany & Chérif, 1990; Said, 1990).

Near East. In contrast to Sinai, the onset of the renewed middle and upper Turonian platform sedimentation was highly diachronous in the Near East. According to Buchbinder *et al.* (2000), platform growth started in the early Turonian on elevated structures of the Judean Hills and northern Negev, prograded successively towards the south and reached the Makhtesh Ramon area and southern Negev in the middle Turonian, 1.5 my later. As in Sinai, the middle Turonian relative sea-level fall (post-Tu1 LST of Buchbinder *et al.,* 2000) is documented by omission and erosion surfaces (Lewy & Avni, 1988), and freshwater lakes with claystones and an angiosperm flora (Dobruskina, 1997) above the platform carbonates. Furthermore, a siliciclastic-evaporite facies ('clastic unit') developed in the Negev and further north with palaeosols, pedogenic alterations and fluvial sandstones. At the Mediterranean coast, coeval outer shelf and basinal sedimentation remained apparently undisturbed (Fig.

12B); neither a SB nor LST-sediments are recorded. The same is true for the southern Negev, owing to a marine ravinement surface that truncated the lowstand deposits and sometimes even parts of the underlying HST-deposits (Buchbinder *et al.,* 2000). A late Turonian return to marine environments is documented by alternating inner-platform and outer-platform deposits. They are interrupted by outer-shelf deposits in the southern Negev, which are interpreted as a short-term, local platform drowning event (SB Tu2 of Buchbinder *et al.,* 2000). However, this drowning unconformity cannot be confirmed in Sinai.

Jordan. The drowned upper Cenomanian platform recovered in middle Turonian times (Schulze & Kuss, 2000). Lagoonal limestones, rudist banks and oyster flats characterise the shallow marine carbonate platform. It was temporally exposed, owing to an inherited basin and swell morphology (Kuss, 1992; Shinaq & Bandel, 1998).

7.4 Latest Turonian - Santonian basins and swells

A basin and swell morphology formed at the end of the Turonian (Fig. 12C) owing to Syrian Arc tectonics and evolved further Senonian doming. Furthermore, an overall deepening of the depositional setting is indicated during the late Coniacian - Santonian (Fig. 8), coinciding with a relative sea-level rise (post-CoSin 1 TST/HST). Senonian palaeogeographic maps of Lewy (1975), Said (1990), Kuss & Bachmann (1996), and Lüning *et al.* (1998b) document deep-water environments in rapidly subsiding depocenters, while coeval shallow-water environments formed on local highs.

Sinai and Eastern Desert. NE-SW striking basins in Egypt and Sinai were successively filled with thick accumulations of sandstones and carbonates since the late Turonian (Kerdany & Chérif, 1990; Said, 1990; El-Hawat, 1997). The North Sinai Basin (Fig. 12C) formed in the latest Turonian (Lewy, 1975), and was separated from the southern inner-shelf realm by an oolitic shoal until the late Coniacian. The Coniacian sediments of north Sinai were deposited on the rapidly subsiding outer shelf, but were locally eroded in pre-Santonian times (Jenkins, 1990). Bartov *et al.* (1980) and Lüning *et al.* (1998b) reported Coniacian open-marine chalks at Gebel Areif El Naqa, overlain by inner-shelf carbonates. In south Sinai (Section V, Fig. 8) and west-central Sinai (Chérif *et al.,* 1998b), a siliciclastic, shallow inner-shelf to fluvialmarine environment was attached. These siliciclastics prograded during post-TuSin 3 HST (Fig. 12C). In the early late Coniacian, the region was locally exposed, and shallow siliciclastics dominate the post-CoSin 1 LST (Fig. 12C). Lewy (1975) reported a particular erosional unconformity in the lower upper Coniacian succession of Sinai, which most probably corresponds to SB CoSin 1 as defined herein. During the late Coniacian - Santonian, the inner-shelf facies retreated (Lewy, 1975). Deep-water chalks and marls developed in local depressions in south Sinai (Section V, Fig. 8), central Sinai (Sections UA and Q), and north Sinai (Bartov *et al.,* 1980; Lüning *et al.,* 1998b), owing to rapid subsidence in combination with the prominent sea-level rise during post-CoSin 1 TST/HST (Fig. 8).

In the Eastern Desert, shallow-marine, siliciclastic, and terrestrial conditions prevailed during the relative sea-level lowstand across the T/C boundary. Middle and upper Coniacian deposits are

limited to isolated occurrences (Kuss, 1992) and reflect a shallow-marine to continental environment (Kuss & Malchus, 1989).

Near East. Compared to Sinai, the region was more strongly affected by Syrian Arc tectonics, and synsedimentary folding and faulting formed an extremely pronounced palaeo-relief with intrashelf-basins and swells (Rosenthal *et al.,* 2000). Differential subsidence, varying sedimentation rates, and erosion resulted in thickness variations of the Senonian successions (Reiss, 1988; Lewy, 1989; Rosenthal *et al.,* 2000). Especially Coniacian deposits are often incomplete, and upper Coniacian - Santonian hemipelagic deposits merely rest disconformally on the Turonian successions in wide areas of the Near East (Lipson-Benitah *et al.,* 1985; Lewy & Avni, 1988; Flexer *et al.,* 1989). Although associated with a relative sea-level fall, this unconformity is mainly tectonically driven (Lewy, 1989) and probably corresponds to SB CoSin 1. In the southern Negev, however, lower Coniacian outer-platform deposits above Turonian inner-platform carbonates are again interpreted as local drowning (SB Co1 of Buchbinder *et al.,* 2000) related to the newly subsiding Eshet-Zenifim Basin (Lewy, 1975). Since the late Coniacian, hemipelagic chalks onlapped the folded highs (Honigstein *et al.,* 1988), and upwelling and high-productivity governed the distribution of local oxygen-depleted sediments (Reiss, 1988; Flexer *et al.,* 1989; Almogi-Labin, 1990).

Jordan. Turonian and lower Coniacian lagoonal and shallow-subtidal environments in north and central Jordan switched to predominately hemipelagic conditions in the middle Coniacian and Santonian (Shinaq & Bandel, 1998). Only in southeast Jordan, a nearshore environment with dolomites and sandstones persisted (Kuss, 1992). As in Egypt and in the Near East, basins and swells were apparent in Jordan, but the highs were not folded during Syrian Arc tectonics (Abu-Jaber *et al.,* 1989). Abed & Amireh (1999) reported a lateral thinning of the stratal packages towards the swells, and reworked and condensed phosphorite belts along the flanks of some of these elevated structures.

8. CONTROLS ON THE SEQUENCE ARCHITECTURE AND PLATFORM CONFIGURATION

8.1 Changes in accommodation

In the sections studied, changes in accommodation are expressed by repeated reorganisation of the depositional system, favouring the progradation/retrogradation of the facies belts and the establishment of specific environments within different systems tracts. Minimum accommodation resulted in local exposure (documented by stratigraphic gaps, emersion and erosion surfaces). Furthermore, supratidal and siliciclastic-evaporite environments formed (LSTs), owing to northward shifts of the shorelines. Increased accommodation triggered the deposition of extended shallow-marine, inner-platform carbonates within the TSTs in north and central Sinai, and also the establishment of temporally high-energy environments. The siliciclastic input decreased and in south Sinai (proximal), and increased accommodation resulted in the retrogradation of protected subtidal and lagoonal TST-deposits.

The maximum flooding of platforms results in highest rates of carbonate production and aggradation (Handford & Loucks, 1993). In the area of investigation, this is reflected by homogenous, dolomitic inner-platform deposits during highstand aggradation, especially in north Sinai. The thick and

uniform lithologies (e.g. post-TuSin 1 HST) were possible during periods of increased accommodation. During periods of highstand progradation, muddy protected inner-platform or lagoonal environments developed in central and south Sinai. In the nearshore realm, siliciclastics derived from the hinterland often prograded and limited the southward extension of the carbonate lithofacies.

8.2 Platform topography

Despite high subsidence in the C-S Basin, the platform topography is considered as rather flat in the late Cenomanian and in the middle to late Turonian, because the depositional environments were not deeper than the shallow subtidal. It is assumed that the studied shallow-marine deposits built up at, or closely to sea level, filling accommodation. This resulted in a generally poised platform topography, which in turn favoured a more or less uniform facies distribution within the individual systems tracts, especially within the HSTs. Moreover, it is assumed that the upper Cenomanian and middle to upper Turonian deposits on the flat topography were highly susceptible to sea-level changes, and even low-amplitude sea-level variations resulted in widespread and more or less synchronous exposure or flooding (compare Hunt & Tucker, 1993; Sharland *et al.*, 2001, p. 50). In contrast, sea-level falls on the structured Coniacian and Santonian morphology probably led to emersion at different times and places (compare Strasser *et al.*, 1999).

8.3 Tectonics

Uplifts. Bartov *et al.* (1980) discuss the late Cenomanian - early Turonian (*Mammites nodosoides* Zone) stratigraphic gap in Section AN (Fig. 8) as a result of sub-marine nondeposition or extreme condensation on an elevated high. This corresponds well to further reports of stratigraphic gaps related to tectonics across the C/T boundary in Egypt and the Near East (see above), North Africa (Camoin, 1991) and Arabia (Philip *et al.*, 1995; Sharland *et al.*, 2001, p. 111). Additionally, Kuss *et al.* (2000b) interpreted a successively thinning of the Turonian sequences along the northern flank of the Gebel Areif El Naqa anticline (locality of Section AN) as synsedimentary onlap geometries on an asymmetrically uplifted area.

Subsidence. Tectonically driven subsidence has been manifested since the late Cenomanian in an increase of sediment accumulation within the halfgrabens of north Sinai and the C-S Basin. Curves of cumulative sediment thickness (Fig. 10) indicate periods of increased subsidence in the basin, with highest subsidence around SB TuSin 2 (segment 6). Because correlatable SBs are missing in adjacent regions of Sinai (see below), it is assumed that this SB was predominantly influenced by local tectonics. During the Coniacian and Santonian, Syrian Arc tectonics formed a structured shelf, and had major influence on the architecture of sequences post-CoSin 1 and post-SaSin 1. A variety of depositional environments document the complex interplay of relative sea-level changes and swell and basin morphology during the late Coniacian - Santonian in north and central Sinai (Lewy, 1975; Bartov & Steinitz, 1977; Kuss & Bachmann, 1996). This is also supported by Late Cretaceous uplift of the Gebel Areif El Naqa anticline (Bartov *et al.*, 1980; Lüning *et al.*, 1998a; Kuss *et al.*, 2000b) and varying thickness of the stratal packages in central Sinai (Chérif *et al.*, 1989b; Kora & Genedi, 1995).

8.4 Lower Turonian lacuna and platform drowning

The late Cenomanian to late early Turonian stratigraphic gap is interpreted herein as a result of long lasting exposure in central and south Sinai, whereas in north Sinai it is probably closely related to uplift movements at Gebel Areif El Naqa anticline (see above). Thus, a diachronous nature of SB CeSin 7 cannot be excluded. Moreover, platform drowning is reflected by the rapid deepening of the depositional system during the post-CeSin 7 TST and possibly also influenced the genesis of the stratigraphic gap, as drowned carbonate platforms are often characterised by extreme condensation or long hiati (Schlager, 1999). For example, platform drowning across the C/T boundary in the Provence (Fig. 13, sequence boundary Sb5) was associated with a long stratigraphic gap in the lower Turonian *Watinoceras coloradoense* biozone (Philip & Airaud-Crumiere, 1991; Philip, 1998). As in Sinai, this gap was followed by condensed deposits in the *Mammites nodosoides* Zone during the TST and the establishment of a new platform in the middle Turonian HST (Philip & Airaud-Crumiere, 1991; Philip, 1998). In the Pyrenees, a shorter highly condensed interval and a stratigraphic gap in the early Turonian were also caused by platform drowning (Drzewiecki & Simo, 1997). In this context, it cannot be excluded that drowning in Sinai started before the onset of the post-CeSin 7 TST-deposits and the stratigraphic gap may possibly be related to the drowning phase.

According to Schlager (1999), platform drowning may be caused either by rapid subsidence or by reduced carbonate production coinciding with a rising eustatic sea level. Restricted carbonate growth is generally attributed to drastic environmental changes, namely flooding of the platforms by oxygen-depleted waters. They were caused by oceanic anoxic events, high nutrient influxes, increased coastal upwelling and eutrophication or changing oceanic circulation and stratification of water masses (e.g. Arthur *et al.,* 1987; Jarvis *et al.,* 1988; Philip & Airaud-Crumiere, 1991; Drzewiecki & Simo, 1997; Weissert *et al.,* 1998). Well known benthic extinction events across the C/T boundary were important issues for the reduction of carbonate production (Philip & Airaud-Crumiere, 1991; Kauffmann, 1995; Kerr, 1998). In Sinai, siliciclastic influxes temporarily reduced the extension of calcareous deposits in the Cenomanian and proximal areas and uplifted highs were exposed in the latest Cenomanian (SB CeSin 7). Thus, the carbonate deposition was already disturbed before the lower Turonian flooding of the platform, and the depositional system would have reacted very sensitively to scenarios of changing environmental factors as described above. Mostafa (1999) and Shahin (1991) interpret the genesis of lower Turonian, organic-rich shales and a δ13C excursion in upper Cenomanian - lower Turonian deposits at the Gulf of Suez coasts as a result of a marked oxygen minimum zone. It is therefore assumed that a flooding of oxygen depleted waters effected the benthic community and delayed the re-establishment of the carbonate deposition in the early Turonian. This is underlined by a decline of diversities and frequencies of benthic foraminifers (Chérif *et al.,* 1989a), ostracods (Shahin, 1991), and specific molluscs (Kassab, 1996) at the C/T boundary. However, in contrast to many other Tethyan shallow carbonate shelves (Philip & Airaud-Crumiere, 1991; Steuber & Löser, 2000), the contribution of rudists to the carbonate production in the Cenomanian was only of minor importance (Bauer *et al.,* in press1). Although a decline of specific rudist taxa is obvious at the C/T boundary, this had little effect on carbonate production.

A further episode of platform drowning is observed during the late Coniacian - Santonian in parts of Sinai and the Near East, coinciding with a widespread deepening of the depositional system and the accumulation of deep-water deposits (post-CoSin 1 TST). This drowning event is also well known in large areas of North Africa (Camoin, 1991) and was induced by rapid subsidence, owing to the renewed tectonic activity ('Santonian tectonic event', Guiraud & Bosworth, 1997).

8.5 Local vs. regional relative sea-level changes

A correlation of the SBs recognised in Sinai with those from Haq *et al.* (1987), Robaszynski *et al.* (1990, 1993), Philip (1998), as well as Buchbinder *et al.* (2000), Bachmann & Kuss (1998), and Lüning *et al.* (1998a,b) is presented in Fig. 13. The timing and correlation of the formerly mentioned SBs is based on Hardenbol & Robaszynski (1998). For practical reasons, equally named sequence boundaries are supplemented in the following by their authors.

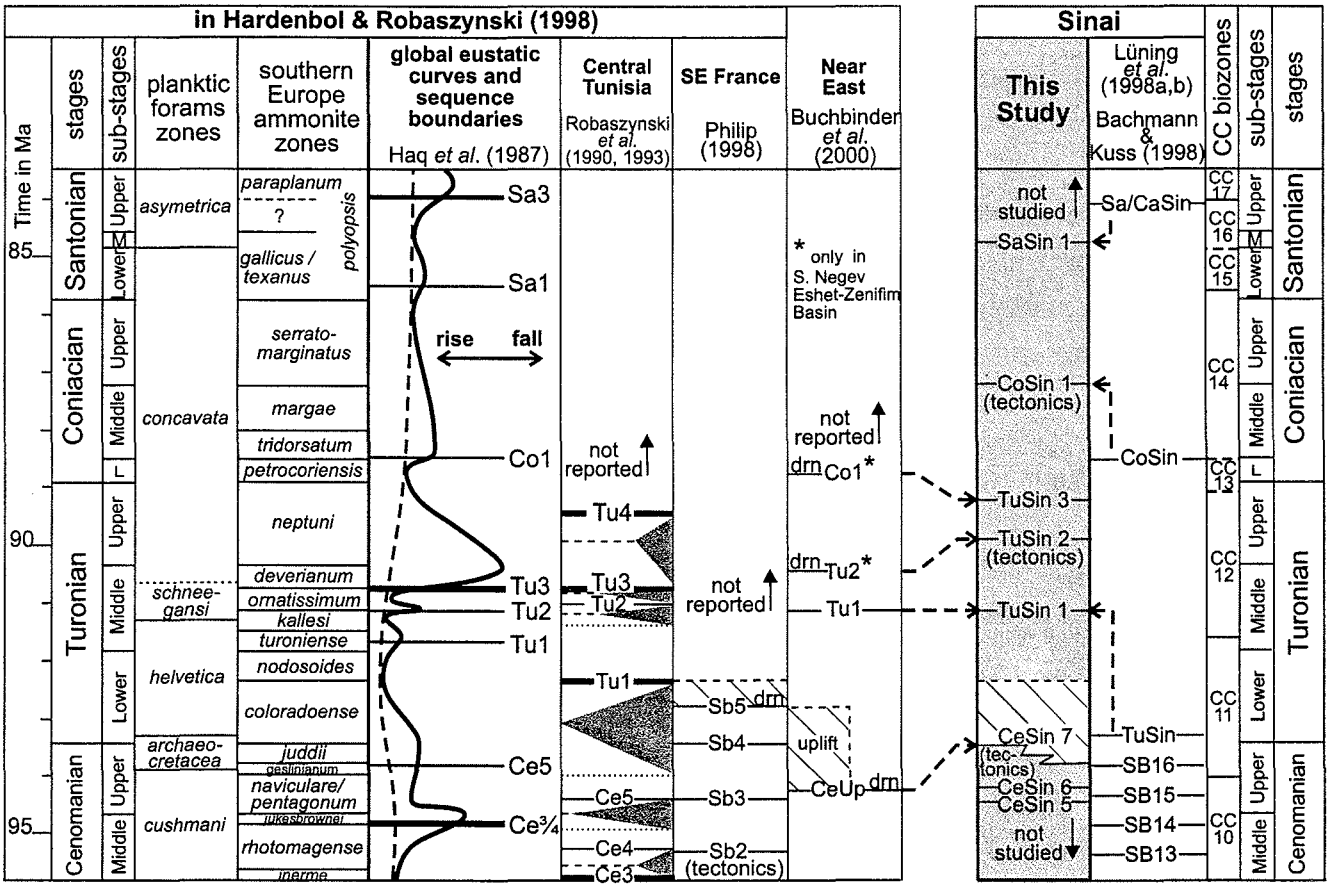

Fig. 13: Correlation of the sequence boundaries in this study, with those of other regional studies and the eustatic concept. Several sequence boundaries of this study were probably markedly influenced by tectonics as indicated. For detailed discussions see text. Stippled lines indicate cross correlation with corresponding sequence boundaries of previous studies in Sinai and in the Near East. Some sequence boundaries in the Near East are regarded to platform drowning (indicated by 'drn'). The biozone schemes in the left columns and the correlation of the global sequence boundaries with those from Tunisia and France are after Hardenbol & Robaszynski (1998).

Correlation with Haq et al. (1987), Robaszynski et al. (1990, 1993), Philip (1998). The correlation (Fig. 13) shows ambiguities regarding TuSin 1, TuSin 3, and stratigraphic mismatches with respect to the remaining sequence boundaries of Sinai are evident. For CeSin 5 and 6, this is most likely due to the limited biostratigraphic data available. Tu1 of Robaszynski and Sb4 and Sb5 (southeast France) fall within the stratigraphic gap in Sinai. TuSin 3 seems to correlate well with Tu4 of Robaszynski. TuSin 1 apparently correlates with Tu2 of Robaszynski/Haq or Tu3 of Robaszynski/Haq. Hardenbol & Robaszynski (1998) propose that Tu2 of Robaszynski/Haq represents a minor sea-level fall, whereas in Sinai and in the Near East, a prominent sea-level fall is recorded. This may suggest that TuSin 1 is equivalent to Tu3 of Robaszynski/Haq and that the minor sea-level fall of Tu2 of Robaszynski/Haq, probably did not leave a recognisable imprint in Sinai and is not preserved (e.g. within the dolomite successions assigned to post-CeSin 7 HST). Alternatively, Tu2 of Robaszynski/Haq and Tu3 of Robaszynski/Haq possibly amalgamated in TuSin 1. However, this would imply a corresponding hiatus, which is not observed in Sinai. Relative sea-level changes related to CeSin 7, TuSin 2, CoSin 1 were influenced by local tectonics in Sinai, especially with respect to the C-S Basin and the Syrian Arc system. This explains their poor correlation with the other studies.

Correlation with Buchbinder et al. (2000). Although the structural evolution and depositional environments in the Negev were very similar to Sinai, the corresponding sequences were clearly diachronous. Buchbinder *et al.* (2000), interpreted their Tu1 and Co1 as a result of drowning (type 3 sequence boundary, *sensu* Schlager, 1999), while the probably corresponding sequences post-TuSin 2 and post-TuSin 3 both clearly exhibit LSTs. The diachronous sequences of Sinai and of the Near East are interpreted herein as predominately controlled by the time transgressive evolution and differing amplitudes of basin subsidence and Syrian Arc tectonics. Additionally, biostratigraphic uncertainties have to be considered.

Correlation with Bachmann & Kuss (1998) and Lüning et al. (1998a,b). Bachmann & Kuss (1998) and Lüning *et al.* (1998a,b) reported some of the SBs described herein, but some biostratigraphic mismatches exist. Comparison of the facies changes strongly suggests that SB16 of Lüning/ Bachmann corresponds to CeSin 7. However, we cannot follow the interpretation of a corresponding uppermost Cenomanian LST (post-SB16 LST), which is restricted to individual sections at Gebel Areif El Naqa and Gebel Minsherah (Bachmann & Kuss, 1998; Lüning *et al.* 1998a). TuSin of Lüning/Bachmann corresponds to TuSin 1, CoSin of Lüning/ Bachmann to CoSin 1 and Sa/CaSin of Lüning/ Bachmann to SaSin 1. Furthermore, two additional Turonian sequence boundaries (TuSin 2 and TuSin 3) have been detected in this study. Lüning *et al.* (1998a,b) placed their SB TuSin in the lower Turonian based on planktic foraminifers, but their biostratigraphic data did not allow to distinguish between the lower and middle Turonian *Whiteinella archaeocretacea* or *Helvetoglobotruncana helvetica* zones. Yet, the interpretations of new biostratigraphic data from calcareous nannoplankton (Bauer *et al.,* in press2) show that the interval post-CeSin 7 TST to post-TuSin 1 LST clearly lies in the biozone CC 12 (middle and upper Turonian). Lüning *et al.* (1998b) assigned their CoSin to the foraminiferal biozones *Dicarinella primitiva* or *D. asymetrica* and to the calcareous nannofossils zones *Micula staurophora* or *Eiffellithus eximus* respectively, and proposed an early Coniacian age after biostratigraphic concepts

of Crux (1982) and Caron (1985). However, the application of new biostratigraphic schemes presented in Hardenbol *et al.* (1998) assign these zones to the middle and upper Coniacian (Fig. 13). This is supported by records of upper Coniacian ammonites at the top of post-TuSin HST. Mismatches between SaSin 1 and Sa/CaSin of Lüning/ Bachmann are also caused by the different biostratigraphic concepts used.

9. IMPLICATIONS FOR THE LARGE-SCALE STRUCTURAL CONTEXT

Differential subsidence along reactivated, deep-seated faults during the late Cenomanian in Sinai corresponds well to similar features in other regions of North Africa (Camoin, 1991), where halokinesis often intensified fault block movements. In contrast, post Cenomanian inversion in Sinai was due to the Syrian Arc tectonics. Bartov *et al.* (1980), Kerdany & Chérif (1990), and Kuss *et al.* (2000b) concluded that the Gebel Areif El Naqa anticline was initially uplifted already in latest Cenomanian - early Turonian times as a result of first pulses of Syrian Arc movements. This correlates well with post Cenomanian compressional regimes described from, e.g., Turkey, Oman and Iran (Patton & O'Connor, 1988; Collins & Robertson, 1997; Sharland *et al.,* 2001, p. 106, 112), and coeval uplifting and folding recorded from the Near East (see above). In contrast to the theory of uplift induced by Syrian Arc tectonics, Gvirtzman & Garfunkel (1998) presented an alternative model of magmatically induced doming since the Early Cretaceous caused by hot spot activities, e.g., in the Maktesh Ramon area. The origin of the C-S Basin and Eshet-Zenifim Basin is little known and scarcely discussed in literature. Gvirtzman & Garfunkel (1998) and Buchbinder *et al.* (2000) suggested that a flexure deviated from pre-existing thermal subsidence of the passive margin; further differential subsidence occurred with the Coniacian Syrian Arc tectonics. Early Turonian structures related to flexural subsidence are also reported from the Arabian Peninsula (Harris *et al.,* 1984; Burchette & Britton, 1985; Philip *et al.,* 1995). On the other hand, it cannot be excluded that in Sinai the fault-induced differential subsidence during the Cenomanian may have persisted throughout the Turonian, and transpressive movements eventually formed the C-S Basin, e.g. in form of a pull-apart basin bounded by horsts in the vicinity of Gebel Areif El Naqa.

Following the tectonic subdivision of Sinai (Said, 1962), fault reactivation and inversion are expressed on the northern 'unstable shelf' of Sinai. However, Bosworth *et al.* (1999) noted that Senonian folding effected the sedimentary cover in the Gulf of Suez region, which was previously considered a stable cratonic setting. Moreover, local depressions along the Gulf of Suez coast (Chérif *et al.,* 1989a) and the periods of increased subsidence in the C-S Basin herein interpreted show that tectonic activity also affected the southern 'stable shelf'.

10. CONCLUSIONS

- Eight sedimentary sequences have been interpreted for the upper Cenomanian to Santonian strata of Sinai. Varying accommodation favoured progradation/retrogradation and the establishment of specific facies belts within different systems tracts. Shallow-water to supratidal and siliciclastic deposits govern the LSTs. Changes of the lithofacies and the palaeogeographic settings were controlled by relative sea-level rises, and extended inner-platform carbonates and occasional

high-energy deposits occur in TSTs; during highstands dolomitic inner-platform deposits aggraded in north Sinai, and protected, muddy inner-platform environments in association with prograding siliciclastics were common in central and south Sinai. In addition, seafloor topography in combination with shifts of the palaeo-coastline left particular imprints on the sequence architecture.

- Palaeogeographic maps allow to reconstruct the platform configuration and to estimate the minimum extensions of the C-S Basin. Several key episodes of the platform evolution have been verified:, the Cenomanian platform was drowned, coinciding with the early Turonian relative sea-level rise, and the formation of the C-S Basin. The C-S Basin was filled by shallow-subtidal sediments and a new platform built up since the middle Turonian. A pronounced shallowing event in the middle Turonian has been observed throughout Sinai. In the upper Coniacian, a further platform drowning is observed, caused by Syrian Arc movements associated with a relative sea-level rise.
- Uplift and subsidence influenced the depositional architectures. Tectonic events were deduced from laterally varying thickness of the stratal packages, which indicate differing synsedimentary subsidence balanced by sediment accumulation. Particular periods of increased subsidence are proposed during: post-CeSin 7 HST, post-TuSin 1 LST, post-TuSin 1 HST, and post-TuSin 2 LST.
- Several stratigraphic mismatches exist between the SBs in Sinai and those elsewhere in the Tethys. Synsedimentary tectonics in combination with relative sea-level changes explain the poor correlation regarding the SBs CeSin 7, TuSin 2, CoSin 1. Diachronous sequence boundaries in the Near East have been attributed to time-transgressive developments and differing amplitudes of basin subsidence and Syrian Arc tectonics.

ACKNOWLEDGEMENTS

Funding was provided by the German Science Foundation (Deutsche Forschungsgemeinschaft Ku 642/15-1). The authors thank M. M. Morsi and A. M. Bassiouni (both Ain Shams University, Cairo) for valuable help in preparing the field work programme, A. Marzouk (University of Tanta, Egypt) for the determination of calcareous nannofossils, F. Wiese (FU Berlin) and P. Luger (TU Berlin) for ammonite determination and U. Heimhofer (ETH Zurich) for his assistance during field work. M. Bachmann, R. Bätzel, E. Friedel and R. Speijer (all Bremen University) are acknowledged for various helpful assistances and comments.

REFERENCES

Abdallah, H., Sassi, S., Meister, C. and **Souissi, R.** (2000) Stratigraphie séquentielle et paléogéographie à la limite Cénomanien-Turonien dans la région de Gafsa-Chott area (Tunisie centrale). *Cretaceous Res.*, **21**, 35-106.

Abed, A.M. and **Amireh, B.S.** (1999) Sedimentology, geochemistry, economic potential and palaeogeography of an Upper Cretaceous phosphorite belt in southeastern desert of Jordan. *Cretaceous Res.*, **20**, 119-133.

Abu-Jaber, N.S., Kimberley, M.M. and **Cavaroc, V.V.** (1989) Mesozoic-Palaeogene basin development within the eastern Mediterranean borderland. *J. Petroleum Geol.*, **12**, 419-436.

Allam, A. and **Khalil, H.** (1988) Geology and stratigraphy of the Arif El-Naqa area, Sinai, Egypt. *Egypt. J. Geol.*, **32**, 199-218.

Almogi-Labin, A., Bein, A. and **Saas, E.** (1990) Agglutinated foraminifera in organic-rich neritic carbonates (Upper Cretaceous, Israel) and their use in identifying oxygen levels in oxygen-poor environments. In:

Paleocology, biostratigraphy, paleoceanography and taxonomy of agglutinated foraminifera (Ed. C. Hemleben), pp. 565-585. Kluwer Academic Publishers, Dordrecht.

Arthur, M.A., Schlanger, S.O. and **Jenkyns, H.C.** (1987) The Cenomanian-Turonian Oceanic Anoxic Event, II. Palaeoceanographic controls on organic-matter production and preservation. In: *Marine petroleum source rocks* (Eds J. Brooks and A.J. Fleets), *Geol. Soc. London Spec. Publ.*, **26,** pp. 401-420.

Bachmann, M. and **Kuss, J.** (1998) The Middle Cretaceous carbonate ramp of the northern Sinai: sequence stratigraphy and facies distribution. In: *Carbonate Ramps* (Eds V.P. Wright and T.P. Burchette), *Geol. Soc. London Spec. Publ.* **149,** 253-280.

Bandel, K., Kuss, J. and **Malchus, N.** (1987) The sediments of Wadi Qena (Eastern Desert, Egypt). *J. African Earth Sci.*, **6,** 427-455.

Bartov, Y. and **Steinitz, G.** (1977) The Judea and Mount Scopus groups in the Negev and Sinai with trend surface analysis of the thickness data. *Isr. J. Earth Sci.*, **26,** 119-148.

Bartov, Y., Lewy, Z., Steinitz, G. and **Zak, I.** (1980) Mesozoic and Tertiary stratigraphy, paleogeography and structural history of the Gebel Areif en Naqa area, eastern Sinai. *Isr. J. Earth Sci*, **29,** 114-139.

Bassoullet, J.-P. and **Damotte, R.** (1969) Quelques ostracodes nouveaux du Cénomano-Turonien de l'atlas saharien occidental (Algérie). *Revue Micropaléontol.*, **12,** 130-144.

Bauer, J., Steuber, T., Kuss, J. and **Heimhofer U.** (in press1) Distribution of shallow-water benthics: The Cenomanian – Turonian carbonate platform sequences of Sinai, Egypt. In: Proceedings of the 5th International Congress on Rudists. *Cour. Forschungsinst. Senckenberg.*

Bauer, J., Marzouk, A.M., Steuber T. and **Kuss J.** (in press2): Lithostratigraphy and biostratigraphy of the Cenomanian - Santonian strata of Sinai, Egypt. Cretaceous Res.

Bentor, Y.K. (1960) *Lexique stratigraphique international, Asie, 3/1,* (Israel), 151 pp. (Centre National de la Rechech Scientifique, Paris).

Bogoch, R., Buchbinder, B. and **Magaritz, M.** (1994) Sedimentology and geochemistry of lowstand peritidal lithofacies at the Cenomanian-Turonian boundary in the Cretaceous carbonate platform of Israel. *J. Sedim. Res.*, **A64,** 733-740.

Bosworth, W., Guiraud, R. and **Kessler, L.G.** (1999) Late Cretaceous (ca. 84 Ma) compressive deformation of the stable platform of northeast Africa (Egypt): far-field stress effects of the 'Santonian event' and origin of the Syrian Arc deformation belt. *Geology*, **27,** 633-636.

Bralower, T.J. (1988) Calcareous nannofossil biostratigraphy and assemblages of the Cenomanian-Turonian boundary interval: implications for the origin and timing of oceanic anoxia. *Paleoceanography*, **3,** 275-316.

Braun, M. and **Hirsch, F.** (1994) Mid Cretaceous (Albian-Cenomanian) carbonate platforms in Israel. *Cuadernos Geol. Ibérica*, **18,** 59-81.

Buchbinder, B., Benjamini, C. and **Lipson-Benitah, S.** (2000) Sequence development of Late Cenomanian-Turonian carbonate ramps, platforms and basins in Israel. *Cretaceous Res.*, **21,** 813-843.

Burchette, T.P. and **Britton, S.R.** (1985) Carbonate facies analysis in the exploration for hydrocarbons: a case-study from the Cretaceous of the Middle East. In: *Sedimentology: recent developments and applied aspects* (Eds P.J. Brenchley and B.P.J. Williams), *Geol. Soc. London Spec. Publ.*, **18,** 311-338.

Burnett, J.A. (1996) Nannofossils and Upper Cretaceous (sub-)stage boundaries - state of the art. *J. Nannoplankton Res.*, **18,** 23-32.

Camoin, G.F. (1991) Sedimentologic and paleotectonic evolution of carbonate platforms on a segmented continental margin: example of the African Tethyan margin during Turonian and early Senonian times. *Palaeogeogr., Palaeoclimatol., Palaeoecol.*, **87,** 29-52.

Caron, M. (1985) Cretaceous planktic foraminifera. In: *Plankton stratigraphy* (Eds H.M. Bolli, J.B. Saunders and K. Perch-Nielsen), pp. 17-86. Cambridge University Press, Cambridge.

Chancellor, G.R., Kennedy, W.J. and **Hancock, J.M.** (1994) Turonian ammonite faunas from central Tunisia. *Spec. Pap. Palaeontol.*, **50,** 118 pp.

Chérif, O.H., Al-Rifaiy, I.A., Al-Afifi, F.I. and **Orabi, O.H.** (1989a) Foraminiferal biostratigraphy and paleoecology of some Cenomanian-Turonian exposures in west-central Sinai (Egypt). *Rev. Micropaléont.*, **31,** 243-262.

Chérif, O.H., Al-Rifaiy, I.A., Al-Afifi, F.I. and **Orabi, O.H.** (1989b) Planktonic foraminifera and chronostratigraphy of Senonian exposures in west-central Sinai, Egypt. *Rev. Micropaléont.*, **32,** 167-184.

Collins, A.S. and **Robertson, A.H.F.** (1997) Lycian melange, southwestern Turkey: an emplaced Late Cretaceous accretionary complex. *Geology*, **25,** 255-258.

Crux, J.A. (1982) Upper Cretaceous (Cenomanian to Campanian) calcareous nannofossils. In: *A stratigraphical index of calcareous nannofossils* (Ed. A.R. Lord), *British Micropalaeontol. Soc.,* pp. 80-135. Ellis Horwood Limited, Chichester.

Davey, S.D. and **Jenkyns, H.C.** (1999) Carbon-isotope stratigraphy of shallow-water limestones and implications for the timing of Late Cretaceous sea-level rise and anoxic events (Cenomanian-Turonian of the peri-Adriatic carbonate platform, Croatia). *Ecolgae geol. Helv.*, **92,** 163-170.

Dobruskina, I.A. (1997) Turonian plants from the southern Negev, Israel. *Cretaceous Res.*, **18,** 87-107.

Drzewiecki, P.A. and **Simo, J.A.** (1997) Carbonate platform drowning and oceanic anoxic events on a mid-Cretaceous carbonate platform, south-central Pyrenees, Spain. *J. Sedim. Res.*, **67,** 698-714.

El-Hawat, A.S. (1997) Sedimentary basins of Egypt: an overview of dynamic stratigraphy. In: *African Basins* (Ed. R.C. Selley), *Sedimentary basins of the World,* **3,** pp. 39-85. Elsevier, Amsterdam.

Eweda, S. and **El-Sorogy, A.S.** (1999) Stratigraphy and facies development of the Upper Cretaceous-Lower Tertiary succession in Wadi Feiran area, southwestern Sinai, Egypt. *Neues Jb Geol. Paläontol. Abh.*, **211,** 263-289.

Flexer, A., Gilat, A., Hirsch, F., Honigstein, A., Rosenfeld, A. and **Rueffer, T.** (1989) Late Cretaceous evolution of the Judean Mountains as indicated by ostracodes. *Terra Nova*, **1,** 349-358.

Freund, R. and **Raab, M.** (1969) Lower Turonian ammonites from Israel. *Spec. Pap. Palaeontol.*, **4,** 83 pp.

Gradstein, F.M., Agterberg, F.P., Ogg, J.G., Hardenbol, J., Van Veen, P., Thierry, J. and **Huang, Z.** (1995) A Triassic, Jurassic and Cretaceous time scale. In: *Geochronology, time scales and global stratigraphic correlation* (Eds W. A. Berggren, D. V. Kent, M.-P. Aubry and J. Hardenbol), *SEPM Spec. Publ.*, **54,** 95-126.

Guiraud, R. (1998) Mesozoic rifting and basin inversion along the northern African Tethyan margin: an overview. In: *Petroleum geology of North Africa* (Eds D.S. Macgregor, R.T.J. Moody and D.D. Clark-Lowes), *Geol. Soc. London Spec. Publ.*, **132,** 217-229.

Guiraud, R. and **Bosworth, W.** (1997) Senonian basin inversion and rejuvenation of rifting in Africa and Arabia: synthesis and implications to plate-scale tectonics. *Tectonophysics*, **282,** 39-82.

Gvirtzman, Z. and **Garfunkel, Z.** (1998) The transformation of southern Israel from a swell to a basin: stratigraphic and geodynamic implications for intracontinental tectonics. *Earth Planetary Sci. Letters*, **163,** 275-290.

Hamza, F.H. (1993) Upper Cretaceous rudist-coral buildups associated with tectonic doming in the Abu Roash area, Egypt. *Neues Jb Geol. Paläontol. Mh.*, **1993,** 75-87.

Hancock, J.M. (1993) Sea-level changes around the Cenomanian-Turonian boundary. *Cretaceous Res.*, **14,** 553-562.

Handford, C.R. and **Loucks, R.G.** (1993) Carbonate depositional sequences and systems tracts - response of carbonate platforms to relative sea-level changes. In: *Carbonate sequence stratigraphy. Recent developments and applications* (Eds R.G. Loucks and J.F. Sarg), *AAPG Mem.*, **57,** pp. 3-41.

Haq, B.U., Hardenbol, J. and **Vail, P.R.** (1987) Chronology of fluctuating sea levels since the Triassic. *Science*, **235,** 1156-1167.

Hardenbol, J., Thierry, J., Farley, M.B., Jacquin, T., Graciansky, P.-C.D. and **Vail, P.R.** (1998) Mesozoic and Cenozoic sequence chronostratigraphic framework of European basins, Cretaceous Biochronostratigraphy. In: *Mesozoic and Cenozoic sequence stratigraphy of European basins* (Ed. P.-C. de Graciansky, J. Hardenbol, T. Jacquin and P.R. Vail), *SEPM Spec. Publ.*, **60,** Chart 5.

Hardenbol, J. and **Robaszynski, F.** (1998) Introduction to the Upper Cretaceous. In: *Mesozoic and Cenozoic Sequence stratigraphy of European basins* (Eds P.-C. de Graciansky, J. Hardenbol, T. Jacquin and P.R. Vail), *SEPM Spec. Publ.*, **60,** pp. 329-332.

Harris, P.M., Frost, S.H., Seiglie, G.A. and **Schneidermann, N.** (1984) Regional unconformities and depositional cycles, Cretaceous of the Arabian Peninsula. In: *Interregional unconformities and hydrocarbon accumulation* (Ed. J.S. Schlee), *AAPG Mem.*, **36,** pp. 67-80.

Hirsch, F., Bassoullet, J.-P., Cariou, É., Conway, B., Feldman, H.R., Grossowicz, L., Honigstein, A., Owen, E.F. and **Rosenfeld, A.** (1998) The Jurassic of the southern Levant. Biostratigraphy, palaeogeography and cyclic events. In: *Peri-Tethys Memoir 4: epicratonic basins of Peri-Tethyan platforms* (Eds S. Crasquin-Soleau and É. Barrier), *Mém. Mus. Natn. Hist. Nat.*, **179,** 213-235.

Honigstein, A., Flexer, A. and **Rosenfeld, A.** (1988) Tectonic activity in the Syrian Arc in Israel, as indicated by

Senonian ostracodes. *Neues Jb Geol. Paläontol. Mh*, **1988,** 173-183.

Honigstein, A., Lipson-Benitah, S., Conway, B., Flexer, A. and **Rosenfeld, A.** (1989) Mid-Turonian anoxic event in Israel - a multidisciplinary approach. *Palaeogeogr., Palaeoclimatol., Palaeoecol.*, **69,** 103-112.

Hunt, D. and **Tucker, M.E.** (1993) Sequence stratigraphy of carbonate shelves with an example from the mid-Cretaceous (Urgonian) of southeast France. In: *Sequence stratigraphy and facies associations* (Eds H.W. Posamentier, C.P. Summerhayes, B.U. Haq and G.P. Allen), *Int. Assoc. Sedimentol. Spec. Publ.*, **18,** 307-341.

Issawi, B., El-Hinnawi, M., Francis, M. and **Mazhar, A.** (1999) The Phanerozoic geology of Egypt: a geodynamic approach. *Egypt. Geol. Surv. Spec. Publ.*, **76,** 462 pp.

Jarvis, I., Carson, G.A., Cooper, M.K.E., Hart, M.B., Leary, P.N., Tocher, B.A., Horne, D. and **Rosenfeld, A.** (1988) Microfossil assemblages and the Cenomanian-Turonian (late Cretaceous) Oceanic Anoxic Event. *Cretaceous Res.*, **9,** 3-103.

Jenkins, D. (1990) north and central Sinai. In: *The Geology of Egypt* (Ed. R. Said), pp. 361-380. Balkema, Rotterdam

Kassab, A.S. (1996) Cenomanian-Turonian boundary in the Gulf of Suez region: towards an inter-regional correlation, based on ammonites. *Geol. Soc. Egypt, Spec. Publ.*, **2,** 61-98.

Kassab, A.S. and **Ismael, M.M.** (1994) Upper Cretaceous invertebrate fossils from the area northwest of Abu Zuneima, Sinai, Egypt. *Neues Jb Geol. Paläontol. Abh.*, **191,** 221-249.

Kassab, A.S. and **Obaidalla, N.A.** (2001) Integrated biostratigraphy and inter-regional correlation of the Cenomanian-Turonian deposits of Wadi Feiran, Sinai, Egypt. *Cretaceous Res.*, **22,** 105-114.

Kauffmann, E.G. (1995) Global change leading to biodiversity crisis in a greenhouse world: the Cenomanian-Turonian (Cretaceous) mass extinction. In: *Effects of past global change on life* (Eds. S.M. Stanley, A.H. Knoll and J. Kennett), pp. 47-71. National Academy Press, Washington D.C.

Kerdany, M.T. and **Chérif, O.H.** (1990) Mesozoic. In: *The geology of Egypt* (Ed. R. Said), pp. 407-438. Balkema, Rotterdam.

Kerr, A.C. (1998) Oceanic plateau formation: a cause of mass extinction and black shale deposition around the Cenomanian-Turonian boundary?. *J. Geol. Soc. London*, **155,** 619-626.

Khalil, B. (1992) The geology of the Ar Rabba area. *1:50,000 Geological Mapping Series Bull.* (Jordan), **22,** 160 pp.

Kora, M., Shahin, A. and **Semeit, A.** (1994) Biostratigraphy and paleoecology of some Cenomanian successions in the west central Sinai, Egypt. *Neues Jb Geol. Paläontol. Mh*, **1994,** 597-617.

Kora, M. and **Genedi, A.** (1995) Lithostratigraphy and facies development of Upper Cretaceous carbonates in east central Sinai, Egypt. *Facies*, **32,** 223-236.

Krenkel, E. (1924) Der syrische Bogen. *Zbl Mineral. Geol. Palaeontol. Abh. B*, **9,** 274-281 and **10,** 301-313.

Kuhnt, W., Nederbragt, A. and **Leine, L.** (1997) Cyclicity of Cenomanian-Turonian organic-carbon-rich sediments in the Tarfaya Atlantic Coastal Basin (Marocco). *Cretaceous Res.*, **18,** 587-601.

Kunow, R., Bauer, J., Bachmann, M. and **Kuss, J.** (1997) Verteilungsmuster benthischer Foraminiferen und Tonmineralassoziationen im Oberapt des Sinai. *Zbl Geol. Paläontol. Teil I*, **H1/2,** 353-371.

Kuss, J. (1992) Facies and stratigraphy of Cretaceous limestones from northeast Egypt, Sinai, and southern Jordan. In: *Geology of the Arab World* (Ed. A Sadek), *Proceedings 1st International Conference on the Geology of the Arab World, Cairo University, 1992,* pp. 283-301.

Kuss, J. and **Bachmann, M.** (1996) Cretaceous paleogeography of the Sinai Peninsula and neighbouring areas. *C.R. Acad. Sci. Paris, Serie IIa,* **322,** 915-933.

Kuss, J. and **Malchus, N.** (1989) Facies and composite biostratigraphy of Late Cretaceous strata from northeast Egypt. In: *Cretaceous of the Western Tethys. Proceedings 3rd International Cretaceous Symposium, Tübingen, 1987* (Ed. J. Wiedmann), pp. 879-910. Schweizerbart, Stuttgart.

Kuss, J., Scheibner, C. and **Gietl, R.** (2000a) Carbonate platform to basin transition along an Upper Cretaceous to Lower Tertiary Syrian Arc uplift, Galala Plateaus, Eastern Desert, Egypt. *GeoArabia,* **5,** 405-424.

Kuss, J., Westerhold, T., Groß, U., Bauer, J. and **Lüning, S.** (2000b) Mapping of Late Cretaceous stratigraphic sequences along a Syrian Arc Uplift - examples from the Areif el Naqa / Eastern Sinai. *Middle East Res. Center, Ain Shams Univ., Earth Sci. Ser.*, **14,** 171-191.

Lewy, Z. (1975) The geological history of southern Israel and Sinai during the Coniacian. *Isr. J. Earth Sci.*, **24,** 19-43.

Lewy, Z. (1989) Correlation of lithostratigraphic units in the upper Judea Group (late Cenomanian-late Coniacian) in Israel. *Isr. J. Earth Sci.*, **38,** 37-43.

Lewy, Z. (1990) Transgressions, regressions and relative sea-level changes on the Cretaceous shelf of Israel and adjacent countries. A critical evaluation of Cretaceous global sea-level correlations. *Paleoceanography*, **5,** 619-637.

Lewy, Z. and **Avni, Y.** (1988) Omission surfaces in the Judea Group, Makhtesh Ramon region, southern Israel, and their paleogeographic significance. *Isr. J. Earth Sci.*, **37,** 105-113.

Lipson-Benitah, S. (1994) Cenomanian stratigraphical micropaleontology of shelf deposits - Israel. *Revista Española Micropaleontol.*, **25,** 83-100.

Lipson-Benitah, S., Honigstein, A. and **Rosenfeld, A.** (1985) Early Turonian to early Senonian biostratigraphy (foraminifera and ostracodes) of Damun-7 borehole, Galilee, northwestern Israel. *Neues Jb Geol. Paläontol. Mh*, **1985,** 100-114.

Lipson-Benitah, S., Flexer, A., Rosenfeld, A., Honigstein, A., Conway, B. and **Eris, H.** (1990) Dysoxic sedimentation in the Cenomanian-Turonian Daliyya Formation, Israel. *AAPG, Studies in Geology*, **30,** 27-39.

Lüning, S., Kuss, J., Bachmann, M., Marzouk, A.M. and **Morsi, A.M.** (1998a) Sedimentary response to basin inversion: Mid Cretaceous - Early Tertiary pre- to syndeformational deposition at the Areif El Naqa anticline (Sinai, Egypt). *Facies*, **38,** 103-136.

Lüning, S., Marzouk, A.M., Morsi, A.M. and **Kuss, J.** (1998b) Sequence stratigraphy of the Upper Cretaceous of central-east Sinai, Egypt. *Cretaceous Res.*, **19,** 153-196.

Morsi, A.M. and Bauer, J. (in press) Cenomanian ostracode faunas from Sinai peninsula, Egypt. *Revue Paléobiologie*, **20.**

Mostafa, A.R. (1999) Organic geochemistry of the Cenomanian-Turonian sequence in the Bakr area, Gulf of Suez, Egypt. *Petroleum Geosci.*, **5,** 43-50.

Moustafa, A.R. and **Khalil, M.H.** (1990) Structural characteristics and tectonic evolution of north Sinai fold belts. In: *The geology of Egypt* (Ed. R. Said), pp. 381-389. Balkema, Rotterdam.

Patton, T.L. and **O'Connor, S.J.** (1988) Cretaceous flexural history of northern Oman mountain foredeep, United Arab Emirates. *AAPG Bull.*, **72,** 797-809.

Philip, J. (1998) Sequences and systems tracts of mixed carbonate-siliciclastic platform-basin settings: the Cenomanian-Turonian stages of Provence (southeastern France). In: *Mesozoic and Cenozoic sequence stratigraphy of European basins* (Ed. P.-C. de Graciansky, J. Hardenbol, T. Jacquin and P.R. Vail), *SEPM Spec. Publ.*, **60,** pp. 387-395.

Philip, J.M. and **Airaud-Crumiere, C.** (1991) The demise of the rudist-bearing carbonate platforms at the Cenomanian/Turonian boundary: a global control. *Coral Reefs*, **10,** 115-125.

Philip, J., Borgomano, J. and **Al-Maskiry, S.** (1995) Cenomanian-early Turonian carbonate platform of northern Oman: stratigraphy and palaeo-environments. *Palaeogeogr., Palaeoclimatol., Palaeoecol.*, **119,** 77-92.

Philip, J. et al. (12 co-authors) (2000) Late Cenomanian. In: *Atlas Peri-Tethys palaeogeographical maps* (Eds J. Dercourt, M. Gaetani, B. Vrielynck, E. Barrier, B. Biju-Duval, M.F. Brunet, J.P. Cadet, S. Crasquin and M. Sandulescu), Map 14. CCGM/CGMW, Paris.

Reiss, Z. (1988) Assemblages from a Senonian high-productivity sea. *Revue Paléobiologie, Spec. Publ. 'Benthos 86'* **2,** 323-332.

Robaszynski, F., Caron, M., Dupuis, C., Amédro, F., Gonzalez Donoso, J.-M., Linares, D., Hardenbol, J., Gartner, S., Calandra, F., and **Deloffre, R.** (1990) A tentative integrated stratigraphy in the Turonian of central Tunisia: formations, zones and sequential stratigraphy in the Kalaat Senan area. *Bull. Centres Rech. Explor.-Product. Elf Aquitaine*, **14,** 214-384.

Robaszynski, F., Hardenbol, J., Caron, M., Amédro, F., Dupuis, C., González Donoso, J.-M., Linares, D., and **Gartner, S.** (1993) Sequence stratigraphy in a distal environment: the Cenomanian of the Kalaat Senan region (Central Tunisia), *Bull. Centres Rech. Explor.-Product. Elf Aquitaine*, **17,** 395-433.

Rosenfeld, A. and **Raab, M.** (1974) Cenomanian-Turonian ostracodes from the Judea Group in Israel. *Geol. Surv. Isr. Bull.*, **62,** 64 pp.

Rosenthal, E., Weinberger, G., Almogi-Labin, A. and **Flexer, A.** (2000) Late Cretaceous-Early Tertiary development of depositional basins in Samaria as a reflection of eastern Mediterranean tectonic evolution. *AAPG Bull.*, **84,** 997-1014.

Sadler, P.M. (1981) Sediment accumulation rates and the completeness of stratigraphic sections. *J. Geol.*, **89,** 569-584.

Said, R. (1962) *The Geology of Egypt.* Elsevier, Amsterdam, 377 pp.

Said, R. (1990) Cretaceous paleogeographic maps. In: *The Geology of Egypt* (Ed. R. Said), pp. 439-449. Balkema, Rotterdam.

Saidi, F., Ben Ismail, M.H. and **M'Rabet, A.** (1997) Le Turonien de Tunisie centro-occidentale: faciès, paléogéographie et stratigraphie séquentielle d'une plate-forme carbonatée ennoyée. *Cretaceous Res.*, **18,** 63-85.

Saint-Marc, P. (1974) Étude stratigraphique et micropaléontologique de l'Albien, du Cénomanien et du Turonien du Liban. *Mus. Natn. Hist. Nat. Paris*, **13,** 298 pp.

Sandler, A. (1996) A Turonian subaerial event in Israel: karst, sandstone and pedogenesis. *Geol. Surv. Isr. Bull*, **85,** 1-52.

Schlager, W. (1999) Type 3 sequence boundaries. In: *Advances in carbonate sequence stratigraphy: application to reservoirs, outcrops and models* (Eds P.M. Harris, A.H. Saller and J.A. Simo), *SEPM Spec. Publ.*, **63,** 35-45.

Schröder, R. and **Neumann, M.** (1985) Les grandes foraminifères du Crétacé moyen de la région Méditerranéenne. *Geobios Mém. Spec.*, **7,** 160 pp.

Schulze, F. and **Kuss, J.** (2000) Biostratigraphy and cyclicities of the late Albian to Turonian carbonate platform in Central Jordan. In: *Abstracts, 6th International Cretaceous Symposium, Vienna*, p. 133.

Scott, R.W., Schlager, W., Fouke, B. and **Nederbragt, S.A.** (2000) Are mid-Cretaceous eustatic events recorded in Middle East carbonate platforms? In: *Middle East models of Jurassic/Cretaceous carbonate systems* (Eds A.S. Alsharhan and R.W. Scott), *SEPM Spec. Publ.*, **69,** 77-88.

Shahar, J. (1994) The Syrian Arc system: an overview. *Palaeogeogr., Palaeoclimatol., Palaeoecol.*, **112,** 125-142.

Shahin, A. (1991) Cenomanian-Turonian ostracods from Gebel Nezzazat, southwestern Sinai, Egypt, with observations on δ13 C values and the Cenomanian/Turonian boundary. *J. Micropalaeontol.*, **10,** 133-150.

Sharland, P.R., Archer, R., Casey, D.M., Davies, R.B., Hall, S.H., Heward, A.P., Horbury, A.D. and **Simmons, M.D.** (2001) *Arabian Plate sequence stratigraphy. GeoArabia Spec. Publ.* **2**, 371 pp.

Shinaq, R. and **Bandel, K.** (1998) Lithostratigraphy of the Belqa Group (Late Cretaceous) in northern Jordan. *Mitt. Geol.-Paläontol. Inst. Univ. Hamburg*, **81,** 163-184.

Steuber, T. and **Löser, H.** (2000) Species richness and abundance patterns of Tethyan Cretaceous rudist bivalves (Mollusca: Hippuritacea) in the central-eastern Mediterranean and Middle East, analysed from a palaeontological database. *Palaeogeogr., Palaeoclimatol., Palaeoecol.*, **162,** 75-104.

Strasser, A., Pittet, B., Hillgärtner, H. and **Pasquier, J.-B.** (1999) Depositional sequences in shallow carbonate-dominated sedimentary systems: concepts for a high-resolution analysis. *Sedim. Geol.*, **128,** 201-221.

Vail, P.R., Audemard, F., Bowman, S.A., Eisner, P.N. and **Perez-Cruz, C.** (1991) The stratigraphic signatures of tectonics, eustasy and sedimentology - an overview. In: *Cycles and events in stratigraphy* (Ed. G. Einsele, W. Ricken and A. Seilacher), pp. 617-659. Springer, Heidelberg.

Van Buchem, F.S.P., Razin, P., Homewood, P.W., Philip, J.M., Eberli, G.P., Platel, J.-P., Roger, J., Eschard, R., Desaubliaux, Guy M.J., Boisseau, et al. (1996) High resolution sequence stratigraphy of the Natih Formation (Cenomanian/Turonian) in northern Oman: distribution of source rocks and reservoir facies. *GeoArabia*, **1,** 65-91.

Van den Bold, W.A. (1964) Ostracoden aus der Oberkreide von Abu-Rawash, Ägypten. *Palaeontographica*, **123,** 111-136.

Van Wagoner, J.C., Posamentier, H.W., Mitchum, R.M., Vail, P.R., Sarg, J.F., Loutit, T.S. and **Hardenbol, J.** (1988) An overview of the fundamentals of sequence stratigraphy and key definitions. In: *Sea-level changes - an integrated approach* (Eds C.K. Wilgus, B.S. Hastings, C.G.St.C. Kendall, H.W. Posamentier, C.A. Ross and J.C. Van Wagoner), *SEPM Spec. Publ.*, **42,** 39-45.

Vidal, N., Alvarez-Marrón, J. and **Klaeschen, D.** (2000) Internal configuration of the Levantine Basin from seismic reflection data (eastern Mediterranean). *Earth Planetary Sci. Letters*, **180,** 77-89.

Walley, C.D. (1998) Some outstanding issues in the geology of Lebanon and their importance in the tectonic evolution of the Levantine region. *Tectonophysics*, **298,** 37–62.

Weissert, H., Lini, A., Föllmi, K.B. and **Kuhn, O.** (1998) Correlation of Early Cretaceous carbon isotope stratigraphy and platform drowning events: a possible link? *Palaeogeogr., Palaeoclimatol., Palaeoecol.*, **137,** 189-203.

Ziko, A., Darwish, M. and **Eweda, S.** (1993) Late Cretaceous - Early Tertiary stratigraphy of the Themed area, east central Sinai, Egypt. *N. Jb Geol. Paläontol. Mh*, **1993,** 135-149.

CHAPTER 4

Distribution of shallow-water benthics (rudists, calcareous algae, benthic foraminifers) in the Cenomanian - Turonian carbonate platform sequences of Sinai, Egypt

Jan Bauer, Thomas Steuber, Jochen Kuss & Ulrich Heimhofer

In press in
Proceedings of the 5th International Congress on Rudists,-
Courier Forschungsinstitut Senckenberg

CHAPTER 4

Distribution of shallow-water benthics (rudists, calcareous algae, benthic foraminifers) in the Cenomanian - Turonian carbonate platform sequences of Sinai, Egypt

Jan Bauer*, Thomas Steuber, Jochen Kuss* & Ulrich Heimhofer#**

Proceedings of the 5th International Congress on Rudists,- Courier Forschungsinstitut Senckenberg, in press

* Bremen University, Department of Geoscience, PO Box 330440, D-28334 Bremen, Germany
** Ruhr-University Bochum, Institute of Geology, Mineralogy and Geophysics, Universitätsstr. 150, D-44801 Bochum, Germany
# Department of Earth Sciences, Geological Institute, ETH Zurich, Sonneggstr. 5, CH-8092 Zuerich, Switzerland

ABSTRACT

Rudist bivalves, benthic foraminifers and calcareous algae are common in the Upper Cenomanian-Turonian Tethyan inner platform deposits of the Sinai peninsula. In this study, special emphasis is placed on the vertical distribution of these benthic organisms across the Cenomanian-Turonian transition, and on laterally varying occurrences along a N-S transect involving a sequence stratigraphic interpretation of Cenomanian and Turonian sediments. A significant disturbance of latest Cenomanian carbonate production was followed by flooding of the Upper Cenomanian inner platform during the Early Turonian and the establishment of a new carbonate platform during the Middle-Late Turonian. Diversities and frequencies of the studied fossils are distinctively different in Cenomanian and Turonian deposits. Rudists and benthic foraminifers are common in the Upper Cenomanian successions but occurrences decline drastically in the Lower Turonian and recover again in the Middle-Upper Turonian. In contrast, calcareous algae of Upper Cenomanian deposits are species-poor and flourished in the Lower and Upper Turonian. In addition to these large scale distribution trends, the occurrences of the studied benthics is closely related to regional facies belts, which prevail in individual systems tracts. Rudists occur mainly in HSTs, benthic foraminifers and calcareous algae mainly in TSTs and HSTs. The correlation of facies, systems tracts and biota distribution suggests a link between repeated reorganisation processes of the depositional system due to relative sea-level changes and the distribution of individual benthic groups.

KEYWORDS: Sinai, Cenomanian, Turonian, carbonate platform, rudists, benthic foraminifers, calcareous algae, sequence stratigraphy

ZUSAMMENFASSUNG

Rudisten, benthische Foraminiferen und Kalkalgen sind häufig in den Obercenoman-Turon Ablagerungen der Tethys Karbonatplattform auf der Sinai-Halbinsel anzutreffen. Diese Studie geht besonders auf die vertikalen Verteilungsmuster dieser Gruppen im Bereich der Cenoman–Turon Grenze ein sowie auf laterale Häufigkeitsvariationen entlang eines über die Halbinsel verlaufenden N-S Längsprofils unter Einbeziehung sequenzstratigraphischer Interpretationen. Eine eingeschränkte Karbonatproduktion im Obercenoman (vermutlich in der *Guerangeri* Ammoniten-Biozone) folgte ein Überfluten der inneren Plattform im Unterturon und dem Aufbauen einer neuen Karbonatplattform im Mittel- und Oberturon. Änderungen in Diversitäten und Häufigkeiten des Benthos sind nach der Cenoman-Turon Grenze deutlich. Die Häufigkeiten der in den Obercenoman-Abfolgen noch weitverbreiteten Rudisten und benthischen Foraminiferen nehmen in den Unterturon Ablagerungen deutlich ab und im Mittel- und Oberturon wieder zu. Dagegen sind Kalkalgen im Obercenoman in geringer Diversität vertreten, Häufigkeiten und Diversitäten nehmen aber im Unter-und Mittelturon deutlich zu. Neben diesen übergeordneten Verteilungsmustern sind die Häufigkeiten der untersuchten Organismen eng mit der regionalen Verteilung von Faziesgürteln verknüpft, die wiederum in einzelnen Systems Tracts überwiegen: Rudisten trteten meist in HSTs auf, benthische Foraminiferen und Kalkalgen sind in TSTs und HSTs häufig. Die Korrelation von Fazies und Systems Tracts mit der Organismenverteilung deutet auf einen Zusammenhang zwischen der wiederholten Umgestaltung des Ablagerungsraumes aufgrund von relativen Meeresspiegelschwankungen und der Verbreitung einzelner Organismengruppen.

1. INTRODUCTION

The biological turnover of benthic biota at the Cenomanian–Turonian boundary and the following recovery patterns are well studied in a variety of different palaeogeographic settings and depositional environments (e.g. JARVIS et al. 1988, PHILIP & AIRAUD-CRUMIERE 1991, HARRIES 1993, HART 1996). The Cenomanian-Turonian boundary event is characterised by anomalous fluctuations of geochemical parameters, such as a positive $\delta^{13}C$ excursion and a widespread oceanic anoxic event (OAE II), coinciding with a maximum sea-level highstand (recent reviews e.g. in ARTHUR et al. 1987, JARVIS et al. 1988, KAUFFMAN 1995, KAUFFMAN & HART 1996, KUYPERS et al. 1999). A stepwise extinction event affected 7% of families and 26 % of all genera (KERR 1998). Only 14% of benthic foraminifers transgressed the boundary (SCHROEDER & NEUMANN 1985), a global extinction affected keeled planktic foraminifers (*Rotalipora*), and a major depletion occurred among the mollusca. Rudist bivalves especially experienced an important selective extinction event at the Cenomanian-Turonian boundary. Predominantly aragonite-dominated genera became extinct and the Hippuritidae which dominated many post-Cenomanian rudist-associations appeared (PHILIP & AIRAUD-CRUMIERE 1991). Rudists recovered in the Middle Turonian with the renewed distribution of the Radiolitidae and the expansion of the Hippuritidae (STEUBER & LÖSER 2000). The Cenomanian-Turonian boundary event is well studied in basinal deposits around the world, while relatively few studies are concerned with its effects on shallow, carbonate shelves (e.g. MERMIGHIS et al. 1991, PHILIP & AIRAUD-CRUMIERE 1991). In this study we focus on the predominantly shallow-marine Upper Cenomanian to Upper Turonian successions of

Sinai. We have analysed the regional distribution of rudists, benthic foraminifers and calcareous algae across the Cenomanian–Turonian boundary with the aim to determine controlling factors of their varying distributions in consideration of laterally and vertically varying facies, that reflect different depositional environments. The Mid-Cretaceous depositional history is reconstructed in terms of sequence stratigraphy, following the subdivisions of Lower Cretaceous platform sediments of the region given by BACHMANN & KUSS (1998) and by LÜNING et al. (1998a) for the Upper Cretaceous successions. Based on a multibiostratigraphic frame, correlations of stratigraphic and facies-related distribution patterns of the examined biota within this sequence stratigraphic model give us a useful tool to delineate the controlling factors of faunal and floral distributions.

Generally, rudists, benthic foraminifers, and calcareous algae reacted sensitively to ecological changes of the depositional environment such as salinity, temperature, nutrient and oxygen conditions, circulation, water energy, bathymetry, and accomodation space. Moreover, these palaeoecologic factors were likely influenced by relative sea-level changes, which may have resulted in changing distribution patterns of these organisms. We compare the distribution charts of three benthic groups within the recognised systems tracts to interpret the interrelationships between benthic-distribution and environmental changes. Special emphasises is given to local 3rd-order relative sea-level changes and the resulting changes of accommodation space, hydrodynamic regimes and detritic input. Moreover, the overall stratigraphically varying occurrences of the examined biota, independent of the systems tracts and/or different positions on the former platform (e.g. distance from the palaeoshoreline), make large-scale trends visible.

2. GEOLOGICAL SETTING

During the Cretaceous, the Sinai peninsula was part of the Arabo-African platform (PHILIP et al. 1993) at the southern margin of the Tethys, while deeper-marine Cretaceous deposits are known from offshore drillings farther north (HIRSCH et al. 1995). In outcrop, the shallow-marine Cretaceous sediments overlie Jurassic and Lower Cretaceous continental sandstones in north Sinai, whereas Cambrian-Triassic sediments and Precambrian basement rocks underlie the Cretaceous successions in south Sinai. Relative sea-level changes clearly influenced the depositional history of the area throughout the Cretaceous (FLEXER et al. 1986, LEWY 1990, BACHMANN & KUSS 1998, LÜNING et al. 1998a, BUCHBINDER et al. 2000) and the Tertiary (LÜNING et al. 1998b). The flooding of the pre- and Lower Cretaceous continental deposits began during the Late Aptian as a consequence of a relative sea-level rise. A north-dipping carbonate ramp established and shallow-marine deposits in the northernmost edge of Sinai interfinger with deltaic sediments further to the south (BACHMANN & KUSS 1998). An Albian transgression led to a subsequent southward retreat of the deltaic facies, although repeated episodes of prograding and retrograding coastlines reflect low-order sea-level fluctuations superimposed on this long-term transgressive trend (BACHMANN & KUSS 1998). In Cenomanian and Turonian times, a broad carbonate platform covered the area, with a N-S extension of at least 200 km. In Sinai, there is no inclination indicated for this platform (in contrast to the Aptian-Albian ramp morphology) and subtidal/peritidal, mainly calcareous sediments were deposited in wide areas. Deep-water

deposits are limited to the Lower Turonian strata in Sinai and reflect a drowning of the platform that re-established in Middle and Late Turonian times (KUSS 1992).

Lateral and vertical facies changes during the Coniacian-Santonian are expressed by hemipelagic deeper-shelf sediments interfingering with shallow-marine deposits over short distances, resulting from synsedimentary tectonic movements (LEWY 1975; BARTOV & STEINITZ 1977, BARTOV et al. 1980). At this time, swell and basin morphologies established in central and north Sinai. The beginning closure of the Neotethyan Ocean caused compressional stress and led to structural inversion of older Mesozoic, rift-induced ENE-trending half-graben structures (e.g. COHEN et al. 1990, MOUSTAFA & KHALIL 1990, BOSWORTH et al. 1999). These Senonian reverse faultings and uplifts marked the onset of Tertiary epeirogenic movements („Syrian Arc" system, KRENKEL 1924) that resulted in domal anticlines extending from present-day central Syria, Near East, north Sinai to western Egypt (JENKINS 1990, CHAIMOV et al. 1992).

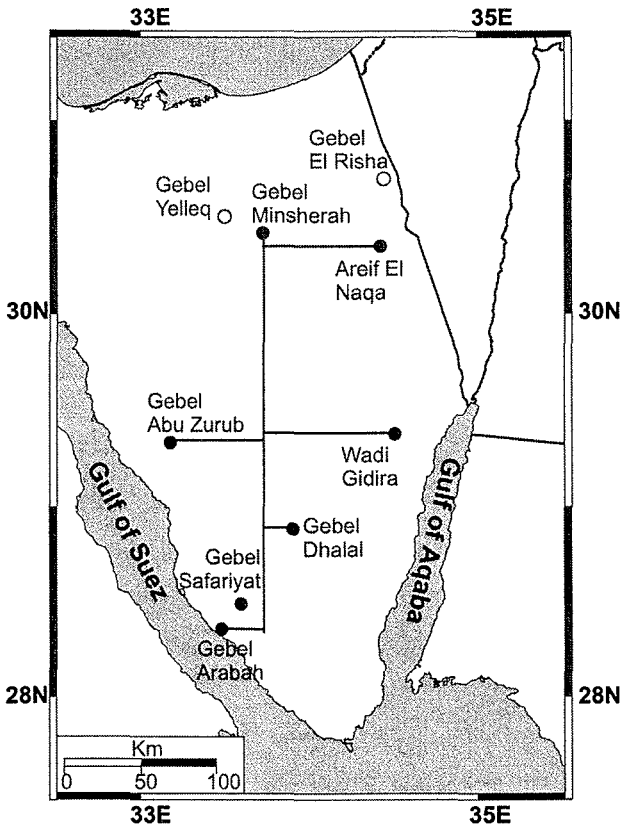

Fig. 1: Location map of the sections presented and traverse of correlation illustrated in Fig. 11. Black dots represent figured sections, white dots represent sections only mentioned in the text.

3. METHODS AND MATERIAL

The sedimentological, cyclostratigraphic and palaeogeographic evolution of 21 Cenomanian and Turonian sections in Sinai (Fig. 1) were studied. The analysis of laterally and vertically changing stacking patterns is based on the analysis of sedimentary structures, microfacies, petrography and biostratigraphy. Benthic foraminifers and calcareous algae were studied in thin sections. The determi-

nations of benthic foraminifers mainly followed HAMAOUI & SAINT-MARC (1970), SAINT-MARC (1974), SCHRÖDER & NEUMANN (1985), LOEBLICH & TAPPAN (1988); those of calcareous algae followed descriptions given by BASSOULLET et al. (1983), BARATTOLO (1991) and KUSS & CONRAD (1991). For the classification of semiquantitative distribution, five abundance classes were defined, using a visual percentage estimation: rare (< 5 %), few (5 %-10 %), common (10 %-30 %), abundant (>30 %), very abundant (rock-forming).

The sequence stratigraphic classification and nomenclature is based on general concepts of SARG (1988), VAN WAGONER et al. (1988) and VAIL et al. (1991) as well as on special concepts for carbonate shelves of BURCHETTE & WRIGHT (1992), HANDFORD & LOUCKS (1993), WRIGHT & BURCHETTE (1996) and regional interpretations by BACHMANN & KUSS (1998) and LÜNING et al. (1998a).

4. STRATIGRAPHY

Biostratigraphy. The biostratigraphic resolution of the studied sections is limited owing to the long ranges of biostratigraphically indicative taxa. To achieve the best possible biostratigraphic resolution, all indicative fossil groups were examined by BAUER et al. (subm.) including ammonites, ostracods and calcareous nannoplankton (Fig. 2). Benthic foraminifers and rudists supplemented the biostratigraphic data.

A diverse fauna of densely packed ammonites occurs in a dolomite unit directly overlying the Cenomanian-Turonian boundary in north (Gebel Areif El Naqa) and central Sinai (Gebel Abu Zurub, Wadi El Gidira, Gebel Dhalal). *Choffaticeras luciae, Choffaticeras segne, Thomasites rollandi, Vascoceras* sp. (determined by F. WIESE and P. LUGER, Berlin) indicate an Early Turonian age. Although these ammonites do not confirm one of the two Lower Turonian biozones (*Watinoceras coloradoense* followed by *Mammites nodosoides)*, BARTOV et al. (1980) and ALLAM & KHALIL (1988) reported the index fossil *Mammites nodosoides* in this bed at Gebel Areif El Naqa. This suggests a hiatus at the Cenomanian-Turonian boundary spanning at least the biozone of *Watinoceras coloradoense.* A hiatus across the Cenomanian-Turonian boundary in the Near East was also described by LEWY (1989).

Ostracods (determined by M. MORSI, Cairo) are abundant in the studied Cenomanian and Turonian deposits. Following the concepts of VAN DEN BOLD (1964), BASSOULLET & DAMOTTE (1969) and ROSENFELD & RAAB (1974) they allow a rough biostratigraphic resolution, and support the lithostratigraphic correlations. Calcareous nannofossils (determined by A. MARZOUK, Tanta, Egypt) occur and allow biostratigraphic assignments of different parts of the sections (BAUER et al. subm.), although the identified Cenomanian and Turonian biozones show long biostratigraphic ranges.

Benthic foraminifers such as *Chrysalidina gradata and Pseudedomia sp.* confirm a Cenomanian age. Rudists such as Ichthyosarcolitidae or Hippuritidae prove Cenomanian or Turonian ages. Planktic foraminifers are rare and mainly comprise hedbergellids, whiteinellids and heterohelicids, which are unsuitable for high-resolution biostratigraphy. Keeled planktic foraminifers are absent in the Cenomanian and Turonian deposits.

Lithostratigraphy. In addition to the biostratigraphic data, the lithostratigraphic subdivision of the sections provides a useful tool for correlation. Formation names are based on Egyptian nomenclature mainly from GHORAB (1961), compared with Israeli lithostratigraphic schemes (Fig. 2). Detailed

lithological descriptions of the formations have been published by BARTOV & STEINITZ (1977), BARTOV et al. (1980), LEWY (1989), ZIKO et al. (1993) and KORA & GENEDI (1995). A correlation of the different schemes is given by e.g. KORA & GENEDI (1995).

The Cenomanian Raha Formation (=Halal Formation in north Sinai) consists of alternating beds of limestones, dolomites, marls, and subordinate sandstones. A conspicuous coral- bearing limestone with branching octocorals (*Polytremacis chalmasi* d'Orbigny, ABDEL-GAWAD & GAMEIL 1995) marks the top of this formation and is used as a uppermost Cenomanian marker-bed in south and central Sinai by field geologists.

In the present study, the Lower Turonian Abu Qada Formation is subdivided into three parts in analogy with the Ora Shales, its Israeli counterpart (BARTOV et al. 1980). The Lower Abu Qada Formation consists of shales and marls underlain by a conspicuous dolomite layer with densely packed Lower Turonian ammonites (see above) which can be traced from north to central Sinai. The Middle Abu Qada Formation is composed of well bedded dolomites and limestones, occasionally oolithic, overlain by gypsum, marls and shales of the Upper Abu Qada Formation (Middle Turonian after BUCHBINDER et al. 2000). The Abu Qada Formation is followed by cyclically bedded dolomites and limestones of the Middle-Upper Turonian Wata Formation.

<table>
<tr><th colspan="2">Stages</th><th>Formations Sinai</th><th>Formations Negev</th><th>Calcareous nannofossil biozones</th><th>Biostratigraphic indicative ostracods</th><th>Biostratigraphic indicative ammonites</th><th colspan="2">Sequence boundaries / depositional setting</th></tr>
<tr><td rowspan="3">Turonian</td><td rowspan="2">Upper - Middle</td><td>Wata Fm.</td><td>Gerofit Fm.</td><td rowspan="2">Lucianorhabdus maleformis (CC 12)</td><td rowspan="3">e.g.
Spinolebris yotvataensis
Paracypris triangularis
Pterygocythere raabi</td><td rowspan="2">Barren</td><td>TuSin 2</td><td rowspan="2">Turonian Platform</td></tr>
<tr><td rowspan="2">Abu Qada Fm.</td><td rowspan="2">Ora Shales</td><td>TuSin 1</td></tr>
<tr><td>Lower</td><td>Quadrum gartneri (CC 11)</td><td>Choffaticeras luciae
Choffaticeras ?segne
Thomasites rollandi
Vascoceras sp.</td><td>Central Sinai Basin</td></tr>
<tr><td colspan="2" rowspan="2">Upper Cenomanian</td><td rowspan="2">Raha Fm. (Halal Fm.)</td><td rowspan="2">Hazera Fm.</td><td rowspan="2">Microrhabdulus decoratus (CC 10)</td><td rowspan="2">e.g.
Cythereis algeriana
Metacytheropteron berbricus
Peloriops ziregensis
Veeniacythereis maghrebensis</td><td rowspan="2">Barren</td><td>Hiatus*</td><td></td></tr>
<tr><td>CeSin 7
CeSin 6
CeSin 5</td><td>Cenomanian Platform</td></tr>
</table>

* after BAUER et al. (subm.)

Fig. 2: Lithostratigraphic subdivisions and compilation of biostratigraphic data of the studied sections. Additional, the stratigraphic positions of interpreted sequence boundaries and depositional settings are shown.

*Sequence stratigraphy.*The sequence stratigraphic interpretation is based on the sedimentological, palaeogeographic and cyclostratigraphic evolution of Cenomanian-Turonian deposits, involving the analysis of lateral and vertical changes of the sedimentary stacking patterns, microfacies, petrographic and biostratigraphic data. Furthermore, sequence stratigraphic reconstructions of Middle and Upper Cretaceous successions of central and east Sinai (BACHMANN & KUSS 1998, LÜNING et al. 1998a) were taken into account. A detailed description of the sequence stratigraphic interpretation of the studied sections will be the subject of forthcoming publications. Nevertheless, a brief compilation of the facies patterns of the individual systems tracts and bounding surfaces is given in Tab. 1 and biostratigraphic

assignments of the sequence boundaries in Fig. 2. The sequence boundaries are numbered according to their basal sequence boundaries in analogy with the sequence TuSin 1: Tu= Turonian, Sin= Sinai, 1= first sequence boundary in the Turonian, following a system used by HARDENBOL et al. (1998). The systems tracts are differentiated by the prefixes "post" and the underlying sequence boundary (e.g. post-TuSin 1 TST: TST above the sequence boundary TuSin 1). BUCHBINDER et al. (2000) presented biostratigraphic assignments for Cenomanian and Turonian sequence boundaries in the Near East. A correlation with our sequence boundaries indicates a Late Cenomanian age (Guerangeri Zone) for sequence boundary CeSin 7 and a Middle Turonian age (Kallesi / Ornatissimum Zone) for sequence boundary TuSin 1.

Sequence Boundaries	Systems Tracts & Surfaces	Characteristics
	TST / HST:	bioclastic dolomites and limestones
	ts:	transition to calcareous deposits
	LST:	deposition of siliciclastics
TuSin 2	SB:	onset of shales or sandstones
	HST:	aggradation of thick bedded dolomites and bioclastic limestones (partly oolithic), locally quartz input in coastal facies
	mfs:	onset of aggradation
	TST:	shallow, open-marine deposits
	ts:	onset of open-marine sedimentation
	LST:	supratidal or intertidal deposits: gypsum beds, siltstones and shales partly with plant remains and brackish ostracods
TuSin 1	SB:	palaeosols or transition from calcareous sediments of HST to shaley-silty deposits of LST
	HST:	aggradation of dolomites and bioclastic partly oolithic limestones, sometimes hardgrounds, ironooids and sandstones in coastal facies.
	mfs:	transition from marls of TST to shallow subtidal-intertidal dolomites and limestones of HST
	TST:	condensed deposits of dolomites with rich ammonites fauna overlain by marls with planktic foraminifers
	ts:	transition to deeper subtidal facies of TST
	LST:	nondeposition or silty marls with plant remains (section Z)
CeSin 7	SB:	hardgrounds
	TST / HST:	dolomites, limestones, marls, abundant macrofossils (rudists, oysters, corals)
	ts:	decrease of quartzose deposits, first limestone beds
	LST:	siltstones and shale with plant remains and ironooids
CeSin 6	SB:	hardgrounds
	HST:	calcareous or dolomitic sandstones especially in south Sinai
	mfs:	marked increase of quartzose deposits
	TST:	marls and limestones with abundant bioclastics
	ts:	first corals and increase of abundance of marine organisms
CeSin 5	LST:	siltstones and shales with ironooids

Tab 1: Compilation of facies characteristics of systems tracts and surfaces.

5. LATE CENOMANIAN-TURONIAN TRANSGRESSIONS

A prominent relative sea-level rise at the Cenomanian-Turonian transition is observed in many regions of the Mediterranean Tethys (cited in ABDALLAH & MEISTER 1997) and is probably of global eustatic origin (PHILIP & AIRAUD-CRUMIERE 1991). In Sinai and in the Negev this transgression coincides with a drowning of the Upper Cenomanian platform (dated within the Upper Cenomanian *Guerangeri* ammonite biozone by BUCHBINDER et al. 2000) and is reflected by deposits of the Central Sinai Intra-shelf-Basin (BARTOV & STEINITZ 1977) and its westward prolongation in the Near East (Eshet-Zenifim Basin, BARTOV & STEINITZ 1977, GVIRTZMAN & GARFUNKEL 1998). In north and central Sinai the drowning event is indicated by Upper Cenomanian platform deposits overlain by a hardground (sequence boundary CeSin 7, Figs. 4, 6, 8, 9); during the following relative sea-level rise, sedimentation started again in the Central Sinai and Eshet-Zenifim Basins in late Early Turonian times with the deposition of densely packed ammonite beds, described above. These beds, represent a condensed interval with very slow sedimentation rates and are overlain by marls with planktic foraminifers. Condensation is also indicated by oysters, which are frequently found attached to ammonites within these beds. During the Middle and Late Turonian, an extended calcareous shelf system re-established, retrograding southwards in Late Turonian times.

6. RESULTS

6.1 Distribution of rudists

Rudist occurrences of Sinai have been studied in detail early last century by DOUVILLÉ (1910, 1913, 1915). The species described in these monographs were frequently referred to in subsequent studies of the geology and stratigraphy of the region, but only PARNES (1987) provided new and detailed descriptions of specimens. Endemism of Cenomanian and Turonian faunas of Sinai is largely expressed on the subspecies-level, but morphological differences from other Mediterranean species have to be re-assessed in the light of modern concepts of intraspecific variability.

Plate 1: Field Photographs of rudists. (1) Bedding plane view of association of *Eoradiolites liratus* (CONRAD); Upper Raha Formation of Gebel Abu Zurub, west Sinai. (2) *Hippurites sp.* and *Vaccinites sp.* in dolomitic limestones of the middle Abu Qada Formation of Areif El Naqa, north Sinai. Diameter of coin is 21.5 mm. (3) Bedding plane view of *Ichthyosarcolites triangularis* (DESMAREST) in recumbent life position. Upper Halal Formation of Gebel Minsherah, north Sinai. (4) Dense growth fabric of *Eoradiolites liratus* (CONRAD); Upper Cenomanian of Gebel Abu Zurub, west Sinai. (5) *Durania sp.;* Wata Formation of Gebel Minsherah, north Sinai.

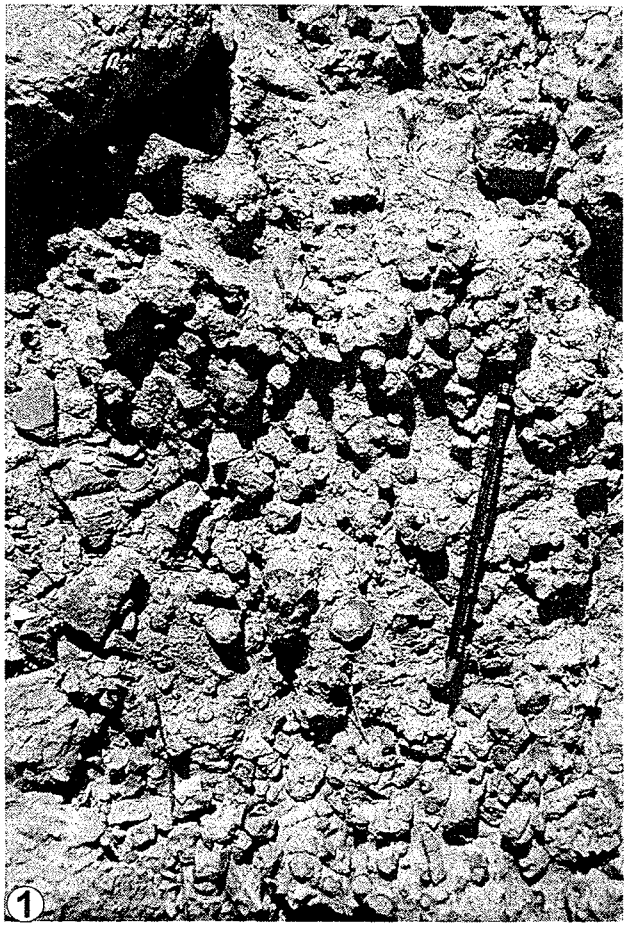

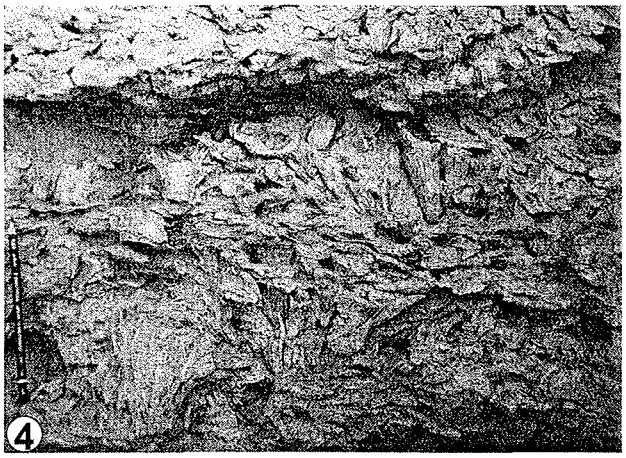

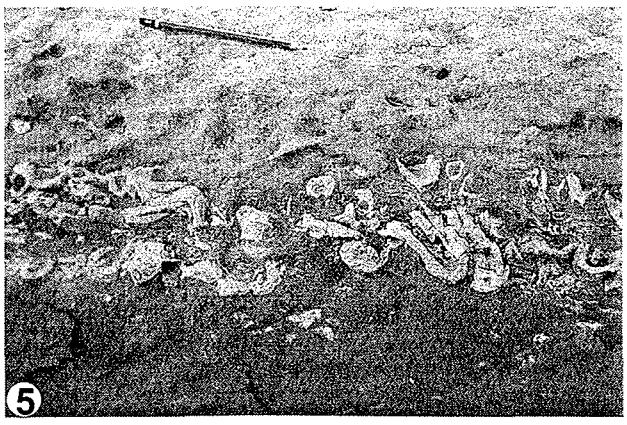

Cenomanian. Cenomanian associations predominantly consist of species of *Eoradiolites* (Pl. 1/1 and Pl. 1/4), *Praeradiolites* and *Radiolites* (e.g. Gebel Minsherah Fig. 4, Gebel Abu Zurub Fig. 8). Caprinidae have not been observed during our field studies and they have yet not been reported from the region, except for a brief note on Cenomanian "calcaires à Caprines du Gebel Gédéra" from north Sinai (DOUVILLÉ & COUYAT-BARTHOUX 1914). Among other typical constituents of Cenomanian rudist associations of the Tethys, *Ichthyosarcolites* (Pl. 1/3) is abundant, although almost exclusively restricted to a single bed of Upper Cenomanian limestones (post-CeSin 6 HST) which can be traced from north Sinai (Gebel Yelleq, Fig. 1) to Gebel Abu Zurub in west Sinai. *Ichthyosarcolites* has not been found in correlative beds further to the south, although the general facies characteristics remain similar and small bushes of branching octocorals (*Polytremacis chalmasi* d'Orbigny, ABDEL-GAWAD & GAMEIL 1995) are consistently found within this bed in central Sinai as far south as Gebel Arabah (uppermost Cenomanian deposits of post-CeSin 6 HST).

Turonian. The condensed Lower Turonian succession (post-CeSin 7 TST) records a significant deepening of depositional environments in Sinai, but further to the south, at Gebel Safariyat (Figs. 1, 10), the type locality of *Durania inermis* DOUVILLÉ is placed in time-equivalent shallow-subtidal deposits, where it forms a laterally extended monospecific rudist-lithosome. Relatively species-rich associations occur in the Middle Turonian successions of north Sinai (post-CeSin 7 HST, Pl. 1/2), specifically at Gebel El Risha (Fig. 1) and in central Sinai at Wadi El Gidira (Fig. 7). The composition of these associations is almost identical at Gebel El Risha and Wadi El Gidira and comprises *Hippurites requieni* MATHERON and species of *Radiolites* and *Durania*. Species-rich associations are also present in Middle-Upper Turonian cyclic deposits (Pl. 1/5) in the post-TuSin 1 HST of north Sinai (Gebel El Minsherah, Fig. 4), but they have not been found further to the south. Uppermost Turonian limestones at Gebel Areif El Naqa and Gebel El Risha contain monospecific clusters of *Bournonia judaica* BLANCKENHORN, which has been reported to be the youngest rudist species in the Near East and Sinai (LEWY & RAAB 1976). However, *Vaccinites rousseli batnenis* (DOUVILLÉ) has been found above this level, in the post-TuSin 2 HST at Gebel Minsherah (Fig. 5).

6.2 Distribution of benthic foraminifers and calcareous algae

Microfacies. Typically, the highest abundance of benthic foraminifers (up to 20 %) in thin section is observed in Cenomanian and Turonian miliolid wackestones (Pl. 2/1) and peloidal packstones (Pl. 2/2, 2/3). Varying amounts of remains of calcareous algae, echinoderms, gastropods, ostracods and bivalves characterise these open lagoon and protected shallow-marine environments without major wave activity. Within more agitated environments, coarse-grained bioclastic packstones (Pl. 2/6) show the highest diversities and frequencies of calcareous algae amongst high amounts of diverse shallow-marine biota (e.g. echinoderms, gastropods, bivalves). Rock-forming frequencies of densely packed debris of udoteaceans and red algae may occur locally in washed packstones, particularly in the Turonian (Pl. 2/4). Associated ooids, frequent oncoids and reworked lithoclasts suggest turbulent shallow and open-marine environments (Pl. 2/5). Very similar Cenomanian and Turonian microfacies with comparable frequencies and diversities of foraminifers and algae have been reported from adja-

cent regions: e.g. north-east Egypt (KUSS & MALCHUS 1989, KUSS 1992), Arabian Gulf (BURCHETTE & BRITTON 1985) or Lebanon (HAMAOUI & SAINT-MARC 1970). However, vertical and lateral variations of diversity and frequency of both groups are clearly visible in the studied sections.

Cenomanian. In Cenomanian deposits of the northern sections at Gebel Minsherah (Fig. 4 and Fig. 5) and Gebel Areif El Naqa (Fig. 6), benthic foraminifers are most abundant and diverse. Although sample density throughout the Cenomanian succession is poor due to extended dolomitisation, few limestone beds show a shallow-subtidal and open-lagoon facies with abundant benthic foraminifers within the HSTs and early TSTs (e.g. post-CeSin 6 TST). Low-energy wackestones and packstones are dominated by miliolids (e.g. *Quinqueloculina* sp., *Triloculina* sp. *Nummoloculina* sp.) and subordinate *Cuneolina* sp., whereas *Nummofallotia* sp., *Pseudolituonella* sp., *Pseudorhapydionina* sp. and *Valvulammina* sp. vary in frequency. *Biconcava ?bentori, Chrysalidina gradata, Cyclogyra.* sp., *Dicyclina* sp., *Nezzazata* sp., *Pseudedomia* sp., *Praealveolina* sp. and *Pyrgo eliptica* occur less frequently in this assemblage. Calcareous algae are nearly absent in the studied samples at Gebel Minsherah and Gebel Areif El Naqa and are limited to few individuals of *Pseudolithothamnium album* and badly preserved individuals of green algae. In west Sinai, at Gebel Abu Zurub, an open-lagoon facies with abundant benthic foraminifers occurs in the post-CeSin 6 HST (Fig. 8). The highly diverse foraminiferal assemblage shows close similarities to that described above, although some genera and species differ in frequency. Calcareous algae (*Bouenia pygmaea, Acicularia sp., Dissocladella undalata* and *Neomeris sp.*) are rare.

In Cenomanian limestones at Gebel Dhalal (Fig. 9) benthic foraminifers are rare. Low-energy lagoonal packstones and wackestones with gastropods, bivalve debris and peloids were deposited during highstand aggradation of sequence CeSin 6. Few miliolids and rare undifferentiated benthic foraminifers indicate an unfavourable, possibly restricted environment for this group, although coral debris suggests temporary open-marine conditions in the post-CeSin 6 HST. Calcareous algae are absent. In the southernmost section at Gebel Arabah (Fig. 10) silty marls, calcareous and siliceous sandstones prevail. Supratidal deposits of the LSTs are predominantly overlain by tidal flat deposits and quartzose shoreface facies in the TSTs and HSTs. Benthic foraminifers and calcareous algae are absent, probably due to the dominant siliciclastic input from the hinterland.

Plate 2: Typical Foraminifers and calcareous algae bearing Cenomanian–Turonian microfacies types (scale bars = 0.5 mm). (1) Cenomanian peloidal packstone with *Cuneolina* sp. (left) and abundant miliolids, Gebel Minsherah, section M2, post-CeSin 5 HST. (2) Cenomanian peloidal packstone with abundant foraminifers: e.g. *Biconcava bentori* (lower left) and *Pseudedomia* sp. (right), Gebel Minsherah, section M1, post-CeSin 6 TST. (3) Turonian packstone with *Cuneolina* sp. (left),*Nezzazata* sp. (upper right) and small *Neomeris cretacea* (central left), Gebel Dhalal, post-TuSin 1 TST. (4) Turonian washed packstone with densely packed udoteaceans and red algae, Gebel Minsherah, section M1, post-TuSin 1 HST. (5) Turonian washed packstone with ooids, oncoids and udoteaceans debris, Gebel El Gidira post-CeSin 7 HST. (6) Turonian coarse-grained bioclastic packstone with abundant udoteaceans, Gebel Abu Zurub post-CeSin 7 HST.

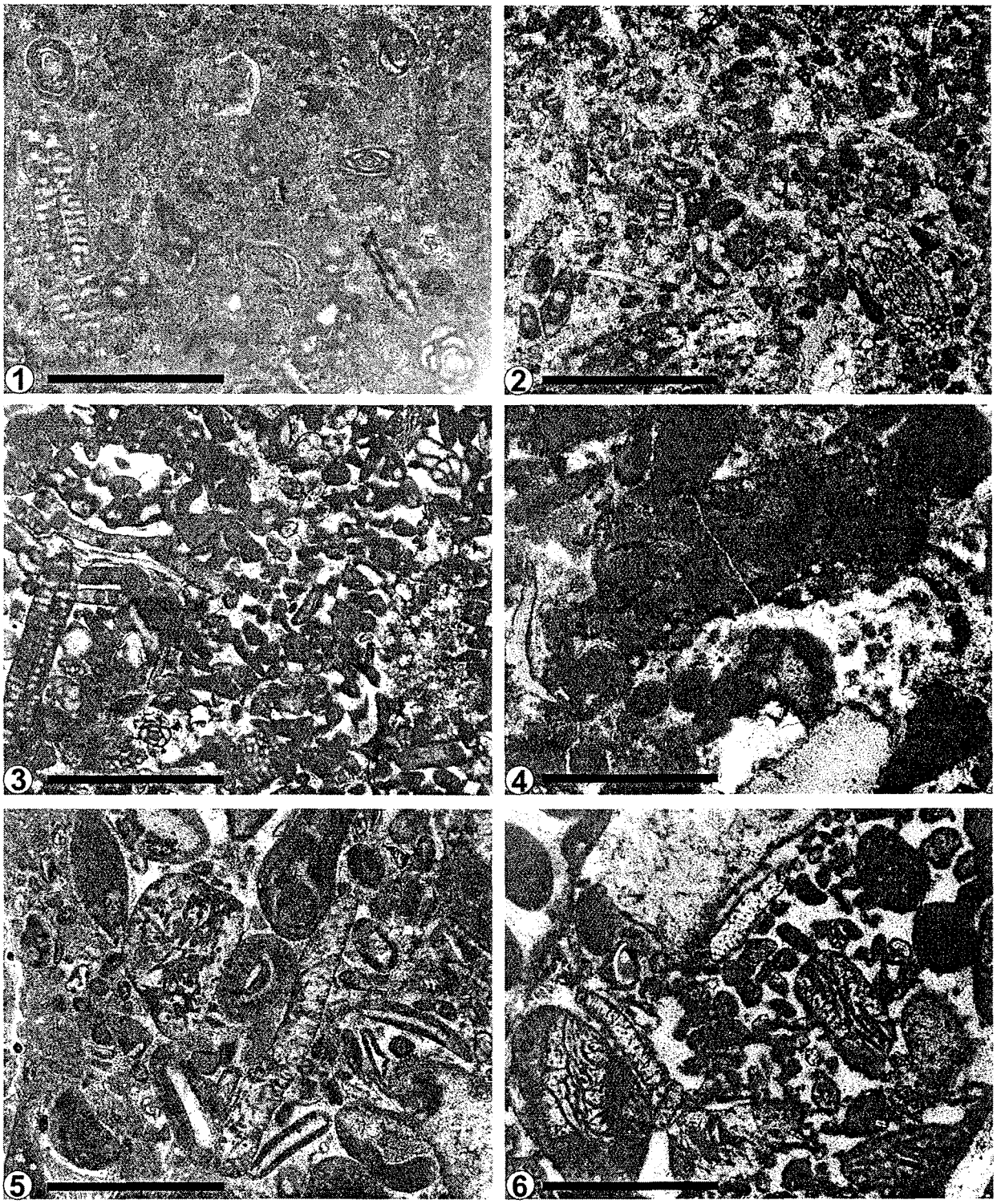
1
2
3
4
5
6

Turonian. Assemblages of benthic foraminifers in the Turonian deposits differ distinctively from those of the Cenomanian deposits and are generally impoverished in abundance and diversity. The Cenomanian *Praealveolina* sp., *Chrysalidina gradata, Pseudedomia* sp., *Biconcava ?bentori* and *Cyclogyra* sp. disappear. The benthic foraminiferal association in the Turonian is dominated by *Cuneolina* sp. *Pseudorhapydionina* sp. *Quinqueloculina* sp. and *Valvulammina* sp.. The distribution of calcareous algae shows an opposite trend, as frequencies increase markedly after the Cenomanian-Turonian transition. Besides *Bouenia pygmaea* and *Neomeris cretacea,* the species *Arabicodium aegagrapiliodes, Bouenia* cf. *hochstetteri, Marinella lugeoni, ?Permocalculus* sp., *Ethelia album* and *Thaumatoporella parvovesiculifera* are recognised.

In the northern sections (Gebel Minsherah and Gebel Areif El Naqa), as well as in the western (Gebel Abu Zurub) and eastern section (Gebel El Gidira), foraminiferal assemblages predominantly consist of miliolids (*Miliolina* sp., *Quinqueloculina* sp., *Nummoloculina* sp., *Triloculina* sp.). More rarely, *Valvulammina* sp., *Nezzazata* sp. and *?Pseudorhapydionina* sp. occur in the mainly open-marine, inner platform deposits of the post-CeSin 7 HST (Middle Abu Qada Formation). Moreover, a diverse algae flora of udoteaceans (*Arabicodium aegagrapiliodes, Bouenia* cf. *hochstetteri, Bouenia pygmaea*), red algae (mainly *Marinella lugeoni*) and dasycladaceans (*Neomeris cretacea*) is present in the post-CeSin 7 HST. It is important to note that the debris of calcareous algae (especially udoteaceans) is particularly abundant in moderate to high-energy settings with occasional ooids and oncoids (e.g. at Gebel El Gidira, Fig. 10, Pl. 2/5). In sequence post-TuSin 1 benthic foraminifers significantly increase in frequency and diversity in the Middle-Upper Turonian limestones in north and central Sinai. Among others, the genera *Cuneolina., Quinqueloculina, Valvulammina, Dicyclina* and *?Pseudorhapydionina* are abundant or common together with miliolids in the shallow-subtidal and lagoonal facies of the TST and HST (e.g. Gebel Dahlal, Fig. 9). Nevertheless, significant changes of frequencies and diversities at the maximum flooding surface are not observed and the foraminifers assemblages are not as diverse as in the Cenomanian deposits (e.g. Gebel Minsherah, Fig. 4), although an extended marine ingression is indicated during sequence post-TuSin 1. In contrast, no distinct differences are observed in the calcareous algae distribution patterns within the Middle and Upper Turonian sequences. In the south, at Gebel Arabah, benthic foraminifers and calcareous algae are nearly absent in the Turonian deposits. However, only 20 km to the north-east, at Gebel Safariat (Fig. 10), the siliciclastic input was less significant and miliolids and dasycladaceans occur in the post-CeSin 7 TST.

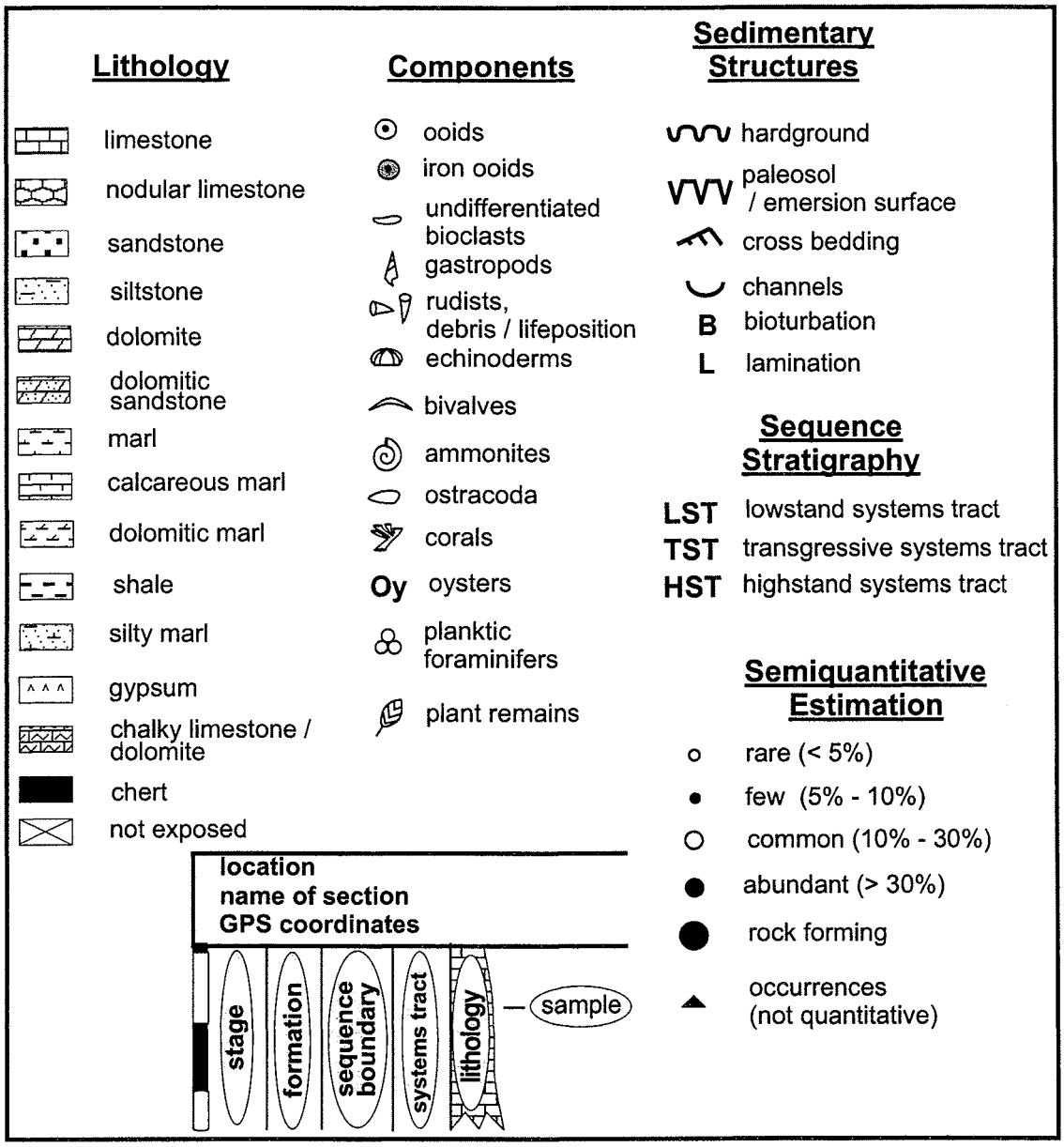

Fig. 3: Explanation of symbols and ornaments used on Figs. 4-10.

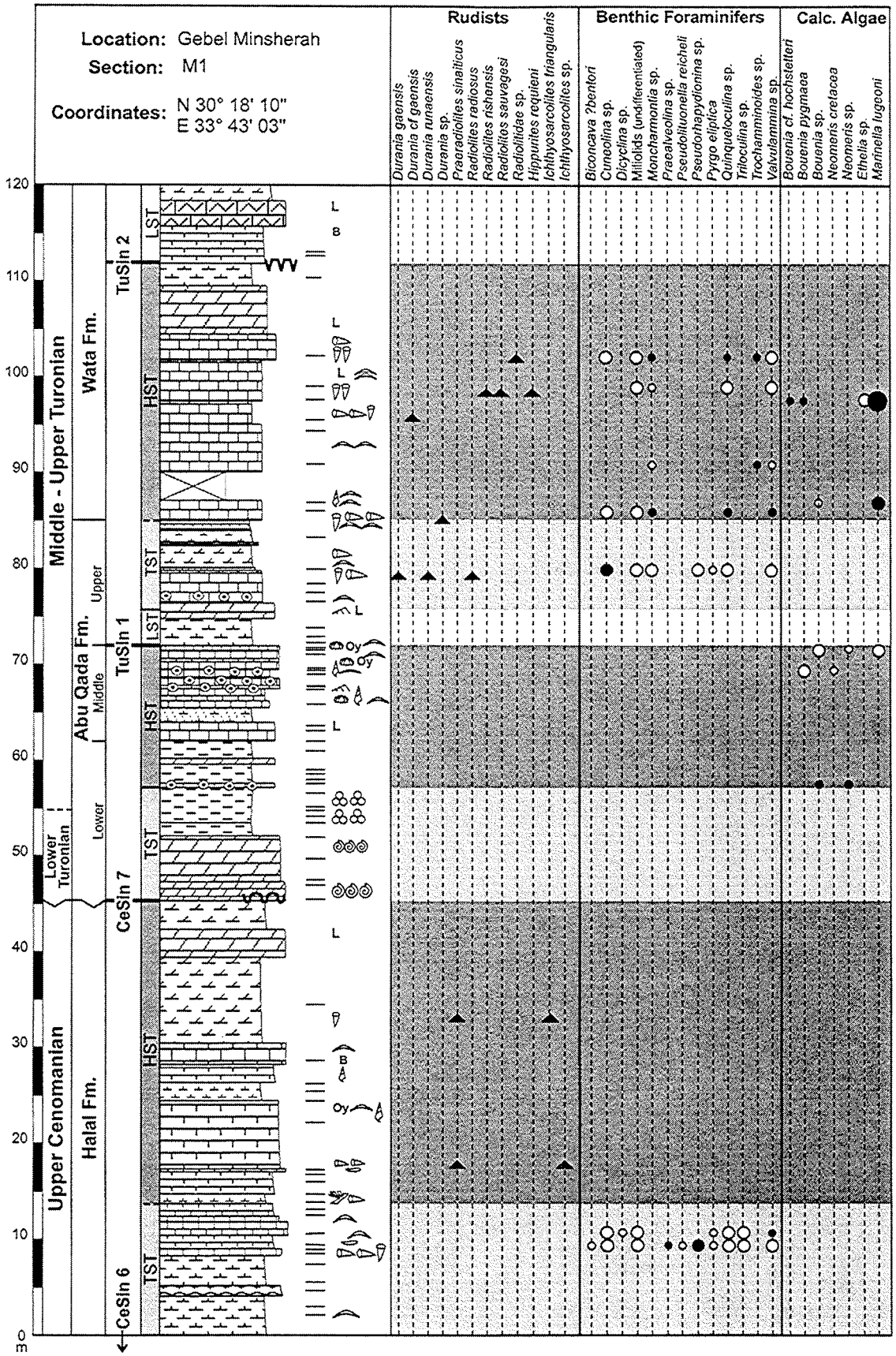

Fig. 4: Section M1 at Gebel Minsherah (north Sinai) with distribution of rudists, benthic foraminifers and calcareous algae. For explanations of symbols and ornaments refer to Fig. 3.

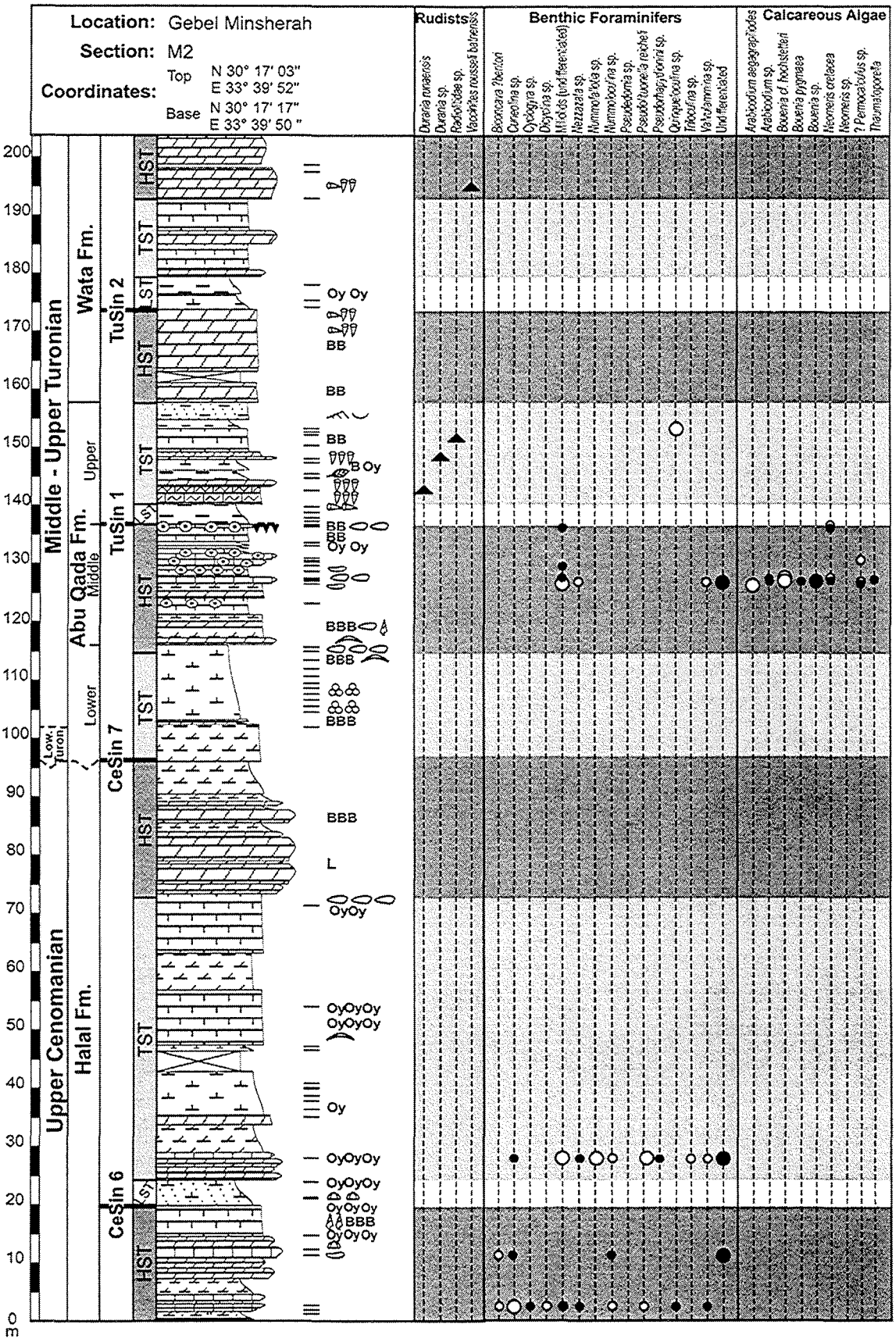

Fig. 5: Section M2 at Gebel Minsherah (north Sinai) with distribution of rudists, benthic foraminifers and calcareous algae. For explanations of symbols and ornaments refer to Fig. 3.

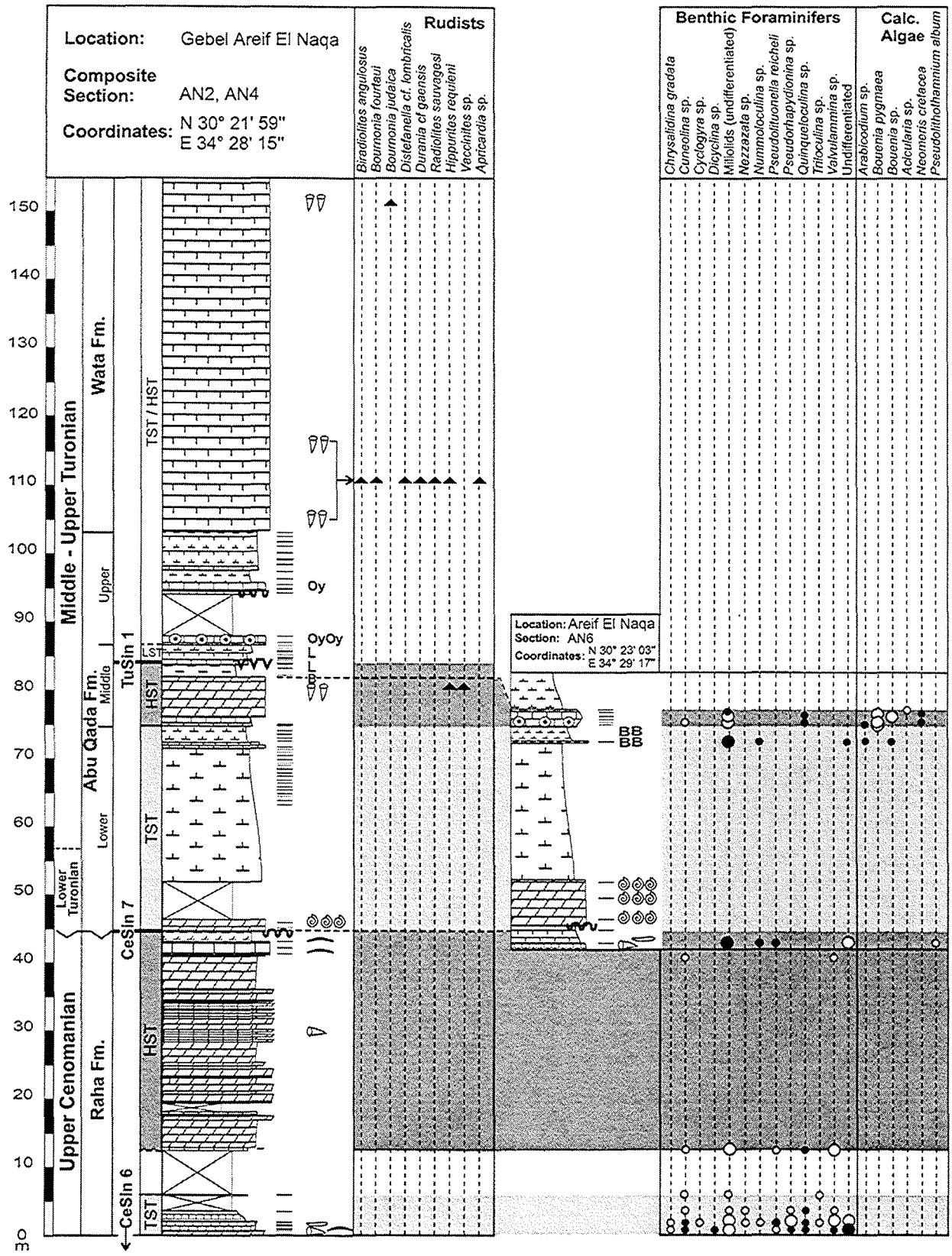

Fig. 6: Two composite sections at Gebel Areif El Naqa (north Sinai) with distribution of rudists (absent in AN6), benthic foraminifers and calcareous algae (absent in AN2, AN4). Explanations of symbols and ornaments are given in Fig. 3.

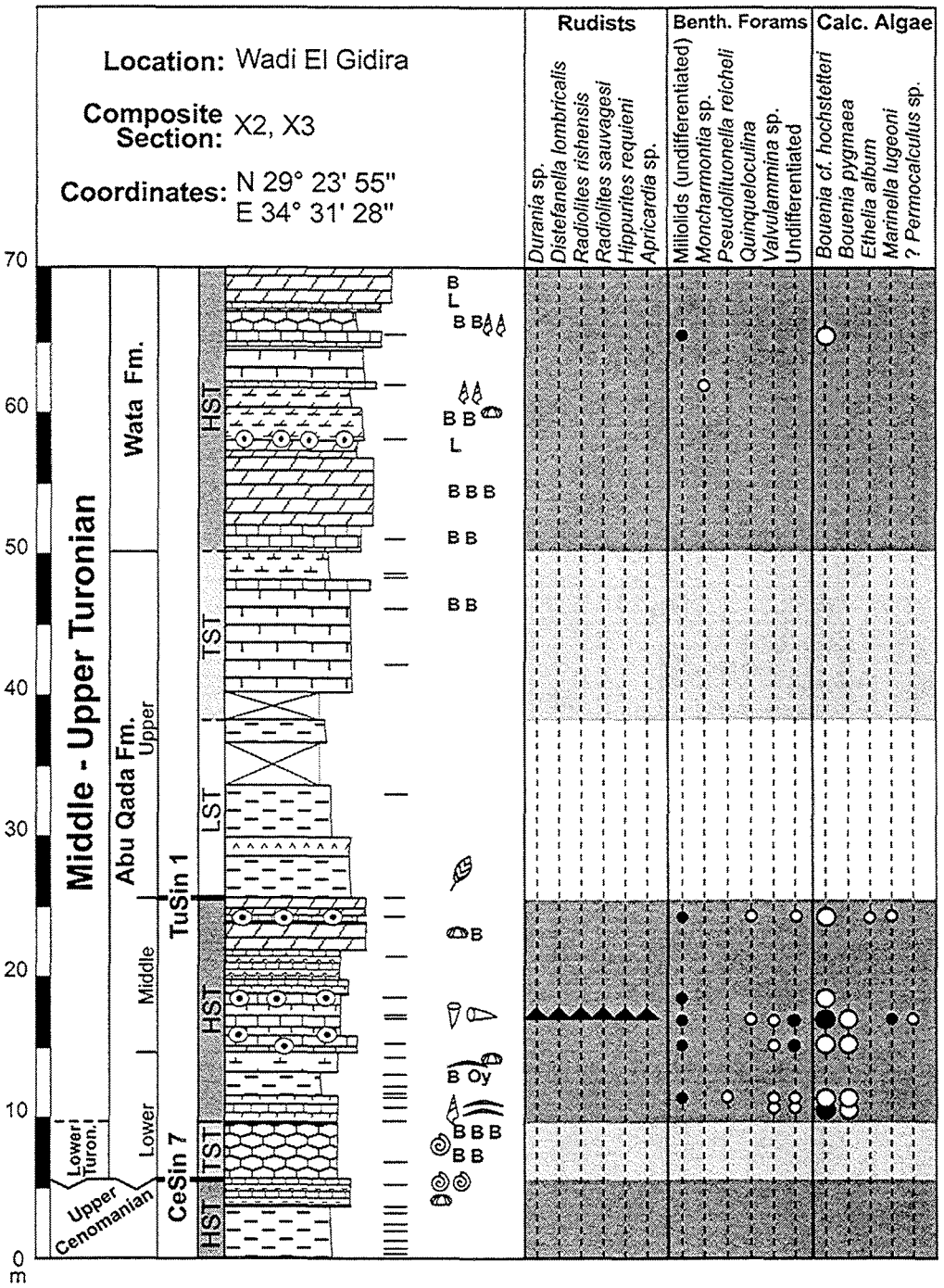

Fig. 7: Composite section at Gebel El Gidira (central Sinai) with distribution of rudists, benthic foraminifers and calcareous algae. For explanations of symbols and ornaments refer to Fig. 3.

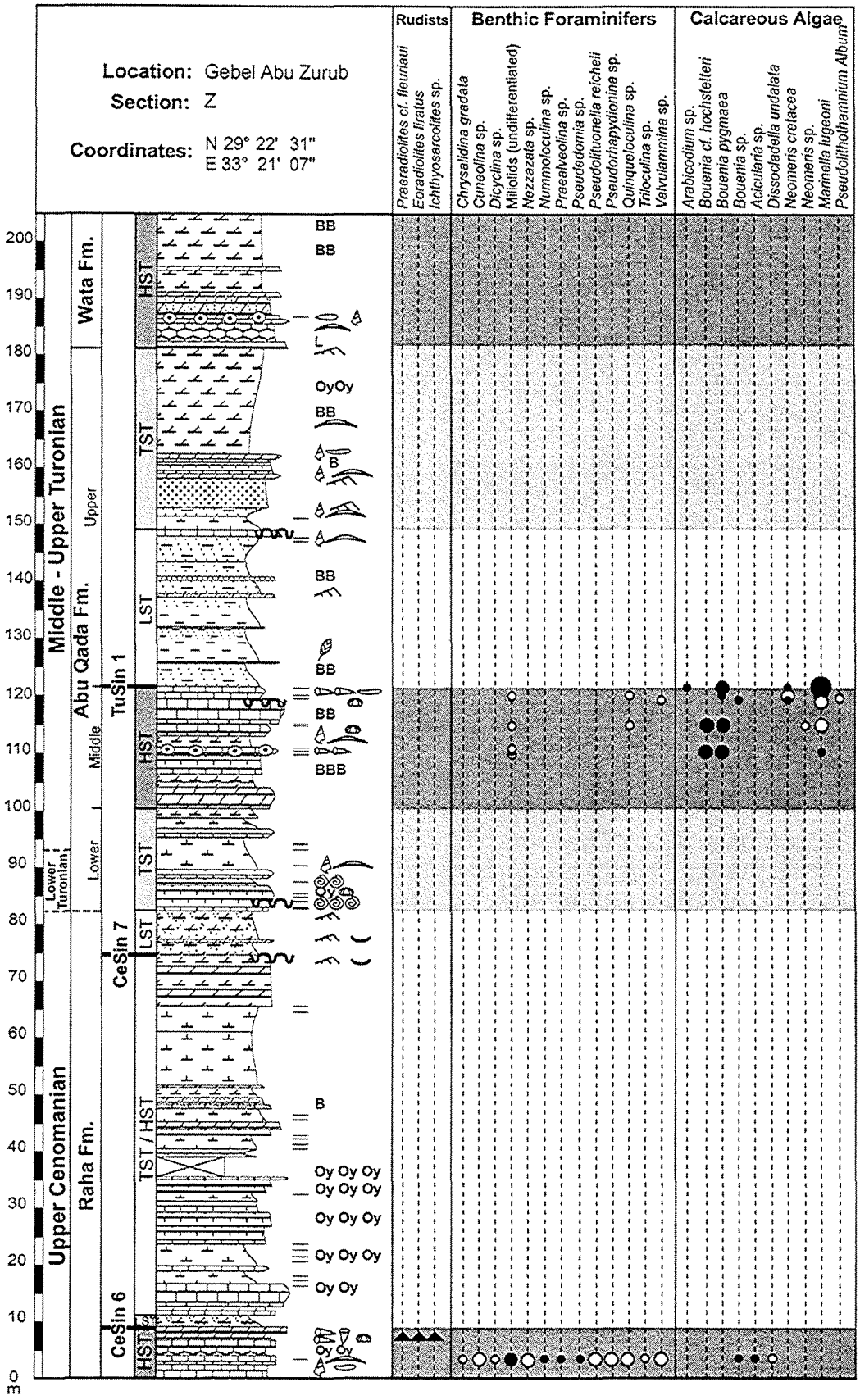

Fig. 8: Section at Gebel Abu Zurub (west Sinai) with distribution of rudists, benthic foraminifers and calcareous algae. For explanations of symbols and ornaments refer to Fig. 3.

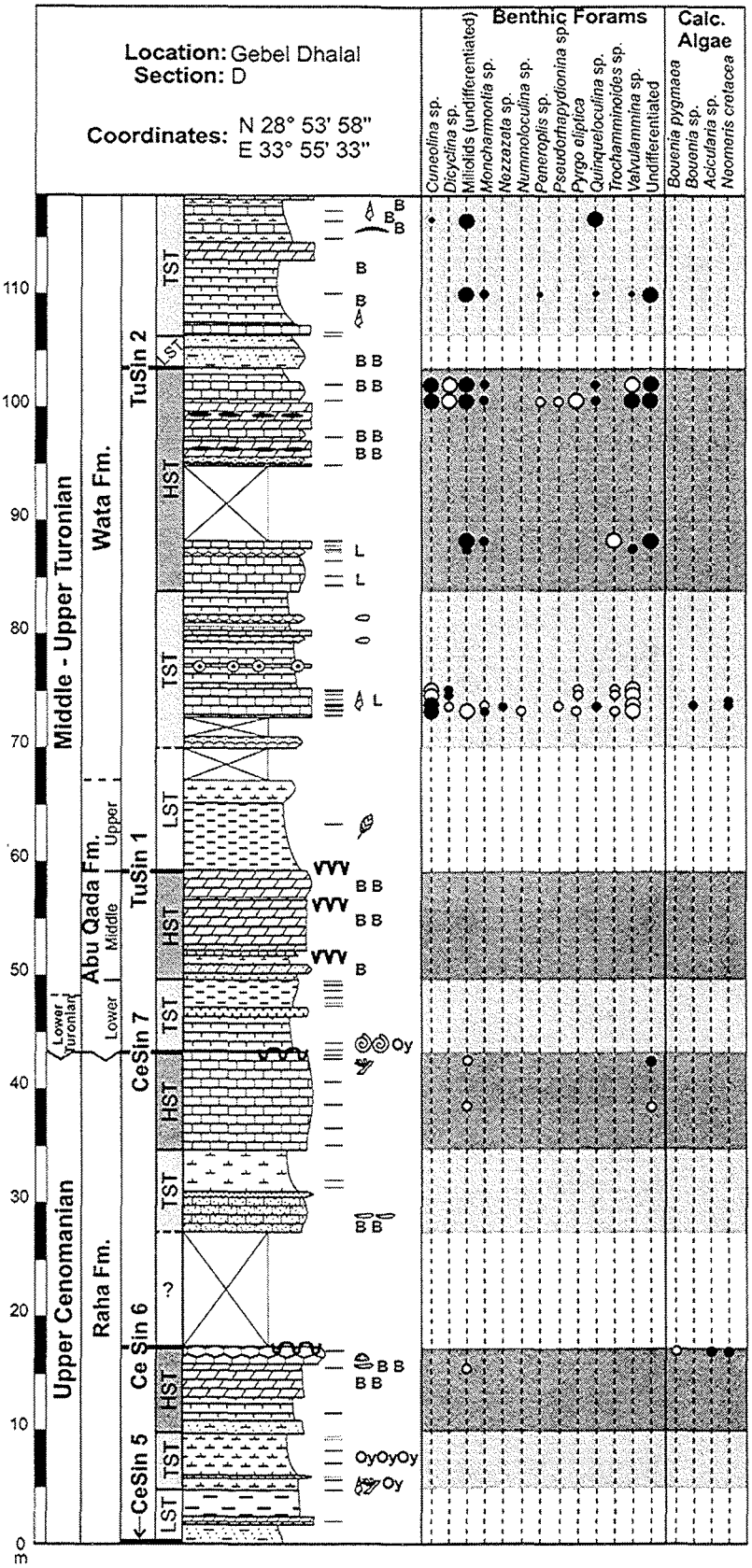

Fig. 9: Section at Gebel Dhalal (central Sinai) with distribution benthic foraminifers and calcareous algae; rudists are absent. For explanations of symbols and ornaments refer to Fig. 3.

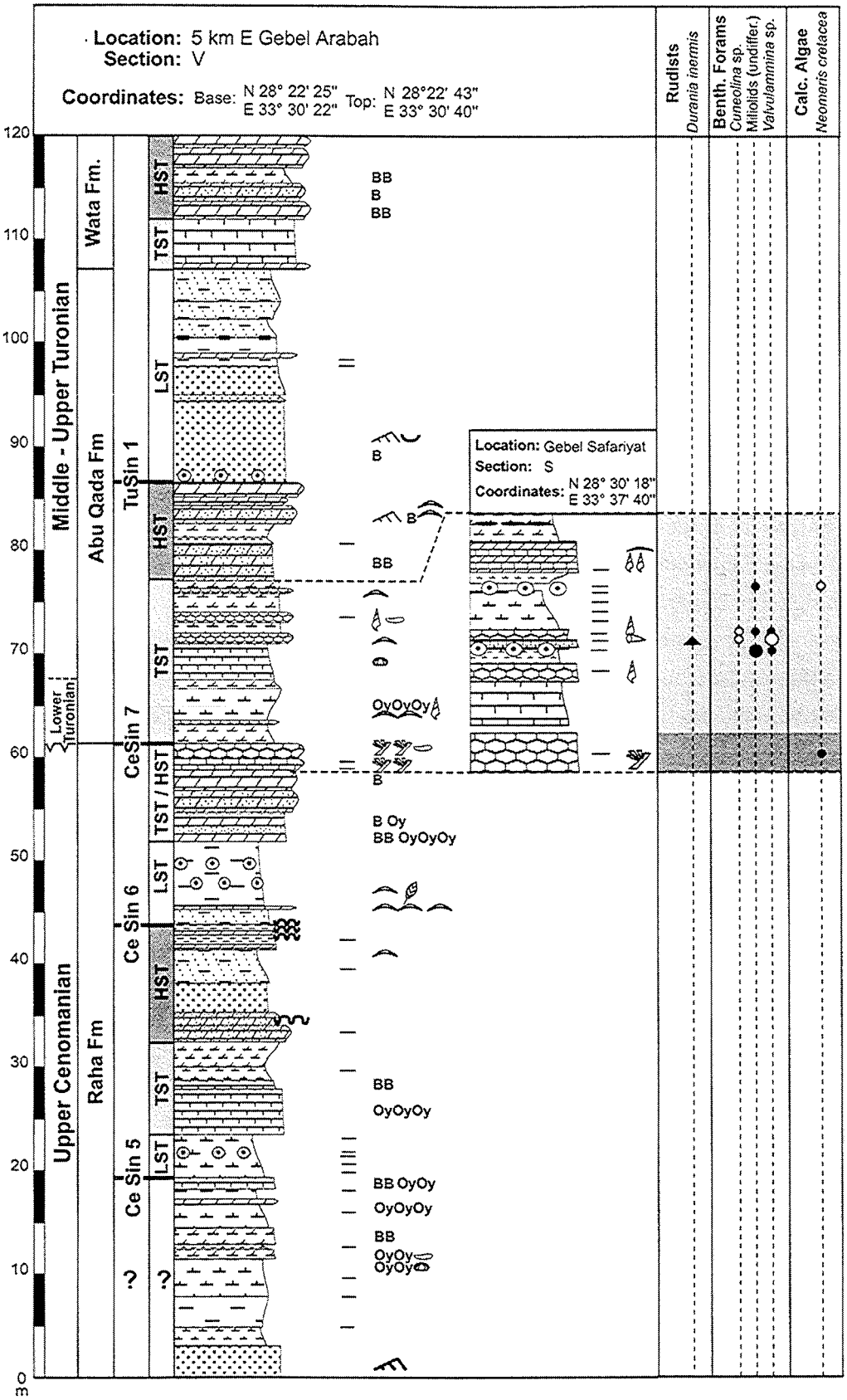

Fig. 10: Sections at Gebel Arabah and Gebel Safariat (south Sinai) with distribution of rudists, benthic foraminifers and calcareous algae. For explanations of symbols and ornaments refer to Fig. 3.

7. DISCUSSION

7.1 Large scale distribution trends

During the Cenomanian, rudists of Sinai were considerably less species-rich when compared to other Tethyan carbonate platforms, e.g. in the central and eastern Mediterranean. Caprinidae are absent in Sinai and generally rare on North African shelves, although abundant in high-energy deposits of Cenomanian platforms in the central areas of the Tethys (e.g. *Mediterranean Seuil* sensu Philip et al. 1993) and northern Tethyan realms (STEUBER & LÖSER, 2000). This may be interpreted as a taphonomic effect, as this aragonite-dominated group possibly has not been preserved in the often dolomitic Cenomanian limestones. On the other hand, *Ichthyosarcolites* with a similar composition and structure of the shell are rather common in Sinai so that the lack of Caprinidae is not regarded as a preservational bias. Middle and Upper Turonian associations are more diverse, e.g. similar to those of the *Mediterranean Seuil*. In contrast to many other Tethyan shallow carbonate shelves (ROSS & SKELTON 1993, CARANNANTE et al. 1999, STEUBER, 2000), the contribution of rudists to the production of calcareous sediment was only minor within the shelf system of Sinai. The establishment of rudist associations during the Cenomanian and Turonian was generally restricted to a few brief periods, often to a single generation of individuals. Rudist debris is restricted to the immediate vicinity of such lithosomes and is absent in most of the studied deposits.

Previous studies on the microfaunal turnover across the Cenomanian-Turonian boundary (e.g. JARVIS et al. 1988, HARRIES 1993, KAUFFMAN 1995, HART 1996, GRÄFE 1999) have shown that the recognition of large-scale extinction and recovery patterns requires continuous sections and that a more precise biostratigraphy is needed than achieved for the successions presented here. However, despite the limited biostratigraphic precision and the hiatus across the Cenomanian-Turonian boundary, our data indicate a decline in diversity and abundance of benthic foraminifers across the Cenomanian-Turonian boundary in Sinai. A recovery during the Middle and Late Turonian is indicated, although the diversity of benthic foraminifers did not reach the same level as in the Cenomanian. The distribution of calcareous algae follows a different trend. This group is limited to only a few species in the Cenomanian deposits, while more diverse assemblages are common in the Turonian successions in Sinai.

The drowning of large areas of the Cenomanian platform of Sinai in Late Cenomanian times, clearly affected the shallow-marine benthic community. Platform drowning and biotic turnover at the Cenomanian-Turonian transition elsewhere are assumed to be closely related to the OAE II by various authors (ARTHUR et al. 1987, JARVIS et al. 1988, KAUFFMAN 1995, KAUFFMAN & HART 1996, KUYPERS et al. 1999). As lowermost Turonian deposits are not recorded in Sinai, the effects of OAE II cannot be investigated in the studied area. However, the re-establishment of a calcareous shelf system after this drowning event was associated with the gradual recovery of the studied biota in the Middle Turonian. A large-scale relative sea-level rise induced a retrogradation of the open-marine environments and a southward retreat of siliciclastic shoreface. Thus, favourable environmental conditions for a diverse benthic community were available in the Middle-Late Turonian.

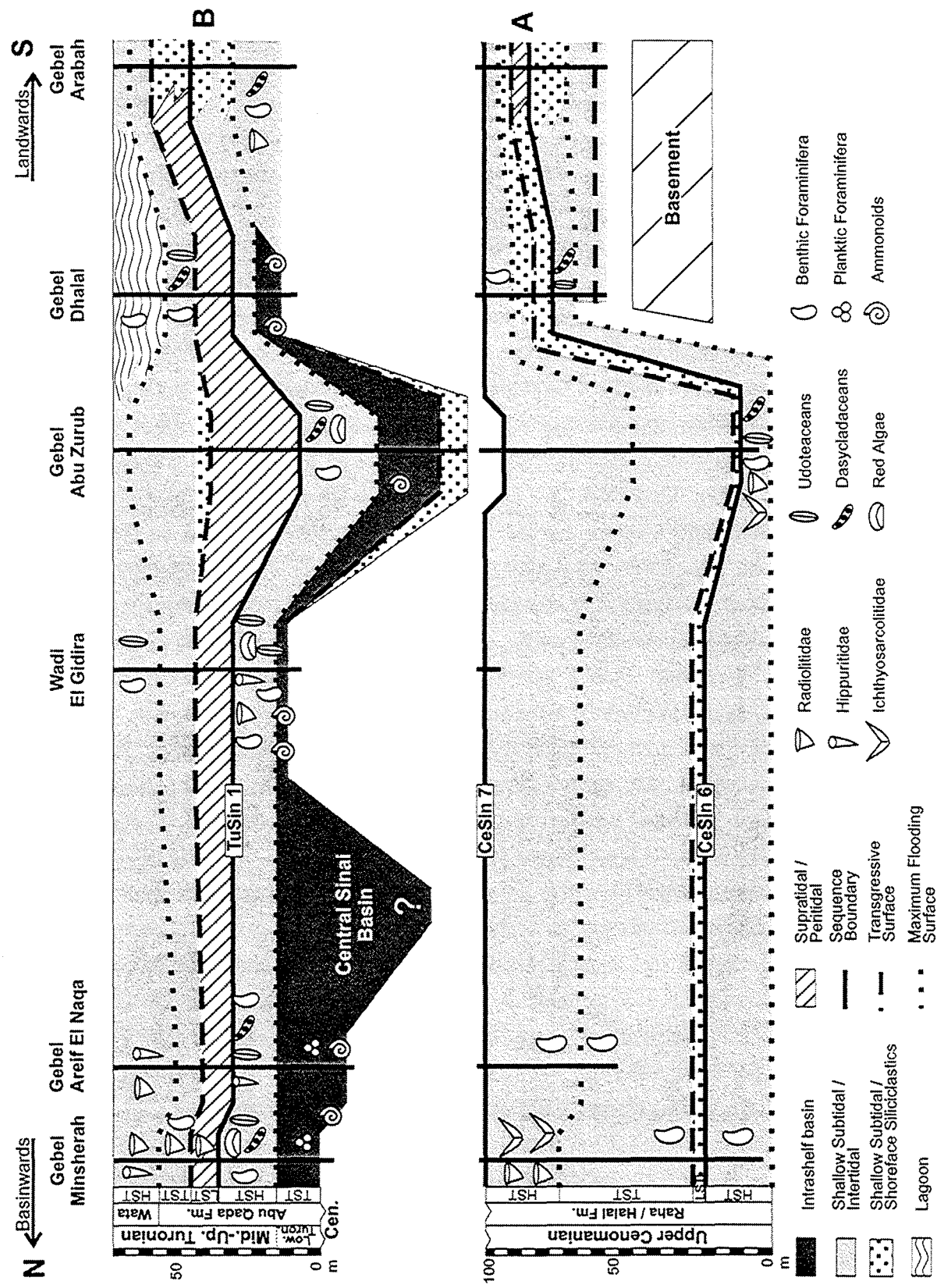

Fig. 11: N-S running sequence stratigraphic correlation and distribution of rudist and calcareous algae families and benthic foraminifers of Upper Cenomanian (A) and Turonian (B) successions. Lateral distance between sections are not to scale. Rudists (Radiolitidae, Hippuritidae, Ichthyosarcolitidae) prevail in HSTs whereas calcareous algae (udoteaneans, dasycladaceans) and benthic foraminifers occur in HSTs and TSTs. Red Algae are limited to HSTs. Localities and traverse in Fig 1.

7.2 Facies and sea-level related distribution trends

The studied biota reacted sensitively on a multitude of ecological conditions of the depositional environment such as salinity, temperature, nutrient and oxygen supply, circulation, water energy, bathymetry and accommodation space, which varied with increasing distance to the shoreline. In the studied sections, diversities and frequencies decrease gradually landwards from the northern sections (Gebel Minsherah and Gebel Areif El Naqa) and central sections (Wadi El Gidira and Gebel Dhalal) to and southern section (Gebel Arabah) (Figs. 11). This is most obvious for the distribution patterns of rudists. Diversity is generally low in north Sinai, but decreases significantly southwards: in central and south Sinai, both Cenomanian and Turonian rudist lithosomes are generally monospecific with *Eoradiolites* in the Cenomanian and *Durania* in the Turonian. Consequently, there is a marked north-south gradient in diversity, and only the northernmost Middle-Upper Turonian associations are similarly species-rich when compared to contemporaneous Tethyan faunas, e.g. in the central and eastern Mediterranean. The benthic foraminifers and calcareous algae are most common in the northern and central sections and show a similar, but less obvious N-S gradient in occurrence when compared to the rudists. Benthic foraminifers were most frequent in open-lagoon and protected shallow-marine settings, while calcareous algae were abundant in shallow, open-marine environments, including high-energy oolithic deposits of the algae debris facies. Both microfossil-groups preferred habitats of the more distal areas of the inner platform, where the highest diversities occurred. Many calcareous algae, however, possibly settled in proximal inner platform areas in Sinai as well; however, the mainly dolomitic lithologies here destroyed the fragile algal skeletons. In south Sinai (sections Gebel Arabah and Gebel Dhalal), all studied biota are absent or rare due to the more landward palaeo-position. Here, supratidal, tidal flats, protected lagoonal and quartzose shoreface facies belts of reduced turbulence and bathymetry prevailed. As a consequence, the depositional environments were more sensitive to sea-level fluctuations and thus were stronger affected by terrigenous siliciclastic input when compared to the northerly exposed more distal environments. These palaeogeographic aspects are interpreted herein as the dominant factors limiting the occurrences of different benthic communities. In contrast, the more distal depositional environments recorded in the northern sections, evidence less ecological stress for the benthic communities. The prevailing shallow open-marine conditions were less influenced by temporary ecological variations such as rapid changes of water circulation and turbulence, or siliciclastic input, favouring the occurrences of diverse benthic assemblages.

Despite the varying distances of the studied sections from the palaeocoastline, the variation of ecological features may have been strongly influenced by relative sea-level changes which, therefore, left imprints on the benthic distribution. A close relation between sequence stratigraphic subdivisions and the distribution of the studied benthics is evident: rudists predominantly occur in HSTs, whereas benthic foraminifers and calcareous algae (including the high-energy algae debris facies) occur in HSTs and TSTs. Red algae are nearly absent in TSTs (Fig. 11, Tab. 2). This suggests that changing environmental parameters such as accommodation space, sedimentation rate and turbulence during TSTs and HSTs were responsible for the dominance or absence of the studied biota. We cannot follow the model of laterally shifting environments that correlate with falling or rising sea level and thus may have controlled the benthics distribution (compare BRETT 1998). For the Middle Cretaceous strata

of north Sinai, BACHMANN & KUSS (1998) showed that 3rd-order sea-level fluctuations resulted in the development of distinct facies patterns within different systems tracts. With respect to the data presented here, the facies-related distribution patterns described above are closely related to an interplay between facies evolution and the development of specific depositional settings within individual systems tracts: During LSTs, restricted very shallow and supratidal palaeoenvironments established, involving siliciclastic terrigenous sedimentation which was unfavourable for the studied benthics. During TSTs, increased accommodation space resulted in an increase of water circulation and turbulence. Additionally, the rise of the base level and retrogradation of the siliciclastic shoreface caused a reduced deposition of siliciclastics. This interplay controlled the onset of extended shallow-marine inner platform conditions, that favoured the growth of foraminifers and algae in the limestones described above and diversities increased as new niches developed during TSTs. In HSTs, platform flooding results in maximum carbonate production (HANDFORD & LOUCKS 1993) and often in the formation of coarse-grained, oolithic sediments (compare SCHLAGER et al. 1994). In Sinai, these features are indicated by abundant reworked algae debris and oolithic lithologies in the studied sections. These high-energetic environments were favoured by recumbent *Ichthyosarcolites* during the Cenomanian in Sinai and by diverse Caprinidae other Tethyan shelves (ROSS & SKELTON 1993), but obviously were not favourable environments for other rudists with different growth strategies neither during the Cenomanian nor during the Turonian in Sinai. Furthermore, shallow-marine environments with abundant foraminifers and algae established during HSTs, while during periods of highstand progradation low-energy environments developed, which were favourable habitats for most of the observed rudist assemblages.

Systems Tracts	Rudists	Foraminifers	Calcareous Algae
HST	*Apricardia, Durania, Hippurites, Ichthyosarcolithes, Praeradiolites, Radiolites, Vaccinites*	*Cuneolina, Dicyclina,* miliolids (undifferentiated) *Pseudolituonella, Pseudorhapydionina, Quinqueloculina, Valvulammina*	*Arabicodium, Bouenia, Neomeris, Marinella*
TST	*Durania, Radiolites*		*Arabicodium, Bouenia, Neomeris*
LST	-	-	-

Tab 2: Compilation of prevailing genera of rudists, benthic foraminifers and calcareous algae within systems tracts.

8. CONCLUSIONS

The regional distribution of rudists, benthic foraminifers, and calcareous algae within a sequence stratigraphic frame allows to determine some of the factors controlling the varying faunal distribution patterns. The following distribution trends are recognised:

- *Large scale trends:* Diversity and frequency of rudists declined across the Cenomanian-Turonian boundary. A recovery is observed in Middle-Late Turonian times. The same is true for benthic foraminifers, even though the diversities did not reach the same level of the Cenomanian assemblages. The distribution patterns of calcareous algae suggest a different trend, with only few species in the Cenomanian and diverse assemblages in the Turonian. The post Cenomanian re-establishment of the drowned carbonate platform since the Middle Turonian allowed the gradual recovery of the studied biota.

- *Trends related to depositional environments and systems tracts:* Diversities and abundances of the studied biota change along a N-S gradient. Varying turbidity, bathymetry and siliciclastic input in the inner platform settings controlled the habitats of the benthic assemblages. The distribution of the studied benthics is closely related to the development of specific depositional settings within individual systems tracts: rudists predominantly occur in HSTs, while benthic foraminifers and calcareous algae prevail in HSTs and TSTs. This suggests that environmental parameters such as accommodation space, sedimentation rate or turbidity, which changed during TSTs and HSTs, controlled the dominance of the studied biota rather than simple lateral shifts of the habitats of these groups with falling or rising sea-level.

ACKNOWLEDGEMENTS

Funding has been provided by the German Science Foundation (DFG Ku 642/15-1/2). We thank M. MORSI and A.M. BASSIOUNI (both Ain Shams University, Cairo) for ostracod determinations and kind help during our stay in Egypt, A. MARZOUK (University of Tanta, Egypt) for the determinations of calcareous nannofossils, and F. WIESE (FU Berlin) / P. LUGER (TU Berlin) for ammonite determinations. H. LÖSER (Dresden) helped with the identification of Cenomanian corals. Various kinds of assistance were provided by M. BACHMANN, E. FRIEDEL and R. BÄTZEL (all University of Bremen). J.P. PLATEL and G.W. HUGHS are acknowledged for their constructive reviews.

REFERENCES

ABDALLAH, H. & MEISTER, C. (1997): The Cenomanian-Turonian boundary in the Gafsa-Chott area (southern part of central Tunisia): biostratigraphy, palaeoenvironments.- Cretaceous Res., **18**: 197-236; London.

ABDEL-GAWAD, G.I. & GAMEIL, M. (1995): Cretaceous and Palaeocene coral faunas in Egypt and Greece.- Coral Res. Bull., **4**: 1-36; Dresden.

ALLAM, A. & KHALIL, H. (1988): Geology and stratigraphy of the Arif El-Naqa area, Sinai, Egypt.- Egypt. J. Geol., **32**: 199-218, Cairo.

ARTHUR, M.A., SCHLANGER, S.O. & JENKYNS, H.C. (1987): The Cenomanian-Turonian Oceanic Anoxic Event, II: Palaeoceanographic controls on organic-matter production and preservation.- In: BROOKS, J. & FLEETS, A.J. (eds): Marine petroleum source rocks.- Geol. Soc. London Spec. Publ., **26**: 401-420; Oxford (Blackwell).

BACHMANN, M. & KUSS, J. (1998): The Middle Cretaceous carbonate ramp of the northern Sinai: sequence stratigraphy and facies distribution.- In: WRIGHT, V.P. & BURCHETTE, T.P. (eds): Carbonate Ramps.- Geol. Soc. London Spec. Publ., **149**: 253-280; Oxford (Blackwell).

BARATTOLO, F. (1991): Mesozoic and Cenozoic marine benthic calcareous algae with particular regard to Mesozoic dasycladaceans.- In: RIDING, R. (ed.): Calcareous algae and stromatolites. 504-540; Berlin (Springer).

BARTOV, Y., LEWY, Z., STEINITZ, G. & ZAK, I. (1980): Mesozoic and Tertiary stratigraphy, paleogeography and structural history of the Gebel Areif en Naqa area, eastern Sinai. - Isr. J. Earth-Sci., **29**: 114-139; Jerusalem.

BARTOV, Y. & STEINITZ, G. (1977): The Judea and Mount Scopus groups in the Negev and Sinai with trend surface analysis of the thickness data.- Isr. J. Earth-Sci., **26**: 119-148; Jerusalem.

BASSOULLET, J.P., BERNIER, P., DELOFFRE, R., GÉNOT, P., PONCET, J. & ROUX, A. (1983): Udoteacea.- Bull. Centres Rech. Explor.-Prod. Elf Aquitaine, **7** (2): 449-621; Pau.

BASSOULLET, J.-P. & DAMOTTE, R. (1969): Quelques ostracodes nouveaux du Cenomano-Turonien de l' atlas Saharien occidental (Algerie).- Rev. Micropaléont., **12** (3): 130-144; Paris.

BAUER, J., MARZOUK, A.M., STEUBER, T. & KUSS, J. (subm.): Lithostratigraphy and biostratigraphy of the Cenomanian-Santonian strata of Sinai, Egypt.- Cretaceous Res.; London.

BOSWORTH, W., GUIRAUD, R. & KESSLER, L.G. (1999): Late Cretaceous (ca. 84 Ma) compressive deformation of the stable platform of northeast Africa (Egypt): Far-field stress effects of the "Santonian event" and origin of the Syrian arc deformation belt.- Geology, **27** (7): 633-636; Boulder.

BRETT, C.E. (1998): Sequence stratigraphy, paleoecology, and evolution: biotic clues and responses to sea-level fluctuations.- Palaios, **13**: 241-262; Tulsa.

BUCHBINDER, B., BENJAMINI, C. & LIPSON-BENITAH, S. (2000): Sequence development of Late Cenomanian-Turonian carbonate ramps, platforms and basins in Israel.- Cretaceous Res., **21**: 813-843; London.

BURCHETTE, T.P. & BRITTON, S.R. (1985): Carbonate facies analysis in the exploration for hydrocarbons: a case-study from the Cretaceous of the Middle East.- In: BRENCHLEY, P.J. & WILLIAMS B.P.J (eds): Sedimentology; recent developments and applied aspects.- Geol. Soc. London Spec. Publ., **18**: 311-338; Oxford (Blackwell).

BURCHETTE, T.P. & WRIGHT, V.P. (1992): Carbonate ramp depositional systems.- Sediment. Geol., **79**: 3-57; Amsterdam.

CARANNANTE, G., GRAZIANO, R., PAPPONE, G., RUBERTI, D. & SIMONE, L. (1999): Depositional system and response to sea level oscillations of the Senonian rudist-bearing carbonate shelves. Examples from central Mediterranean areas.- Facies, **40**: 1-24; Erlangen.

CHAIMOV, T.A., BARAZANGI, M., AL-SAAD, D., SAWAF, T., & GEBRAN, A. (1992): Mesozoic and Cenozoic deformation inferred from seismic stratigraphy in the southwestern intracontinental Palmyride fold-thrust belt, Syria.- Geol. Soc. Amer. Bull., **104**: 704-715; Boulder.

COHEN, Z., KAPTSAN, V., & FLEXER, A. (1990): The tectonic mosaic of the southern Levant: implications for hydrocarbon prospects.- J. Petrol. Geol., **13** (4): 437-462; Beaconsfield.

DOUVILLÉ, H. (1910): Etudes sur les rudistes. Rudistes de Sicile, d'Algérie, d'Egypte, du Liban et de la Perse.- Mém. Soc. géol. France, **41**: 1-83.; Paris.

DOUVILLÉ, H. (1913): Description des rudistes de l'Egypte.- Mém. Inst. Egypt., **6**: 237-256; Al Qahirah.

DOUVILLÉ, H. (1915): Sur quelques rudistes d'Egypte.- Bull. Inst. Egyptien, **8** (5): 162-167; Al Qahirah.

DOUVILLÉ, H. & COUYAT-BARTHOUX, (1914): Le massif du Moghara, à l'est du listhme de Suez.- C. R. Acad. Sci., **159**: 565-570; Paris.

FLEXER, A., ROSENFELD, A., LIPSON-BENITAH, S., & HONIGSTEIN, A. (1986): Relative sea level changes during the Cretaceous in Israel.- Amer. Assoc. Petrol. Geol. Bull, **70** (11): 1685-1699; Tulsa.

GHORAB, M.A. (1961): Abnormal stratigraphic feature in Ras Gharib oil fields.- 3rd Arab. Petrol. Congr., Alexandria, Egypt: 1-10; Alexandria.

GRÄFE, K.-U. (1999): Foraminiferal evidence for Cenomanian sequence stratigraphy and palaeoceanography of the Boulonnais (Paris Basin, northern France).- Palaeogeogr., Palaeoclimat., Palaeoecol., **153**: 41-70; Amsterdam.

Gvirtzman, Z. & Garfunkel, Z. (1998): The transformation of southern Israel from a swell to a basin: stratigraphic and geodynamic implications for intracontinental tectonics.- Earth and Planetary Sci. Letters, **163**: 275-290; Amsterdam.

HAMAOUI, M. & SAINT-MARC P. (1970): Microfaunes et microfaciès du Cénomanien du proche-orient.- Bull. Centre Rech. Pau-SNPA, **4** (2): 257-352; Pau.

HANDFORD, C.R. & LOUCKS, R.G. (1993): Carbonate depositional sequences and systems tracts - responses of carbonate platforms to relative sea-level changes.- In: LOUCKS, R.G. & SARG, J.F. (eds): Carbonate

sequence stratigraphy-recent events and applications.- Amer. Assoc. Petrol. Geol. Mem., **57**: 3-41; Tulsa.

HARDENBOL, J., THIERRY, J., FARLEY, M. B.; JACQUIN, T., DE GRACIANSKY, P.-C. & VAIL, P.R. (1998): Cretaceous sequence chronostratigraphy.- In: DE GRACIANSKY, P.-C., HARDENBOL, J., JACQUIN, T. & VAIL, P.R.(eds): Mesozoic and Cenozoic sequence stratigraphy of European basins.- Soc. Econ. Paleontol. Mineral. Spec. Publ., **60**: Chart 4; Tulsa.

HARRIES, P.J. (1993): Dynamics of survival following the Cenomanian-Turonian (Upper Cretaceous) mass extinction event.- Cretaceous Res., **14**: 563-583; London.

HART, M.B. (1996): Recovery of the food chain after the Late Cenomanian extinction event.- In: Hart, M.B. (ed.): Biotic recovery from mass extinction events.- Geol. Soc. London Spec. Publ., **102**: 265-277; Oxford (Blackwell).

HIRSCH, F., FLEXER, A., ROSENFELD, A. & YELLIN-DROR, A. (1995): Palinspastic and crustal setting of the eastern Mediterranean.- J. Petrol. Geol., **18** (2): 149-170; Beaconsfield.

JARVIS, I., CARSON, G.A., COOPER, M.K.E., HART, M.B., LEARY, P.N., TOCHER, B.A., HORNE, D. & ROSENFELD, A. (1988): Microfossil assemblages and the Cenomanian-Turonian (Late Cretaceous) oceanic anoxic event.- Cretaceous Res., **9**: 3-103; London.

JENKINS, D. A. (1990): North and Central Sinai. In: Said, R. (ed.): The geology of Egypt.- 361-380; Rotterdam (Balkema).

KAUFFMAN, E.G. (1995): Global change leading to biodiversity crisis in a greenhouse world: the Cenomanian-Turonian (Cretaceous) mass extinction.- In: STANLEY, S.M., KNOLL, A.H. & KENNETT, J. (eds): Effects of past global change on life.- Studies in Geophysics: 47-71; Washington D.C. (National Academy Press).

KAUFFMAN, E.G. & HART M.B. (1996): Cretaceous bio-events.- In: WALLISER, O.H. (ed.): Global events and event stratigraphy in the Phanerozoic.- 285-312; Berlin (Springer).

KERR, A.C. (1998): Oceanic plateau formation: a cause of mass extinction and black shale deposition around the Cenomanian-Turonian boundary.- J. Geol. Soc. London, **155**: 619-626; London.

KORA, M. & GENEDI, A. (1995): Lithostratigraphy and facies development of the Upper Cretaceous carbonates in East Central Sinai, Egypt.- Facies, **32**: 223-236; Erlangen.

KRENKEL, E. (1924): Der syrische Bogen.- Zbl. Mineral., Geol. und Paläont. Abh., **B 9** & **B 10:** 274-281 & 301-313; Stuttgart.

KUSS, J. (1992): Facies and stratigraphy of Cretaceous limestones from northeast Egypt, Sinai and southern Jordan.- In: SADEK, A. (ed.): Geology of the Arab world.- 283-301; Cairo.

KUSS, J. & CONRAD, M.-A. (1991): Calcareous algae from Cretaceous carbonates of Egypt, Sinai, and southern Jordan. J. Paleont., **65** (5): 869-882; Lawrence, Kansas.

KUSS, J. & MALCHUS, N. (1989): Facies and composite biostratigraphy of Late Cretaceous strata from Northeast Egypt.- In: WIEDMANN, J. (ed.): Cretaceous of the Western Tethys. Proceedings 3rd International Cretaceous Symposium, Tübingen 1987.- 879-910; Stuttgart (Schweizerbart).

KUYPERS, M.M.M., PANCOST, R.D. & DAMSTÉ, J.S.S. (1999): A large and abrupt fall in atmospheric CO2 concentration during Cretaceous times.- Nature, **399**: 342-345; London.

LEWY, Z. (1975): The geological history of southern Israel and Sinai during the Coniacian.- Isr. J. Earth-Sci, **24**: 19-43; Jerusalem.

LEWY, Z. (1989): Correlation of lithostratigraphic units in the upper Judea Group (Late Cenomanian-Late Coniacian) in Israel.- Isr. J. Earth-Sci, **38**: 37-43; Jerusalem.

LEWY, Z. (1990): Transgressions, regressions and relative sea level changes on the Cretaceous shelf of Israel and adjacent countries. A critical evaluation of Cretaceous global sea level correlations.- Paleoceanography, **5** (4): 619-637; Washington, DC.

LEWY, Z. & RAAB, M. (1976): Mid-Cretaceous stratigraphy of the Middle East.- Ann. Mus. Hist. Nat. Nice, **4**: XXXII.1-XXXII.20; Nice.

LOEBLICH, A.R. & TAPPAN H. (1988): Foraminiferal genera and their classification.- **I** & **II**, 1-970; New York (Van Nostrand Reinhold).

LÜNING, S., MARZOUK, A. M., MORSI, M. & KUSS, J. (1998a): Sequence stratigraphy of the Upper Cretaceous of central-east Sinai, Egypt.- Cretaceous Res., **19**: 153-196; London.

LÜNING, S., MARZOUK, A.M. & KUSS, J. (1998b): The Paleocene of Central East Sinai, Egypt: 'sequence stratigraphy' in monotonous hemipelagites.- J. Foram. Res., **28** (1): 19-39; Washington, DC.

MERMIGHIS, A., PHILIP, J. & TRONCHETTI, G. (1991): Séquences et cortèges de dépôts de plate-forme carbonatée au passage Cénomanien-Turonien dans les Hellénides internes (Péloponnèse, Grèce).- Bulletin de la Société géologique de France, **162**: 547-552; Paris.

MOUSTAFA, A.R. & KHALIL, M.H. (1990): Structural characteristics and tectonic evolution of north Sinai fold belts.- In: SAID, R. (ed.): The geology of Egypt. 381-389; Rotterdam (Balkema).

PARNES, A. (1987): Radiation of species of the genus *Radiolites* from the Upper Turonian at Gebel Er-Risha (NE Sinai, Egypt).- Israel J. Earth-Sci., **36**: 133-153; Jerusalem.

PHILIP, J. & AIRAUD-CRUMIERE, C. (1991): The demise of the rudist-bearing carbonate platforms at the Cenomanian/Turonian boundary: a global control.- Coral Reefs, **10**: 115-125; Berlin.

PHILIP, J., BABINOT, J.F., TRONCHETTI, G., FOURCADE, E., GUIRAUD, R., BELLION, Y., HERBIN, J.P., COMBES, P.J., CORNEE, J.J., DERCOURT, J. & RICOU, L.E. (1993): Late Cenomanian (94-92 Ma).- In: DERCOURT, J., RICOU, L.E. & VRIELYNCK, B. (eds): Atlas Tethys palaeoenvironmental maps- explanatory notes. 153-178; Paris (Gauthier-Villars).

ROSENFELD, A. & RAAB, M. (1974): Cenomanian-Turonian ostracodes from the Judea Group in Israel.- Geol. Surv. Isr. Bull., **62**: 1-64; Jerusalem.

ROSS, D.J. & SKELTON, P.W. (1993): Rudist formations of the Cretaceous: a palaeoecological, sedimentological and stratigraphic review. - In: WRIGHT, P. (ed.), Sedimentology Review. - **1**: 73-91; Oxford (Blackwell).

SAINT-MARC, P. (1974): Étude stratigraphique et micropaléontologique de l'Albien, du Cénomanien et du Turonien du Liban.- Notes et mémoires sur le moyen-orient, **13**: 1- 298; Paris.

SARG, J. F. (1988): Carbonate sequence stratigraphy. - In: WILGUS, C.K., HASTINGS, B.S., KENDALL, C.G.ST.C., POSAMENTIER, H.W., ROSS, C.A. & VAN WAGONER, J.C. (eds): Sea-level changes: an integrated approach. - Soc. Econ. Paleontol. Mineral. Spec. Publ., **42**: 155-181; Tulsa.

SCHLAGER, W., REIJMER, J.J.G. & DOXLER, A. (1994): Highstand shedding of carbonate platforms.- J. Sediment. Res., **B64** (3): 270-281; Tulsa.

SCHRÖDER R. & NEUMANN M. (1985): Les grandes foraminifères du Crétacé moyen de la region Méditerranéenne.- Geobios Mém. Spéc., **7**: 1-160; Lyon.

STEUBER, T. (2000): Skeletal growth rates of Upper Cretaceous rudist bivalves: implications for carbonate production and organism-environment feedbacks.- In: INSALACO, E., SKELTON, P.W. & PALMER, T.J. (eds): Carbonate Platform Systems: components and interactions.- Geol. Soc. London Spec. Publ.: **178**: 21-32; Oxford (Blackwell).

STEUBER, T. & LÖSER, H. (2000): Species richness and abundance patterns of Tethyan Cretaceous rudist bivalves (Mollusca: Hippuritacea) in the central-eastern Mediterranean and Middle East, analysed from a palaeontological database. Palaeogeogr., Palaeoclimat., Palaeoecol., **162**: 75-104; Amsterdam.

VAIL, P. R., AUDEMARD, F., BOWMAN, S. A., EISNER, P. N. & PERZ-CRUZ, C. (1991): The stratigraphic signatures of tectonics, eustasy and sedimentology - an overview.- In: EINSELE, G., RICKEN, W. & SEILACHER, A. (eds): Cycles and events in stratigraphy.- 617-659; Berlin (Springer).

VAN DEN BOLD, W.A. (1964): Ostracoden aus der Oberkreide von Abu-Rawash, Ägypten. – Palaeontographica, **123**: 111-136; Stuttgart.

VAN WAGONER, J.C., POSAMENTIER, H.W., MITCHUM, R. M., VAIL, P.R., SARG, J.F., LOUTIT, T.S. & HARDENBOL, J. (1988): An overview of the fundamentals of sequence stratigraphy and key definitions.- In: WILGUS, C.K., HASTINGS, B.S., KENDALL, C.G.ST.C., POSAMENTIER, H.W., ROSS, C.A: & VAN WAGONER, J.C.(eds): Sea-level changes: an integrated approach.- Soc. Econ. Paleontol. Mineral. Spec. Publ., **42**: 39-45; Tulsa.

WRIGHT, P. & BURCHETTE, T.P. (1996): Shallow-water carbonate environments.- In: READING, H.G. (ed.): Sedimentary environments: processes, facies and stratigraphy.- 325-394; Oxford (Blackwell).

Ziko, A., Darwish, M. & Eweda, S.(1993): Late Cretaceous-Early Tertiary stratigraphy of the Themed area, East Central Sinai, Egypt.- N. Jb. Geol. Paläont. Mh., **1993** (H.3): 135-149; Stuttgart.

CHAPTER 5

Platform environments, microfacies and systems tracts of the upper Cenomanian - lower Santonian of Sinai, Egypt

Jan Bauer, Jochen Kuss & Thomas Steuber

Submitted to Facies

CHAPTER 5

Platform environments, microfacies and systems tracts of the upper Cenomanian - lower Santonian of Sinai, Egypt

Jan Bauer*, Jochen Kuss* & Thomas Steuber**

Facies, submitted

* Bremen University, Department of Geoscience, PO Box 330440, D-28334 Bremen, Germany
** Ruhr-University Bochum, Institute of Geology, Mineralogy and Geophysics, Universitätsstr. 150, D-44801 Bochum, Germany

KEYWORDS: Microfacies analysis, inner-carbonate platform, Sinai, Egypt

SUMMARY

Factors controlling grain composition and depositional environments of upper Cenomanian - Santonian shallow-water, inner-platform limestones of Sinai are discussed. The inner-platform setting investigated is subdivided into five major facies belts, each represented by several microfacies types (MFTs). The lateral distribution patterns of the MFTs and their components underline the proximal-distal zonation across the platform and mirror the distance from the palaeocoastline.

The microfacies of the Cenomanian - Santonian sediments differ obviously, and are evaluated with respect to the local and regional large-scale environmental changes. Among other features, the prevalence of calm, protected subtidal environments, and the scarceness of ooids and oncoids during the late Cenomanian contrast with occasional high-energy facies belts in the Turonian. We consider variations of the platform morphology as a major controlling factor. In addition, a higher siliciclastic input, decline of calcareous algae, and reduced quantities of coated grains correspond to an increase of humidity and a decrease of water temperature at least since the early Coniacian.

The interplay between sea-level changes, accommodation, hydrodynamics and siliciclastic input is reflected by the correlation of lithofacies and biofacies within individual systems tracts. In particular, increasing accommodation and carbonate production intensified circulation and wave-agitation and controlled the distribution of high-energy environments in TSTs, and to a minor extent, in HSTs, where protected environments prevailed.

1. INTRODUCTION

We present the results of microfacies and semiquantitative component analyses of upper Cenomanian - Santonian limestones of Sinai to (1) evaluate the environmental influences on the inner-platform

lithofacies and biofacies; to (2) recognise ecological variations with respect to the local and regional depositional history; and to (3) examine the relations between microfacies and the sequence-stratigraphical architecture. This paper is based on semiquantitative examinations of 450 thin sections from 20 stratigraphical sections, of which the most representative sections (Fig. 1) are referred to herein.

Detailed microfacies analyses of Cenomanian and Turonian rocks of Sinai were previously presented by, e.g., EL-AZABI & EL-ARABY (1996), KUSS (1992), BACHMANN & KUSS (1998), LÜNING et al. (1998a), HEIMHOFER (1999), and ZALAT (1999). However, some of these studies refer to single sections or relatively small areas of Sinai; others do not focus on lateral and vertical microfacies distribution patterns within a high-resolution stratigraphical framework. Microfacies analysis of the upper Turonian - Santonian deposits of Sinai, Egypt, Israel, and Palestine are rare (KUSS & MALCHUS,1989; AHMED, 1995; ORABI & RAMADAN, 1995; EWEDA & EL-SOROGY, 1999; BUCHBINDER et al., 2000). While BAUER et al. (in press) concentrate on the distribution of benthics (rudists, calcareous algae, and benthic foraminifers) to examine the factors controlling their occurrences and to document their decline and recovery patterns across the Cenomanian/Turonian (C/T) boundary, this study is based on comprehensive microfacies analyses, including Coniacian and Santonian successions.

Well known extrinsic perturbations, such as oceanographical and climatical changes and oceanic anoxia effected many Cretaceous Afro-Arabian platforms at the C/T boundary (PHILIP & AIRAUD-CRUMIERE, 1991; KERR, 1998; KUYPERS et al., 1999). Key issues of the Cenomanian - Santonian depositional history of Sinai are (1) relative sea-level changes, (2) platform drowning at the C/T boundary, (3) post-Cenomanian 'Syrian Arc' tectonics, and (4) Late Cretaceous upwelling along the Afro-Arabian Plate margin, (LEWY, 1975; ALMOGI-LABIN et al., 1993; ESHET et al., 1994; LÜNING et al., 1998b; KUSS et al. 2000, BAUER et al., submitted). The aim of this contribution is to specify the effects of these issues on the sedimentary record.

2. GEOLOGICAL FRAMEWORK

In late Cenomanian times, Sinai was part of the wide carbonate platform (Fig. 2) along the passive continental margin of the Afro-Arabian Plate (PHILIP et al., 2000), where shallow inner-shelf environments with predominantly subtidal and peritidal calcareous sediments and sandstones established (Fig. 2). The Sinai platform extended over a maximum of about 200 km from north to south (distal - proximal) and was differentiated in the Turonian by a shallow intrashelf basin (BARTOV & STEINITZ, 1977), the Central Sinai Basin (C-S Basin). Its eastward prolongation was the Eshet-Zenifim Basin (BUCHBINDER et al. 2000). This configuration is similar to the Cretaceous inner-platform setting of Oman (HARRIS et al., 1984; Fig. 2). During the early Turonian, the Sinai platform was drowned (BAUER et. al., 2001) which is documented by condensed deep-water deposits of the C-S Basin (Fig. 2). Carbonate platform environments recovered in the middle Turonian and shallow calcareous inner-platform deposits prevailed until the late Turonian. From the Coniacian onwards, the siliciclastic input from the hinterland increased markedly, and a basin and swell morphology developed with mixed siliciclastic-carbonate deposits (LEWY, 1975; KUSS & BACHMANN, 1996).

The platform examined was characterised by six major facies belts (Fig. 2) including a supratidal facies belt which is, however, represented by soft lithologies (siltstones, claystones,

gypsum) only and is therefore not considererd in the microfacies analysis. Siliciclastic shoreface and lagoons occurred nearshore, shallow subtidal, and high-energy subtidal (mainly isolated, platform interior shoals) facies belts governed the inner-platform setting, and deep-water deposits occurred in the C-S Basin. An overview of the main lithological characteristics is given in Tab. 1. It is important to note that comparisons with sections from south Sinai in Tab. 1 highlight the lithofacies variations, but as limestones are rare, these sections were not used for microfacies analysis.

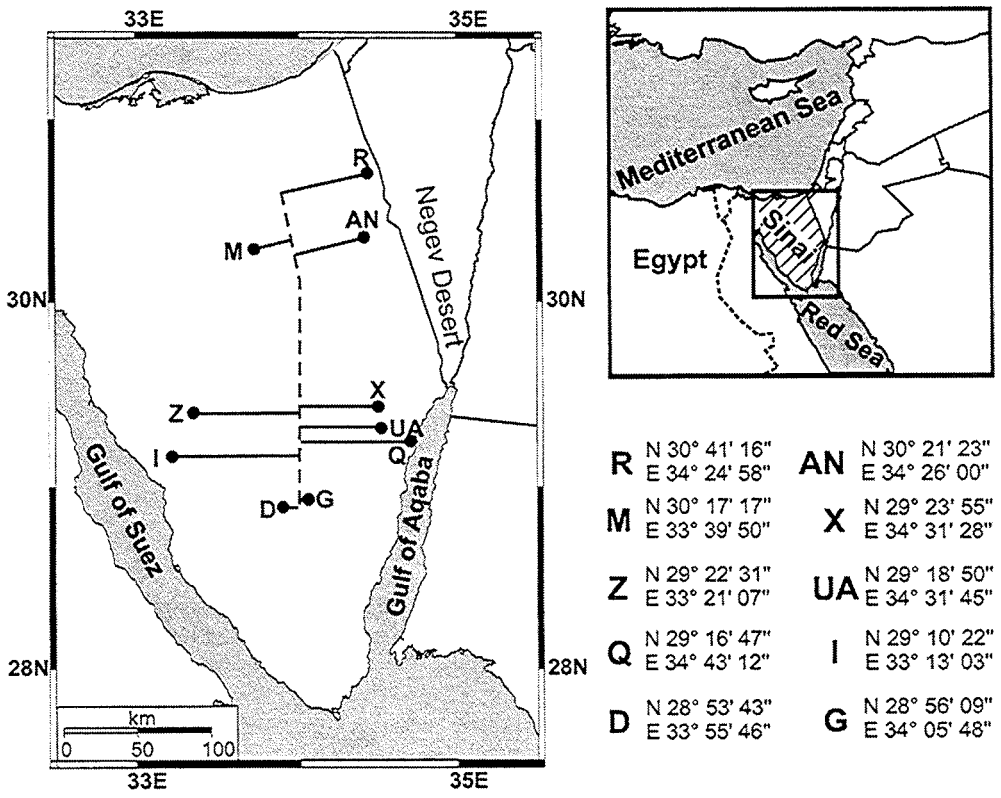

Fig. 1: Location map and co-ordinates of the sections studied, projected on the transect (stippled line) of correlation (Fig. 4). R, Gebel Risha; AN, Gebel Areif El Naqa; M, Gebel Minsherah; X, Wadi Gidira; Z, Gebel Abu Zurub; UA, Gebel Um Alda; Q, Ain Quseiyib; I, Gebel Iseila; G, Gebel Gunna; D, Gebel Dhalal.

In Sinai, 'Early Alpine' transpression since the Turonian resulted in the structural inversion of older half grabens (MOUSTAFA & KHALIL, 1990). The beginning closure of the Neotethys coincides with several episodes of the strike-slip faulting and folding in mid and Late Cretaceous times in parts of North Africa and Near East (SHAHAR, 1994; GUIRAUD & BOSWORTH, 1997; BOSWORTH et al., 1999). A resulting belt of domal anticlines ('Syrian Arc') extends from present-day central Syria, Israel, Palestine, north Sinai to western Egypt (SHAHAR, 1994; WALLEY, 1998; KUSS et al., 2000).

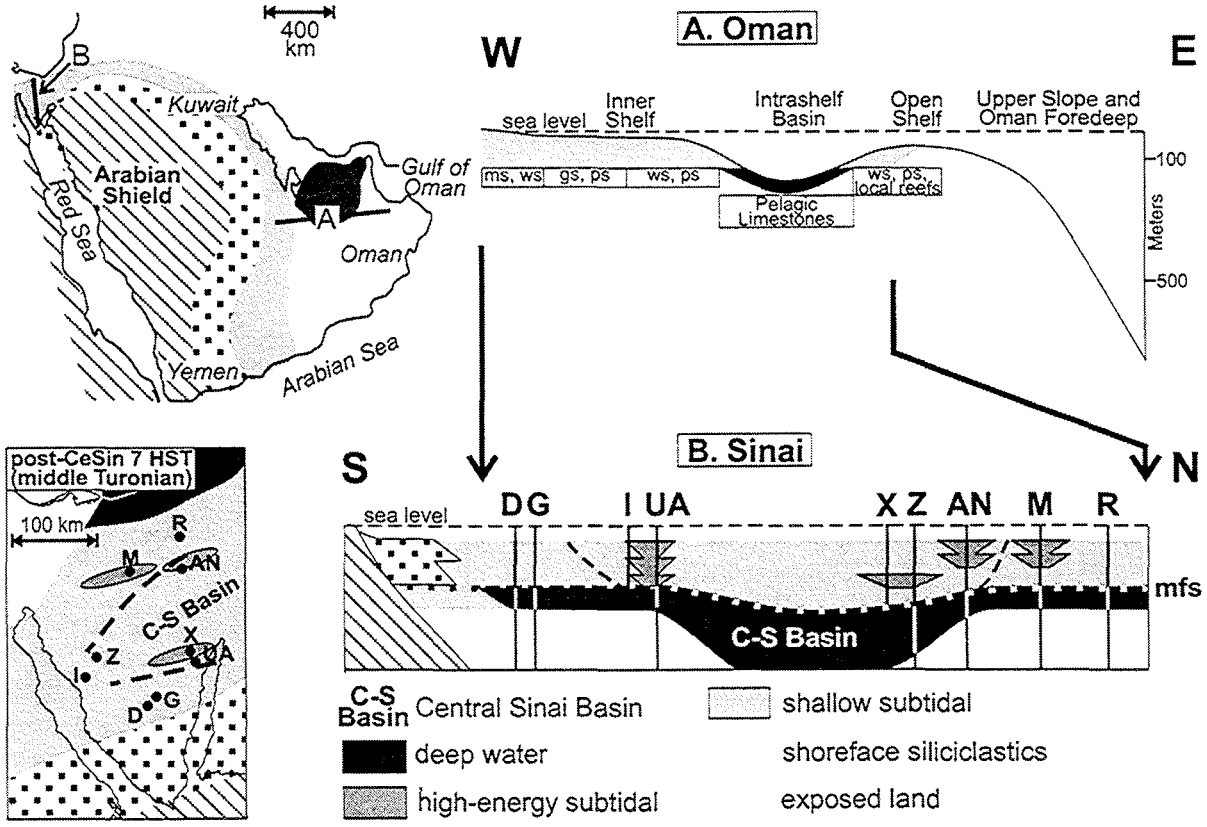

Fig. 2: Schematic middle Turonian (post-CeSin 7 HST) palaeogeographical map and cross-section of the Sinai platform (B), including the C-S Basin. The sections studied are indicated on the map and in the cross section. Close similarities between the Sinai platform geometry and the Cretaceous shelf of Oman (A), modified after HARRIS et al. (1984, Fig. 1), are obvious. The schematic palaeogeographical map (top left) shows the general depositional setting of the Arabian Plate (modified after HARRIS et al., 1984, Fig. 1), the position of the Oman cross section and the Sinai Peninsula are also indicated.

3. STRATIGRAPHY

Biostratigraphical data and the lithostratigraphical correlation of most sections presented herein have been integrated into a multistratigraphical framework (BAUER et al., 2001) on which a sequence-stratigraphical interpretation is based (BAUER et al., submitted). Thus, we give only a brief overview of the upper Cenomanian - Santonian stratigraphy of Sinai.

3.1 Biostratigraphy

The biostratigraphical framework of the sections studied (Fig. 3) is based on the combination and cross-correlation of data from different groups of fossils (ammonites, calcareous nannofossils, benthic foraminifers, ostracods and rudists). Keeled planktic foraminifers or inoceramids are absent in the successions presented in this paper.

	Facies Belts	North Sinai (sections R, AN, M)	Central Sinai (sections Z, X, UA, Q, I, G, D)	South Sinai	MFT
Nearshore	Supratidal	- Emersion surfaces, karstification evaporites and foliated claystones with plant remains.		- Emersion surfaces, plant remains, silicified wood, caliche beds.	—
	Shoreface siliciclastics	- Reddish mottled siltstone and fine sandstones. - Coarse and medium grained sandstones. - Bioclastic (cross-bedded) calcareous sandstones		- Reddish siltstones and sandstones with ferruginous ooids. - Bioclastic (cross-bedded) sandstones.	S1, S2
Platform	Lagoon	- Marls, paucispecific, hypersaline to brackish ostracods and oysters assemblages	- Stromatolitic and laminated calcareous marls. - Wackestones and packstones with miliolids, ostracods peloids, birds eyes. - Mudstones with benthic foraminifers.	- Marls with paucispecific ostracods assemblages.	L1, L2, L3
	Shallow subtidal	- Coarse bioclastic, dolomites, limestones and calcareous marls with bivalves (e.g., rudists, oysters), corals, chaetatids, gastropods, echinoderms. - Bioclastic packstones and wackestones (benthic foraminifers, calcareous algae, ostracods, echinoderms, bivalves, peloids).		- Bioclastic marls and packstones (e.g., oysters, gastropods). - wackestones with benthic foraminifers and ostracods.	P1, P2, P3, P4, P5
	High-energy subtidal	- Winnowed packstones and grainstones with ooids, oncoids, reworked debris (e.g., algae debris, ostracods). - Cross-bedding, channels, rip-up structures, reworking textures.		*not developed*	W1, W2, W3, W4
Basin	Deep-water	- Marls and chalks with frequent ammonites, planktic foraminifers and calcareous nannofossils.		*not developed*	B1

Tab. 1: Lithofacies and biofacies characteristics of the major facies belts and their local occurrences in Sinai. Dominant microfacies types (MFT) of individual facies belts are indicated in the right column.

Abundant ammonites are mainly limited to a relatively thin interval of lower Turonian deposits ('ammonite bed', see section 3.2). The reported species indicate an earliest Turonian stratigraphical gap in large parts of Sinai (BARTOV et al., 1980; KASSAB & OBAIDALLA, 2001; BAUER et al., 2001), which is also indicated by biostratigraphical data of CHÉRIF et al. (1989) and elswhere in the Near East (LEWY, 1989; BUCHBINDER et al., 2000). *Paratexanites desmondi* is characteristical of the upper Coniacian successions studied.

The chronostratigraphical assignments of the calcareous nannofossil zones identified, follow the scheme of VON SALIS in HARDENBOL et al. (1998), although two exceptions are discussed by BAUER et al. (2001): the lower boundary of CC 11 is placed in the uppermost Cenomanian, and the lower

boundary of CC 12 is placed in the middle Turonian. Some benthic foraminifers allow to differentiate the stages (Fig. 3) after SAINT-MARC (1974) and SCHRÖDER & NEUMANN (1985). The biostratigraphical ranges of ostracods recovered from the sections presented herein were given previously by MORSI & BAUER (in press), those from the Turonian and Santonian are after ROSENFELD & RAAB (1974). In addition, the last occurrence of the rudist bivalve *Ichthyosarcolites* and the first occurrence of the Hippuritidae mark the C/T boundary (PHILIP & AIRAUD-CRUMIERE, 1991). In the sections studied, the first Hippuritidae occur in the middle Turonian (Middle Abu Qada Formation, see section 3.2).

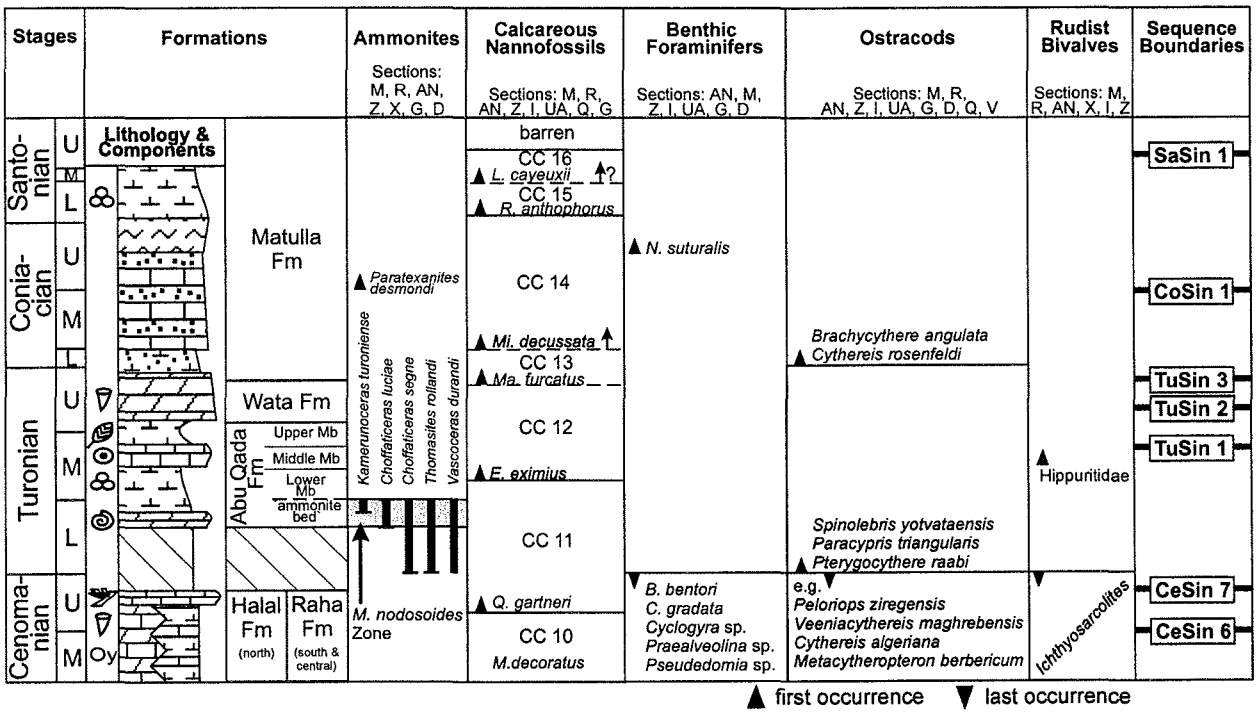

Fig. 3: Multistratigraphical framework of the sections studied. The standard section on the left shows a compilation of the generalised lithologies and lithostratigraphical subdivision. For a key to the symbols and lithologies, see Fig. 4. Abbreviations: calcareous nannofossils: *E.*, *Eiffellithus*; *L.*, *Lucianorhabdus*; *M.*, *Microrhabdulus*; *Ma.*, *Marthasterites*; *Mi.*, *Micula*; *Q.*,*Quadrum*; *R.*, *Reinhardtites*; benthic foraminifers: B., *Biconcava*; *C.*, *Chrysalidina*; *N.*, *Neoflabellina*. Sequence boundaries (right) are after BAUER et al. (submitted).

3.2 Lithostratigraphy

In north Sinai, the Cenomanian Halal Formation consists of dolostones, with some intercalations of marls and bioclastic limestones (Fig. 3). In central and south Sinai, the Cenomanian deposits correspond to the Raha Formation with fossiliferous limestones and dolostones; marls and sandstones are more frequent in the Raha Formation.

The Turonian Abu Qada Formation is subdivided into three members: marls with intercalated limestone beds represent the Lower and Upper members, and they are separated by well bedded dolostones and limestones of the Middle Member. Nodular dolostone layers with densely packed lower Turonian ammonites (´ammonite bed`) represent the base of the formation. The Wata Formation (mainly upper Turonian) consists of cliff-forming, cyclically bedded deposits of dolostones, bioclastic

limestones, and calcareous marls. Detailed microfacies analyses by HEIMHOFER (1999) indicated parasequences which originated from high order relative sea-level changes.

The lithologies of the Coniacian - Santonian Matulla Formation show small-scale lateral variations. Cross-bedded sandstones, marls, bioclastic limestones and dolostones interfinger with chalks with concretional chert. Siliciclastic detritus is common in most of the lithologies. Rare macrofossils are oysters; rudists are absent.

3.3 Sequence Stratigraphy

A compilation of the sequence-stratigraphical interpretation and correlation by BAUER et al. (submitted) is shown in Tab. 2 and Fig.4. The classification and nomenclature schemes follow the 'Exxon concepts' e.g. by Van Wagoner *et al.* (1988) and Vail *et al.* (1991).

Relative sea-level falls resulted in exposure surfaces. These sequence boundaries are documented by stratigraphical gaps, emersion or erosion surfaces. During lowstands, shorelines shifted northwards (i.e. basinwards) and shallow-water to supratidal environments evolved in Sinai. Carbonate production on the platform was reduced and, thus, siliciclastics and evaporites are typical lithologies of the lowstand systems tracts (LSTs).

Relative sea-level rises resulted in palaeogeographical modifications and are well recognisable from the lithofacies and biofacies of the transgressive systems tracts (TSTs). The siliciclastic influx was reduced in north and central Sinai, and extended shallow-marine, inner-platform carbonates retrograded. Relative sea-level highstands are generally characterised by thick accumulations of homogenous, dolomitic highstand systems tracts (HSTs) in north Sinai and protected, muddy subtidal or lagoonal environments in central and south Sinai. Prograding siliciclastics imply that the marine ingression reached the siliciclastic hinterland and limited the southward extension of the calcareous deposits.

4. METHODS

The detailed microfacies analysis is based on semiquantitative component analysis and on textural (including sorting and roundness of the components) and diagenetical features. For limestone classification we use the schemes of DUNHAM (1962) and EMBRY & KLOVAN (1972): mudstones (ms), wackestones (ws), floatstones (fs), packstones (ps), grainstones (gs). The thin sections investigated have been grouped into 15 microfacies types (MFTs) according to their components, textures, and environments of deposition (Fig. 5). In order to give a closer description of the MFTs, textural names have been supplemented by typical components and/or important textural features. In addition, the terms 'with' and 'rich in' express (in ascending order) the relative quantity of other important components (e.g. algal ps rich in coated grains).

The main skeletal and non-skeletal components of the limestones studied are listed in Fig. 5. However, further accessory constituents were also considered for the facies interpretation, such as debris from corals, rudists, and oysters, as well as glauconite, and phosphorite grains. Systematical determinations of microfossils (e.g. genera and species of calcareous algae and benthic foraminifers) mainly follow descriptions of SAINT-MARC (1974), SCHRÖDER & NEUMANN (1985), BARATTOLO (1991),

KUSS & CONRAD (1991), BASSOULLET et al. (1983) and SALAJ & MAAMOURI (1998). For semiquantitative component analysis, techniques described by FLÜGEL (1982) were used for visual percentage estimation. Three abundance classes were defined: rare (< 10 %), common (10 %-30 %), abundant (>30 %).

Sequence Boundaries	Systems Tracts & Surfaces	Characteristics
SaSin 1	SB / LST	Transition to shallow subtidal calcareous sandstones
	ts, TST / HST	Lithologic break at ts to chalky limestones and chalks with planktic foraminifers
	LST	Sandstones (calcareous) and siltstones
CoSin 1	SB	Hardgrounds
	mfs, HST	Condensation at mfs, dolostones alternate with calcareous sandstones
	ts, TST	Onset of carbonates, in parts oolitic with reworked components
	LST	Marls, shales and siltstones with gypsum, plant remains, ferruginous ooids and caliche intercalations
TuSin 3	SB	Emersions surfaces, hardgrounds, karstification, caliche beds
	TST / HST	Bioclastic dolostones and limestones
	LST	Deposition of siliciclastics
TuSin 2	SB	onset of shales and sandstones
	mfs, HST	Aggradation of thick bedded dolomites and bioclastic limestones (in parts oolitic), locally quartz grains in shoreface facies
	ts, TST	Onset of shallow-subtidal deposits
	LST	Gypsum beds, siltstones and shales, in parts with plant remains and brackish ostracods
TuSin 1	SB	Palaeosols or transition to shaley-silty deposits
	mfs, HST	Aggradation of dolostones and bioclastic, parts oolitic limestones; sometimes hardgrounds, ferruginous ooids and sandstones in coastal facies.
	ts, TST	Transition to deep-water facies at the ts; condensed deposits of dolostones with abundant ammonites overlain by marls with planktic foraminifers
	LST	Nondeposition or silty marls with plant remains (section Z)
CeSin 7	SB	Hardgrounds
	ts, TST/ HST	Decrease of quartzose deposits at the ts; dolostones, limestones, and marls with abundant macrofossils (rudists, oysters, corals)
	LST	Siltstones and shales with plant remains and ferruginous ooids
CeSin 6	SB	Hardgrounds

Tab. 2: Facies characteristics of upper Cenomanian - Santonian systems tracts and corresponding surfaces.

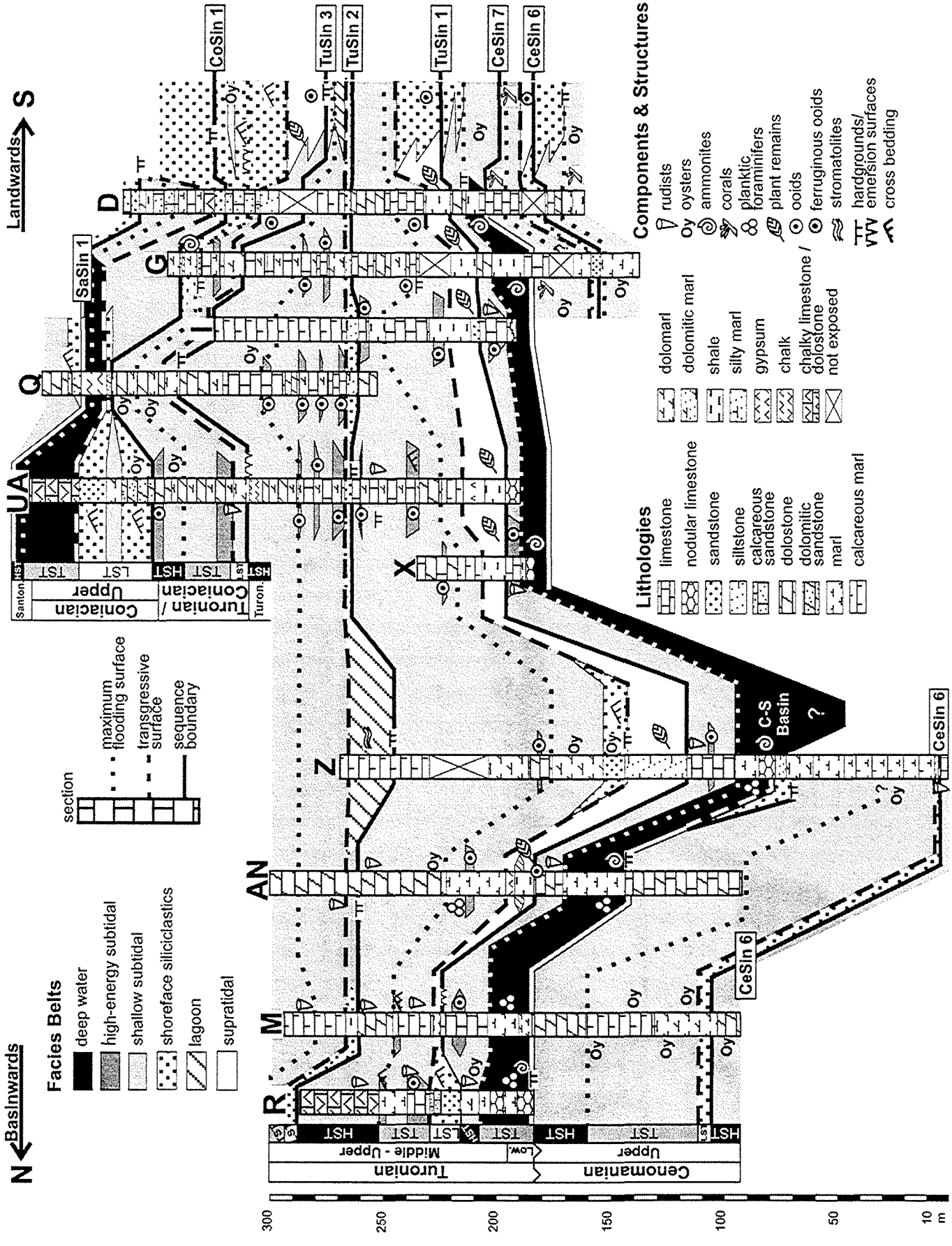

Fig. 4: Facies belt configuration, sequence architecture and platform-basin configuration along a N-S transect across Sinai (compare Fig. 1, stippled line).

5. RESULTS

5.1 Texture, Diagenesis, and Components

In the following, components, textural and diagenetical features are described with respect to their general characteristics and importance for facies interpretation.

Texture and diagenesis: Most thin sections studied show mud-supported textures (ms and ws). Among the grain-supported textures, packstones with micrite matrix prevail over washed packstones and grainstones. We do not differentiate between micrite and recrystallized microsparite. The relative quantities of micrite versus sparite and the abundance of packstones and grainstones describe general hydrodynamical energy conditions in the area of deposition. However, packing density may have prevented the transport of intergranular micrite, or vice versa, wave currents possibly infiltrated mud into the pores. Furthermore, grain orientation and componential sorting and roundness were considered for hydrodynamical estimations. Other indicative textural features are birdseyes and stromatactis. Bioturbation is occasionally recognised in thin sections. Borings occur in many clasts (Pl. 1/2). Intense microbe borings are common taphonomical features and resulted in completely micritized grains or in micrite envelopes (Pl. 4/13), which originated from micrite filling of microborings. The internal, destructive micrite envelopes have been differentiated from external, constructive micrite layers of coated grains (see below), which formed in association with biofilms. Studies on recent sediments of Jamaica (PERRY, 1998, 1999) show that (1) microendolithic organisms are most active in shallow, low-energy back-reef environments, (2) their bathymetrical distributions are mainly controlled by light penetration and (3) the microbes tend to infest predominantly corals, molluscs and foraminifers, whereas algae (e.g. *Halimeda*) and echinoderms are rarely affected.

Several cement types have been identified in this study and were investigated in detail by HEIMHOFER (1999). Intergranular calcite spar cement is most frequent; marine phreatic precipitation of syntaxial overgrowths and radial fibrous cements (Pl. 4/14) are sometimes present in intergranular pores of oolitic and bioclastic grainstones. These rocks may also comprise vadose dripstone (Pl. 4/15) and meniscus cements (compare e.g. FLÜGEL, 1982, p. 75; HILLGÄRTNER et al., 2001). Sparry calcite cement often filled moulds of dissolved grains (probably within the phreatic zone), which are often outlined by micrite envelopes (Pl. 4/13).

Skeletal components: Lagoonal and protected subtidal environments are often characterised by diverse assemblages of benthic foraminifers, e.g. *Biconcava bentori, Chrysalidina gradata* (Pl. 3/1, 2), *Cuneolina* sp. (Pl. 2/1), *Cyclogyra* sp. (Pl. 3/5), *Dicyclina* sp. (Pl. 3/3), *Nezzazata* sp., *Nummofallotia* sp. (Pls. 3/8, 2/1), *Pseudedomia* sp. (Pl. 3/4), *Pseudolituonella reicheli* (Pl. 3/11), *Pseudorhapydionina* sp. (Pl. 3/9, 10), and *Valvulammina* sp. (Pl. 3/6). Miliolids are typical of lagoonal environments and CARANNANTE et al. (2000) discuss that their thick tests indicate shallow and turbulent environments. Planktic foraminifers (Pl. 2/8, 9) are indicators of deep-water deposits. In the sections studied, this group comprises only non-keeled forms (hedbergellids, whiteinellids, heterohelicids); keeled morphotypes, typical of deeper water depths (HART, 1999), are absent.

Calcareous algae are common constituents of tropical inner-platform environments. In the thin sections studied, dasycladaceans are mainly represented by *Neomeris cretacea* (Pl. 3/14, 15) and minor amounts of *Acicularia* sp. (Pls. 3/13, 1/7) and ?*Cylindroporella* sp. (Pl. 1/3); udoteaceans (Pl. 2/4) mainly record *Bouenia pygmaea* (Pl. 4/3), *B.* cf. *hochstetteri* (Pl. 4/2) and *Arabicodium aegagrapiliodes* (Pl. 4/1). Rhodophytes are represented mainly by *Marinella lugeoni* (Pl. 4/4) and by rare gymnocodiaceans (Pl. 4/6). Furthermore, *Pseudolithothamnium album* (Pl. 3/16), *Thaumatoporella* sp. and *Bacinella* sp. may be present (Pl. 4/5).

Varying amounts of bivalves, gastropods, echinoderms, spicules (biaxial and monaxial), ostracods, bryozoans, and serpulids (Pl. 4/7) occur in most facies belts and are considered as shallow marine biota. Individual representatives of these groups are not indicative of a specific depositional environment, but together with other components they represent constituents of facies-indicative assemblages. Accessory grains identified as bioclasts of sponges, oysters, rudists, and corals (Pl. 4/8, 9). Although the latter may rarely occur in the Turonian deposits, coral debris occurs especially in the protected subtidal facies belts in the uppermost Cenomanian (Fig. 4). Rudists debris is rare in thin sections, but when present, disarticulated elements (laminae and muri) of the cellular shell structure of Radiolitidae (Pl. 4/8) produced a large amount of fine-grained carbonate. SANDERS (2001), underlined that shell dissolution by bioturbation and microbial infestation in combination with spalling of the thin-walled cellular structure are important taphonomic aspects with respect to disintegration of radiolitid shells.

Non-skeletal components: Peloids are frequent constituents of most MFTs, sometimes in rock-forming quantities. A variety of definitions and polygenetical interpretations of peloids exist in literature (for a review, see FLÜGEL, 1982, p. 131). In this study we use peloids as a non-genetical term for sand-sized, structureless, mostly spherical micrite grains (TUCKER & WRIGHT, 1990, p. 10). They are probably representatives of entirely micritized grains (ooids, algae, shell fragments) or reworked (consolidated) carbonate mud (TUCKER & WRIGHT, 1990, p. 11; RIDING, 2000). A more detailed genetical interpretation is mostly not possible. Some occurrences have been identified as faecal pellets due to their ovoid shape, good sorting, and high concentrations in clusters. Large coprolites may occur (Pls. 1/7, 4/11), but taxonomical classifications after SENOWBARI-DARYAN & KUSS (1992) have not been attempted.

Coated grains have been defined as components with a constructive, external micrite layer, such as ooids (Pl. 2/5), superficial ooids, and oncoids (Pl. 4/12), in contrast to micrite envelopes (see above). Ooids originated in high-energy settings and have been defined in this study as being *normal* ooids with several laminae, in contrast to superficial ooids with one to three laminae. The nuclei are composed of quartz or diverse bioclasts. The layers are micritized or show tangential structures; radial structures are rare. In the sections studied, ooids were linked to the formation of carbonate sand sheets and shoals. Yet, some were also transported into calmer environments, which is indicated by truncated rims and mismatches between nuclei and grain composition of the surrounding sediment. In the samples studied, superficial ooids occurred in both, high-energy settings, where ooid diameter and amount of layers depended on water energy, and in low-energy environments, as a result of microbial coatings (RIDING, 2000). Diagenetical origins have not been recognised.

Oncoids mostly have dark micrite layers (Pl. 2/2) in the thin sections studied, probably originated by bacterial biofilms (RIDING, 2000). Large algal oncoids (e.g. rhodolithes; compare BOSENCE, 1983) with typically wavy laminae have also been recognised.

Mud-intraclasts originated from reworking of partly consolidated carbonate mud by currents. Carbonate extraclasts are represented by allochthonous limestone fragments. They occur mostly in winnowed limestones and are characterised by differing grain composition and cements when compared to those of the host-rock, by truncated particles at their boundaries and by oxidation boundaries.

Quartz grains mirror the detritic input from the hinterland, and the textural maturities (sorting and roundness) have allowed estimations of water energy. Further accessory non-skeletal components are phosphate and glauconite grains, which may indicate reduced sedimentation rates.

Plate 1: Microfacies types of the siliciclastic shoreface, lagoonal and shallow subtidal facies belts. Scale bars are 1 mm.

Fig. 1. MFT S1, quartzose ps with ooids. Angular and subrounded quartz grains (1) in a micrite matrix are associated with normal ooids (2) and superficial ooids (3). Note *Acicularia* sp. (2) as ooid nucleus. Sample D3-13, Coniacian of section D (Gebel Dhalal), post-TuSin 3 HST.

Fig. 2. MFT S2, quartzose ps rich in bioclasts. Rock-forming quartz grains (fine to medium sand, subrounded, well sorted) occur within a micrite matrix. Thick bivalve fragments are commonly rounded and extensively bored (1). Coated grains are absent, in contrast to MFT S1. Sample D3-11, Coniacian of section D (Gebel Dhalal), post-TuSin 3 TST.

Fig. 3. MFT L1, monotonous ms, probably with ?*Cylindroporella* sp. (1). Sample D2-18, Turonian of section D (Gebel Dhalal), post-TuSin 1 HST.

Fig. 4. MFT L3, peloidal ps with foraminifers. Thick agglutinated miliolids, e.g. *Quinqueloculina* sp. (1), dominate among the benthic foraminifers with *Pseudorhapydionina* sp. (2). Sample G-5, Cenomanian of section G (Gebel Gunna), post-CeSin 5 TST.

Fig. 5. MFT P1, peloidal ps rich in molluscs. Coarse, poorly sorted and poorly rounded bivalves and gastropods are abundant, and sometimes represent coated grains; peloids and intraclasts are typical; a protected, environment is reflected by the muddy matrix. Sample AN2-19, Turonian of section AN (Gebel Areif el Naqa), post-CeSin 7 TST.

Fig. 6. MFT P2, fs rich in bivalves. Coarse bivalve shells are associated with intraclasts (1) and rare micritized ooids (2). A thick horizontal burrow (3) occurs in the mud supported texture. Sample M1-46, Turonian of section M (Gebel Minsherah), post-CeSin 7 HST.

Fig. 7. MFT P3, bioclastic ps with algae. Calcareous algae, *Neomeris cretacea* (1) and *Acicularia* sp. (2), occur together with miliolids, coprolites (3) and micritized intraclasts. Sample G2-4, Turonian of section G (Gebel Gunna), post-TuSin 2 TST.

Fig. 8. MFT P4, foraminiferal ps. The sample is dominated by thick agglutinated miliolids and other benthic foraminifers. Peloids are abundant and intraclasts indicate reworked lagoonal components. Sample M2-8, Cenomanian of section M (Gebel Minsherah), post-CeSin 6 TST.

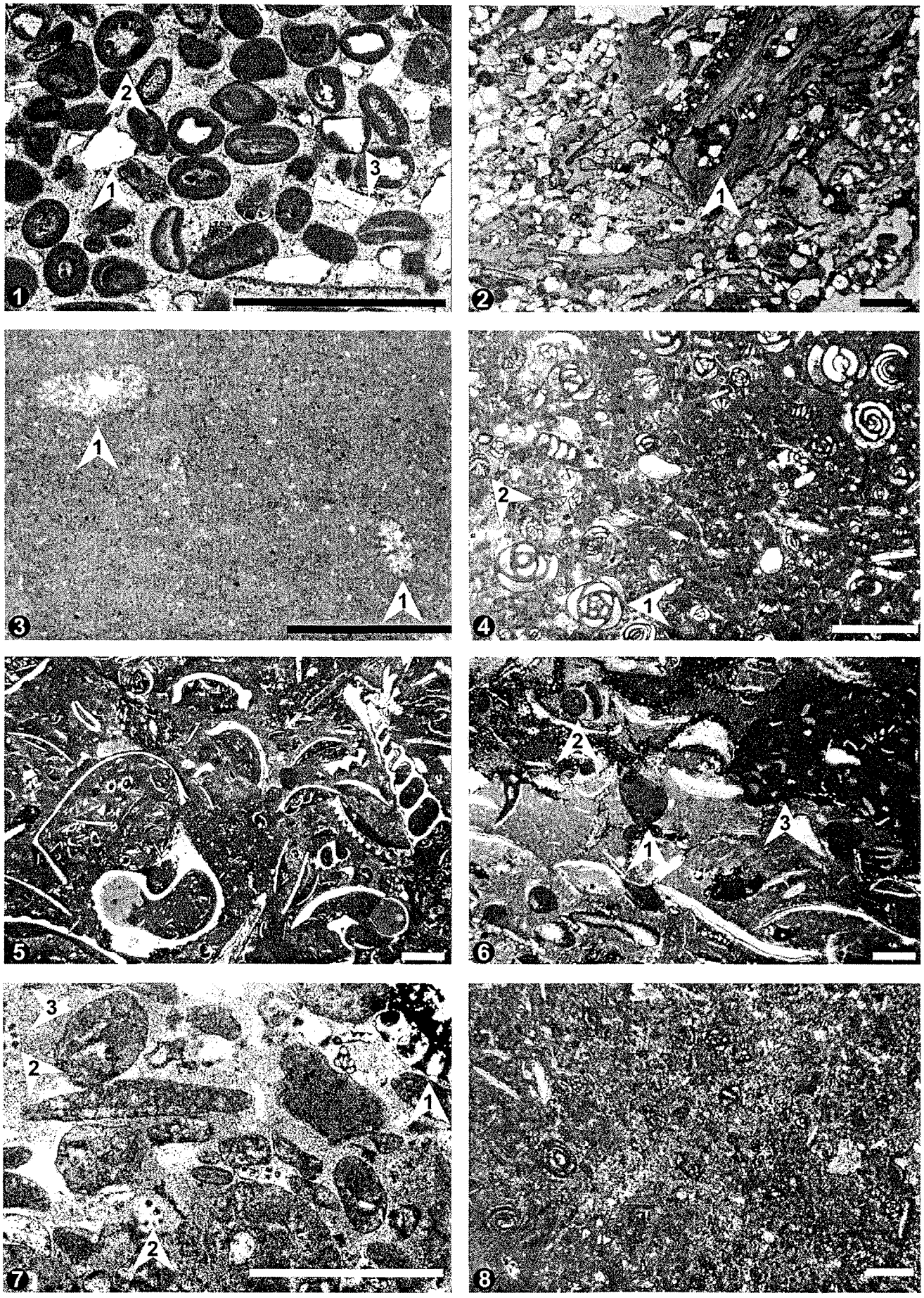
1
2
3
1
2
1
3
1
1
4
2
1
5
6
2
1
3
7
3
2
1
2
8

5.2 Microfacies Types of the Facies Belts

The limestones investigated show a wide spectrum of different MFTs (Fig. 5), which correspond to the five major facies belts. Lateral and vertical distribution patterns of components and MFTs are illustrated in Figs 6, 7.

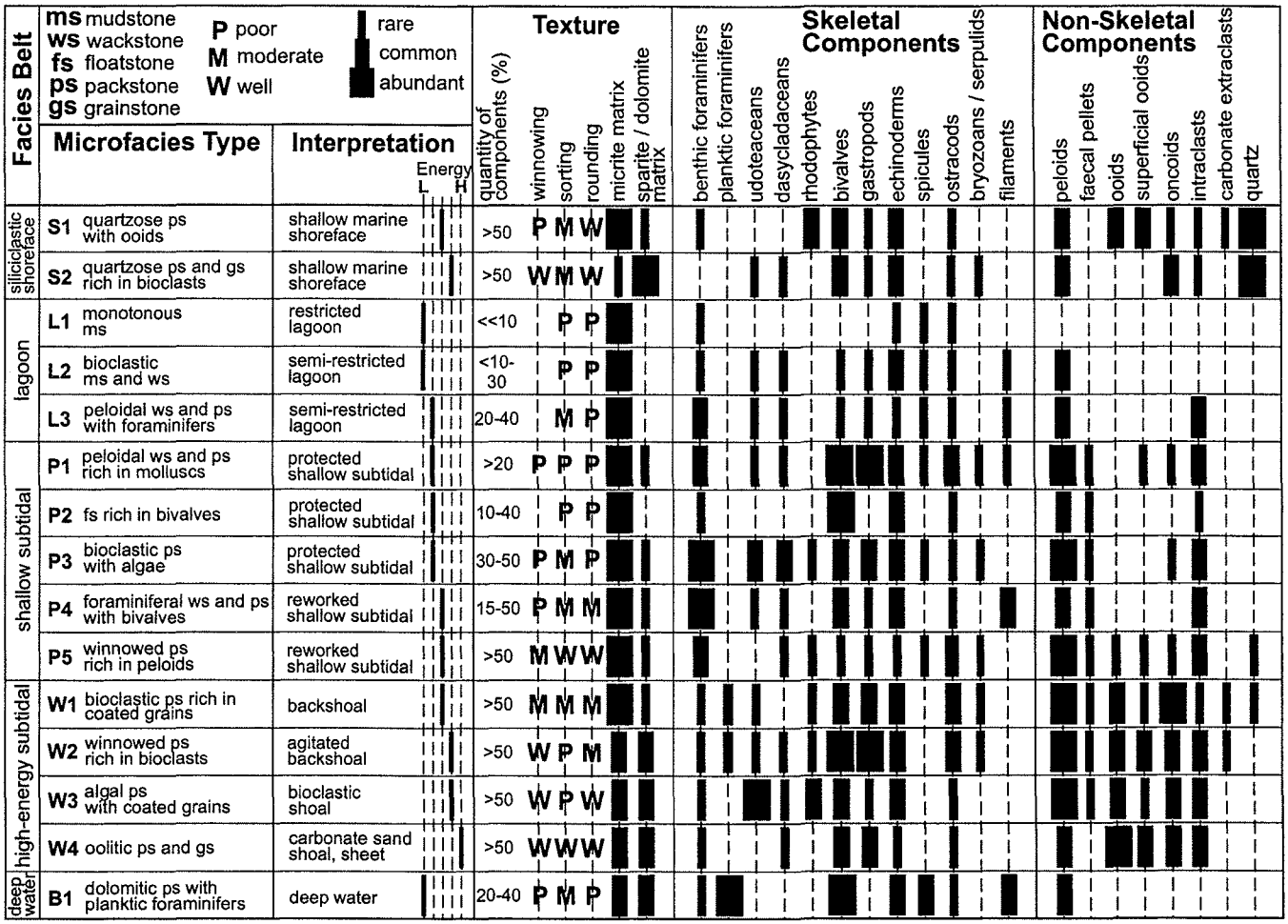

Fig. 5: Compilation of microfacies types, textures and semiquantitative component distributions. Accessory constituents, such as debris from corals, rudists and oysters, glauconite and phosphorite grains are not listed.

5.2.1 Siliciclastic Shoreface

MFT S1, quartzose ps with ooids (Pl. 1/1)*:* Diverse shallow-water bioclasts (bivalves, echinoderms, gastropods, ostracods, bryozoans, calcareous algae) are associated with rock-forming contents of quartz (fine to medium grained, moderately sorted, rounded) and accessory detrital glauconite. Peloids and coated grains (ooids, superficial ooids, oncoids) are common (Pl. 1/1). However, allochthonous ooids are indicated by rare quartz nuclei, despite abundant quartz grains in the surrounding sediment. The matrix mainly consists of micrite; silica and phosphate replacements of bioclasts are common as well as sparite-filled moulds with micrite envelopes. MFT S1 was deposited in a shallow, open marine, siliciclastic nearshore realm.

MFT S2, quartzose ps and gs rich in bioclasts: Apart from rock-forming amounts of quartz grains (fine to medium sand, sub-rounded to rounded, well sorted), similar shallow-water bioclasts occur as in MFT S1. Fish teeth are very rare (Pl. 4/10). Coated grains are absent. MFT S2 (Pl. 1/2) was deposited in a similar siliciclastic nearshore realm, but the higher textural maturity and the predominant sparite matrix indicats higher energy conditions, when compared with MFT S1.

5.2.2 Lagoon

MFT L1, monotonous ms: This MFT is characterised by extreme low amounts of components (thin bivalve shells, spicules, ostracods, calcareous algae). Birdseyes and mud cracks may occur. MFT L1 (Pl. 1/3) represents shallow, extremely low-energy and highly restricted lagoons or tidal ponds (compare WILSON, 1975, SFZ 8-9).

MFT L2, bioclastic ms and ws: The low diverse benthic assemblage is composed of molluscs, echinoderms, ostracods, and benthic foraminifers. Spicules, calcareous algae, and cyanophyceans may also occur. Peloids are sometimes common to abundant, especially in ws. Bioturbation and stromatactis may occur. We interpret a shallow, low-energy lagoonal environment of deposition. However, in contrast to MFT L1, bioturbation as well as a higher biotic diversity suggests semi-restricted conditions. This is also indicated by the occurrence of miliolids (WILSON, 1975).

MFT L3, peloidal ws and ps with foraminifers: Benthic foraminifers predominate the skeletal components; further biogenic constituents are rare bivalves, gastropods, echinoderms, calcareous algae, spicules, and ostracods. Peloids and intraclasts are the most important non-skeletal grains. Bioturbation, stromatactis, and birdseyes may be present. Common thick agglutinated miliolids (Pl. 1/4), *Dicyclina* sp., and *Cuneolina* sp. as well as rare calcareous algae indicate a semi-restricted lagoonal environment. Rounded intraclasts, preferred orientations of the components and scarce reworking features indicate a higher degree of turbulence when compared to MFT L2.

5.2.3 Shallow Subtidal

MFT P1, peloidal ws and ps rich in molluscs: Bivalves and gastropods (Pl. 1/5) are abundant. In addition, diverse assemblages of occasionally coarse-grained bioclasts of shallow-water benthics (miliolids, calcareous algae, spicules, bryozoans, serpulids, rudist debris, corals) are typical. Peloids are abundant non-skeletal grains, besides rare superficial ooids, oncoids, and intraclasts. The poorly sorted and poorly rounded components are often densely packed and occur within a predominantly micrite matrix. Sparite-filled bioclast moulds, sometimes outlined by micrite envelopes, are typical diagenetical features. Micritized and bored clasts are common. MFT P1 documents a normal-marine, shallow-subtidal environment. A protected, low-energy area of deposition is reflected by the muddy matrix.

MFT P2, fs rich in bivalves: Coarse bivalve shells (e.g. oysters, rudists debris) are characteristic (Pl. 1/6). Subordinate benthic foraminifers (miliolids), echinoderms, and ostracods as well as peloids, intraclasts, and glauconite grains occur in varying quantities. The components are sometimes micritized and bored. Burrows and dolomite patches are sometimes found in the mud supported texture (Pl. 1/6). MFT P2 was formed in a protected shallow subtidal environment.

MFT P3 bioclastic ps with algae: The diverse benthic assemblage contains benthic foraminifers, calcareous algae debris (Pl. 1/7), bivalves, gastropods, echinoderms, spicules, ostracods, bryozoans, and serpulids. Some peloids were identified as faecal pellets. Oncoids and rounded intraclasts indicate reworking. Sparry calcite-filled moulds and micrite envelopes are common. The components of MFT P3 are very similar to MFT P1, but the higher content of calcareous algae debris (udoteaceans, dasycladaceans, rhodophytes) and further reworked grains indicate re-deposition of lagoonal components in the shallow subtidal realm.

MFT P4, foraminiferal ws and ps rich in bivalves: The foraminiferal assemblage is dominated by thick agglutinated miliolids (Pl. 1/8), supplemented by smaller quantities of further benthic foraminifers. Furthermore, bivalves and echinoderms prevail. Calcareous algae, gastropods, and ostracods occur rarely. Sub-rounded intraclasts, peloids (some identified as faecal pellets) are common non-skeletal components. MFT P4 comprises reworked lagoonal components, but differs from MFT L3 by abundant foraminifers.

MFT P5, winnowed ps rich in peloids: Skeletal grains are rare. However, species-rich benthic foraminifers are abundant occasionally (Pl. 2/1). Non-skeletal grains comprise high amounts of very well sorted peloids and common rounded intraclasts; coated grains (superficial ooids, tangential ooids, oncoids) may occur rarely. Moderate turbulence during deposition is indicated by very well sorted, rounded and preferentially oriented components within a micrite and sparite matrix (Pl. 2/1), and probably also by the thick tests of foraminifers (see section 5.1). High packing density of the grains probably hampered the transport of intergranular mud. Reworked miliolids, dasycladaceans, and rudist debris may indicate occasional re-deposition of lagoonal deposits.

5.2.4 High-Energy Subtidal

MFT W1, bioclastic ps rich in coated grains: Within MFT W1 the quantities of coarse, shallow-water bioclasts vary strongly. Non-skeletal grains are peloids and, more rarely, rounded intraclasts; oncoids typically dominate among the coated grains (Pl. 2/2), besides common superficial ooids and concentrical ooids. Quartz, phosphates and glauconite grains are rare. The matrix is mainly micrite, in parts associated with blocky sparite and rare syntaxial rim cements. Calcite-filled moulds outlined by distinct micrite envelopes are common, borings and burrows are sometimes present. The moderate energy-level and components derived from both, the protected shallow subtidal facies belt (e.g. calcareous algae, foraminifers, oncoids) and high-energy shoals (e.g. ooids, see below), suggest a transitional facies. Protected shallow subtidal deposits were reworked within this backshoal realm.

Plate 2: Microfacies types of the shallow subtidal, high-energy subtidal and deep-water facies belts. Scale bars are 1 mm.

Fig. 1 MFT P5, winnowed gs rich in peloids. Abundant benthic foraminifers comprise *Nummoloculina* sp. (1), other miliolids, and *Cuneolina* sp.(2); well sorted peloids are typical; the gs texture with sparry calcite cement is however not characteristic of the MFT. Sample G-6, Cenomanian of section G (Gebel Gunna), post-CeSin 5 TST.

Fig. 2. MFT W1, bioclastic ps rich in coated grains. Coarse bioclasts are nuclei of oncoids (1). Note their typical irregular and dark micrite layers; probably an encrusting foraminifer (2) infested a skeletal grain before coating; associated components in the micrite matrix are peloids, rare quartz and micritized grains. Sample AN6-1, Turonian of section AN (Gebel Areif el Naqa), post-CeSin 7 HST.
Fig. 3. MFT W2, winnowed ps rich in bioclasts. Densely packed components are molluscs, peloids, intraclasts and large oncoids; within the winnowed texture sparry calcite cement is present. Sample Z-27a, Turonian of section Z (Gebel Abu Zurub), post-CeSin 7 HST.

Fig. 4. MFT W3, algal ps with coated grains. Calcareous algae debris is represented by rock-forming quantities of udoteaceans (*Boueina* sp.) chips (1) in a winnowed texture with sparry calcite cement. Abundant peloids and well rounded intraclasts characterise the non-skeletal grains. Sample Z-29, Turonian of section Z (Gebel Abu Zurub), post-CeSin 7 HST.

Fig. 5. MFT W4, oolitic gs. Well sorted coated grains are abundant normal ooids and some superficial ooids; micritized grains, probably ooids are common; well rounded carbonate extraclasts (1) and ostracods (2) are shown; sparry calcite cement is typical. Sample D2-15, Turonian of section D (Gebel Dhalal), post-TuSin 1 TST.

Fig. 6. MFT W4, oolitic gs. Ostracods (1) are common nuclei of ooids (2), and rock-forming amounts of disarticulated ostracods valves (2) are often clustered and interlocked. The sample AN2-41 (Gebel Areif el Naqa) was taken near the transgressive surface of post-TuSin 1 TST.

Fig. 7. MFT B1, ps with planktic foraminifers. Skeletal grains are planktic foraminifers (1), monaxial and biaxial (2) spicules, as well as echinoderm and bivalve fragments; abundant peloids and accessory quartz occur. Sample R-3a, Turonian of section R (Gebel Risha), post-CeSin 7 TST.

Figs. 8.-9. MFT B1, ws with *Whiteinella ?baltica* (Fig. 8) and *?Hedbergella* sp. (Fig. 9). Sample R-0, Turonian of section R (Gebel Risha), post-CeSin 7 TST.


1
1
2


2
1
1
2


3


1
1
1
1
4


1
2
2
5


3
2
1
1
3
1
6

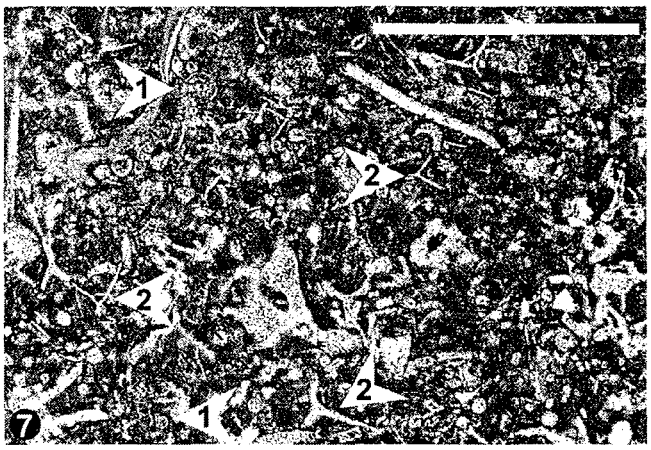
1
2
2
2
1
2
7

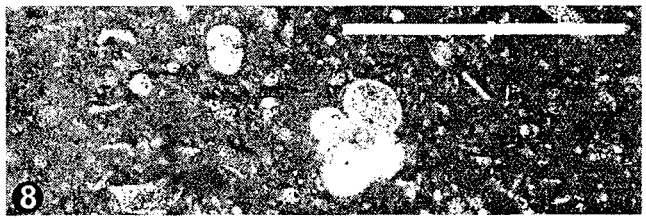
8

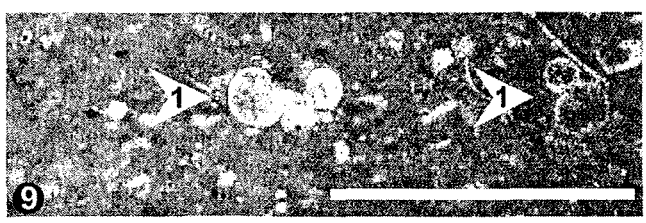
1
1
9

MFT W2, winnowed ps rich in bioclasts: MFT W2 is very similar to MFT W1, with respect to the grain composition and diagenetical features, but has a more winnowed fabric (Pl. 2/3). In addition to ooids, common sparry calcite cement and reworked components indicate more turbulent conditions when compared to MFT W1.

MFT W3, algal ps with coated grains: The diverse calcareous algae assemblage is dominated by udoteacean debris (Pl. 2/4), which may occur in rock-forming quantity, besides varying amounts of rhodophytes and dasycladaceans. Benthic foraminifers, bivalves, gastropods, echinoderms, and ostracods are also present. In addition to abundant peloids and well rounded intraclasts, non-skeletal grains are ooids, superficial ooids and/or oncoids. The components are poorly sorted, but well rounded. Matrix micrite as well as sparry calcite is common (Pl. 2/4). Further diagenetical features are syntaxial and granular rim cements, calcite-filled moulds, micrite envelopes, and micritized grains. The winnowed fabrics, ooids and redeposited bioclasts indicate high-energy, oolitic and bioclastic shoal deposits above wave base. Especially concentrations of allochthonous calcareous algae debris in the bioclastic shoals indicate that these bioclasts were preventially eroded in protected shallow subtidal and lagoonal environments (compare e.g. MFTs P1, P3 and L2) because of their fragile skeletons. This MFT was also described from Egypt, Jordan and the Near East (KUSS & CONRAD, 1991; KUSS, 1992; BUCHBINDER et al., 2000).

MFT W4, oolitic ps and gs: MFT W4 (Pl. 2/5) reveals high amounts of shallow-water benthics and is typified by coated grains (abundant ooids, common superficial ooids and oncoids). Further non-skeletal grains are peloids and rounded intraclasts. A notable variety of MFT W4 in north Sinai shows rock-forming amounts of reworked, disarticulated ostracod valves, which are often clustered and interlocked or represent nuclei of ooids (Pl. 2/6). The components of MFT W4 are very well sorted, rounded, and preferentially oriented. Sparry calcite cement is typical, whereas densely packed components sometimes prevented washing of intergranular mud. Radial fibrous (Pl. 4/14) and syntaxial rim cements as well as meniscus cements occur occasionally. Sparite-filled moulds with micrite envelopes are common. Occasionally, ooids are entirely micritized and are identified only by their size, sorting and circular shape. MFT W4 reflects a very high-energy, shallow subtidal environment above wave base. Components from other facies belts (e.g. ostracods) were re-deposited and formed, together with ooids, carbonate sand shoals and sheets. The MFT is typical at Turonian transgressive surfaces in north Sinai.

5.2.5 Deep Water

MFT B1, dolomitic ws - ps with planktic foraminifers: Skeletal grains are abundant planktic foraminifers (hedbergellids and/or whiteinellids, heterohelicids), as well as bivalve and echinoderm debris, spicules, benthic foraminifers, and ostracods (Pl. 2/7). Peloids and accessory quartz, glauconite, and phosphorite grains represent the non-skeletal composition. It is worth mentioning that faecal pellets (probably coprolites) may be frequent (Pl. 4/11). Dolomitisation affected predominantly the matrix of the grain

supported texture, but the components are often preserved. A deep-water environment of MFT B1 is evident, owing to the characteristic planktic foraminifer assemblages (Pl. 2/8, 9).

5.3 Distribution of Components and Microfacies Types

5.3.1 Spatial Distribution

The lateral distribution of some important components with respect to the facies belts is shown in Fig. 6. Diverse benthic foraminiferal assemblages are dominated by the genera *Pseudolituonella, Pseudorhapydionia, Cuneolina, Valvulammina* and miliolids (*Triloculina, Quinqueloculina* and *Nummoloculina*), within shallow subtidal MFTs (P1, P4) in north Sinai. In contrast, assemblages are less diverse in shallow subtidal ws and ps (P1 and P5) and lagoonal ms and ws (L1, L2, L3) in central Sinai.

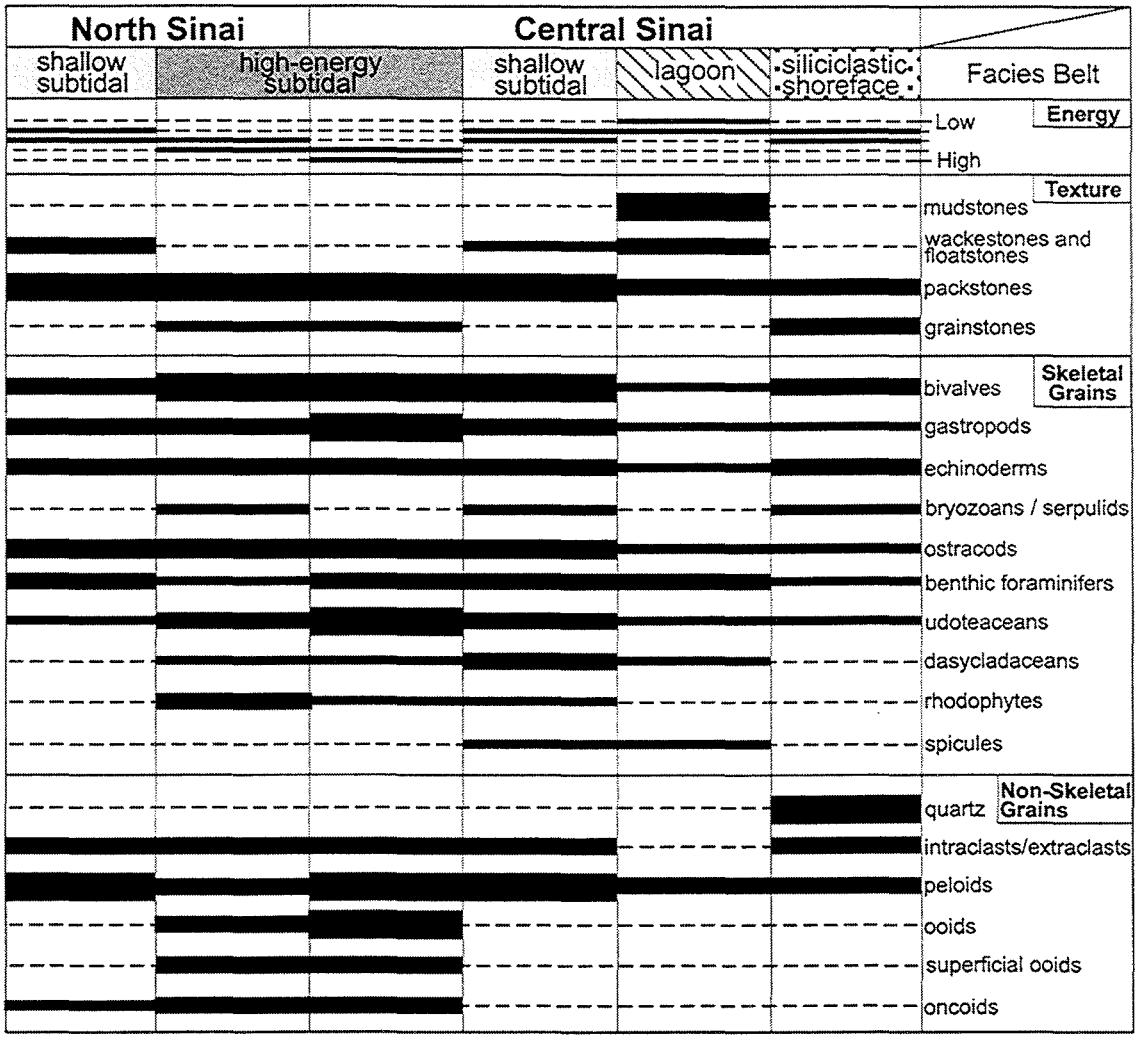

Fig. 6: Composite inner-platform transect. The semiquantitative distribution of important components and textures across the platform in the Turonian are shown with respect to the facies belts.

Calcareous algae are represented by rare udoteaceans (*Bouenia* sp.) and single individuals of dasycladaceans (*Neomeris cretacea*) and rhodophytes in the shallow subtidal deposits of north Sinai. Rhodophytes were common in high-energy settings, whereas dasycladaceans were common in the protected shallow subtidal environments (e.g. P3, bioclastic ps with algae). Udoteacean quantity is more or less constant in both facies belts, except for rock-forming amounts of algal debris in bioclastic shoals (W3, algal ps).

Bioclasts of molluscs and echinoderms are common to abundant in most facies belts. They are particularly frequent in high-energy (in parts oolitic) ps and gs of shoals (W3 and W4) and in agitated backshoal environments (W2) due to re-deposition. Reworked ostracods are also common in such deposits.

Peloids and, to a minor extent, intraclasts dominate the non-skeletal grains in almost all facies belts, except for monotonous ms and some bioclastic ws of restricted lagoons (L1 and L2). Coated grains are typical components in the high-energy, subtidal environments of central and north Sinai. Ooids are common in bioclastic shoals (e.g. W3, algal ps), or were re-deposited within winnowed, bioclastic ps in backshoal areas (W1 and W2). However, high amounts of ooids are limited to bioclastic and oolitic ps and gs (W4), which represented very high-energy carbonate sand shoals and sheets, especially in central Sinai. In addition, oncoids were present in these environments, but also occurred in more protected subtidal environments of north Sinai (e.g. P1, peloidal ws and ps).

5.3.2 Stratigraphical Distribution

Stratigraphical variations of the important skeletal and non-skeletal components, independent of their palaeogeographical setting, are illustrated in Fig. 7. We suggest an inner-platform sedimentation during the late Cenomanian, without particular environmental disturbances. This is supported by: (1) relatively uniform lithologies, (2) the prevalence of protected shallow subtidal deposits, which are characterised by mud-dominated, bioclastic ws, fs and ps (P1, P2), and (3) minor variations of the vertical and lateral distribution patterns of components (Fig. 7). Although reworked, shallow subtidal deposits (P4) occur within the Cenomanian successions, oncoids and high-energy deposits with ooids are scarce. It is also important to note that shales, marls and sandstones within the Raha Formation confirm a considerable Cenomanian siliciclastic input. However, in the Cenomanian limestones, quartz grains are rare (Fig. 7).

The Cenomanian conditions contrast with more variegated Turonian lithologies. High-energy, winnowed ps and gs, sometimes with coated grains, (P5, W1, W2, W3, W4) are present in the Turonian successions. Oncoids are abundant in the lower middle Turonian, but quantities decrease successively and are low in the upper Turonian. Abundance and diversity of benthic foraminifers decline after the C/T boundary; calcareous algae are rare in the Cenomanian, but abundant in the middle Turonian and again rare in the upper Turonian.

The Coniacian - Santonian Matulla Formation consists of high amounts of siliciclastics (marlstones, claystones and sandstones; Fig. 4), which correspond to large quantities of quartz in the bioclastic ps and gs studied (e.g. S2). Ooids and oncoids (which are common in the Turonian) are absent in the Coniacian successions studied; benthic foraminifers occur rarely, and calcareous algae are

nearly absent. However, LEWY (1975) reported oolitic deposits in north-west Sinai, which indicates that ooids were not entirely absent in the Coniacian. Coniacian bioclastic ps also contain debris of various benthic organisms such as gastropods, echinoderms, oysters, spicules, bryozoans and serpulids.

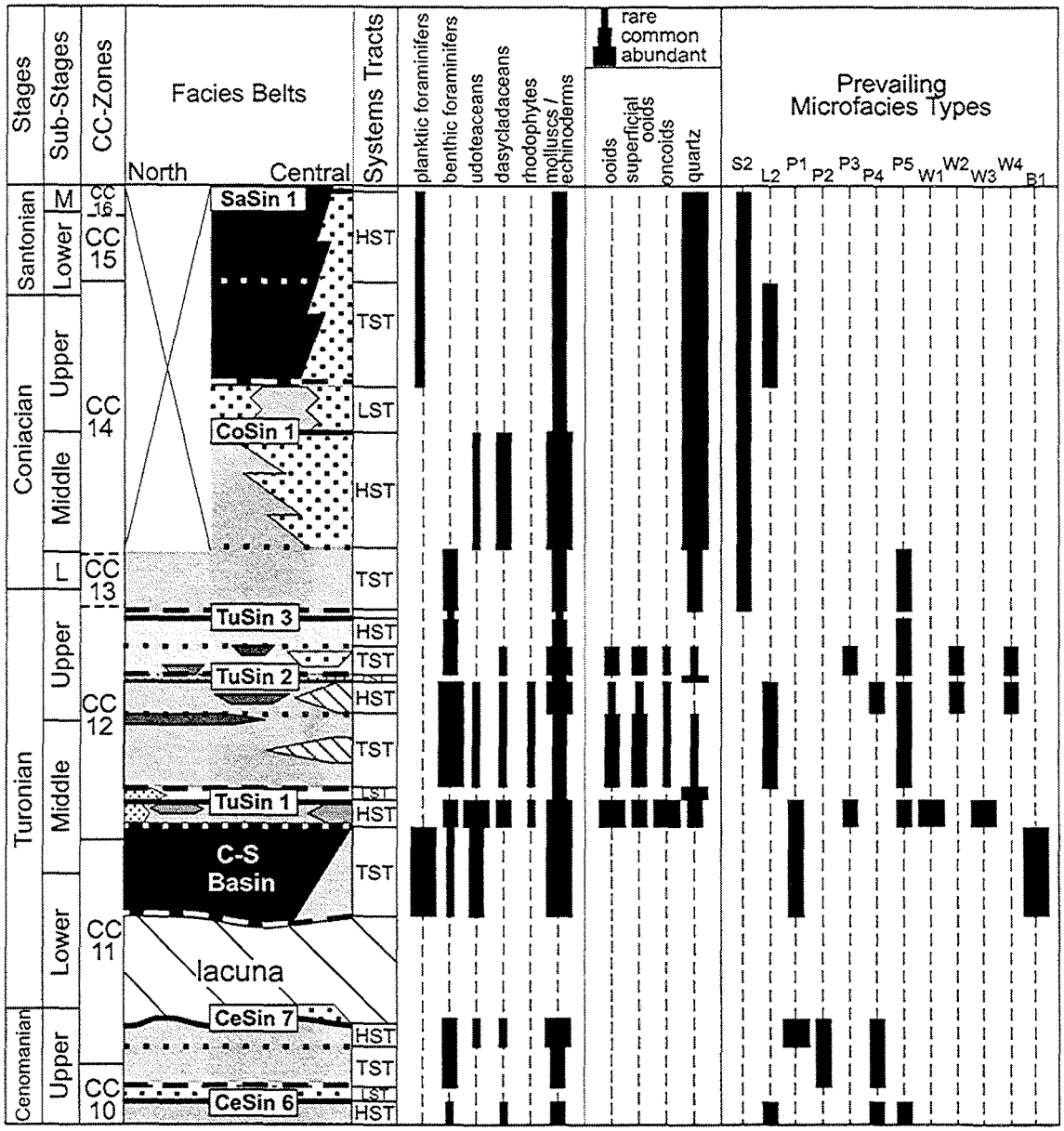

Fig. 7: Stratigraphical distribution of the major facies belts (for a key of fill patterns and symbols, see Fig. 4) as well as systems tracts and corresponding surfaces. Semiquantitative distribution patterns of important components are shown.

5.3.3 Distribution within Systems Tracts

Figures 7, 8 and 9 show the distribution of MFTs and selected components within individual systems tracts defined by BAUER et al. (submitted). As LSTs are mainly represented by soft, supratidal lithologies and sandstones (Tab. 1), microfacies analysis is restricted to quartzose ps and gs (S2) LST-deposits only. However, in the TST-deposits, the quartz content is at a minimum (Figs. 7, 9). Apart

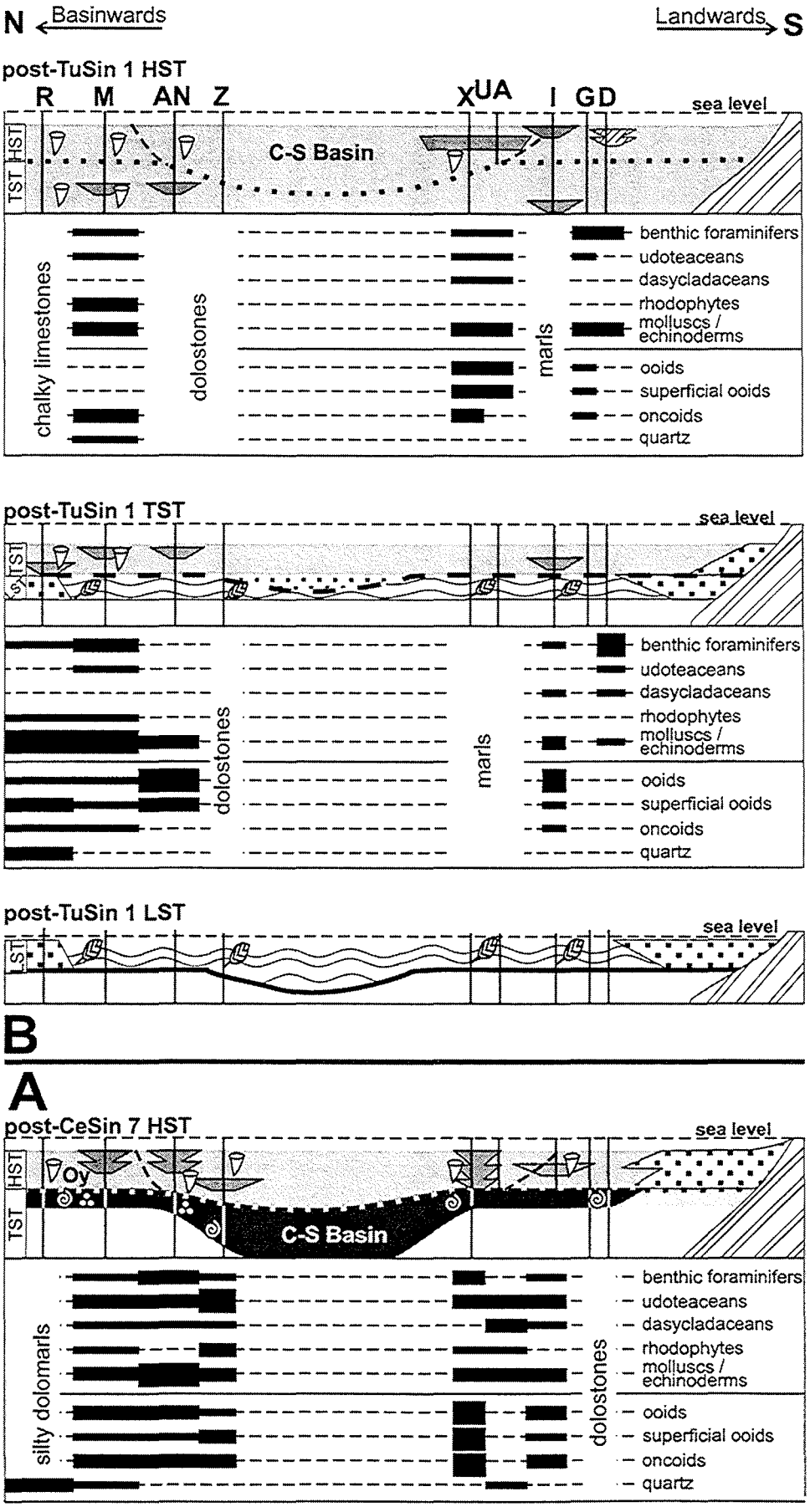
N
Basinwards
Landwards
S
post-TuSin 1 HST
R
M
AN
Z
XUA
I
GD
sea level
HST
TST
C-S Basin
chalky limestones
dolostones
marls
benthic foraminifers
udoteaceans
dasycladaceans
rhodophytes
molluscs / echinoderms
ooids
superficial ooids
oncoids
quartz
post-TuSin 1 TST
sea level
TST
dolostones
marls
benthic foraminifers
udoteaceans
dasycladaceans
rhodophytes
molluscs / echinoderms
ooids
superficial ooids
oncoids
quartz
post-TuSin 1 LST
sea level
LST
B
A
post-CeSin 7 HST
sea level
HST
TST
Oy
C-S Basin
silty dolomarls
dolostones
benthic foraminifers
udoteaceans
dasycladaceans
rhodophytes
molluscs / echinoderms
ooids
superficial ooids
oncoids
quartz

Fig. 8: (Previous page) Schematic N-S transects (compare Figs. 1, 2) display the lateral distribution of the major facies belts within different systems tracts: (A) post-CeSin 7 HST and (B) post-TuSin 1 LST, TST, HST (for a key of the fill patterns see Fig. 4). The semiquantitative distributions of important components refer to the respective systems tracts on top of each transect. Note the larger quantities of calcareous algae and frequent shoals in both HSTs, which contrast to the HSTs of other sequences (Fig. 7). The post-TuSin 1 LST is not represented by limestones in the sections studied.

from deep marine planktic foraminiferal ps (B1) within the C-S Basin, the TSTs are normally composed of coarse bioclastic limestones which characterise the protected shallow subtidal or semi-restricted lagoonal background sedimentation (e.g. P1, P3, L3). Typical components are diverse shallow-water biota. During periods of increased wave-action, the bioclasts (among others molluscs, foraminifers and calcareous algae) were reworked and re-deposited together with peloids and intraclasts in ws and winnowed ps (P4, P5). In addition, high-energy bioclastic packstones and grainstones with ooids and oncoids (W4) are occasionally associated with carbonate sand shoals. It is worth mentioning that especially the ostracod-rich variety of W4 (Pl. 2/6) is an indicative MFT of the Turonian post-TuSin 1 TST in north Sinai, and sometimes marks the transgressive surface.

The HSTs mainly comprise shallow subtidal deposits as well as occasional semi-restricted lagoonal ms to ws (L2). However, in comparison to the TST-deposits, distinct differences in the grain composition have been recognised. These are: (1) coarse-grained MFTs (e.g. P1, P2) occur; (2) quartz grains are more frequent; (3) reworked shallow-subtidal ws and winnowed ps (P4, P5) may be present, but high-energy, bioclastic and oolitic shoal ps and gs (W4), and winnowed backshoal ps (W2) are normally rare; and (4) udoteaceans (*Bouenia* sp.), dasycladaceans (*Neomeris cretacea*), and rhodophytes (*Marinella lugeoni*) are more frequent within algal ps (P3) of the HSTs (in contrast to previous interpretations of BAUER et al., in press). The abundance of calcareous algae within two HSTs is documented in Fig. 8, including the lateral distribution of important components MFTs and carbonate lithologies. However, these examples also display some exceptions of the distribution patterns within the systems tracts described; these are (1) frequent bioclastic shoals along the C-S Basin margin and (2) restricted lagoonal deposits (L1, monotonous ms) in the post-TuSin1 HST of section D (Fig. 8).

6. DISCUSSION

6.1 Lateral Platform Organisation

The generalised lateral distribution patterns of components (Fig. 6) reflect a proximal-distal zonation of the upper Cenomanian - Turonian platform. A clear relation exists between grain composition, the corresponding depositional environments and their platform position. The lateral trends recorded were most probably dependent on environmental changes with increasing distance from the palaeocoastline, e.g. turbulence, oxygenation, nutrient influx, salinity or light, rather than simple variations of bathymetry (see section 6.3). However, it is important to bear in mind that biochemical carbonate dissolution may have in parts masked the original composition (PERRY, 1998).

Supratidal, protected lagoonal and quartzose shoreface facies belts of reduced turbulence and bathymetry prevailed in south Sinai. High siliciclastic input in the nearshore realms most likely led to minor light penetration and/or high nutrient input and eutrophication. These factors probably

decreased carbonate productivity. It may also be speculated that the ferruginous ooids, typical of the nearshore environment (Fig. 4), originated from the re-deposition of iron-rich soils. Similar interpretations have been given for the origin of Jurassic and Lower Cretaceous ferruginous ooids elsewhere in the Near East (ROHRLICH et al., 1980) and for Upper Cretaceous occurrences in southern Egypt and Sudan (MÜCKE, 2000). In the vicinity of this siliciclastic shoreline, in-situ mixing of carbonate mud and grains with sand and silt, probably enhanced by bioturbation, resulted in quartzose bioclastic ps and gs (MFTs S1, S2).

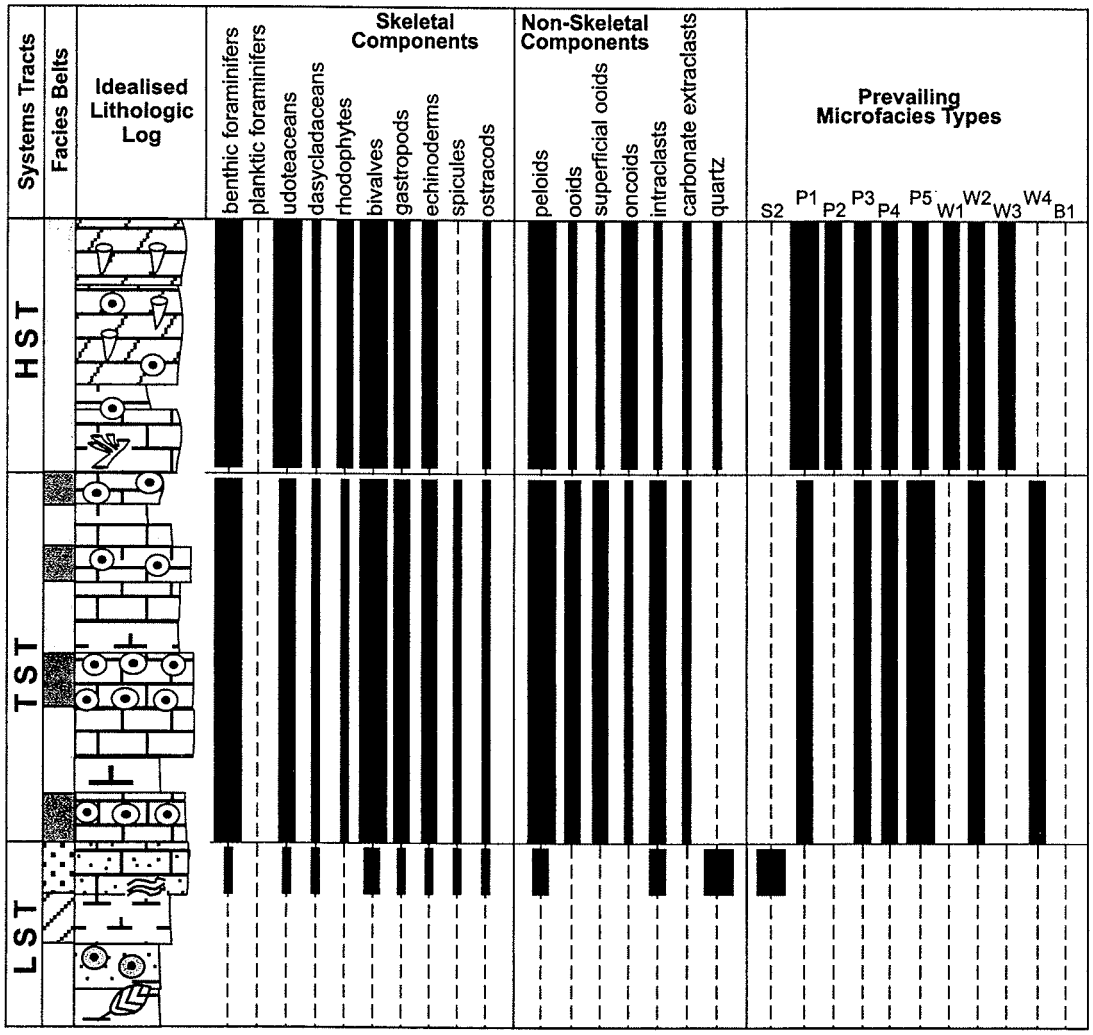

Fig. 9: Idealised lithological section (left) of the Turonian systems tracts and dominating facies belts (for a key to symbols and lithologies, see Fig. 4). Semiquantitative distribution of important components and microfacies types within individual systems tracts is shown. Accessory constituents, such as debris from corals, rudists and oysters, bryozoans, serpulids, faecal pellets, glauconite and phosphorite grains are not listed.

In the lagoonal facies belts, carbonate mud prevailed and only minor amounts of siliciclastics reached this area. Among the components identified, especially monospecifical or paucispecifical assemblages of miliolids (*Quinqueloculina* sp., *Triloculina* sp., *Nummoloculina* sp.) are considered to

be typical of (semi-)restricted shallow-water environments, which are proposed for MFTs L1, L2 and L3 (for a discussion, see CARANNANTE et al., 2000).

The shallow subtidal facies belt was less influenced by temporary ecological stress, regarding changes of water circulation, turbulence and siliciclastic input. Low-energy regimes dominated with mainly protected, shallow subtidal conditions across the platform. It has been shown by BAUER et al. (in press) that highest diversities of benthic foraminifers, calcareous algae, and rudists occurred in north and central Sinai, and thus, these groups preferred habitats of the distal areas of the inner platform. Although benthic foraminifers generally occupied a wide range of habitats, they tended to be frequent and species-rich in protected subtidal facies belts in Sinai. *Biconcava bentori*, *Cuneolina* sp., *Dicyclina* sp., *Nezzazata* sp., *Pseudedomia* sp., and *Valvulammina* sp. are also typical in open lagoonal environments elsewhere, e.g. in the Cenomanian - Turonian Mishrif Formation of the Arabian Gulf (EL-NAGGAR & AL-RIFAIY, 1973). Calcareous algae are abundant in shallow, open-marine environments of north and in parts of central Sinai. Yet, many calcareous algae possibly also settled in proximal inner platform areas, but dolomitisation may have destroyed their fragile skeletons. Dasycladaceans and udoteaceans are indicators for protected, shallow (3 - 5 m), warm environments, with normal marine salinity or semi-restricted environments (ELLIOT, 1991; MU, 1991). *Thaumatoporella* sp. and *Bacinella* sp. are typical of very shallow protected environments or more agitated shallow environments, respectively (BARATTOLO, 1991; CARANNANTE et al., 2000).

Winnowed, sometimes oolitic, MFTs (W2, W3, W4) are mostly bounded to isolated interior shoals within the inner platform. These high-energy environments occurred especially in central Sinai along the margins of the C-S Basin. Although sedimentation generally balanced subsidence within the C-S Basin, which resulted in a persisting shallow water-depth, shallow depressions may have formed occasionally with high turbulence at the margins. Although calcareous algae are valuable facies indicators, it is important to note that their disarticulated debris (algae chips) was easily transported across the platform by currents. This is indicated by high concentrations of algae chips in winnowed limestones studied herein (e.g. MFT W3) as well as in similar MFTs in Egypt, Jordan, Lebanon, Oman, Israel, and Palestine (HAMAOUI & SAINT-MARC, 1970; BURCHETTE & WRIGHT, 1992; KUSS & CONRAD, 1991; KUSS 1992; BUCHBINDER et al., 2000).

6.2 Large-Scale Environmental Perturbations

The stratigraphical changes in microfacies composition make long-term trends visible (Fig. 7) which are related to large-scale environmental perturbations. Stratigraphically characteristic lithologies and facies associations are: the relative uniform upper Cenomanian platform deposits, the laterally varying middle Turonian - middle Coniacian platform deposits, and upper Coniacian - Santonian deep-water deposits. Different factors controlled the depositional regimes, such as (1) variation of grain composition and biotic turnover across the C/T boundary, (2) platform morphology, and (3) a combination of Syrian Arc tectonics and climatic variabilities.

1. Variations in the grain composition are documented across the C/T boundary. High-energy deposits, especially oolites, are more or less only observed in the Turonian, and generally absent in the Cenomanian (Fig. 7). The data presented in this study does not allow to detect diversity variations

of the benthic groups on a higher taxonomical level, which is needed for correlation with the global benthic extinction event at the C/T boundary. BAUER et al. (in press) previously reported biotic turnovers of rudists and benthic foraminifers in the Cenomanian - Turonian successions of Sinai. Other studies on benthic foraminifers (CHÉRIF et al., 1989), ostracods (SHAHIN, 1991) and specific molluscs (KASSAB, 1996) reported a faunal turnover at the C/T boundary in Sinai, which possibly resulted from a platform flooding by oxygen depleted waters related to the oceanic anoxic event.

2. Platform morphology is generally considered as an important factor for currents and turbulence (compare HANDFORD & LOUCKS, 1993; WRIGHT & BURCHETTE, 1996). Therefore we assume that a change of the platform morphology allowed an occasional increase of turbulence in the Turonian, which was responsible for the formation of carbonate sands and oolitic shoals. This contrasts to the extended Cenomanian low-energy inner-platform setting. This issue was probably closely related to the reorganisation of the platform in the early Turonian after the late Cenomanian platform drowning (see section 2). It may be speculated that circulation was reduced in the late Cenomanian by extended barriers at the outer platform (such as carbonate sand bars or rudist patches, which were typical of the early Cenomanian successions in north Sinai, BACHMANN & KUSS, 1998), but after the platform drowning, these rims were not able to recover in the early Turonian. Yet, arguments against this speculation are, (1) pronounced upper Cenomanian platform rims are not reported in Sinai, neither in outcrop nor subsurface, (2) a considerable amount of ooids or rudist debris would probably have been transported into the inner platform, and (3) BAUER et al. (in press) showed that rudists were subordinate carbonate producers in the Cenomanian of Sinai in contrast to other contemporaneous Tethyan platforms (STEUBER & LÖSER, 2000).

Alternatively, the lack of upper Cenomanian high-energy facies belts may have been a result of the flat platform topography proposed (see section 6.1). The carbonate deposits tended to build up at, or closely to sea level, filling accommodation and probably resulted in a restricted circulation on the poised topography. It may be assumed that in this setting, the water depth was possibly too shallow for high carbonate production and the formation of ooids (compare PITTET & STRASSER, 1998). However, this assumption contrasts with the thick TST and HST-deposits, which suggest strong carbonate accumulation and high activity of carbonate producing organisms.

3. The Coniacian - Santonian platform evolution was strongly controlled by Syrian Arc tectonics, which generated a basin and swell morphology and the interfingering of deep-water and platform deposits. In addition, siliciclastic influxes increased markedly (Fig. 7), mainly derived from the southern Arabian Shield and adjacent areas, and reduced carbonate productivity of the inner platform. Tectonics probably governed the availability of these siliciclastics, yet, we assume that a relative increase of humidity since the Coniacian intensified continental weathering and controlled the supply into the sedimentary system. Relatively humid Coniacian conditions have also been reported from Egypt (IBRAHIM & ABDEL-KIREEM, 1997) and contrast with the Cenomanian and Turonian tropical to arid climate in Egypt and adjacent regions (ABDEL-KIREEM et al., 1996; SANDLER, 1996; PHILIP & FLOQUET, 2000). Water physicochemistry (e.g. temperature, HCO_3^--concentration etc.) are often discussed as controlling factors for microbial carbonate precipitation and ooid formation (FLÜGEL, 1982, p. 156; TUCKER & WRIGHT, 1990, p. 7, 32; PERRY, 1998, 1999; RIDING, 2000). In analogy to the depositional model of PITTET et al.

(1995) for a Jurrassic carbonate platform, we suggest that a decrease in frequencies of ooids and oncoids versus an increase in siliciclastics (Fig. 7) reflects the influence of humidity. A decrease in water temperature is also indicated, which may have prevented the formation of ooids from the Coniacian onwards. A general decrease of turbulence in the Coniacian is not probable, because cross-bedding and reworking structures indicate wave-agitated environments (Fig. 4). A considerable Coniacian - Santonian cooling episode is also indicated (1) in Sinai by the decline of calcareous algae, which require warm water, and (2) from oxygen isotope data from the Near East (KOLODNY & RAAB, 1988). This may correspond to upwelling along the Coniacian - Maastrichtian Afro-Arabian Plate margin, which generated high productivity conditions and favoured the accumulation of thick phosphorites and/or black shales in Sinai, Egypt, and in other parts of the Afro-Arabian Plate (GLENN, 1990; ALMOGI-LABIN et al., 1993; ESHET et al., 1994; LÜNING et al., 1998b; ABED & AMIREH; 1999). However, a Late Cretaceous cooling trend is also recorded in other Tethyan regions (FRAKES et al. 1992; WIESE, 1999; Stoll & Schrag, 2000).

Plate 3: Benthic foraminifers (Figs. 1.-12.) and calcareous algae (Figs. 13.-16.) of the Cenomanian - Turonian platforms.

Figs. 1.-2. Different sections of *Chrysalidina gradata* from the Cenomanian of north Sinai. Fig. 1 sample M1p-4, section M, post-CeSin 6 TST; Fig. 2 sample AN4-3, section AN, post-CeSin 6 HST. Scale bars are 1 mm.

Figs. 3.-5. *Dicyclina* sp. (Fig. 3), *Pseudedomia* sp. (Fig. 4), and *Cyclogyra* sp. (Fig. 5). Sample M2-3, Cenomanian of section M (Gebel Minsherah), post-CeSin 5 HST. Scale bars are 1 mm.

Figs. 6, 8. *Valvulammina* sp. (Fig. 6), and *Nummoloculina* sp. (Fig. 8). Sample D2-3, Turonian of section D (Gebel Dhalal), post-TuSin 1 TST. Scale bars are 0.5 mm.

Fig. 7. Unidentified benthic foraminifer. Sample G-5, Cenomanian of section G (Gebel Gunna), post-CeSin 5 TST. Scale bar is 1 mm.

Figs. 9.-10. Different sections of *Pseudorhapydionina* sp. Fig. 9 sample G-6, section G, post-CeSin 5 TST; scale bar is 1 mm. Fig. 10 sample M2-3, section M, Cenomanian, post-CeSin 5 HST; scale bar is 0.5 mm.

Figs. 11.-12. *Pseudolituonella reicheli,* Fig. 11 (scale bar is 1 mm; sample M2-1), and *Nummofallotia* sp.,Fig. 12 (scale bar is 0.5 mm; sample M2-8). Both from the Cenomanian of section M (Gebel Minsherah), post-CeSin 6 TST.

Fig. 13. *Acicularia* sp. Sample AN6-4, Turonian of section AN (Gebel Areif el Naqa), post-CeSin 7 HST. Scale bar is 0.25 mm.

Figs. 14.-15. Different sections of *Neomeris cretacea.* Samples Z-32 and Z-33, Turonian of section Z (Gebel Abu Zurub), post-CeSin 7 HST. Scale bars are 1 mm.

Fig. 16. *Pseudolithothamnium album.* Sample AN6-20, Turonian of section AN (Gebel Areif el Naqa) post-CeSin 6 HST. Scale bar is 1 mm.

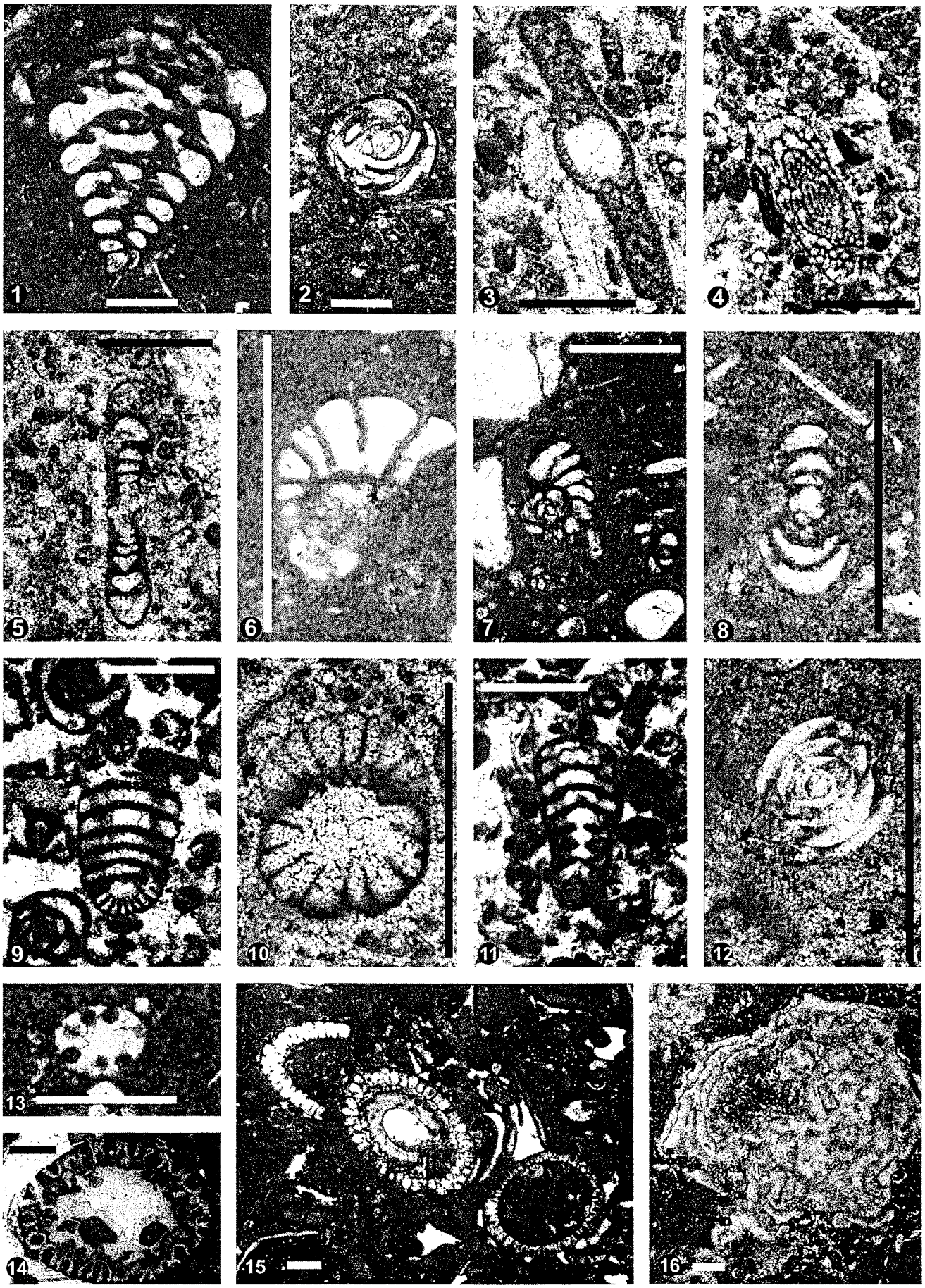
1
2
3
4
5
6
7
8
9
10
11
12
13
14
15
16

6.3 Relative Sea-Level Changes

BAUER et al. (in press) showed that the occurrence of selected benthics of the herein studied sections, is closely related to the formation of local facies belts within the individual systems tracts. Rudists occurred mainly in HSTs, benthic foraminifers and calcareous algae mainly in TSTs and HSTs. The correlation of microfacies distribution patterns and systems tracts presented in this study (Figs 7-9) also reflects the reorganisation of the platform, which was related to relative sea-level changes. During the late Cenomanian, and middle and late Turonian, the platform topography was probably almost flat (BAUER et al., 2001). On such low-angle and wide carbonate shelves, relative sea-level changes have particular infuences on the depositional patterns (HUNT & TUCKER, 1993; STRASSER et al., 1999; SHARLAND et al., 2001, p. 31, 50). However, water-depth did not increase significantly basinwards in Sinai, and the depositional environments ranged from shallow subtidal to exposure (Fig. 4) the poised platform topography. Besides progradation/retrogradation patterns (Fig. 4), the correlation of MFTs and grain compositions with the systems tracts shows that relative sea-level changes controlled accommodation and influenced environmental parameters, e.g. hydrodynamics and detritic influxes. In turn, these features governed the development and sediment composition of the facies belts (Fig. 9), rather than laterally shifting environments that correlate with relative sea-level changes (compare BRETT, 1998).

In Sinai, the siliciclastic influx was reduced during relative sea-level and base-level rises and extended inner-platform TST-carbonates (including high-energy deposits) dominated in nearly all sequences (Fig. 7). In addition, increased accommodation in more proximal areas generally favoured the retrogradation of protected subtidal deposits (P1, peloidal ws and ps; P3, bioclastic ps with algae) and lagoonal TST-deposits (L3, peloidal ws and ps with foraminifers) in central and south Sinai. In north Sinai, the progressive creation of accommodation resulted in the aggradation of thick shallow-subtidal sediments (BAUER et al., 2001). Platform interior and shoreline shoals normally tend to form only where sediment supply exceeds erosion and where accommodation is adequate (WRIGHT & BURCHETTE, 1996). These conditions existed during transgressive periods in north and central Sinai (Figs 4, 8). Increased accommodation resulted in an improved water circulation, and increased wave action sometimes triggered the formation of high-energy inner-platform deposits, e.g. carbonate sand sheets and shoals (W4, oolitic ps and gs) and agitated backshoals (W2, winnowed ps). Similar high-energy MFTs were described from TSTs of the Aptian - middle Cenomanian carbonate ramp of Sinai (BACHMANN & KUSS, 1998), and processes of increased accommodation and the formation of high-energy TST-deposits are also known from other Tethyan platforms (BURCHETTE & WRIGHT, 1992; SPENCE & TUCKER, 1999; D'ARGENIO et al., 1999; DI STEFANO & RUBERTI, 2000).

Aggrading, thick and uniform inner-platform HST-deposits of north Sinai (e.g. P2, bivalves-bearing fs) reflect increased carbonate production rates, owing to the maximum flooding of the carbonate platform (HANDFORD & LOUCKS, 1993; SHARLAND et al., 2001, p. 31). In central Sinai, protected shallow-subtidal (P1, peloidal ws and ps) and lagoonal HST-deposits (L2, bioclastic ms and ws) also reveal more or less stable depositional environments. However, sediment transport, coarse-grained carbonates, oolites and shoals are generally common on platforms during highstands (JAMES & KENDALL, 1992; SCHLAGER et al., 1994). Yet in Sinai, low-energy shallow subtidal environments pre-

vailed during highstands (Fig. 9), although coarse-grained (P1, P2) and reworked (P4, P5) shallow-subtidal ws and ps occurred. This indicates minor sediment transport and circulation on the wide inner platform, which resulted in fine-grained, matrix supported lithologies. High-energy HST-deposits were mostly limited to laterally restricted shallow oolitic and bioclastic shoals at the C-S Basin margins (Figs 4, 8), but probably did not significantly affect circulation. Reduced water depths especially in the late highstands probably restricted the vertical growth of these shoals and also limited the formation of ooids. However, although the platform margin is not exposed, it may be speculated that further shoals may have prograded basinwards on the outer platform, out of the area of investigation. These barriers possibly protected the inner platform from high wave action and allowed the wide distribution of low-energy, shallow subtidal environments (compare WRIGHT & BURCHETTE, 1996).

Plate 4: Turonian calcareous algae (Figs. 1.-6.), bioclasts (Figs. 7.-10.), non-skeletal grains (Figs. 11.-12.) and diagenetical features (Figs. 13.-15.). Scale bars are 1 mm, scale bar of Fig. 15 is 0.5 mm.

Fig. 1. Vertical section of *Arabicodium aegagrapiliodes.* Sample AN6-0, Turonian of section AN (Gebel Areif El Naqa), post-CeSin 7 HST.

Fig. 2. Horizontal section of *Bouenia* cf. *hochstetteri.* Sample M2-34a, Turonian of section M (Gebel Minsherah), post-CeSin 7 HST.

Fig. 3. Vertical section of *Bouenia pygmaea.* Sample X3-12, Turonian of section X (Gebel Gidira), post-CeSin 7 TST.

Fig. 4. *Marinella lugeoni.* Sample R-11, Turonian of section R (Gebel Risha), post-TuSin 1 TST.

Fig. 5. *Bacinella* sp. (1) associated with *Thaumatoporella* sp. (2). Sample M2-34a, Turonian of section M (Gebel Minsherah), post-CeSin 7 HST.

Fig. 6. Gymnocodiaceae, note the reproductive structures in the cortex (1). Sample M2-33, Turonian of section M (Gebel Minsherah), post-CeSin 7 HST.

Fig. 7. Serpulid colony. Sample AN2-26, Turonian of section AN (Gebel Areif El Naqa), post-CeSin 7 HST.

Fig. 8. Rudist (Radiolitidae) fragments. Note the cellular shell structure. When disarticulated, these vertical (muri) and horizontal (laminae) elements may produce fine-grained carbonate. Sample M1-55, Turonian of section M (Gebel Minsherah), post-TuSin 1 TST.

Fig. 9. Horizontal section of a solitary coral. Sample V-17. Cenomanian / Turonian boundary in south Sinai, post-CeSin 6 HST.

Fig. 10. Phosphatic fish tooth. Note the typical bone structure. White grains are quartz. Sample D3-26, Santonian of section D (Gebel Dhalal), post-SaSin 1 LST.

Fig. 11. Faecal pellets (probably coprolites). Note the internal structures, which are important taxonomical characteristics. The thin section is from a horizontal section of an ammonite. Sample ANII-4, Cenomanian / Turonian boundary of section AN (Gebel Areif El Naqa), post-CeSin 7 TST.

Fig. 12. Large oncoid. Note the dark micrite and wavy and irregular laminae around a intraclast with bivalve fragments. Sample AN6-1, Turonian of section AN (Gebel Areif El Naqa), post-CeSin 7 HST.

Fig. 13. Micrite envelopes. Note the internal destructive nature (1) of the micrite-filled microbe borings, which outline calcite-filled moulds of clasts. Sample R-12b, Turonian of section R (Gebel Risha), post-TuSin 1 TST.

Fig. 14. Cement types: early diagenetical radial fibrous cements (1) outline the clasts (mainly ooids); the intergaranular pores were filled later by sparry calcite cement (2). Sample M2-42, Turonian of section M, (Gebel Minsherah), post-CeSin 7 HST.

Fig. 15. Vadose dripstone cement along a mollusc fragment. The rim cement (1) hangs from the roof of the pore (1). Sample X5-11, section X (Gebel Gidira).

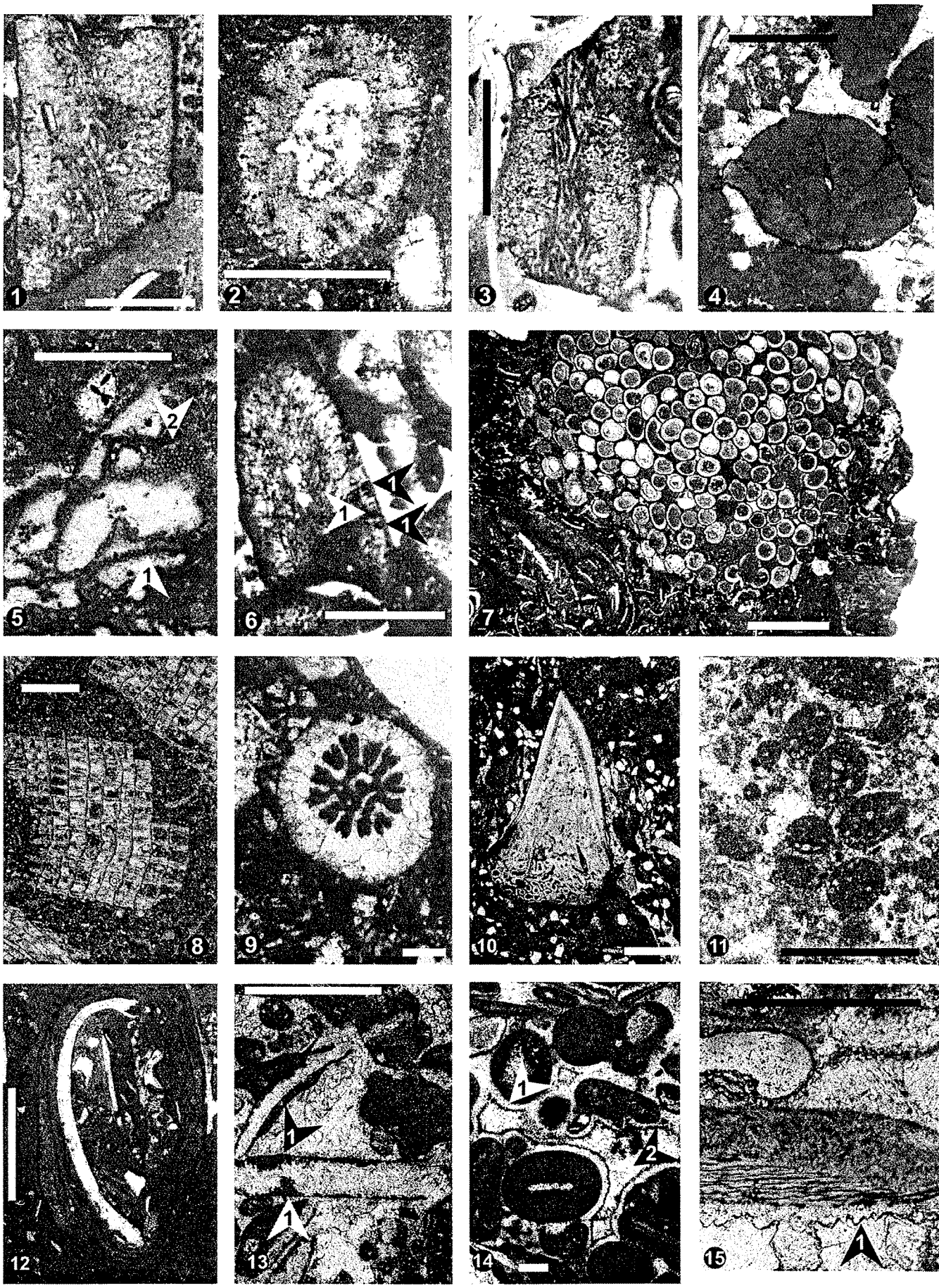
1
2
3
4
5
1
2
6
1
1
1
7
8
9
10
11
12
13
1
1
14
1
2
15
1

7. CONCLUSIONS

Microfacies and semiquantitative component analysis of the upper Cenomanian - Santonian platform carbonates of Sinai allowed to define 15 microfacies types, which characterise the main areas and environments of deposition. Distinct proximal-distal gradients in grain composition reflect the lateral zonation of the platform and environmental changes (turbulence, nutrient influx, light penetration) with increasing distance to the palaeocoastline, rather than variations of bathymetry. The inner-platform settings in central and north Sinai were characterised by protected, shallow subtidal deposits. Winnowed, oolitic deposits were restricted to isolated shoals within the inner platform especially along the margins of the C-S Basin.

Stratigraphically varying changes in microfacies composition reflect large-scale environmental perturbations. High-energy deposits, especially oolites, are only observed in the Turonian. In the Coniacian - Santonian, a decrease in the frequencies of ooids, oncoids, and calcareous algae versus an increasing in siliciclastics indicates changes to lower water temperatures and to a more humid climate.

The distribution of the MFTs and selected components correlates with the systems tracts and reflects changes of accommodation, hydrodynamics and detritic influxes, caused by relative sea-level changes. Increased accommodation triggered wave-agitation and the formation of (oolitic) high-energy TST-deposits, e.g. carbonate sand sheets and shoals. Protected shallow-subtidal deposits dominate the HSTs and reworked shallow-subtidal and high-energy shoals are normally rare.

ACKNOWLEDGEMENTS

This study has been funded by the German Research Foundation (DFG; Ku 642/15-1,2). We thank M.M. Morsi and A.M. Bassiouni of Ain Shams University (Cairo, Egypt) for their help in preparing the field work programme in Sinai. We would like to express our special thanks to U. Heimhofer (ETH Zurich), F. Wiese (FU Berlin), P. Luger (TU Berlin), and A.M Marzouk (Tanta University, Egypt). M. Bachmann, R. Bätzel, E. Friedel, and R. Speijer of Bremen University are also acknowledged for various kinds of help and advises.

REFERENCES

ABDEL-KIREEM, M.R., SCHRANK, E., SAMIR, A.M. & IBRAHIM, M.I.A. (1996): Cretaceous palaeoecology, palaeogeography and palaeoclimatology of the northern Western Desert, Egypt.- J. Afric. Earth Sci., **22**, 93-112, Amsterdam.

ABED, A.M. & AMIREH, B.S. (1999): Sedimentology, geochemistry, economic potential and palaeogeography of an Upper Cretaceous phosphorite belt in southeastern desert of Jordan.- Cretaceous Res., **20**, 119-133, London.

AHMED, S. M. (1995): Facies characteristics of the Upper Cretaceous exposures, Taba area, Sinai, Egypt.- Egypt. J. Geol., **39**, 159-178, Cairo.

ALMOGI-LABIN, A., BEIN, A. & SAAS, E. (1993): Late Cretaceous upwelling systems along the southern Tethys margin (Israel): interrelationship between productivity, bottom water environments, and organic matter preservation.- Paleoceanography, **8**, 671-690, Washington, DC.

BACHMANN, M. & KUSS, J. (1998): The Middle Cretaceous carbonate ramp of the northern Sinai: sequence stratigraphy and facies distribution.- In: WRIGHT, V.P. & BURCHETTE, T.P. (Eds.): Carbonate Ramps.- Geol. Soc. London Spec. Publ., **149**, 253-280, Oxford (Blackwell).

BARATTOLO, F. (1991): Mesozoic and Cenozoic marine benthic calcareous algae with particular regard to Mesozoic dasycladaceans.- In: RIDING, R. (Ed.): Calcareous algae and stromatolites. - 504-540, Berlin (Springer).

BARTOV, Y. & STEINITZ, G. (1977): The Judea and Mount Scopus groups in the Negev and Sinai with trend surface analysis of the thickness data.- Isr. J. Earth-Sci., **26,** 119-148, Jerusalem.

BARTOV, Y., LEWY, Z., STEINITZ, G. & ZAK, I. (1980): Mesozoic and Tertiary stratigraphy, paleogeography and structural history of the Gebel Areif en Naqa area, eastern Sinai.- Isr. J. Earth-Sci., **29,** 114-139, Jerusalem.

BASSOULLET, J.P., BERNIER, P., DELOFFRE, R., GÉNOT, P., PONCET, J. & ROUX, A. (1983): Udoteacea.- Bull. Centres Rech. Explor.-Prod. Elf Aquitaine, **7,** 449-621, Pau.

BAUER, J., MARZOUK, A.M., STEUBER, T. & KUSS, J. (2001): Lithostratigraphy and biostratigraphy of the Cenomanian - Santonian strata of Sinai, Egypt.- Cretaceous Res., **22,** 497-526, London.

BAUER, J., STEUBER, T., KUSS, J. & HEIMHOFER U. (in press): Distribution of shallow-water benthics: The Cenomanian - Turonian carbonate platform sequences of Sinai, Egypt.- In: Proceedings of the 5th International Congress on Rudists.- Cour. Forschungsinst. Senckenberg, Frankfurt.

BOSENCE, D.W.J. (1983): Description and classification of rhodoliths (rhodoids, rhodolites).- In: PERYT, T. (Ed.): Coated grains. - 217-224, Berlin (Springer).

BOSWORTH, W., GUIRAUD, R. & KESSLER, L.G. (1999): Late Cretaceous (ca. 84 Ma) compressive deformation of the stable platform of northeast Africa (Egypt): far-field stress effects of the 'Santonian event' and origin of the Syrian arc deformation belt.- Geology, **27,** 633-636, Boulder.

BRETT, C.E. (1998): Sequence stratigraphy, paleoecology, and evolution: biotic clues and responses to sea-level fluctuations.- Palaios, **13,** 241-262, Tulsa.

BUCHBINDER, B., BENJAMINI, C. & LIPSON-BENITAH, S. (2000): Sequence development of Late Cenomanian - Turonian carbonate ramps, platforms and basins in Israel.- Cretaceous Res., **21,** 813-843, London.

BURCHETTE, T.P. & WRIGHT, V.P. (1992): Carbonate ramp depositional systems.- Sediment. Geol., **79,** 3-57, Amsterdam.

CARANNANTE, G., RUBERTI, D. & SIRNA, M. (2000): Upper Cretaceous ramp limestones from Sorrento Peninsula (southern Apennines, Italy): micro- and macrofossil associations and their significance in depositional sequences.- Sedim. Geol., **132,** 89-123, Amsterdam.

CHÉRIF, O.H., AL-RIFAIY, I.A., AL-AFIFI, F.I. & ORABI, O.H. (1989): Foraminiferal biostratigraphy and paleoecology of some Cenomanian-Turonian exposures in west-central Sinai, (Egypt).- Rev. Micropaléont., **31,** 243-262, Paris

D'ARGENIO, B., FERRERI, V., RASPINI, A., AMODIO, S. & BUONOCUNTO, F.P. (1999): Cyclostratigraphy of a carbonate platform as a tool for high-precision correlation.- Tectonophysics, **315,** 357-384, Amsterdam.

DI STEFANO, P. & RUBERTI, D. (2000): Cenomanian rudist-dominated shelf-margin limestones from the Panormide carbonate platform (Sicily, Italy): facies analysis and sequence stratigraphy.- Facies, **42,** 133-160.

DUNHAM, R.J. (1962): Classification of carbonate rocks according to depositional texture.- In: HAM, W.E. (Ed.): Classification of carbonate rocks.- Amer. Assoc. Petrol. Geol. Mem., **1,** 108-121, Tulsa.

EL-AZABI, M.H. & EL-ARABY, A. (1996): Depositional facies and palaeoenvironments of the Albian - Cenomanian sediments in Gabal El-Minshera, north central Sinai, Egypt.- Geol. Soc. Egypt Spec. Publ., **2,** 151-198, Cairo.

EL-NAGGAR, Z. R. & AL-RIFAIY, I. A. (1973): Stratigraphy and microfacies of type Magwa Formation of Kuwait, Arabia; Part 2: Mishrif Limestone Member.- Amer. Assoc. Petrol. Geol. Bull., **57,** 2263-2279, Tulsa.

ELLIOT, G.F. (1991): Dasycladalean algae of the Palaeozoic and Mesozoic.- In: RIDING, R. (Ed.): Calcareous algae and stromatolites. - 125-130, Berlin (Springer).

EMBRY, A.F. & KLOVEN, S.E. (1972): Absolute water depth limits of late Devonian paleoecological zones.- Geologische Rundschau, **61,** 672-686, Stuttgart.

ESHET, Y., ALMOGI-LABIN, A. & BEIN, A. (1994): Dinoflagellate cysts, paleoproductivity and upwelling systems: A Late Cretaceous example from Israel.- Marine Micropaleont., **23,** 231-240, Amsterdam.

EWEDA, S. & EL-SOROGY, A.S. (1999): Stratigraphy and facies development of the Upper Cretaceous - Lower Tertiary succession in Wadi Feiran area, southwestern Sinai, Egypt.- N. Jb. Geol. Paläontol. Abh., **211,** 263-289, Stuttgart.

FLÜGEL, E. (1982): Microfacies analysis of limestones. - 633 p., Berlin (Springer).

FRAKES, L.A., FRANCIS, J.E. & SYKTUS, J.I. (1992): Climate modes of the Phanerozoic: the history of the earth's climate over the past 600 million years.- 274 p. Cambridge (Cambridge University Press).

GLENN, C.R. (1990): Depositional sequences of the Duwi, Sibâîya and phoshate formations, Egypt: phosphogenesis and glauconitization in a Late Cretaceous epeiric sea. In: NOTHOLT, A. J. G. & JARVIS, I. (Eds.): Phosphorite research and development.- Geol. Soc. London Spec. Publ., **52,** 205-222, Oxford (Blackwell).

GUIRAUD, R. & BOSWORTH, W. (1997): Senonian basin inversion and rejuvenation of rifting in Africa and Arabia: synthesis and implications to plate-scale tectonics.- Tectonophysics, **282,** 39-82, Amsterdam.

HAMAOUI, M. & SAINT-MARC P. (1970): Microfaunes et microfaciès du Cénomanien du proche-orient.- Bull. Centre Rech. Pau-SNPA, **4,** 257-352, Pau.

HANDFORD, C.R. & LOUCKS, R.G. (1993): Carbonate depositional sequences and systems tracts - responses of carbonate platforms to relative sea-level changes.- In: LOUCKS, R.G. & SARG, J.F. (Eds.): Carbonate sequence stratigraphy-recent events and applications.- Amer. Assoc. Petrol. Geol. Mem., **57,** 3-41, Tulsa.

HARDENBOL, J., THIERRY, J., FARLEY, M. B., JACQUIN, T., DE GRACIANSKY, P.-C. & VAIL, P.R. (1998): Mesozoic and Cenozoic sequence chronostratigraphic framework of European basins, Chart 5.- In: DE GRACIANSKY, P.-C., HARDENBOL, J., JACQUIN, T. & VAIL, P.R. (Eds.): Mesozoic and Cenozoic sequence stratigraphy of European basins.- (SEPM) Soc. Econ. Paleontol. Mineral. Spec. Publ., **60,** Tulsa.

HARRIS, P.M., FROST, S.H., SEIGLIE, G.A. & SCHNEIDERMANN, N. (1984): Regional unconformities and depositional cycles, Cretaceous of the Arabian Peninsula.- In: SCHLEE, J.S. (Ed.): Interregional unconformities and hydrocarbon accumulation.- Amer. Assoc. Petrol. Geol. Mem., **36,** 67-80, Tulsa.

HART, M.B. (1999): The evolution and biodiversity of Cretaceous planktonic foraminiferida.- Geobios, **32,** 247-255, Lyon.

HEIMHOFER, U. (1999): Mikrofazies, Zyklostratigraphie und Diagenese zweier Profile der oberturonen Wata-Formation (E' Sinaihalbinsel / Ägypten). - 85 p., unpublished Diploma thesis, Institute for Geology and Mineralogy, Erlangen University.

HILLGÄRTNER H., DUPRAZ, C. & HUG, W. (2001): Microbially induced cementation of carbonate sands: are micritic meniscus cements good indicators of vadose diagenesis?- Sedimentology, **48,** 117-132, Oxford.

HUNT, D. & TUCKER, M. E. (1993): Sequence stratigraphy of carbonate shelves with an example from the mid-Cretaceous (Urgonian) of southeast France.- In: POSAMENTIER, H.W., SUMMERHAYES, C.P., HAQ, B.U. & ALLEN, G.P. (Eds.): Sequence stratigraphy and facies associations.- Int. Assoc. Sedimentol. (IAS) Spec. Publ., **18,** 307-341, Oxford (Blackwell).

IBRAHIM, M.I.A. & ABDEL-KIREEM, M.R. (1997): Late Cretaceous palynofloras and foraminifera from Ain El-Wadi area, Farafra Oasis, Egypt.- Cretaceous Res., **18,** 633-660, London.

JAMES, N.P. & KENDALL, A.C. (1992): Introduction to carbonate and evaporite facies models.- In: WALKER, R.G. (Ed.): Facies models: response to seal-level changes. - 265-275, Geological Association of Canada.

KASSAB, A.S. (1996): Cenomanian-Turonian boundary in the Gulf of Suez region: towards an inter-regional correlation, based on ammonites.- Geol. Soc. Egypt, Spec. Publ., **2,** 61-98, Cairo.

KASSAB, A.S. & OBAIDALLA, N.A. (2001): Integrated biostratigraphy and inter-regional correlation of the Cenomanian-Turonian deposits of Wadi Feiran, Sinai, Egypt. Cretaceous Res., **22,** 105-114, London.

KERR, A.C. (1998): Oceanic plateau formation: a cause of mass extinction and black shale deposition around the Cenomanian-Turonian boundary?- J. Geol. Soc. London, **155,** 619-626.

KOLODNY, Y. & RAAB, M. (1988): Oxygen isotopes in phosphatic fish remains from Israel: paleothermometry of tropical Cretaceous and Tertiary shelf waters.- Palaeogeogr., Palaeoclimatol., Palaeoecol., **64,** 59-67, Amsterdam.

KUSS, J. (1992): The Aptian - Paleocene shelf carbonates of northeast Egypt and southern Jordan: establishment and break-up of carbonate platforms along the southern Tethyan shores.- Zeitschrift der Deutschen Geologischen Gesellschaft, **143,** 107-132, Hannover.

KUSS, J. & BACHMANN, M. (1996): Cretaceous paleogeography of the Sinai peninsula and neighbouring areas.- Comptes Rendus de l'Académie des Sciences, Serie IIa, **322,** 915-933, Paris.

KUSS, J. & CONRAD, M.-A. (1991): Calcareous algae from Cretaceous carbonates of Egypt, Sinai, and southern Jordan.- J. Paleont., **65,** 869-882, Lawrence, Kansas.

KUSS, J. & MALCHUS, N. (1989): Facies and composite biostratigraphy of Late Cretaceous strata from Northeast Egypt.- In: WIEDMANN, J. (Ed.): Cretaceous of the Western Tethys. Proceedings 3rd International Cretaceous Symposium, Tübingen 1987. - 879-910, Stuttgart (Schweizerbart).

KUSS, J., SCHEIBNER, C. & GIETL., R. (2000). Carbonate platform to basin transition along an Upper Cretaceous to Lower Tertiary Syrian Arc uplift, Galala Plateaus, Eastern Desert, Egypt.- GeoArabia, **5,** 405-424, Bahrain.

KUYPERS, M.M.M., PANCOST, R.D. & DAMSTÉ, J.S.S. (1999): A large and abrupt fall in atmospheric CO2 concentration during Cretaceous times.- Nature, **399** (May), 342-345, London.

LEWY, Z. (1975): The geological history of southern Israel and Sinai during the Coniacian.- Isr. J. Earth-Sci, **24**, 19-43, Jerusalem.

LEWY, Z. (1989): Correlation of lithostratigraphic units in the upper Judea Group (Late Cenomanian - Late Coniacian) in Israel.- Isr. J. Earth-Sci, **38**, 37-43, Jerusalem.

LÜNING, S., KUSS, J., BACHMANN, M., MARZOUK, A. M. & MORSI, A. M. (1998a): Sedimentary response to basin inversion: Mid Cretaceous - Early Tertiary pre- to syndeformational deposition at the Areif El Naqa anticline (Sinai, Egypt).- Facies, **38**, 103-136, Erlangen.

LÜNING, S., MARZOUK, A.M., MORSI, M. & KUSS, J. (1998b): Sequence stratigraphy of the Upper Cretaceous of central-east Sinai, Egypt.- Cretaceous Res., **19**, 153-196, London.

MORSI, A.M. & BAUER, J. (in press): Cenomanian ostracode faunas from Sinai peninsula, Egypt.- Revue Paléobiologie, **20**, Genève.

MOUSTAFA, A.R. & KHALIL, M.H. (1990): Structural characteristics and tectonic evolution of north Sinai fold belts.- In: SAID, R. (Ed.): The geology of Egypt. - 381-389, Rotterdam (Balkema).

MU, X. (1991): Fossil Udoteaceae and Gymnocodiaceae.- In: RIDING, R. (Ed.): Calcareous algae and stromatolites. - 146-166, Berlin (Springer).

MÜCKE, A. (2000): Environmental conditions in the Late Cretaceous African Tethys: conclusions from a microscopic-microchemical study of ooidal ironstones from Egypt, Sudan and Nigeria.- J. Afric. Earth Sci., **30**, 25-46, Amsterdam.

ORABI, O.H. & RAMADAN, F.S. (1995): Contribution to the stratigraphy and microfacies of the Matulla Formation in southern Wadi Feiran and Wadi Abuira, west-central Sinai, Egypt.- Egypt. J. Geol., **39**, 339-360, Cairo.

PERRY, C.T. (1998): Grain susceptibility to the effects of microboring; implications for the preservation of skeletal carbonates.- Sedimentology, **45**, 39-51, Oxford.

PERRY, C.T. (1999): Biofilm-related calcification, sediment trapping and constructive micrite envelopes: a criterion for the recognition of ancient grass-bed environments?- Sedimentology, **46**, 33-45, Oxford.

PHILIP, J. & AIRAUD-CRUMIERE, C. (1991): The demise of the rudist-bearing carbonate platforms at the Cenomanian/Turonian boundary: a global control.- Coral Reefs, **10**, 115-125, Berlin.

PHILIP, J. & FLOQUET, M. (2000): Late Cenomanian (94.7-93.5 Ma). In: DERCOURT, J., GAETANI, M., VRIELYNCK, B., BARRIER, E., BIJU-DUVAL, B., BRUNET, M. F., CADET, J.P., CRASQUIN, S. & SANDULESCU, M. (Eds.): Peri-Tethys atlas palaeogeographical maps, explanatory notes. - 129-136, Paris (CCGM/CGMW).

PHILIP, J. et al. (12 co-authors) (2000): Late Cenomanian.- In: J. DERCOURT, J., GAETANI M., VRIELYNCK B., BARRIER E., BIJU-DUVAL B., BRUNET M.F., CADET J.P., CRASQUIN S. & M. SANDULESCU (Eds.): Atlas Peri-Tethys palaeogeographical maps. - Map 14, Paris (CCGM/CGMW).

PITTET, B. & STRASSER, A. (1998): Depositional sequences in deep-shelf environments formed through carbonate-mud import from the shallow platform (Late Oxfordian, German Swabian Alb and eastern Swiss Jura).- Eclogae Geol. Helv., **91**, 149-169, Basel.

PITTET, B., STRASSER, A. & DUPRAZ, C. (1995): Palaeoecology, palaeoclimatology and cyclostratigraphy of shallow-water carbonate-siliciclastic transitions in the Oxfordian of the Swiss Jura.- 16th IAS Regional Meeting of Sedimentology, Field Trip Book, 254 p., Paris.

RIDING, R. (2000): Microbial carbonates: the geological record of calcified bacterial-algal mats and biofilms.- Sedimentology, **47**, 179-214, Oxford.

ROHRLICH, V., METZER, A. & ZOHAR, E. (1980): Potential iron ores in the Lower Cretaceous of Israel and their origin.- Isr. J. Earth Sci., **29**, 73-80, Jerusalem.

ROSENFELD, A. & RAAB, M. (1974): Cenomanian-Turonian ostracodes from the Judea Group in Israel.- Geol. Surv. Isr. Bull., **62**, 1-64, Jerusalem.

SAINT-MARC, P. (1974): Étude stratigraphique et micropaléontologique de l'Albien, du Cénomanien et du Turonien du Liban.- Notes et Mémoires sur le Moyen-Orient, **13**, 1- 298, Paris (Muséum National d'Histoire Narturelle).

SALAJ, J. & MAAMOURI, A.-L. (1998): Upper Cretaceous microbiofacies of Tunisia, III part.- In: SALAJ, J. & MAAMOURI, A.-L. (Eds.): Atlas of Tunisian microbiofacies and its relation to some circum-tethydian types.- Zemný Plyn A Nafta, **43**, 339-433, (MND, Hodonín, Czech Republic).

SANDERS, D. (2001): Burrow-mediated carbonate dissolution in rudist biostromes (Aurisina, Italy): implications for taphonomy in tropical, shallow subtidal carbonate environments.- Palaeogeogr., Palaeoclimatol., Palaeoecol., **168**, 39-74, Amsterdam.

SANDLER, A. (1996): A Turonian subaerial event in Israel: karst, sandstone and pedogenesis.- Geol. Surv. Isr. Bull., **85,** 52 p., Jerusalem.

SCHLAGER, W., REIJMER, J.J.G. & DOXLER, A. (1994): Highstand shedding of carbonate platforms.- J. Sediment. Res., **B64**, 270-281, Tulsa.

SCHRÖDER, R. & NEUMANN, M. (Eds.) (1985): Les grandes foraminifères du Crétacé moyen de la region Méditerranéenne.- Geobios Mém. Spéc., **7,** 1-160, Lyon.

SENOWBARI-DARYAN, B. & KUSS, J. (1992): Anomuren-Koprolithen aus der Kreide von Ägypten.- Mitt. Geol.-Paläont. Inst. Univ. Hamburg, **73,** 129-157, Hamburg.

SHAHAR, J. (1994): The Syrian Arc system: an overview.- Palaeogeogr., Palaeoclimatol., Palaeoecol., **112,** 125-142, Amsterdam.

SHAHIN, A. (1991): Cenomanian-Turonian ostracods from Gebel Nezzazat, southwestern Sinai, Egypt, with observations on δ13 C values and the Cenomanian/Turonian boundary.- J. Micropalaeontol., **10,** 133-150, London.

SHARLAND, P.R., ARCHER, R., CASEY, D.M., DAVIES, R.B., HALL, S.H., HEWARD, A.P., HORBURY, A.D. & SIMMONS, M.D. (2001): Arabian Plate sequence stratigraphy.- GeoArabia Spec. Publ. **2,** 371 p., Bahrain.

SPENCE, G.H. & TUCKER, M.E. (1999): Modeling carbonate microfacies in the context of high-frequency dynamic relative sea-level and environmental changes.- J. Sedim. Res., **69,** 947-961, Tulsa.

STEUBER, T. & LÖSER, H. (2000): Species richness and abundance patterns of Tethyan Cretaceous rudist bivalves (Mollusca: Hippuritacea) in the central-eastern Mediterranean and Middle East, analysed from a palaeontological database.- Palaeogeogr., Palaeoclimatol., Palaeoecol., **162,** 75-104, Amsterdam.

STOLL, H.M. & SCHRAG, D.P. (2000): High-resolution stable isotope records from the Upper Cretaceous rocks of Italy and Spain: Glacial episodes in a greenhouse planet?- Geological Society of America Bulletin, **112,** 308-319, Boulder.

STRASSER, A., PITTET, B., HILLGÄRTNER, H. & PASQUIER, J.-B. (1999): Depositional sequences in shallow carbonate-dominated sedimentary systems: concepts for a high-resolution analysis.- Sedim. Geol., **128,** 201-221, Amsterdam.

TUCKER, M. & WRIGHT, P. (1990): Carbonate sedimentology. - 482 p., Oxford (Blackwell).

VAIL, P. R., AUDEMARD, F., BOWMAN, S. A., EISNER, P. N. & PERZ-CRUZ, C. (1991): The stratigraphic signatures of tectonics, eustasy and sedimentology - an overview.- In: EINSELE, G., RICKEN, W. & SEILACHER, A. (Eds.): Cycles and events in stratigraphy. - 617-659, Berlin (Springer).

VAN WAGONER, J.C., POSAMENTIER, H.W., MITCHUM, R. M., VAIL, P.R., SARG, J.F., LOUTIT, T.S. & HARDENBOL, J. (1988): An overview of the fundamentals of sequence stratigraphy and key definitions.- In: WILGUS, C.K., HASTINGS, B.S., KENDALL, C.G.ST.C., POSAMENTIER, H.W., ROSS, C.A. & VAN WAGONER, J.C. (Eds.): Sea-level changes: an integrated approach.- (SEPM) Soc. Econ. Paleontol. Mineral. Spec. Publ., **42,** 39-45, Tulsa.

WALLEY, C.D. (1998): Some outstanding issues in the geology of Lebanon and their importance in the tectonic evolution of the Levantine region.- Tectonophysics, **298,** 37–62, Amsterdam.

WIESE, F. (1999): Stable isotope data (δ13C, δ18O) from middle - upper Turonian (Upper Cretaceous) of Liencres (Cantabria, northern Spain) with a comparison to northern Germany (Söhlde & Salzgitter-Salder).- Newsletter Stratigraphy, **37,** 37-62, Stuttgart.

WILSON, J.L. (1975): Carbonate facies in geologic history. - 471 p., Berlin (Springer).

WRIGHT, P. & BURCHETTE, T.P. (1996): Shallow-water carbonate environments.- In: READING, H.G. (Ed.): Sedimentary environments: processes, facies and stratigraphy. - 325-394, Oxford (Blackwell).

ZALAT, A.A. (1999): Dolomitization of Cenomanian-Turonian limestones in central Sinai, Egypt.- *Middle East Research Center, Ain Shams University, Earth Sci. Ser.,* **13,** 173-186, Cairo.

CHAPTER 6

Conclusions and Perspectives

CHAPTER 6

Conclusions and perspectives

Lithostratigraphy and biostratigraphy: A chronostratigraphic framework of the sections investigated is developed by integrating and correlating lithostratigraphic and biostratigraphic data. It is shown that (1) ammonites and calcareous nannofossils enable a fairly well biostratigraphic resolution, complemented by benthic and planktic foraminifers, ostracods and rudists; (2) considerable differences exist between the chronostratigraphic assignments of calcareous nannofossil biozones in Sinai and those of other regional and global schemes, owing to ecologic factors and taphonomic effects; (3) a major hiatus straddles the Cenomanian / Turonian boundary,which is probably related to initial Syrian Arc tectonics; (3) considering the stratigraphic resolution achieved, chronostratigraphic synchroneity is proposed for the upper Cenomanian - upper Turonian lithologic units whereas the lower Coniacian - Santonian units are probably diachronous as a response to Syrian Arc tectonics.

Sequence stratigraphy: The sequence-stratigraphic interpretation shows that (1) progradation and retrogradation patterns and specific facies belts are typical within individual systems tracts. Shallow-water to supratidal and siliciclastic deposits occur in the LSTs, subtidal carbonates with occasional high-energy deposits are typical in TSTs, and aggrading protected inner-platform deposits are associated with prograding nearshore siliciclastics in HSTs; (2) eight sedimentary sequences are distinguished for the upper Cenomanian - Santonian; (3) several stratigraphic mismatches exist between the sequence boundaries in Sinai and those elsewhere in the Tethys. These reflect the effects of local synsedimentary tectonics in combination with relative sea-level changes.

Palaeogeography and synsedimentary tectonics: (1) Palaeogeographic maps allow to reconstruct the platform configuration and to estimate the minimum extensions of the C-S Basin; (2) uplift and subsidence influenced the depositional architecture and tectonic events are deduced from laterally varying thickness of the stratal packages; (3) in particular increased subsidence is proposed for the following systems tracts: post-CeSin 7 HST, post-TuSin 1 LST, post-TuSin 1 HST, and post-TuSin 2 LST.

Lithofacies and biofacies proxies: Lithofacies and biofacies analysis and distribution patterns of skeletal and non-skeletal components reflect ecological changes within the depositional environments. The main results are: (1) protected, shallow subtidal deposits occur in central and north Sinai and winnowed deposits are restricted to isolated shoals along the margins of the C-S Basin; (2) proximal-distal gradients in grain composition and the lateral zonation of the platform reflect and environmental changes with increasing distance to the palaeocoastline, rather than variations of bathymetry; (3) facies composition was controlled by platform morphology and long-term environmental changes, such as platform drowning at the Cenomanian/Turonian boundary, middle Turonian platform recovery, and an increase of humidity and cooling from the Coniacian onwards; (4) distinct facies belts, the habitats of rudists, benthic foraminifers and calcareous algae and the distribution of skeletal and non-skeletal components are closely related to relative sea-level changes. Apart from simple lateral shifts of the

facies belts, variations of accommodation with falling or rising sea-level influenced wave-agitation, siliciclastic input and light penetration.

The present thesis does not cover all aspects related to the depositional history of the Sinai platform and several uncertainities remain. For example, the palaeo water-depths within the C-S Basin are unclear, the same is true for the lateral subsurface expansion of the basin to Egypt and Jordan and the factors controlling its subsidence (e.g. faults). Also, the sedimentary response and driving mechanism of platform drowning at the Turonian/Coniacian boundary (e.g. decline of carbonate production or tectonically driven subsidence?) are not well understood. Closer verifications of climatic perturbations, e.g. in the Coniacian - Santonian, are needed for further palaeoecological interpretations. With respect to the anticlines in north Sinai and Syrian Arc tectonics, the ages of initial uplifts in the the vincinity of Gebel Areif el Naqa are not known precisely. Promissing appraoches to solve these questions are:

- Palaeoecologic studies on e.g. ostracods and benthic foraminifers and comparisons with existing palaeoslope models probably enable more precise palaeodepth estimations of the C-S Basin deposits.
- Geophysical investigations of the Basin and its margins may give further information on its E-W expansions and its subsidence history.
- Fossil distribution patterns across the Turonian/Coniacian boundary give important insights on the platform drowning event and studies on stable isotopes are promising methods for the identification of climatic changes.
- High resolution sequence-stratigraphic interpretations and small scale correlations along the flanks of other anticlines in north Sinai are required to reconstruct the tectonic evolution of the region in detail.

APPENDIX 1

Abstract collection of closely related publications

Kunow, R., Bauer, J., Bachmann, M. & Kuss, J. (1997): Verteilungsmuster benthischer Foraminiferen und Tonmineralassoziationen im Oberapt des Sinai. *Zbl. Geol. Paläontol. Teil I,* H1/2, 353-371. I

Kuss, J., Westerhold, T., Groß, U., Bauer, J. & Lüning, S. (2000): Mapping of Late Cretaceous stratigraphic sequences along a Syrian Arc Uplift - examples from the Areif el Naqa / Eastern Sinai. *Middle East Res. Center, Ain Shams Univ., Earth Sci. Ser.*, 14, 171-191. II

Morsi, A.M. & Bauer, J. (in press): Cenomanian ostracode faunas from Sinai peninsula, Egypt. *Revue de Paléobiologie,* 20 (2). III

Zbl. Geol. Paläont. Teil I	1997	H. 1/2	353–371	Stuttgart, Juni 1998

Verteilungsmuster benthischer Foraminiferen und Tonmineralassoziationen im Oberapt des Sinai

Distribution patterns of benthic foraminifera and clay mineral associations of Late Aptian sediments, Sinai

von R. Kunow, J. Bauer, M. Bachmann und J. Kuss, Bremen

mit 5 Abbildungen und 1 Tabelle im Text

Zusammenfassung: Die lateralen und vertikalen Verteilungsmuster benthischer Foraminiferen (exkl. Orbitolinen) und der Tonmineralvergesellschaftungen ermöglichen die Definition charakteristischer Fazieszonen auf der Oberapt-Rampe des Nordsinai. Unter Einbeziehung weiterer sedimentologischer und mikrofazieller Parameter werden diese Verteilungsmuster im Hinblick auf primär faziesbedingte Unterschiede innerhalb vier verschiedener Ablagerungsbereiche diskutiert.

Es konnten 43 Gattungen benthischer Foraminiferen identifiziert werden, die zu fünf Morphogruppen agglutinierter bzw. sechs Morphogruppen kalkschaliger Foraminiferen zusammengefaßt wurden. Deren semiquantitative Verteilungsmuster stehen in enger Verbindung zum jeweiligen Mikrohabitat und ermöglichen weitere detaillierte palökologische Zuordnungen. Unter Einbeziehung der Tonmineralvergesellschaftungen wurden zusätzliche fazieskritische Parameter definiert, die die Veränderungen der Ablagerungsbedingungen in lateraler und vertikaler Abfolge widerspiegeln. Darüber hinaus zeichnen diese die Oszillationen des relativen Meeresspiegels nach und kennzeichnen verschiedene Systems Tracts bzw. deren Grenzflächen im sequenzstratigraphischen Sinn.

Abstract: The lateral and vertical distribution patterns of benthic foraminifera (excl. orbitolines) and clay-mineral assemblages allow the recognition of characteristic facies zones of the Late Aptian carbonate ramp of the northern Sinai. We discuss these patterns with respect to their primary facies-controlled differences, which reflect different environments of deposition.

43 genera of benthic foraminifera have been identified and served as the basis for five agglutinated morphogroups and six calcareous morphogroups. Their semiquantitative distribution allows the reconstruction and correlation of their respective microhabitats, and as a consequence, reflects palaeoecologic conditions. Additional facies parameters have been defined based on the distribution of clay minerals. All these parameters reflect changes of the environmental conditions, both in lateral and vertical order. Moreover, they indicate oscillations of the relative sea level and thus different systems tracts and their boundary surfaces under a sequence stratigraphic aspect.

M.E.R.C. Ain Shams Univ., Earth Sci. Ser., Vol. 14, 2000, p. 171-191.

Mapping of Late Cretaceous stratigraphic sequences along a Syrian Arc uplift - Examples from the Areif el Naqa, Eastern Sinai

By Jochen KUSS, Thomas WESTERHOLD, Ulrike GROß, Jan BAUER & Sebastian LÜNING
University of Bremen, FB5 - P.O. Box 330440, D-28334, Bremen, Germany

ABSTRACT. *The Areif el Naqa (AeN) is an anticline in the Syrian Arc of eastern Sinai that exposes a Cretaceous succession composed of mainly marine near-shore (Upper Albian to Coniacian) and deeper shelf (Upper Coniacian to Maastrichtian) deposits. The Cretaceous strata have been mapped on a 1:10,000 scale, with special emphasis placed on lateral facies variations within two sedimentary sequences: the Early Turonian (post-CeSin7 to post-TuSin1) and the Late Campanian-Early Maastrichtian (post-CaSin to post-MaSin1). The depositional characteristics of both units exhibit facies changes, progressive thinning and condensation towards and along the anticlinal flanks that are interpreted as a result of synsedimentary tectonic movements. Moreover, detailed correlations of sedimentary sequences show evidence for a submarine swell that existed during deposition of Lower Turonian sediments and evolved into a local structural high elevated above sea-level during Campanian-Maastrichtian times. This high coincides with the present-day roughly E-W striking anticlinal core. The westward deepening facies zones of both units, however, indicate a W-dipping fold-axis. Although detailed tectonic analyses are missing for the AeN, our mapping results and combined sedimentologic and sequence-stratigraphic interpretations favour the model of a right-stepped E-W oriented fold, situated north of (and sub-parallel to) the major border fault that developed as a submarine high during the late Early Turonian and was situated above the sea-level during the Late Campanian–Maastrichtian.*

INTRODUCTION

Sequence stratigraphy allows the interpretation of geologic and stratigraphic data of rock units within a genetic framework and the understanding of the factors controlling deposition in different areas or coeval non-deposition in others. Our sequence-stratigraphic interpretations are based on the determination of depositional environments within a high-resolution biostratigraphic frame. We interpret regional sea-level fluctuations and compare these signals to those from neighbouring areas and to "global" signals. This technique allows to filter the various exogenic and endogenic factors influencing the Late Cretaceous sedimentation processes in Sinai that have been markedly influenced by synsedimentary tectonic movements during the "Syrian Arc" deformation (Fig. 1).

Recently, the Cretaceous strata of Sinai and neighbouring areas on the western side of the Gulf of Suez have been described with a focus on sequence stratigraphy (Bachmann & Kuss 1998, Lüning et al. 1998b, Scheibner et al. 2000) and on the major synsedimentary tectonic processes (Lüning et al. 1998a, Kuss et al. 2000). In this paper, we illustrate how these models can be used for geologic interpretations of results from field-mapping, including lateral comparisons and detailed correlations of two Late Cretaceous units deposited around sequence boundaries CeSin7-TuSin1 and CaSin-Ca/MaSin (Lüning et al. 1998a). The Areif el Naqa (AeN) represents a fine area for such a study because of the excellent outcrops and the detailed biostratigraphic and lithostratigraphic data available (Bartov et al. 1980, Lüning et al. 1998a).

Revue Paléobiol., Genève (2001) 20 (2): x-xx ISSN 0253-6730

Cenomanian ostracode faunas from Sinai Peninsula, Egypt

Abdel-Mohsen M. MORSI & Jan BAUER

Abstract
Detailed study of the ostracode fauna from the Cenomanian sequence of Sinai yielded 39 ostracode species belonging to 22 genera. Out of these, six species namely *Cytherella dhalalensis*, *Cytherella gunnaensis*, *Neocyprideis boukharyi*, *Sarlatina babinoti*, *Glenocythere abdulrazzaqae* and *Peloriops aegyptiaca* are new to literature. Stratigraphically, three kinds of ostracode species are distinguished: three species known since the Albian, sixteen species restricted to the Cenomanian and five species extending higher into the lower Turonian. The recorded ostracode fauna are dominated by open marine species, however, levels yielding transitional marine and brackish water species are also recognized. Most of the elements recorded here have a wide geographic distribution along the southern Tethyan realm from Morrocco in the west to the Arabian Gulf region in the east.

Key Words
Cenomanian, Ostracoda, Taxonomy, Biostratigraphy, Paleoecology, Paleobiogeography, Sinai, Egypt.

Résumé
Faune cénomanienne d'ostracodes de la péninsule du Sinai, Egypte.- 39 espèces d'ostracodes appartenant à 22 genres ont été étudiées dans la séquence cénomanienne du Sinai. Parmi celles-ci, 6 espèces sont nouvelles. Du point de vue stratigraphique, trois sortes d'espèces sont distinguées: 3 espèces connues dès l'Albien, 17 espèces propres au Cénomanien et 5 espèces montent dans le Turonien inférieur. Cette faune d'ostracodes est dominée par des espèces de mer ouverte; cependant certains niveaux indiquent un milieu saumâtre. La plupart des espèces étudiées ont une grande répartition géographique au sud de la Tethys, du Maroc à l'ouest au Golfe Arabique à l'est.

Mots-clés
Cénomanien, Ostracoda, Taxonomie, Biostratigraphie, Paléoécologie, Paléobiogéographie, Sinai, Egypte.

INTRODUCTION

The present research is concerned with the study of Cenomanian ostracode associations in Sinai Peninsula. It is mainly directed to their taxonomy and paleobiogeography. Stratigraphic distribution as well as paleoecologic implications are also included. Nine sections have been investigated for their ostracode content. These sections are distributed in the northern, central and southern parts of Sinai Peninsula (Fig. 1). In northern Sinai, one section (Y) is located at Gebel Yelleq and two sections (M1 and M2) are located at Gebel Minsherah (Fig. 2). From central Sinai, three sections (I, Z and KT) are taken respectively at Gebel Iseila, Gebel Abu Zurub and Gebel Khashm El Tarif (Fig. 3). In southern Sinai, three sections (D, G and V) are situated respectively at Gebel Dhalal, Gebel Gunna and Gebel Arabah (Fig. 4). Some of these sections were also previously studied by BAUER *et al.* (subm. 1) for their benthic foraminifers, calcareous algae and rudist bivalves. The biostratigraphic characterization of the studied sections is based essentially here on ostracodes. Most of the yielded assemblages are those typically known for the Cenomanian of the South Tethyan areas. The one exception is at the highest investigated level in the sections of Gebel Minsherah which could be Cenomanian or lower Turonian. Certain species among the recorded Cenomanian fauna as well as integrated nannofossil data (BAUER *et al.*, subm.2) even suggest a late Cenomanian age for the studied sections.

Previous studies dealing with the Cenomanian ostracodes of Egypt are those of BOLD (1964) on Abu Rawash area in the northeastern part of the Western Desert, ISMAIL & SOLIMAN (1997) on the north Western Desert, HATABA & AMMAR (1990) on the Western Desert and Gulf of Suez areas, COLIN & EL

APPENDIX 2

Sections

Localities

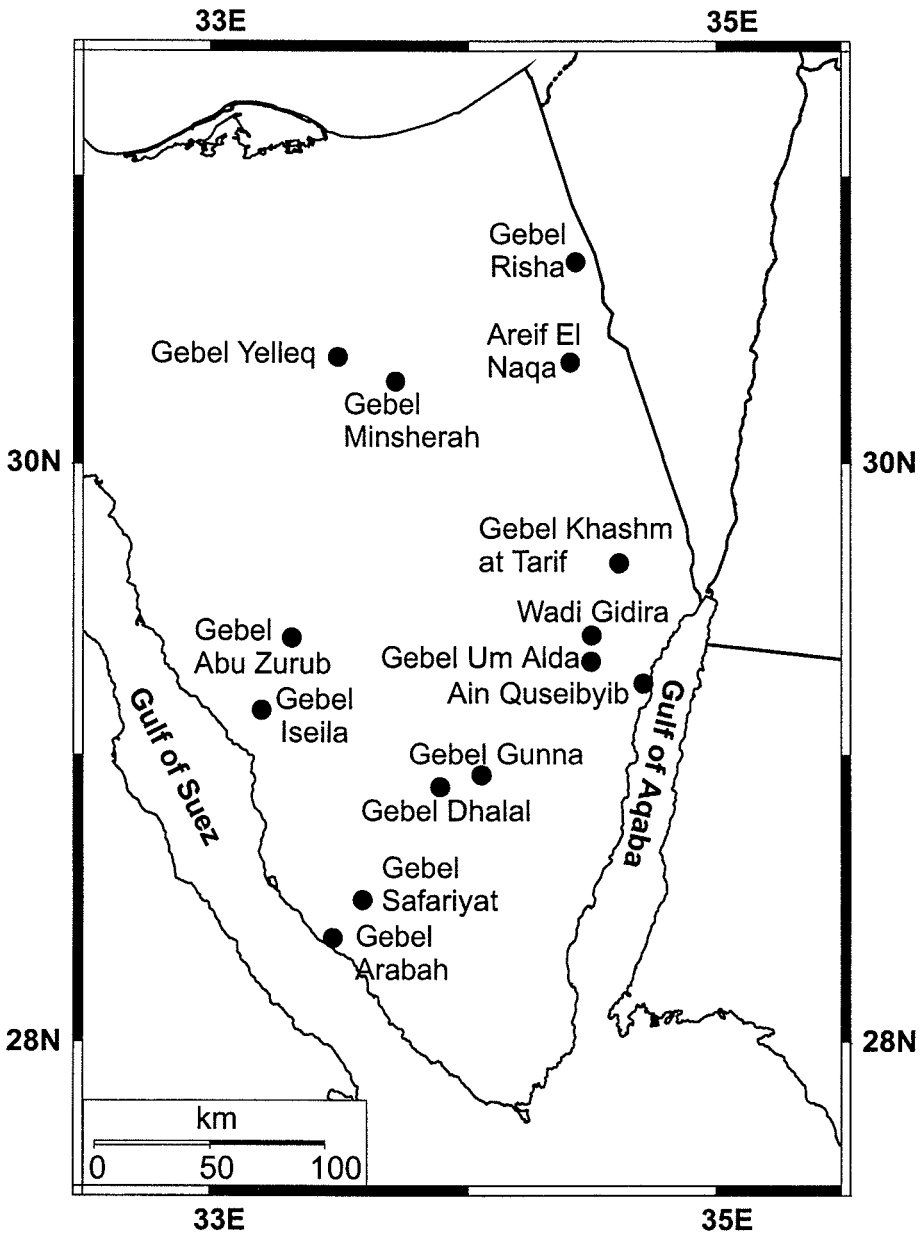
33E
35E
30N
28N
Gebel Risha
Areif El Naqa
Gebel Yelleq
Gebel Minsherah
Gebel Khashm at Tarif
Wadi Gidira
Gebel Abu Zurub
Gebel Um Alda
Ain Quseibyib
Gebel Iseila
Gebel Gunna
Gebel Dhalal
Gebel Safariyat
Gebel Arabah
Gulf of Suez
Gulf of Aqaba
km
0
50
100

Localities and Measured Sections

Legend for Sections

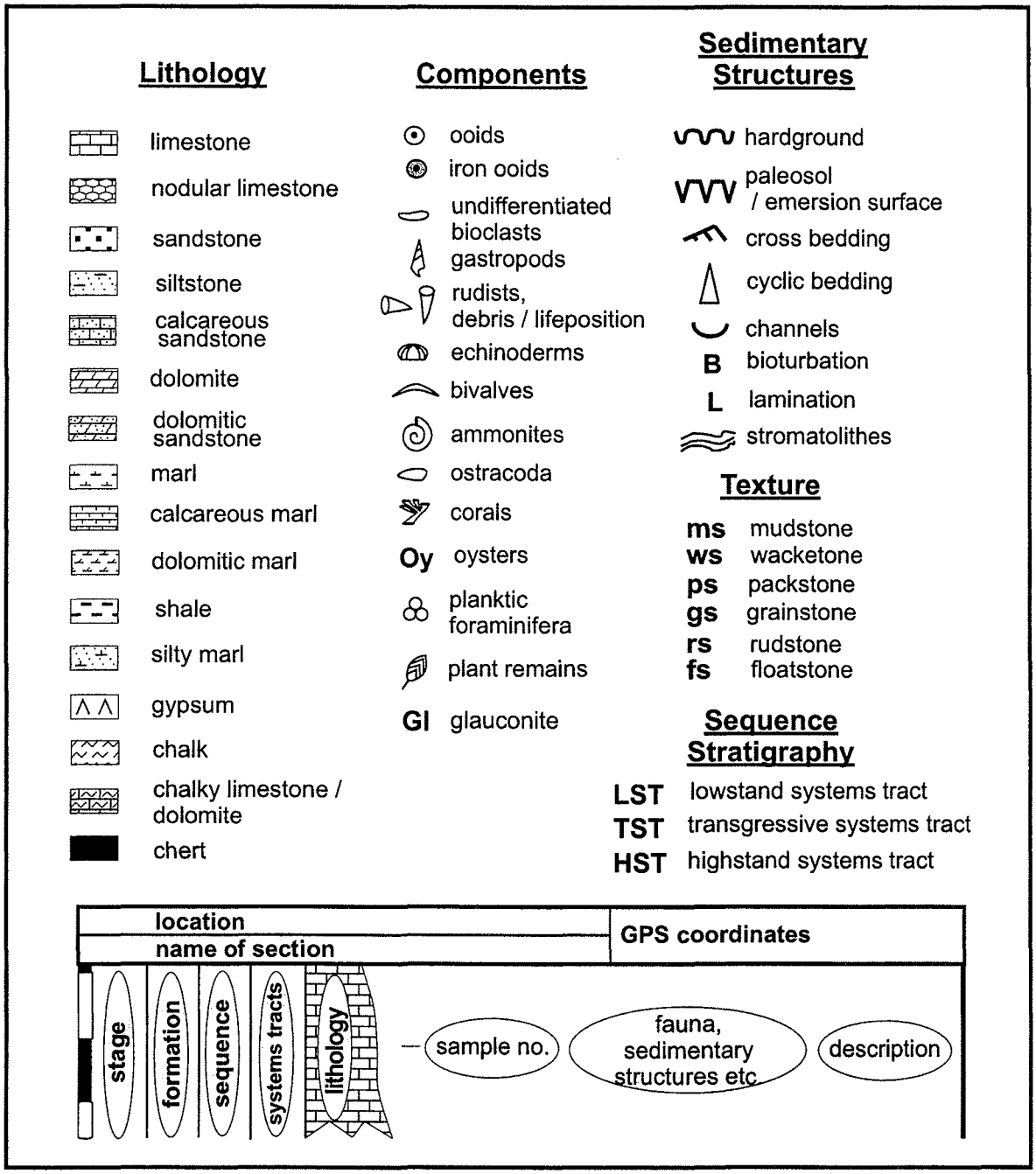

Location: Gebel Areif El Naqa
Section: AN1

Coordinates: N 30° 22,582'
E 34° 27,117'

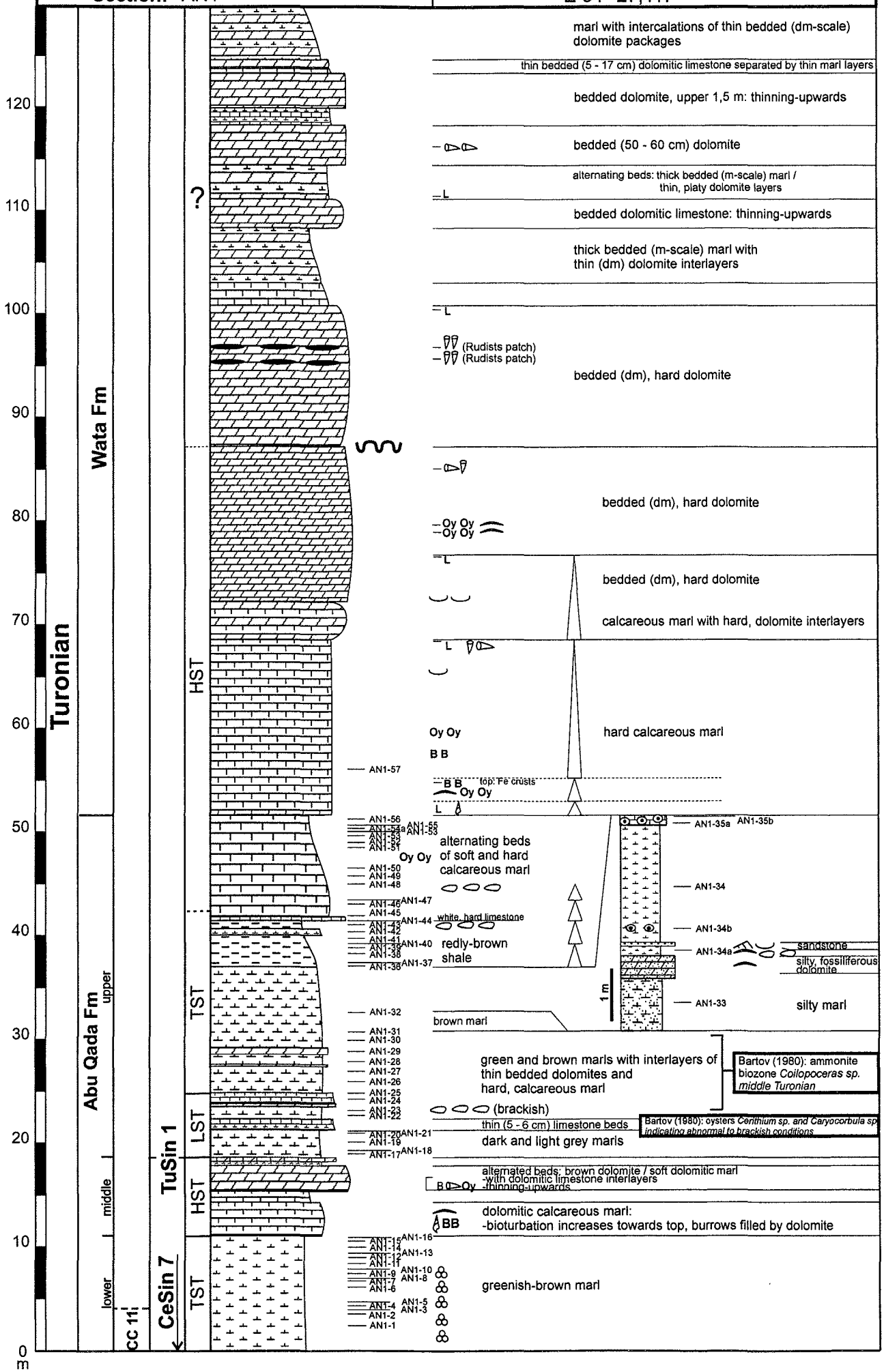

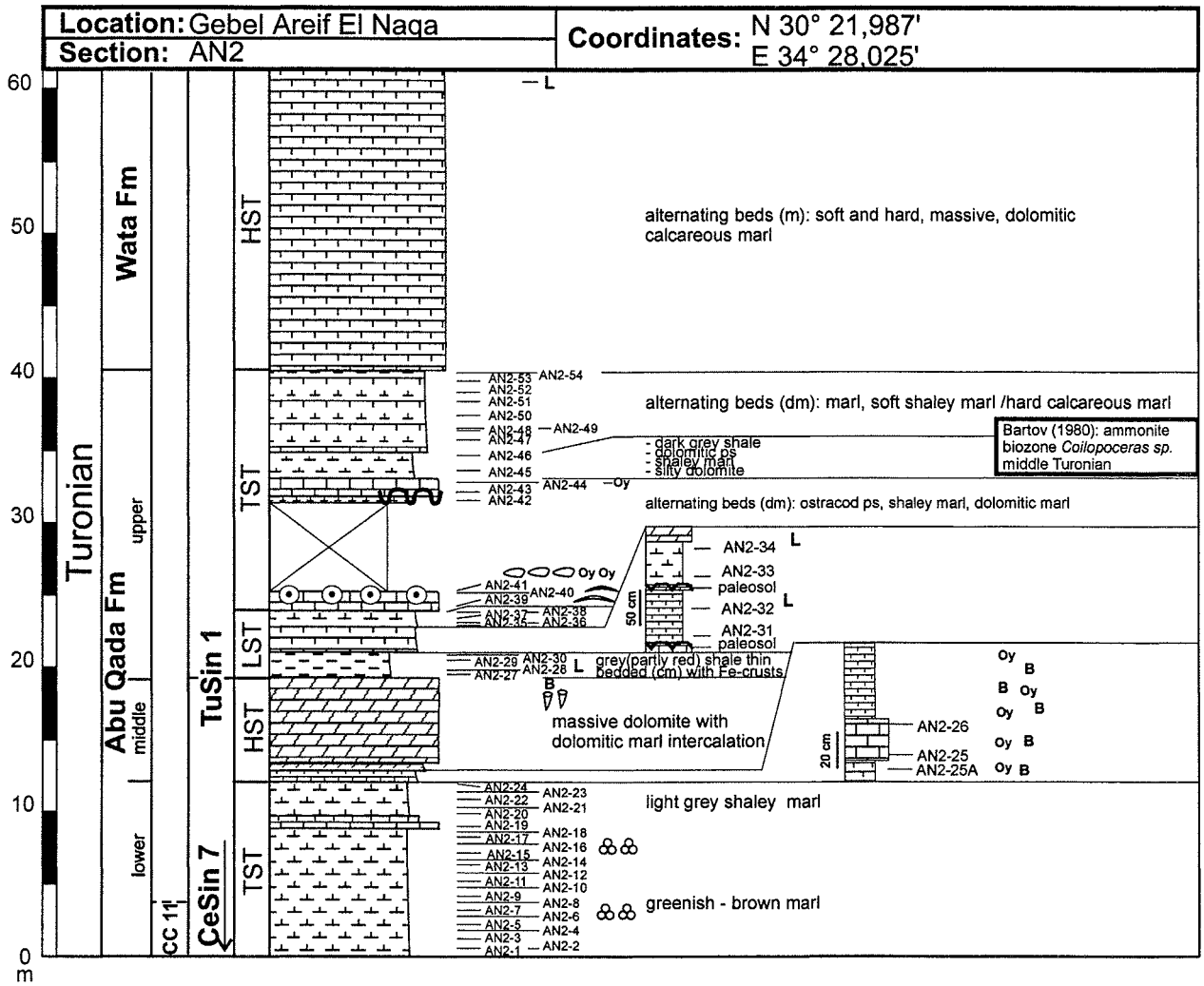
Location: Gebel Areif El Naqa
Section: AN2
Coordinates: N 30° 21,987'
E 34° 28,025'
Turonian
Wata Fm
Abu Qada Fm
upper
middle
lower
cc 11
TuSin 1
CeSin 7
HST
TST
LST
HST
TST
60
50
40
30
20
10
0
m
alternating beds (m): soft and hard, massive, dolomitic calcareous marl
alternating beds (dm): marl, soft shaley marl /hard calcareous marl
- dark grey shale
- dolomitic ps
- shaley marl
- silty dolomite
Bartov (1980): ammonite biozone Coilopoceras sp. middle Turonian
alternating beds (dm): ostracod ps, shaley marl, dolomitic marl
AN2-34
AN2-33
paleosol
AN2-32
AN2-31
paleosol
50 cm
grey(partly red) shale thin bedded (cm) with Fe-crusts
massive dolomite with dolomitic marl intercalation
AN2-26
AN2-25
AN2-25A
20 cm
light grey shaley marl
greenish - brown marl

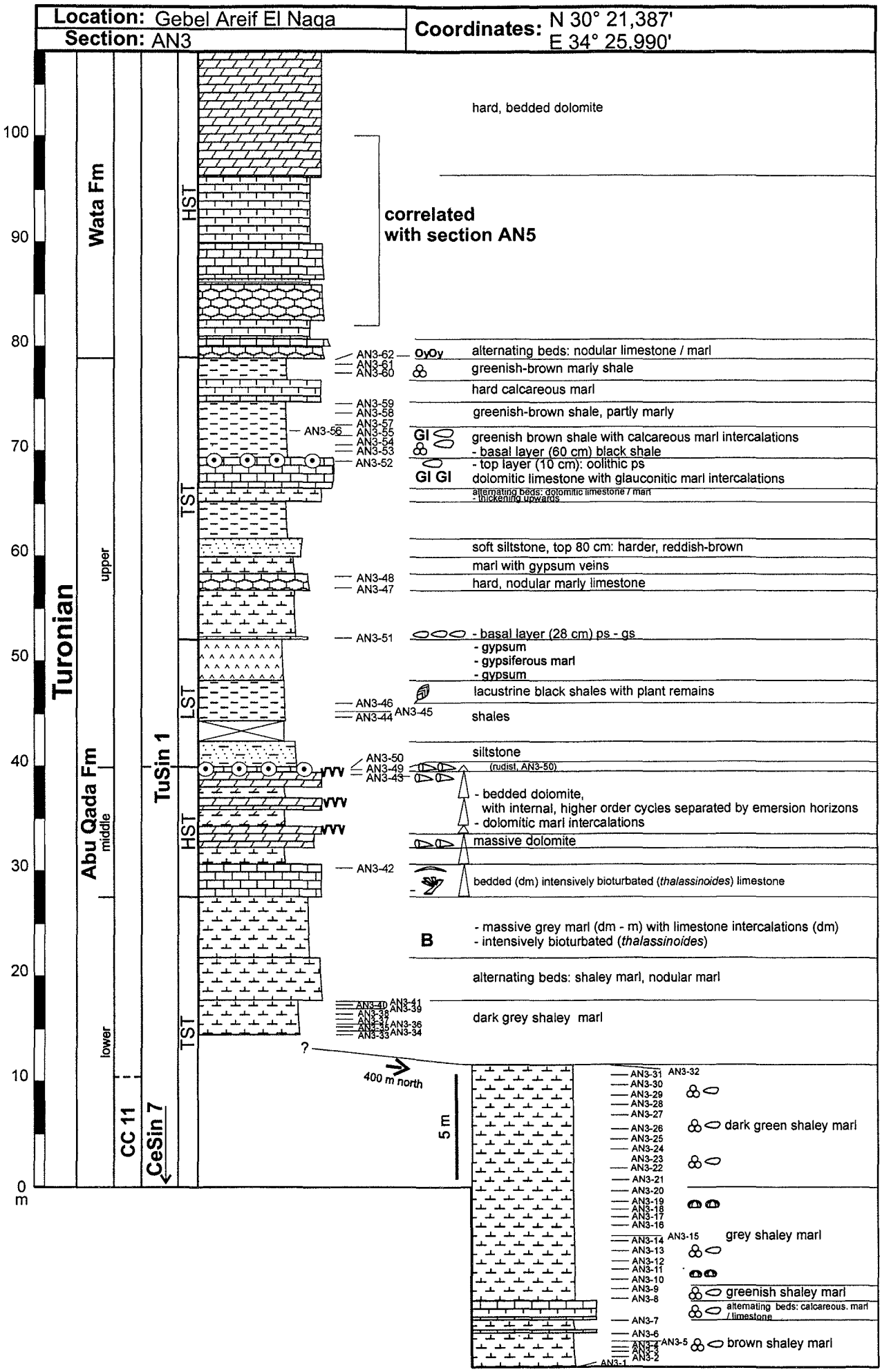
Location: Gebel Areif El Naqa
Section: AN3
Coordinates: N 30° 21,387'
E 34° 25,990'
Turonian
Wata Fm
Abu Qada Fm
upper
middle
lower
CC 11
CeSin 7
TuSin 1
HST
TST
LST
HST
TST
100
90
80
70
60
50
40
30
20
10
0
m
hard, bedded dolomite
correlated
with section AN5
AN3-62
AN3-61
AN3-60
OyOy
alternating beds: nodular limestone / marl
greenish-brown marly shale
hard calcareous marl
AN3-59
AN3-58
AN3-57
AN3-56
AN3-55
AN3-54
AN3-53
AN3-52
greenish-brown shale, partly marly
Gl
greenish brown shale with calcareous marl intercalations
- basal layer (60 cm) black shale
- top layer (10 cm): oolithic ps
Gl Gl
dolomitic limestone with glauconitic marl intercalations
alternating beds: dolomitic limestone / marl
- thickening upwards
soft siltstone, top 80 cm: harder, reddish-brown
marl with gypsum veins
AN3-48
AN3-47
hard, nodular marly limestone
AN3-51
- basal layer (28 cm) ps - gs
- gypsum
- gypsiferous marl
- gypsum
lacustrine black shales with plant remains
AN3-46
AN3-44
AN3-45
shales
siltstone
AN3-50
AN3-49
AN3-43
(rudist, AN3-50)
- bedded dolomite,
with internal, higher order cycles separated by emersion horizons
- dolomitic marl intercalations
massive dolomite
AN3-42
bedded (dm) intensively bioturbated (thalassinoides) limestone
- massive grey marl (dm - m) with limestone intercalations (dm)
B
- intensively bioturbated (thalassinoides)
alternating beds: shaley marl, nodular marl
AN3-40
AN3-41
AN3-39
AN3-38
AN3-37
AN3-36
AN3-35
AN3-34
AN3-33
dark grey shaley marl
?
400 m north
5 m
AN3-31
AN3-32
AN3-30
AN3-29
AN3-28
AN3-27
AN3-26
AN3-25
AN3-24
AN3-23
AN3-22
AN3-21
AN3-20
AN3-19
AN3-18
AN3-17
AN3-16
AN3-14
AN3-15
AN3-13
AN3-12
AN3-11
AN3-10
AN3-9
AN3-8
AN3-7
AN3-6
AN3-4
AN3-5
AN3-3
AN3-2
AN3-1
dark green shaley marl
grey shaley marl
greenish shaley marl
alternating beds: calcareous. marl / limestone
brown shaley marl

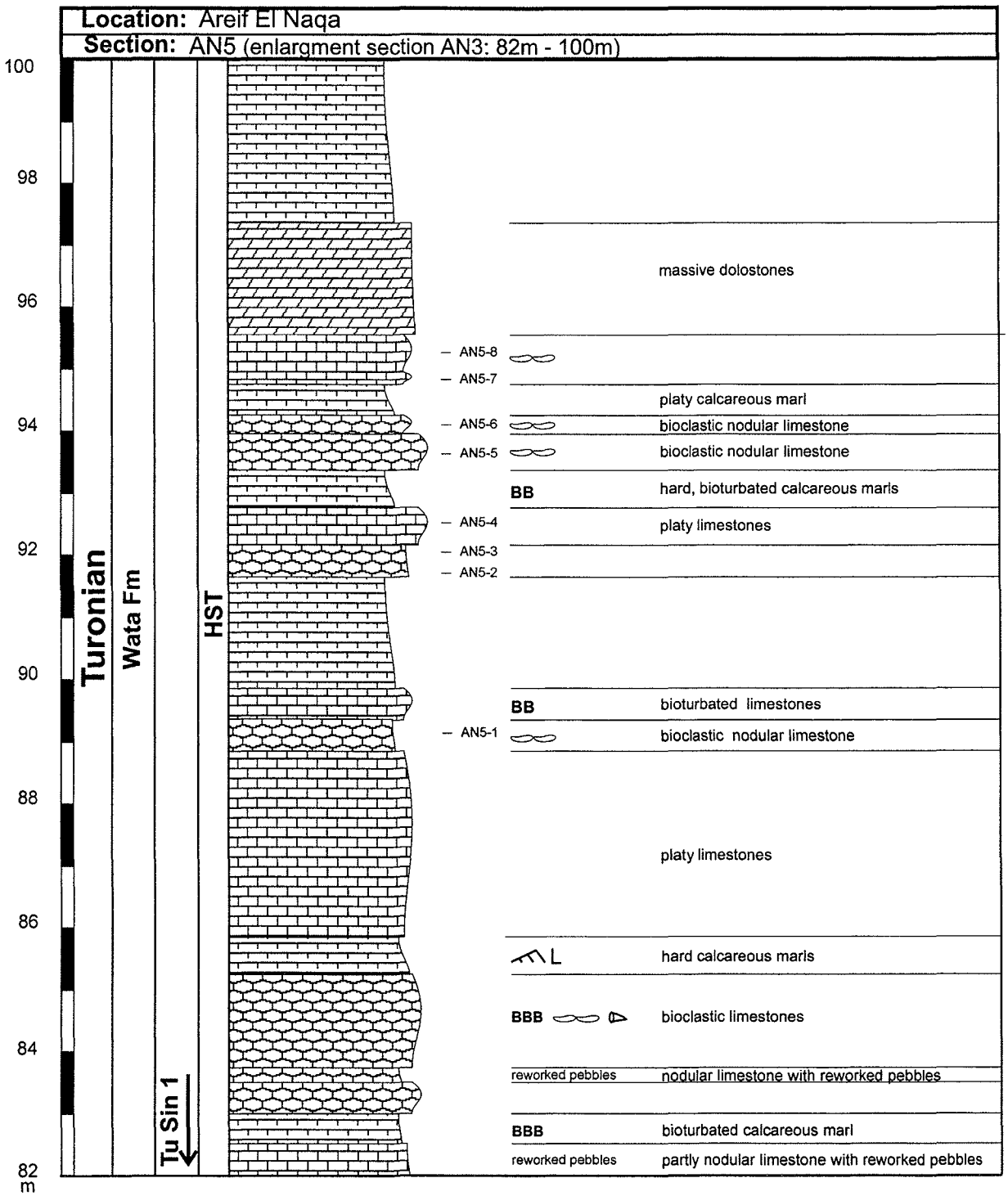
Location: Areif El Naqa
Section: AN5 (enlargment section AN3: 82m - 100m)
100
98
96
94
92
90
88
86
84
82
m
Turonian
Wata Fm
HST
Tu Sin 1
AN5-8
AN5-7
AN5-6
AN5-5
AN5-4
AN5-3
AN5-2
AN5-1
massive dolostones
platy calcareous marl
bioclastic nodular limestone
bioclastic nodular limestone
BB
hard, bioturbated calcareous marls
platy limestones
BB
bioturbated limestones
bioclastic nodular limestone
platy limestones
L
hard calcareous marls
BBB
bioclastic limestones
reworked pebbles
nodular limestone with reworked pebbles
BBB
bioturbated calcareous marl
reworked pebbles
partly nodular limestone with reworked pebbles

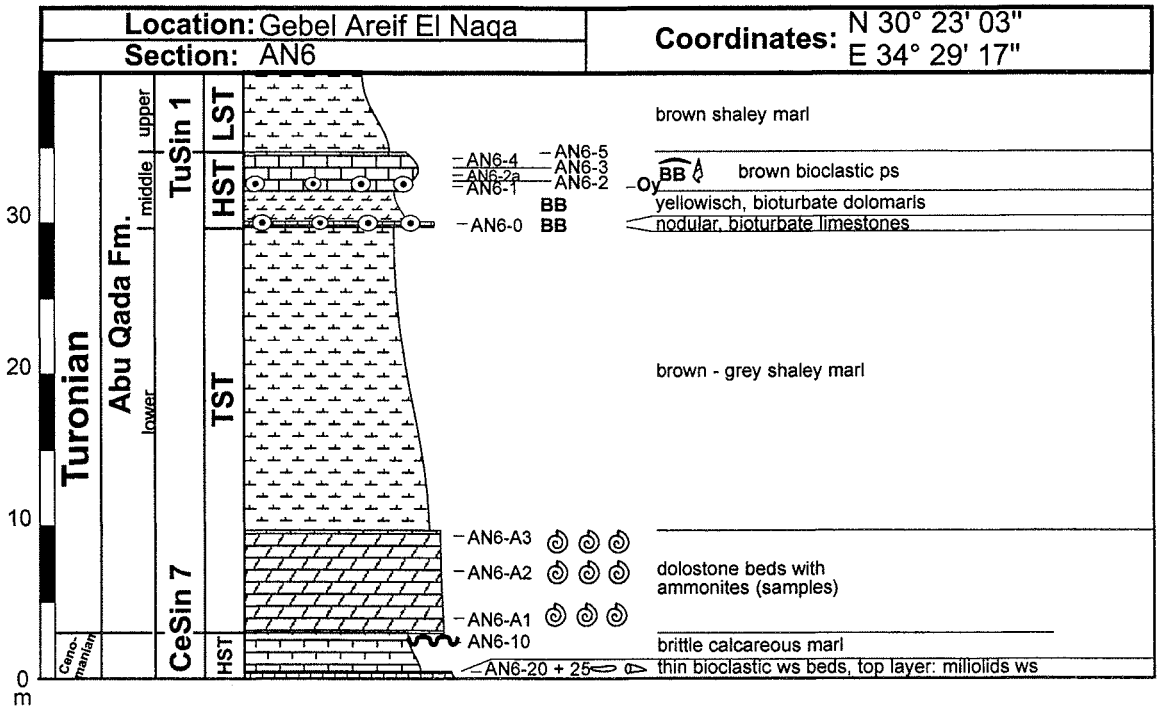
Location: Gebel Areif El Naqa
Section: AN6
Coordinates: N 30° 23' 03"
E 34° 29' 17"
Turonian
Abu Qada Fm.
upper
middle
lower
TuSin 1
CeSin 7
LST
HST
TST
Cenomanian
HST
brown shaley marl
AN6-4
AN6-5
AN6-3
AN6-2a
AN6-2
AN6-1
BB
Oy
brown bioclastic ps
yelliowisch, bioturbate dolomarls
AN6-0
BB
nodular, bioturbate limestones
brown - grey shaley marl
AN6-A3
AN6-A2
AN6-A1
dolostone beds with ammonites (samples)
AN6-10
brittle calcareous marl
AN6-20 + 25
thin bioclastic ws beds, top layer: miliolids ws
30
20
10
0
m

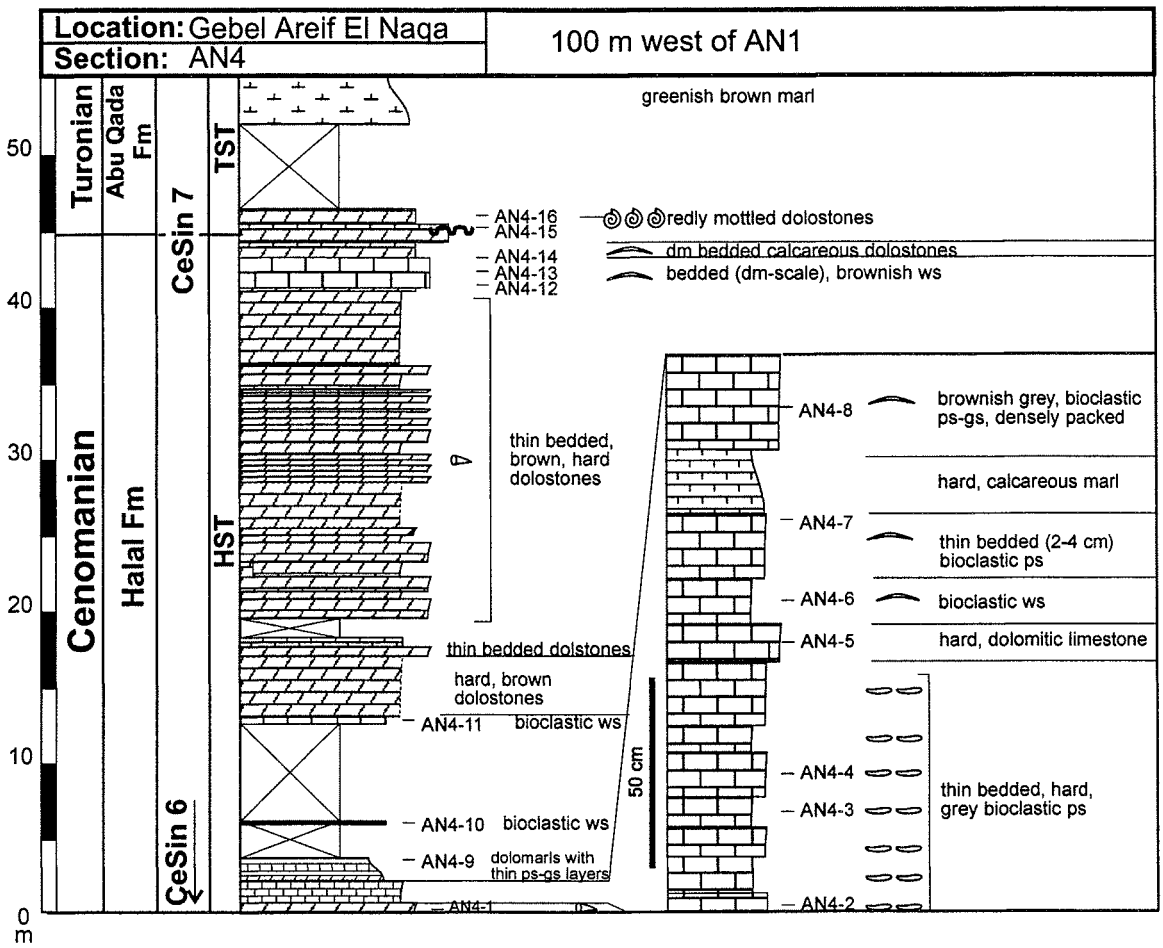
Location: Gebel Areif El Naqa
Section: AN4
100 m west of AN1
Turonian
Abu Qada Fm
Cenomanian
Halal Fm
CeSin 7
CeSin 6
TST
HST
greenish brown marl
AN4-16
AN4-15
redly mottled dolostones
AN4-14
dm bedded calcareous dolostones
AN4-13
AN4-12
bedded (dm-scale), brownish ws
thin bedded, brown, hard dolostones
thin bedded dolstones
hard, brown dolostones
AN4-11
bioclastic ws
AN4-10
bioclastic ws
AN4-9
dolomarls with thin ps-gs layers
AN4-1
50 cm
AN4-8
brownish grey, bioclastic ps-gs, densely packed
hard, calcareous marl
AN4-7
thin bedded (2-4 cm) bioclastic ps
AN4-6
bioclastic ws
AN4-5
hard, dolomitic limestone
AN4-4
AN4-3
thin bedded, hard, grey bioclastic ps
AN4-2
50
40
30
20
10
0
m

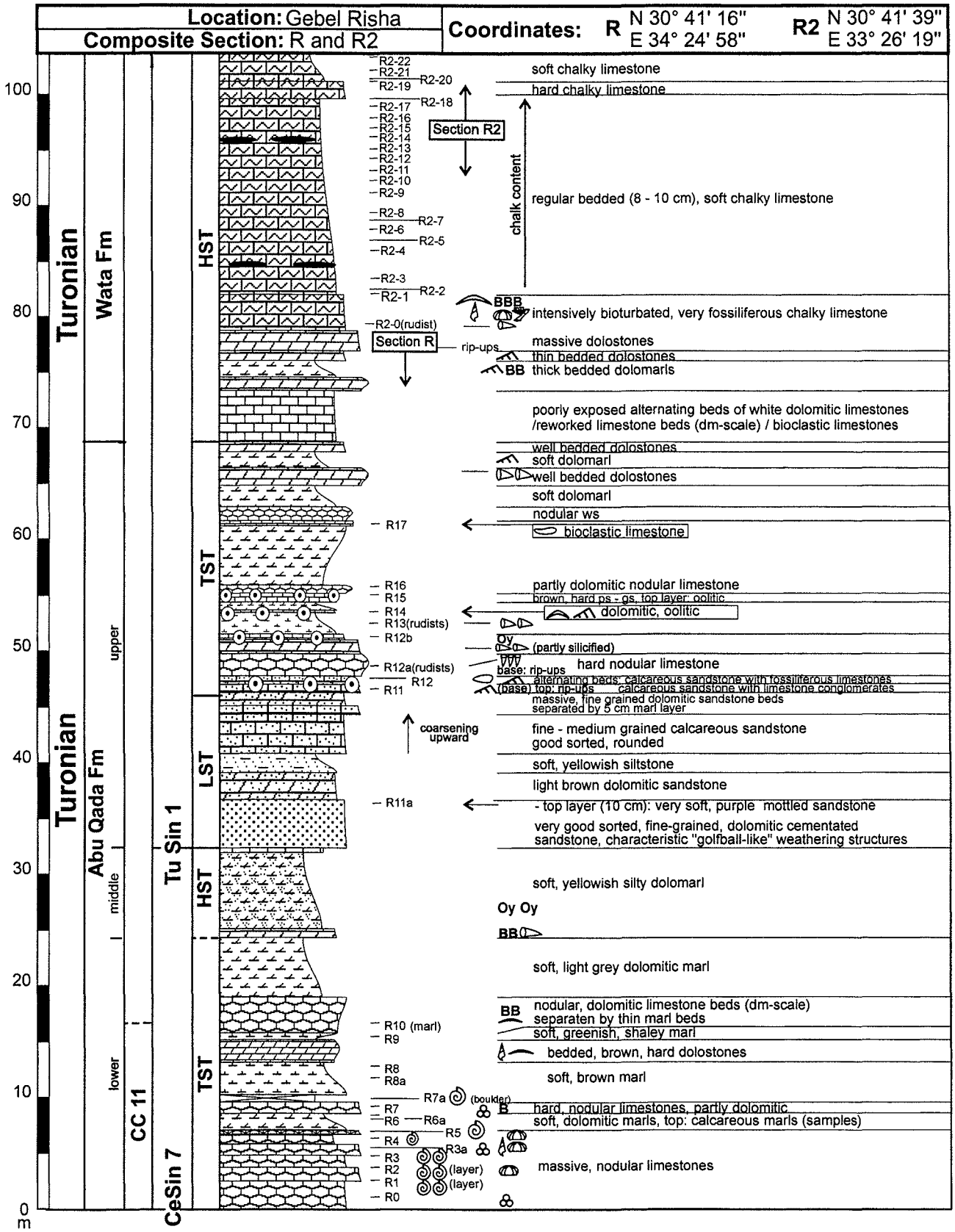
Location: Gebel Risha
Composite Section: R and R2
Coordinates: R N 30° 41' 16" E 34° 24' 58"
R2 N 30° 41' 39" E 33° 26' 19"
Turonian
Wata Fm
Abu Qada Fm
upper
middle
lower
CC 11
Tu Sin 1
CeSin 7
HST
TST
LST
HST
TST
100
90
80
70
60
50
40
30
20
10
0
m
R2-22
R2-21
R2-19
R2-20
R2-18
R2-17
R2-16
R2-15
R2-14
R2-13
R2-12
R2-11
R2-10
R2-9
R2-8
R2-7
R2-6
R2-5
R2-4
R2-3
R2-1
R2-2
R2-0(rudist)
Section R2
Section R
chalk content
soft chalky limestone
hard chalky limestone
regular bedded (8 - 10 cm), soft chalky limestone
BBB
intensively bioturbated, very fossiliferous chalky limestone
massive dolostones
rip-ups
thin bedded dolostones
BB
thick bedded dolomarls
poorly exposed alternating beds of white dolomitic limestones
/reworked limestone beds (dm-scale) / bioclastic limestones
well bedded dolostones
soft dolomarl
well bedded dolostones
soft dolomarl
nodular ws
R17
bioclastic limestone
R16
R15
R14
R13(rudists)
R12b
R12a(rudists)
R12
R11
partly dolomitic nodular limestone
brown, hard ps - gs, top layer: oolitic
dolomitic, oolitic
Oy
(partly silicified)
base: rip-ups
hard nodular limestone
(base) top: rip-ups
alternating beds: calcareous sandstone with fossiliferous limestones
calcareous sandstone with limestone conglomerates
massive, fine grained dolomitic sandstone beds
separated by 5 cm marl layer
coarsening upward
fine - medium grained calcareous sandstone
good sorted, rounded
soft, yellowish siltstone
light brown dolomitic sandstone
R11a
- top layer (10 cm): very soft, purple mottled sandstone
very good sorted, fine-grained, dolomitic cementated
sandstone, characteristic "golfball-like" weathering structures
soft, yellowish silty dolomarl
Oy Oy
BB
soft, light grey dolomitic marl
R10 (marl)
R9
R8
R8a
R7a
(boulder)
R7
R6
R6a
R5
R4
R3a
R3
R2
R1
R0
(layer)
(layer)
BB
nodular, dolomitic limestone beds (dm-scale)
separaten by thin marl beds
soft, greenish, shaley marl
bedded, brown, hard dolostones
soft, brown marl
B
hard, nodular limestones, partly dolomitic
soft, dolomitic marls, top: calcareous marls (samples)
massive, nodular limestones

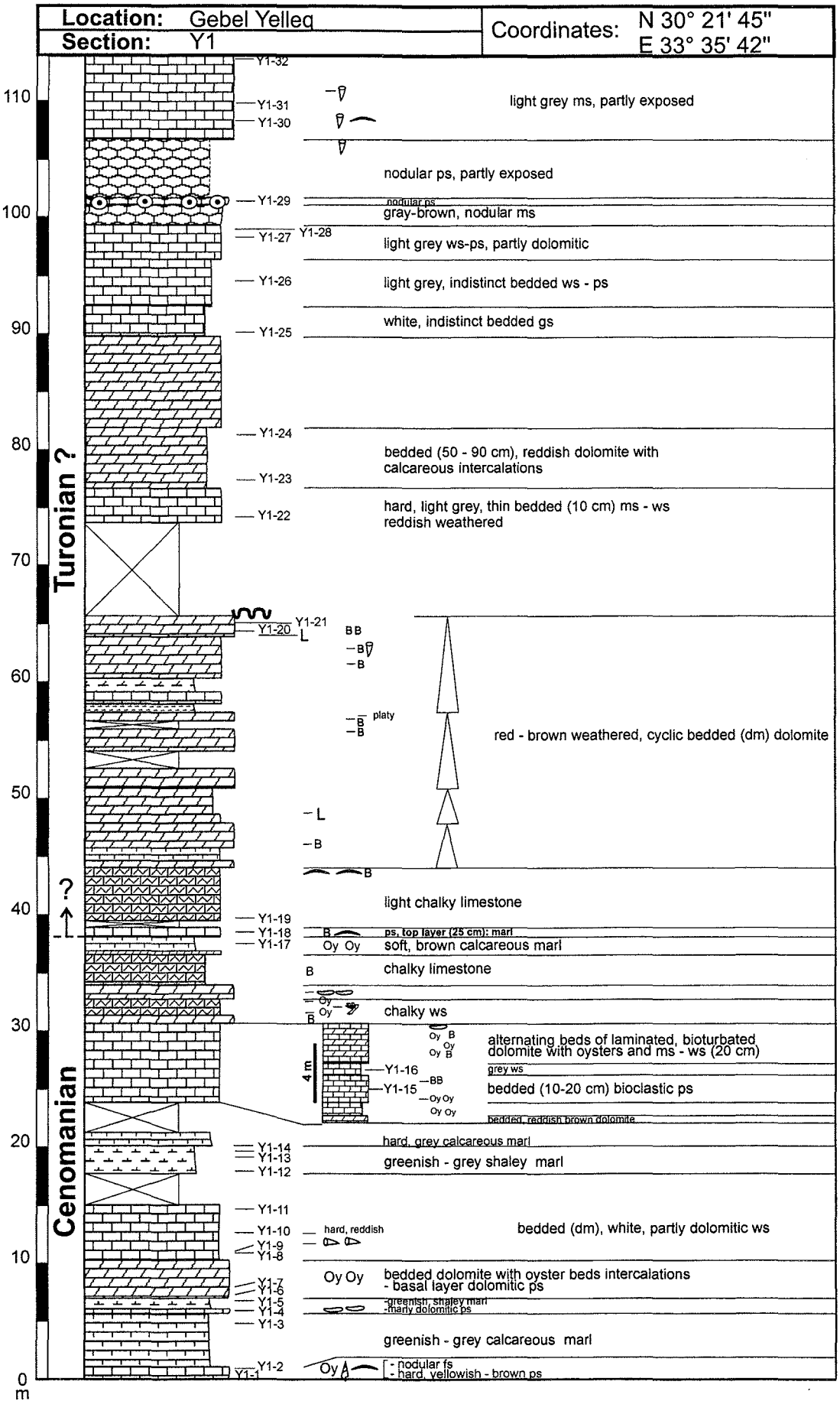
Location: Gebel Yelleq
Section: Y1
Coordinates: N 30° 21' 45"
E 33° 35' 42"
Turonian ?
Cenomanian
?
110
100
90
80
70
60
50
40
30
20
10
0
m
Y1-32
Y1-31
Y1-30
Y1-29
Y1-28
Y1-27
Y1-26
Y1-25
Y1-24
Y1-23
Y1-22
Y1-21
Y1-20
Y1-19
Y1-18
Y1-17
Y1-16
Y1-15
Y1-14
Y1-13
Y1-12
Y1-11
Y1-10
Y1-9
Y1-8
Y1-7
Y1-6
Y1-5
Y1-4
Y1-3
Y1-2
Y1-1
4 m
light grey ms, partly exposed
nodular ps, partly exposed
nodular ps
gray-brown, nodular ms
light grey ws-ps, partly dolomitic
light grey, indistinct bedded ws - ps
white, indistinct bedded gs
bedded (50 - 90 cm), reddish dolomite with calcareous intercalations
hard, light grey, thin bedded (10 cm) ms - ws reddish weathered
platy
red - brown weathered, cyclic bedded (dm) dolomite
light chalky limestone
ps, top layer (25 cm): marl
soft, brown calcareous marl
chalky limestone
chalky ws
alternating beds of laminated, bioturbated dolomite with oysters and ms - ws (20 cm)
grey ws
bedded (10-20 cm) bioclastic ps
bedded, reddish brown dolomite
hard, grey calcareous marl
greenish - grey shaley marl
hard, reddish
bedded (dm), white, partly dolomitic ws
bedded dolomite with oyster beds intercalations
- basal layer dolomitic ps
-greenish, shaley marl
-marly dolomitic ps
greenish - grey calcareous marl
- nodular fs
- hard, yellowish - brown ps

X

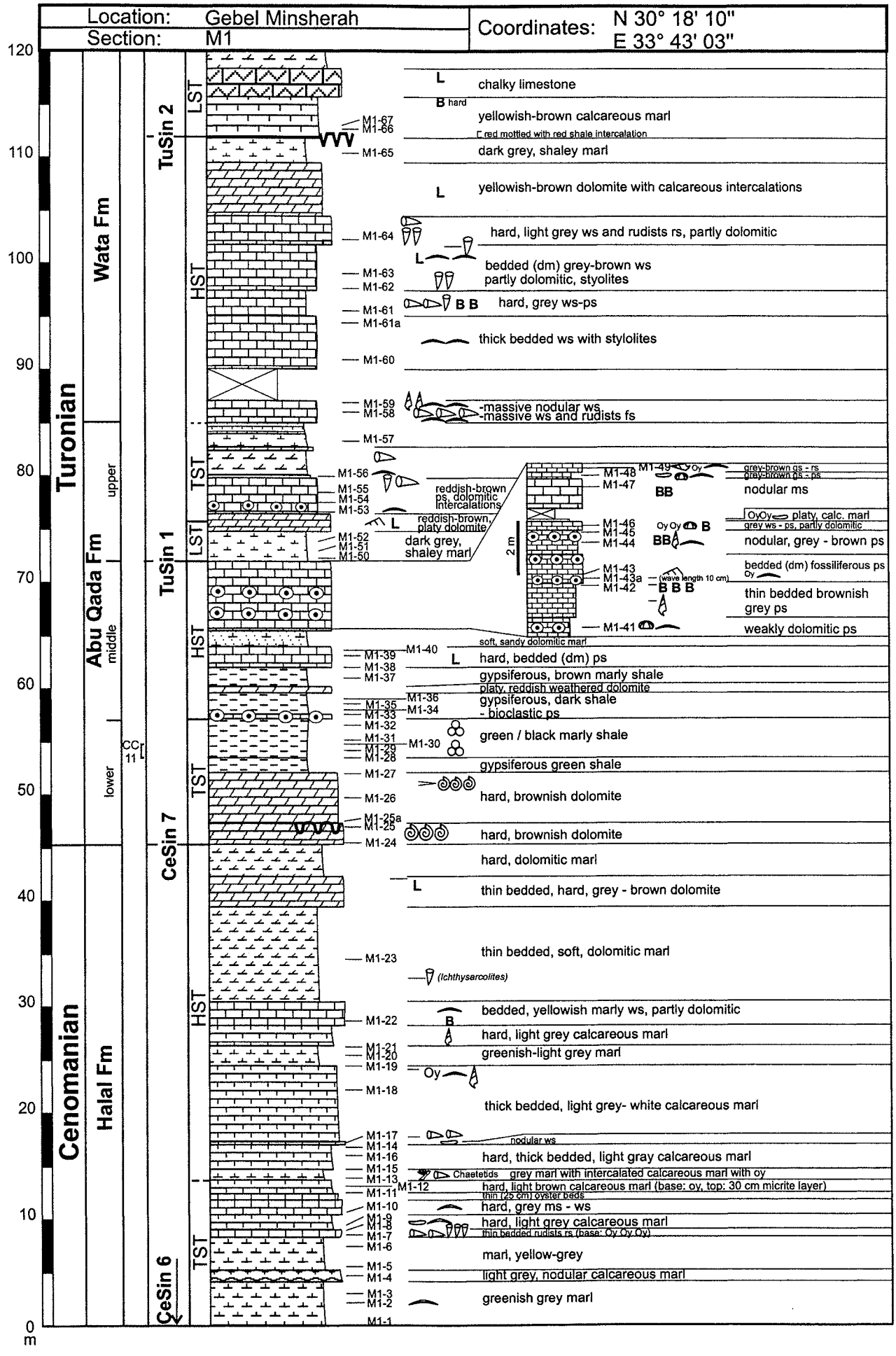
Location: Gebel Minsherah
Section: M1
Coordinates: N 30° 18' 10"
E 33° 43' 03"
Turonian
Cenomanian
Wata Fm
Abu Qada Fm
upper
middle
lower
Halal Fm
TuSin 2
TuSin 1
CeSin 7
CeSin 6
CC 11
LST
HST
TST
chalky limestone
yellowish-brown calcareous marl
red mottled with red shale intercalation
dark grey, shaley marl
yellowish-brown dolomite with calcareous intercalations
hard, light grey ws and rudists rs, partly dolomitic
bedded (dm) grey-brown ws
partly dolomitic, stylolites
hard, grey ws-ps
thick bedded ws with stylolites
-massive nodular ws
-massive ws and rudists fs
reddish-brown ps, dolomitic intercalations
reddish-brown, platy dolomite
dark grey, shaley marl
grey-brown gs - rs
grey-brown gs - ps
nodular ms
platy, calc. marl
grey ws - ps, partly dolomitic
nodular, grey - brown ps
bedded (dm) fossiliferous ps
thin bedded brownish grey ps
weakly dolomitic ps
soft, sandy dolomitic marl
hard, bedded (dm) ps
gypsiferous, brown marly shale
platy, reddish weathered dolomite
gypsiferous, dark shale
- bioclastic ps
green / black marly shale
gypsiferous green shale
hard, brownish dolomite
hard, brownish dolomite
hard, dolomitic marl
thin bedded, hard, grey - brown dolomite
thin bedded, soft, dolomitic marl
(Ichthysarcolites)
bedded, yellowish marly ws, partly dolomitic
hard, light grey calcareous marl
greenish-light grey marl
thick bedded, light grey- white calcareous marl
nodular ws
hard, thick bedded, light gray calcareous marl
Chaetetids
grey marl with intercalated calcareous marl with oy
hard, light brown calcareous marl (base: oy, top: 30 cm micrite layer)
thin (25 cm) oyster beds
hard, grey ms - ws
hard, light grey calcareous marl
thin bedded rudists rs (base: Oy Oy Oy)
marl, yellow-grey
light grey, nodular calcareous marl
greenish grey marl
2 m
(wave length 10 cm)
m

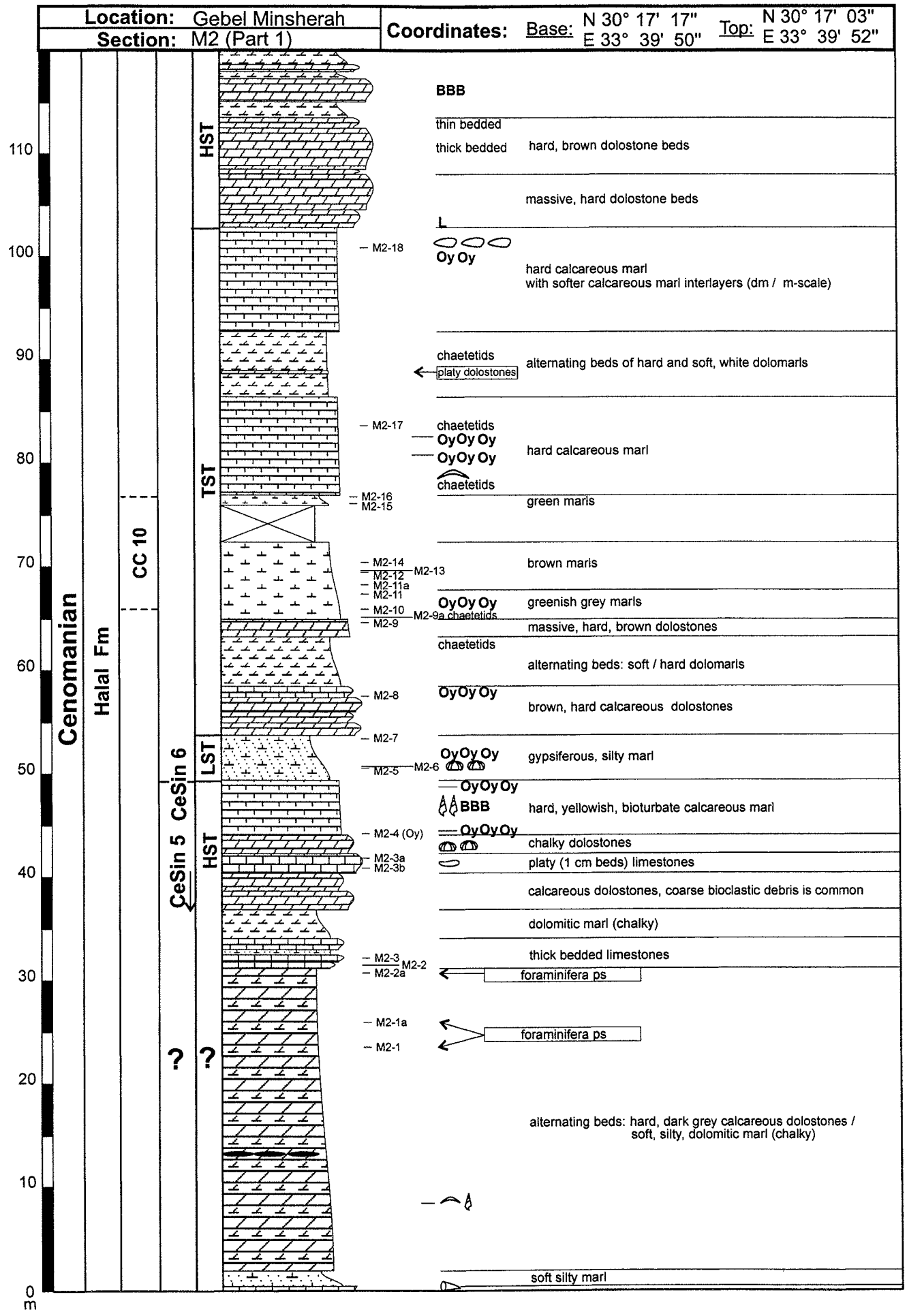
Location: Gebel Minsherah
Section: M2 (Part 1)
Coordinates: Base: N 30° 17' 17" E 33° 39' 50" Top: N 30° 17' 03" E 33° 39' 52"
Cenomanian
Halal Fm
CC 10
CeSin 6
CeSin 5
HST
TST
LST
HST
?
?
BBB
thin bedded
thick bedded
hard, brown dolostone beds
massive, hard dolostone beds
L
M2-18
Oy Oy
hard calcareous marl
with softer calcareous marl interlayers (dm / m-scale)
chaetetids
platy dolostones
alternating beds of hard and soft, white dolomarls
M2-17
chaetetids
Oy Oy Oy
Oy Oy Oy
hard calcareous marl
chaetetids
M2-16
M2-15
green marls
M2-14
M2-13
M2-12
M2-11a
M2-11
brown marls
M2-10
M2-9a chaetetids
M2-9
Oy Oy Oy
greenish grey marls
massive, hard, brown dolostones
chaetetids
alternating beds: soft / hard dolomarls
M2-8
Oy Oy Oy
brown, hard calcareous dolostones
M2-7
M2-6
M2-5
Oy Oy Oy
gypsiferous, silty marl
Oy Oy Oy
BBB
hard, yellowish, bioturbate calcareous marl
M2-4 (Oy)
Oy Oy Oy
chalky dolostones
M2-3a
M2-3b
platy (1 cm beds) limestones
calcareous dolostones, coarse bioclastic debris is common
dolomitic marl (chalky)
thick bedded limestones
M2-3
M2-2
M2-2a
foraminifera ps
M2-1a
M2-1
foraminifera ps
alternating beds: hard, dark grey calcareous dolostones / soft, silty, dolomitic marl (chalky)
soft silty marl
110
100
90
80
70
60
50
40
30
20
10
0
m

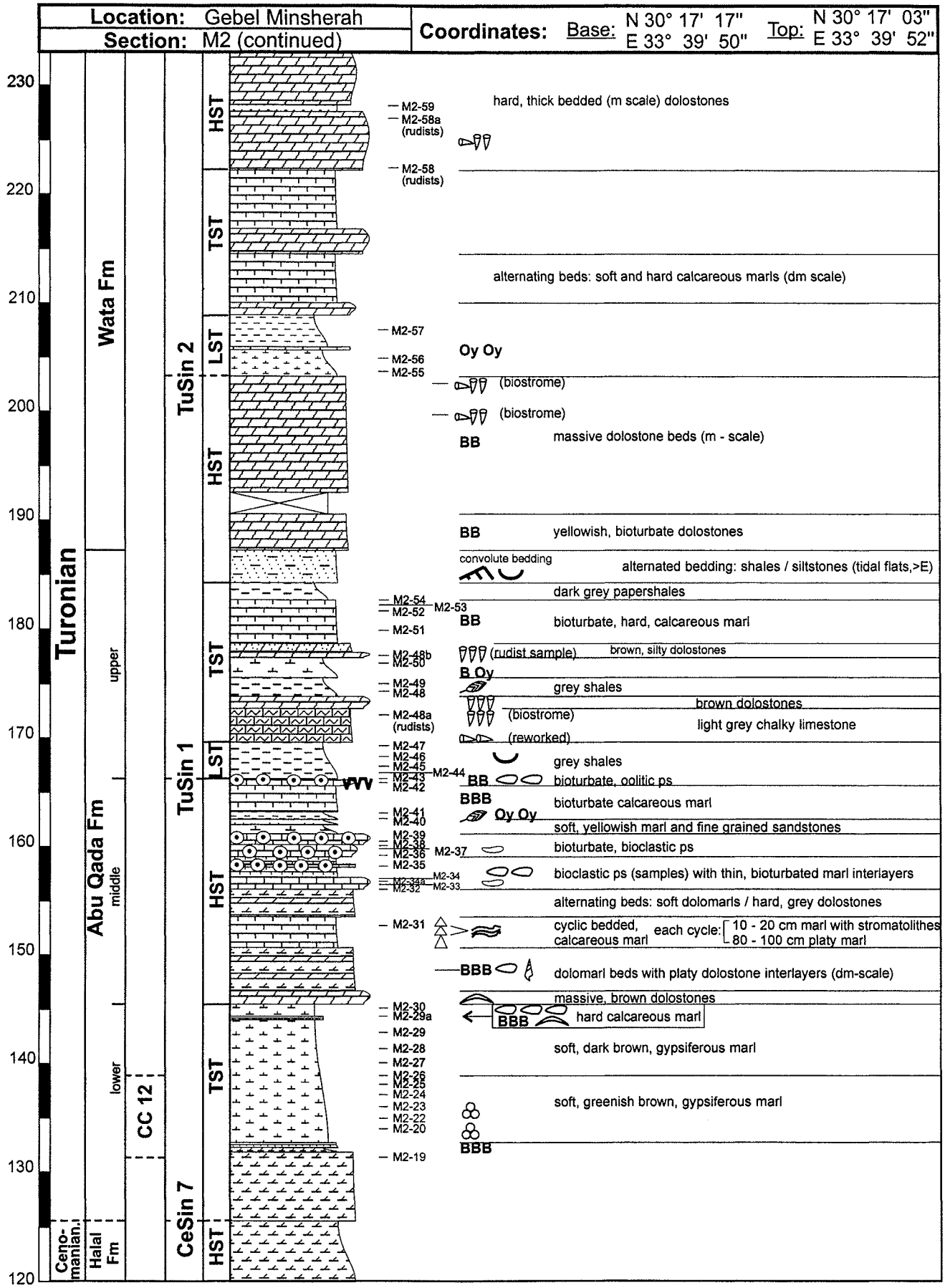
Location: Gebel Minsherah
Section: M2 (continued)
Coordinates: Base: N 30° 17' 17" E 33° 39' 50" Top: N 30° 17' 03" E 33° 39' 52"
230
220
210
200
190
180
170
160
150
140
130
120
Turonian
Ceno-manian
Wata Fm
Abu Qada Fm
upper
middle
lower
Halal Fm
CC 12
TuSin 2
TuSin 1
CeSin 7
HST
TST
LST
HST
TST
LST
HST
TST
HST
M2-59
M2-58a (rudists)
M2-58 (rudists)
M2-57
M2-56
M2-55
M2-54
M2-52
M2-53
M2-51
M2-48b
M2-50
M2-49
M2-48
M2-48a (rudists)
M2-47
M2-46
M2-45
M2-43
M2-44
M2-42
M2-41
M2-40
M2-39
M2-38
M2-36
M2-37
M2-35
M2-34a
M2-34
M2-32
M2-33
M2-31
M2-30
M2-29a
M2-29
M2-28
M2-27
M2-26
M2-25
M2-24
M2-23
M2-22
M2-20
M2-19
hard, thick bedded (m scale) dolostones
alternating beds: soft and hard calcareous marls (dm scale)
Oy Oy
(biostrome)
(biostrome)
BB
massive dolostone beds (m - scale)
BB
yellowish, bioturbate dolostones
convolute bedding
alternated bedding: shales / siltstones (tidal flats,>E)
dark grey papershales
BB
bioturbate, hard, calcareous marl
(rudist sample)
brown, silty dolostones
B Oy
grey shales
brown dolostones
(biostrome)
light grey chalky limestone
(reworked)
grey shales
BB
bioturbate, oolitic ps
BBB
bioturbate calcareous marl
Oy Oy
soft, yellowish marl and fine grained sandstones
bioturbate, bioclastic ps
bioclastic ps (samples) with thin, bioturbated marl interlayers
alternating beds: soft dolomarls / hard, grey dolostones
cyclic bedded, calcareous marl
each cycle:
10 - 20 cm marl with stromatolithes
80 - 100 cm platy marl
BBB
dolomarl beds with platy dolostone interlayers (dm-scale)
massive, brown dolostones
BBB
hard calcareous marl
soft, dark brown, gypsiferous marl
soft, greenish brown, gypsiferous marl
BBB

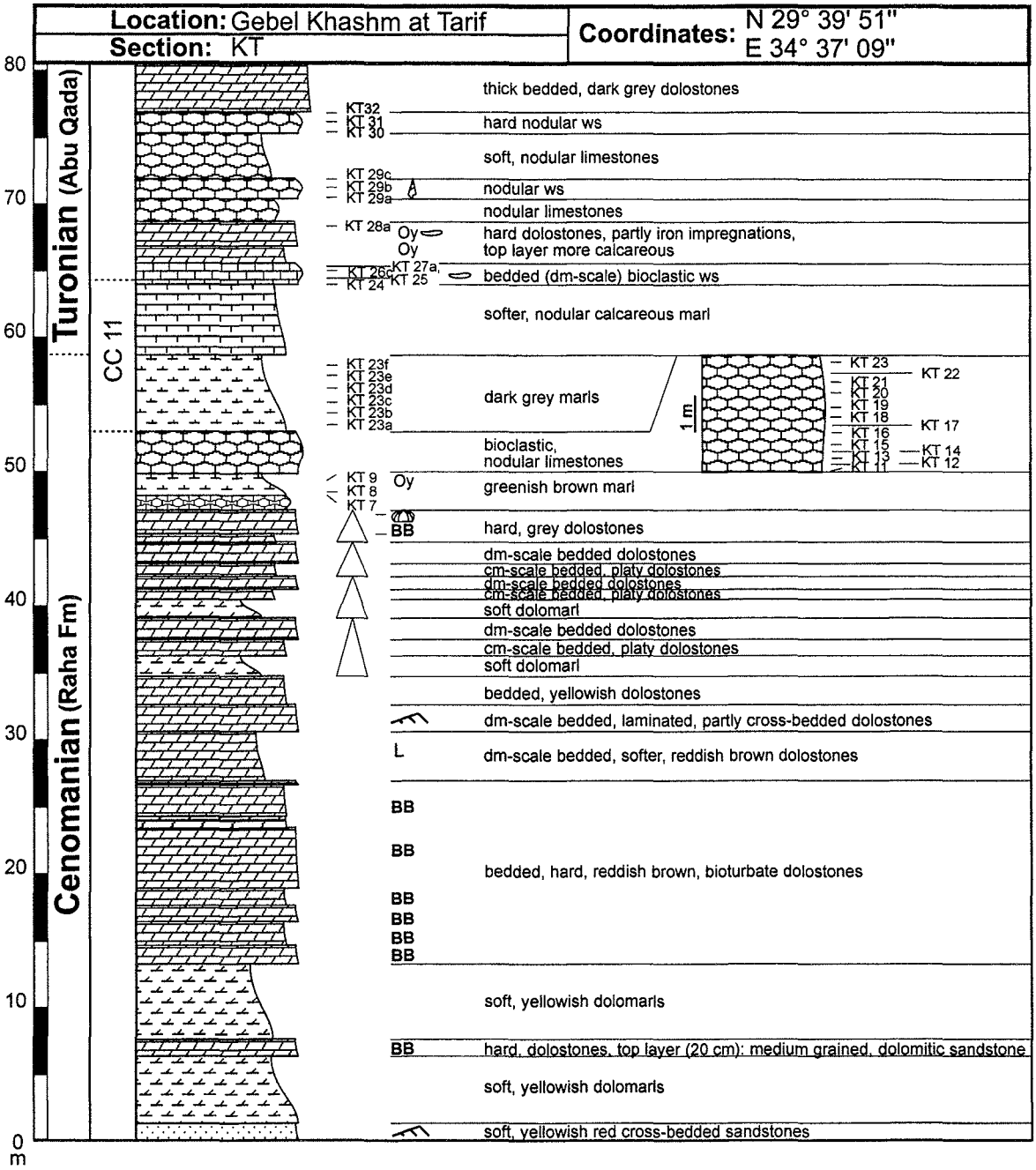
Location: Gebel Khashm at Tarif
Section: KT
Coordinates: N 29° 39' 51"
E 34° 37' 09"
Turonian (Abu Qada)
Cenomanian (Raha Fm)
CC 11
80
70
60
50
40
30
20
10
0
m
KT32
KT 31
KT 30
KT 29c
KT 29b
KT 29a
KT 28a
KT 26c
KT 27a
KT 25
KT 24
KT 23f
KT 23e
KT 23d
KT 23c
KT 23b
KT 23a
KT 9
KT 8
KT 7
Oy
Oy
BB
BB
BB
BB
BB
BB
L
thick bedded, dark grey dolostones
hard nodular ws
soft, nodular limestones
nodular ws
nodular limestones
hard dolostones, partly iron impregnations,
top layer more calcareous
bedded (dm-scale) bioclastic ws
softer, nodular calcareous marl
dark grey marls
bioclastic,
nodular limestones
greenish brown marl
hard, grey dolostones
dm-scale bedded dolostones
cm-scale bedded, platy dolostones
dm-scale bedded dolostones
cm-scale bedded, platy dolostones
soft dolomarl
dm-scale bedded dolostones
cm-scale bedded, platy dolostones
soft dolomarl
bedded, yellowish dolostones
dm-scale bedded, laminated, partly cross-bedded dolostones
dm-scale bedded, softer, reddish brown dolostones
bedded, hard, reddish brown, bioturbate dolostones
soft, yellowish dolomarls
hard, dolostones, top layer (20 cm): medium grained, dolomitic sandstone
soft, yellowish dolomarls
soft, yellowish red cross-bedded sandstones
1 m
KT 23
KT 22
KT 21
KT 20
KT 19
KT 18
KT 17
KT 16
KT 15
KT 14
KT 13
KT 12
KT 11

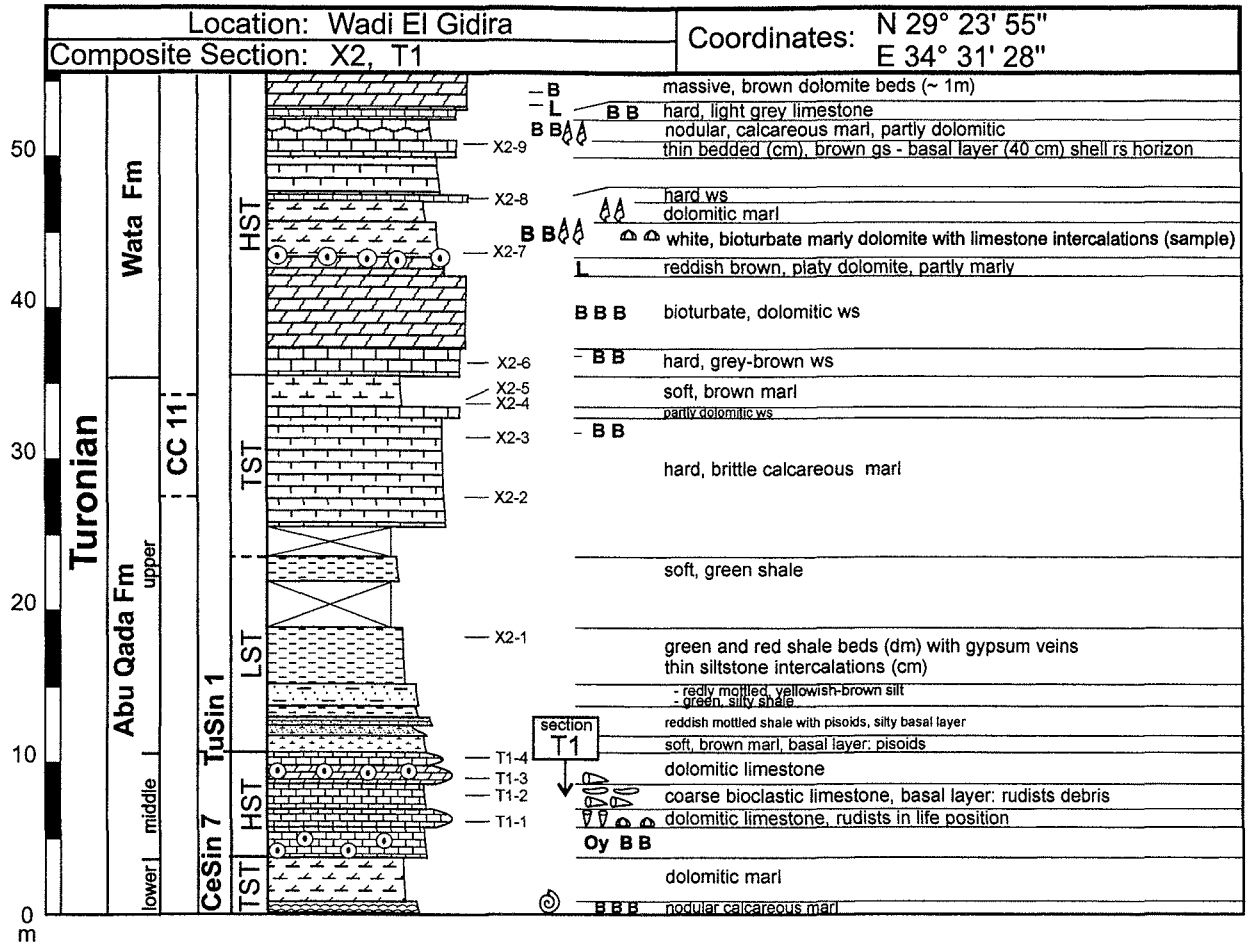
Location: Wadi El Gidira
Composite Section: X2, T1
Coordinates: N 29° 23' 55"
E 34° 31' 28"
Turonian
Wata Fm
Abu Qada Fm
upper
middle
lower
CC 11
CeSin 7
TuSin 1
HST
TST
LST
HST
TST
X2-9
X2-8
X2-7
X2-6
X2-5
X2-4
X2-3
X2-2
X2-1
T1-4
T1-3
T1-2
T1-1
section T1
massive, brown dolomite beds (~ 1m)
hard, light grey limestone
nodular, calcareous marl, partly dolomitic
thin bedded (cm), brown gs - basal layer (40 cm) shell rs horizon
hard ws
dolomitic marl
white, bioturbate marly dolomite with limestone intercalations (sample)
reddish brown, platy dolomite, partly marly
bioturbate, dolomitic ws
hard, grey-brown ws
soft, brown marl
partly dolomitic ws
hard, brittle calcareous marl
soft, green shale
green and red shale beds (dm) with gypsum veins
thin siltstone intercalations (cm)
- redly mottled, yellowish-brown silt
- green, silty shale
reddish mottled shale with pisoids, silty basal layer
soft, brown marl, basal layer: pisoids
dolomitic limestone
coarse bioclastic limestone, basal layer: rudists debris
dolomitic limestone, rudists in life position
dolomitic marl
nodular calcareous marl
0
10
20
30
40
50
m

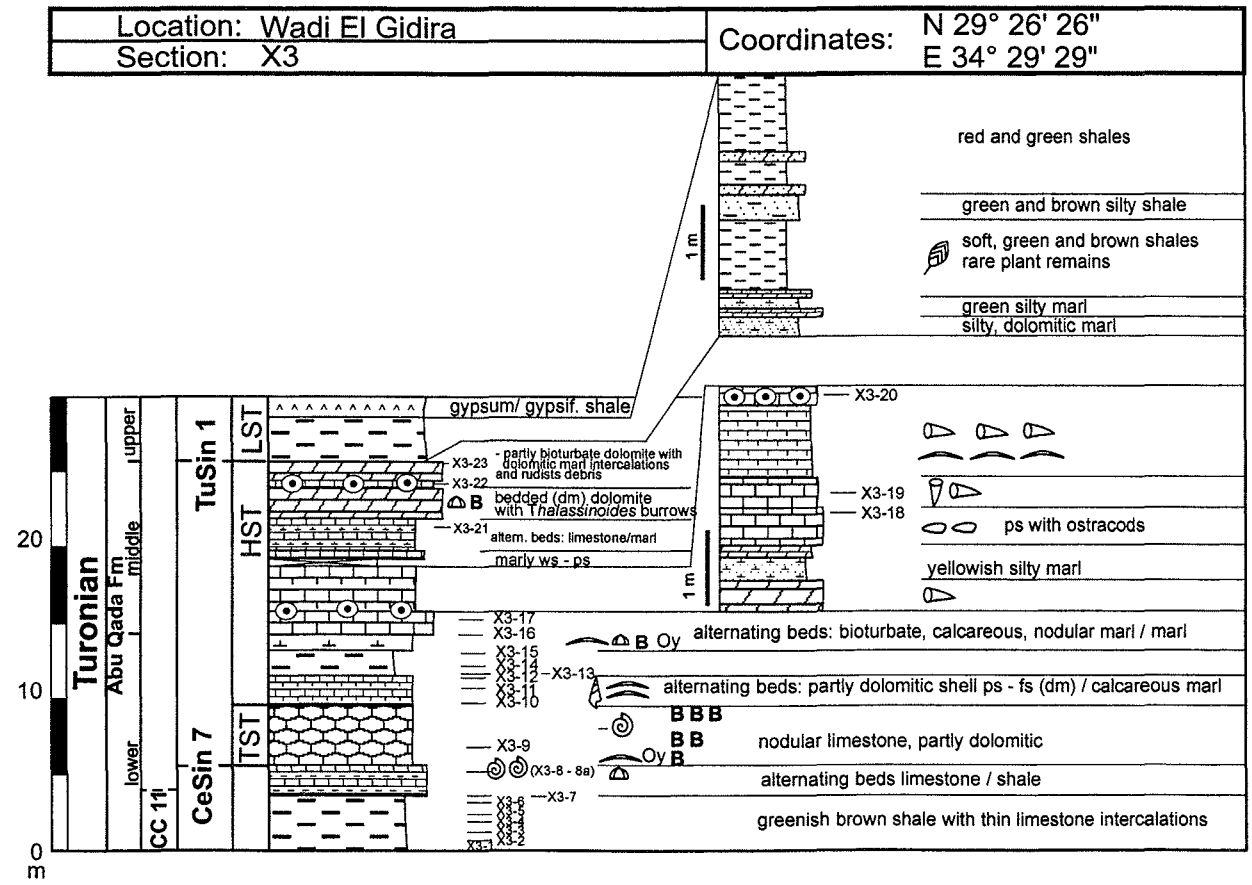
Location: Wadi El Gidira
Section: X3
Coordinates: N 29° 26' 26"
E 34° 29' 29"
Turonian
Abu Qada Fm
upper
middle
lower
CC 11
CeSin 7
TuSin 1
LST
HST
TST
red and green shales
green and brown silty shale
soft, green and brown shales
rare plant remains
green silty marl
silty, dolomitic marl
1 m
gypsum/ gypsif. shale
X3-23
X3-22
X3-21
partly bioturbate dolomite with dolomitic marl intercalations and rudists debris
bedded (dm) dolomite with Thalassinoides burrows
altern. beds: limestone/marl
marly ws - ps
X3-20
X3-19
X3-18
ps with ostracods
yellowish silty marl
X3-17
X3-16
X3-15
X3-14
X3-13
X3-12
X3-11
X3-10
X3-9
X3-8 - 8a
X3-7
X3-6
X3-5
X3-4
X3-3
X3-2
X3-1
alternating beds: bioturbate, calcareous, nodular marl / marl
alternating beds: partly dolomitic shell ps - fs (dm) / calcareous marl
nodular limestone, partly dolomitic
alternating beds limestone / shale
greenish brown shale with thin limestone intercalations
0
10
20
m

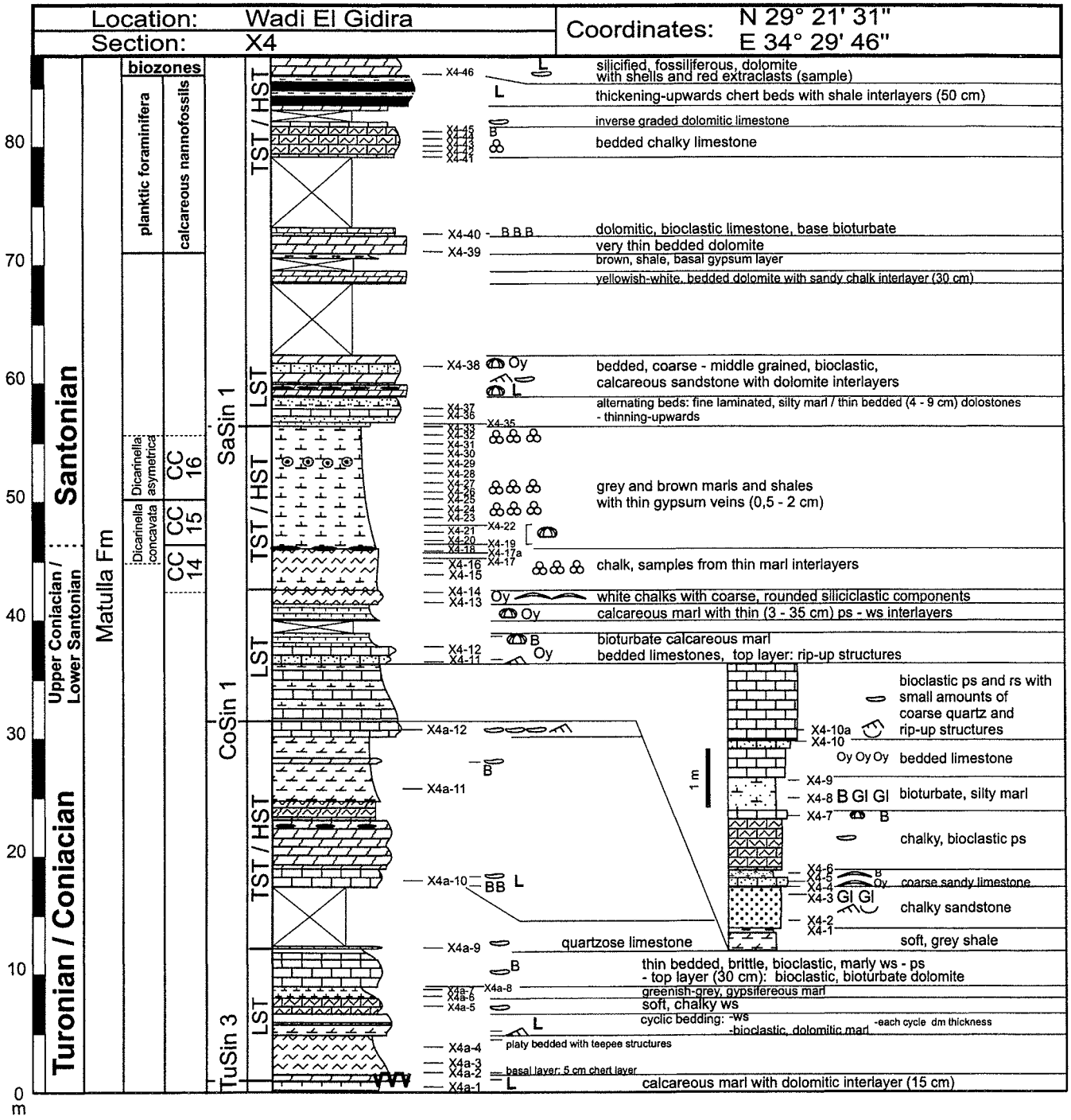
Location: Wadi El Gidira
Section: X4
Coordinates: N 29° 21' 31"
E 34° 29' 46"
biozones
planktic foraminifera
calcareous nannofossils
Santonian
Upper Coniacian / Lower Santonian
Turonian / Coniacian
Matulla Fm
Dicarinella asymetrica
Dicarinella concavata
CC 16
CC 15
CC 14
TST / HST
LST
SaSin 1
CoSin 1
TuSin 3
0 m
10
20
30
40
50
60
70
80
silicified, fossiliferous, dolomite with shells and red extraclasts (sample)
thickening-upwards chert beds with shale interlayers (50 cm)
inverse graded dolomitic limestone
bedded chalky limestone
dolomitic, bioclastic limestone, base bioturbate
very thin bedded dolomite
brown, shale, basal gypsum layer
yellowish-white, bedded dolomite with sandy chalk interlayer (30 cm)
bedded, coarse - middle grained, bioclastic, calcareous sandstone with dolomite interlayers
alternating beds: fine laminated, silty marl / thin bedded (4 - 9 cm) dolostones - thinning-upwards
grey and brown marls and shales with thin gypsum veins (0,5 - 2 cm)
chalk, samples from thin marl interlayers
white chalks with coarse, rounded siliciclastic components
calcareous marl with thin (3 - 35 cm) ps - ws interlayers
bioturbate calcareous marl
bedded limestones, top layer: rip-up structures
bioclastic ps and rs with small amounts of coarse quartz and rip-up structures
bedded limestone
bioturbate, silty marl
chalky, bioclastic ps
coarse sandy limestone
chalky sandstone
soft, grey shale
quartzose limestone
thin bedded, brittle, bioclastic, marly ws - ps
- top layer (30 cm): bioclastic, bioturbate dolomite
greenish-grey, gypsiferous marl
soft, chalky ws
cyclic bedding: -ws
-bioclastic, dolomitic marl
-each cycle dm thickness
platy bedded with teepee structures
basal layer: 5 cm chert layer
calcareous marl with dolomitic interlayer (15 cm)
1 m

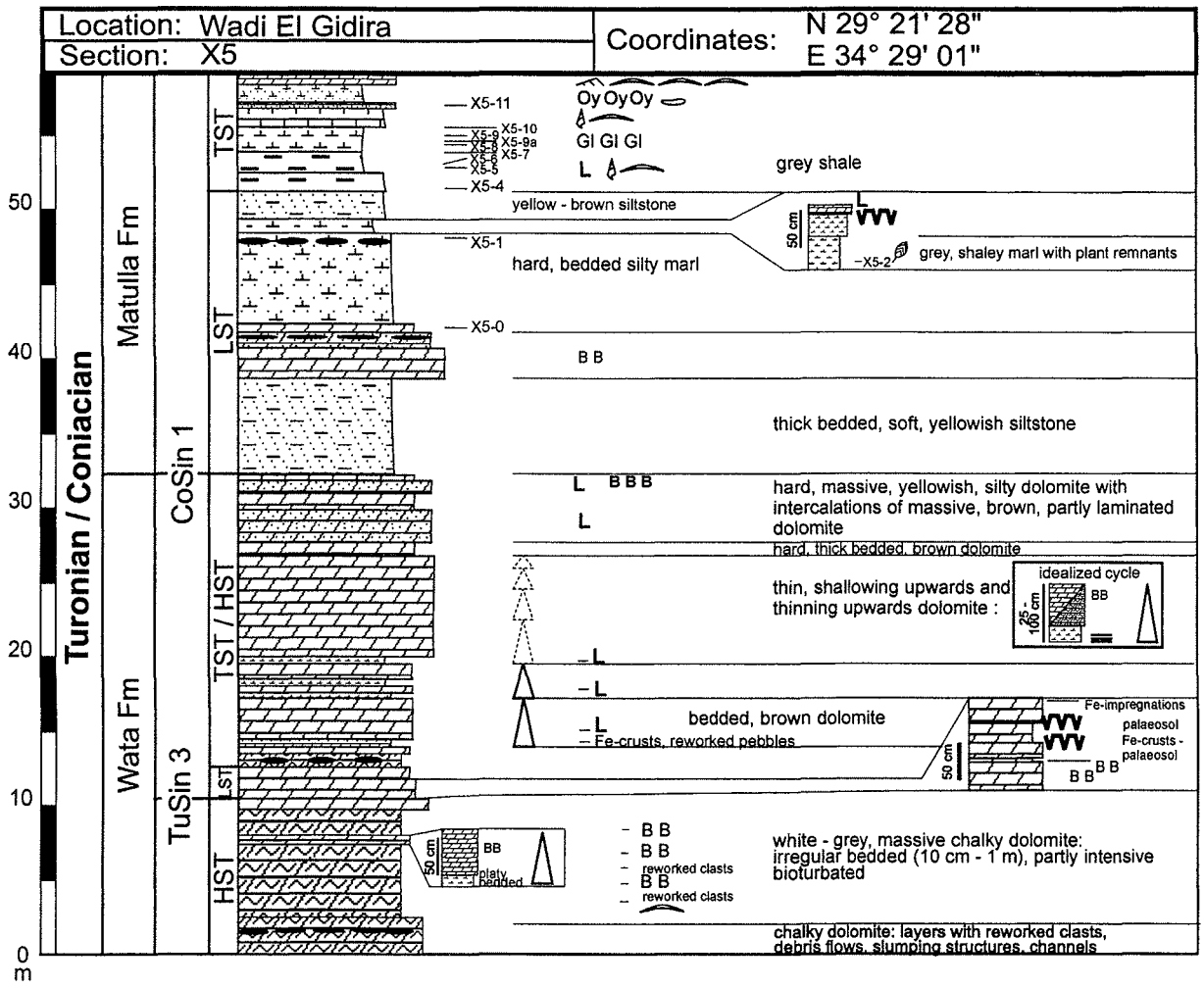
Location: Wadi El Gidira
Section: X5
Coordinates: N 29° 21' 28"
E 34° 29' 01"
Turonian / Coniacian
Matulla Fm
Wata Fm
CoSin 1
TuSin 3
TST
LST
TST / HST
LST
HST
X5-11
X5-10
X5-9a
X5-9
X5-8
X5-7
X5-6
X5-5
X5-4
X5-1
X5-0
Oy Oy Oy
Gl Gl Gl
grey shale
yellow - brown siltstone
hard, bedded silty marl
50 cm
X5-2
grey, shaley marl with plant remnants
B B
thick bedded, soft, yellowish siltstone
L B B B
hard, massive, yellowish, silty dolomite with intercalations of massive, brown, partly laminated dolomite
hard, thick bedded, brown dolomite
thin, shallowing upwards and thinning upwards dolomite :
idealized cycle
25 - 100 cm
BB
bedded, brown dolomite
Fe-crusts, reworked pebbles
Fe-impregnations
palaeosol
Fe-crusts -
palaeosol
50 cm
BB
platy bedded
reworked clasts
reworked clasts
white - grey, massive chalky dolomite: irregular bedded (10 cm - 1 m), partly intensive bioturbated
chalky dolomite: layers with reworked clasts, debris flows, slumping structures, channels
50
40
30
20
10
0
m

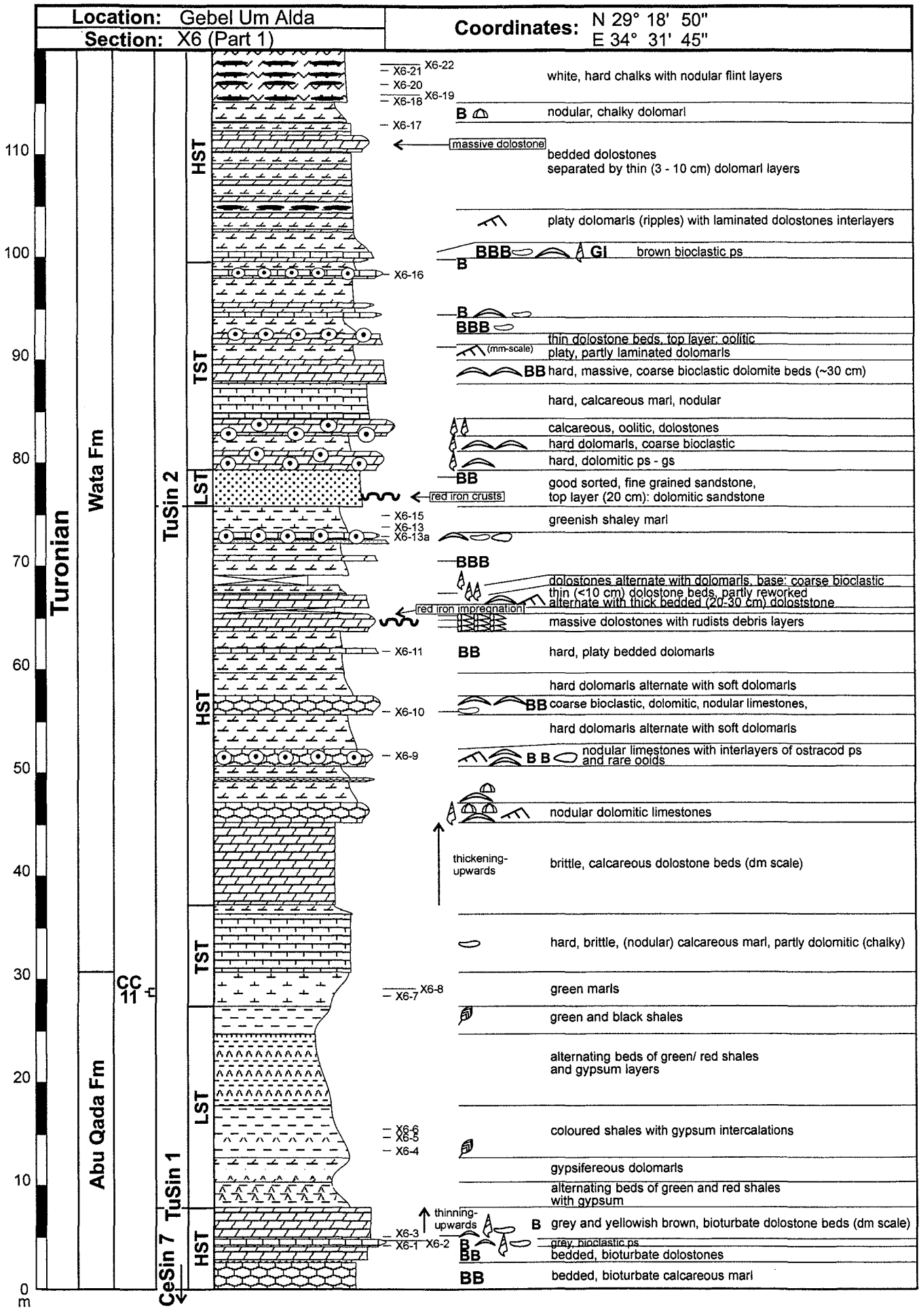
Location: Gebel Um Alda
Section: X6 (Part 1)
Coordinates: N 29° 18' 50"
E 34° 31' 45"
Turonian
Wata Fm
Abu Qada Fm
TuSin 2
TuSin 1
CeSin 7
HST
TST
LST
HST
TST
LST
HST
CC 11
X6-22
X6-21
X6-20
X6-19
X6-18
X6-17
X6-16
X6-15
X6-13
X6-13a
X6-11
X6-10
X6-9
X6-8
X6-7
X6-6
X6-5
X6-4
X6-3
X6-2
X6-1
white, hard chalks with nodular flint layers
nodular, chalky dolomarl
massive dolostone
bedded dolostones
separated by thin (3 - 10 cm) dolomarl layers
platy dolomarls (ripples) with laminated dolostones interlayers
brown bioclastic ps
thin dolostone beds, top layer: oolitic
platy, partly laminated dolomarls
(mm-scale)
hard, massive, coarse bioclastic dolomite beds (~30 cm)
hard, calcareous marl, nodular
calcareous, oolitic, dolostones
hard dolomarls, coarse bioclastic
hard, dolomitic ps - gs
good sorted, fine grained sandstone,
top layer (20 cm): dolomitic sandstone
red iron crusts
greenish shaley marl
dolostones alternate with dolomarls, base: coarse bioclastic
thin (<10 cm) dolostone beds, partly reworked
alternate with thick bedded (20-30 cm) dolostone
red iron impregnation
massive dolostones with rudists debris layers
hard, platy bedded dolomarls
hard dolomarls alternate with soft dolomarls
coarse bioclastic, dolomitic, nodular limestones,
hard dolomarls alternate with soft dolomarls
nodular limestones with interlayers of ostracod ps
and rare ooids
nodular dolomitic limestones
thickening-upwards
brittle, calcareous dolostone beds (dm scale)
hard, brittle, (nodular) calcareous marl, partly dolomitic (chalky)
green marls
green and black shales
alternating beds of green/ red shales
and gypsum layers
coloured shales with gypsum intercalations
gypsifereous dolomarls
alternating beds of green and red shales
with gypsum
thinning-upwards
grey and yellowish brown, bioturbate dolostone beds (dm scale)
grey, bioclastic ps
bedded, bioturbate dolostones
bedded, bioturbate calcareous marl
0
10
20
30
40
50
60
70
80
90
100
110
m

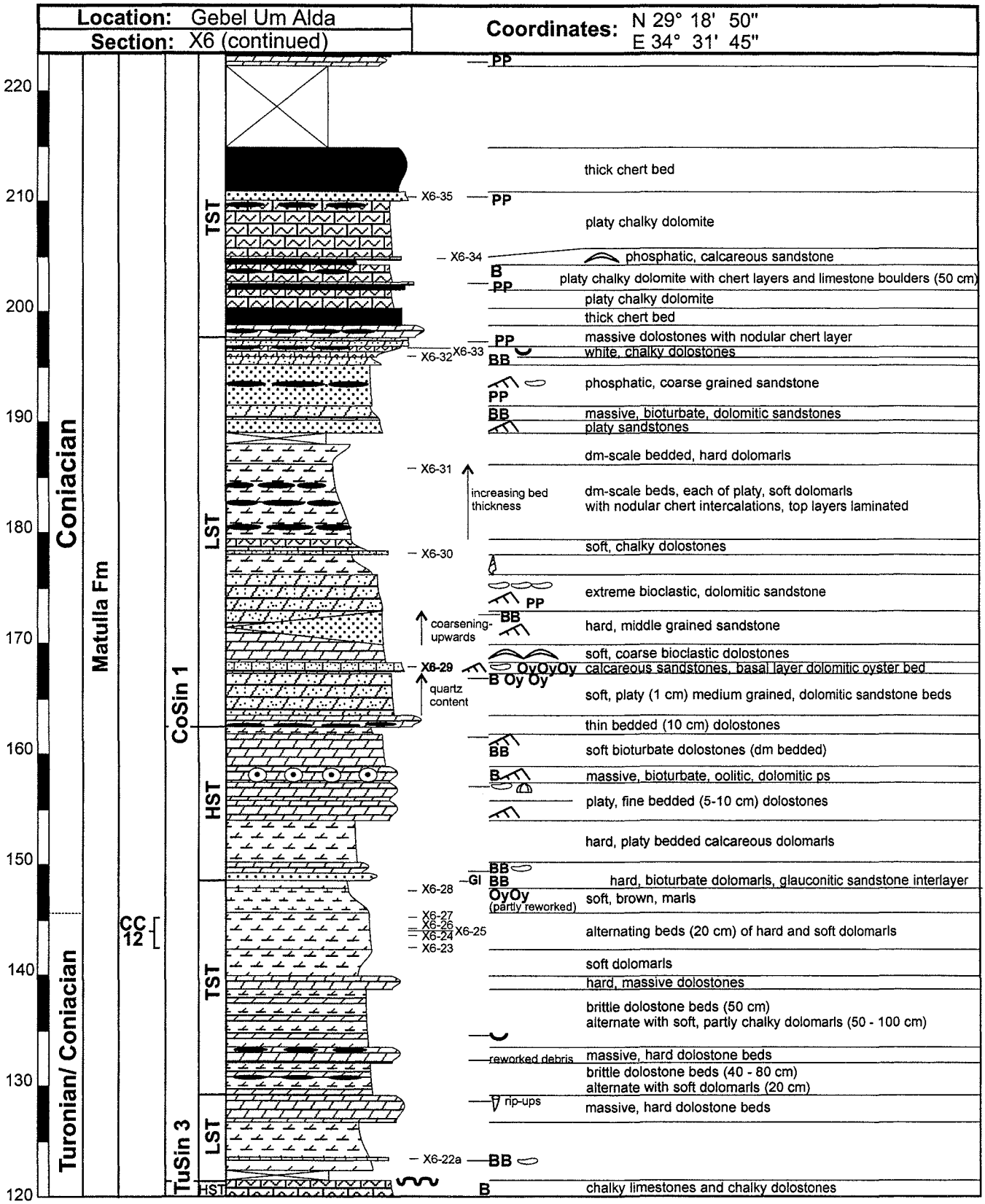
Location: Gebel Um Alda
Section: X6 (continued)
Coordinates: N 29° 18' 50"
E 34° 31' 45"
220
210
200
190
180
170
160
150
140
130
120
Coniacian
Turonian/ Coniacian
Matulla Fm
CC 12
CoSin 1
TuSin 3
TST
LST
HST
TST
LST
HST
TST
LST
HST
X6-35
X6-34
X6-33
X6-32
X6-31
X6-30
X6-29
X6-28
X6-27
X6-26
X6-25
X6-24
X6-23
X6-22a
PP
B
PP
PP
BB
PP
BB
increasing bed thickness
coarsening-upwards
PP
BB
OyOyOy
B Oy Oy
quartz content
BB
B
BB
GI
BB
OyOy
(partly reworked)
reworked debris
rip-ups
BB
B
thick chert bed
platy chalky dolomite
phosphatic, calcareous sandstone
platy chalky dolomite with chert layers and limestone boulders (50 cm)
platy chalky dolomite
thick chert bed
massive dolostones with nodular chert layer
white, chalky dolostones
phosphatic, coarse grained sandstone
massive, bioturbate, dolomitic sandstones
platy sandstones
dm-scale bedded, hard dolomarls
dm-scale beds, each of platy, soft dolomarls with nodular chert intercalations, top layers laminated
soft, chalky dolostones
extreme bioclastic, dolomitic sandstone
hard, middle grained sandstone
soft, coarse bioclastic dolostones
calcareous sandstones, basal layer dolomitic oyster bed
soft, platy (1 cm) medium grained, dolomitic sandstone beds
thin bedded (10 cm) dolostones
soft bioturbate dolostones (dm bedded)
massive, bioturbate, oolitic, dolomitic ps
platy, fine bedded (5-10 cm) dolostones
hard, platy bedded calcareous dolomarls
hard, bioturbate dolomarls, glauconitic sandstone interlayer
soft, brown, marls
alternating beds (20 cm) of hard and soft dolomarls
soft dolomarls
hard, massive dolostones
brittle dolostone beds (50 cm)
alternate with soft, partly chalky dolomarls (50 - 100 cm)
massive, hard dolostone beds
brittle dolostone beds (40 - 80 cm)
alternate with soft dolomarls (20 cm)
massive, hard dolostone beds
chalky limestones and chalky dolostones

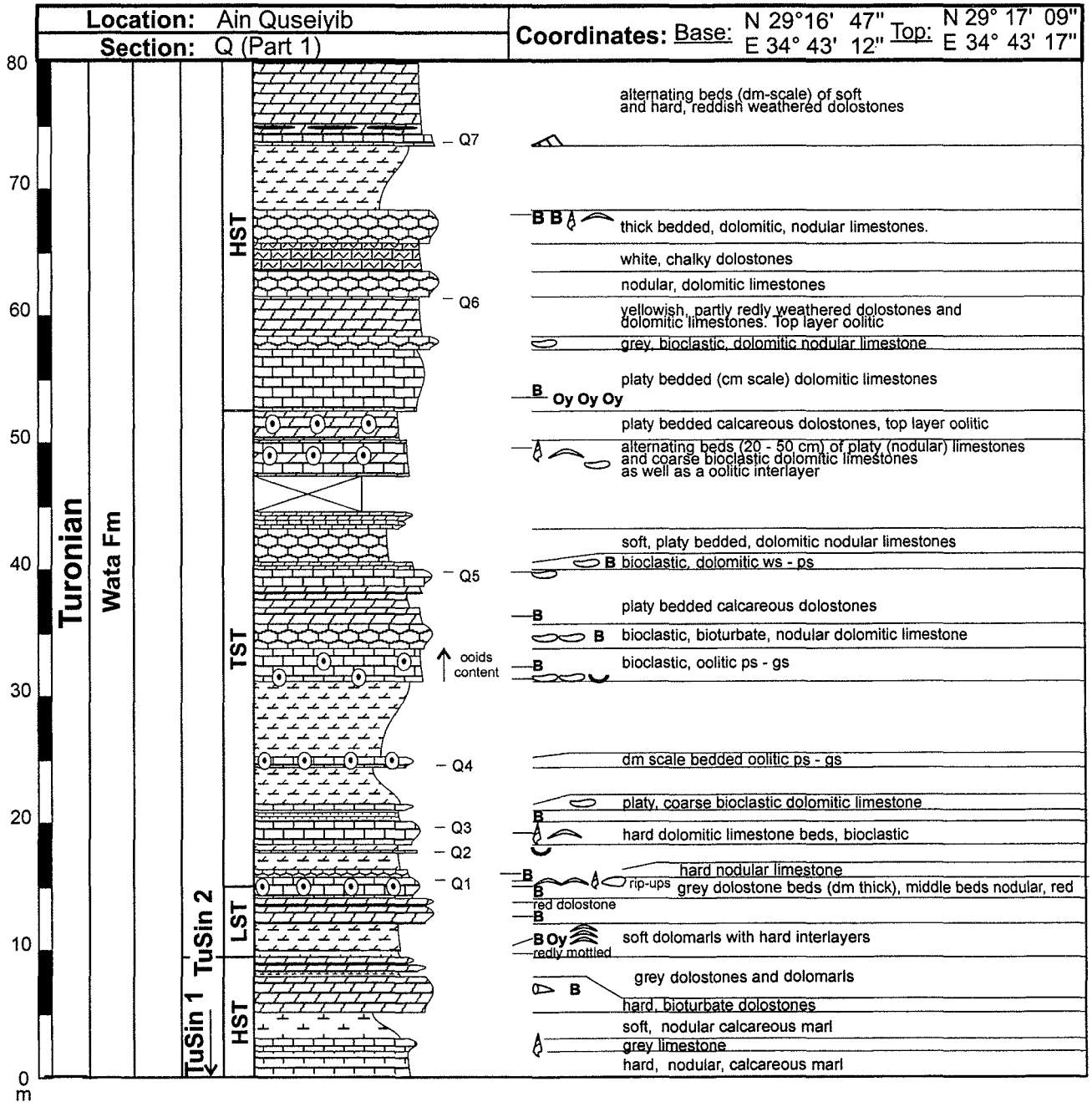
Location: Ain Quseiyib
Section: Q (Part 1)
Coordinates: Base: N 29°16' 47" E 34° 43' 12" Top: N 29° 17' 09" E 34° 43' 17"
Turonian
Wata Fm
TuSin 1
TuSin 2
HST
TST
LST
HST
Q7
Q6
Q5
Q4
Q3
Q2
Q1
ooids content
alternating beds (dm-scale) of soft and hard, reddish weathered dolostones
thick bedded, dolomitic, nodular limestones.
white, chalky dolostones
nodular, dolomitic limestones
yellowish, partly redly weathered dolostones and dolomitic limestones. Top layer oolitic
grey, bioclastic, dolomitic nodular limestone
platy bedded (cm scale) dolomitic limestones
Oy Oy Oy
platy bedded calcareous dolostones, top layer oolitic
alternating beds (20 - 50 cm) of platy (nodular) limestones and coarse bioclastic dolomitic limestones as well as a oolitic interlayer
soft, platy bedded, dolomitic nodular limestones
bioclastic, dolomitic ws - ps
platy bedded calcareous dolostones
bioclastic, bioturbate, nodular dolomitic limestone
bioclastic, oolitic ps - gs
dm scale bedded oolitic ps - gs
platy, coarse bioclastic dolomitic limestone
hard dolomitic limestone beds, bioclastic
hard nodular limestone
rip-ups
grey dolostone beds (dm thick), middle beds nodular, red
red dolostone
soft dolomarls with hard interlayers
redly mottled
grey dolostones and dolomarls
hard, bioturbate dolostones
soft, nodular calcareous marl
grey limestone
hard, nodular, calcareous marl
80
70
60
50
40
30
20
10
0
m

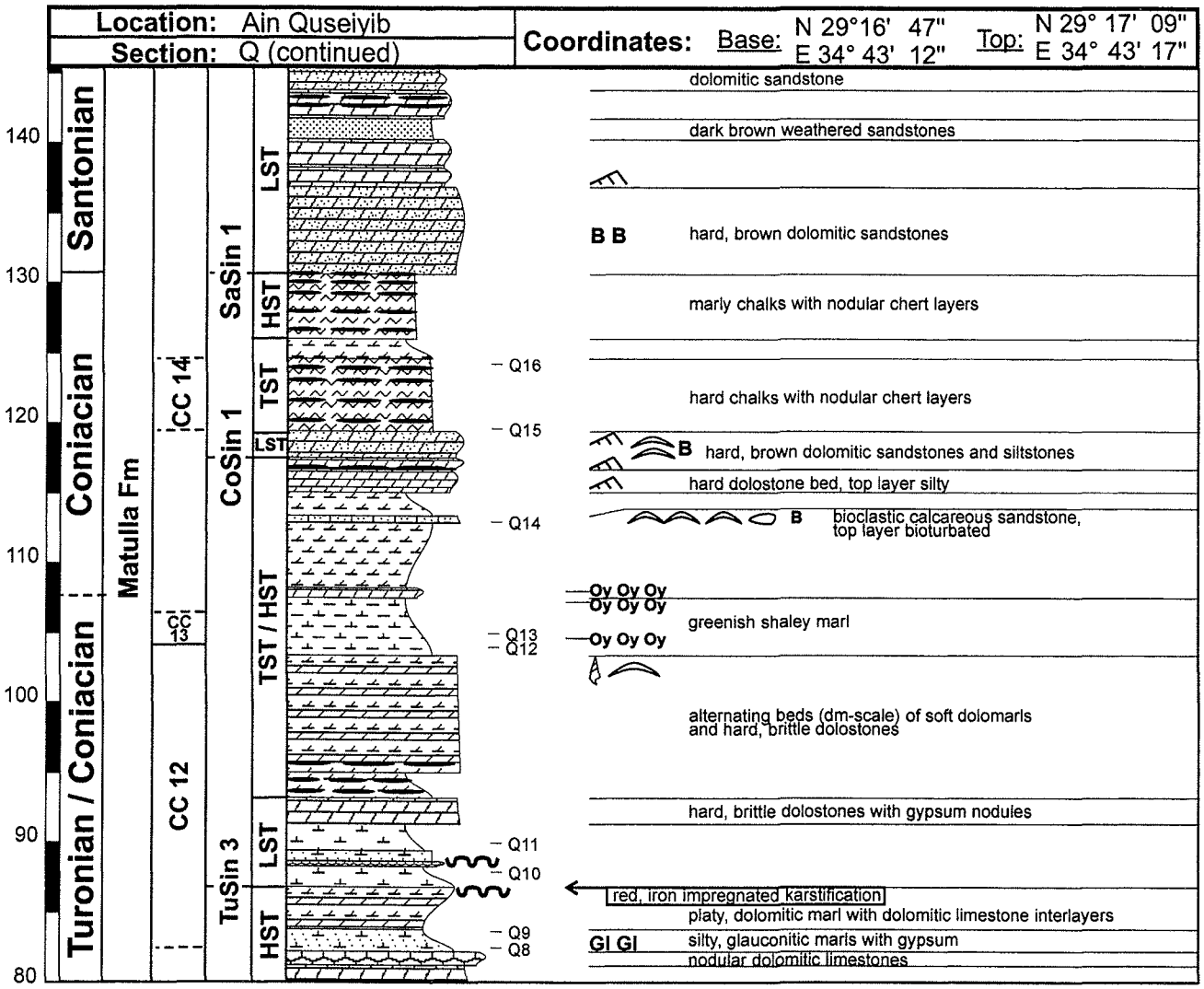
Location: Ain Quseiyib
Section: Q (continued)
Coordinates: Base: N 29°16' 47" E 34° 43' 12" Top: N 29° 17' 09" E 34° 43' 17"
Santonian
Coniacian
Turonian / Coniacian
Matulla Fm
CC 14
CC 13
CC 12
SaSin 1
CoSin 1
TuSin 3
LST
HST
TST
LST
TST / HST
LST
HST
Q16
Q15
Q14
Q13
Q12
Q11
Q10
Q9
Q8
140
130
120
110
100
90
80
dolomitic sandstone
dark brown weathered sandstones
B B
hard, brown dolomitic sandstones
marly chalks with nodular chert layers
hard chalks with nodular chert layers
B
hard, brown dolomitic sandstones and siltstones
hard dolostone bed, top layer silty
B
bioclastic calcareous sandstone, top layer bioturbated
Oy Oy Oy
Oy Oy Oy
greenish shaley marl
Oy Oy Oy
alternating beds (dm-scale) of soft dolomarls and hard, brittle dolostones
hard, brittle dolostones with gypsum nodules
red, iron impregnated karstification
platy, dolomitic marl with dolomitic limestone interlayers
Gl Gl
silty, glauconitic marls with gypsum
nodular dolomitic limestones

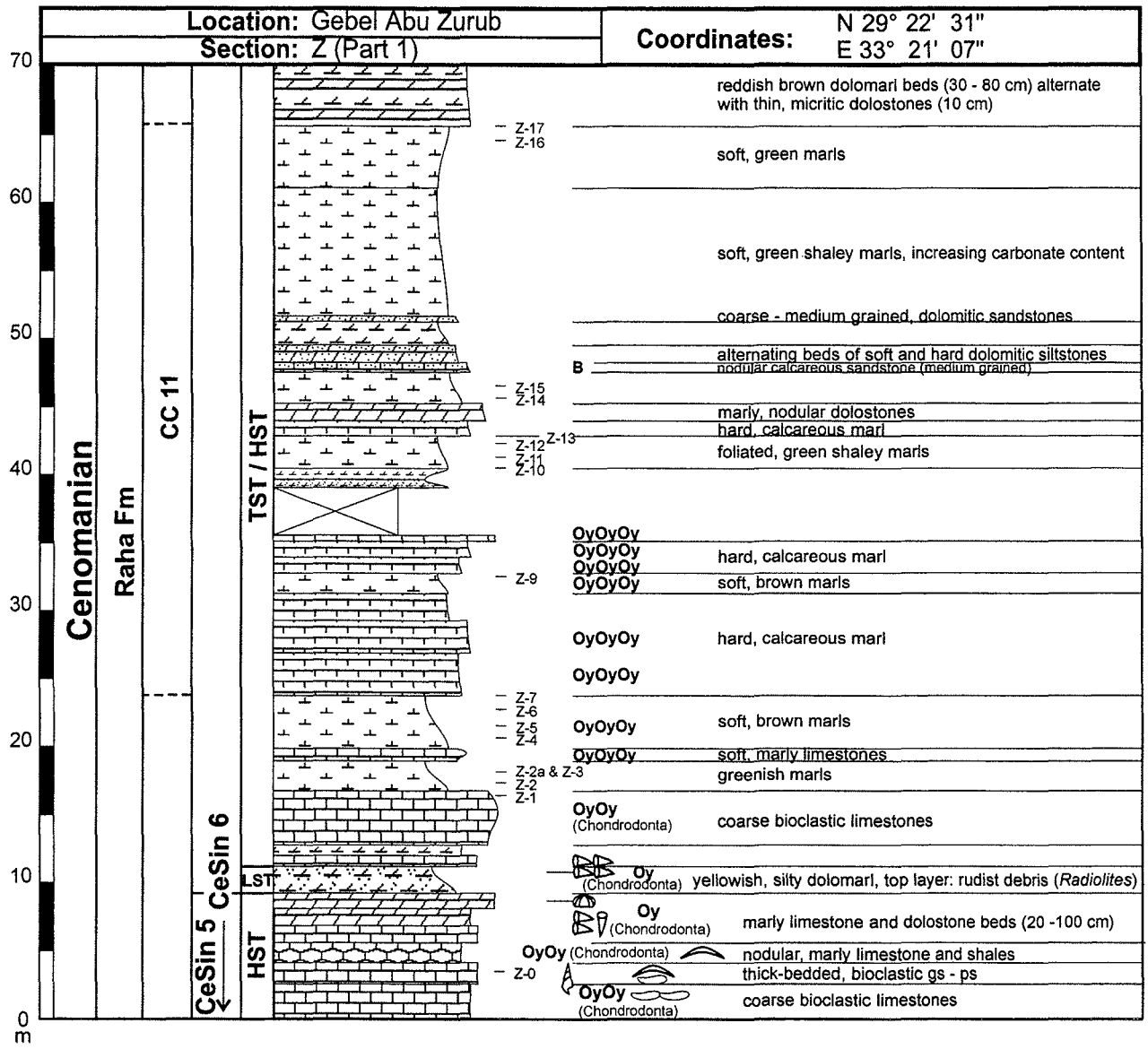
Location: Gebel Abu Zurub
Section: Z (Part 1)
Coordinates: N 29° 22' 31"
E 33° 21' 07"
Cenomanian
Raha Fm
CC 11
CeSin 5
CeSin 6
TST / HST
LST
HST
70
60
50
40
30
20
10
0
m
Z-17
Z-16
Z-15
Z-14
Z-13
Z-12
Z-11
Z-10
Z-9
Z-7
Z-6
Z-5
Z-4
Z-2a & Z-3
Z-2
Z-1
Z-0
B
reddish brown dolomarl beds (30 - 80 cm) alternate with thin, micritic dolostones (10 cm)
soft, green marls
soft, green shaley marls, increasing carbonate content
coarse - medium grained, dolomitic sandstones
alternating beds of soft and hard dolomitic siltstones
nodular calcareous sandstone (medium grained)
marly, nodular dolostones
hard, calcareous marl
foliated, green shaley marls
OyOyOy
hard, calcareous marl
soft, brown marls
hard, calcareous marl
soft, brown marls
soft, marly limestones
greenish marls
OyOy (Chondrodonta)
coarse bioclastic limestones
Oy (Chondrodonta)
yellowish, silty dolomarl, top layer: rudist debris (Radiolites)
Oy (Chondrodonta)
marly limestone and dolostone beds (20 -100 cm)
OyOy (Chondrodonta)
nodular, marly limestone and shales
thick-bedded, bioclastic gs - ps
OyOy (Chondrodonta)
coarse bioclastic limestones

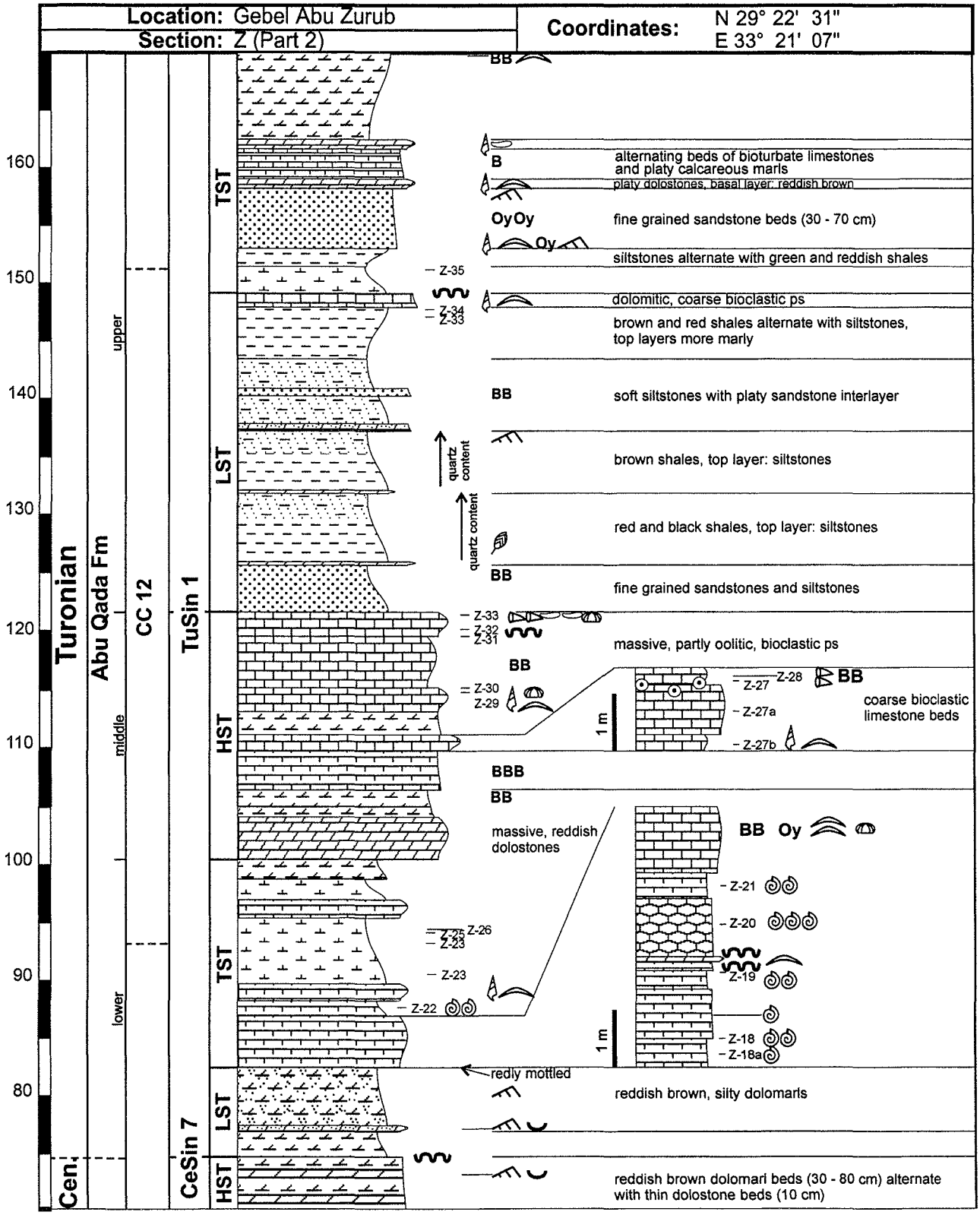
Location: Gebel Abu Zurub
Section: Z (Part 2)
Coordinates: N 29° 22' 31"
E 33° 21' 07"
Turonian
Cen.
Abu Qada Fm
upper
middle
lower
CC 12
TuSin 1
CeSin 7
TST
LST
HST
160
150
140
130
120
110
100
90
80
BB
B
alternating beds of bioturbate limestones and platy calcareous marls
platy dolostones, basal layer: reddish brown
OyOy
Oy
fine grained sandstone beds (30 - 70 cm)
siltstones alternate with green and reddish shales
Z-35
dolomitic, coarse bioclastic ps
Z-34
Z-33
brown and red shales alternate with siltstones, top layers more marly
soft siltstones with platy sandstone interlayer
quartz content
brown shales, top layer: siltstones
red and black shales, top layer: siltstones
fine grained sandstones and siltstones
Z-32
Z-31
massive, partly oolitic, bioclastic ps
Z-30
Z-29
Z-28
Z-27
Z-27a
Z-27b
1 m
coarse bioclastic limestone beds
BBB
massive, reddish dolostones
Z-26
Z-25
Z-24
Z-23
Z-22
Oy
Z-21
Z-20
Z-19
Z-18
Z-18a
redly mottled
reddish brown, silty dolomarls
reddish brown dolomarl beds (30 - 80 cm) alternate with thin dolostone beds (10 cm)

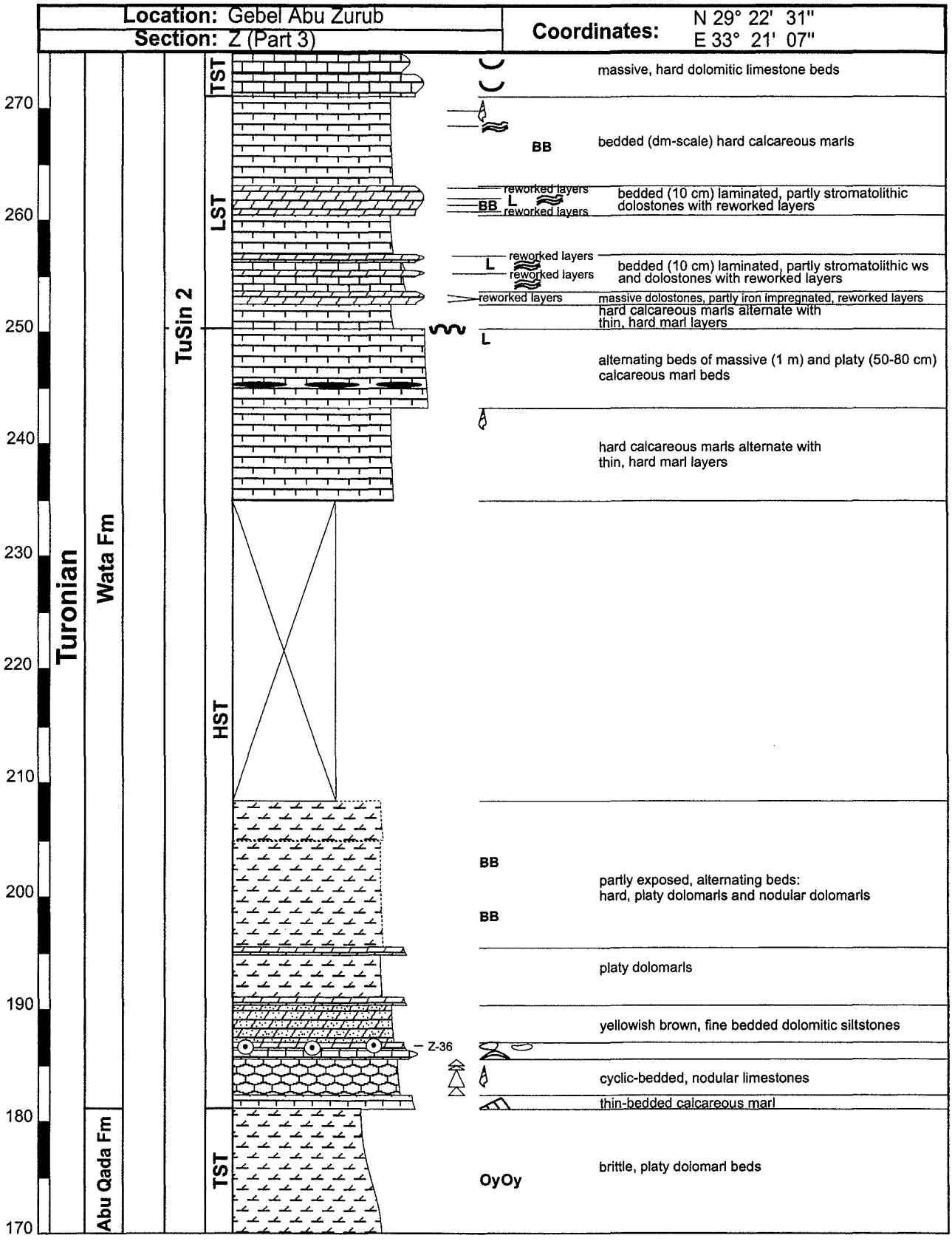
Location: Gebel Abu Zurub
Section: Z (Part 3)
Coordinates: N 29° 22' 31"
E 33° 21' 07"
Turonian
Wata Fm
Abu Qada Fm
TuSin 2
TST
LST
HST
TST
270
260
250
240
230
220
210
200
190
180
170
massive, hard dolomitic limestone beds
BB
bedded (dm-scale) hard calcareous marls
reworked layers
BB
L
reworked layers
bedded (10 cm) laminated, partly stromatolithic dolostones with reworked layers
L
reworked layers
reworked layers
bedded (10 cm) laminated, partly stromatolithic ws and dolostones with reworked layers
reworked layers
massive dolostones, partly iron impregnated, reworked layers
hard calcareous marls alternate with thin, hard marl layers
L
alternating beds of massive (1 m) and platy (50-80 cm) calcareous marl beds
hard calcareous marls alternate with thin, hard marl layers
BB
BB
partly exposed, alternating beds: hard, platy dolomarls and nodular dolomarls
platy dolomarls
yellowish brown, fine bedded dolomitic siltstones
Z-36
cyclic-bedded, nodular limestones
thin-bedded calcareous marl
OyOy
brittle, platy dolomarl beds

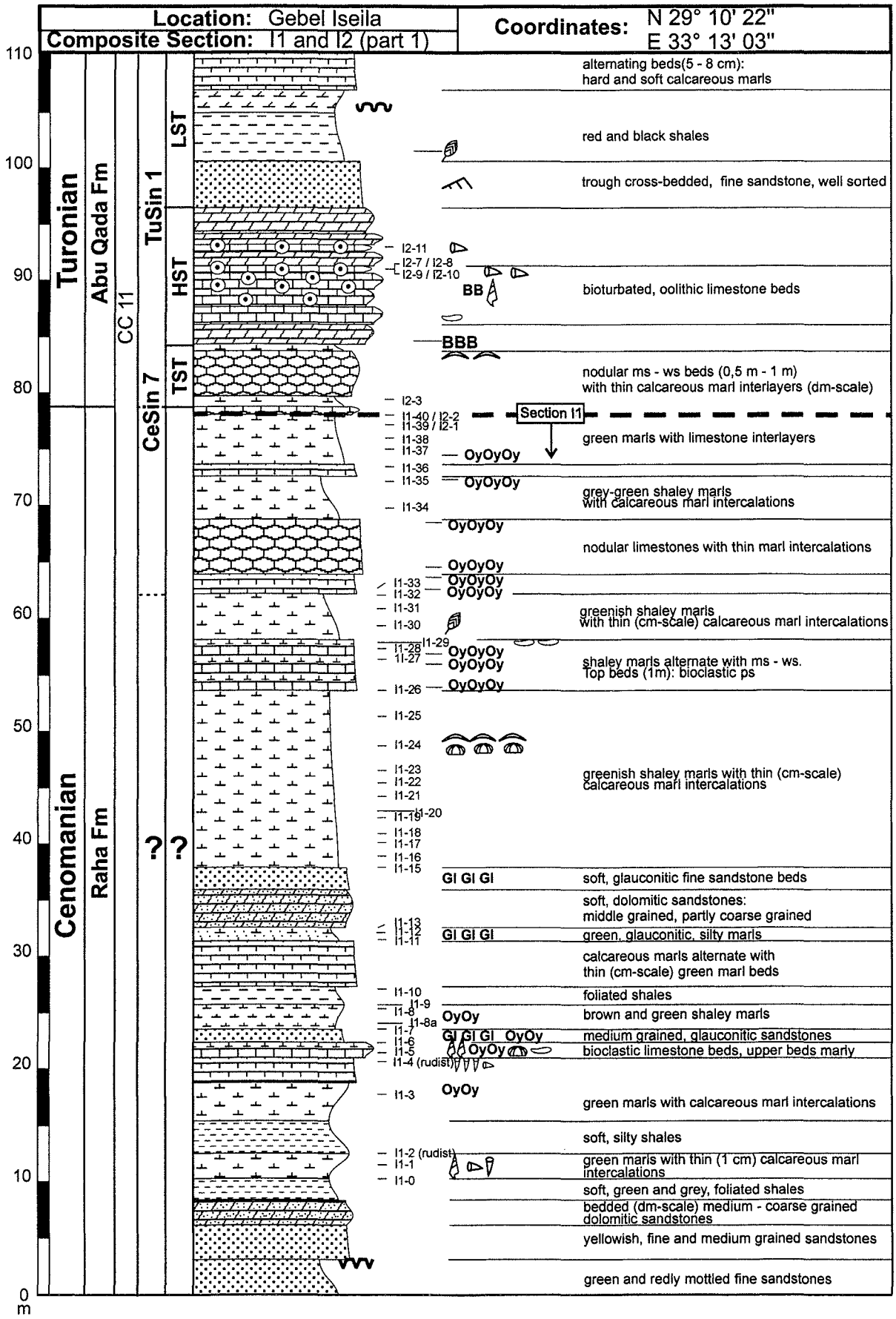
Location: Gebel Iseila
Composite Section: I1 and I2 (part 1)
Coordinates: N 29° 10' 22"
E 33° 13' 03"
Turonian
Cenomanian
Abu Qada Fm
Raha Fm
CC 11
TuSin 1
CeSin 7
LST
HST
TST
110
100
90
80
70
60
50
40
30
20
10
0
m
I2-11
I2-7 / I2-8
I2-9 / I2-10
BB
BBB
I2-3
I1-40 / I2-2
I1-39 / I2-1
Section I1
I1-38
I1-37
I1-36
I1-35
I1-34
I1-33
I1-32
I1-31
I1-30
I1-29
I1-28
I1-27
I1-26
I1-25
I1-24
I1-23
I1-22
I1-21
I1-20
I1-19
I1-18
I1-17
I1-16
I1-15
I1-13
I1-12
I1-11
I1-10
I1-9
I1-8
I1-8a
I1-7
I1-6
I1-5
I1-4 (rudist)
I1-3
I1-2 (rudist)
I1-1
I1-0
OyOyOy
Gl Gl Gl
OyOy
alternating beds(5 - 8 cm):
hard and soft calcareous marls
red and black shales
trough cross-bedded, fine sandstone, well sorted
bioturbated, oolithic limestone beds
nodular ms - ws beds (0,5 m - 1 m)
with thin calcareous marl interlayers (dm-scale)
green marls with limestone interlayers
grey-green shaley marls
with calcareous marl intercalations
nodular limestones with thin marl intercalations
greenish shaley marls
with thin (cm-scale) calcareous marl intercalations
shaley marls alternate with ms - ws.
Top beds (1m): bioclastic ps
greenish shaley marls with thin (cm-scale)
calcareous marl intercalations
soft, glauconitic fine sandstone beds
soft, dolomitic sandstones:
middle grained, partly coarse grained
green, glauconitic, silty marls
calcareous marls alternate with
thin (cm-scale) green marl beds
foliated shales
brown and green shaley marls
medium grained, glauconitic sandstones
bioclastic limestone beds, upper beds marly
green marls with calcareous marl intercalations
soft, silty shales
green marls with thin (1 cm) calcareous marl
intercalations
soft, green and grey, foliated shales
bedded (dm-scale) medium - coarse grained
dolomitic sandstones
yellowish, fine and medium grained sandstones
green and redly mottled fine sandstones

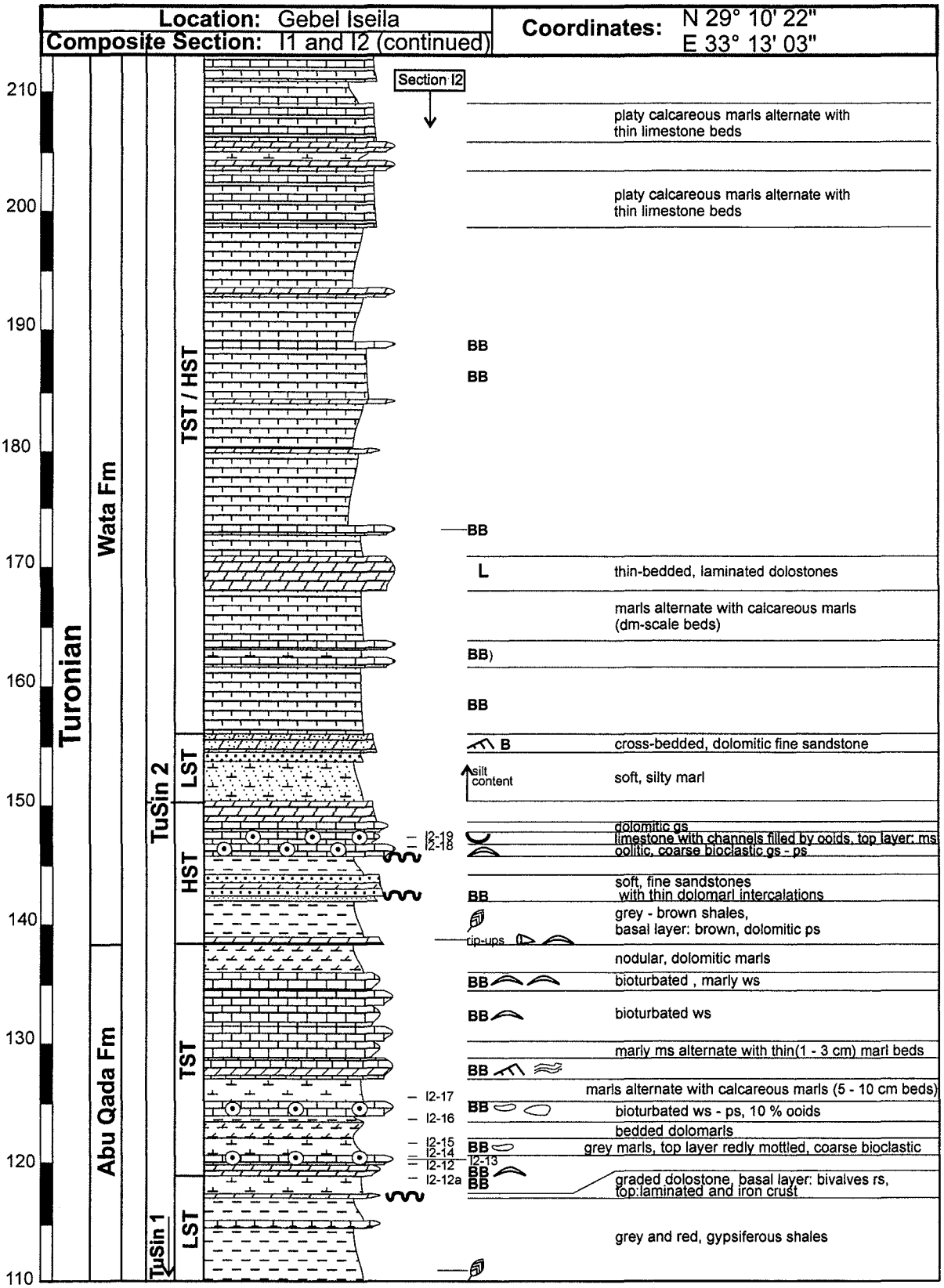
Location: Gebel Iseila
Composite Section: I1 and I2 (continued)
Coordinates: N 29° 10' 22" E 33° 13' 03"
Section I2
platy calcareous marls alternate with thin limestone beds
platy calcareous marls alternate with thin limestone beds
BB
BB
BB
L
thin-bedded, laminated dolostones
marls alternate with calcareous marls (dm-scale beds)
BB)
BB
B
cross-bedded, dolomitic fine sandstone
silt content
soft, silty marl
dolomitic gs
limestone with channels filled by ooids, top layer: ms
oolitic, coarse bioclastic gs - ps
soft, fine sandstones with thin dolomarl intercalations
BB
grey - brown shales, basal layer: brown, dolomitic ps
tip-ups
nodular, dolomitic marls
BB
bioturbated , marly ws
BB
bioturbated ws
marly ms alternate with thin(1 - 3 cm) marl beds
BB
marls alternate with calcareous marls (5 - 10 cm beds)
BB
bioturbated ws - ps, 10 % ooids
bedded dolomarls
BB
grey marls, top layer redly mottled, coarse bioclastic
BB
BB
graded dolostone, basal layer: bivalves rs, top:laminated and iron crust
grey and red, gypsiferous shales
I2-19
I2-18
I2-17
I2-16
I2-15
I2-14
I2-13
I2-12
I2-12a
210
200
190
180
170
160
150
140
130
120
110
Turonian
Wata Fm
Abu Qada Fm
TuSin 2
TuSin 1
TST / HST
LST
HST
TST
LST

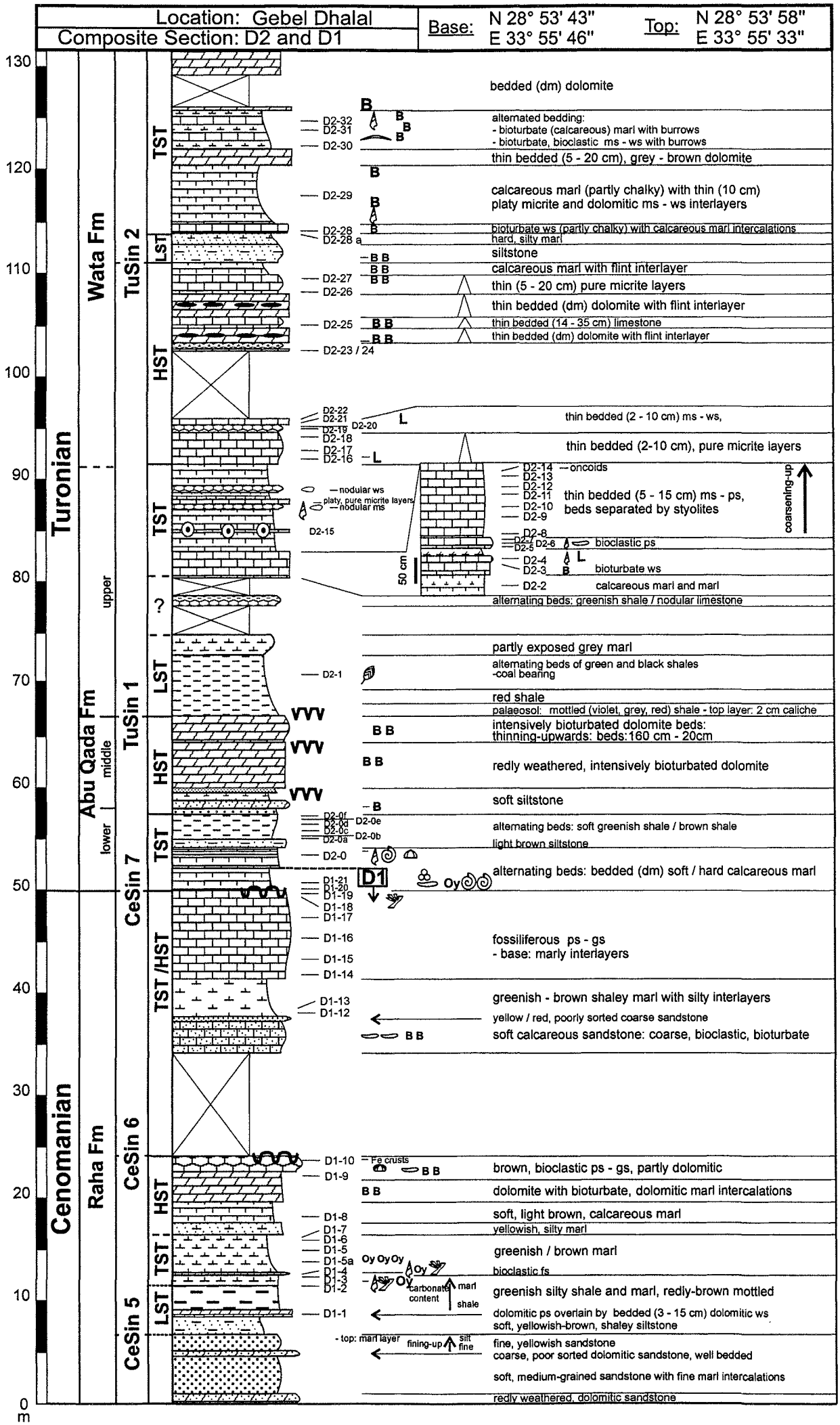
Location: Gebel Dhalal
Composite Section: D2 and D1
Base: N 28° 53' 43" E 33° 55' 46"
Top: N 28° 53' 58" E 33° 55' 33"
Turonian
Cenomanian
Wata Fm
Abu Qada Fm
upper
middle
lower
Raha Fm
TuSin 2
TuSin 1
CeSin 7
CeSin 6
CeSin 5
TST
LST
HST
TST /HST
?
D2-32
D2-31
D2-30
D2-29
D2-28
D2-28 a
D2-27
D2-26
D2-25
D2-23 / 24
D2-22
D2-21
D2-20
D2-19
D2-18
D2-17
D2-16
D2-15
D2-14
D2-13
D2-12
D2-11
D2-10
D2-9
D2-8
D2-7
D2-6
D2-5
D2-4
D2-3
D2-2
D2-1
D2-0f
D2-0d
D2-0c
D2-0a
D2-0e
D2-0b
D2-0
D1-21
D1-20
D1-19
D1-18
D1-17
D1-16
D1-15
D1-14
D1-13
D1-12
D1-10
D1-9
D1-8
D1-7
D1-6
D1-5
D1-5a
D1-4
D1-3
D1-2
D1-1
D1
50 cm
bedded (dm) dolomite
alternated bedding:
- bioturbate (calcareous) marl with burrows
- bioturbate, bioclastic ms - ws with burrows
thin bedded (5 - 20 cm), grey - brown dolomite
calcareous marl (partly chalky) with thin (10 cm) platy micrite and dolomitic ms - ws interlayers
bioturbate ws (partly chalky) with calcareous marl intercalations
hard, silty marl
siltstone
calcareous marl with flint interlayer
thin (5 - 20 cm) pure micrite layers
thin bedded (dm) dolomite with flint interlayer
thin bedded (14 - 35 cm) limestone
thin bedded (dm) dolomite with flint interlayer
thin bedded (2 - 10 cm) ms - ws,
thin bedded (2-10 cm), pure micrite layers
nodular ws
platy, pure micrite layers
nodular ms
oncoids
thin bedded (5 - 15 cm) ms - ps, beds separated by styolites
coarsening-up
bioclastic ps
bioturbate ws
calcareous marl and marl
alternating beds: greenish shale / nodular limestone
partly exposed grey marl
alternating beds of green and black shales -coal bearing
red shale
palaeosol: mottled (violet, grey, red) shale - top layer: 2 cm caliche
intensively bioturbated dolomite beds: thinning-upwards: beds:160 cm - 20cm
redly weathered, intensively bioturbated dolomite
soft siltstone
alternating beds: soft greenish shale / brown shale
light brown siltstone
alternating beds: bedded (dm) soft / hard calcareous marl
fossiliferous ps - gs
- base: marly interlayers
greenish - brown shaley marl with silty interlayers
yellow / red, poorly sorted coarse sandstone
soft calcareous sandstone: coarse, bioclastic, bioturbate
Fe crusts
brown, bioclastic ps - gs, partly dolomitic
dolomite with bioturbate, dolomitic marl intercalations
soft, light brown, calcareous marl
yellowish, silty marl
greenish / brown marl
bioclastic fs
greenish silty shale and marl, redly-brown mottled
carbonate content
marl
shale
dolomitic ps overlain by bedded (3 - 15 cm) dolomitic ws
soft, yellowish-brown, shaley siltstone
- top: marl layer
fining-up
silt
fine
fine, yellowish sandstone
coarse, poor sorted dolomitic sandstone, well bedded
soft, medium-grained sandstone with fine marl intercalations
redly weathered, dolomitic sandstone
0
10
20
30
40
50
60
70
80
90
100
110
120
130
m

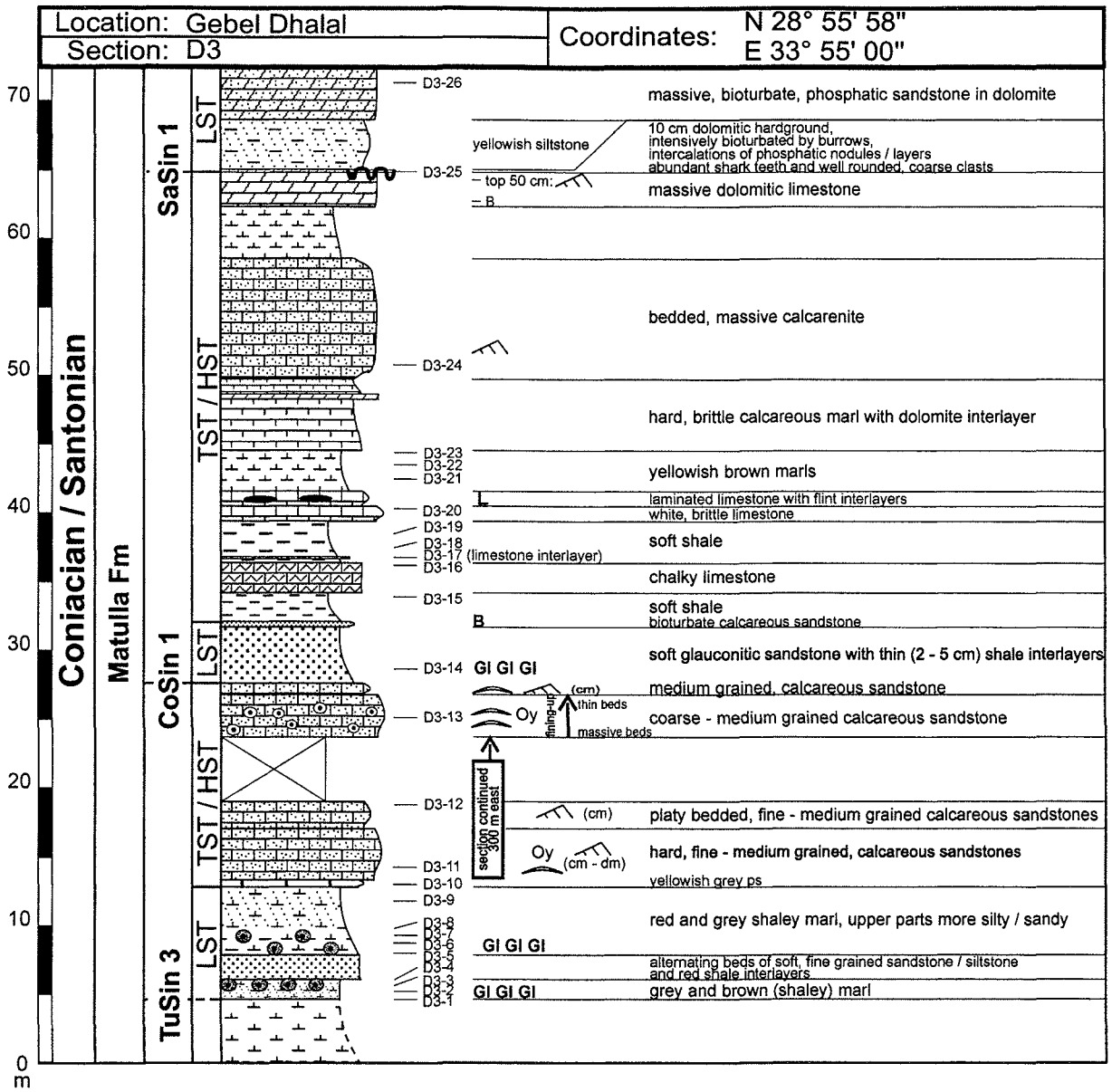
Location: Gebel Dhalal
Section: D3
Coordinates: N 28° 55' 58" E 33° 55' 00"
Coniacian / Santonian
Matulla Fm
SaSin 1
CoSin 1
TuSin 3
LST
TST / HST
LST
TST / HST
LST
70
60
50
40
30
20
10
0 m
D3-26
D3-25
D3-24
D3-23
D3-22
D3-21
D3-20
D3-19
D3-18
D3-17
D3-16
D3-15
D3-14
D3-13
D3-12
D3-11
D3-10
D3-9
D3-8
D3-7
D3-6
D3-5
D3-4
D3-3
D3-2
D3-1
massive, bioturbate, phosphatic sandstone in dolomite
yellowish siltstone
10 cm dolomitic hardground, intensively bioturbated by burrows, intercalations of phosphatic nodules / layers abundant shark teeth and well rounded, coarse clasts
top 50 cm:
massive dolomitic limestone
B
bedded, massive calcarenite
hard, brittle calcareous marl with dolomite interlayer
yellowish brown marls
laminated limestone with flint interlayers
white, brittle limestone
soft shale
(limestone interlayer)
chalky limestone
soft shale
B
bioturbate calcareous sandstone
Gl Gl Gl
soft glauconitic sandstone with thin (2 - 5 cm) shale interlayers
(cm)
medium grained, calcareous sandstone
fining-up
thin beds
Oy
coarse - medium grained calcareous sandstone
massive beds
section continued 300 m east
(cm)
platy bedded, fine - medium grained calcareous sandstones
Oy
(cm - dm)
hard, fine - medium grained, calcareous sandstones
yellowish grey ps
red and grey shaley marl, upper parts more silty / sandy
Gl Gl Gl
alternating beds of soft, fine grained sandstone / siltstone and red shale interlayers
Gl Gl Gl
grey and brown (shaley) marl

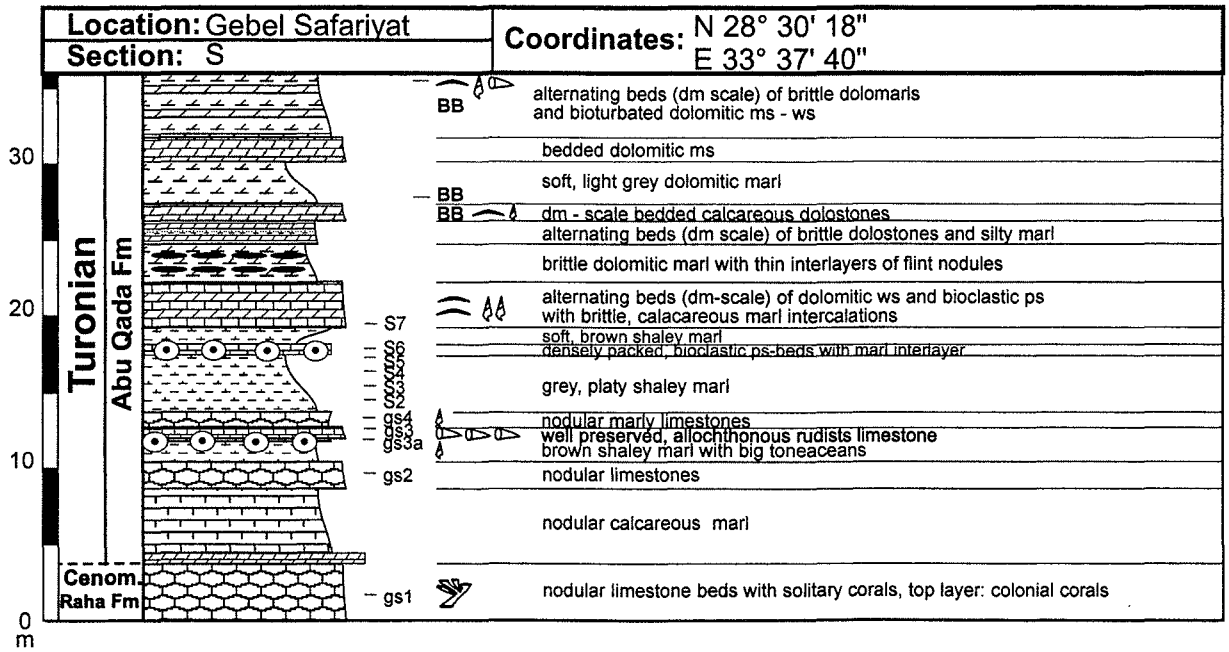
Location: Gebel Safariyat
Section: S
Coordinates: N 28° 30' 18" E 33° 37' 40"
Turonian
Abu Qada Fm
Cenom.
Raha Fm
30
20
10
0 m
BB
alternating beds (dm scale) of brittle dolomarls and bioturbated dolomitic ms - ws
bedded dolomitic ms
soft, light grey dolomitic marl
BB
BB
dm - scale bedded calcareous dolostones
alternating beds (dm scale) of brittle dolostones and silty marl
brittle dolomitic marl with thin interlayers of flint nodules
alternating beds (dm-scale) of dolomitic ws and bioclastic ps with brittle, calacareous marl intercalations
S7
soft, brown shaley marl
densely packed, bioclastic ps-beds with marl interlayer
S6
S5
S4
S3
S2
grey, platy shaley marl
gs4
nodular marly limestones
gs3
gs3a
well preserved, allochthonous rudists limestone
brown shaley marl with big toneaceans
gs2
nodular limestones
nodular calcareous marl
gs1
nodular limestone beds with solitary corals, top layer: colonial corals

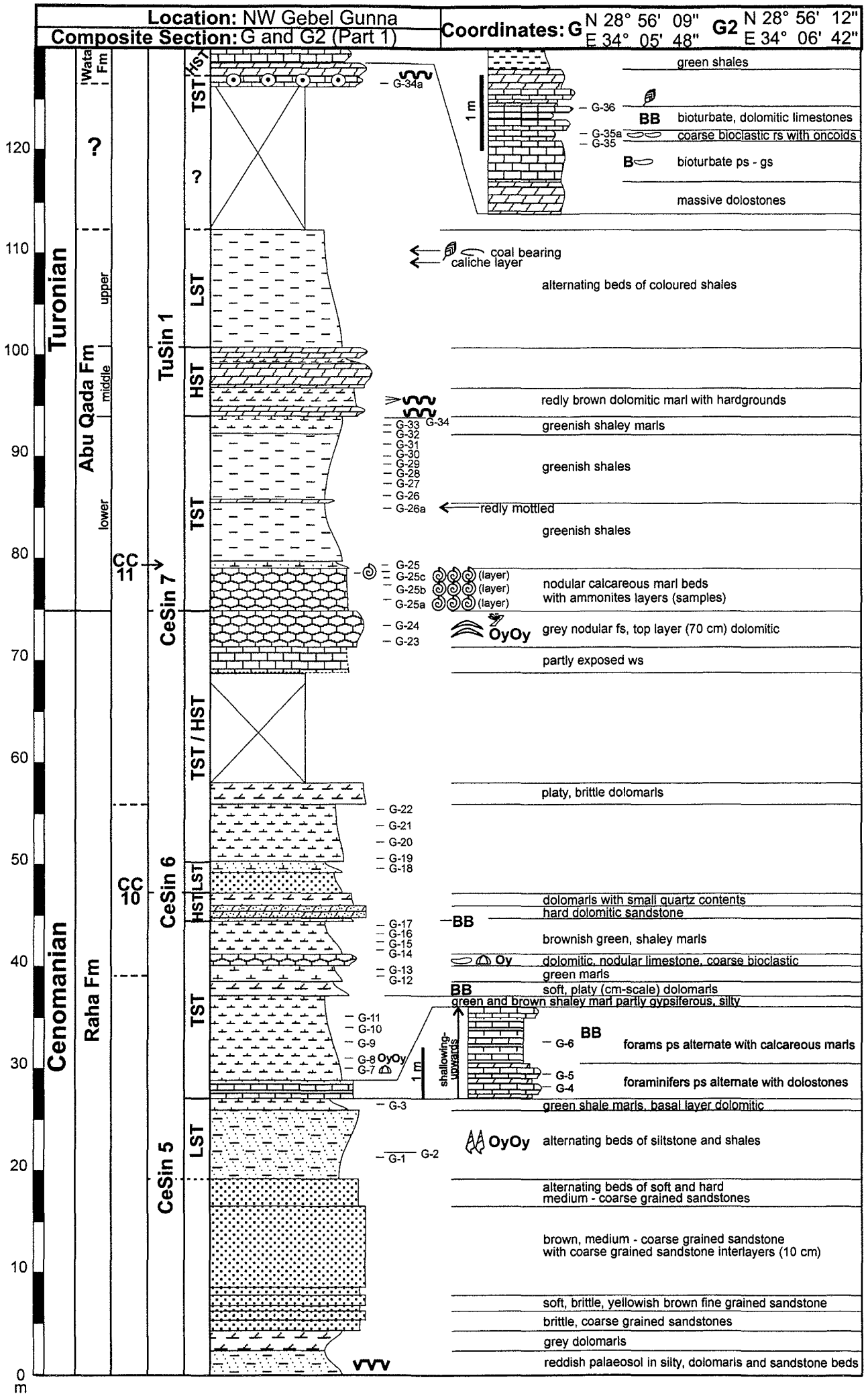
Location: NW Gebel Gunna
Composite Section: G and G2 (Part 1)
Coordinates: G N 28° 56' 09" E 34° 05' 48"
G2 N 28° 56' 12" E 34° 06' 42"
Turonian
Cenomanian
Wata Fm
Abu Qada Fm
upper
middle
lower
Raha Fm
CC 11
CC 10
TuSin 1
CeSin 7
CeSin 6
CeSin 5
TST
LST
HST
TST / HST
HST/LST
120
110
100
90
80
70
60
50
40
30
20
10
0
m
green shales
bioturbate, dolomitic limestones
coarse bioclastic rs with oncoids
bioturbate ps - gs
massive dolostones
coal bearing
caliche layer
alternating beds of coloured shales
redly brown dolomitic marl with hardgrounds
greenish shaley marls
greenish shales
redly mottled
greenish shales
nodular calcareous marl beds with ammonites layers (samples)
grey nodular fs, top layer (70 cm) dolomitic
partly exposed ws
platy, brittle dolomarls
dolomarls with small quartz contents
hard dolomitic sandstone
brownish green, shaley marls
dolomitic, nodular limestone, coarse bioclastic
green marls
soft, platy (cm-scale) dolomarls
green and brown shaley marl partly gypsiferous, silty
forams ps alternate with calcareous marls
foraminifers ps alternate with dolostones
green shale marls, basal layer dolomitic
alternating beds of siltstone and shales
alternating beds of soft and hard medium - coarse grained sandstones
brown, medium - coarse grained sandstone with coarse grained sandstone interlayers (10 cm)
soft, brittle, yellowish brown fine grained sandstone
brittle, coarse grained sandstones
grey dolomarls
reddish palaeosol in silty, dolomarls and sandstone beds
shallowing-upwards
1 m

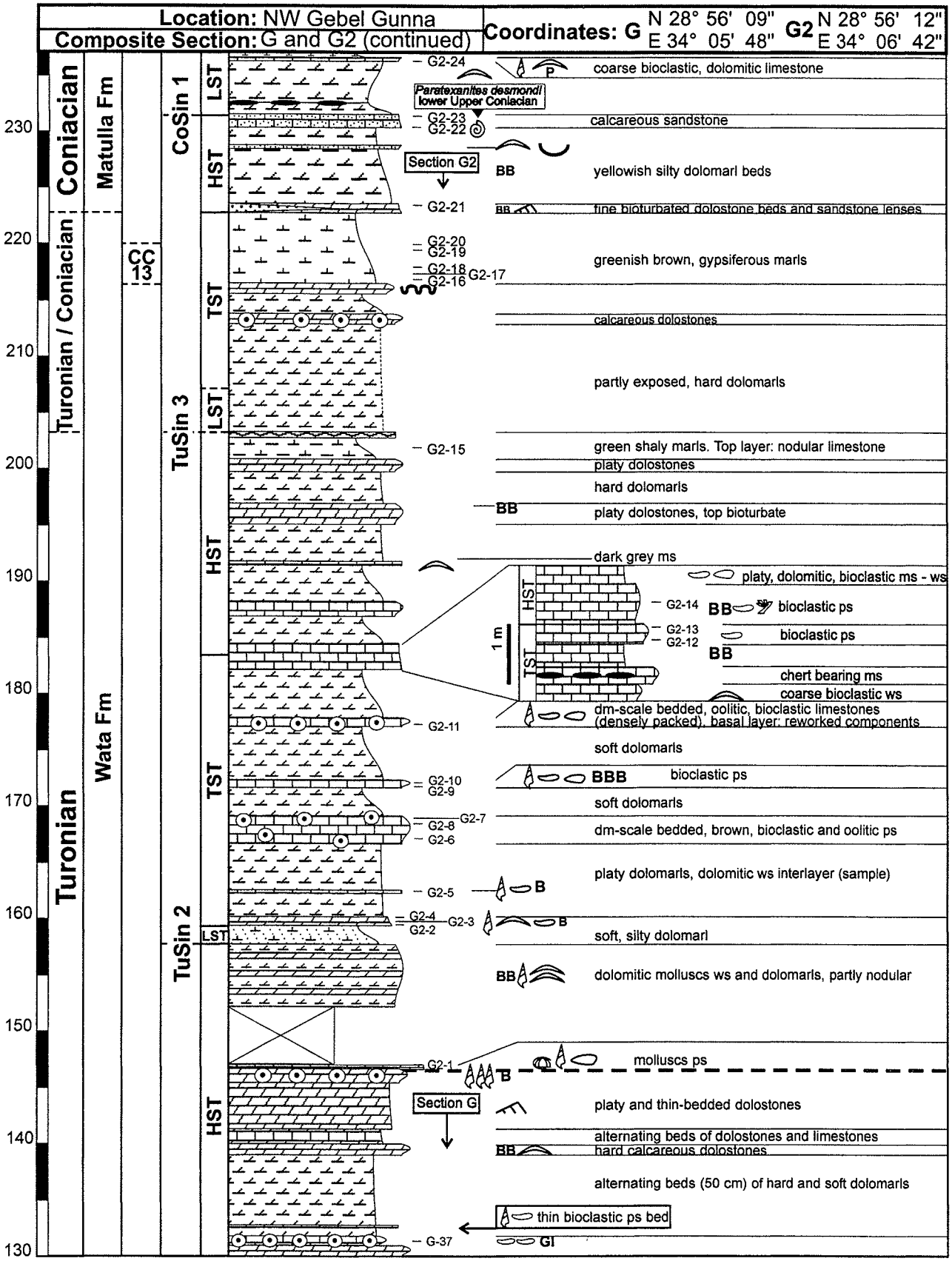
Location: NW Gebel Gunna
Composite Section: G and G2 (continued)
Coordinates: G N 28° 56' 09" E 34° 05' 48" G2 N 28° 56' 12" E 34° 06' 42"
Coniacian
Turonian / Coniacian
Turonian
Matulla Fm
Wata Fm
CC 13
CoSin 1
TuSin 3
TuSin 2
LST
HST
TST
230
220
210
200
190
180
170
160
150
140
130
G2-24
Paratexanites desmoidi lower Upper Coniacian
G2-23
G2-22
Section G2
G2-21
G2-20
G2-19
G2-18
G2-16
G2-17
G2-15
G2-14
G2-13
G2-12
1 m
G2-11
G2-10
G2-9
G2-8
G2-7
G2-6
G2-5
G2-4
G2-3
G2-2
G2-1
Section G
G-37
coarse bioclastic, dolomitic limestone
calcareous sandstone
yellowish silty dolomarl beds
fine bioturbated dolostone beds and sandstone lenses
greenish brown, gypsiferous marls
calcareous dolostones
partly exposed, hard dolomarls
green shaly marls. Top layer: nodular limestone
platy dolostones
hard dolomarls
platy dolostones, top bioturbate
dark grey ms
platy, dolomitic, bioclastic ms - ws
bioclastic ps
bioclastic ps
chert bearing ms
coarse bioclastic ws
dm-scale bedded, oolitic, bioclastic limestones (densely packed), basal layer: reworked components
soft dolomarls
bioclastic ps
soft dolomarls
dm-scale bedded, brown, bioclastic and oolitic ps
platy dolomarls, dolomitic ws interlayer (sample)
soft, silty dolomarl
dolomitic molluscs ws and dolomarls, partly nodular
molluscs ps
platy and thin-bedded dolostones
alternating beds of dolostones and limestones
hard calcareous dolostones
alternating beds (50 cm) of hard and soft dolomarls
thin bioclastic ps bed
GI

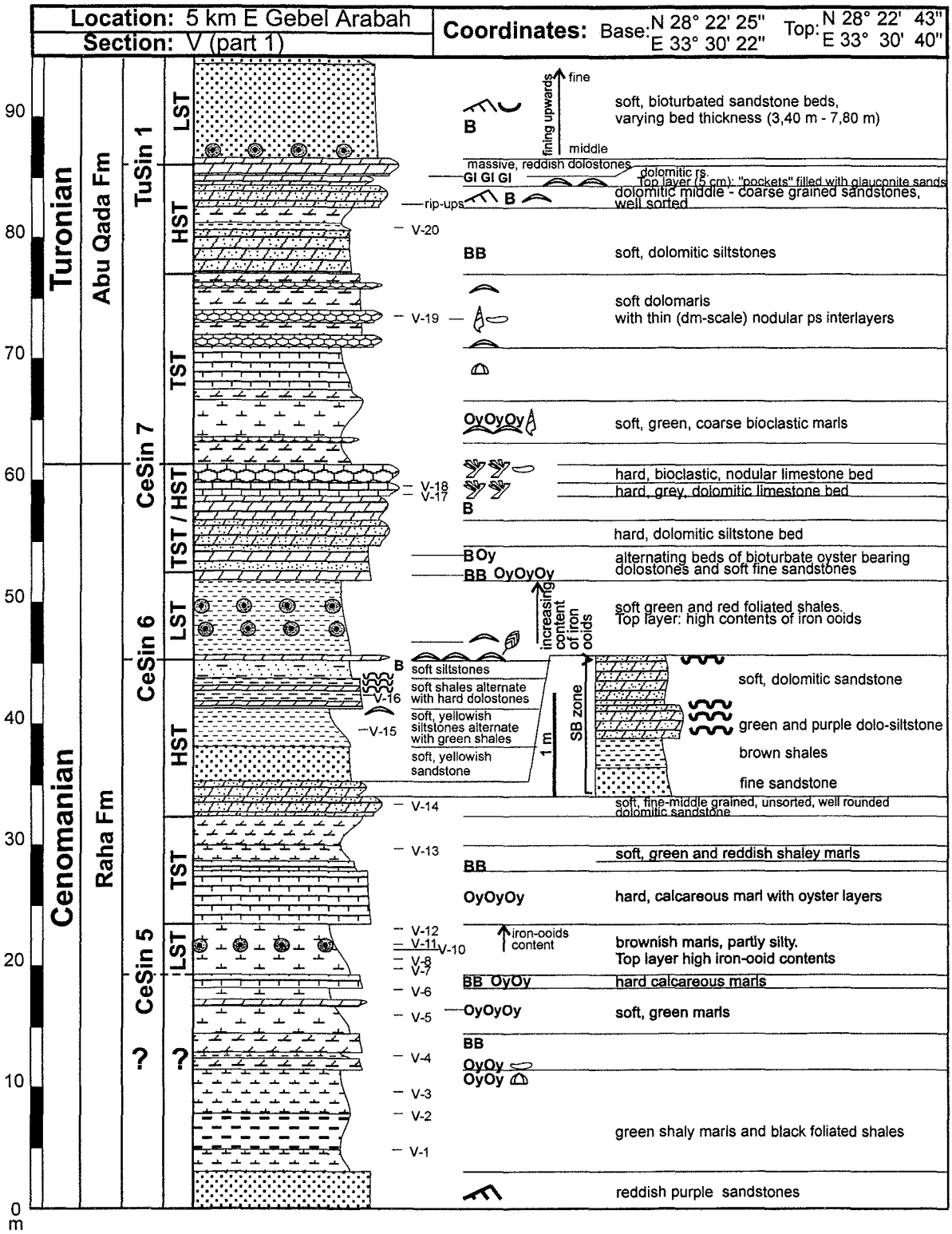
Location: 5 km E Gebel Arabah
Section: V (part 1)
Coordinates: Base: N 28° 22' 25" E 33° 30' 22" Top: N 28° 22' 43" E 33° 30' 40"
Turonian
Cenomanian
Abu Qada Fm
Raha Fm
TuSin 1
CeSin 7
CeSin 6
CeSin 5
? ?
LST
HST
TST
TST / HST
LST
HST
TST
LST
90
80
70
60
50
40
30
20
10
0 m
fining upwards
fine
middle
B
soft, bioturbated sandstone beds, varying bed thickness (3,40 m - 7,80 m)
massive, reddish dolostones
Gl Gl Gl
dolomitic rs.
Top layer (5 cm): "pockets" filled with glauconite sands
rip-ups
B
dolomitic middle - coarse grained sandstones, well sorted
V-20
BB
soft, dolomitic siltstones
V-19
soft dolomarls
with thin (dm-scale) nodular ps interlayers
OyOyOy
soft, green, coarse bioclastic marls
hard, bioclastic, nodular limestone bed
V-18
V-17
hard, grey, dolomitic limestone bed
B
hard, dolomitic siltstone bed
BOy
BB OyOyOy
alternating beds of bioturbate oyster bearing dolostones and soft fine sandstones
increasing content of iron ooids
soft green and red foliated shales.
Top layer: high contents of iron ooids
B
soft siltstones
soft shales alternate with hard dolostones
V-16
V-15
soft, yellowish siltstones alternate with green shales
soft, yellowish sandstone
1 m
SB zone
soft, dolomitic sandstone
green and purple dolo-siltstone
brown shales
fine sandstone
V-14
soft, fine-middle grained, unsorted, well rounded dolomitic sandstone
V-13
soft, green and reddish shaley marls
BB
OyOyOy
hard, calcareous marl with oyster layers
V-12
V-11
V-10
V-8
V-7
iron-ooids content
brownish marls, partly silty.
Top layer high iron-ooid contents
BB OyOy
hard calcareous marls
V-6
V-5
OyOyOy
soft, green marls
BB
V-4
OyOy
OyOy
V-3
V-2
V-1
green shaly marls and black foliated shales
reddish purple sandstones

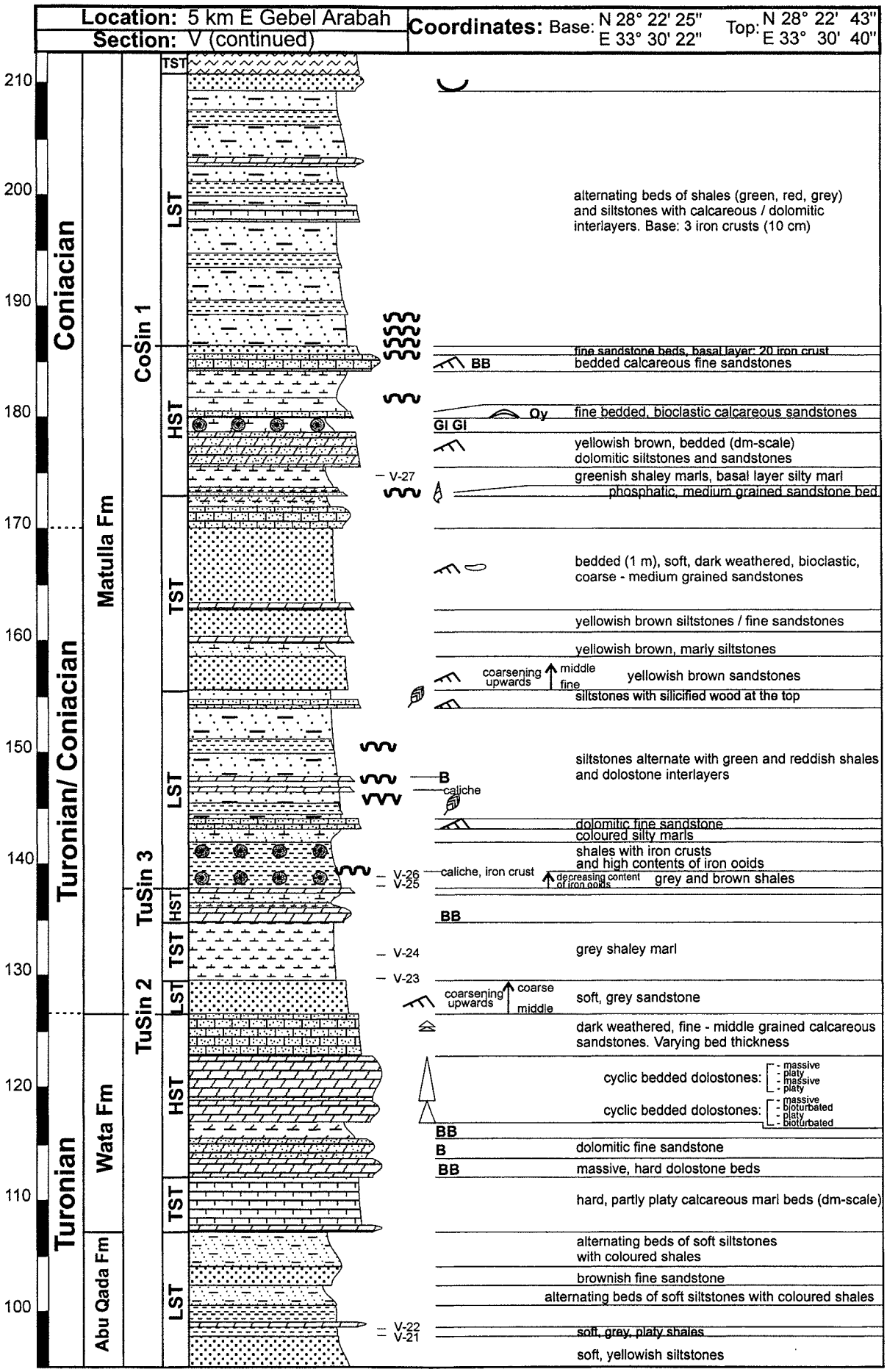
Location: 5 km E Gebel Arabah
Section: V (continued)
Coordinates: Base: N 28° 22' 25" E 33° 30' 22" Top: N 28° 22' 43" E 33° 30' 40"
Coniacian
Turonian/ Coniacian
Turonian
Matulla Fm
Wata Fm
Abu Qada Fm
CoSin 1
TuSin 3
TuSin 2
TST
LST
HST
TST
HST
TST
LST
HST
TST
LST
210
200
190
180
170
160
150
140
130
120
110
100
alternating beds of shales (green, red, grey) and siltstones with calcareous / dolomitic interlayers. Base: 3 iron crusts (10 cm)
fine sandstone beds, basal layer: 20 iron crust
BB
bedded calcareous fine sandstones
Oy
fine bedded, bioclastic calcareous sandstones
Gl Gl
yellowish brown, bedded (dm-scale) dolomitic siltstones and sandstones
V-27
greenish shaley marls, basal layer silty marl
phosphatic, medium grained sandstone bed
bedded (1 m), soft, dark weathered, bioclastic, coarse - medium grained sandstones
yellowish brown siltstones / fine sandstones
yellowish brown, marly siltstones
coarsening upwards
middle
fine
yellowish brown sandstones
siltstones with silicified wood at the top
siltstones alternate with green and reddish shales and dolostone interlayers
B
caliche
dolomitic fine sandstone
coloured silty marls
shales with iron crusts and high contents of iron ooids
V-26
V-25
caliche, iron crust
decreasing content of iron ooids
grey and brown shales
BB
grey shaley marl
V-24
V-23
coarsening upwards
coarse
middle
soft, grey sandstone
dark weathered, fine - middle grained calcareous sandstones. Varying bed thickness
cyclic bedded dolostones: - massive - platy - massive - platy
cyclic bedded dolostones: - massive - bioturbated - platy - bioturbated
BB
B
dolomitic fine sandstone
BB
massive, hard dolostone beds
hard, partly platy calcareous marl beds (dm-scale)
alternating beds of soft siltstones with coloured shales
brownish fine sandstone
alternating beds of soft siltstones with coloured shales
V-22
V-21
soft, grey, platy shales
soft, yellowish siltstones

Publications of this series:

No. 1 **Wefer, G., E. Suess and cruise participants**
Bericht über die POLARSTERN-Fahrt ANT IV/2, Rio de Janeiro - Punta Arenas, 6.11. - 1.12.1985.
60 pages, Bremen, 1986.

No. 2 **Hoffmann, G.**
Holozänstratigraphie und Küstenlinienverlagerung an der andalusischen Mittelmeerküste.
173 pages, Bremen, 1988. (out of print)

No. 3 **Wefer, G. and cruise participants**
Bericht über die METEOR-Fahrt M 6/6, Libreville - Las Palmas, 18.2. - 23.3.1988.
97 pages, Bremen, 1988.

No. 4 **Wefer, G., G.F. Lutze, T.J. Müller, O. Pfannkuche, W. Schenke, G. Siedler, W. Zenk**
Kurzbericht über die METEOR-Expedition No. 6, Hamburg - Hamburg, 28.10.1987 - 19.5.1988.
29 pages, Bremen, 1988. (out of print)

No. 5 **Fischer, G.**
Stabile Kohlenstoff-Isotope in partikulärer organischer Substanz aus dem Südpolarmeer (Atlantischer Sektor). 161 pages, Bremen, 1989.

No. 6 **Berger, W.H. and G. Wefer**
Partikelfluß und Kohlenstoffkreislauf im Ozean.
Bericht und Kurzfassungen über den Workshop vom 3.-4. Juli 1989 in Bremen.
57 pages, Bremen, 1989.

No. 7 **Wefer, G. and cruise participants**
Bericht über die METEOR - Fahrt M 9/4, Dakar - Santa Cruz, 19.2. - 16.3.1989.
103 pages, Bremen, 1989.

No. 8 **Kölling, M.**
Modellierung geochemischer Prozesse im Sickerwasser und Grundwasser.
135 pages, Bremen, 1990.

No. 9 **Heinze, P.-M.**
Das Auftriebsgeschehen vor Peru im Spätquartär. 204 pages, Bremen, 1990. (out of print)

No. 10 **Willems, H., G. Wefer, M. Rinski, B. Donner, H.-J. Bellmann, L. Eißmann, A. Müller, B.W. Flemming, H.-C. Höfle, J. Merkt, H. Streif, G. Hertweck, H. Kuntze, J. Schwaar, W. Schäfer, M.-G. Schulz, F. Grube, B. Menke**
Beiträge zur Geologie und Paläontologie Norddeutschlands: Exkursionsführer.
202 pages, Bremen, 1990.

No. 11 **Wefer, G. and cruise participants**
Bericht über die METEOR-Fahrt M 12/1, Kapstadt - Funchal, 13.3.1990 - 14.4.1990.
66 pages, Bremen, 1990.

No. 12 **Dahmke, A., H.D. Schulz, A. Kölling, F. Kracht, A. Lücke**
Schwermetallspuren und geochemische Gleichgewichte zwischen Porenlösung und Sediment im Wesermündungsgebiet. BMFT-Projekt MFU 0562, Abschlußbericht. 121 pages, Bremen, 1991.

No. 13 **Rostek, F.**
Physikalische Strukturen von Tiefseesedimenten des Südatlantiks und ihre Erfassung in Echolotregistrierungen. 209 pages, Bremen, 1991.

No. 14 **Baumann, M.**
Die Ablagerung von Tschernobyl-Radiocäsium in der Norwegischen See und in der Nordsee.
133 pages, Bremen, 1991. (out of print)

No. 15 **Kölling, A.**
Frühdiagenetische Prozesse und Stoff-Flüsse in marinen und ästuarinen Sedimenten.
140 pages, Bremen, 1991.

No. 16 **SFB 261 (ed.)**
1. Kolloquium des Sonderforschungsbereichs 261 der Universität Bremen (14.Juni 1991):
Der Südatlantik im Spätquartär: Rekonstruktion von Stoffhaushalt und Stromsystemen.
Kurzfassungen der Vorträge und Poster. 66 pages, Bremen, 1991.

No. 17 **Pätzold, J. and cruise participants**
Bericht und erste Ergebnisse über die METEOR-Fahrt M 15/2, Rio de Janeiro - Vitoria,
18.1. - 7.2.1991. 46 pages, Bremen, 1993.

No. 18 **Wefer, G. and cruise participants**
Bericht und erste Ergebnisse über die METEOR-Fahrt M 16/1, Pointe Noire - Recife,
27.3. - 25.4.1991. 120 pages, Bremen, 1991.

No. 19 **Schulz, H.D. and cruise participants**
Bericht und erste Ergebnisse über die METEOR-Fahrt M 16/2, Recife - Belem, 28.4. - 20.5.1991.
149 pages, Bremen, 1991.

No. 20 **Berner, H.**
Mechanismen der Sedimentbildung in der Fram-Straße, im Arktischen Ozean und in der Norwegischen See. 167 pages, Bremen, 1991.

No. 21 **Schneider, R.**
Spätquartäre Produktivitätsänderungen im östlichen Angola-Becken: Reaktion auf Variationen im Passat-Monsun-Windsystem und in der Advektion des Benguela-Küstenstroms.
198 pages, Bremen, 1991. (out of print)

No. 22 **Hebbeln, D.**
Spätquartäre Stratigraphie und Paläozeanographie in der Fram-Straße. 174 pages, Bremen, 1991.

No. 23 **Lücke, A.**
Umsetzungsprozesse organischer Substanz während der Frühdiagenese in ästuarinen Sedimenten.
137 pages, Bremen, 1991.

No. 24 **Wefer, G. and cruise participants**
Bericht und erste Ergebnisse der METEOR-Fahrt M 20/1, Bremen - Abidjan, 18.11.- 22.12.1991.
74 pages, Bremen, 1992.

No. 25 **Schulz, H.D. and cruise participants**
Bericht und erste Ergebnisse der METEOR-Fahrt M 20/2, Abidjan - Dakar, 27.12.1991 - 3.2.1992.
173 pages, Bremen, 1992.

No. 26 **Gingele, F.**
Zur klimaabhängigen Bildung biogener und terrigener Sedimente und ihrer Veränderung durch die Frühdiagenese im zentralen und östlichen Südatlantik. 202 pages, Bremen, 1992.

No. 27 **Bickert, T.**
Rekonstruktion der spätquartären Bodenwasserzirkulation im östlichen Südatlantik über stabile Isotope benthischer Foraminiferen. 205 pages, Bremen, 1992. (out of print)

No. 28 **Schmidt, H.**
Der Benguela-Strom im Bereich des Walfisch-Rückens im Spätquartär. 172 pages, Bremen, 1992.

No. 29 **Meinecke, G.**
Spätquartäre Oberflächenwassertemperaturen im östlichen äquatorialen Atlantik.
181 pages, Bremen, 1992.

No. 30 **Bathmann, U., U. Bleil, A. Dahmke, P. Müller, A. Nehrkorn, E.-M. Nöthig, M. Olesch, J. Pätzold, H.D. Schulz, V. Smetacek, V. Spieß, G. Wefer, H. Willems**
Bericht des Graduierten Kollegs. Stoff-Flüsse in marinen Geosystemen.
Berichtszeitraum Oktober 1990 - Dezember 1992. 396 pages, Bremen, 1992.

No. 31 **Damm, E.**
Frühdiagenetische Verteilung von Schwermetallen in Schlicksedimenten der westlichen Ostsee.
115 pages, Bremen, 1992.

No. 32 **Antia, E.E.**
Sedimentology, Morphodynamics and Facies Association of a mesotidal Barrier Island Shoreface (Spiekeroog, Southern North Sea). 370 pages, Bremen, 1993.

No. 33 **Duinker, J. and G. Wefer (ed.)**
Bericht über den 1. JGOFS-Workshop. 1./2. Dezember 1992 in Bremen. 83 pages, Bremen, 1993.

No. 34 **Kasten, S.**
Die Verteilung von Schwermetallen in den Sedimenten eines stadtbremischen Hafenbeckens.
103 pages, Bremen, 1993.

No. 35 **Spieß, V.**
Digitale Sedimentographie. Neue Wege zu einer hochauflösenden Akustostratigraphie.
199 pages, Bremen, 1993.

No. 36 **Schinzel, U.**
Laborversuche zu frühdiagenetischen Reaktionen von Eisen (III) - Oxidhydraten in marinen Sedimenten.189 pages, Bremen, 1993.

No. 37 **Sieger, R.**
CoTAM - ein Modell zur Modellierung des Schwermetalltransports in Grundwasserleitern.
56 pages, Bremen, 1993. (out of print)

No. 38 **Willems, H. (ed.)**
Geoscientific Investigations in the Tethyan Himalayas. 183 pages, Bremen, 1993.

No. 39 **Hamer, K.**
Entwicklung von Laborversuchen als Grundlage für die Modellierung des Transportverhaltens von Arsenat, Blei, Cadmium und Kupfer in wassergesättigten Säulen. 147 pages, Bremen, 1993.

No. 40 **Sieger, R.**
Modellierung des Stofftransports in porösen Medien unter Ankopplung kinetisch gesteuerter Sorptions- und Redoxprozesse sowie thermischer Gleichgewichte. 158 pages, Bremen, 1993.

No. 41 **Thießen, W.**
Magnetische Eigenschaften von Sedimenten des östlichen Südatlantiks und ihre paläozeanographische Relevanz. 170 pages, Bremen, 1993.

No. 42 **Spieß, V. and cruise participants**
Report and preliminary results of METEOR-Cruise M 23/1, Kapstadt - Rio de Janeiro, 4.-25.2.1993. 139 pages, Bremen, 1994.

No. 43 **Bleil, U. and cruise participants**
Report and preliminary results of METEOR-Cruise M 23/2, Rio de Janeiro - Recife, 27.2.-19.3.1993 133 pages, Bremen, 1994.

No. 44 **Wefer, G. and cruise participants**
Report and preliminary results of METEOR-Cruise M 23/3, Recife - Las Palmas, 21.3. - 12.4.1993 71 pages, Bremen, 1994.

No. 45 **Giese, M. and G. Wefer (ed.)**
Bericht über den 2. JGOFS-Workshop. 18../19. November 1993 in Bremen. 93 pages, Bremen, 1994.

No. 46 **Balzer, W. and cruise participants**
Report and preliminary results of METEOR-Cruise M 22/1, Hamburg - Recife, 22.9. - 21.10.1992. 24 pages, Bremen, 1994.

No. 47 **Stax, R.**
Zyklische Sedimentation von organischem Kohlenstoff in der Japan See: Anzeiger für Änderungen von Paläoozeanographie und Paläoklima im Spätkänozoikum. 150 pages, Bremen, 1994.

No. 48 **Skowronek, F.**
Frühdiagenetische Stoff-Flüsse gelöster Schwermetalle an der Oberfläche von Sedimenten des Weser Ästuares. 107 pages, Bremen, 1994.

No. 49 **Dersch-Hansmann, M.**
Zur Klimaentwicklung in Ostasien während der letzten 5 Millionen Jahre: Terrigener Sedimenteintrag in die Japan See (ODP Ausfahrt 128). 149 pages, Bremen, 1994.

No. 50 **Zabel, M.**
Frühdiagenetische Stoff-Flüsse in Oberflächen-Sedimenten des äquatorialen und östlichen Südatlantik. 129 pages, Bremen, 1994.

No. 51 **Bleil, U. and cruise participants**
Report and preliminary results of SONNE-Cruise SO 86, Buenos Aires - Capetown, 22.4. - 31.5.93 116 pages, Bremen, 1994.

No. 52 **Symposium: The South Atlantic: Present and Past Circulation.**
Bremen, Germany, 15 - 19 August 1994. Abstracts. 167 pages, Bremen, 1994.

No. 53 **Kretzmann, U.B.**
^{57}Fe-Mössbauer-Spektroskopie an Sedimenten - Möglichkeiten und Grenzen. 183 pages, Bremen, 1994.

No. 54 **Bachmann, M.**
Die Karbonatrampe von Organyà im oberen Oberapt und unteren Unteralb (NE-Spanien, Prov. Lerida): Fazies, Zyklo- und Sequenzstratigraphie. 147 pages, Bremen, 1994. (out of print)

No. 55 **Kemle-von Mücke, S.**
Oberflächenwasserstruktur und -zirkulation des Südostatlantiks im Spätquartär. 151 pages, Bremen, 1994.

No. 56 **Petermann, H.**
Magnetotaktische Bakterien und ihre Magnetosome in Oberflächensedimenten des Südatlantiks. 134 pages, Bremen, 1994.

No. 57 **Mulitza, S.**
Spätquartäre Variationen der oberflächennahen Hydrographie im westlichen äquatorialen Atlantik. 97 pages, Bremen, 1994.

No. 58 **Segl, M. and cruise participants**
Report and preliminary results of METEOR-Cruise M 29/1, Buenos-Aires - Montevideo, 17.6. - 13.7.1994
94 pages, Bremen, 1994.

No. 59 **Bleil, U. and cruise participants**
Report and preliminary results of METEOR-Cruise M 29/2, Montevideo - Rio de Janiero 15.7. - 8.8.1994. 153 pages, Bremen, 1994.

No. 60 **Henrich, R. and cruise participants**
Report and preliminary results of METEOR-Cruise M 29/3, Rio de Janeiro - Las Palmas 11.8. - 5.9.1994. Bremen, 1994. (out of print)

No. 61 **Sagemann, J.**
Saisonale Variationen von Porenwasserprofilen, Nährstoff-Flüssen und Reaktionen in intertidalen Sedimenten des Weser-Ästuars. 110 pages, Bremen, 1994. (out of print)

No. 62 **Giese, M. and G. Wefer**
Bericht über den 3. JGOFS-Workshop. 5./6. Dezember 1994 in Bremen.
84 pages, Bremen, 1995.

No. 63 **Mann, U.**
Genese kretazischer Schwarzschiefer in Kolumbien: Globale vs. regionale/lokale Prozesse.
153 pages, Bremen, 1995. (out of print)

No. 64 **Willems, H., Wan X., Yin J., Dongdui L., Liu G., S. Dürr, K.-U. Gräfe**
The Mesozoic development of the N-Indian passive margin and of the Xigaze Forearc Basin in southern Tibet, China. – Excursion Guide to IGCP 362 Working-Group Meeting "Integrated Stratigraphy". 113 pages, Bremen, 1995. (out of print)

No. 65 **Hünken, U.**
Liefergebiets - Charakterisierung proterozoischer Goldseifen in Ghana anhand von Fluideinschluß - Untersuchungen. 270 pages, Bremen, 1995.

No. 66 **Nyandwi, N.**
The Nature of the Sediment Distribution Patterns in ther Spiekeroog Backbarrier Area, the East Frisian Islands. 162 pages, Bremen, 1995.

No. 67 **Isenbeck-Schröter, M.**
Transportverhalten von Schwermetallkationen und Oxoanionen in wassergesättigten Sanden. - Laborversuche in Säulen und ihre Modellierung -. 182 pages, Bremen, 1995.

No. 68 **Hebbeln, D. and cruise participants**
Report and preliminary results of SONNE-Cruise SO 102, Valparaiso - Valparaiso, 95.
134 pages, Bremen, 1995.

No. 69 **Willems, H. (Sprecher), U.Bathmann, U. Bleil, T. v. Dobeneck, K. Herterich, B.B. Jorgensen, E.-M. Nöthig, M. Olesch, J. Pätzold, H.D. Schulz, V. Smetacek, V. Speiß. G. Wefer**
Bericht des Graduierten-Kollegs Stoff-Flüsse in marine Geosystemen.
Berichtszeitraum Januar 1993 - Dezember 1995.
45 & 468 pages, Bremen, 1995.

No. 70 **Giese, M. and G. Wefer**
Bericht über den 4. JGOFS-Workshop. 20./21. November 1995 in Bremen. 60 pages, Bremen, 1996. (out of print)

No. 71 **Meggers, H.**
Pliozän-quartäre Karbonatsedimentation und Paläozeanographie des Nordatlantiks und des Europäischen Nordmeeres - Hinweise aus planktischen Foraminiferengemeinschaften.
143 pages, Bremen, 1996. (out of print)

No. 72 **Teske, A.**
Phylogenetische und ökologische Untersuchungen an Bakterien des oxidativen und reduktiven marinen Schwefelkreislaufs mittels ribosomaler RNA. 220 pages, Bremen, 1996. (out of print)

No. 73 **Andersen, N.**
Biogeochemische Charakterisierung von Sinkstoffen und Sedimenten aus ostatlantischen Produktions-Systemen mit Hilfe von Biomarkern. 215 pages, Bremen, 1996.

No. 74 **Treppke, U.**
Saisonalität im Diatomeen- und Silikoflagellatenfluß im östlichen tropischen und subtropischen Atlantik. 200 pages, Bremen, 1996.

No. 75 **Schüring, J.**
Die Verwendung von Steinkohlebergematerialien im Deponiebau im Hinblick auf die Pyritverwitterung und die Eignung als geochemische Barriere. 110 pages, Bremen, 1996.

No. 76 **Pätzold, J. and cruise participants**
Report and preliminary results of VICTOR HENSEN cruise JOPS II, Leg 6, Fortaleza - Recife, 10.3. - 26.3. 1995 and Leg 8, Vítoria - Vítoria, 10.4. - 23.4.1995.
87 pages, Bremen, 1996.

No. 77 **Bleil, U. and cruise participants**
Report and preliminary results of METEOR-Cruise M 34/1, Cape Town - Walvis Bay, 3.-26.1.1996.
129 pages, Bremen, 1996.

No. 78 **Schulz, H.D. and cruise participants**
Report and preliminary results of METEOR-Cruise M 34/2, Walvis Bay - Walvis Bay, 29.1.-18.2.96
133 pages, Bremen, 1996.

No. 79 **Wefer, G. and cruise participants**
Report and preliminary results of METEOR-Cruise M 34/3, Walvis Bay - Recife, 21.2.-17.3.1996.
168 pages, Bremen, 1996.

No. 80 **Fischer, G. and cruise participants**
Report and preliminary results of METEOR-Cruise M 34/4, Recife - Bridgetown, 19.3.-15.4.1996. 105 pages, Bremen, 1996.

No. 81 **Kulbrok, F.**
Biostratigraphie, Fazies und Sequenzstratigraphie einer Karbonatrampe in den Schichten der Oberkreide und des Alttertiärs Nordost-Ägyptens (Eastern Desert, N'Golf von Suez, Sinai). 153 pages, Bremen, 1996.

No. 82 **Kasten, S.**
Early Diagenetic Metal Enrichments in Marine Sediments as Documents of Nonsteady-State Depositional Conditions. Bremen, 1996.

No. 83 **Holmes, M.E.**
Reconstruction of Surface Ocean Nitrate Utilization in the Southeast Atlantic Ocean Based on Stable Nitrogen Isotopes. 113 pages, Bremen, 1996.

No. 84 **Rühlemann, C.**
Akkumulation von Carbonat und organischem Kohlenstoff im tropischen Atlantik: Spätquartäre Produktivitäts-Variationen und ihre Steuerungsmechanismen. 139 pages, Bremen, 1996.

No. 85 **Ratmeyer, V.**
Untersuchungen zum Eintrag und Transport lithogener und organischer partikulärer Substanz im östlichen subtropischen Nordatlantik. 154 pages, Bremen, 1996.

No. 86 **Cepek, M.**
Zeitliche und räumliche Variationen von Coccolithophoriden-Gemeinschaften im subtropischen Ost-Atlantik: Untersuchungen an Plankton, Sinkstoffen und Sedimenten. 156 pages, Bremen, 1996.

No. 87 **Otto, S.**
Die Bedeutung von gelöstem organischen Kohlenstoff (DOC) für den Kohlenstoffffluß im Ozean. 150 pages, Bremen, 1996.

No. 88 **Hensen, C.**
Frühdiagenetische Prozesse und Quantifizierung benthischer Stoff-Flüsse in Oberflächensedimenten des Südatlantiks. 132 pages, Bremen, 1996.

No. 89 **Giese, M. and G. Wefer**
Bericht über den 5. JGOFS-Workshop. 27./28. November 1996 in Bremen. 73 pages, Bremen, 1997.

No. 90 **Wefer, G. and cruise participants**
Report and preliminary results of METEOR-Cruise M 37/1, Lisbon - Las Palmas, 4.-23.12.1996. 79 pages, Bremen, 1997.

No. 91 **Isenbeck-Schröter, M., E. Bedbur, M. Kofod, B. König, T. Schramm & G. Mattheß**
Occurrence of Pesticide Residues in Water - Assessment of the Current Situation in Selected EU Countries. 65 pages, Bremen 1997.

No. 92 **Kühn, M.**
Geochemische Folgereaktionen bei der hydrogeothermalen Energiegewinnung. 129 pages, Bremen 1997.

No. 93 **Determann, S. & K. Herterich**
JGOFS-A6 "Daten und Modelle": Sammlung JGOFS-relevanter Modelle in Deutschland. 26 pages, Bremen, 1997.

No. 94 **Fischer, G. and cruise participants**
Report and preliminary results of METEOR-Cruise M 38/1, Las Palmas - Recife, 25.1.-1.3.1997, with Appendix: Core Descriptions from METEOR Cruise M 37/1. Bremen, 1997.

No. 95 **Bleil, U. and cruise participants**
Report and preliminary results of METEOR-Cruise M 38/2, Recife - Las Palmas, 4.3.-14.4.1997. 126 pages, Bremen, 1997.

No. 96 **Neuer, S. and cruise participants**
Report and preliminary results of VICTOR HENSEN-Cruise 96/1. Bremen, 1997.

No. 97 **Villinger, H. and cruise participants**
Fahrtbericht SO 111, 20.8. - 16.9.1996. 115 pages, Bremen, 1997.

No. 98 **Lüning, S.**
Late Cretaceous - Early Tertiary sequence stratigraphy, paleoecology and geodynamics of Eastern Sinai, Egypt. 218 pages, Bremen, 1997.

No. 99 **Haese, R.R.**
Beschreibung und Quantifizierung frühdiagenetischer Reaktionen des Eisens in Sedimenten des Südatlantiks. 118 pages, Bremen, 1997.

No. 100 **Lührte, R. von**
Verwertung von Bremer Baggergut als Material zur Oberflächenabdichtung von Deponien - Geochemisches Langzeitverhalten und Schwermetall-Mobilität (Cd, Cu, Ni, Pb, Zn). Bremen, 1997.

No. 101 **Ebert, M.**
Der Einfluß des Redoxmilieus auf die Mobilität von Chrom im durchströmten Aquifer. 135 pages, Bremen, 1997.

No. 102 **Krögel, F.**
Einfluß von Viskosität und Dichte des Seewassers auf Transport und Ablagerung von Wattsedimenten (Langeooger Rückseitenwatt, südliche Nordsee). 168 pages, Bremen, 1997.

No. 103 **Kerntopf, B.**
Dinoflagellate Distribution Patterns and Preservation in the Equatorial Atlantic and Offshore North-West Africa. 137 pages, Bremen, 1997.

No. 104 **Breitzke, M.**
Elastische Wellenausbreitung in marinen Sedimenten - Neue Entwicklungen der Ultraschall Sedimentphysik und Sedimentechographie. 298 pages, Bremen, 1997.

No. 105 **Marchant, M.**
Rezente und spätquartäre Sedimentation planktischer Foraminiferen im Peru-Chile Strom. 115 pages, Bremen, 1997.

No. 106 **Habicht, K.S.**
Sulfur isotope fractionation in marine sediments and bacterial cultures. 125 pages, Bremen, 1997.

No. 107 **Hamer, K., R.v. Lührte, G. Becker, T. Felis, S. Keffel, B. Strotmann, C. Waschkowitz, M. Kölling, M. Isenbeck-Schröter, H.D. Schulz**
Endbericht zum Forschungsvorhaben 060 des Landes Bremen: Baggergut der Hafengruppe Bremen-Stadt: Modelluntersuchungen zur Schwermetallmobilität und Möglichkeiten der Verwertung von Hafenschlick aus Bremischen Häfen. 98 pages, Bremen, 1997.

No. 108 **Greeff, O.W.**
Entwicklung und Erprobung eines benthischen Landersystemes zur *in situ*-Bestimmung von Sulfatreduktionsraten mariner Sedimente. 121 pages, Bremen, 1997.

No. 109 **Pätzold, M. und G. Wefer**
Bericht über den 6. JGOFS-Workshop am 4./5.12.1997 in Bremen. Im Anhang: Publikationen zum deutschen Beitrag zur Joint Global Ocean Flux Study (JGOFS), Stand 1/1998. 122 pages, Bremen, 1998.

No. 110 **Landenberger, H.**
CoTReM, ein Multi-Komponenten Transport- und Reaktions-Modell. 142 pages, Bremen, 1998.

No. 111 **Villinger, H. und Fahrtteilnehmer**
Fahrtbericht SO 124, 4.10. - 16.10.199. 90 pages, Bremen, 1997.

No. 112 **Gietl, R.**
Biostratigraphie und Sedimentationsmuster einer nordostägyptischen Karbonatrampe unter Berücksichtigung der Alveolinen-Faunen. 142 pages, Bremen, 1998.

No. 113 **Ziebis, W.**
The Impact of the Thalassinidean Shrimp *Callianassa truncata* on the Geochemistry of permeable, coastal Sediments. 158 pages, Bremen 1998.

No. 114 **Schulz, H.D. and cruise participants**
Report and preliminary results of METEOR-Cruise M 41/1, Málaga - Libreville, 13.2.-15.3.1998. Bremen, 1998.

No. 115 **Völker, D.J.**
Untersuchungen an strömungsbeeinflußten Sedimentationsmustern im Südozean. Interpretation sedimentechographischer Daten und numerische Modellierung. 152 pages, Bremen, 1998.

No. 116 **Schlünz, B.**
Riverine Organic Carbon Input into the Ocean in Relation to Late Quaternary Climate Change. 136 pages, Bremen, 1998.

No. 117 **Kuhnert, H.**
Aufzeichnug des Klimas vor Westaustralien in stabilen Isotopen in Korallenskeletten. 109 pages, Bremen, 1998.

No. 118 **Kirst, G.**
Rekonstruktion von Oberflächenwassertemperaturen im östlichen Südatlantik anhand von Alkenonen. 130 pages, Bremen, 1998.

No. 119 **Dürkoop, A.**
Der Brasil-Strom im Spätquartär: Rekonstruktion der oberflächennahen Hydrographie während der letzten 400 000 Jahre. 121 pages, Bremen, 1998.

No. 120 **Lamy, F.**
Spätquartäre Variationen des terrigenen Sedimenteintrags entlang des chilenischen Kontinentalhangs als Abbild von Klimavariabilität im Milankovi- und Sub-Milankovi-Zeitbereich. 141 pages, Bremen, 1998.

No. 121 **Neuer, S. and cruise participants**
Report and preliminary results of POSEIDON-Cruise Pos 237/2, Vigo – Las Palmas, 18.3.-31.3.1998. 39 pages, Bremen, 1998

No. 122 **Romero, O.E.**
Marine planktonic diatoms from the tropical and equatorial Atlantic: temporal flux patterns and the sediment record. 205 pages, Bremen, 1998.

No. 123 **Spiess, V. und Fahrtteilnehmer**
Report and preliminary results of RV SONNE Cruise 125, Cochin – Chittagong, 17.10.-17.11.1997. 128 pages, Bremen, 1998.

No. 124 **Arz, H.W.**
Dokumentation von kurzfristigen Klimaschwankungen des Spätquartärs in Sedimenten des westlichen äquatorialen Atlantiks. 96 pages, Bremen, 1998.

No. 125 **Wolff, T.**
Mixed layer characteristics in the equatorial Atlantic during the late Quaternary as deduced from planktonic foraminifera. 132 pages, Bremen, 1998.

No. 126 **Dittert, N.**
Late Quaternary Planktic Foraminifera Assemblages in the South Atlantic Ocean: Quantitative Determination and Preservational Aspects. 165 pages, Bremen, 1998.

No. 127 **Höll, C.**
Kalkige und organisch-wandige Dinoflagellaten-Zysten in Spätquartären Sedimenten des tropischen Atlantiks und ihre palökologische Auswertbarkeit. 121 pages, Bremen, 1998.

No. 128 **Hencke, J.**
Redoxreaktionen im Grundwasser: Etablierung und Verlagerung von Reaktionsfronten und ihre Bedeutung für die Spurenelement-Mobilität. 122 pages, Bremen 1998.

No. 129 **Pätzold, J. and cruise participants**
Report and preliminary results of METEOR-Cruise M 41/3, Vitoria, Brasil – Salvador de Bahia, Brasil, 18.4. - 15.5.1998. Bremen, 1999.

No. 130 **Fischer, G. and cruise participants**
Report and preliminary results of METEOR-Cruise M 41/4, Salvador de Bahia, Brasil – Las Palmas, Spain, 18.5. – 13.6.1998. Bremen, 1999.

No. 131 **Schlünz, B. und G. Wefer**
Bericht über den 7. JGOFS-Workshop am 3. und 4.12.1998 in Bremen. Im Anhang: Publikationen zum deutschen Beitrag zur Joint Global Ocean Flux Study (JGOFS), Stand 1/ 1999. 100 pages, Bremen, 1999.

No. 132 **Wefer, G. and cruise participants**
Report and preliminary results of METEOR-Cruise M 42/4, Las Palmas - Las Palmas - Viena do Castelo; 26.09.1998 - 26.10.1998. 104 pages, Bremen, 1999.

No. 133 **Felis, T.**
Climate and ocean variability reconstructed from stable isotope records of modern subtropical corals (Northern Red Sea). 111 pages, Bremen, 1999.

No. 134 **Draschba , S.**
North Atlantic climate variability recorded in reef corals from Bermuda. 108 pages, Bremen, 1999.

No. 135 **Schmieder, F.**
Magnetic Cyclostratigraphy of South Atlantic Sediments. 82 pages, Bremen, 1999.

No. 136 **Rieß, W.**
In situ measurements of respiration and mineralisation processes – Interaction between fauna and geochemical fluxes at active interfaces. 68 pages, Bremen, 1999.

No. 137 **Devey, C.W. and cruise participants**
Report and shipboard results from METEOR-cruise M 41/2, Libreville – Vitoria, 18.3. – 15.4.98. 59 pages, Bremen, 1999.

No. 138 **Wenzhöfer, F.**
Biogeochemical processes at the sediment water interface and quantification of metabolically driven calcite dissolution in deep sea sediments. 103 pages, Bremen, 1999.

No. 139 **Klump, J.**
Biogenic barite as a proxy of paleoproductivity variations in the Southern Peru-Chile Current. 107 pages, Bremen, 1999.

No. 140 **Huber, R.**
Carbonate sedimentation in the northern Northatlantic since the late pliocene. 103 pages, Bremen, 1999.

No. 141 **Schulz, H.**
Nitrate-storing sulfur bacteria in sediments of coastal upwelling. 94 pages, Bremen, 1999.

No. 142 **Mai, S.**
Die Sedimentverteilung im Wattenmeer: ein Simulationsmodell. 114 pages, Bremen, 1999.

No. 143 **Neuer, S. and cruise participants**
Report and preliminary results of Poseidon Cruise 248, Las Palmas - Las Palmas, 15.2.-26.2.1999.
45 pages, Bremen, 1999.

No. 144 **Weber, A.**
Schwefelkreislauf in marinen Sedimenten und Messung von *in situ* Sulfatreduktionsraten.
122 pages, Bremen, 1999.

No. 145 **Hadeler, A.**
Sorptionsreaktionen im Grundwasser: Unterschiedliche Aspekte bei der Modellierung des Transportverhaltens von Zink. 122 pages, 1999.

No. 146 **Dierßen, H.**
Zum Kreislauf ausgewählter Spurenmetalle im Südatlantik: Vertikaltransport und Wechselwirkung zwischen Partikeln und Lösung. 167 pages, Bremen, 1999.

No. 147 **Zühlsdorff, L.**
High resolution multi-frequency seismic surveys at the Eastern Juan de Fuca Ridge Flank and the Cascadia Margin – Evidence for thermally and tectonically driven fluid upflow in marine sediments. 118 pages, Bremen 1999.

No. 148 **Kinkel, H.**
Living and late Quaternary Coccolithophores in the equatorial Atlantic Ocean: response of distribution and productivity patterns to changing surface water circulation. 183 pages, Bremen, 2000.

No. 149 **Pätzold, J. and cruise participants**
Report and preliminary results of METEOR Cruise M 44/3, Aqaba (Jordan) - Safaga (Egypt) – Dubá (Saudi Arabia) – Suez (Egypt) - Haifa (Israel), 12.3.-26.3.-2.4.-4.4.1999. 135 pages, Bremen, 2000.

No. 150 **Schlünz, B. and G. Wefer**
Bericht über den 8. JGOFS-Workshop am 2. und 3.12.1999 in Bremen. Im Anhang:
Publikationen zum deutschen Beitrag zur Joint Global Ocean Flux Study (JGOFS), Stand 1/ 2000.
95 pages, Bremen, 2000.

No. 151 **Schnack, K.**
Biostratigraphie und fazielle Entwicklung in der Oberkreide und im Alttertiär im Bereich der Kharga Schwelle, Westliche Wüste, SW-Ägypten. 142 pages, Bremen, 2000.

No. 152 **Karwath, B.**
Ecological studies on living and fossil calcareous dinoflagellates of the equatorial and tropical Atlantic Ocean. 175 pages, Bremen, 2000.

No. 153 **Moustafa, Y.**
Paleoclimatic reconstructions of the Northern Red Sea during the Holocene inferred from stable isotope records of modern and fossil corals and molluscs. 102 pages, Bremen, 2000.

No. 154 **Villinger, H. and cruise participants**
Report and preliminary results of SONNE-cruise 145-1 Balboa – Talcahuana, 21.12.1999 – 28.01.2000.
147 pages, Bremen, 2000.

No. 155 **Rusch, A.**
Dynamik der Feinfraktion im Oberflächenhorizont permeabler Schelfsedimente. 102 pages, Bremen, 2000.

No. 156 **Moos, C.**
Reconstruction of upwelling intensity and paleo-nutrient gradients in the northwest Arabian Sea derived from stable carbon and oxygen isotopes of planktic foraminifera. 103 pages, Bremen, 2000.

No. 157 **Xu, W.**
Mass physical sediment properties and trends in a Wadden Sea tidal basin. 127 pages, Bremen, 2000.

No. 158 **Meinecke, G. and cruise participants**
Report and preliminary results of METEOR Cruise M 45/1, Malaga (Spain) - Lissabon (Portugal),
19.05. - 08.06.1999. 39 pages, Bremen, 2000.

No. 159 **Vink, A.**
Reconstruction of recent and late Quaternary surface water masses of the western subtropical Atlantic Ocean based on calcareous and organic-walled dinoflagellate cysts. 160 pages, Bremen, 2000.

No. 160 **Willems, H. (Sprecher), U. Bleil, R. Henrich, K. Herterich, B.B. Jørgensen, H.-J. Kuß, M. Olesch, H.D. Schulz,V. Spieß, G. Wefer**
Abschlußbericht des Graduierten-Kollegs Stoff-Flüsse in marine Geosystemen.
Zusammenfassung und Berichtszeitraum Januar 1996 - Dezember 2000. 340 pages, Bremen, 2000.

No. 161 **Sprengel, C.**
Untersuchungen zur Sedimentation und Ökologie von Coccolithophoriden im Bereich der Kanarischen Inseln: Saisonale Flussmuster und Karbonatexport. 165 pages, Bremen, 2000.

No. 162 **Donner, B. and G. Wefer**
Bericht über den JGOFS-Workshop am 18.-21.9.2000 in Bremen:
Biogeochemical Cycles: German Contributions to the International Joint Global Ocean Flux Study.
87 pages, Bremen, 2000.

No. 163 **Neuer, S. and cruise participants**
Report and preliminary results of Meteor Cruise M 45/5, Bremen – Las Palmas, October 1 – November 3, 1999. 93 pages, Bremen, 2000.

No. 164 **Devey, C. and cruise participants**
Report and preliminary results of Sonne Cruise SO 145/2, Talcahuano (Chile) - Arica (Chile), February 4 – February 29, 2000. 63 pages, Bremen, 2000.

No. 165 **Freudenthal, T.**
Reconstruction of productivity gradients in the Canary Islands region off Morocco by means of sinking particles and sediments. 147 pages, Bremen, 2000.

No. 166 **Adler, M.**
Modeling of one-dimensional transport in porous media with respect to simultaneous geochemical reactions in CoTReM. 147 pages, Bremen, 2000.

No. 167 **Santamarina Cuneo, P.**
Fluxes of suspended particulate matter through a tidal inlet of the East Frisian Wadden Sea (southern North Sea). 91 pages, Bremen, 2000.

No. 168 **Benthien, A.**
Effects of CO_2 and nutrient concentration on the stable carbon isotope composition of C37:2 alkenones in sediments of the South Atlantic Ocean. 104 pages, Bremen, 2001.

No. 169 **Lavik, G.**
Nitrogen isotopes of sinking matter and sediments in the South Atlantic. 140 pages, Bremen, 2001.

No. 170 **Budziak, D.**
Late Quaternary monsoonal climate and related variations in paleoproductivity and alkenone-derived sea-surface temperatures in the western Arabian Sea. 114 pages, Bremen, 2001.

No. 171 **Gerhardt, S.**
Late Quaternary water mass variability derived from the pteropod preservation state in sediments of the western South Atlantic Ocean and the Caribbean Sea. 109 pages, Bremen, 2001.

No. 172 **Bleil, U. and cruise participants**
Report and preliminary results of Meteor Cruise M 46/3, Montevideo (Uruguay) – Mar del Plata (Argentina), January 4 – February 7, 2000. Bremen, 2001.

No. 173 **Wefer, G. and cruise participants**
Report and preliminary results of Meteor Cruise M 46/4, Mar del Plata (Argentina) – Salvador da Bahia (Brazil), February 10 – March 13, 2000. With partial results of METEOR cruise M 46/2. 136 pages, Bremen, 2001.

No. 174 **Schulz, H.D. and cruise participants**
Report and preliminary results of Meteor Cruise M 46/2, Recife (Brazil) – Montevideo (Uruguay), December 2 – December 29, 1999. 107 pages, Bremen, 2001.

No. 175 **Schmidt, A.**
Magnetic mineral fluxes in the Quaternary South Atlantic: Implications for the paleoenvironment.
97 pages, Bremen, 2001.

No. 176 **Bruhns, P.**
Crystal chemical characterization of heavy metal incorporation in brick burning processes.
93 pages, Bremen, 2001.

No. 177 **Karius, V.**
Baggergut der Hafengruppe Bremen-Stadt in der Ziegelherstellung. 131 pages, Bremen, 2001.

No. 178 **Adegbie, A. T.**
Reconstruction of paleoenvironmental conditions in Equatorial Atlantic and the Gulf of Guinea Basins for the last 245,000 years. 113 pages, Bremen, 2001.

No. 179 **Spieß, V. and cruise participants**
Report and preliminary results of R/V Sonne Cruise SO 149, Victoria - Victoria, 16.8. - 16.9.2000.
100 pages, Bremen, 2001.

No. 180 **Kim, J.-H.**
Reconstruction of past sea-surface temperatures in the eastern South Atlantic and the eastern South Pacific across Termination I based on the Alkenone Method. 114 pages, Bremen, 2001.

No. 181 **von Lom-Keil, H.**
Sedimentary waves on the Namibian continental margin and in the Argentine Basin – Bottom flow reconstructions based on high resolution echosounder data. 126 pages, Bremen, 2001.

No. 182 **Hebbeln, D. and cruise participants**
PUCK: Report and preliminary results of R/V Sonne Cruise SO 156, Valparaiso (Chile) - Talcahuano (Chile), March 29 - May 14, 2001. 195 pages, Bremen, 2001.

No. 183 **Wendler, J.**
Reconstruction of astronomically-forced cyclic and abrupt paleoecological changes in the Upper Cretaceous Boreal Realm based on calcareous dinoflagellate cysts. 149 pages, Bremen, 2001.

No. 184 **Volbers, A.**
Planktic foraminifera as paleoceanographic indicators: production, preservation, and reconstruction of upwelling intensity. Implications from late Quaternary South Atlantic sediments. 122 pages, Bremen, 2001.

No. 185 **Bleil, U. and cruise participants**
Report and preliminary results of R/V METEOR Cruise M 49/3, Montevideo (Uruguay) - Salvador (Brasil), March 9 - April 1, 2001. 99 pages, Bremen, 2001.

No. 186 **Scheibner, C.**
Architecture of a carbonate platform-to-basin transition on a structural high (Campanian-early Eocene, Eastern Desert, Egypt) – classical and modelling approaches combined. 173 pages, Bremen, 2001.

No. 187 **Schneider, S.**
Quartäre Schwankungen in Strömungsintensität und Produktivität als Abbild der Wassermassen-Variabilität im äquatorialen Atlantik (ODP Sites 959 und 663): Ergebnisse aus Siltkorn-Analysen. 134 pages, Bremen, 2001.

No. 188 **Uliana, E.**
Late Quaternary biogenic opal sedimentation in diatom assemblages in Kongo Fan sediments. 96 pages, Bremen, 2001.

No. 189 **Esper, O.**
Reconstruction of Recent and Late Quaternary oceanographic conditions in the eastern South Atlantic Ocean based on calcareous- and organic-walled dinoflagellate cysts. 130 pages, Bremen, 2001.

No. 190 **Wendler, I.**
Production and preservation of calcareous dinoflagellate cysts in the modern Arabian Sea. 117 pages, Bremen, 2002.